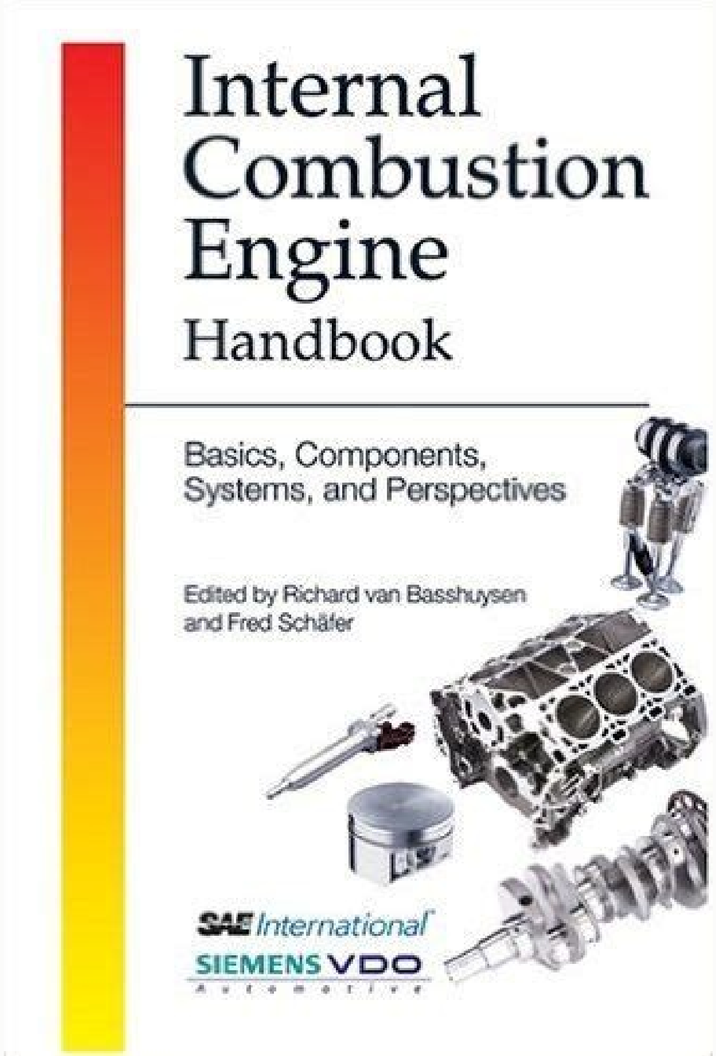


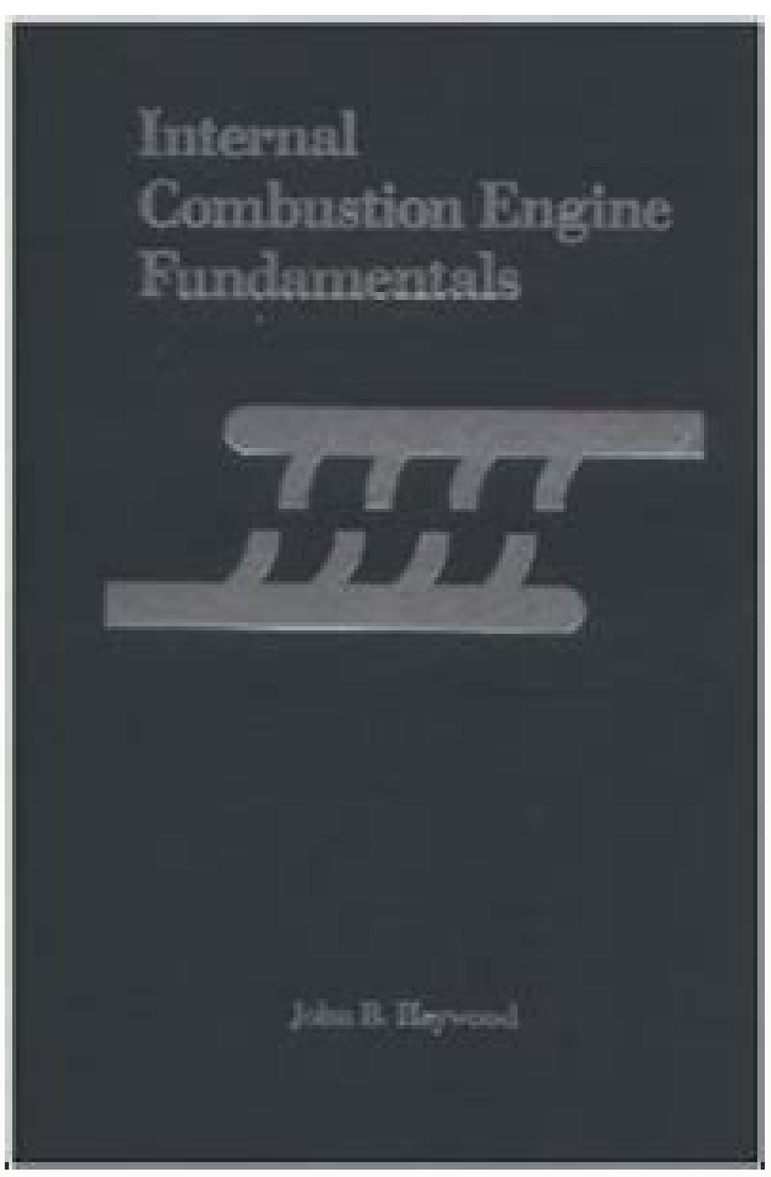
Continue

Internal combustion engine fundamentals 2020 pdf

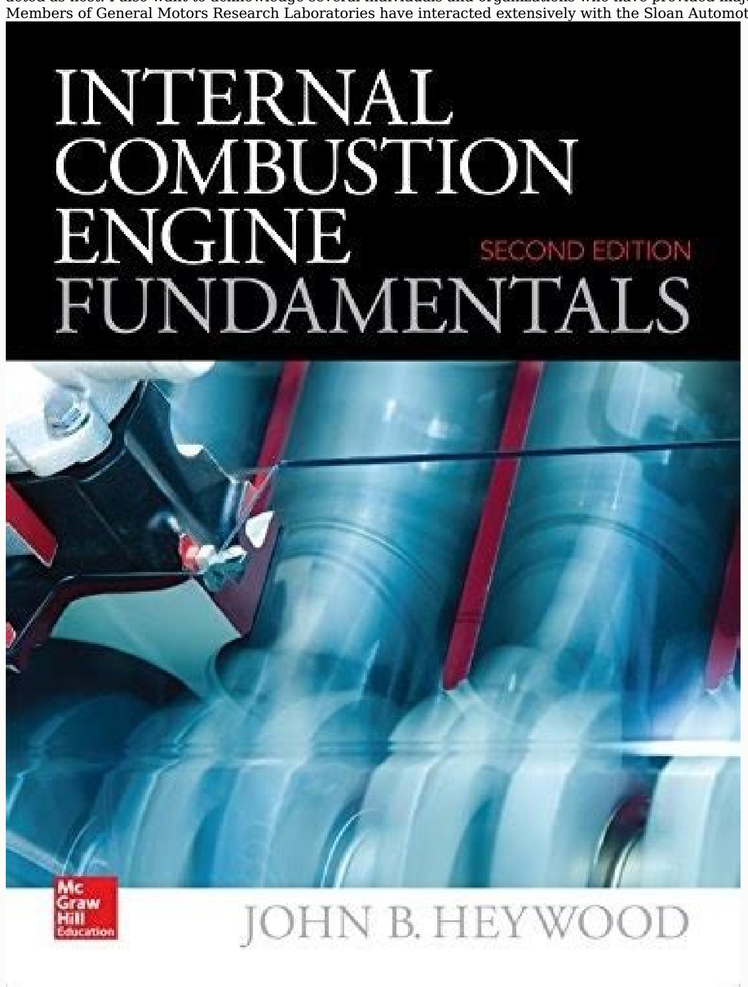
Academia.edu uses cookies to personalize content, tailor ads and improve the user experience.
By using our site, you agree to our collection of information through the use of cookies. To learn more, view our Privacy Policy. VDOC.PUB Authors: John Heywood PDF Technique , Transport Download Embed This document was uploaded by our user. The uploader already confirmed that they had the permission to publish it. If you are author/publisher or own the copyright of this documents, please report to us by using this DMCA report form. honeywell chronotherm t8095 manual Report DMCA This text, by a leading authority in the field, presents a fundamental and factual development of the science and engineering underlying the design of combustion engines and turbines. An extensive illustration program supports the concepts and theories discussed. McGraw-Hill Series in Mechanical Engineering Jack P. Holman, Southern Methodist University Consulting Editor Anderson: Modern Compressible Flow: With Historical Perspective Dieter: Engineering Design: A Materials and Processing Approach Eckert and Drake: Analysis of Heat and Mars Transfer Heywood: Internal Combwtion Engine Fundamentals H i m : Turbulence,2/e Hutton: Applied Mechanical Vibrations Juvinall: Engineering Considerations of Stress, Strain, and Strength Kane and Levinson: Dynamics: Theory and Applications Kays and Crawford: Convective Heat and Mass Transfr Mutin: Kinematics and Dynamics of Machines Pklan: Dynamics of Machinery Pbelan: Fundamentals of Mechanical Design, 3/e Pierce: Acoustics: An Introduction to Its Physical Principles and Applications Raven: Automatic Control Engineering, 4/e Rosenberg aod Karnopp: Introduction to Physics Schlichting: Boundary-Layer Theory, 7/e Shames: Mechanics of Fluiak, 2/e Shigley: Kinematic Analysis of Mechanisms, 2/e Sbigley and Mitchell: Mechanical Engineering Design, 4/e Sbigley and Uicker: Theory of Machines and Mechanisms Stoecker and Jones: Refrigeration and Air Conditioning, 2/e Vanderplaats: Numerical Optimization Techniquesfor Engineering Design: With Applications - INTERNAL COMBUSTION ENGINE John B.LHeywood Professor of Mechanical Engineering Director, Sloan Automotive Laboratory Massachusetts Institute of Technology Xnderung nur iiber Fechbibliothek BFV21 (S!V McGraw-Hill, Inc. New York St. Louis San Francisco Auckland Bogoti Caracas Lisbon London Madrid Mexico City Milan Montreal New Delhi San Juan Singapore Sydney Tokyo Toronto INTERNAL COMBUSTION ENGINE FUNDAMENTALS This book was set in Times Roman. The editors were Anne Duffy and John M. M o m s ; the designer was Joan E. O'Connor; the production supervisor was Denise L. Puryear. New drawings were done by ANCO. Project Supervision was done by Santype International Ltd. R. R. Donnelley & Sons Company was printer and binder. ABOUT THE AUTHOR See acknowledgements on page xxi. Copyright 0 1988 by McGraw-Hill, Inc. All rights rese~ed. Printed in the United States of America. Except as permitted under the United States Copyright Act of 1976, no part of this publication may be reproduced or distributed in any form or by any means, or stored in a data base or retrieval system, without the prior written permission of the publisher. ISBN - 0-07-028637-X Library of Congress Cataloging-iP.PublicationData Heywood, John B. Internal combustion engine fundamentals. rage quit games for android (McGraw-Hill series in mechanical engineering) Bibliography: p. Includes index.
I. Internal combustion engines. I. papier_millimetre_rouge.pdf Title. 11. Series. TJ755.H45 1988 621.43 87-15251 This book is printed on acid-free paper. Dr. John B. Heywood received the Ph.D. degree in mechanical engineering from the Massachusetts Institute of Technology in 1965.
Following an additional postdoctoral year of research at MIT, he worked as a research officer at the Central Electricity Generating Board's Research Laboratory in England on magnetohydrodynamic power generation. In 1968 he joined the faculty at MIT where he is Professor of Mechanical Engineering. At MIT he is Director of the Sloan Automotive Laboratory. He is currently Head of the Fluid and Thermal Science Division of the Mechanical Engineering Department, and the Transportation Energy Program Director in the MIT Energy Laboratory. He is faculty advisor to the MIT Sports Car Club. Professor Heywood's teaching and research interests lie in the areas of thermodynamics, combustion, energy, power, and propulsion. During the past two decades, his research activities have centered on the operating characteristics and fuels requirements of automotive and aircraft engines. A major emphasis has been on computer models which predict the performance, efficiency, and emissions of spark-ignition, diesel, and gas turbine engines; and in carrying out experiments to develop and validate these models. He is also actively involved in technology assessments and policy studies related to automotive engines, automobile fuel utilization, and the control of air pollution. He consults frequently in &he automotive and petroleum industries, and for the U.S. Government. His extensive research in the field of eogines has been supported by the U.S. Army, Department of Energy, Environmental Protection Agency, NASA, National Science Foundation, automobile and diesel engine manufacturers, and petroleum companies. He has presented or published over a hundred papers on ~i ABOUT THE A U T H O R his research in technical conferences and journals. He has co-authored two previous books: Open-Cycle MHD Power Generation published by Pergamon Press in 1969 and The Automobile and the Regulation of Its Impact on the Environment published by University of Oklahoma Press in 1975. He is a member of the American Society of Mechanical Engineers, an associate fellow of the American Institute of Aeronautics and Astronautics, a fellow of the British Institution of Mechanical Engineers, and in 1982 was elected a Fellow of the U.S. Society of Automotive Engineers for his technical contributions to automotive engineering. He is a member of the editorial boards of the journals Progress in Energy and Combustion Science and the International Journal of Vehicle Design. His research publications on internal combustion engines, power generation, and gas turbine combustion have won numerous awards.
He was awarded the Ayreton Premium in 1969 by the British Institution of Electrical Engineers. Professor Heywood received a Ralph R. Teetor Award as an outstanding young engineering educator from the Society of Automotive Engineers in 1971. He has twice been the recipient of an SAE Arch T.
Colwell Merit Award for an outstanding technical publication (1973 and 1981). He received SAE's Horning Memorial Award for the best paper on engines and fuels in 1984.



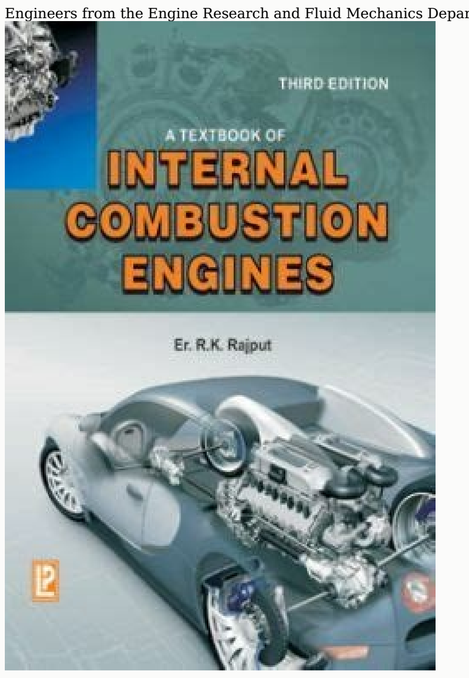
In 1984 he received the Sc.D. degree from Cambridge University for his published contributions to engineering research. He was selected as the 1986 American Society of Mechanical Engineers Freeman Scholar for a major review of "Fluid Motion within the Cylinder of Internal Combustion Engines." ' THISBooK IS DEDICATED TO MY FATHER, Harold Heywood : I have followed many of the paths he took. vii . ' - CONTENTS Preface xvii Commonly Used Symbols, Subscripts, and Abbreviations xxiii Chapter 1 Engine Types and Their Operation 1.1 1.2 1.3 1.4 1.5 1.6 1.7 1.8 1.9 Introduction and Historical Perspective Engine Classifiytions Engine Operating Cycles Engine Components Spark-Ignition Engine Operation Examples of Spark-Ignition Engines Compression-Ignition Engine Operation Examples of Diesel Engines Stratified-ChargeEngines Chapter 2 Engine Design and Operating Parameters 2.1 2.2 23 2.4 2.5 2.6 2.7 2.8 2.9 Important Engine Characteristics Geometrical Properties of Reciprocating Engines Brake Torque and Power Indicated Work Per Cycle Mechanical Efficiency Road-Load Power Mean Effective Pressure Specific Fuel Consumption and Efficiency Air/Fuel and Fuel/Air Ratios X CONTENTS 2.10 2.11 2.12 2.13 2.14 2.15 Volumetric Efficiency Engine Specific Weight and Specific Volume Correction Factors for Power and Volumetric Efficiency Specific Emissions and Emissions Index Relationships between Performance Parameters Engine Design and Performance Data Chapter 5 Ideal Models of Engine Cycles 5.1 5.2 5.3 5.4 Chapter 3 Thermochemistry of Fuel-Air Mixtures 3.1 3.2 3.3 3.4 3.5 Characterization of Flames Ideal Gas Model Composition of Air and Fuels Combustion Stoichiometry The First Law of Thermodynamics and Combustion 3.5.1 Energy and Enthalpy Balances 3.5.2 Enthalpies of Formation 3.5.3 Heating Values 3.5.4 Adiabatic Combustion Processes 3.5.5 Combustion Efiency of an Internal Combustion Engine The Second Law of Thermodynamics Applied to Combustion 3.6.1 Entropy 3.6.2 Maximum Work from an Internal Combustion Engine and Efficiency Chemically Reacting Gas Mixtures 3.7.1 Chemical Equilibrium 3.7.2 Chemical Reaction Rates 5.8 Chapter 6 Gas Exchange Processes 6.1 6.2 Chapter 4 Properties of Working Fluids 4.1 4.2 4.3 4.4 4.5 Introduction Unburned Mixture Composition Gas Property Relationships A Simple Analytic Ideal Gas Model Thermodynamic Charts 4.5.1 Unburned Mixture Charts 4.5.2 Burned Mixture Charts 4.5.3 Relation between Unburned and Burned Mixture Charts Tables of Properties and Composition Computer Routines for Property and Composition Calculations 4.7.1 Unburned Mixtures 4.7.2 Burned Mixtures Transport Properties Exhaust Gas Composition 4.9.1 Species Concentration Data 4.9.2 Equivalence Ratio Determination from Exhaust Gas Constituents 4.9.3 Effects of Fuel/Air Ratio Nonuniformity 4.9.4 Combustion Inefficiency Introduction Ideal Models of Engine Processes Thermodynamic Relations for Engine Processes Cycle Analysis with Ideal Gas Working Fluid with c, and Constant 5.4.1 Constant-Volume Cycle 5.4.2 Limited- and Constant-Pressure Cycles 5.4.3 Cycle Comparison Fuel-Air Cycle Analysis 5.5.1 SI Engine Cycle Simulation 5.5.2 CI Engine Cycle Simulation 5.5.3 Results of Cycle Calculations Overexpanded Engine Cycles Availability Analysis of Engine Processes 5.7.1 Availability Relationships 5.7.2 Entropy Changes in Ideal Cycles 5.7.3 Availability Analysis of Ideal Cycles 5.7.4 Effect of Equivalence Ratio Comparison with Real Engine Cycles 6.4 6.5 6.6 6.7 6.8 Inlet and Exhaust Processes in the Four-Stroke Cycle Volumetric Efficiency 6.2.1 Quasi-Static Effects 6.2.2 Combined Quasi-Static and Dynamic Ekects 'iming 6.2.3 Variation with Speed. and Valve Area, Lift, and 'I Flow Through Valves 6.3.1 Poppet Valve Geometry and Timing . 6.3.2 Flow Rate and Discharge Coefficients Residual Gas Fraction Exhaust Gas Flow Rate and Temperature Variation Scavenging in Two-Stroke Cycle Engines 6.6.1 Two-Stroke Engine Configurations 6.6.2 Scavenging Parameters and Models 6.6.3 Actual Scavenging Processes Flow Through Ports Supercharging and Turbocharging 6.8.1 Methods of Power Boosting 6.8.2 Basic Relationships 6.8.3 Compressors 6.8.4 Turbines 6.8.5 Wave-Compression Devices Chapter 7 SI Engine Fuel Metering and Manifold Phenomena 7.1 7.2 Spark-Ignition Engine Mixture Requirements Carburetors xii CONTENTS 7.2.1 Carburetor Fundamentals 7.2.2 Modem Carburetor Design 7.3 Feedback Systems Flow Past Throttle Plate Flow in Intake Manifolds 7.6.1 Design Requirements 7.6.2 Air-Flow Phenomena 7.6.3 Fuel-Flow Phenomena Chapter 10 Combustion in Compression-Ignition Engines 10.1 10.2 Chapter 8 Charge Motion within the Cylinder 8.1 8.2 8.3 8.4 8.5 8.6 8.7 Intake Jet Flow Mean Velocity and Turbulence Characteristics 8.2.1 Definitions 8.2.2 Application to Engine Velocity Data Swirl 8.3.1 Swirl Measurement 8.3.2 Swirl Generation during Induction 8.3.3 Swirl Modification within the Cylinder Squish Prechamber Engine Flows Crevice Flows and Blowby Flows Generated by Piston-Cylinder Wall Interaction Chapter 9 Combustion in Spark-Ignition Engines 9.1 9.2 9.3 9.4 9.5 9.6 Knock Fundamentals Fuel Factors Fuel-Injection Systems 7.3.1 Multipoint Port Injection 7.3.2 Single-Point Throttle-Body Injection 7.4 7.5 7.6 9.6.2 9.6.3 Essential Features of Process Thermodynamic Analysis of SI Engine Combustion 9.2.1 Burned and Unburned Mixture States 9.2.2 Analysis of Cylinder Pressure Data 9.2.3 Combustion Process Characterization Flame Structure and Speed 9.3.1 Experimental Observations 9.3.2 Flame Structure 9.3.3 Laminar Burning Speeds 9.3.4 Flame Propagation Relations Cyclic Variations in Combustion, Partial Burning, and Misfire 9.4.1 Observations and Definitions ' 9.4.2 Causes of Cycle-by-Cycle and Cylinder-to-Cylinder Variations 9.4.3 Partial Burning, Misfire, and Engine Stability Spark Ignition 9.5.1 Ignition Fundamentals 9.5.2 Conventional Ignition Systems 9.5.3 Alternative Ignition Approaches Abnormal Combustion: Knock and Surface Ignition 9.6.1 Description of Phenomena Essential Features of Process Types of Diesel Combustion Systems 10.2.1 Direct-Injection Systems 10.2.2 Indirect-Injection Systems 10.2.3 Comparison of Different Combustion Systems Phenomenological Model of Compression-Ignition Engine Combustion 10.3.1 Photographic Studies of Engine Combustion 10.3.2 Combustion in Direct-Injection, Multispray Systems 10.3.3 Application of Model to Other Combustion Systems Analysis of Cylinder Pressure Data 10.4.1 Combustion Efficiency 10.4.2 Direct-Injection Engines 10.4.3 Indirect-Injection Engines Fuel Spray Behavior 10.5.1 Fuel Injection 10.5.2 Overall Spray Structure 10.5.3 Atomization 10.5.4 Spray Penetration 10.5.5 Droplet Size Distribution 10.5.6 Spray Evaporation Ignition Delay 10.6.1 Definition and Discussion 10.6.2 Fuel Ignition Quality 10.6.3 Autoignition Fundamentals 10.6.4 Physical Factors Affecting Delay 10.6.5 Effect of Fuel Properties 10.6.6 Correlations for Ignition Delay in Engines Mixing-Controlled Combustion 10.7.1 Background 10.7.2 Spray and Flame Structure 10.7.3 Fuel-Air Mixing and Burning Rates Chapter 11 Pollutant Formation and Control 11.1 11.2 Nature and Extent of Problem Nitrogen Oxides 11.2.1 Kinetics of NO Formation 11.2.2 Formation of NO, 11.2.3 NO Formation in Spark-Ignition Engines 11.2.4 NO, Formation in Compression-Ignition Engines Carbon Monoxide Unburned Hydrocarbon Emissions 11.4.1 Background 11.4.2 Flame Quenching and Oxidation Fundamentals xiv CONTENTS 13.3.1 Lubricated Friction 13.3.2 Turbulent Dissipation 13.3.3 Total Friction 11.4.3 HC Emissions from Spark-Ignition Engines 11.4.4 Hydrocarbon Emission Mechanisms in Diesel Engines 11.5 11.6 Particulate Emissions 11.5.1 Spark-Ignition Engine Particulates 11.5.2 Characteristics of Diesel Particulates 11.5.3 Particulate Distribution within the Cylinder 11.5.4 Soot Formation Fundamentals 11.5.5 Soot Oxidation 11.5.6 Adsorption and Condensation Exhaust Gas Treatment 11.6.1 Available Options 11.6.2 Catalytic Converters 11.6.3 Thermal Reactors 11.6.4 Particulate Traps 13.4 13.5 13.6 13.7 13.8 Chapter 12 Engine Heat Transfer 12.1 12.2 12.3 12.4 12.5 12.6 12.7 Importance of Heat Transfer Modes of Heat Transfer 12.2.1 Conduction 12.2.2 Convection 12.2.3 Radiation 12.2.4 Overall Heat-Transfer Process Heat Transfer and Engine Energy Balance Convective Heat Transfer 12.4.1 Dimensional Analysis 12.4.2 Correlations for Time-Averaged Heat Flux 12.4.3 Correlations for Instantaneous Spatial Average Coefficients 12.4.4 Correlations for Instantaneous Local Coefficients 12.4.5 Intake and Exhaust System Heat Transfer Radiative Heat Transfer 12.5.1 Radiation from Gases 12.5.2 Flame Radiation 12.5.3 Prediction Formulas Measurements of Instantaneous Heat-Transfer Rates 12.6.1 Measurement Methods 12.6.2 Spark-Ignition Engine Measurements 12.6.3 Diesel Engine Measurements 12.6.4 Evaluation of Heat-Transfer Correlations 12.6.5 Boundary-Layer Behavior Thermal Loading and Component Temperatures 12.7.1 Component Temperature Distributions 12.7.2 Effect of Engine Variables Chapter 13 Engine Friction and Lubrication 13.1 13.2 13.3 Background Definitions Friction Fundamentals Measurement Methods Engine Friction Data 13.5.1 SI Engines 13.5.2 Diesel Engines Engine Friction Components 13.6.1 Motored Engine Breakdown Tests 13.6.2 Pumping Friction 13.6.3 Piston Assembly Friction 13.6.4 Crankshaft Bearing Friction 13.6.5 Valve Train Friction Accessory Power Requirements Lubrication 13.8.1 Lubrication System 13.8.2 Lubricant Requirements Chapter 14 Modeling Real Engine Flow and Combustion Processes 14.1 14.2 14.3 14.4 14.5 Purpose and Classification of Models Governing Equations for Open Thermodynamic System 14.2.1 Conservation of Mass 14.2.2 Conservation of Energy Intake and Exhaust Flow Models 14.3.1 Background 14.3.2 Quasi-Steady Flow Models 14.3.3 Filling and Emptying Methods 14.3.4 Gas Dynamic Models Thermodynamic-Based In-Cylinder Models 14.4.1 Background and Overall Model Structure 14.4.2 Spark-Ignition Engine Models 14.4.3 Direct-Injection Engine Models 14.4.4 Prechamber Engine Models 14.4.5 Multicylinder and Complex Engine System Models 14.4.6 Second Law Analysis of Engine Processes Fluid-Mechanic-Based Multidimensional Models - 14.5.1 Basic Approach and Governing Equations 14.5.2 Turbulence Models 14.5.3 Numerical Methodology 14.5.4 Flow Field Predictions 14.5.5 Fuel Spray Modeling 14.5.6 Combustion Modeling Chapter 15 Engine Operating Characteristics 15.1 15.2 Engine Performana Parameters Indicated and Brake Power and MEP xvi CONTENTS 15.3 15.4 15.5 15.6 Operating Variables That Affect SI Engine Performance, Efficiency, and Emissions 15.3.1 Spark Timing 15.3.2 Mixture Composition 15.3.3 Load and Speed 15.3.4 Compression Ratio SI Engine Combustion Chamber Design 15.4.1 Design Objectives and Options 15.4.2 Factors That Control Combustion 15.4.3 Factors That Control Performance 15.4.4 Chamber Octane Requirement 15.4.5 Chamber Optimization Strategy Variables That Affect CI Engine Performance, Efficiency, and Emissions 15.5.1 Load and Speed 15.5.2 Fuel-Injection Parameters 15.5.3 Air Swirl and Bowl-in-Piston Design Supercharged and Turbocharged Engine Performance 15.6.1 Four-Stroke Cycle SI Engines 15.6.2 Four-Stroke Cycle CI Engines 15.6.3 Two-Stroke Cycle SI Engines 15.6.4 Two-Stroke Cycle CI Engines Engine Performance Summary Appendixes A B C D Unit Conversion Factors Ideal Gas Relationships B.l Ideal Gas Law B.2 The Mole B.3 Thermodynamic Properties B.4 Mixtures of Ideal Gases Equations for Fluid Flow through a Restriction C.1 Liquid Flow C.2 Gas Flow Data on Working Fluids Index - PREFACE Internal combustion engines date back to 1876 when Otto first developed the spark-ignition engine and 1892 when Diesel invented the compression-ignition engine. Since that time these engines have continued to develop as our knowledge of engine processes has increased, as new technologies became available, as demand for new types of engine arose, and as environmental constraints on engine use changed. Internal combustion engines, and the industries that develop and manufacture them and support their use, now play a dominant role in the fields of power, propulsion, and energy. The last twenty-five years or so have seen an explosive growth in engine research and development as the issues of air pollution, fuel cost, and market competitiveness have become increasingly important. An enormous technical literature on engines now exists which has yet to be adequately organized and summarized. This book has been written as a text and a professional reference in response to that need. slither io ölümsüzlük hilesi apk indir It contains a broadly based and extensive review of the fundamental principles which govern internal combustion engine design and operation. It attempts to provide a simplifying framework for the vast and complex mass of technical material that now exists on spark-ignition and compression-ignition engines, and at the same time to include sufficient detail to convey the real world dimensions of this pragmatic engineering field. It is the author's conviction that a sound knowledge of the relevant fundamentals in the many disciplines that contribute to this field, as well as an awareness of the extensive practical knowledge base which has been built up over many decades, are essential tools for engine research, development, and design. Of course, no one text can include everything about engines. The emphasis here is on the thermodynamics, combustion physics and chemistry, fluid flow, heat transfer, friction, and lubrication processes relevant to internal combustion engine design, performance, efficiency, emissions, and fuels requirements. xviii PREFACE From a fundamental point of view, how the fuel-air mixture within an internal combustion engine cylinder is ignited appropriately organizes the field. From the method of ignition-spark-ignition or compression-ignition-follows each type of engine's important features: fuel requirements, method of mixture prep aration, combustion chamber design, details of the combustion process, method of load control, emission formation mechanisms, and performance and efficiency characteristics. While many engine processes (such as intake and exhaust flows, convective heat transfer, and friction) are similar in both types of engines, this distinction is fundamental and lies behind the overall organization of the book. The book is arranged in four major sections. The first (Chapters 1 to 5) provides an introduction to, and overview of, the major characteristics of sparkignition and compression-ignition engines, defines the parameters used to describe engine operation, and develops the necessary thermodynamics and combustion theory required for a quantitative analysis of engine behavior. loi d' ohm exercices corrigés It concludes with an integrated treatment of the various methods of analyzing idealized models of internal combustion engine cycles. The second section (Chapters 6 to 8) focuses on engine flow phenomena. The details of the gas exchange processintake and exhaust processes in four-stroke and scavenging in two-stroke cycles-and the various methods of supercharging engines-are reviewed. Fuel metering methods for spark-ignition engines and air- and fuel-flow phenomena in intake manifolds are described. The essential features of the various types of fluid motion within the engine cylinder are then developed. These flow processes control the amount of air an engine will induct (and therefore its power), and largely govern the rate at which the fuel-air mixture will burn during combustion. The third section of the book focuses on engine combustion phenomena. These chapters (9, 10, and 11) are especially important. The combustion process releases the fuel's energy within the engine cylinder for eventual conversion to useful work. What fraction of the fuel's energy is converted depends strongly on how combustion takes place. The spark-ignition and compression-ignition engine combustion processes (Chapters 9 and 10, respectively) therefore influence essentially all aspects of engine behavior. Air pollutants are undesirable byproducts of combustion. download beat saber for android Our extensive knowledge of how the major pollutants form during these combustion processes and how such emissions can be controlled is reviewed in Chapter 11. The last section of the book focuses on engine operating characteristics. First, the fundamentals of engine heat transfer and friction, both of which detract from engine performance, are developed in Chapters 12 and 13. Chapter 14 then focuses on the methods available for predicting important aspects of engine behavior based on realistic models of engine flow and combustion processes. Since the various thermodynamic-based and fluid-mechanic-based models which have been developed over the past fifteen years or so are increasingly used in engine research and development, a knowledge of their basic structure and capabilities is most important. Then, Chapter 15 presents a summary of how the operating characteristics-power, efficiency, and emissions--of spark-ignition and compression-ignition engines depend on the major engine design and oper- PREFACE X~X sting variables. These final two chapters effectively integrate the analytical understanding and practical knowledge of individual engine processes together to describe overall spark-ignition and compression-ignition engine behavior. Material on internal combustion engine fuels is distributed appropriately the book. Each chapter is extensively illustrated and referenced, and includes problems for both undergraduate and graduate level courses. While this book contains much advanced material on engine design and operation intended for the practitioner, each major topic is developed from its beginnings and the more sophisticated chapters have introductory sections to facilitate their use in undergraduate courses. The chapters are extensively crossand indexed. Thus several arrangements of the material for a course on engines can be followed. For example, an introductory course on internal combustion engines could begin with Chapters 1 and 1,which review the different types of engines and how their performance is characterized, and continue with the parts of Chapters 3 and 5, which introduce the key combustion concepts necessary to understand the effects of fuellair ratio, and ideal cycle analysis. Selections from the introductory sections of Chapters 6,9, 10, l l , and 15 could then be used to explain several of the practical and design aspects of spark-ignition and diesel engine intake and exhaust processes, combustion, emissions, and performance. A more advanced course would review this introductory material more rapidly, and then move on to those sections of Chapters 4 and 5, which cover fuel-air cycle analysis, a more extensive discussion of engine breathing using additional sections of Chapter 6, and more in-depth treatment of engine combustion and emissions processes based on the appropriate sections of Chapters 9, 10, and 11. Material on engine heat transfer and friction selected from Chapters 12 and 13 could be included next. While Chapter 14 on modeling the thermodynamics and fluid dynamics of real engine processes is primarily intended for the professional scientist and engineer, material from this chapter along with selections from Chapter 15 could be used to illustrate the performance, efficiency, and emissions characteristics of the different types of internal combustion engines. I have also used much of the more sophisticated material in Chapters 6 through 15 for review seminars on individual engine topics and more extensive courses for professional engineers, an additional important educational and reference opportunity. Many individuals and organizations have assisted me in various ways as I have worked on this book over the past ten or so years. I am especially indebted to my colleagues in the Sloan Automotive Laboratory at M.I.T., Professors Wai K. Cheng, Ahmed F.



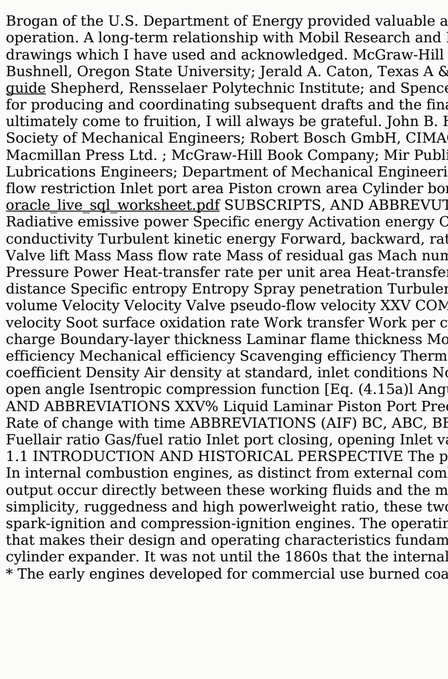
Ghoniem, and James C. Keck, and Drs. Jack A. Ekchian, David P. Hoult, Joe M. Rife, and Victor W. Wong, for providing a stimulating environment in which to carry out engine research and for assuming additional burdens as a result of my writing. Many of the Sloan Automotive Laboratory's students have made significant contributions to this text through their research; their names appear in the reference lists. The U.S. Department of Energy provided support during the early stages of the text development and funded the work on engine cycle simulation used extensively in Chapters 14 and 15. I am grateful , XX PREFACE to Churchill College, Cambridge University, for a year spent as a Richard C. Mellon Visiting Fellow, 1977-78, and the Engineering Department, Cambridge University, for acting as my host while I developed the outline and earlier chapters of the book. The M.I.T. sabbatical leave fund supported my full-time writing for eight months in 1983, and the Mechanical Engineering Department at Imperial College graciously acted as host. I also want to acknowledge several individuals and organizations who have provided major inputs to this book beyond those cited in the references.
Members of General Motors Research Laboratories have interacted extensively with the Sloan Automotive Laboratory over many years and provided valuable advice on engine research developments.



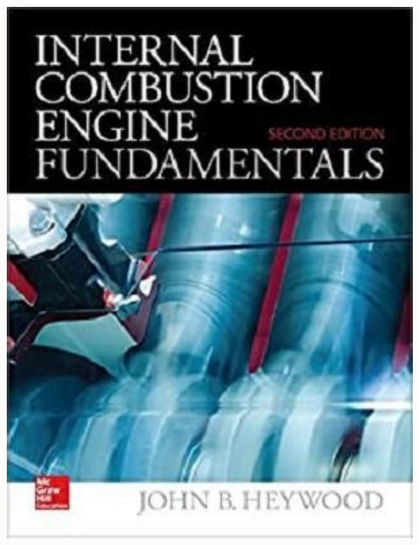
Engineers from the Engine Research and Fluid Mechanics Departments at General Motors Research Laboratories reviewed and critiqued the final draft manuscript for me. Charles A. winipog.pdf Amann, Head of the Engine Research Department, made especially helpful inputs on engine performance. John J.



Brogan of the U.S. Department of Energy provided valuable assistance with the initial organization of this effort. My regular interactions over the years with the Advanced Powertrain Engineering Ofiice and Scientific Research Laboratories of the Ford Motor Company have given me a broad exposure to the practical side of engine design and operation. A long-term relationship with Mobil Research and Development Corporation has provided comparable experiences in the area of engine-fuels interactions. Many organizations and individuals supplied specific material and illustrations for the text. I am especially grateful to those who made available the high-quality photographs and line drawings which I have used and acknowledged. McGraw-Hill and the author would like to express their thanks to the following reviewers for their useful comments and suggestions: Jay A. Bolt, University of Michigan; Gary L. best_two_player_tablet_games_android.pdf Borman and William L. Brown, University of Wisconsin at Madison; Dwight Bushnell, Oregon State University; Jerald A. Caton, Texas A & M University; David E. Cole, University of Michigan; Lawrence W. Evers, Michigan Technological University; Samuel S. Lestz, Pennsylvania State University; Willard Pulkrabek, University of Wisconsin; Robert F. Sawyer, University of California at Berkeley; Joseph E. minix neo u1 setup guide Shepherd, Rensselaer Polytechnic Institute; and Spencer C. Sorenson, The Technical University of Denmark. Special thanks are due to my secretaries for their faithful and thoughtful assistance with the manuscript over these many years, beyond the "call of duty "; Linda Pope typed an earlier draft of the book, and Karla Stryket was responsible for producing and coordinating subsequent drafts and the final manuscript. My wife Peggy, and sons James, Stephen, and Ben have encouraged me throughout this long and time-consuming project which took many hours away from them. Without their continuing support it would never have been finished; for their patience, and faith that it would ultimately come to fruition, I will always be grateful. John B. Heywood - ACKNOWLEDGMENTS The author wishes to acknowledge the following organizations and publishers for permission to reproduce figures and tables from their publications in this text: The American Chemical Society; American Institute of Aeronautics & Astronautics; American Society of Mechanical Engineers; Robert Bosch GmbH, CIMAC, Cambridge University Press; The Combustion Institute; Elsevier Science Publishing Company; G. T. Foulis & Co. Ltd.; General Motors Corporation; Gordon & Breach Science Publishers; The Institution of Mechanical Engineers; The Japan Society of Mechanical Engineers; M.I.T. Press; Macmillan Press Ltd. ; McGraw-Hill Book Company; Mir Publishers; Mobil Oil Corporation; Morgan-Grampian Publishers; Pergamon Journals, Inc.; Plenum Press Corporation; The Royal Society of London; Scientific Publications Limited; Society of Automotive Engineers; Society of Automotive Engineers of Japan, Inc.; Society of Tribologists and Lubrications Engineers; Department of Mechanical Engineering, Stanford University. xxi COMMONLY USED SYMBOLS, SUBSCRIPTS, AND ABBREVIATIONS 1. SYMBOLS a a A Ac A,, 4 AE Ai 4 B c C~ CS CD C Crank radius Sound speed Specific availability Acceleration Area Valve cu.rtain area Cylinder head area Exhaust port area Effective area of flow restriction Inlet port area Piston crown area Cylinder bore Steady-flow availability Specific heat Specific heat at constant pressure Soot concentration (mass/volume) Specific heat at constant volume Absolute gas velocity t Nomenclature specific to a section or chapter is defined in that section or chapter. xxiii COMMONLY USED SYMBOLS. oracle_live_sql_worksheet.pdf SUBSCRIPTS, AND ABBREVUTIONS X X ~ V COMMONLY USED SYMBOLS, SUBSCRIPTS, AND ABBREVIATIONS Swirl coefficient Discharge coefficient Vehicle drag coefficient Diameter Fuel-injection-nozzle orifice diameter Diameter Diffusion coefficient Droplet diameter Sauter mean droplet diameter Valve diameter Radiative emissive power Specific energy Activation energy Coefficient of friction Fuel mass fraction Force Gravitational acceleration Specific Gibbs free energy Gibbs free energy Clearance height Oil flm thickness Specific enthalpy Heat-transfer coefficient Port open height Sensible specific enthalpy Enthalpy Moment of inertia Flux Thermal conductivity Turbulent kinetic energy Forward, backward, rate constants for ith reaction Constant Equilibrium constant expressed in concentrations Equilibrium constant expressed in partial pressures Characteristic length scale Connecting rod length Characteristic length scale of turbulent flame Piston stroke Fuel-injection-nozzle orifice length Valve lift Mass Mass flow rate Mass of residual gas Mach number Molecular weight n "R N P P 4 8 Qch QHV Q. r rc R R+,R Rs S S s* SL SP t T u u' "9 'T U 1) v Number of moles Polytropic exponent Number of crank revolutions per power stroke Crankshaft rotational speed Soot particle number density Turbocharger shaft speed Cylinder pressure Pressure Power Heat-transfer rate per unit area Heat-transfer rate per unit mass of fluid Heat transfer Heat-transfer rate Fuel chemical energy release or gross heat release Fuel heating value Net heat release Radius Compression ratio Connecting rod lengthlcrank radius Gas constant Radius One-way reaction rates Swirl ratio Crank axis to piston pin distance Specific entropy Entropy Spray penetration Turbulent burning speed Laminar flame speed Piston speed Time Temperature Torque Specific internal energy Velocity Turbulence intensity Sensible specific internal energy Characteristic turbulent velocity Compressorlturbine impellor tangential velocity Fluid velocity Internal energy Specific volume Velocity Velocity Valve pseudo-flow velocity XXV COMMONLY USED SYMBOLS, SUBSCRIPTS, AND ABBREVIATIONS X X V ~ COMMONLY USED SYMBOLS. SUBSCRIPTS. AND ABBREVIATIONS 'I0 'Ic 'Ic 'lch 'If 'I, 'Ise 'It 'IT 'It, 'Iv e 1 A Squish velocity Cylinder volume Volume Clearance volume Displaced cylinder volume Relative gas velocity Soot surface oxidation rate Work transfer Work per cycle Pumping work Spatial coordinates Mass fraction Mole fraction Burned mass fraction Residual mass fraction H/C ratio of fuel Volume fraction Concentration of species a per unit mass Inlet Mach index Angle Thermal diffusivity k/(pc) Angle Specific heat ratio cJc, Angular momentum of charge Boundary-layer thickness Laminar flame thickness Molal enthalpy of formation of species i Rapid burning angle Flame development angle 4/(4 + y): y = H/C ratio of fuel Turbulent kinetic energy dissipation rate Availability conversion efficiency Combustion efficiency Compressor isentropic efficiency Charging efficiency Fuel conversion efficiency Mechanical efficiency Scavenging efficiency Thermal conversion efficiency Turbine isentropic efficiency Trapping efficiency Volumetric efficiency Crank angle Relative air/fuel ratio Delivery ratio Dynamic viscosity Chemical potential of species i Kinematic viscosity p / p Stoichiometric coefficient of species i /' /'I 1, vi i P , Flow friction coefficient Density Air density at standard, inlet conditions Normal stress Standard deviation Stefan-Boltzmann constant Surface tension Characteristic time Induction time Shear stress Ignition delay time Fuellair equivalence ratio Flow compressibility function [Eq. (C.1.1)] Isentropic compression function [Eq. (4.15b)l Molar N/O ratio Throttle plate open angle Isentropic compression function [Eq. (4.15a)l Angular velocity Frequency SUBSCRIPTS Air Burned gas Coolant Cylinder Compression stroke Compressor Crevice Equilibrium Exhaust Expansion stroke Flame Friction Fuel Gas Indicated Intake Species i Gross indicated Net indicated XXV~~ COMMONLY USED SYMBOLS SUBSCRIPTS, AND ABBREVIATIONS XXV% Liquid Laminar Piston Port Prechamber r, 8, z components Reference value Isentropic Stoichiometric Nozzle or orifice throat Turbine Turbulent Unburned Valve Wall x, y, z components Reference value Stagnation value NOTATION Difference Average or mean value Value per mole Concentration, moles/vol Mass fraction Rate of change with time ABBREVIATIONS (AIF) BC, ABC, BBC CN Da EGR EI EPC, EPO EVC, EVO (FIA) (GIF) IPC, IPO IVC, IVO mep Nu Airlfuel ratio Bottom-center crank position, after BC, before BC Fuel cetane number Damkohler number T = / T ~ Exhaust gas recycle Emission index Exhaust port closing, opening Exhaust valve closing, opening Fuellair ratio Gas/fuel ratio Inlet port closing, opening Inlet valve closing, opening Mean effective pressure Nusselt number h, Ilk ON Re sfc TC, ATC, BTC We Fuel octane number Reynolds number pul/p Specificfuel consumption Topcenter crank position, after TC, before TC Weber number p, u2D/a CHAPTER ENGINE TYPES AND THEIR OPERATION 1.1 INTRODUCTION AND HISTORICAL PERSPECTIVE The purpose of internal combustion engines is the production of mechanical power from the chemical energy contained in the fuel.



In internal combustion engines, as distinct from external combustion engines, this energy is released by burning or oxidizing the fuel inside the engine. The fuel-air mixture before combustion and the burned products after combustion are the actual working fluids. discours indirect exercices pdf The work transfers which provide the desired power output occur directly between these working fluids and the mechanical components of the engine. The internal combustion engines which are the subject of this book are spark-ignition engines (sometimes called Otto engines, or gasoline or petrol engines, though other fuels can be used) and compression-ignition or diesel engines.t Because of their simplicity, ruggedness and high powerlweight ratio, these two types of engine have found wide application in transportation (land, sea, and air) and power generation. It is the fact that combustion takes place inside the work- t The gas turbine is also, by this definition, an "internal combustion engine." Conventionally, however, the term is used for spark-ignition and compression-ignition engines. The operating prinn p l a of gas turbines are fundamentally different, and they are not discussed as separate en$nes in this book. noco_genius_g26000_not_working.pdf 2 ' ENGINE N P E S AND THEIR OPERATION INTERNAL COMBUSTION ENGINE FUNDAMENTALS producing part of these engines that makes their design and operating characteristics fundamentally different from those of other types of engine. Practical heat engines have served mankind for over two and a half centuries. For the first 150 years, water, raised to steam, was interposed between the combustion gases produced by burning the fuel and the work-producing pistonin-cylinder expander. It was not until the 1860s that the internal combustion engine became a practical reality.'.
* The early engines developed for commercial use burned coal-gas air mixtures at atmospheric pressurethere was no compression before combustion. J.



J. E. Lenoir (1822-1900) developed the first marketable engine of this type. Gas and air were drawn into the cylinder during the first half of the piston stroke. The charge was then ignited with a spark, the pressure increased, and the burned gases then delivered power to the piston for the second half of the stroke.
The cycle was completed with an exhaust stroke. Some 5000 of these engines were built between 1860 and 1865 in sizes up to six horsepower. Efficiency was at best about 5 percent. A more successful development-an atmospheric engine introduced in 1867 by Nicolaus A. Otto (1832-1891) and Eugen Langen (1833-1895)-used the pressure rise resulting from combustion of the fuel-air charge early in the outward stroke to accelerate a free piston and rack assembly so its momentum would generate a vacuum in the cylinder. Atmospheric pressure then pushed the piston inward, with the rack engaged through a roller clutch to the output shaft. Production engines, of which about 5000 were built, obtained thermal efficiencies of up to 11 percent. A slide valve controlled intake, ignition by a gas flame, and exhaust. To overcome this engine's shortcomings of low thermal efficiency and excessive weight, Otto proposed an engine cycle with four piston strokes: an intake stroke, then a compression stroke before ignition, an expansion or power stroke where work was delivered to the crankshaft, and finally an exhaust stroke. He also proposed incorporating a stratified-charge induction system, though this was not achieved in practice. His prototype four-stroke engine first ran in 1876. A comparison between the Otto engine and its atmospheric-type predecessor indicates the reason for its success (see Table 1.1): the enormous reduction in engine weight and volume. This was the breakthrough that effectively founded the internal combustion engine industry. By 1890, almost 50,000 of these engines had been sold in Europe and the United States. In 1884, an unpublished French patent issued in 1862 to Alphonse Beau de Rochas (1815-1893) was found which described the principles of the four-stroke cycle. This chance discovery cast doubt on the validity of Otto's own patent for this concept, and in Germany it was declared invalid. Beau de Rochas also outlined the conditions under which maximum efficiency in an internal combustion engine could be achieved.
These were: 1. The largest possible cylinder volume with the minimum boundary surface 2. The greatest possible working speed 3 TABLE 1.1 comparison of Otto four-stroke cycle and Otto-Langen engines2 Otto a d h n g e n Otto four-stroke Brake horsepower Weight, lb, approx. Piston displacement, in3 Power strokes per min Shaft speed, rev/min Mechanical efficiency, % Overall efficiency, % Expansion ratio 3.
The greatest possible expansion ratio 4. The greatest possible pressure at the beginning of expansion The first two conditions hold heat losses from the charge to a minimum. The third condition recognizes that the greater the expansion of the postcombustion gases, the greatet the work extracted. The fourth condition recognizes that higher initial pressures make greater expansion possible, and give higher pressures throughout the process, both resulting in greater work transfer. Although Beau de Rochas' unpublished writings predate Otto's developments, he never reduced these ideas to practice. Thus Otto, in the broader sense, was the inventor of the modern internal combustion engine as we know it today. Further developments followed fast once the full impact of what Otto had achieved became apparent.
By the 1880s several engineers (e.g., Dugald Clerk, 1854-1913,; and James Robson, 1833-1913, in England and Karl Benz, 18441929, in Germany) had successfully developed two-stroke internal combustion engines where the exhaust and intake processes occur during the end of the power stroke and the beginning of the compression stroke. James Atkinson (1846-1914) in England made an engine with a longer expansion than compression stroke, which had a high efficiency for the times but mechanical weaknesses. It was recognized that efficiency was a direct function of expansion ratio, yet compression ratios were limited to less than four if serious knock problems were to be avoided with the available fuels. Substantial carburetor and ignition system developments were required, and occurred, before high-speed gasoline engines suitable for automobiles became available in the late 1880s. Stationary engine progress also continued. By the late 1890s, large single-cylinder engines of 1.3-m bore fueled by low-energy blast furnace gas produced 600 bhp at 90 revlmin. In Britain, legal restrictions on volatile fuels turned their engine builders toward kerosene. Low compression ratio "oil" engines with heated external fuel vaporizers and .electric ignition were developed with efficiencies comparable to those of gas engines (14 to 18 percent). The Hornsby-Ackroyd engine became the most 4 INTERNAL COMBUSTION ENGINE FUNDAMENTALS popular oil engine in Britain, and was also built in large numbers in the United States2 In 1892, the German engineer Rudolf Diesel (1858-1913) outlined in his patent a new form of internal combustion engine. His concept of initiating combustion by injecting a liquid fuel into air heated solely by compression permitted a doubling of efficiency over other internal combustion engines. debt snowball spreadsheet Much greater expansion ratios, without detonation or knock, were now possible. However, even with the efforts of Diesel and the resources of M.A.N. in Ausburg combined, it took five years to develop a practical engine. Engine developments, perhaps less fundamental but nonetheless important to the steadily widening internal combustion engine markets, have continued ever ~ince.~ One - ~ more recent major development has been the rotary internal combustion engine. Although a wide variety of experimental rotary engines have been proposed over the years,' the first practical rotary internal combustion engine, the Wankel, was not successfully tested until 1957. That engine, which evolved through many years of research and development, was based on the designs of the German inventor Felix WankeL6* Fuels have also had a major impact on engine development. The earliest engines used for generating mechanical power burned gas. dommage bigflo et oli paroles pdf Gasoline, and lighter fractions of crude oil, became available in the late 1800s and various types of carburetors were developed to vaporize the fuel and mix it with air. Before 1905 there were few problems with gasoline; though compression ratios were low (4 or less) to avoid knock, the highly volatile fuel made starting easy and gave good cold weather performance.
However, a serious crude oil shortage developed, and to meet the fivefold increase in gasoline demand between 1907 and 1915, the yield from crude had to be raised.
Through the work of William Burton (1865-1954) and his associates of Standard Oil of Indiana, a thermal cracking process was developed whereby heavier oils were heated under pressure and decomposed into less complex more volatile compounds. These thermally cracked gasolines satisfied demand, but their higher boiling point range created cold weather starting problems. Fortunately, electrically driven starters, introduced in 1912, came along just in time. On the farm, kerosene was the logical fuel for internal combustion engines since it was used for heat and light. Many early farm engines had heated carburetors or vaporizers to enable them to operate with such a fuel. The period following World War I saw a tremendous advance in our understanding of how fuels affect combustion, and especially the problem of knock. The antiknock effect of tetraethyl lead was discovered at General ~otors,' and it became commercially available as a gasoline additive in the United States in 1923. In the late 1930s, Eugene Houdry found that vaporized oils passed over an activated catalyst at 450 to 480•‹C were converted to highquality gasoline in much higher yields than was possible with thermal cracking. These advances, and others, permitted fuels with better and better antiknock properties to be produced in large quantities; thus engine compression ratios steadily increased, improving power and efficiency. ' ENGINE TYPES AND THEIR OPERATION 5 During the past three decades, new factors for change have become important and now significantly affect engine design and operation. 74335909165.pdf These factors are, first, the need to control the automotive contribution to urban air pollution and, second, the need to achieve significant improvements in automotive fuel consumption.
The automotive air-pollution problem became apparent in the 1940s in the ~ o Angeles s basin. In 1952, it was demonstrated by Prof. constitutional law 1 matrix worksheet answers A. J. Haagen-Smit that the smog problem there resulted from reactions between oxides of nitrogen and hydrocarbon compounds in the presence of sunlight.' In due course it became clear that theJautomobile was a major contributor to hydrocarbon and oxides of nitrogen emissions, as well as the prime cause of high carbon monoxide levels in urban areas. Diesel engines are a significant source of small soot or smoke particles, as well as hydrocarbons and oxides of nitrogen. Table 1.2 outlines the dimensions of the problem. As a result of these developments, emission standards for automobiles were introduced first in California, then nationwide in the United States, starting in the early 1960s. Emission standards in Japan and Europe, and for other engine applications, have followed. Substantial reductions in emissions from spark-ignition and diesel engines have been achieved. Both the use of catalysts in spark-ignition engine exhaust systems for emissions control and concern over the toxicity of lead antiknock additives have resulted in the reappearance of unleaded gasoline as a major part of the automotive fuels market. Also, the maximum lead content in leaded gasoline has been substantially reduced. The emission-control requirements and these fuel developments have produced significant changes in the way internal combustion engines are designed and operated. Internal combustion engines are also an important source of noise. There are several sources of engine noise: the exhaust system, the intake system, the fan used for cooling, and the engine block surface. The noise may be generated by aerodynamic effects, may be due to forces that result from the combustion process, or may result from mechanical excitation by rotating or reciprocating engine components.
Vehicle noise legislation to reduce emissions to the environment was first introduced in the early 1970s. During the 1970s the price of crude petroleum rose rapidly to several times its cost (in real terms) in 1970, and concern built up regarding the longer-term availability of petroleum. Pressures for substantial improvements in internal combustion engine efficiency (in all its many applications) have become very substantial indeed. Yet emission-control requirements have made improving engine fuel consumption more difficult, and the removal and reduction of lead in gasoline has forced spark-ignition engine compression ratios to be reduced. Much work is being done on the use of alternative fuels to gasoline and diesel. Of the non-petroleum-based fuels, natural gas, and methanol and ethanol (methyl and ethyl alcohols) are receiving the greatest attention, while synthetic gasoline and diesel made from shale oil or coal, and hydrogen could be longer-term possibilities. It might be thought that after over a century of development, the internal ENGINE N P E S AND THEIR OPERATION TABLE 12 The automotive urban air-pollution problem Automobile emissiom PoUutnnt Impact Oxides of nitrogen (NO and NO,) Reactant in photochemical smog; NO, is toxic Toxic Carbon monoxide (CO) Unburned hydrocarbons (HC, many hydrocarbon compounds) Particulates (soot and absorbed hydrocarbon compounds) Mobile source emissiom as % of totalt Uncontrolled vehicles, g/kmt Reduction in new vehicles, "/. 7 Truck emissionsti SI engines, dlun Diesel, g/km Reactant in photochemical smog Reduces visibility; some of HC compounds mutagenic t Depends on typc of urban area and source mix.
t Average values for pre-1968 automobiles which had no emission controls, determined by U.S. test procedure which simulates typical urban and highway driving. Exhaust emissions, except for HC where 55 percent are exhaust emissions, 20 percent are evaporative emissions from fuel tank and carburetor, and 25 percent are crankcase blowby gases. 9 Diesel engine automobiles only. Particulate emissions from spark-ignition engines a n negligible. f Compares emissions from new spark-ignition engine automobiles with uncontrolled automobile levels in previous column. Varies from country to country. The United States, Canada, Western Europe, and Japan have standards with different degrrn of severity. The United States, Europc, and Japan have dierent test procedures. Standards are strictest in the United States and Japan. tt Representativeaverage emission levels for trucks. f $ With 95 percent exhaust emissions and 5 percent evaporative emissions. n negligible. - combustion engine has reached its peak and little potential for further improvement remains. Such is not the case. Conventional spark-ignition and diesel engines continue to show substantial improvements in efficiency, power, and degree of emission control. New materials now becoming available offer the possibilities of reduced engine weight, cost, and heat losses, and of different and more efficient internal combustion engine systems. Alternative types of internal combustion engines, such as the stratifiedcharge (which combines characteristics normally associated with either the spark-ignition or diesel) with its wider fuel tolerance, may become sufficiently attractive to reach large-scale production. The engine development opportunities of the future are substantial. While they 7 present a formidable challenge to automotive engineers, they will be made pos&le in large part by the enormous expansion of our knowledge of engine proasses which the last twenty years has witnessed. 1.2 ENGINE CLASSIFICATIONS There are many different types of internal combustion engines. They can be classified by: 1. .lpplication. Automobile, truck, locomotive, light aircraft, marine, portable power system, power generation 2. 69869983201.pdf Basic engine design. Reciprocating engines (in turn subdivided by arrange- ment of cylinders: e.g., in-line, V, radial, opposed), rotary engines (Wankel and other geometries) 3. Working cycle. Four-stroke cycle: naturally aspirated (admitting atmospheric air), supercharged (admitting precompressed fresh mixture), and turbocharged (admitting fresh mixture compressed in a compressor driven by an exhaust turbine), two-stroke cycle: crankcase scavenged, supercharged, and turbocharged 4. Valve or port design and location. Overhead (or I-head) valves, underhead (or L-head) valves, rotary valves, cross-scavenged porting (inlet and exhaust ports on opposite sides of cylinder at one end), loop-scavenged porting (inlet and exhaust ports on same side of cylinder at one end), through- or uniflowscavenged (inlet and exhaust ports or valves at different ends of cylinder) 5. ripugegusefiri.pdf Fuel. Gasoline (or petrol), fuel oil (or diesel fuel), natural gas, liquid petroleum gas, alcohols (methanol, ethanol), hydrogen, dual fuel 6. Method of mixture preparation. Carburetion, fuel injection into the intake ports or intake manifold, fuel injection into the engine cylinder 7.
Method of ignition. Spark ignition (in conventional engines where the mixture is uniform and in stratified-charge engines where the mixture is non-uniform), compression ignition (in conventional diesels, as well as ignition in gas engines by pilot injection of fuel oil) 8. Combustion chamber design. Open chamber (many designs: e.g., disc, wedge, hemisphere, bowl-in-piston), divided chamber (small and large auxiliary chambers; many designs: e.g., swirl chambers, prechambers) 9. Method of load control. Throttling of fuel and air flow together so mixture composition is essentially unchanged, control of fuel flow alone, a combination of these 10. Method of cooling. Water cooled, air cooled, uncooled (other than by natural convection and radiation) All these distinctions are important and they illustrate the breadth of engine designs available. Because this book approaches the operating and emissions 8 ENGINE TYPES AND THEIR OPERATION INTERNAL COMBUSTION ENGINE FUNDAMENTALS TABLE 13 the predominant type of engine used in each classification listed, and the approximateengine power range in each type of service. Classification of reciprocating engines by application Clrss Service Road vehicles Motorcycles, scooters Small passenger cars Large passenger cars Light commercial Heavy (long-distance) commercial Light vehicles (factory, airport, etc.) Agricultural Earth moving Military Rail cars Locomotives Outboard Inboard motorcrafts Light naval craft Ships Ships' auxiliaries Airplanes Helicopters Lawn mowers Snow blowers Light tractors Building service Electric power Gas pipeline OK-road vehicles Railroad Marine Airborne vehicles Home use Stationary Approximate engine power range, kW 9 Predominant type D or SI Cycle Cooling SI SI SI SI, D D SI SI, D D D D D SI SI, D D D D SI SI SI SI SI D D SI 13 ENGINE OPERATING ~ o s oft this book is about reciprocating engines, where th, piston moves back and forth in a cylinder and transmits power through a connecting rod and crank mechanism to the drive shaft as shown in Fig. 1-1. The steady rotation of the crank produces a cyclical piston motion. The piston comes to rest a t the t o p center (TC) crank position and .bottom-center (BC) crank position when the cylinder volume is a minimum or maximum, respective1y.t The minimum cylinder volume is called the clearance volume V,.
The volume swept out by the t These crank positions are also referred to as top-dead-center (TDC) and bottom-dead-center (BDC).
Stroke SI = spark-ignition; D =; diuel; A = air cooled; W = water cooled. Sowee: Adapted from Taylor? characteristics of internal combustion engines from a fundamental point of view, the method of ignition has been selected as the primary classifying feature. From the method of ignition-spark-ignition or compression-ignitiont-follow the important characteristics of the fuel used, method of mixture preparation, combustion chamber design, method of load control, details of the combustion process, engine emissions, and operating characteristics. Some of the other classifications are used as subcategories within this basic classification. The engine operating cycle-four-stroke or two-stroke-is next in importance; the principles of these two cycles are described in the following section. Table 1.3 shows the most common applications of internal combustion BC I '..-+-' I \ \ ,/ 180•‹ t In the remainder of the book, these terms will often be abbreviated by SI and CI, respectively. CYCLES BC FIGURE 1-1 Basic geometry of the reciprocating internal combustion engine.
V,, Y, and & indicate clearance. displaced, and total cylinder volumes. 10 INTERNAL COMBUSTION ENGINE FUNDAMENTALS lnlet Exhaust lnlet Exhaust ENGINE TYPES AND THEIR OPERATION lnlet Exhaust lnlet Exhaust J. 11 the piston approaches BC the exhaust valve opens to initiate the exhaust process and drop the cylinder pressure to close to the exhaust pressure. .qn r,~lrarrststroke, where the remaining burned gases exit the cylinder: first, hecause the cylinder pressure may be substantially higher than the exhaust pressure: then as they are swept out by the piston as it moves toward TC. As tile p~stonapproaches TC the inlet valve opens. Just after TC the exhaust \.11\ccloses and the cycle starts again. i I l t ~ p hoften called the Otto cycle after its inventor, Nicolaus Otto, who built 111c I;rst engine operating on these principles in 1876, the more descriptive four- stroke nomenclature is preferred. The four-stroke cycle requires, for each engine cylinder, two crankshaft revolut~onsfor each power stroke. To obtain a higher power output from a given criptnc 47e. and a simpler valve design, the two-stroke cycle was developed. The IN'!-\trokccycle is applicable to both SI and CI engines. k'lpurc 1-3 shows one of the simplest types of two-stroke engine designs. I'or[\ I r i the cylinder liner, opened and closed by the piston motion, control the cxh,iust and inlet flows while the piston is close to BC. The two strokes are: (a) Intake (b) Compression (c) Expans~on (d) Exhaust FIGURE 1-2 The four-stroke operating cycle.10 I. A co~rpressionstroke, which starts by closing the inlet and exhaust ports, and ~hencompresses the cylinder contents and draws fresh charge into the crankc.~\c.As the piston approaches TC, combustion is initiated.
piston, the difference between the maximum or total volume (L and the clearance volume, is called the displaced or swept volume V,. The ratio of maximum volume to minimum volume is the compression ratio r, .
Typical values of r, are 8 to 12 for SI engines and 12 to 24 for CI engines. The majority of reciprocating engines operate on what is known as the four-stroke cycle. Each cylinder requires four strokes of its piston-two revolutions of the crankshaft-to complete the sequence of events which produces one power stroke. Both SI and CI engines use this cycle which comprises (see Fig. 1-2) : 1.
An intake stroke, which starts with the piston at T C and ends with the piston at BC, which draws fresh mixture into the cylinder. To increase the mass inducted, the inlet valve opens shortly before the stroke starts and closes after it ends. 2. A compression stroke, when both valves are closed and the mixture inside the cylinder is compressed to a small fraction of its initial volume. Toward the end of the compression stroke, combustion is initiated and the cylinder pressure rises more rapidly. 3. A power stroke, or expansion stroke, which starts with the piston at TC and ends at BC as the high-temperature, high-pressure, gases push the piston down and force the crank to rotate. About five times as much work is done on the piston during the power stroke as the piston had to do during compression. Exhaust blowdown Scavenging FIGURE 1-3 The two-stroke operating cycle.
A crankcase-scavengedengine is shown.'O 12 INTERNAL COMBUSTION ENGINE FUNDAMENTALS 2. A power or expansion stroke, similar to that in the four-stroke cycle until the Air Cleaner piston approaches BC, when first the exhaust ports and then the intake ports are uncovered (Fig. 1-3).
Most of the burnt gases exit the cylinder in an exhaust blowdown process. When the inlet ports are uncovered, the fresh charge which has been compressed in the crankcase flows into the cylinder.
The piston and the ports are generally shaped to deflect the incoming charge from flowing directly into the exhaust ports and to achieve effective scavenging of the residual gases. Each engine cycle with one power stroke is completed in one crankshaft revolution. However, it is diffcult to fill completely the displaced volume with fresh charge, and some of the fresh mixture flows directly out of the cylinder during the scavenging process.? The example shown is a cross-scavenged design; other approaches use loop-scavenging or unflow systems (see Sec. 6.6). 1.4 ENGINE COMPONENTS Labeled cutaway drawings of a four-stroke SI engine and a two-stroke CI engine are shown in Figs. 1-4 and 1-5, respectively. The spark-ignition engine is a fourcylinder in-line automobile engine. The diesel is a large V eight-cylinder design with a uniflow scavenging process. The function of the major components of these engines and their construction materials will now be reviewed. The engine cylinders are contained in the engine block. The block has traditionally been made of gray cast iron because of its good wear resistance and low cost. Passages for the cooling water are cast into the block. Heavy-duty and truck engines often use removable cylinder sleeves pressed into the block that can be replaced when worn. These are called wet liners or dry liners depending on whether the sleeve is in direct contact with the cooling water. Aluminum is being used increasingly in smaller SI engine blocks to reduce engine weight. Iron cylinder liners may be inserted at the casting stage, or later on in the machining and assembly process. The crankcase is often integral with the cylinder block. The crankshaft has traditionally been a steel forging; nodular cast iron crankshafts are also accepted normal practice in automotive engines.
The crankshaft is supported in main bearings. The maximum number of main bearings is one more than the number of cylinders; there may be less. The crank has eccentric portions (crank throws); the connecting rod big-end bearings attach to the crank pin on each throw. Both main and connecting rod bearings use steelbacked precision inserts with bronze, babbit, or aluminum as the bearing materials. The crankcase is sealed at the bottom with a pressed-steel or cast aluminum oil pan which acts as an oil reservoir for the lubricating system. It is primarily for this reason that two-stroke SI engines are at a disadvantage because the lost fresh charge contains fuel and air. Sprocket - FIGURE 1-4 Cutaway drawing of Chrysler 2.2-liter displacement four-cylinder spark-ignition engine.'' Bore 87.5 mm, stroke 92 mm,compression ratio 8.9, maximum power 65 kW at MOO revfmin. Pistons are made of aluminum in small engines or cast iron in larger slower-speed engines. The piston both seals the cylinder and transmits the combustion-generated gas pressure to the crank pin via the connecting rod. The connecting rod, usually a steel or alloy forging (though sometimes ahuninum in small engines), is fastened to the piston by means of a steel piston pin through the rod upper end.
The piston pin is usually hollow to reduce its weight. FIGURE 1-5 Cross-section drawing of an Electro-Motive two-stroke cycle diesel engine.
This engine uses a uniflow scavenging process with inlet ports in the cylinder liner and four exhaust valves in the cylinder head. Bore 230.2 mm, stroke 254 mm, displaced volume per cylinder 10.57 liters, rated speed 750400 revfmin. (Courtesy Electro-Motive Dioision, General Motors Corporation.) The oscillating motion of the connecting rod exerts an oscillating force on the cylinder walls via the piston skirt (the region below the piston rings).
The piston skirt is usually shaped to provide appropriate thrust surfaces. The piston is fitted with rings which ride in grooves cut in the piston head to seal against gas leakage and control oil flow. The upper rings are compression rings which are forced outward against the cylinder wall and downward onto the groove face. The lower rings scrape the surplus oil from the cylinder wall and return it to the crankcase. The crankcase must be ventilated to remove gases which blow by the piston rings, to prevent pressure buildup. The cylinder head (or heads in V engines) seals off the cylinders and is made of cast iron or aluminum. It must be strong and rigid to distribute the gas forces acting on the head as uniformly as possible through the engine block. The cylinder head contains the spark plug (for an SI engine) or fuel injector (for a CI engine), and, in overhead valve engines, parts of the valve mechanism. The valves shown in Fig. 1-4 are poppet valves, the valve type normally used in four-strokeengines.
Valves are made from forged alloy steel; the cooling of the exhaust valve which operates at about 700•‹Cmay be enhanced by using a hollow stem filled with sodium which through evaporation and condensation carries heat from the hot valve head to the cooler stem. Most modern sparkignition engines have overhead valve locations (sometimes called valve-in-head or l-head configurations) as shown in Fig. 1-4. This geometry leads to a compact combustion chamber with minimum heat losses and flame travel time, and improves the breathing capacity. Previous geometries such as the L head where valves are to one side of the cylinder are now only used in small engines. The valve stem moves in a valve guide, which can be an integral part of the cylinder head (or engine block for L-head engines), or may be a separate unit pressed into the head (or block). The valve seats may be cut in the head or block metal (if cast iron) or hard steel inserts may be pressed into the head or block. A valve spring, attached to the valve stem with a spring washer and split keeper, holds the valve closed. A valve rotator turns the valves a few degrees on opening to wipe the valve seat, avoid local hot spots, and prevent deposits building up in the valve guide. A camshaft made of cast iron or forged steel with one cam per valve is used to open and close the valves. The cam surfaces are hardened to obtain adequate life. In four-stroke cycle engines, camshafts turn at one-half the crankshaft speed. Mechanical or hydraulic lifters or tappets slide in the block and ride on the cam. Depending on valve and camshaft location, additional members are required to transmit the tappet motion to the valve stem; e.g., in in-head valve engines with the camshaft at the side, a push rod and rocker arm are used.
A recent trend in automotive engines is to mount the camshaft over the head with the cams acting either directly or through a pivoted follower on the valve. Camshafts are gear, belt, or chain driven from the crankshaft. An intake manifold (aluminum or cast iron) and an exhaust manifold (generally of cast iron) complete the SI engine assembly. Other engine components specific to spark-ignition engines-arburetor, fuel injectors, ignition systems-are described more fully in the remaining sections in this chapter. The two-stroke cycle CI engine shown in Fig. 1-5 is of the uniflow scavenged design. The burned gases exhaust through four valves in the cylinder head. These valves are controlled through cam-driven rocker arms. Fresh air is compressed and fed to the air box by a Roots blower. The air inlet ports a t the bottom of each cylinder liner are uncovered by the descending piston, and the scavenging air flows upward along the cylinder axis.
The fuel injectors are mounted in the cylinder' head and are driven by the camshaft through rocker arms. Diesel fuel-injection systems are discussed in more detail in Sec.
1.7. 1.5 SPARK-IGNITION ENGINE OPERATION In SI engines the air and fuel are usually mixed together in the intake system prior to entry to the engine cylinder, using a carburetor (Fig. 1-6) or fuel-injection system (Fig. 1-7). In automobile applications, the temperature of the air entering 16 INTERNAL COMBUSTION ENGINE FUNDAMENTALS ENGINE TYPES AND THEIR OPERATION idle air bleed float chamber venttlatton alr correctton let emulston tube full load enr~chmen auxhary alr bleec fuel mlet aux~haryfuel let float needle valve boost venturt tdle jet float matn let part load control adle mtxture control screw ' throt'le valve , aux~ltarymtxture control Screw FIGURE 1-6 Cross section of single-barrel downdraft carburetor.12(Courtesy Robert Bosch GmbH and SAE.) the intake system is controlled by mixing ambient air with air heated by contact with the exhaust manifold. The ratio of mass flow of air to mass flow of fuel must be held approximately constant at about 15 to ensure reliable combustion. The FIGURE 1-7 Schematic drawing of LJetronic port electronic fuel-injection system." (Courtesy Robert Bosch GmbH and SAE.) 17 meters an appropriate fuel flow for the engine air flow in the following manner. The air flow through the venturi (a converging-diverging nozzle) sets up a pressure difference between the venturi inlet and throat which is used to meter an appropriate amount of fuel from the float chamber, through a series of orifices, into the air flow at the venturi throat. Just downstream of the venturi is a throttle valve or plate which controls the combined air and fuel flow, and thus the engine output. The intake flow is throttled to below atmospheric pressure by reducing the flow area when the power required (at any engine speed) is below the maximum which is obtained when the throttle is wide open.
The intake manifold is usually heated to promote faster evaporation of the liquid fuel and obtain more uniform fuel distribution between cylinders. Fuel injection into the intake manifold or inlet port is an increasingly common alternative to a carburetor. With port injection, fuel is injected through individual injectors from a low-pressure fuel supply system into each intake port. There are several different types of systems: mechanical injection using an injection pump driven by the engine; mechanical, driveless, continuous injection; electronically controlled, driveless, injection. Figure 1-7 shows an example of an electronically controlled system. In this system, the air flow rate is measured directly; the injection valves are actuated twice per cam shaft revolution by injection pulses whose duration is determined by the electronic control unit to provide the desired amount of fuel per cylinder per cycle.12 An alternative approach is to use a single fuel injector located above the throttle plate in the position normally occupied by the carburetor. This approach permits electronic control of the fuel flow at reduced cost. The sequence of events which take place inside the engine cylinder is illustrated in Fig. 1-8. Several variables are plotted against crank angle through the entire four-stroke cycle. Crank angle is a useful independent variable because engine processes occupy almost constant crank angle intervals over a wide range of engine speeds. The figure shows the valve timing and volume relationship for a typical automotive spark-ignition engine. To maintain high mixture flows at high engine speeds (and hence high power outputs) the inlet valve, which opens before TC, closes substantially after BC. During intake, the inducted fuel and air mix in the cylinder with the residual burned gases remaining from the previous cycle.
After the intake valve closes, the cylinder contents are compressed to above atmospheric pressure and temperature as the cylinder volume is reduced. Some heat transfer to the piston, cylinder head, and cylinder walls occurs but the effect on unburned gas properties is modest. Between 10 and 40 crank angle degrees before TC an electrical discharge across the spark plug starts the combustion process. A distributor, a rotating switch driven off the camshaft, interrupts the current from the battery through the primary circuit of the ignition coil. The secondary winding of the ignition coil, connected to the spark plug, produces a high voltage across the plug electrodes as the magnetic field collapses. Traditionally, cam-operated breaker points have been used; in most automotive engines, the switching is now done electronically. A turbulent flame develops from the spark discharge, propagates - 2000 Combustion 300.- kPa Exhaust Compression Expansion 1000 Ivo EVC O I I TC NO IVC fi BC TC BC TC 0 Unburned Crank position and angle FIGURE 1-8 Saquena of events in four-stroke spark-ignition engine operating cycle. Cylinder pressure p (solid Line, firing cycle; dashed line, motored cycle), cylinder volume V/V,,, and mass fraction burned xb are plotted against crank angle. brake-torque (MBT) timing,? this optimum timing is an empirical compromise between starting combustion too early in the compression stroke (when the work transfer is to the cylinder gases) and completing combustion too late in the stroke (and so lowering peak expansion stroke pressures). About two-thirds of the way through the expansion stroke, the exhaust valve starts to open. The cylinder pressure is greater than the exhaust manifold pressure and a blowdown process occurs.
The burned gases flow through the valve into the exhaust port and manifold until the cylinder pressure and exhaust pressure equilibrate. The duration of this process depends on the pressure level in the cylinder. The piston then displaces the burned gases from the cylinder into the manifold during the exhaust stroke. The exhaust valve opens before the end of the expansion stroke to ensure that the blowdown process does not last too far into the exhaust stroke. The actual timing is a compromise which balances reduced work transfer to the piston before BC against reduced work transfer to the cylinder contents after BC.
The exhaust valve remains open until just after TC; the intake opens just before TC. The valves are opened and closed slowly to avoid noise and excessive cam wear.
To ensure the valves are fully open when piston velocities are at their highest, the valve open periods often overlap. If the intake flow is throttled to below exhaust manifold pressure, then backflow of burned gases into the intake manifold occurs when the intake valve is first opened. 1.6 EXAMPLES OF SPARK-IGNITION ENGINES across the mixture of air, fuel, and residual gas in the cylinder, and extinguishes at the combustion chamber wall. The duration of this burning process varies with .engine design and operation, but is typically 40 to 60 crank angle degrees, as shown in Fig. 1-8. As fuel-air mixture bums in the flame, the cylinder pressure in Fig. 1-8 (solid line) rises above the level due to compression alone (dashed line). This latter curve-called the motored cylinder pressure-is the pressure trace obtained from a motored or nonfiring engine.? Note that due to differences in the flow pattern and mixture composition between cylinders, and within each cylinder cycle-by-cycle, the development of each combustion process differs somewhat. As a result, the shape of the pressure versus crank angle curve in each cylinder, and cycle-by-cycle, is not exactly the same. There is an optimum spark timing which, for a given mass of fuel and air inside the cylinder, gives maximum torque. More advanced (earlier) timing or retarded (later) timing than this optimum gives lower output. Called maximum This section presents examples of production spark-ignition engines to illustrate the different types of engines in common use. Small SI engines are used in many applications: in the home (e.g., lawn mowers, chain saws), in portable power generation, as outboard motorboat engines, and in motorcycles. These are often single-cylinder engines. In the above applications, light weight, small bulk, and low cost in relation to the power generated are the most important characteristics;fuel consumption, engine vibration, and engine durability are less important. A single-cylinder engine gives only one power stroke per revolution (two-stroke cycle) or two revolutions (four-stroke cycle). Hence, the torque pulses are widely spaced, and engine vibration and smoothness are significant problems. Multicylinder engines are invariably used in automotive practice. As rated power increases, the advantages of smaller cylinders in regard to size, weight, and improved engine balance and smoothness point toward increasing the number of t in practice, the intake and compression processes of a firing engine and a motored engine are not t MBT timing has traditionally been defined as the minimum spark advance for best torque. Since the torque first increases and then decreases as spark timing is advanced, the definition used here is more precise. exactly the same due to the presence of burned gases from the previous cycle under firing conditions. 20 INTERNAL COMBUSTION ENGINE FUNDAMENTALS cylinders per engine. An upper limit on cylinder size is dictated by dynamic considerations: the inertial forces that are created by accelerating and decelerating the reciprocating masses of the piston and connecting rod would quickly limit the maximum speed of the engine. Thus, the displaced volume is spread out amongst several smaller cylinders. The increased frequency of power strokes with a multicylinder engine produces much smoother torque characteristics. Multicylinder engines can also achieve a much better state of balance than single-cylinder engines. A force must be applied to the piston to accelerate it during the first half of its travel from bottom-center or top-center. The piston then exerts a force as it decelerates during the second part of the stroke. It is desirable to cancel these inertia forces through the choice of number and arrangement of cylinders to achieve a primary balance. Note, however, that the motion of the piston is more rapid during the upper half of its stroke than during the lower half (a consequence of the connecting rod and crank mechanism evident from Fig. 1-1; see also Sec. 2.2). The resulting inequality in piston acceleration and deceleration produces corresponding differences in inertia forces generated.
Certain combinations of cylinder number and arrangement will balance out these secondary inertia force effects. Four-cylinder in-line engines are the most common arrangements for automobile engines up to about 2.5-liter displacement. An example of this in-line arrangement was shown in Fig. 1-4. It is compact-an important consideration for small passenger cars. It provides two torque pulses per revolution of the crankshaft and primary inertia forces (though not secondary forces) are balanced.
V engines and opposed-piston engines are occasionally used with this number of cylinders. The V arrangement, with two banks of cylinders set at 90" or a more acute angle to each other, provides a compact block and is used extensively for larger displacement engines. Figure 1-9 shows a V-6 engine, the six cylinders being arranged in two banks of three with a 60' angle between their axis. Six cylinders are usually used in the 2.5- to 4.5-liter displacement range. Six-cylinder engines provide smoother operation with three torque pulses per revolution. The in-line arrangement results in a long engine, however, giving rise to crankshaft torsional vibration and making even distribution of air and fuel to each cylinder more ditlicult. The V-6 arrangement is much more compact, and the example shown provides primary balance of the reciprocating components. With the V engine, however, a rocking moment is imposed on the crankshaft due to the secondary inertia forces, which results in the engine being less well balanced than the in-line version. The V-8 and V-12 arrangements are also commonly used to provide compact, smooth, low-vibration, larger-displacement, spark-ignition engines. Turbochargers are used to increase the maximum power that can be obtained from a given displacement engine. The work transfer to the piston per cycle, in each cylinder, which controls the power the engine can deliver, depends on the amount of fuel burned per cylinder per cycle. This depends on the amount of fresh air that is inducted each cycle. Increasing the air density prior to entry into the engine thus increases the maximum power that an engine of given dis- 22 ENGINE TYPES AND THEIR OPERATION INTERNAL COMBUSTION ENGINE FUNDAMENTALS placement can deliver. Figure 1-10 shows an example of a turbocharged fourcylinder spark-ignition engine. The turbocharger, a compressor-turbine combination, uses the energy available in the engine exhaust stream to achieve compression of the intake flow. The air flow passes through the compressor (2), intercooler (3), carburetor (4), manifold (5), and inlet valve (6) as shmn. Engine inlet pressures (or boost) of up to about 100 kPa above atmospheric pressure are typical. The exhaust flow through the valve (7) and manifold (8) drives the turbine (9) which powers the compressor. A wastegate (valve) just upstream of the turbine bypasses some of the exhaust gas flow when necessary to prevent the boost pressure becoming too high. The wastegate linkage (1 1) is controlled by a boost pressure regulator.
While this turbocharged engine configuration has the carburetor downstream of the compressor, some turbocharged spark-ignition engines have the carburetor upstream of the compressor so that it operates at or below atmospheric pressure. Figure 1-11 shows a cutaway drawing of a small automotive turbocharger. The arrangements of the compressor and turbine 1 Lubricatmg passage 23 r ~ o c plate k Compressed alr Outlet Compressor housmg Compressor wheel bypass passage f?Exhaust gas Inlet stde FIGURE 1-11 Cutaway view of small automotive engine turbocharger. (Courtesy Nissan Motor Co., Ltd.) FIGURE 1-10 Turbocharged four-cylinderautomotive spark-ignition engine. (Courtesy Regie Nationole des Usines.) rotors connected via the central shaft and of the turbine and compressor flow passages are evident. Figure 1-12 shows a two-stroke cycle spark-ignition engine. The two-stroke cycle spark-ignition engine is used for small-engine applications where low cost and weighttpower ratio are important and when the use factor is low. Examples of such applications are outboard motorboat engines, motorcycles, and chain saws. All such engines are of the carburetor crankcase-compression type which is one of the simplest prime movers available. It has three moving parts per cylinder: the piston, connecting rod, and the crank. The prime advantage of the twostroke cycle spark-ignition engine relative to the four-stroke cycle engine is its higher power per unit displaced volume due to twice the number of power strokes per crank revolution.
This is offset by the lower fresh charge density achieved by the two-stroke cycle gas-exchange process and the loss of fresh mixture which goes straight through the engine during scavenging. Also, oil consumption is higher in two-stroke cycle engines due to the need to add oil to the fuel to lubricate the piston ring and piston surfaces. The Wankel rotary engine is an alternative to the reciprocating engine geometry of the engines illustrated above. It is used when its compactness and higher engine speed (which result in high powerlweight and power/volume ratios), and inherent balance and smoothness, offset its higher heat transfer, and 24 INTERNAL COMBUSTION ENGINE FUNDAMENTALS Fied timing gear ,-Center housing Intake pon Eccentric shaft 1 Coolant passages Side housing Induction FIGURE 1

engines. In-line pumps are used in the mid-engine-size range. In the larger diesels, individual singlebarrel injection pumps, close mounted to each cylinder with an external drive as shown in Fig. 1-5, are normally used. 1.8 EXAMPLES OF DIESEL ENGINES A large number of diesel engine configurations and designs are in common use. The very large marine and stationary power-generating diesels are two-stroke 32 ENGINE TYPES AND THEIR OPERATION INTERNAL COMBUSTION ENGINE FUNDAMENTALS Overflow valve I Control lever - s u p p l y &mpl) Presupply pump //I Govern& ~ l i d i n g s l r e v t~l ~ S z e v e r Drive Governor Cam \ hiaximumeffectke stroke, start drive plate T ~ m i n gdevice') 1 1) Shown additionally turned hub - 33 of diesel engine, it is often necessary to use a swirling air flow rotating about the cylinder axis, which is created by suitable design of the inlet port and valve, to achieve adequate fuel-air mixing and fuel burning rates. The fuel injector, shown left-of-center in the drawing, has a multihole nozzle, typically with three to five holes. The fuel jets move out radially from the center of the piston bowl into the (swirling) air flow. The in-line fuel-injection pump is normally used with this type of diesel engine. Figure 1-21 shows a four-cylinder in-line overhead-valve-cam design automobile diesel engine. The smallest diesels such as this operate at higher engine speed than larger engines; hence the time available for burning the fuel is less and the fuel-injection and combustion system must achieve faster fuel-air mixing rates.
This is accomplished by using an indirect-injection type of diesel. Fuel is injected into an auxiliary combustion chamber which is separated from the main combustion chamber above the piston by a flow restriction or nozzle.
During the latter stages of the compression process, air is forced through this nozzle from the through 90' ') S h o w n turned t h r o u g h 90- FIGURE 1-19 Diesel fuel system with distributor-type fuel-injection pump with mechanical govern~r.'~ (Courtesy Robert Boxh GmbH.) cycle engines. Small- and medium-size engines use the four-stroke cycle. Because air capacity is an important constraint on the amount of fuel that can be burned in the diesel engine, and therefore on the engine's power, turbocharging is used extensively. All large engines are turbocharged. The majority of smaller diesels are not turbocharged, though they can be turbocharged and many are. The details of the engine design also vary significantly over the diesel size range. In particular, different combustion chamber geometries and fuel-injection characteristics are required to deal effectively with a major diesel engine design problemachieving suffciently rapid fuel-air mixing rates to complete the fuel-burning process in the time available. A wide variety of inlet port geometries, cylinder head and piston shapes, and fuel-injection patterns are used to accomplish this over the diesel size range. Figure 1-20 shows a diesel engine typical of the medium-duty truck application. The design shown is a six-cylinder in-line engine. The drawing indicates that diesel engines are generally substantially heavier than spark-ignition engines because stress levels are higher due to the significantly higher pressure levels of the diesel cycle. The engine shown has a displacement of 10 liters, a compression ratio of 16.3, and is usually turbocharged.
The engine has pressed-in cylinder liners to achieve better cylinder wear characteristics. This type of diesel is called a direct-injection diesel. The fuel is injected into a combustion chamber directly above the piston crown. The combustion chamber shown is a " bowl-in-pistonn design, which puts most of the clearance volume into a compact shape. With this FIGURE 1-20 ,Direct-injection four-stroke cycle six-cylinder turbocharged Cummins diesel engine.
Displaced volume 10 liters, bore 125 mm, stroke 136 mm, compression ratio 16.3, maximum power 168 to 246 kW at rated speed of 2100 rev/min. (Courtesy Cwnmins Engine Company, Inc.) 34 INTERNAL COMBUSTION ENGINE F W A M E N T A L S ENGINE N P E S AND THEIR OPERATION 35 Diesel engines are turbocharged to achieve higher powerlweight ratios. By increasing the density of the inlet air, a given displaced volume can induct more air. Hence more fuel can be injected and burned, and more power delivered, while avoiding excessive black smoke in the exhaust. All the larger diesels are turbocharged; smaller diesels can be and often are. Figure 1-22 shows how a turbocharger connects to a direct-injection diesel. All the above diesels are water cooled; some production diesels are air cooled. Figure 1-23 shows a V-8 air-cooled direct-injection naturally aspirated FIGURE 1-21 Four-cylinder naturally aspirated indirect-injection automobile Volkswagen diesel engine.14 Displaced volume 1.47 liters, bore 76.5 mm, stroke 80 mm, maximum power 37 kW at 5000 rev/min. cylinder into the prechamber at high velocity. Fuel is injected into this highly turbulent and often rapidly swirling flow in this auxiliary or prechamber, and very high mixing rates are achieved.
Combustion starts in the prechamber, and the resulting pressure rise in the prechamber forces burning gases, fuel, and air into the main chamber. Since this outflow is also extremely vigorous, rapid mixing then occurs in the main chamber as the burning jet mixes with the remaining air and combustion is completed. A distributor-type fuel pump, which is normally used in this engine size range, driven off the camshaft at half the crankshaft speed by a toothed belt, is shown on the right of the figure. It supplies high-pressure fuel pulses to the pintle-type injector nozzles in turn. A glow plug is also shown in the auxiliary chamber; this plug is electrically heated prior to and during cold engine start-up to raise the temperature of the air charge and the fuel sufficiently to achieve autoignition. The compression ratio of this engine is 23.
Indirect-injection diesel engines require higher compression ratios than directinjection engines to start adequately when cold. FIGURE 1-22 Turbocharged aftercooled direct-injection four-stroke cycle Caterpillar six-cylinder in-line heavy-duty truck diesel engine. Bore 137.2 mm, stroke 165.1 mm, rated power 200-300 kW and rated speed of 1600-2100 revlmin depending on application.
(Courtesy Caterpillar Tractor Company.) 36 INTERNAL COMBUSTION ENGINE FUNDAMENTALS FIGURE 1-23 V-8 air-cooled direct-injection naturally aspirated diesel engine. Displacement 13.4 liter, bore 128 mm, stroke 130 mm, compression ratio 17, maximum rated power 188 kW at rated speed of 2300 rev/min. (Courtesy Kliieker-Humboldt-Deutz AG.") diesel.
The primary advantage compared to the water-cooled engines is lower engine weight. The fins on the cylinder block and head are necessary to increase the external heat-transfer surface area to achieve the required heat rejection. An air blower, shown on the right of the cutaway drawing, provides forced air convection over the block. The blower is driven off the injection pump shaft, which in turn is driven off the camshaft. The in-line injection pump is placed between the two banks of cylinders. The injection nozzles are located at an angle to the cylinder axis. The combustion chamber and fuel-injection characteristics are similar to those of the engine in Fig. 1-22. The nozzle shown injects four fuel sprays into a reentrant bowl-in-piston combustion chamber. Diesels are also made in very large engine sizes. These large engines are used for marine propulsion and electrical power generation and operate on the two-stroke cycle in contrast to the small- and medium-size diesels illustrated above. Figure 1-24 shows such a two-stroke cycle marine engine, available with from 4 to 12 cylinders, with a maximum bore of 0.6-0.9 m and stroke of 2-3 m, which operates at speeds of about 100 revlmin. These engines are normally of the crosshead type to reduce side forces on the cylinder. The gas exchange between cycles is controlled by first opening the exhaust valves, and then the piston uncovering inlet ports in the cylinder liner.
Expanding exhaust gases leave the cylinder via the exhaust valves and manifold and pass through the turbocharger ENGINE TYPES AND THEIR OPERATION 37 FIGURE 1-24 Large Sulzer two-stroke turbocharged marine diesel engine. Bore 840 mm, stroke 2900 mm, rated power 1.9 MW per cylinder at 78 revlmin, 4 to 12 cylinders. (CourtesySulzer Brothers Ltd.) turbine. Compressed air enters via the inlet ports and induces forced scavenging; air is supplied from the turbocharger and cooler. At part load electrically driven blowers cut in to compress the scavenge air. Because these large engines operate at low speed, the motion induced by the centrally injected fuel jets is sufficient to mix the fuel with air and bum it in the time available. A simple open combustion chamber shape can be used, therefore, which achieves efficient combustion even with the low-quality heavy fuels used with these types of engines. The pistons are water cooled in these very large engines. The splash oil piston cooling used in medium- and small-size diesels is not adequate. 1.9 STRATIFIED-CHARGE ENGINES Since the 1920s, attempts have been made to develop a hybrid internal combustion engine that combines the best features of the spark-ignition engine and the diesel. The goals have been to operate such an engine at close to the optimum compression ratio for efficiency (in the 12 to 15 range) by: (1) injecting the fuel directly into the combustion chamber during the compression process (and thereby avoid the knock or spontaneous ignition problem that limits conventional spark-ignition engines with their premixed charge); (2) igniting the fuel as it mixes with air with a spark plug to provide direct control of the ignition process ENGINE TYPES AND THEIR OPERATION 39 (and thereby avoid the fuel ignition-quality requirement of the diesel); (3) controlling the engine power level by varying the amount of fuel injected per cycle (with the air flow unthrottled to minimize work done pumping the fresh charge into the cylinder). Such engines are often called stratified-chargeengines from the need to produce in the mixing process between the fuel jet and the air in the cylinder a "stratified" fuel-air mixture, with an easily ignitable composition at the spark plug at the time of ignition. Because such engines avoid the spark-ignition engine requirement for fuels with a high antiknock quality and the diesel requirement for fuels with high ignition quality, they are usually fuel-tolerant and will operate with a wide range of liquid fuels. Many different types of stratified-charge engine have been proposed, and some have been partially or fully developed. A few have even been used in practice in automotive applications. The operating principles of those that are truly fuel-tolerant or multifuel engines are illustrated in Fig. 1-25.
The combustion chamber is usually a bowl-in-piston design, and a high degree of air swirl is created during intake and enhanced in the piston bowl during compression to achieve rapid fuel-air mixing. Fuel is injected into the cylinder, tangentially into the bowl, during the latter stages of compression. A long-duration spark discharge ignites the developing fuel-air jet as it passes the spark plug. The flame spreads downstream, and envelopes and consumes the fuel-air mixture. Mixing continues, and the final stages of combustion are completed during expansion. Most successful designs of this type of engine have used the four-stroke cycle. This concept is usually called a direct-injection stratified-charge engine. The engine can be turbocharged to increase its power density. Texaco M.A.N. FIGURE 1-26 Sectional drawing of M.A.N. high-speed multifuel four-cylinder direct-injection stratified-charge engine. Bore 94.5 mm, stroke 100 mm, displacement 2.65 liters, compression ratio 16.5, rated power 52 kW at 3800 rev/min.17 Late injection FIGURE 1-25 Two multifuel stratified-charge engines which have been used in commercial practice: the Texaco Controlled Combustion System (TCCS)16and the M.A.N.-FM System.17 A commercial multifuel engine is shown in Fig.
1-26.
In this particular design, the fuel injector comes diagonally through the cylinder head from the upper left and injects the fuel onto the hot wall of the deep spherical piston bowl. The fuel is carried around the wall of the bowl by the swirling flow, evaporated off the wall, mixed with air, and then ignited by the discharge at the spark plug which enters the chamber vertically on the right.
This particular engine is air cooled, so the cylinder block and head are finned to increase surface area. An alternative stratified-charge engine concept, which has also been mass produced, uses a small prechamber fed during intake with an auxiliary fuel system to obtain an easily ignitable mixture around the spark plug. This concept, first Proposed by Ricardo in the 1920s and extensively developed in the Soviet Union and Japan, is often called a jet-ignition or torch-ignition stratified-charge engine. Its operating principles are illustrated in Fig. 1-27 which shows a three-valve ' IN~AKE CO~.'FRES~W COMBUSTIOF! FIGURE 1-27 Schematic of three-valve torch-ignition stratified-chargespark-ignitionengine. 1J. The two-stroke cycle has twice as many power strokes per crank revolution as the four-stroke cycle. However, two-stroke cycle engine power outputs per unit displaced volume are less than twice the power output of an equivalent four-stroke cycle engine at the same engine speed. Suggest reasons why this potential advantage of the twocycle is offset in practice. 1.6. Suggest reasons why multicylinder engines prove more attractive than single-cylinder once the total engine displaced volume exceeds a few hundred cubic centimeters.
1.7. The Wankel rotary spark-ignition engine, while lighter and more compact than a reciprocating :park-ignition engine of equal maximum power, typically has worse eficisncy due t o significantly higher gas leakage from the combustion chamber and higher total heat loss from the hot combustion gases to the chamber walls. Based on the design details in Figs. 1 4 1 - 1 3 , and 1-14 suggest reasons for these higher losses.
REFERENCES carbureted version of the concept.'' A separate carburetor a n d intake manifold feeds a fuel-ech mixture (which contains fuel beyond the a m o u n t that c a n be b u r n e d with the available air) through a separate small intake valve i n t o the prechamber which contains the spark plug. At the same time, a very lean mixture (which contains excess air beyond t h a t required to burn the fuel completely) is fed to the m a i n combustion chamber through the main carburetor and intake manifold. D u r i n g intake the rich prechamber flow fully purges the prechamber volume. After intake valve closing, lean mixture from the main chamber is compressed i n t o the prechamber bringing the mixture a t the spark plug t o a n easily ignitable, slightly rich, composition.
After combustion starts in the prechamber, rich b u r n i n g mixture issues as a jet through the orifice i n t o the m a i n chamber, entraining and igniting the lean m a i n chamber charge. Though called a stratifiedcharge engine, this engine is really a jet-ignition concept whose primary function is t o extend the operating limit of conventionally ignited spark-ignition engines t o mixtures leaner than could normally be burned. PROBLEMS 1.1. Describe the major functions of the following reciprocating engine components: piston, connecting rod, crankshaft, cams and camshaft, valves, intake and exhaust manifolds. 1.2. Indicate on an appropriate sketch the different forces that act on the piston, and the direction of these forces, during the engine's expansion stroke with the piston, connecting rod, and crank in the positions shown in Fig. 1-1. 13. List five important differences between the design and operating characteristics of spark-ignition and compression-ignition (diesel) engines. 1.4. Indicate the approximate crank angle at which the following events in the four-stroke and two-stroke internal combustion engine cycles occur on a line representing the full cycle (720" for the four-stroke cycle; 360' for the two-stroke cycle): bottom- and topcenter crank positions, inlet and exhaust valve or port opening and closing, start of combustion process, end of combustion process, maximum cylinder pressure. I. Cummins, Jr., C. L.: Internal Fire. Carnot Press Lake Oswego, Oreg., 1976. 2 Cummins, Jr., C. L.: "Early IC and Automotive Engines," SAE paper 760604 in A History of the Automotive Internaf Com6ustion Engine, SP-409, SAE Trans., vol.
85,1976. 3. Hempson, J. G. G.: "The Automobile Engine 1920-1950," SAE paper 760605 in A History of the Automotive Internal Combustion Engine, SP-409, SAE, 1976. 4. Agnew, W. G.: "Fifty Years of Combustion Research at General Motors," Progress in Energy and Combustion Science, vol. 4, pp. 115-156, 1978. 5. Wankel. F.: Rotary Piston Machines.
Iliffe Books. London, 1965. 6. Ansdale, R. F.: The Wankel RC Engine Design and Performance, Iliffe Books, London, 1968. 7. Yamamoto, K.: Rotary Engine, Toyo Kogyo Co. Ltd., Hiroshima, 1969. 8.
Haagen-Smit, A. J.: "Chemistry and Physiology of Los Angeles Smog," Ind. Eng. Chem., vol. 44, p. 1342, 1952. 9. Taylor, C. F.: The Internal Combustion Engine in Theory and Practice, vol. 2, table 10-1, MIT Press, Cambridge, Mass, 1968.
10. Rogowski, A. R.: Elements of Internal Combustion Engines, McGraw-Hill, 1953.
11. Weertman, W. L, and Dean, J. W.: "Chrysler Corporation's New 2.2 Liter 4 Cylinder Engine," SAE paper 810007,1981. 12. Bosch: Automotive Handbook, 1st English edition, Robert Bosch GmbH, 1976. 13. Martens, D. A.: "The General Motors 2.8 Liter 60" V-6 Engine Designed by Chevrolet," SAE paper 790697,1979. 14. Hofbauer, P., and Sator, K.: "Advanced Automotive Power Systems-Part 2: A Diesel for a Subcompact Car," SAE paper 770113, SAE Trans., vol. 86,1977. 15.
Garthe, H.: "The Deutz BF8L 513 Aircooled Diesel Engine for Truck and Bus Application," SAE paper 852321,1985. 16 Alperstein, M., Schafer. G. H., and Villforth, F. J.: "Texaco's Stratified Charge EngineMultifuel, Efficient,Clean, and Practical," SAE paper 740563.1974.
17. Urlaub, A. G., and Chmela, F. G.: "High-speed, Multifucl Engine: L9204 FMV," SAE paper 740122,1974. 18. Date, T., and Yagi, S.: "Research and Development of the Honda CVCC Engine," SAE paper 740605,1974. ENGINE DESIGN AND OPERATING PARAMETERS CHAPTER 43 Engine performance is more precisely defined by: 1. The maximum power (or the maximum torque) available at each speed within the useful engine operating range 2. The range of speed and power over which engine operation is satisfactory The following performance definitions are commonly used: ENGINE DESIGN AND OPERATING PARAMETERS Maximum rated power. The highest power an engine is allowed to develop for short periods of operation. Normal rated power. The highest power an engine is allowed to develop in continuous operation. Rated speed. The crankshaft rotational speed at which rated power is developed. 2.2 GEOMETRICAL PROPERTIES OF RECIPROCATING ENGINES The following parameters define the basic geometry ,of a reciprocating engine (see Fig. 2-1): Compression ratio rc : rc = 2.1 IMPORTANT ENGINE CHARACTERISTICS (2.1) where V, is the displaced or swept volume and V, is the clearance volume. Ratio of cylinder bore to piston stroke: In this chapter, some basic geometrical relationships and the parameters commonly used to characterize engine operation are developed. The factors important to an engine user are: Ratio of connecting rod length to crank radius: 1. The engine's performance over its operating range 2. The engine's fuel consumption within this operating range and the cost of the required fuel 3. The engine's noise and air pollutant emissions within this operating range 4. The initial cost of the engine and its installation 5. The reliability and durability of the engine, its maintenance requirements, and how these affect engine availability and operating costs These factors control total engine operating costs-usually the primary consideration of the user-and whether the engine in operation can satisfy environmental regulations. This book is concerned primarily with the performance, efficiency, and emissions characteristics of engines; the omission of the other factors listed above does not, in any way, reduce their great importance. maximum cylinder volume --V, + I/, minimum cylinder volume I/, In addition, the stroke and crank radius are related by i I I Typical values of these parameters are: rc = 8 to 12 for SI engines and rc = 12 to 24 for CI engines; B/L = 0.8 to 1.2 for small- and medium-size engines, decreas-. ing to about 0.5 for large slow-speed CI engines; R = 3 to 4 for small- and medium-size engines, increasing to 5 to 9 for large slow-speed.CI engines. The cylinder volume V at any crank position 8 is nB2 V = K+-(l+a-s) 4 I (2.4) 44 ENGINE DESIGN AND OPERATING PARAMETERS INTERNAL COMBUSTION ENGINE FUNDAMENTALS FIGURE 2-1 Geometry of cylinder, piston, connecting rod, and crankshaft where B = bore, L = stroke, I = connecting road length, a = crank radius, 0 = crank angle. where s is the distance between the crank axis and the piston pin axis (Fig. 2-I), and is given by s = a cos 8 + (I2 - a2 sin2 @'I2 K TC Crank angle, 8 BC FIGURE 2-2 Instantaneous piston speedfmean piston speed as a function of crank angle for R = 3.5. more appropriate parameter than crank rotational speed for correlating engine behavior as a function of speed. For example, gas-flow velocities in the intake and the cylinder all scale with S,. The instantaneous piston velocity S, is obtained from (2.5) The angle 8, defined as shown in Fig. 2-1, is called the crank angle. Equation (2.4) with the above definitions can be rearranged: v = 1 + 4 (r, - 1)[R + 1 - cos 8 - (R2 - sin2 8)'12) - 180 45 (2.6) The piston velocity is zero at the beginning of the stroke, reaches a maximum near the middle of the stroke, and decreases to zero at the end of the stroke. Differentiation of Eq. (2.5) and substitution gives The combustion chamber surface area A at any crank position 8 is given by A = A,, + A, + xB(1 + a - s) (2.7) where A,, is the cylinder head surface area and A, is the piston crown surface area. For flat-topped pistons, A, = xB2/4. Using Eq. (2.5), Eq. (2-7) can be rearranged : Figure 2-2 shows how S, varies over each stroke for R = 3.5. Resistance to gas flow into the engine or stresses due to the inertia of the moving parts limit the maximum mean piston speed to within the range 8 to 15 m/s (1500 to 3000 ft/min). Automobile engines operate at the higher end of this range; the lower end is typical of large marine diesel engines. 2 3 BRAKE TORQUE AND POWER An important characteristic speed is the mean piston speed S,: 3, = 2LN (2.9) where N is the rotational speed of the crankshaft.
Mean piston speed is often a Engine torque is normally measured with a dynamometer.' The engine is clamped on a test bed and the shaft is connected to the dynamometer rotor. Figure 2-3 illustrates the operating principle of a dynamometer. The rotor is 46 ENGINE DESIGN AND OPERATING PARAMETERS INTERNAL COMBUSTION ENGINE FUNDAMENTALS 47 FIGURE 2-3 Schematic of principle of operation of dynamometer.
TC coupled electromagnetically, hydraulically, or by mechanical friction to a stator, which is supported in low friction bearings.
The stator is balanced with the rotor stationary. The torque exerted on the stator with the rotor turning is measured by balancing the stator with weights, springs, or pneumatic means. Using the notation in Fig. 2-3, if the torque exerted by the engine is T: T = Fb RGURE 24 Examples of pV diagrams for (a) a twostroke cycle engine, (b) a four-stroke cycle engine; (c) a four-strokecycle spark-ignitionengine exhaust and intake strokes (pumpingloop) at part load. area enclosed on the diagram: (2.13~) where N is the crankshaft rotational speed. In SI units: or in U.S.units: )= TC C o m ~ - ~ Vol ~ ~. BC (2.12) The power P delivered by the engine and absorbed by the dynamometer is the product of torque and angular speed: P = 2xNT Vol. BC N(rev/min) T(1bf. ft) 5252 Note that torque is a measure of an engine's ability to do work; power is the rate at which work is done. The value of engine power measured as described above is called brake power P b . This power is the usable power delivered by the engine to the load-in this case, a "brake." With two-stroke cycles (Fig. 2-4a), the application of Eq. (2.14) is straightforward. With the addition of inlet and exhaust strokes for the four-stroke cycle, some ambiguity is introduced as two definitions of indicated output are in common use. These will be defined as: Gross indicated work per cycle W,,i,. Work delivered to the piston over the compression and expansion strokes only. Net indicated work per cycle W,,. Work delivered to the piston over the entire four-stroke cycle. + Pressure data for the gas in the cylinder over the operating cycle of the engine can be used to calculate the work transfer from the gas to the piston. The cylinder pressure and corresponding cylinder volume throughout the engine cycle can be plotted on a p-V diagram as shown in Fig. 2-4.
The indicated work per cycle WGit (per cylinder) is obtained by integrating around the curve to obtain the is (area A area C) In Fig. 2-4b and c, Wc,i, is (area A + area C) and Wc,in - (area B + area C), which equals (area A - area B), where each of these areas is regarded as a positive quantity. Area B + area C is the work transfer between the piston and the cylinder gases during the inlet and exhaust strokes and is called the pumping work W, (see Chaps. 5 and 13). The pumping work transfer will be to the cylinder gases if the pressure during the intake stroke is less than the pressure during the exhaust stroke. This is the situation with naturally aspirated engines. The pumping work transfer will be from the cylinder gases to the piston if the exhaust stroke pressure is lower than the intake pressure, which is normally the case with highly loaded turbocharged engines.? f The term indicated is used because such pV diagrams used to be generated directly with a device called an engine indicator. t With some two-stroke engine concepts there is a piston pumping work term associated with compressing the scavenging air in the crankcase. 2.4 INDICATED WORK PER CYCLE ENGINE DESIGN AND OPERATING PARAMETERS The power per cylinder is related to the indicated work per cycle by Suppliedby the dynamometer to overcome all these frictional losses. The engine speed, throttle setting, oil and water temperatures, and ambient conditions are kept the same in the motored test as under firing conditions. The major sources of inaccuracy with this method are that gas pressure forces on the piston and rings are lower in the motored test than when the engine is firing and that the oil temperatures on the cylinder wall are also lower under motoring conditions. The ratio of the brake (or useful) power delivered by the engine to the indicated power is called the mechanical efficiency q, : where nR is the number of crank revolutions for each power stroke per cylinder. For four-stroke cycles, nR equals 2; for two-stroke cycles, n, equals 1. This power is the indicated power; i.e., the rate of work transfer from the gas within the cylinder to the piston. It differs from the brake power by the power absorbed in overcoming engine friction, driving engine accessories, and (in the case of gross indicated power) the pumping power. In discussing indicated quantities of the four-stroke cycle engine, such as work per cycle or power, the definition used for "indicated" (i.e., gross or net) should always be explicitly stated. The gross indicated output, the definition most commonly used, will be chosen where possible in this book for the following reasons. Indicated quantities are used primarily to identify the impact of the compression, combustion, and expansion processes on engine performance, etc. The gross indicated output is, therefore, the most appropriate definition. It represents the sum of the useful work available at the shaft and the work required to overcome all the engine losses. Furthermore, the standard engine test codes2 define procedures for measuring brake power and friction power (the friction power test provides a close approximation to the total lost power in the engine). The sum of brake power and friction power provides an alternative way of estimating indicated power; the value obtained is a close approximation to the gross indicated power. The terms brake and indicated are used to describe other parameters such as mean effective pressure, specific fuel consumption, and specific emissions (see the following sections) in a manner similar to that used for work per cycle and power. Since the friction power includes the power required to pump gas into and out of the engine, mechanical efficiencydepends on throttle position as well as engine design and engine speed. Typical values for a modern automotive engine at wideopen or full throttle are 90 percent at speeds below about 30 to 40 rev/s (1800 to ~ 0 rev/min), 0 decreasing to 75 percent at maximum rated speed. As the engine is throttled, mechanical efficiencydecreases, eventually to zero at idle operation. 2.6 ROAD-LOAD POWER A part-load power level useful as a reference point for testing automobile engines is the power required to drive a vehicle on a level road at a steady speed. Called road-load power, this power overcomes the rolling resistance which arises from the friction of the tires and the aerodynamic drag of the vehicle. Rolling resistance and drag coefficients, C, and C,, respectively, are determined empirically. An approximate formula for road-load power Pr is where C, = coefficient of rolling resistance (0.012 < C, < 0.015)3 M u = mass of vehicle [for passenger cars: curb mass plus passenger load of 68 kg (150 Ibm); in U.S.units W,= vehicle weight in lbfl g = acceleration due to gravity pa = ambient air density C, = drag coefficient (for cars: 0.3 < C, 5 0.5)3 A, = frontal area of vehicle S, = vehicle speed 2.5 MECHANICAL EFFICIENCY We have seen that part of the gross indicated work per cycle or power is used to expel exhaust gases and induct fresh charge. An additional portion is used to overcome the friction of the bearings, pistons, and other mechanical components of the engine, and to drive the engine accessories.
All of these power requirements are grouped together and calledfriction power P, .t Thus: Friction power is difficult to determine accurately. One common approach for high-speed engines is to drive or motor the engine with a dynamometer (i.e., operate the engine without firing it) and measure the power which has to be t The various components of friction power are examined in detail in Chap. 13. 49 I With the quantities in the units indicated: 50 INTERNAL COMBUSTION ENGINE FUNDAMENTALS 2.7 MEAN EFFECTIVE PRESSURE While torque is a valuable measure of a particular engine's ability to d o work, it depends on engine size. A more useful relative engine performance measure is obtained by dividing the work per cycle by the cylinder volume displaced per cycle. The parameter so obtained has units of force per unit area and is called the mean effective pressure (mep). Since, from Eq. (2.15), Pn, Work per cycle = N where n, is the number of crank revolutions for each power stroke per cylinder (two for four-stroke cycles; one for two-stroke cycles), then Pn, mep = V,N For SI and U.S. units, respectively, 1b,'in2)range, with the bmep at the maximum rated power of about 700 kPa (100 1b/in2).~urbochargedfour-stroke diesel maximum bmep values are typically in the range 1000 to 1200 kPa (145 to 175 lb/in2); for turbocharged aftercooled this can rise to 1400 kPa. At maximum rated power, bmep is about 850 to 950 kPa (125 to 140 lb/in2). Two-stroke cycle diesels have comparable performance to four-stroke cycle engines.
Large low-speed two-stroke cycle engines can achieve bmep values of about 1600 kPa. An example of how the above engine performance parameters can be used 10 initiate an engine design is given below. Example. A four-cylinder automotive spark-ignition engine is being designed to provide a maximum brake torque of 150 N-m (110 Ibf-ft)in the mid-speed range (3000 rev/min). Estimate the required engine displacement, bore and stroke, and the maximum brake power the engine will deliver. Equation (2.204 relates torque and mep. Assume that 925 kPa is an appropriate value for bmep at the maximum engine torque point. Equation (2.20~)gives - For a four-cylinder engine, the displaced volume, bore, and stroke are related by Mean effective pressure can also be expressed in terms of torque by using Eq. (2.13): mep(lb/in2) = 75.4nRT(lbf.ft) &(in3) The maximum brake mean effective pressure of good engine designs is well established, and is essentially constant over a wide range of engine sizes. Thus, the actual bmep that a particular engine develops can be compared with this norm, and the effectiveness with which the engine designer has used the engine's displaced volume can be assessed.
Also, for design calculations, the engine displacement required to provide a given torque or power, at a specified speed, can be estimated by assuming appropriate values for bmep for that particular application. Typical values for bmep are as follows. For naturally aspirated sparkignition engines, maximum values are in the range 850 to 1050 kPa (125 to 150 lb/in2) at the engine speed where maximum torque is obtained (about 3000 rev/min). At the maximum rated power, bmep values are 10 to 15 percent lower.
For turbocharged automotive spark-ignition engines the maximum bmep is in the 1250 to 1700 kPa (180 to 250 lb/in2) range. At the maximum rated power, bmep is in the 900 to 1400 kPa (130 to 200 lb/in2) range. For naturally aspirated four-stroke diesels, the maximum bmep is in the 700 to 900 kPa (100 to 130 - Assume B = L; this gives B = L = 86 mm. The maximum rated engine speed can be estimated from an appropriate value for the maximum mean piston speed, 15 m/s (see Sec. 2.2): The maximum brake power can be estimated from the typical bmep value at maximum power, 800 kPa (116 lb/in2),using Eq.(2.196): 2.8 SPECIFIC FUEL CONSUMPTION AND EFFICIENCY In engine tests, the fuel consumption is measured as a flow rate-mass flow p r unit time m,. A more useful parameter is the specijc fuel consumption (s f c t t h e fuel flow rate per unit power output. It measures how efficiently an engine is using the fuel supplied to produce work: 52 ENGINE DESIGN AND OPERATING PARAMETERS INTERNAL COMBUSTION ENGINE FUNDAMENTALS 53 or with units: With units, Low values of sfc are obviously desirable. For SI engines typical best values of brake specific fuel consumption are about 75 pg/J = 270 g/kW h = 0.47 lbm/ hp .h. For CI engines, best values are lower and in large engines can go below 55 pg/J = 200 g/kW h = 0.32 lbm/hp- h. The specific fuel consumption has units. A dimensionless parameter that relates the desired engine output (work per cycle or power) to the necessary input (fuel flow) would have more fundamental value. The ratio of the work produced per cycle to the amount of fuel energy supplied per cycle that can be released in the combustion process is commonly used for this purpose. It is a measure of the engine's efficiency.
The fuel energy supplied which can be released by combustion is given by the mass of fuel supplied to the engine per cycle times the heating value of the fuel. The heating value of a fuel, QHv,defines its energy content. It is determined in a standardized test procedure in which a known mass of fuel is fully burned with air, and the thermal energy released by the combustion process is absorbed by a calorimeter as the combustion products cool down to their original temperature. This measure of an engine's "efficiency," which will be called the fuel conversion eficiency qf ,t is given by - Typical heating values for the commercial hydrocarbon fuels used in engines are in the range 42 to 44 MJ/kg (18,000 to 19,000 Btu/lbm). Thus, specific fuel consumption is inversely proportional 'to fuel conversion efficiency for normal hydrocarbon fuels. Note that the fuel energy supplied to the engine per cycle is not fully released as thermal energy in the combustion process because the actual combustion process in incomplete. When enough air is present in the cylinder to .
oxidize the fuel completely, almost all (more than about 96 percent) of this fuel energy supplied is transferred as thermal energy to the working fluid. When insufficient air is present to oxidize the fuel completely, lack of oxygen prevents this fuel energy supplied from being fully released. This topic is discussed in more detail in Secs. 3.5 and 4.9.4. 2.9 AIRIFUEL AND FUEL/AIR RATIOS In engine testing, both the air mass flow rate ma and the fuel mass flow rate rit/ are normally measured. The ratio of these flow rates is useful in defining engine operating conditions: Airlfuel ratio (A10 = % mf Fuellair ratio (F/A) = % 4 where mf is the mass of fuel inducted per cycle. Substitution for P/mf from Eq. (2.2 1) gives (2.26) The normal operating range for a conventional SI engine using gasoline fuel is 12 S AIF I 18 (0.056 < F/A 5 0.083); for CI engines with diesel fuel, it is 18 s AIF I70 (0.014 I F/A 10.056). 2.10 VOLUMETRIC EFFICIENCY t This empirically defined engine effciency has previously been called thermal effciency or enthalpy efficiency. The term fuel conversion effciency is preferred because it describes this quantity more precisely, and distinguishes it clearly from other definitions of engine effciehcy which will be developed in Sec. 3.6. Note that there are several different definitions of heating value (see Scc. 3.5). The numerical values do not normally d f i r by more than a few pcmnt, however.
In this text, the lower heating value at constant pressure is used in evaluating the fuel convenion effciency.
The intake system-the air filter, carburetor, and throttl; plate (in a sparkignition engine), intake manifold, intake port, intake valve--restricts the amount of air which an engine of given displacement can induct.
The parameter used to measure the effectivenessof an engine's induction process is the volumetric eficiency q,,. Volumetric efficiencyis only used with four-stroke cycle engines which have a distinct induction process. It is defined as the volume flow rate of air into 54 ENGINE DESIGN AND OPERATING PARAMETERS INTERNAL COMBUSTION ENGINE FUNDAMENTALS 55 the intake system divided by the rate at which volume is displaced by the piston: where pa,i is the inlet air density. An alternative equivalent definition for volumetric efficiency is where ma is the mass of air inducted into the cylinder per cycle. The inlet density may either be taken as atmosphere air density (in which case q, measures the pumping performance of the entire inlet system) or may be taken as the air density in the inlet manifold (in which case q, measures the pumping performance of the inlet port and valve only). Typical maximum values of q,, for naturally aspirated engines are in the range 80 to 90 percent. The volumetric efficiency for diesels is somewhat higher than for SI engines. Volumetric efficiency is discussed more fully in Sec. 6.2. 2.11 ENGINE SPECIFIC WEIGHT AND SPECIFIC VOLUME Engine weight and bulk volume for a given rated power are important in many applications.
Two parameters useful for comparing these attributes from one engine to another are: engine weight Specific weight = rated power Specific volume = Dry air pressure Water vapour pressure Temperature 736.6 mmHg 29.00 inHg 9.65 mmHg 0.38 inHg 29.4"C 85•‹F The basis for the correction factor is the equation for one-dimensional steady compressible flow through an orifice or flow restriction of effective area A, (see App. C): 1" deriving this equation, it has been assumed that the fluid is an ideal gas with gas constant R and that the ratio of specific heats (cJc, = 7) is a constant; po and T, are the total pressure and temperature upstream of the restriction and p is the pressure at the throat of the restriction. If, in the engine, plp, is assumed constant at wide-open throttle, then for a given intake system and engine, the mass flow rate of dry air ma varies as For mixtures containing the proper amount of fuel to use all the air available (and thus provide maximum power), the indicated power at full throttle Pi will bt proportional to rit,, the dry air flow rate. Thus if (2.32) Pi,. = CFPi,m where the subscripts s and m denote values at the standard and measured conditions, respectively, the correction factor CFis given by engine volume rated power For these parameters to be useful in engine comparisons, a consistent definition of what components and auxiliaries are included in the term "enginen must be adhered to. These parameters indicate the effectiveness with which the engine designer has used the engine materials and packaged the engine components? where p , = ~ standard dry-air absolute pressure pm = measured ambient-air absolute pressure p,., = measured ambient-water vapour partial pressure Tm = measured ambient temperature, K T, = standard ambient temperature, K The rated brake power is corrected by using Eq. (2.33) to correct the indi- 2.12 CORRECTION FACTORS FOR POWER AND VOLUMETRIC EFFICIENCY The pressure, humidity, and temperature of the ambient air inducted into an engine, at a given engine speed, affect the air mass flow rate and the power output. Correction factors are used to adjust measured wide-open-throttle power and volumetric efficiencyvalues to standard atmospheric conditions to provide a more accurate basis for comparisons between engines. Typical standard ambient w e d power and making the assumption that friction power is unchanged. Thus Pb.s = CFPi,m - P1.m (2.34) Volumetric efficiency is proportional to mJpa [see Eq. (2.2711. Since pa is Proportional to p/T, the correction factor for volumetric efficiency, CF, is 112 (2.35) ENGINE DESIGN AND OPERATING PARAMETERS 2.13 SPECIFIC EMISSIONS AND EMISSIONS INDEX 57 For four-stroke cycle engines, volumetric efficiency can be introduced: Levels of emissions of oxides of nitrogen (nitric oxide, NO, and nitrogen dioxide, NO,, usually grouped together as NO,), carbon monoxide (CO), unburned hydrocarbons (HC), and particulates are important engine operating characteristics. The concentrations of gaseous emissions in the engine exhaust gases are usually measured in parts per million or percent by volume (which corresponds to the mole fraction multiplied by lo6 or by lo2, respectively). Normalized indicators of emissions levels are more useful, however, and two of these are in common use. Specific emissions are the mass flow rate of pollutant per unit power output: litco sC0 =P (2.36b) ~ H C sHC = - (2.36~) P For torque T: For mean effective pressure: The power per unit piston area, often called the specific power, is a measure of the engine designer's success in using the available piston area regardless of cylinder size. From Eq. (2.39), the specific power is Mean piston speed can be

Typically the proportion by mass is about 1 percent, though it can rise to about 4 percent under extreme conditions. The relative humidity compares the water vapor content of air with that required to saturate. It is defined as: The ratio of the partial pressure of water vapor actually present to the saturation pressure at the same temperature. Water vapor content is measured with a wet- and dry-bulb psychrometer.
This consists of two thermometers exposed to a stream of moist air. The dry-bulb temperature is the temperature of the air. The bulb of the other thermometer is wetted by a wick in contact with a water reservoir. The wet-bulb temperature is lower than the dry-bulb temperature due to evaporation of water from the wick.
It is a good approximation to assume that the wet-bulb temperature is the adiabatic saturation temperature. Water vapor pressure can be obtained from observed wet- and dry-bulb temperatures and a psychrometric chart such as Fig. 3-1." The effect of humidity on the properties of air is given in Fig. 3-2.5 The fuels most commonly used in internal combustion engines (gasoline or petrol, and 'diesel fuels) are blends of many different hydrocarbon compounds obtained by refining petroleum or crude oil. These fuels are predominantly carbon and hydrogen (typically about 86 percent carbon and 14 percent hydrogen by weight) though diesel fuels can contain up to about 1 percent sulfur. Other fuels of interest are alcohols (which contain oxygen), gaseous fuels (natural gas and liquid petroleum gas), and single hydrocarbon compounds (e.g., methane, propane, isooctane) which are often used in engine research. Properties of the more common internal combustion engine fuels are summarized in App. D. Some knowledge of the different classes of organic compounds and their FIGURE 3-2 ~ f of ~humidity t on properties of air: R is the gas constant; c, and c, are specific heats at constant tolurne and pressure, respectively; y = cdc,; k is the thermal conductivity.(From T ~ ~ l o r . 3 molecular structure is necessary in order to understand combustion mechanism~.~ The different classes are as follows: Alkyl Compounds Parafins (alkanes) H H I I I H H H-C-C-H CnHzn + z C~cloparafins or napthenes (cyclanes) H H I I H- 0 If Ci v, = 0, changes in pressure have no effect on the composition. If (dissociation reactions), then the mole fractions of the dissociation products decrease as pressure increases. If C, v, < 0 (recombination reactions), the converse is true. An equilibrium constant, Kc, based on concentrations (usually expressed in gram moles per cubic centimeter) is also used: Kc = n [MilVi i Equation (3.40) can be used to relate K, and Kc: - The equilibrium relation [Eq. (3.40)J gives which can be solved to give a = 0.074. The composition of the products in mole fractions is, therefore. x", = -- 0.037 "P The pressure of the product mixture is p = 5.555np = 5.76 atm for p, = 1 atmosphere. For xi vi = 0, K, and Kc are equal. Example 3.4. A stoichiometric mixture of CO and 0, in a closed vessel, initially at 1 atm and 300 K, is exploded.
Calculate the composition of the products of combustion at 2500 K and the gas pressure.
The combustion equation is CO + 40, = C 0 , The JANAF tables give log,, K, (equilibrium constants of formation from the elements in their standard state) at 2500 K of CO,, CO, and 0, as 8.280,6.840, and 0, respectively. Thus, the equilibrium constant for the CO combustion reaction above is, from Eq. (3.41), log,, Kp = 8.280 - 6.840 = 1.440 which gives K, = 27.5. Example 35. In fuel-rich combustion product mixtures, equilibrium between the species CO, , H20, CO, and H, is often assumed to determine the burned gas composition. For 4 = 1.2, for C,H,,-air combustion products, determine the mole fractions of the product species at 1700 K. The reaction relating these species (often called the water gas reaction) is C 0 2 + H2 CO +H20 From the JANAF tables, log,, K, of formation for these species at 1700 K are: CO,, 12.180; H2,0 ; CO, 8.011; Hz%), 4.699.
The equilibrium constant for the above reaction is, from Eq. (3.41), log,, K, = 8.011 + 4.699 - 12.180 = 0.530 from which K, = 3.388. The combustion reaction for CBHl,-air with 4 = 1.2 can be written For gases, the chemical potential A carbon balance gives: A hydrogen balance gives: An oxygen balance gives: is a+c=8 + 2d = 18 2a + b + c = 20.83 2b The equilibrium relation gives (bc)/(ad)= 3.388 (since the equilibrated reaction has the same number of moles as there are reactants or products, the moles of each species can be substituted for the partial pressures). These four equations can be solved to obtain where ji; is the chemical potential in the standard state and p is the mixture pressure in atmospheres. Using the method of lagrangian multipliers, the term I n is defined.
The condition for equilibrium then becomes which gives c = 2.89, a = 5.12, b = 7.72, and d = 1.29.
The total number of moles of products is Treating the variations 6nj and 6Ai as independent gives and the mole fractions of the species in the burned gas mixture are CO2, 0.0908; HzO, 0.137; CO, 0.051; Hz, 0.023; N2, 0.698 Our development of the equilibrium relationship for one reaction has placed no restrictions on the occurrence of simultaneous equilibria. Consider a mixture of N reacting gases in equilibrium. If there are C chemical elements, conservation of elements will provide C equations which relate the concentrations of these N species. Any set of (N - C) chemical reactions, each in equilibrium, which includes each species at least once will then provide the additional equations required to determine the concentration of each species in the mixture. Unfortunately, this complete set of equations is a coupled set of C linear and (N - C) nonlinear equations which is difficult to solve for cases where (N - C) > 2. For complex systems such as this, the following approach to equilibrium composition calculations is now more widely used. Standardized computer methods for the calculation of complex chemical equilibrium compositions have been developed. A generally available and welldocumented example is the NASA program of this type.14 The approach taken is to minimize explicitly the Gibbs free energy of the reacting mixture (at constant temperature and pressure) subject to the constraints of element mass conservation. The basic equations for the NASA program are the following. If the stoichiometric coefficients aij are the number of kilomoles of element i per kilomole of species j, br is the number of kilomoles of element i per kilogram of mixture, and nj is the number of kilomoles of speciesj per kilogram of mixture, element mass balance constraints are The Gibbs free energy per kilogram of mixture is and the original mass balance equation (3.44). Equations (3.44) and (3.48) permit the determination of equilibrium compositions for thermodynamic states specified by a temperature T and pressure p. In the NASA program, the thermodynamic state may be specified by other pairs of state variables: enthalpy and pressure (useful for constant-pressure combustion processes); temperature and volume; internal energy and volume (useful for constant-volume combustion processes); entropy and pressure, and entropy and volume (useful for isentropic compressions and expansions). The equations required to obtain mixture composition are not all linear in the composition variables and an iteration procedure is generally required to obtain their solution. Once the composition is determined, additional relations, such as those in App.
B which define the thermodynamic properties of gas mixtures, must then be used. For each species, standard state enthalpies I;" are obtained by combining standard enthalpies of formation at the datum temperature (298.15 K) ~h;,,, with sensible enthalpies (I;" - Rg,), i.e., 6 is zero ; [the ~ elements ~ ~ important For the elements in their reference state, ~ in combustion are C (solid, graphite), H,(g), O,(g), N,(g)]. For each species, the thermodynamic quantities specific heat, enthalpy, and entropy as functions of temperature are given in the form: 92 INTERNAL COMBUSTION ENGINE FUNDAMENTALS The coefficients are obtained by least-squares matching with thermodynamic property data from the JANAF tables. Usually two sets of coefficients are included for two adjacent temperature intervals (in the NASA program these are 300 to 1000 K and 1000 to 5000 K) (see Sec. 4.7). In some equilibrium programs, the species to be included in the mixture must be specified as an input to the calculation.
In the NASA program, all allowable species are included in the calculation, though species may be specifically omitted from consideration. For each reactant composition and pair of thermodynamic state variables, the program calculates and prints out the following: 1. Thermodynamic mixture properties (obtained from the equilibrium composition and the appropriate gas mixture rule; see App. B). p, T, p, h, s, M , (a In V/a In p), ,(a In V/a In T),,c,, y,, and a (sound speed) 2. Equilibrium composition. Mole fractions of each species (which are present in significant amounts), f Figure 3-10 shows how the equilibrium composition of the products of combustion of isooctane-air mixtures at selected temperatures and 30 atm pressure varies with the equivalence ratio. At low temperatures, the products are N,, CO, ,-H,O, and 0, for lean mixtures and N, , CO,, H,O, CO, and Hzfor rich mixtures.
As temperature increases, the burned-gas mixture composition becomes much more complex with dissociation products such as OH, 0, and H becoming significant. Figure 3-1 1 shows adiabatic flame temperatures for typical engine conditions as a function of the equivalence ratio, obtained with the NASA program using the methodology of Sec. 3.5.4. The isooctane-air unburned mixture state was 700 K and 10 atm. Flame temperatures for adiabatic combustion at constant pressure (where pR and HR are specified) and at constant volume (where VR and U Rare specified) are shown.
Flame temperatures at constant volume are higher, because the final pressure is higher and dissociation is less. Maximum flame temperatures occur slightly rich of stoichiometric. 3.7.2 Chemical Reaction Rates Whether a system is in chemical equilibrium depends on whether the time constants of the controlling chemical reactions are short compared with time scales over which the system conditions (temperature and pressure) change. Chemical processes in engines are often not in equilibrium. Important examples of nonequilibrium phenomena are the flame reaction zone where the fuel is oxidized, and the air-pollutant formation mechanisms.
Such nonequilibrium processes are controlled by the rates at which the actual chemical reactions which convert 94 THERMOCHEMISTRY OF FUEL-AIR MMTURES INTERNAL COMBUSTION ENGINE FUNDAMENTALS 95 M is any molecule (such as N,) which takes part in the collision and carries away the excess energy. The law of mass action states that the rate at which product species are pduced and the rate at which reactant species are removed is proportional to the product of the concentrations of reactant species, with the concentration of each species raised to the power of its stoichiometric coefficient v,. ~ h & ,for reaction (3.51) above, the reaction rate R + in the forward (+) direction, reactants to is given by If the reaction can also proceed in the reverse (-) direction, then the backward rate R- is given by I 0!2 0:4 ' 66 0!8 lb Fuellair equivalence ratio 9 r! k + and k - are the rate constants in the forward and reverse directions for this reaction. The net rate of production of products or removal of reactants is, there- 0 1 : I fore, FIGURE %I1 Equilibrium product temperatures for constant-volume (T,.
3 and constant-pnssure (Tp.S adiabatic combustion of isooctane-air mixture initially at 700 K and 10 atm, as a function of fuellair equivalena ratio.
Pressure @,,,)isequilibrium pressure for adiabatic wnstant-volume combustion. reactants to products occur. The rates at which chemical reactions proceed depend on the concentration of the reactants, temperature, and whether any catalyst is present. This field is called chemical kinetics and some of its basic relations will now be reviewed.' Most of the chemical reactions of interest in combustion are binary reactions, where two reactant molecules, Ma and M,, with the capability of reacting together collide and form two product molecules, M, and M,; i.e., M,+Mb=Mc+Md (3.51) These results can be stated more generally as follows. Any reaction can be written as where vi is the stoichiometric coefficient of species Mi, subscripts R and P denote reactants and products, respectively, and there are n reactant species and m product species.
The forward reaction rate R+ and the reverse reaction rate R are given by An important example of such a reaction is the rate-controlling step in the process by which the pollutant nitric oxide, NO, forms: O+N1=NO+N This is a second-order reaction since the stoichiometric coefficients of the reactants v, and v, are each unity and sum to 2. (The only first-order reactions are decomposition processes.) Third-order reactions are important in combustion, also. Examples are the recombination reactions by which radical species such as H, 0, and O H combine during the final stage of the fuel oxidation process: e.g., H+H+M=H2+M* (3.52) The net rate of removal of reactant species MR,is THERMOCHEMXSTRY OF FUEL-AIR MIXTURES 96 a7 INTERNAL COMBUSTION ENGINE FUNDAMENTALS The molar composition of dry exhaust gas of a propane-fueled SI engine is given below (water was removed before the measurement).Calculate the equivalenceratio. and the net rate of production of product species M,, is M. The rate constants, k, usually follow the Anhenius form: 35.
where A is called the frequency o r preexponential factor a n d may be a (moderate) function of temperature; EA is the activation energy. The Boltzmann factor exp (-E,,/RT) defines the fraction of all collisions that have a n energy greater than E,-i.e., sufficient energy t o make the reaction take place. The functionaldependence of k on T and the constants in the Arrhenius form, Eq. (3.59), if that is appropriate, are determined experimentally. At equilibrium, the forward and reverse reaction rates are equal. Then, from Eq. (3.59, with R + - R- = 0: where Kc is the equilibrium constant based on concentrations defined by Eq. (3.42). It can be related t o K,, the equilibrium constant based on partial pressures, by Eq. (3.43). The chemical reaction mechanisms of importance in combustion are much more complex than the above illustrations of rate-controlled processes. Such mechanisms usually involve both parallel and sequential interdependent reactions.
The methodology reviewed above still holds; however, one must sum algebraically the forward and reverse rates of all the reactions which produce (or remove) a species of interest. I n such complex mechanisms it is often useful to assume that (some of) the reactive intermediate species o r radicals are in steady state. That is, these radicals react so quickly once they are formed that their concentrations d o not rise but are maintained in steady state with the species with which they react. The net rate at which their concentration changes with time is set equal to zero. PROBLEMS 3.1. 3.2. Isooctane is supplied to a four-cylinder spark-ignition engine at 2 4s. Calculate the air flow rate for stoichiometric combustion. If the engine is operating at 1500 rev/ min, estimate the mass of fuel and air entering each cylinder per cycle. The engine displaced volume is 2.4 liters. What is the volumetric efficiency? Calculate the exhaust gas composition of a butane-fueled spark-ignition engine ope[ating with equivalence ratio of 0.9. Assume the fuel is fully burned within the . Butane is C,H,, . 3 . 3.7. 3.8. Evaluate and compare the lower heating values per unit mass of stoichiometric mixture and per unit volume of stoichiometric mixture (at standard atmospheric conditions) for methane, isooctane, methyl alwhol, and hydrogen. Assume the fuel is fully vaporized. The measured engine fuel flow rate is 0.4 g/s, air flow rate is 5.6 g/s, and exhaust gas composition (measured dry) is CO, = 13.0%, CO = 2.8% with 0,essentially zero. Unburned hydrocarbon emissions can be neglected. Compare the equivalence ratio calculated from the fuel and air flow with the equivalence ratio calculated from exhaust gas composition. The fuel is gasoline with a H/C ratio of 1.87. Assume a H, concentration equal to one-third the CO concentration. The brake fuel conversion efficiency of an engine is 0.3. The mechanical efficiency is 0.8. The combustion efficiency is 0.94.
The heat losses to the coolant and oil are 60 kW. The fuel chemical energy entering the engine per unit time, mQ ,, is 190 kW. What percentage of this energy becomes (a) brake work; (b) friction work; (c) heat losses; (d) exhaust chemical energy; (e) exhaust sensible energy. An upper estimate can be made of the amount of NO formed in an engine from considering the equilibrium of the reaction N, 0, = 2N0. Calculate the N O concentration at equilibrium at 2500 K and 30 atm. log,, K, = - 1.2 for this reaction at 2500 K. Assume N/O ratio in the combustion products is 15. N,, O,, and NO are the only species present. Carbon monoxide reacts with air at 1 atm and 1000 K in an exhaust gas reactor. The mole fractions of the exhaust gas-air mixture flowing into the reactor are CO, 3%; 02, 7% ; N2,74%; C o t , 6%; H20, 10%. (a) Calculate the concentration of CO and 0, in gram moles per cmqn the entering mixture. (b) The rate of reaction is given by + d[CO]/dt = -4.3 x 10, x [CO][O JO."exp [- E / (R q [I denotes concentration in gram moles per cm3, E/R = 20,000 K.,Calculate the initial reaction rate of CO, d[CO]/dt: time is in seconds. (c) The equilibrium constant K, for the reaction CO + 40, = CO, at 1000 K is 10l0.Find the equilibrium CO concentration. (d) Determine the time to reach this equilibrium concentration of CO using the initial reaction rate. (The actual time will be longer but this calculation indicates approximately the time required.) 3.9. The exhaust gases of a hydrogen-fueled engine contain 22.3 percent H,O, 7.44 percent 0,, and 70.2 percent N, .At what equivalence ratio is it operating?
3-10. Gas is sampled at 1 atmosphere pressure from the exhaust manifold of an internal combustion engine and analyzed. The mole fractions of species in the exhaust are: Other species such as CO and unburned hydrocarbons can be neglected. (4 The fuel is a synthetic fuel derived from wal containing only carbon and hydrogen. What is the ratio of hydrogen atoms to carbon atoms in the fuel? 98 INTERNAL COMBUSTION E N G M FUNDAMENTALS THERMOCHEMISTRY OF FUEL-NR MIXTURES (b) Calculate the fuellair equivalence ratio at which this engine is operating. (c) Is the internal combustion engine a conventional spark-ignition or a diesel engine? Explain. (d) The engine has a displaced volume of 2 liters. Estimate approximately the percentage by which the fuel flow rate would be increased if this engine were operated at its maximum load at this same speed (2000 revlmin). Explain briefly what limits the equivalence ratio at maximum load.
3.11. The following are approximate values of the relative molecular mass (molecular weights): oxygen O,, 32; nitrogen N, ,28; hydrogen Hz, 2; carbon C, 12. Determine the stoichiometric fuellair and airlfuel ratios on a mass basis, and the lower heating value per unit mass of stoichiometric mixture for the following fuels: Methane (CHJ, isooctane (C,H,,), alcohol (CH,OH) benzene (C,H6), hydrogen (H,), methyl Heating values for these fuels are given in App. D. 3.12. Liquid petroleum gas (LPG) is used to fuel spark-ignition engines. A typical sample of the fuel consists of 70 percent by volume propane C3H, 5 percent by volume butane C,H,, 25 percent by volume propene C3H6 The higher heating values of the fuels are: propane, 50.38 MJ/kg; butane, 49.56 MJ/kg; propylene (propene), 48.95 MJ/kg. (a) Work out the overall combustion reaction for stoichiometric combustion of 1 mole of LPG with aii, and the stoichiometric FIA and AIF.
(b) What are the higher and lower heating values for combustion of this fuel with excess air, per unit mass of LPG? 3.13. A spark-ignition engine is operated on isooctane fuel (C,H,,). The exhaust gases are cooled, dried to remove water, and then analyzed for CO, ,CO, H, , 0,. Using the overall combustion reaction for a range of equivalence ratios from 0.5 to 1.5, calculate the mole fractions of CO,, CO, H z , and 0, in the dry exhaust gas, and plot the results as a function of equivalence ratio. Assume: (a) that all the fuel is burnt inside the engine (almost true) and that the r'atio of moles CO to moles H, in the exhaust is 3 : 1, and (b) that there is no hydrogen in the exhaust for lean mixtures. For high-power engine operation the airlfuel ratio is 14 :1. What is the exhaust gas composition, in mole fractions, before the water is removed? REFERENCES 1. Fristrom, R.
M., and Westenberg, A. A.: Flame Structure, McGraw-Hill, 1965. 2. Glassman, I.: Combustion,Academic Press, 1977. 3. Kaye, G. W. C., and Laby, T. H.: Tables of Physical and Chemical Constants, Longmans, London. 1973. 4.
Reynolds, W. C.: Thermodynamic Properties in S1, Department of Mechanical Engineering, Stanford University, 1979. 5. Taylor, C. F.: The Internal Combustion Engine in Theory and Practice, vol. 1, MIT Press, Cambridge, Mass., 1960. 99 6. Goodger, E. M.: Hydrocarbon Fuels, Macmillan, London, 1975.
7. Spalding D. B.. and Cole. E.H.:Engineering Thermodynamics, M ed., Edward Arnold. 1973. 8. JANAF Thennochemical Tables, National Bureau of Standards Publication NSRDS-NBS37, 1971. 9.
Maxwell, J. B.: Data Book on Hydrocarbons,Van Nostrand, New York, 1950. 10. Rossink F. D.,Pitzer, K.
S., Arnelt, R L.. Braun, R. M., and Primentel, G. C.: Selected Valws of physical and Thennodynamic Properties of Hydrocarbons and Related Compounds, Carnegie Press, Pittsburgh, Pa, 1953. 11. Stull, D. R.. Westrum, E. F, and Sinke, G. C.: The Chemical Thennodynamics of Organic Cornpounds, John Wiley, New York, 1969. 12. Matthews, R. D.: "Relationship of Brake Power to Various Energy mciencies and Other Engine Parameters: The EfficiencyRule," Int. J. of VehicleDesign, vol. 4, no. 5, pp. 491-500,1983. 13. Keenan, J. H.:Thermodynamics. John Wiley, New York, 1941 (MIT -Press, Cambridge, Mass., 1970). 14. Svehla, R. A., and McBride, B. J.: "Fortran IV Computer Program for Calculation of Thermody- namic and Transport Properties of Complex Chemical Systems," NASA Technical Note TN D-7056, NASA Lewis Research Center, 1973. PROPERTIES OF WORKING FLUIDS 101 TABLE 4.1 CHAPTER Working fluid collstituents Air Fuel7 Recycled exhaust$ Residual ga.4 Air Recycled exhaust$ i om press ion Air Fuel vapor Recycled exhaust Residual gas Air Recycled exhaust Residual gas Expansion Combustion products (mixture of N, ,HzO, CQg CO, Hz, Og NO, OH, 0 , H, ...) Combustion products (mixture of Nz ,HzO, Cog, CO, Hz, 0 2 , NO, OH, 0 , H, ...) Exhaust Combustion products [mainly Nz, C o p , HzO. and either O2(4 < 1) or CO and Hz (4 > I)] Combustion products (mainly Nz, COZ, HzO, and 0 3 Intake PROPERTIES OF WORKING FLUIDS f dual & Liquid and vapor in the intake; mainly vapor within the cylinder. ;Sometimesusad to wntrol NO, emissions (see Sccs.
11.2, 15.3.2, and 15.5.1). g Within the cylinder.
4.1 INTRODUCTION The study of engine operation through an analysis of the processes that occur inside the engine has a long and productive history. The earliest attempts at this analysis used the constant-volume and constant-pressure ideal cycles as approximations to real engine processes (see Chap. 5). With the development of highspeed digital computers, the simulation of engine processes has become much more sophisticated and accurate (see Chap. 14). All these engine simulations (from the simplest to the most complex) require models for the composition and properties of the working fluids inside the engine, as well as models for the individual processes-induction, compression, combustion, expansion, and exhaustthat make up the engine operating cycle. This chapter deals with models for the working fluid composition, and thermodynamic and transport properties. The composition of the working fluid, which changes during the engine operating cycle, is indicated in Table 4.1. The unburned mixture for a sparkignition engine during intake and compression consists of air, fuel, and previously burned gases. It is, therefore, a mixture of N,, O,, CO,, H 2 0 , CO, and H, for fuel-rich mixtures, and fuel (usually vapor). The composition of the unburned mixture does not change significantly during intake and compression. It is suffi- ciently accurate to assume the composition is frozen.
For the compressionignition engine, the unburned mixture prior to injection contains no fuel; it consists of air and previously burned gas. The combustion products or burned mixture gases, during the combustion process and much of the expansion process, are close to thermodynamic equilibrium. The composition of such mixtures has already been discussed (Sec. 3.7.1). As these combustion products cool, recombination occurs as indicated in Fig. 3-10. Towards the end of the expansion process, the gas composition departs from the equilibrium composition; recombination can no longer occur fast enough to maintain the reacting mixture in equilibrium. During the exhaust process, reactions are sufficiently slow so that for calculating thermodynamic properties the composition can be regarded asfrozen. The models used for predicting the thermodynamic properties of unburned and burned mixtures can be grouped into the five categories listed in Table 4.2. The first category is only useful for illustrative purposes since the specific heats of unburned and burned mixtures are significantly different. While the specific heats of the working fluids increase with increasing temperature in the range of interest, a constant-specific-heat model can be matched to the thermodynamic data over a limited temperature range. This approach provides a simple analytic model which can be useful when moderate accuracy of prediction will sufice. The appropriateness of frozen and equilibrium assumptions has already been discussed above. Approximations to thermodynamic equilibrium calculations are useful because of 102 INTERNAL COMBUSTION ENGINE FUNDAMENTALS TABLE 4.2 Categories of models for thermodynamic properties -- Unburned mixture Burned mixture 1. Single ideal gas throughout operating cycle with c, (and hence c ,) constant 2. Ideal gas; c,, constant 3. Frozen mixture of ideal gases; c , m Frozen mixture of ideal gases; c,AT) 4. 5. Frozen mixture of ideal gam; c , m he percent of exhaust gas recycled (%EGR) is defined as the percent of the total intake mixture which is recycled exhaust,? Ideal gas; c,, constant Frozen mixture of ideal where mEGR is the mass of exhaust gas recycled, then the burned gas fraction in h e fresh mixture is gases; c , . m Approximations fitttd to equilibrium thermodynamic properties Mixture of reacting ideal gases in thermodynamic equilibrium x, = ~ + fi = E G R mc (E) - + 1 x,) x, u p to about 30 percent of the exhaust can be recycled; the burned gas fraction during compression can, therefore, approach 30 to 40 percent. The composition of the burned gas fraction in the unburned mixture can be calculated as follows. The combustion equation for a hydrocarbon fuel of average molar H/C ratio y [e.g., Eq. (3.511 can be written per mole 0, as Note: Subscripts i, u, and b denote species i io the gas mixture, the unburned mixture, and burned mixture properties, respectively. the savings in computational time, relative to full equilibrium calculations, which can result from their use. Values of thermodynamic properties of unburned and burned mixtures relevant to engine calculations are available from charts, tables, and algebraic relationships developed to match tabulated data. A selection of this material is included in this chapter and App. D. The references indicate additional sources. where $ = the molar N/O ratio (3.773 for air) y = the molar H/C ratio of the fuel 4 = fuellair equivalence ratio ni = moles of species i per mole 0, reactant The n, are determined using the following assumptions: 4.2 UNBURNED MIXTURE COMPOSITION The mass of charge trapped in the cylinder (me) is the inducted mass per cycle (mJ, plus the residual mass (m,) left over from the previous cycle.
The residual fraction (x,) is Typical residual fractions in spark-ignition engines range from 20 percent at light load to 7 percent at full load.
In diesels, the residual fraction is smaller (a few percent) due to the higher compression ratio, and in naturally aspirated engines is approximately constant since the intake is unthrottled. If the inducted mixture is fuel and air (or air only), then the burned gas fraction (x,) in the unburned mixture during compression equals the residual fraction. In some engines, a fraction of the engine exhaust gases is recycled to the intake to dilute the fresh mixture for control of NO, emissions (see Sec. 11.2). If 1. For lean and stoichiometricmixtures (4 a; 1) CO and Hz can be neglected. 2 For rich and stoichiometricmixtures (4 2 1) 0, can be neglected. 3. For rich mixtures, either (a) the water gas reaction t An alternative definition of percent EGR is also used based on the ratio of EGR to fresh mixture (h l and air): The two definitions are related by EGR* 100 -= EGR 100-EGR and EGR -100 EGR* - 100 + EGR* PROPERTIES OF WORKING FLUIDS can be assumed to be in equilibrium with the equilibrium constant K(T): where where K(T) can be determined from a curve fit to JANAF table data? If we write 4* = (4 where T is in K, or (b) K can be assumed constant over the normal engine operating range. A value of 3.5 is often assumed (see Sec. 4.9), which corresponds to evaluating the equilibrium constant at 1740 K. The ni obtained from an element balance and the above assumptions are shown in Table 4.3. The value of c is obtained by solving the quadratic: The mole fractions are given by $* = (1 - ;)c$ (4.7~) the reactant expression (4.74 becomes which is identical in form to the reactant expression for a hydrocarbon fuel (4.4). ~ h u sTable 4.3 can still be used to give the composition of the burned gas residual fraction in the unburned mixture, except that 4 * replaces 4 and $* replaces $ in the expressions for n, . Now consider the unburned mixture. The number of moles of fuel per mole 0,in the mixture depends on the molecular weight of the fuel, M,. If the average molecular formula of the fuel is (CH,),then x, where n, = ni is given in the bottom line of Table 4.3. While Eq. (4.4) is for a fuel containing C and H only, it can readily be modified for alcohols or alcohol-hydrocarbon blends. For a fuel of molar composition CH,O,, the reactant mixture and 105 Mf = u(12 + y) The fresh fuel-air mixture (not yet diluted with EGR or residual), e4C + 2(1 - &)#Hz+ O2 + $N2 then becomes can be rearranged per mole of 0, reactant as The unburned mixture (fuel, air, and a burned gas fraction), per mole 0, in the mixture, can be written: TABLE 43 Burned gas composition under 1700 K n,, co, H2O CO H, 0, N2 Sum:n, t c defined by Eq.(4.6). rnoka/rnole 0, reactant The number of moles of each species in the unburned mixture, per mole 02,is summarized in Table 4.4. The mole fractions of each species are obtained by dividing by the total number of moles of unburned mixture nu, where n, is given in Table 4.3. The molecular weights of the unburned and unburned PROPERTIES OF WORKING FLUIDS 107 TABLE 4.5 TABLE 4A ~pctorsfor relating properties on molar anti mass basis Unburned mixture composition n,, moles/mole 0, reactant Species Fuel w n t i t y , per mole 0, tbe mixture General equation^ Equation for C,H,,-air Mola of burned mixture nb nb= (1 -814 n~= (2 - 814 0 2 co, H2O CO Hi ass of mixture7 + 1 + $, Mr n b = 32 4 1 4>1 + JI. 4(1 + %)# ~ o l e of s unburned mixture n. N2 mixtures + '+$1' xbnb {: + 4#1 + 2s)+ 28.16$ :: + 4.773 + 3.773 n, = 0.084 + 4.773 +0 .
2 8 ~4 ~ n,, = 0.084 + 4.773 nb= 0.364 nb= 1.364 +xdl.284 138.2 - 1) + 9.124 (burned or unburned) Sum7 Mass of air7 t Given by Eq.(4.8). 32 + 28.1w 138.2 t Units: kg/kmol or Ibm/lb.mol. For hydrocarbon fuek $ for air = 3.773; for fuels containing oxygen, +* and $* given by Eq. (4.7~) are substituted for 4 and S,respectively.
: mixture can now be determined. The mass of mixture (burned or unburned) per mole 0,in the mixture, m,,, is given by m, = 32 + 4#1 + 28) + 28.16$ The molecular weight of the unburned mixture, Mu,is The molecular weight of the burned mixture, Mb,is therefore Figure 4-1 gives M, and Mb for a range of 4 and x, for air, isooctane, burned gas mixtures. Frequently, thermodynamic properties of unburned and burned mixtures are expressed per unit mass of air in the original mixture (for burned mixture this is the mixture before combustion). To obtain properties in these units, we need the mass of original air, per mole 0,in the mixture, which is with units of kilograms per kilomole or pound-mass per pound-mole. Table 4.5 summarizes the factors needed to relate properties expressed on a molar and a mass basis. 4 3 GAS PROPERTY RELATIONSHIPS FIGURE 4-1 Equivalence ratio @ Molecular weight of unburned and lowtemperature burned isooctane-air mixtures as a function of fuel/air quivalena ratio and burned gas fraction. - The individual species in the unburned and burned gas mixtures can with SUEcient accuracy be modeled as ideal gases. Ideal gas relationships are reviewed in App. B. The most important relationships for property determination for engine calculations are summarized below. 108 INTERNAL COMBUSTION FNGINE FUNDAMENTALS PROPERTIES OF WORKING FLUIDS Since internal energy and enthalpy are functions of temperature only, the specific heats at constant volume and constant pressure are given by and 109 In these equations, the units of u and h can be on a per unit mass or molar basis [i.e., joules per kilogram (British thermal units per pound-mass) or joules per kilomole (British thermal units per pound-mole)]; similarly, s, c,, c,, R, Y, and @ can be in joules per kilogram-kelvin (British thermal units per poundrnass-degree Rankine) or joules per kilomole-kelvin (British thermal units per pound-mole-degree Rankine). For gas mixtures, once the composition is known, mixture properties are determined either on a mass or molar basis from u=Cxiui h=Cxihi s = C xisi and The entropy s(T, o) or s(T, p) is given by cu = C xi cv.i cp = The integrals in Eqs. (4.14a, b) are functions of temperature only, and are useful in evaluating entropy changes and in following isentropic processes. If we define (4.1Sa) and then Thus, for example, the entropy change between states (TI, p,) and (T2,p,) is s, - s, = cD2 For an isentropic process, - a,- R In (4.17) C xi cP,i 4.4 A SIMPLE ANALYTIC IDEAL GAS MODEL While the first category of model listed in Table 4.2 is too inaccurate for other than illustrative purposes, the second category-constant but different specific heats for the unburned and burned gas mixtures--can with careful choice of specific heat values be made much more precise. The advantages of a simple analytic model may be important for certain problems. Figure 4-2 shows an internal energy versus temperature plot for a stoichiometric mixture. It is a quantitative version of Fig. 3-5.
The unburned mixture line is for a burned gas fraction of 0.1. The fuel is isooctane. Data to construct such graphs can be obtained from charts or tables or computer programs (see Secs. 4.5 to 4.7). The units for u are kilojoules per kilogram of air in the original mixture (the units of the charts in Sec.
4.5). The datum is zero enthalpy for O , , N,, H z , and C (solid) at 298 K. Note that the specific heats of the unburned and burned mixtures (the slopes of the lines in Fig. 4-2) are a function of temperature; at high temperatures, the internal energy of the burned mixture is a function of temperature and pressure. However, the temperature range of interest for the unburned mixture in an SI engine is 400 to 900 K (700 to 16W0R); for the burned gas mixture, the extreme end states are approximately 2800 K, 35 atm (5000•‹R, 500 lb/in2 abs) and 1200 K, 2 atm (2200"R, 30 lb/in2 abs).
Linear approximations to the unburned and burned mixture curves which minimize the error in u over the temperature (and pressure) ranges of interest are shown as dashed lines. The error in T for a given u is less than 50 K.
110 INTERNAL PROPERTIES OF WORKING FLUIDS COMBUSnON ENGINE FUNDAMENTALS 111 For a constant-pressure adiabatic combustion process, hu = h, and it can similarly be shown that To use the model, suitable values of y,, y,, Mu, (MJM,,), and Ah,/Ru must be determined. Values for Mu and Mb can be obtained from Eqs. (4.10) and (4.1 I).? Values of Y,, yb, and Ah#, can be obtained from graphs such as Fig.
4-2 (see Example 4.1 below).
Values for y,, y,, and Ah,/R, are available in the literature (e.g., Refs. 1 and 2) for a range of 4 and x b . However, values used for computations should always be checked over the temperature range of interest, to ensure that the particular linear fit to u(T)used is appropriate. Example 4.1. Determine the values of y,, y,, and Ah,/& which correspond to the straight-line fits for u,(T) and u,(T)in Fig. 4-2. Equations for the straight lines in Fig. 4-2 are u, (kJ/kg air) = 0.96T(K)- 700 I 500 t 1 l low lsoo 1 2000 I 2500 I 3000 Temperature, K FIGURE 4 2 Internal energy versus temperature plot for stoichiometric unburned and burned gas mixtures: isooctane fuel; unburned residual fraction 0.1. ub (kJ/kg air) = 1.5T(K)- 4250 From Table 4.5, for isooctane fuel with 4 = 1.0 and x, moles of unburned mixture per mole 0,in the mixture is and = 0.1, the number of n, = 0.08 x 1 + 4.773 + 0.28 x 0.1 x 1 = 4.881 The mass of air per mole 0,in the mixture is 138.2. Thus, the number of moles of unburned mixture per unit mass of air in the original mixture is The basis for this ideal gas model is The molar specific heat of the unburned mixture i., is therefore where h , , and hIc are the enthalpies 9f formation of unburned and burned gas mixture, respectively, at 0 K. Then, for a constant-volume adiabatic combustion process, Since a = 8.314 kJ/kmol. K , uu = ub or C,,U T, + hfeU= c , s Tb + h1.b If we solve for T, and use the relations (RdRJ = (MJM,)and c,JR = l/(y - 11, we obtain where Ah, = h,, - h,,, . The number of moles of burned mixture per mole 0,is (from Table 4.5) nb = 0.36 x 1 + 4.773 = 5.133 t The error in ignoring the effect of dissociation on M, is small. 112 PROPERTIES OF WORKXNG FLUIDS INTERNAL COMBUSTION ENGINE FUNDAMENTALS The number of moles of burned mixture per unit mass of air in the original mixture is t;i -- - 0.0371 The molar specific heat ,Z is therefore and y, is To find AhJR,, R, is given by R, = 8.314 x 0.0353 = 0.293 k3/kg air K and so 4 5 THERMODYNAMIC CHARTS One method of presenting thermodynamic properties of unburned and burned gas mixtures for internal combustion engine calculations is on charts. Two sets of charts are in common use: those developed by Hottel et aL3 and those developed by Newhall and Starkman.4*' Both these sets of charts use U.S. units. We have developed a new set of charts in SI units, following the approach of Newhall and Starkman. Charts are no longer used extensively for engine cycle calculations; computer models for the thermodynamic properties of working fluids have replaced the charts. Nonetheless, charts are useful for illustrative purposes, and afford an easy and accurate method where a limited number of calculations are required. The charts presented below are for isooctane fuel, and the following equivalence ratios: 4 = 0.4,0.6,0.8, 1.0, 1.2. 113 TABLE 4 6 unburned mixture composition for charts ~qrivrleaee rntio $ (FIA) K h p m s of mixtnre Mdcs of mixture Kilomole of mixture PI,, Rt per kilognm of air per mole of 0 2 per kilogram of air J/kg air.^ 0.4 0.6 08 1.o 1.2 1.0264 1.0396 1.0528 1.0661 1.0792 t For r, 0.0264 0.0396 0.0528 0.0661 0.0792 E 4.805 4.821 4.837 4.853 4.869 + 0.112~. 0.0348 + 0 . 0 0 0 8 1 ~ ~ 289 + 0 . 1 6 8 ~ ~ 0.0349 + 0 . 0 0 1 2 2 ~ ~ 290 + 0 . 2 2 4 ~ ~ 0.030350 + 0 .
0 0 1 6 2 ~ ~ 291 + 0.28Oxb 0.0351 + 0 . 0 0 2 0 3 ~ ~ 292 + 0 . 5 3 6 ~ ~ 0.0352 + 0 . 0 0 3 8 8 ~ ~ 292 0. Error h neglecting X, is usually mall. 2. The fuel is in the vapor phase. 3. The mixture composition is homogeneous and frozen (no reactions between the fuel and air). 4. Each species in the mixture can be modeled as an ideal gas.
5. The burned gas fraction is zero.? It pro

equivalence ratio Molecular weight of equilibrium burned gases & a function bf equivalence ratio at T = 1750, 2250, and 2750 K, and 30 atm. Fuel: isooctane. FIGURE 4-15 Specific heat at constant pressure of equilibrium burned gases as a function of equivalence ratio at T = 1750, 22% and2750K,and30atm.Fuel:isooctane. Units: kJFg mixture-K. 0.2 0.4 0.6 0.8 1.0 Fuellair equivalence ratio 1.2 Ratio of specific heats, y, = c,dcdc,,, for equilibrium burned gases as a function of equivalence ratio at T = 1750, 2250, 1.4 a n d 2 7 5 0 K , a n d 3 0 a t m . F u e l : i s o octane. A computer program for calculating properties of equilibrium combustion products, designed specifically for use in internal combustion engine applications, has been developed by Olikara and Borman and is readily available.18 The fuel composition (C,H,O,N,), fuellair equivalence raho, and product pressure and temperature are specified. The species included in the product mixture are: CO,, H,O, CO, H,,0 2 , N,, Ar, NO, OH, 0 , H, and N. The element balance equations and equilibrium constants for seven nonredundant reactions provide the set of 11 equations required for solution of these species concentrations (see Sec. 3.7). The equilibrium constants are curve fitted from data in the JANAF table^.^ The initial estimate of mole fractions to start the iteration procedure is the nondissociated composition. Once the mixture composition is determined, the thermodynamic properties and their derivatives with respect to temperature, pressure, and equivalence ratio are computed. This limited set of species has been found to be sufficiently accurate for engine burned gas calculations, and is much more rapid than the extensive NASA equilibrium program?.
l o Several techniques for estimating the thermodynamic properties of hightemperature burned gases for engine applications have been developed. One commonly used approach is that developed by Krieger and Borman.lg The internal energy and gas constant of undissociated combustion products were first described by polynomials in gas temperature. The second step was to limit the range of T and p to values found in internal combustion engines. Then the deviations between the equilibrium thermodynamic property data published by Newhall and Starkman4. and the calculated nondissociated values were fitted 500 I I 1000 1500 I I 2000 2500 Temperature, K I 3000 3500 500 I loo0 I 1500 (a) 500 1000 1500 2000 2500 Temperature, K 3000 3MO 500 (b) I I loo0 I500 I I 2000 2500 Temperature, K (4 I I 2000 2500 Temperature, K (b) I 3000 I 3000 3500 3500 FIGURE 4-17 S p d c heat at constant pressure for equilibrium, frozen, and tixed composition burned gases as a function of temperature and pressure: (a) equivalence ratio q5 5 1.0; (b) equivalence ratio 4 > 1. Units :J/kg mixture. K. Fuel: C,H,, . C.H2,. by an exponential function of T, p, and 4. For 4 I 1, a single set of equations resulted. For 4 2 1, sets of equations were developed, each set applying to a specific value of equivalence ratio (see Ref. 19). In general, the fit for internal energy is within 24 percent over the pressure and temperature range of interest and the error over most of the range is less than 1 percent. For many applica- 'ions, the undissociated equations for thermodynamic properties are sufficiently accurate. An alternative approach for property calculations, applicable to a wide range of hydrocarbon and alcohol fuels, is used extensively in the author's laboratoty.'' With this method, the products of combustion of hydrocarbon (or FlGURE 4-18 Ratio of specific heats, yb = c,,Jc,, for equilibrium, frozen, and fmed compaition burned gases as a fmtion of temperature and pressure: (a) equivalena ratio 4 z 1. Fuel: 4 3 TRANSPORT PROPERTIES alcohol)-air mixtures are divided into triatomic, diatomic, and monatomic molecules, M, , M,, and MI, respectively.
Then, if Y is the extra number of moles of diatomic molecules due to dissociation of triatomic molecules and U is the extra number of monatomic molecules due to dissociation of diatomic molecules, the combustion reaction can be written as + + + $N2 ~)4 2Y]M3 + [I- 4 + 3Y- &4C 2(1- &)&Hz O2 [(2- + U + $]MI + 2UM1 for [(2 ne processes by which mass, momentum, and energy are transferred from one point in a system to another are called rate processes. In internal combustion engines,examples of such processes are evaporation of liquid fuel, fuel-air mixin& friction at a gaslsolid interface, and heat transfer between gas and the walls of the combustion chamber. In engines, most of these processes are turbulent and are therefore strongly influenced by the properties of the fluid flow. However, rate processes are usually characterized by correlations between dimensionless numbers (e.g., Reynolds, Prandtl, Nusselt numbers, etc.), which contain the fluid's transport properties of viscosity, thermal conductivity, and diffusion coe&cient as well as the flow properties. The simplest approach for computing the transport properties is based on [he application of kinetic theory to a gas composed of hard-sphere molecules. By analyzing the momentum flux in a plarie Couette flow,? it can be shown (Chapman and Cowling, Ref. 21, p. 218) that the viscosity p of a monatomic hard-sphere gas [where p = r/(du/dx), t being the shear stress and (du/&) the velocity gradient] is given by 4I 1 (4.45) - 4) 4 - 2 U M 3 + [2(4 - 1) + 3Y - U + $]M, + 2UM1 for 4>1 The method is based upon a fitting of data obtained from sets of detailed chemical equilibrium calculations to this functional form. Two general dissociation reactions : 2M3 =3M2 and M, =2M, are then used with fitted equilibrium constants Kl(T) and K,(T) to calculate the relative species concentrations. This approach has been developed to -give equations for enthalpy which sum the translational, rotational, and vibrational contributions to the specific heat, and the enthalpy of formation: T, R + ~ R h,P *ph = - (8N3 + 7N2 SN1)T R(3N3 2) exp (T J ~1 2 (4.46) + + + where N,, N,, and N, are the number of moles of triatomic, diatomic, and monatomic molecules respectively per mole 0, reactant, T, is a fitted vibrational temperature, mRpis the mass of products per mole 0,reactant [Eq. (4.911, and fi, is the average specific enthalpy of formation of the products. The molecular weight is given by M, = M* = or ~ R P 1+(1-&)4+*+Y+U ~ R P (2-&)4+*+ Y + U for 4I 1 (4.47) for 4 > 1 U and Y are found using an approximate solution to the equations obtained by applying the fitted equilibrium constants to the dissociation reactions; h, is obtained by fitting a correction to the undisssociated products enthalpy of formation. Equations are presented for the partial derivatives of enthalpy h and density p with respect to T; p, and 4.'' These relationships have been tested for fuels with H/C ratios of 4 to 0.707, equivalence ratios 0.4 to 1.4, pressures 1 to 30 a m and temperatures 1000 to 3000 K. The error for burned mixture temperatures relevant to engine calculations is always less than f 10 K. The errors in density are less than 0.2 percent. + 1 3 where m is the mass of the gas molecule, d is the molecular diameter, and is Boltmann's constant, 1.381 x lo-', J/K. For such a gas, the viscosity varies as T1I2, but will not vary with gas pressure or density. Measurements of viscosity show it does only vary with temperature, but generally not proportionally to T1l2. The measured temperature dependence can only be explained with more sophisticated models for the intermolecular potential energy than that of a hard sphere. Effectively, at higher temperatures, the higher average kinetic energy of a pair of colliding molecules requires that they approach closer to each other and experience a greater repulsive force to be deflected in the collision. As a result, the molecules appear to be smaller spheres as the temperature increases. An expression for the thermal conductivity k of a monatomic hard-sphere gas Ck = U(dT/dx), where q is the heat flux per unit area and dT/dx is the temperature gradient] can be derived from an analysis of the thermal equivalent of plane Couette flow (Ref. 21, p.
235): ' IQ Couette flow, the fluid is contained between two infinite plane parallel surfaces, one at rest and moving with constant velocity.
In the absence of pressure gradients, the fluid velocity varies hearly across the distance between the surfaces. Om PROPERTIES OF WORKING FLUIDS which has the same temperature dependence as p. Equations (4.48) and (4.49) can be combined to give 143 "vjty, and ~randtlnumber in addition to the thermodynamic calculations described in Secs. 3.7 and 4.7 for high-temperature equilibrium and frozen gas mixtures. The procedures used in the NASA program to compute these transport properties are based on the techniques described in Hirschfelder ,t d.Z2The NASA program has been used to compute the transport properties of hydro~arbon-aircombustion products.17 These quantities are functions of temperature T, equivalence ratio 4, and (except for viscosity) pressure p. Approximate correlations were then fitted to the calculated data of viscosity and Prandtl number. The principal advantage of these correlations is computational speed. For Prandtl number WJk), it was found convenient to use y, the specific heat ratio (cJc,,), as an independent variable. Values of y and c, then permit determination of the thermal conductivity. The viscosity of hydrocarbon-air combustion products over the temperature range 500 up to 4000 K, for pressures from 1 up to 100 atm, for 4 = o up to 4 = 4 is shown in Fig. 4-19. The viscosity as a function of temperature of hydrocarbon-air combustion products differs little from that of air. Therefore, a power law based on air viscosity data was used to fit the data: k = %.% since, for a monatomic gas, the specific heat at constant volume is 3k/(2m). This simple equality is in good agreement with measurements of p and k for mon. atomic gases. The above model does not take into account the vibrational and rotational energy exchange in collisions between polyatomic molecules which contribute to energy transport in gases of interest in engines. Experimental measurements of k and p show that k is less than jpc, for such polyatomic gases, where c, is the sum of the translational specific heat and the specific heat due to internal degrees of freedom. It was suggested by Eucken that transport of vibrational and rotational energy was slower than that of translational energy. He proposed an empirical expression where T is in kelvins. The viscosity of combustion products is almost indepenwhere Pr is the Prandtl number, which is in good agreement with experimental data. A similar analysis of a binary diffusion process, where one gas diffuses through another, leads to an expression for the binary diffusion coefficient D,,. Dij is a transport property of the gas mixture composed of species i and j, delined by Fick's law of molecular diffusion which relates the fluxes of species i and j, T, and Txj, in the x direction to the concentration gradients, dnJdx and dnjdx (n is the molecular number density): 1.5 X I I 4 0.0 1.0 NASA 0 0 I Eq(4.53) - ----- I I I II C The binary diffusion coefticient for a mixture of hard-sphere molecules is (Ref. 21, p. 545) where mij is the reduced mass mi mi/(mi + mj). A more rigorous treatment of gas transport properties, based on more redistic intermolecular potential energy models, can be found in Hirschfelder et d.?' who also present methods for computing the transport properties of mixtures of gases. The NASA computer program "Thermodynamic and Transport Properties of Complex Chemical system^"'^ computes the viscosity, thermal conduc- k f V'lscosit~,kg/m-s, of combustion products as a fundion of temperature and equivalence ratio.
Equalions shown are (4.52) and (4.53). 144 INTERNAL COMBUSTION ENGINE FUNDAMENTALS dent of pressure. This correlation was corrected to include the effect of the equivalence ratio 4 on the viscosity of hydrocarbon-air combustion prodpcts: =1 Ppd I - 1) - 6.7(y - 1)' cosity of a multicomponent gas mixture is where 5i and M iare the mole fraction and molecular weight of the ith species, pi is the viscosity of the ith species, v is the number of species in the mixture, and Di, is the binary diffusioncoefficient for species i and j.12 4.9 EXHAUST GAS COMPOSITION 451 The values of Pr predicted with Eq. (4.54) are within 5 percent of the equilibrium Pr values calculated with the NASA program. For rich mixtures the following equation is a good fit to the equilibrium values of Pr using equilibrium values of y, for temperatures greater than 2000 K: -: $ % ; The predicted values of Pr in this case are also close to the calculated values of Pr, with less than 10 percent error. Equation (4.55) is also a reasonable fit to the frozen values* of Pr for rich mixtures, using frozen values of y, for the temperature range 1200 to 2000 K. As there are no data for Pr of rich mixtures at low temperatures, we suggest that where a fixed composition for the mixture is appropriate (e.g., during the exhaust process in an internal combustion engine), Eq. (4.55) can also be used with fixed Composition values of y. The Prandtl number can be obtained from the above relations if y is known. The thermal conductivity can be obtained from the Prandtl number if values of p and c, are known. Values of y, and c,,~ as functions of temperature, pressure, and equivalence ratio are given in Figs. 4-15 to 4-18. Since the fundamental relations for viscosity and thermal conductivity are complicated, various approximate methods have been proposed for evaluating these transport properties for gas mixtures. A good approximation for the vis- t In the NASA program, "frozen"means the gas composition is in equilibrium at the given T and PI While the formulas for the products of combustion used in Sec. 3.4 are useful for determining unburned mixture stoichiometry, they do not correspond closely to the actual burned gas composition. At high temperatures (e.g., during combustion and the early part of the expansion stroke) the burned gas composition corresponds closely to the equilibrium composition at the local temperature, pressure, and equivalence ratio. During the expansion process, recombination reactions simplify the burned gas composition. However, late in the expansion stroke and during exhaust blowdown, the recombination reactions are unable to maintain the gases in chemical equilibrium and, in the exhaust process, the composition becomes frozen. In addition, not all the fuel which enters the engine is fully burned inside the cylinder; the combustion inefficiency even when excess air is present is a few percent (see Fig. 3-9). Also, the contents of each cylinder are not necessarily uniform in composition, and the amounts of fuel and air fed to each cylinder of a multicylinder engine are not exactly the same. For all these reasons, the composition of the engine exhaust gases cannot easily be calculated. It is now routine to measure the composition of engine exhaust gases. This is done to determine engine emissions (e.g., CO, NO,, unburned hydrocarbons, and particulates). It is also done to determine the relative proportions of fuel and air which enter the engine so that its operating equivalence ratio can be computed. In this section, typical engine exhaust gas composition will be reviewed, and techniques for calculating the equivalence ratio from exhaust gas composition will be given. 4.9.1 Species Concentration Data f but is frozen as c,, c,, and k arc computed. 145 Pair + 0.0274 Figure 4-19 shows that the viscosity predicted using Eqs. (4.52) and (4.53) is very close to the viscosity values calculated with the NASA program. There is less than 4 percent error. The Prandtl number of hydrocarbon-air combustion products has also been correlated over the above ranges of temperatures, pressures, and equivalence ratios. Since the expression for Prandtl number of a monatomic hardsphere molecule gas is a function of y, a second-order polynomial of y was used to curve-fit the calculated Prandtl number data. A good fit to the data for lean combustion product mixtures was the following: Pr = 0.05 + 4.2(y PROPERTtES OF WORKING FLUIDS 3 Standard instrumentation for measuring the concentrations of the major exhaust gas species has been de~eloped.'~ Normally a small fraction of the engine exhaust gas stream is drawn off into a sample line. Part of this sample is fed directly to the instrument used for unburned hydrocarbon analysis, a flame ionization detecfor (FID). The hydrocarbons present in the exhaust gas sample are burned in a Small hydrogen-air flame, producing ions in an amount proportional to the number of carbon atoms burned. The FID is effectively a carbon atom counter. It calibrated with sample gases containing known amounts of hydrocarbons. Unburned hydrocarbon concentrations are normally expressed as a mole fraction 146 MTERNAL COMBUSnON ENGME FUNDAMENTALS or volume fraction in parts per million @pm) as C,. Sometimes results are expressed as ppm propane (C3H,) or ppm hexane (C,H,,); to convert these to ppm C, multiply by 3 or 6, respectively. Older measurements of unburned hydrocarbons were often made with a nondispersive infrared (NDIR) analyzer, where the infrared absorption by the hydrocarbons in a sample cell was used to determine their ~oncentration.'~ Values of HC concehtrations in engine exhaust gases measured by an FID are about two times the equivalent values measured by an NDIR analyzer (on the same carbon number basis, e.g., C,). NDIR-obtained concentrations are usually multiplied by 2 to obtain an estimate of actual HC concentrations. Substantial concentrations of oxygen in the exhaust gas affect the FID measurements. Analysis of unburned fuel-air mixtures should be done with special care." To prevent condensation of hydrocarbons in the sample line (especially important in diesel exhaust gas), the sample line is often heated. NDIR analyzers are used for CO, and CO concentration measurements. Infrared absorption in a sample cell containing exhaust gas is compared to absorption in a reference cell. The detector contains the gas being measured in two compartments separa~edby a diaphragm. Radiation not absorbed in the sample cell is absorbed by the gas in the detector on one side of the diaphragm. Radiation not absorbed in the reference cell is absorbed by the gas in the other half of the detector. Different amounts of absorption in the two halves of the detector result in a pressure difference being built up which is measured in terms of diaphragm distention. NDIR detectors are calibrated with sample gases of known composition. Since water vapor IR absorption overlaps CO, and CO absorption bands, the exhaust gas sample is dried with an ice bath and chemical dryer before it enters the NDIR instrument. Oxygen concentrations are usually measured with paramagnetic analyzers. Oxides of nitrogen, either the amount of nitric oxide (NO) or total oxides of nitrogen (NO + NO,, NOJ, are measured with a chemiluminescent analyzer.
The NO in the exhaust gas sample stream is reacted with ozone in a flow reactor. The reaction produces electronically excited NO, molecules which emit radiation as they decay to the ground state. The amount of radiation is measured with a photomultiplier and is proportional to the amount of NO. The instrument can also convert any NO, in the sample stream to NO by decomposition in a heated stainless steel tube so that the total NO, (NO + NO,) concentration can be determined.23 Gas chromatography can be used to determine all the inorganic species (N, , CO,, 0 , , CO, Hz) or can be used to measure the individual hydrocarbon compounds in the total unburned hydrocarbon mixture. Particulate emission are measured by filtering the particles from the exhaust gas stream onto a previously weighed filter, drying the filter plus particulate, and reweighing. SPARK-IGNITION ENGINE DATA. Dry exhaust gas composition data, as a function of the fuel/air equivalence ratio, for several different multi- and singlecylinder automotive spark-ignition engines over a range of engine speeds and loads are shown in Fig. 4-20. The fuel compositions (gasolines and isooctane) had H/C ratios ranging from 2.0 to 2.25. Exhaust gas composition is subs tan ti all^ PROPERTIES OF WORKING FLUIDS 147 Exhaust equivalence ratio FIGURE 4-20 Spark-ignition engine exhaust gas composition data in mole fractions as a function of fuelfair equivalence ratio. Fuels: gasoline and isooctane, H/C 2 to 2.25. (From D'Alleva and L o ~ e l l ?StiCendm?' ~ Harrington and Shish~,'~S~indt,~' and data from the author's laboratory at MIT,) different on the lean and the rich side of the stoichiometric airlfuel or fuellair ratios; thus, the fuellair equivalence ratio 4 (or its inverse, the relative airjfuel ratio 1)is the appropriate correlating parameter. On the lean side of stoichiornetric, as 4 decreases, CO, concentrations fall, oxygen concentrations increase, and CO levels are low but not zero (-0.2 percent). On the rich side of stoichiometric, CO and H, concentrations rise steadily as 4 increases and CO, concentrations fall. 0, levels are low (-0.2 to 0.3 percent) but are not zero. At stoichiometric operation, there is typically half a percent 0, and three-quarters of a percent CO. Fuel composition has only a modest effect on the magnitude of the species concentrations shown. Measurements with a wide range of liquid fuels show that CO concentrations depend only on the equivalence ratio or relative fuellair ratio (see Fig. 11-20).26 A comparison of exhaust CO concentrations with gasoline, Propane (C3H8),and natural gas (predominantly methane, CH,) show that only with the high H/C ratio of methane, and then only for CO 2 4 percent, is fuel composition significant." The values of CO, concentration at a given 4 are slightly affected by the fuel H/C ratio.
For example, for stoichiometric mixtures with 0.5 percent 0, and 0.75 percent CO, as the H/C ratio decreases CO, concentrations increase from 13.7 percent for isooctane (H/C = 2.25).
t o 14.2 to 14.5 percent for typical gasolines (H/C in range 2-1.8), to 16 for toluene (H/C= 1.14).29 Exhaust equivalence ratio Carbon monoxide, % by MI. FIGURE 4-21 Hydrogen conantration in spark-ignition engine exhaust as a function of carbon monoxide conantration. Units: percent by v o l u n ~ .
~ ~ * f Unburned hydrocarbon exhaust concentrations vary substantially with engine design and operating conditions. Spark-ignition engine exhaust levels in a modern low-emission engine are typically of the order of 2000 ppm C, with liquid hydrocarbon fuels, and about half that level with natural gas .and propane fuels. Hydrogen concentrations in engine exhaust are not routinely measured. However, when the mixture is oxygen-deficient-fuel rich-hydrogen is present with CO as an incomplete combustion product. Figure 4-21 summarizes much of the available data on H, concentrations plotted as a function of C0.30 DIESEL EXHAUST DATA. Since diesels normally operate significantly lean of stoichiometric (4 5; 0.8) and the diesel combustion process is essentially complete (combustion inefficiency is 1 2 percent), their exhaust gas composition is straightforward. Figure 4-22 shows that 0, and CO, concentrations vary linearly with the fuellair equivalence ratio over the normal operating range. Diesel emissions of CO and unburned HC are low. the composition of fuel can be represented as C,H,O,.
For conventional petroleum-based fuels, oxygen will be absent; for fuels containing alcohols, oxygen will be present.
The overall combustion reaction can be written as Fuel + oxidizer -,products The fuel is C,H,O,; the oxidizer is air (0, + 3.773N2). The products are CO,, H,O, CO, Hz, O,, NO,, N,, unburned hydrocarbons (unburned fuel and products of partial fuel reaction), and soot particles (which are mainly solid carbon). The amount of solid carbon present is usually sufficiently small (s0.5 percent of the fuel mass) for it to be omitted from the analysis. The overall combustion reaction can be written explicitly as , + -I-%NO~NO, + ji.H20H,0 5&2) (4.57) where 4 is the measured equivalence ratio [(F/A)ac,uaJ(F/A)swch*.nn J,nor is the number of 0, molecules required for complete combustion (n m/4 - r/2), n, is the total number of moles of exhaust products, and 2, is the mole fraction of the ith component. There are several methods for using Eq. (4.57) to determine 4, the equivalence ratio, depending on the amount of information available. Normally CO,, % O,, NO, concentrationr as mole fractions and unburned hydrocarbon (as + 49.2 Equivalence Ratio Determination from Exhaust Gas Constituents & Exhaust gas composition depends on the relative proportions of fuel and air fed to the engine, fuel composition, and completeness of combustion. These relationships can be used to determine the operating fuelfair equivalence ratio of an engine from a knowledge of its exhaust gas composition. A general formula for FIGURE 4-22 Exhaust gas composition from several diesel engines in mole fractions on a dry basis as a function of fuel/air equivalence ratio.31 $ $ $ PROPERTIES OF WORKING FLUIDS mole fraction or ppm C,, i.e., ZJ, are measured. The concentration of the inorganic gases are usually measured dry (i.e., with H,O removed) or partially dry. Unburned hydrocarbons may be measured wet or dry or partially dry. NO, is mainly nitric oxide (NO); its concentration is usually sufficiently low (pe: The net and gross indicated mean effective pressures are related by 'I Definition of system boundary for thermodynamic analysis of ideal cycle processes. the open system in Fig. 5-4. Application of the first law between points 6 and 1 gives + U 1 - U 6 = -pi(Vl - V6) (ml - m6)hi (5.19~) The net indicated fuel conversion efficie;cy is related to the gross indicated fuel conversion efficiencyby 5.4 CYCLE ANALYSIS WITH IDEAL GAS WORKING FLUID WITH c, AND c, CONSTANT If the working fluid in these ideal cycles is assumed to be an ideal gas, with cu and c, constant throughout the engine operating cycle, the equations developed in the where hi is the specific enthalpy of the inlet mixture and p, = pi. Note that when pi < pe, part of the residual gas in the cylinder at the end of the exhaust stroke will flow into the intake system when the intake valve opens. This flow will cease when the cylinder pressure equals pi.
However, provided no heat transfer occurs, this backflow will not affect Eqs. (5.19) above, since the flow of residual through the intake valve is a constant enthalpy process. In many engines, the closing of the exhaust valve and the opening of the intake valve overlap. Flow of exhausted gases from the exhaust system through the cylinder into the intake system can then occur. Equations (5.18) and (5.19) would have to be modified to account for valve overlap.
In the four-stroke engine cycle, work is done on the piston during the intake and the exhaust processes.
The work done by the cylinder gases on the piston during exhaust is The work done by the cylinder gases on the piston during intake is W = PXVI - V2) previous section which describe engine performance and efficiency can be further simplified. We will use the notation of Fig. 5-2.
5.4.1 Constant-Volume Cycle The compression work (Eq. 5.6) becomes Wc= mc,,(Tl - T2) The expansion work (Eq. 5.9) becomes WE= mc,,(T3 - T,) The denominator in Eq. (5.14), m, QLHv,can be related to the temperature rise during combustion. For the working fluid model under consideration, the U(T)lines for the reactants and products on a U - T diagram such as Fig. 3-5 are parallel and have equal slopes, of magnitude c,. Hence, for a constant-volume adiabatic combustion process (5.21) The net work to the piston over the exhaust and intake strokes, the pumping work, is (5.22) Wp = (Pi - P~XVI - V2) which, for the cylinder gas system, is negative for pi < pe and positive for pi > PI- t Note that if insutficient air is available for complete combustion of the fuel, Eq. (5.28) must be modified. The right-hand side of the equation should then be E m,QLHv. where E is the combustion dtiency given by Eq. (3.27). Note that the heating values at constant volume and constant pressure are the same for this working fluid. For convenience we will define Q* is the specific internal energy (and enthalpy) decrease, during isothermal com. bustion, per unit mass of working fluid. The relation for indicated fuel conversion efficiency (Eq. 5.14) becomes The indicated mean effectivepressure, using Eqs. (5.2) and (5.31), becomes The dimensionless numbers r,, y, and Q*/(c,T,) are sufficient to describe [he characteristics of the constant-volume ideal gas standard cycle, relative to its initial conditions pl, Tl. 1t is useful to compare the imep-a measure of the effectiveness with which [he displaced volume of the engine is used to produce work-and the maximum pressure in the cycle, p3. The ratio p31pl can be determined from the ideal gas applied at points 2 and 3, and the relation Since 1-2 and 3-4 are isentropic processes between the same volumes, Vl and V2, obtained from Eq. (5.28). Equations (5.32) and (5.33) then give where y = cJc, . Hence: and Eq. (5.30) can be rearranged as Values of q,,, for different values of y are shown in Fig. 5-5. The indicated fuel conversion efficiency increases with increasing compression ratio and decreases as y decreases. A high value of imeplp, is desirable.
Engine weight will increase with increasing p, to withstand the increasing stresses in components. The indicated fuel conversion efficiency and the ratios imeplp, and imep/p3 for this ideal cycle model do not depend on whether the cycle is throttled or supercharged. However, the relationships between the working fluid properties at points 1 and 6 do depend on the degree of throttling or supercharging. For throttled engine operation, the residual gas mass fraction x, can be determined as follows. From Eq. (5.17), since state 5 corresponds to an isentropic expansion from state 4 to p = p,, x, is given by it follows that FIGURE 5-5 Ideal gas constant-volume cycle fuel conversion dficiency as a function of cornpression ratio; y = E#,. The residual mass fraction increases as pi decreases below pe, decreases as r, increases, and decreases as Q*/(c, T,)increases. Through a similar analysis, the temperature of the residual gas T, can be determined: The mixture temperature at point 1 in the cycle can be related to the inlet mixture temperature, T , with Eq. (5.19). For a working fluid with c , and c, con. stant, this equation becomes The mean effective pressure is related to p, and p3 via Use of Eqs. (5.36) and (5.37)leads to the relation 5.43 Cycle Comparison Extensive results for the constant-voluine cycle with y = 1.4 can be found in Taylor.' 5.4.2 Limited- and ConstantPressure Cycles The constant-pressure cycle is a limited-pressure cycle with p3 = p2. For the limited-pressure cycle, the compression work remains The expansion work, from Eq. (5.13), becomes w~= mCcdGb - T4) + ~ 3 (u 3 b- u3a)I The above expressions are most useful if values for y and Q*/(cuT I)are chosen to match real working fluid properties. Figure 5-5 has already shown the sensitivity of llj for the constant-volume cycle t o the value of y chosen. In Sec. 4.4, average values of y, and yb were determined which match real working fluid properties over the compression and expansion strokes, respectively. Values for a stoichiometric mixture appropriate to an SI engine are y, x 1.3, yb z 1.2. However, analysis of pressure-volume data for real engine cycles indicates that pVn, where n 1.3, is a good fit to the expansion stroke p-V data.' Heat transfer from the burned gases increases the exponent above the value corresponding to yb. A value of y = 1.3 for the entire cycle is thus a reasonable compromise. Q*, defined by Eq. (5.29), is the enthalpy decrease during isothermal combustion per unit mass of working fluid. Hence For the combustion process, Eqs.
(5.7g, h) give for a working fluid with c, and c, constant throughout the cycle. Combining Eqs. (5.1),(5.3),and (5.39)to (5.41)and simplifying gives ._ ttjJ = 1 - T-4 - Tl - T2) + d T 3 b (T3~ - T3a) Use of the isentropic relationships for the working fluid along 1-2 and 3b-4, with the substitutions leads to the result For p = 1 this result becomes the constant-volume cycle eficiency (Eq. 5.31). For a = 1, this result gives the constant-pressure cycle efficiency as a special case. A simple approximation for (mdm) is (r, - l)/r,; i.e., fresh air fills the displaced volume and the residual gas fills the clearance volume at the same density. Then, for isooctane fuel, for a stoichiometric mixture, Q* is given by 2.92 x lo6 (rc - l)/rc J/kg air. For y = 1.3 and an average molecular weight M = 29.3, c, = 946 J/kg - K.
For Tl = 333 K , Q*/(c, T I)becomes 9.3 (r, - l)/r,. For this value of Q+/(c, Ti) all cycles would be burning a stoichiometric mixture with an appropriate residual gas fraction. Pressure-volume diagrams for the three ideal cycles for the same compression ratio and unburned mixture composition are shown in Fig. 5-6. For each cycle, y = 1.3, r, = 12, Q*/(c, T I)= 9.3(rc - l)/r, = 8.525. Overall performance characteristics for each of these cycles are summarized in Table 5.2. The constantvolume cycle has the highest efficiency, the constant-pressure cycle the lowest cficiency. This can be seen from Eq. (5.43) where the term in square brackets is equal to unity for the constant-volume cycle and greater than unity for the limited- and constant-pressure cycles. The imep values are proportional t o tl/,i since the mass of fuel burned per cycle is the same in all three cases. As the peak pressure p3 is decreased, the ratio of imep to p3 increases. This ratio is important because imep is a measure of the useful pressure on the piston, and the maximum pressure chiefly affects the strength required of the engine structure. Constant volume \ --- Constant volume Limited pnssure ? -- ----- constant pressure Limited pressure Fuel conversion etliciency as a function of compression ratio, for constant-volume,constant-pressure, limited-pressure ideal gas cycles. y = 1.3, Q*/(c, TI) = 9.3(r, - l)/r,. For limited-pressure cycle. and pJp, = 33.67.100.
FIGURE S6 Pressure-volume diagrams for constant-volume, limited-pressure, and constant-pressure ideal gac standard cycles.
re = 12, y = 1.3, Q*/(c,Tl) = 9 . y ~ ~l)/r, = 8.525, pJp, = 67. TABLE 52 Comparison of ideal cycle results Vf.i Constant volume Limited pressure Constant pressure 0.525 0.500 0.380 y = 1.3; r, = 12; Q*/(c, T,) = 8.525. Pimep imep m P1 P3 16.3 15.5 11.8 0.128 0.231 0.466 u A more extensive comparison of the three cycles is given in Figs. 5-7 and 5-8, over a range of compression ratios. For all cases y = 1.3 and Q*/(c, TI) = 9.3(rC- l)/r,. At any given r,, the constant-volume cycle has the highest emciency and lowest imeplp,. For a given maximum pressure p,, the constantpressure cycle has the highest efficiency (and the highest compression ratio). For the limited-pressure cycle, at constant p3/pl, there is little improvement in efficiency and imep above a compression ratio of about 8 to 10 as r, is increased.
Example 5.1 shows how ideal cycle equations relate residual and intake conditions with the gas state at point 1 in the cycle. An iterative procedure is required if intake conditions are specified. P1 128 67 25.3 Example 5.1. For y =. 1.3, compression ratio r, = 6, and a stoichiometric mixture with intake temperature 300 K. find the residual gas fraction, residual gas temperature, and mixture temperature at point 1 in the constant-volume cycle for pJpi = 1 (unthrottled operation)and 2 (throttled operation). -= 300 1-x, 1 - ClM1.3 x 6)]@Jp, + 0.3) (4 A trial-and-error solution of Eqs. (a) to (4 is required. It is easiest to estimate x,, solve for Tlfrom (4, evaluate Q*/(c, Tl)from (a), and check the value of x, assumed with that given by (b). For @JpJ = 1(unthrottled operation) the following solution is obtained: For (pJpi) = 2 the following solution is obtained: 5.5 FUELAIR CYCLE ANALYSIS FIGURE 5-8 Indicated mean effective pressure (imep) divided by maximum cycle pressure (p,) a s function of wm~ressionratio for constant-volume, constant-pressure, and limited-pressure cycles. Details same For a stoichiometric mixture, for isooctane, 44.38 (1 - x.1- 2.7W - xd Q* = Q w = = eg)~~~~ For y = 1.3, c, = 946 J/kgSK and Q* 2.75 x lo6 (1 c, TI 94611 -= Equations (5.35). (5.36), and (5.381 for r, = 2 [l = 6 and y = 1.3,become + Q*/(c, TIx 6•‹.3)]0.769 2 t)"'I3(' = TI 1-2 Reversible adiabatic compression of a mixture of air, fuel vapor, and residual gas without change in chemical composition. 2-3 Complete combustion (at constant volume or limited pressure or constant pressure), without heat loss, to burned gases in chemical equilibrium. 3-4 Reversible adiabatic expansion of the burned gases which remain in chemical equilibrium. 4-5-6 Ideal adiabatic exhaust blowdown and displacement processes with the burned gases fixed in chemical composition. 6-7-1 Ideal intake process with adiabatic mixing between residual gas and fresh mixture, both of which are fixed in chemical composition. (.Pd~d~.~~~ I Xr - x,) = 2910 -(1 - x,) A more accurate representation of the properties of the working fluid inside the engine cylinder is to treat the unburned mixture as frozen in composition and the burned gas mixture as in equilibrium. Values for thermodynamic properties for these working fluid models can be obtained with the charts for unburned and burned gas mixtures described in Sec. 4.5, or the computer codes summarized in Sec. 4.7. When these working fluid models are combined with the ideal engine process models in Table 5.1, the resulting cycles are called fuel-air cycles.' The sequence of processes and assumptions are (with the notation of Fig. 5-2): + r9 T,Q* 60.3 The basic equations for each of these processes have already been presented in Sec.
5.3. The use of the charts for a complete engine cycle calculation will now be Ilustrated.
55.1 SI Engine Cycle Simulation The mixture conditions at point 1 must be known or must be estimated. The following approximate relationships can be used for this purpose:3 can be checked against the calculated values and an additional cycle computation carried out with the new calculated values if required. The convergence is rapid.
The indicated fuel conversion efficiencyis obtained from Eq. (5.1). The indicated mean effective pressure is obtained from Eq. (5.2). The volumetric efficiency (see Sec. 2.10) for a four-stroke cycle engine is given by where T, = 1400 K and (y - l)/y = 0.24 are appropriate average values to use for initial estimates. Given the equivalence ratio 4 and initial conditions T' (K), p, = pi (Pa), and vl (m3/kg air), the state at point 2 at the end of compression through a volume ratio vl/v2 = r, is obtained from Eq. (4.25~)and the isentropic compression chart (Fig. 4-4).
The compression work Wc (J/kg air) is found from Eq. (5.6) with the internal energy change determined from the unburned mixture chart (Fig. 4-3). The use of charts to relate the state of the burned mixture to the state of the unburned mixture prior to combustion, for adiabatic constant-volume and constant-pressure combustion, has already been illustrated in Sec. 4.5.3. For the constant-volume cycle, where pa,i is the inlet air density (in kilograms per cubic meter) and u, is the chart mixture specific volume (in cubic meters per kilogram of air in the original mixture). + u3 = ua2 Au;,, J/kg air (5.49) where us, is the sensible internal energy of the unburned mixture at T, from Fig. 4-3 and Au;, is the internal energy of formation of the unburned mixture [given by Eq. (4.3211. Since 0, = v,, the burned gas state at point 3 can be located on the appropriate burned gas chart (Figs. 4-5 to 4-9). For the constant-pressure cycle, h, = hrs + Ah;,, J/kg air (5.50) Since p, = p,, the burned gas state at point 3 can be located (by iteration) on the high-temperature burned gas charts, as illustrated by Example 4.5. For the limited-pressure cycle, application of the first law to the mixture between states 2 and 3b gives J/kg air (5.51) h3b = uja + p3 vjb = u2 + p3 02 = uS2 A u ; ~+ p3 v2 + Since p, for a limited-pressure cycle is given, point 3b can be located on the appropriate burned gas chart. The expansion process 3-4 follows an isentropic line from v, to v4 (v4 = ol) on the burned mixture charts. Equation (5.9) [or (5.11) or (5.13)] now gives the The state of the residual gas at points 5 and 6 in the cycle is expansion work WE. obtained by continuing this isentropic expansion from state 4 to p = p,.
The residual gas temperature can be read from the equilibrium burned gas chart; the residual gas fraction is obtained from Eq. (5.17). If values of T, and x, were assumed at the start of the cycle calculation to determine TI, the assumed values Example 5.2. Calculate the performance characteristics of the constant-volume fuelair cycle defined by the initial conditions of Examples 4.2,4.3, and 4.5. The compression ratio is 8; the fuel is isooctane and the mixture is stoichiometric; the pressure and temperature inside the cylinder at the start of compression are 1 atm and 350 K, respectively. Use the notation of Fig. 5-21 to define the states at the beginning and end of each process. Example 4.2 analyzed the compression process: Tl = 350 K, pl = 101.3 kPa, v , = 1 m3/kgair, T, = 682 K , p, = 1.57 MPa, v, = 0.125 m3/kg air, usl = 40 kJ/kg air us, = 350 kl/kg air W,-, = W, = -310 kJ/kg air Example 4.5 analyzed the constant-volume adiabatic combustion process (it was assumed that the residual gas fraction was 0.08): ub3= UU2 = us,, + Au;,, = -5 v3 = v , = 0.125 m3/kgair, kJ/kg air, s3 = 9.33 kJ/kg air. K T3 = 2825 K, p3 = 7100 kPa Example 4.3 analyzed the expansion process, from these conditions after combustion at TC, to the volume v

compression starts later, close to the time that the i& valve closes some 40 to 60" after BC. This matching process is approximate. cycle will be lower. During expansion, heat transfer will cause the gas pressure in the real cycle to fall below an isentropic expansion line as the volume increases. A decrease in efficiency results from this heat loss. t Finite combustion time. In an SI engine with spark-timing adjusted for optimum efficiency,combustion typically starts 10 to 40 crank angle degrees before TC, is half complete at about 10" after TC, and is essentially complete 30 to 40" after TC. Peak pressure occurs at about 15" after TC (see Fig. 1-8).
In a diesel engine, the burning process starts shortly before TC. The pressure rises rapidly to a peak some 5 to 10" after TC since the initial rate of burning is fast. However, the final stages of burning are much slower, and combustion continues until 40 to 50" after TC (see Fig.
1-15). Thus, the peak pressure in the engine is substantially below the fuel-air cycle peak pressure value, because combustion continues until well after TC, when the cylinder volume is much greater than the clearance volume. After peak pressure, expansion stroke pressures in the engine are higher than fuel-air cycle values in the absence of other loss mechanisms, because less work has been extracted from the cylinder gases.
A comparison of the constant-volume and limited-pressure cycles in Fig. 5-6 demonstrates this point. For spark or fuel-injection timing which is retarded from the optimum for maximum efficiency, the peak pressure in the real cycle will be lower, and expansion stroke pressures after the peak pressure will be higher than in the optimum timing cycle.
3. Exhaust blowdown loss. In the real engine operating cycle, the exhaust valve is opened some 60" before BC to reduce the pressure during the first part of the exhaust stroke in four-stroke engines and to allow time for scavenging in twostroke engines. The gas pressure at the end of the expansion stroke is therefore reduced below the isentropic line. A decrease in expansion-stroke work transfer results. 4. Crevice efects and leakage. As the cylinder pressure increases, gas flows into crevices such as the regions between the piston, piston rings, and cylinder wall. These crevice regions can comprise a few percent of the clearance volume. This flow reduces the mass in the volume above the piston crown, and this flow is cooled by heat transfer to the crevice walls. In premixed charge engines, some of this gas is unburned and some of it will not burn. Though much of this gas returns to the cylinder later in the expansion, a fraction, from behind and between the piston rings, flows into the crankcase. However, leakage in a well-designed and maintained engine is small (usually less than one percent of the charge). All these effects reduce the cylinder pressure during the latter stages of compression, during combustion, and during expansion below the value that would result if crevice and leakage effects were absent.
5.
Incomplete combustion. Combustion of the cylinder charge is incomplete; the exhaust gases contain combustible species. For example, in spark-ignition engines the hydrocarbon emissions from a warmed-up engine (which come largely from the crevice regions) are 2 to 3 percent of the fuel mass under normal operating conditions; carbon monoxide and hydrogen in the exhaust contain an additional 1 to 2 percent or more of the fuel energy, even with excess air present (see Sec. 4.9). Hence, the chemical energy of the fuel which is released in the actual engine is about 5 percent less than the chemical energy of the fuel inducted (the combustion efficiency, see Sec. 3.5.5, is about 95 percent). The fuel-air cycle pressures after combustion d l be higher because complete combustion is assumed. In diesel engines, the combustion inefficiency is usually less, about 1to 2 percent, so this effect is smaller. SUMMARY.
The effect of all these loss mechanisms on engine efficiency is best defined by an availability balance for the real engine cycle. A limited number of such calculations have been published (e.g., Refs. 8, 10, and 11). Table 5.4 shows the magnitude of the loss in availability (as a fraction of the initial availability) that occurs due to real cycle effects in a typical naturally aspirated diesel engine.1•‹ The combustion and exhaust losses are present in the ideal cycle models also (they are smaller, howeverg). The loss in availability due to heat losses, flow or aerodynamic losses, and mechanical friction are real engine effects. Figure 5-19 shows standard and fuel-air cycle efficiencies as a function of the compression ratio compared with engine indicated efficiency data. The top three sets of engine data are for the best efficiency airlfuel ratio. Differences in the data are in part due to different fuels [(12) isooctane; (13) gasoline; (14) propane] which affect efficiency slightly through their different composition and heating values (see Table D.4). They also result from different combustion chamber shapes which affect the combustion rate and heat transfer. The trends in the data with increasing compression ratio and the 6 = 0.8 fuel-air cycle curve (which corresponds approximately to the actual airffuel ratios used) are similar. The factor of 0.8 relating real engine and fuel-air cycle efficiencies holds roughly. At compression ratios above about 14, however, the data show that the indicated efficiency of actual engines is essentially constant.
Increasing crevice and heat ta $ ..* I +. Compression ratio r, FIGURE S19 Indicated fuel conversion efficiency as a function of compression ratio for ideal gas constant-volume cycle (dashed lines, y = 1.25, 1.3, 1.4) and fuel-air cycle (solid lines, I$ = 0.4.0.8, 1.0). Also shown are available engine data for equivalence ratios given: best dfkiency b = l.l4 TABLE 5 4 Availability losses in naturally aspirated diesel Loas, fraction of fuel availability Combustion Exhaust Heat transfer Aerodynamic Mechanical friction Total losses Availability conversion efficiency (brake) Source: Traupel."' losses offset the calculated ideal cycle elfiency increase as the compression ratio is raised above this value. The standard ideal gas cycle analysis results, with an appropriate choice for the value of y (1.25 to 1.3), correspond closely to the fuelair cycle analysis results. The ideal cycle provides a convenient but crude approximation to the real engine operating cycle. It is useful for illustrating the thermodynamic aspects of engine operation. It can also provide approximate estimates of trends as major engine parameters change. The weakest link in these ideal cycles is the modeling of the combustion processes in SI and CI engines. None of the models examined in this chapter are sufficiently close to reality to provide accurate predictions of engine performance. More sophisticated models of the spark-ignition and diesel %ne operating cycles have been developed and are the subject of Chap. 14. 198 INTERNAL COMBUSTION ENGINE FUNDAMENTALS 16. Use a limited-pressure cycle analysis to obtain a plot of indicated fuel conversion PROBLEMS 5.1. Many diesel engines can be approximated by a limited-pressure cycle. In a limitedpressure cycle, a fraction of the fuel is burnt at constant volume and the remaining fuel is burnt at constant pressure. Use this cycle approximation with y = cJc, = 1.3 to analyze the following problem: Inlet conditions: Compression ratio: Heat added during combustion: Overall fuellair ratio: 5.2. 5.3. (a) Half of the fuel is burnt at constant volume, then half at constant pressure. Draw a p-V diagram and compute the fuel conversion efficiency of the cycle. (b) Compare the efficiency and peak pressure of the cycle with the efficiency and peak pressure that would be obtained if all of the fuel were burnt at constant pressure or at constant volume. It is desired to increase the output of a spark-ignition engine by either (1) raising the compression ratio from 8 to 10 or (2) increasing the inlet pressure from 1.0 atm to 1.5 atm.
Using the constant-volume cycle as a model for engine operation, which procedure will give: (a) The highest pressure of the cycle? (b) The highest efficiency? (c) The highest mep? Assume g = 1.3 and (m, Q,)/(mc, Tl) = 9.3(rC- l)/r,.
When a diesel engine, originally designed to be naturally aspirated, is turbocharged the fuellair equivalence ratio 4 at full load must be reduced to maintain the maximum cylinder pressure essentially constant. If the naturally aspirated engine was deslgned for 4 = 0.75 at full load, estimate the maximum permissible value of 4 for the turbocharged engine at full load if the air pressure at the engine inlet is 1.6 atm. Assume that the engine can be modeled with the limited-pressure cycle, with half the injected fuel burned at constant volume and half at constant pressure. The compression ratio is 16. The fuel heating value is 42.5 MJ/kg fuel. Assume y = cJcD = 1.35, that the air temperature at the start of compression is 325 K, and (FIA),,, = 0.0666. A spark-ignition engine is throttled when operating at part load (the inlet pressure is reduced) while the fuellair ratio is held essentially constant. Part-load operation of the engine is modeled by the cycle shown in Fig. 5-2d; the inlet air is at pressure PI* the exhaust pressure is atmospheric pa, and the ambient temperature is T,. Derive an expression for the decrease in net indicated fuel conversion efficiency due to throttling from the ideal constant-volume cycle efficiency and show that it is proportional to (pdp, - 1). Assume mass fuel < mass air. (a) Use the ideal gas cycle with constant-volume combustion to describe the OPeration of an SI engine with a compression ratio of 9. Find the pressure and ternperature at points 2,3,4, and 5 on Fig. 5-2a. Assume a pressure of 100 kPa and 1 temperature of 320 K at point 1. Assume mf/m = 0.06, c, = 946 J/kg.K, y = 1-30 Q,, for gasoline is 44 MJ/kg. (b) Find the indicated fuel conversion eficiency and imep for this engine under thoperating conditions. , 5.4. 55.
p, = 1.0 bar, T, = 289 K 15: 1 43,000 kJ/kg of fuel 0.045 kg fuelkg air versus p,/p, for a compression ratio of 15 with light diesel oil as fuel. Assume mf/m = 0.04, T, = 4S•‹C.Use y = 1.3 and c, = 946 J/kgSK. 57. Explain why constant-volume combustion gives a higher indicated fuel conversion efficiencythan constant-pressure combustion for the same compression ratio. 53. Two engines are running at a bmep of 250 kPa. One is an SI engine with the throttle partially closed to maintain the correct load. The second engine is a naturally aspirated CI engine which requires no throttle. Mechanical friction mep for both engines is 100 kPa. If the intake manifold pressures for the SI and CI engines are 25 kPa and 100 kPa respectively, and both exhaust manifold pressures are 105 kPa, use an ideal cycle model to estimate and compare the gross imep of the two engines.
You may neglect the pressure drop across the valves during the intake and exhaust processes. 5.9. (a) Plot net imep versus pi for 20 kPa < pi < 100 kPa for a constant-volume cycle using the following conditions : m,/m = 0.06, T, = 40•‹C, c, = 946 J/kg. K, g = 1.3, r, = 9.5, QmV = 44 MJ/kg fuel. Assume p, = 100 k P a (b) What additional information is necessary to draw a similar plot for the engine's indicated torque, and indicated power?
~ 1 0 (a) . Draw a diagram similar to those in Fig. 5-2 for a supercharged cycle with constant-pressure combustion. (b) Use the ideal gas cycle with constant-pressure combustion to model an engine with a compression ratio of 14 through such a supercharged cycle. Find the pressure and temperature at points corresponding to 2, 3, 4, and 5 in Fig. 5-2. Assume a pressure of 200 kPa and temperature of 325 K at point 1, and a pressure of 100 kPa at points 5 and 6. m,/m = 0.03 and the fuel is a light diesel oil. (c) Calculate the gross and net indicated fuel conversion efficiency and imep for this engine under these operating conditions. 5.11. Use the appropriate tables and charts to carry out a constant-pressure fuel-air cycle calculation for the supercharged engine described in Prob. 5.10. Assume the same initial conditions at point 1, with 4 = 0.4 and a residual gas fraction of 0.025. A single cycle calculation is sulcient. (a) Determine the pressure and temperature at points 2, 3, 4, and 5. Calculate the compression stroke, expansion stroke, and pumping work per cycle per kg air. (b) Find the gross and net indicated fuel conversion efficiency and imep. (c) Compare the calculated residual gas fraction with the assumed value of 0.025. 5.12. One method proposed for reducing the pumping work in throttled spark-ignition engines is early intake valve closing (EIVC). The ideal cycle p-V diagram shown illustrates the concept. The EIVC cycle is 1-2-3-4-5-6-7-8-1 (the conventional throttled cycle is 1-2-3-4-5-6-7'-1). With EIVC, the inlet manifold is held at a pressure pi (which is higher than the normal engine intake pressure, p:), and the inlet valve is closed during the inlet stroke at 8. The trapped fresh charge and residual is then expanded to the normal cycle (lower) intake pressure, p.: You can assume that both cycles have the same mass of gas in the cylinder, temperature, and pressure at state 1 of the cycle. (a) On a sketch of the intake and exhaust process p V diagram, shade in the area that corresponds to the difference between the pumping work of the EIVC cycle and that of the normal cycle. (b) What value of pi and V,, will give the maximum reduction in pumping work for the EIVC cycle. 200 IDEAL MODELS OF ENGINE CYCLES INTERNAL COMBUSTION ENGINE FUNDAMENTALS I v, v,, I v, FIGURE PSI2 (c) Derive an expression for this maximum difference in pumping work between the normal cycle and the EIVC cycle in terms of p,, p f , V , , and V,. You can make the appropriate ideal cycle assumptions. 5.13. Calculate the following parameters for a constant-volume fuel-air cycle (Fig. 5-2a): (a) The pressures and temperatures at states 1,2,3,4,5, and 6 (b) The indicated fuel conversion efficiency (c) The imep (d) The residual fraction (e) The volumetric efli&ency Inlet pressure = 1 atm, exhaust pressure = 1 atm, inlet temperature = 300 K, compression ratio = 8 : 1, equivalence ratio = 4 = 1. Calculate the above parameters (points a+) using the SI units charts. Use 44.4 MJ/kg for heating value of the fuel. Hint: Start the calculations using the residual mass fraction 0.03 and the residual gas temperature 1370 K. 5.14. The cycle 1-2-3-4-5-6-1 is a conventional constant-volume fuel-air cycle with a compression ratio of 8. The fuel is isooctane, C,H,,, with a lower heating value of 44.4 MJ/kg. The gas state at 1 is T, = 300 K, p, = 1 atmosphere with an equivalence ratio of 1.0 and zero residual fraction.
The specific volume at state 1 is 0.9 m3/kgair in the mixture. The temperature at the end of compression at state 2 is 600 K. (a) Find the indicated fuel conversion efficiency and mean effective pressure of this fuel-air cycle model of a spark-ignition engine. (b) The efficiency of the cycle can be increased by increasing the expansion ratio r, while maintaining the same compression ratio rc (cycle 1-2-3-44-5A-6-1). (Thk 201 can be done with valve timing.) If the expansion ratio r, is 12, while the compression ratio and other details of the cycle remain the same as in (a), what is the indicated efficiency and mean effective pressure (based on the new, larger, displaced volume) of this new engine cycle? 515. In spark-ignition engines, exhaust gas is recycled to the intake at part load to reduce the peak burned gas temperatures and lower emissions of nitrogen oxides. (a) Calculate the reduction in burned gas temperature that occurs when, due to exhaust gas recycle, the burned gas fraction in the unburned gas mixture (x,) inside the cylinder is increased from 10 percent (the normal residual fraction) to 30 percent. Assume combustion occurs at top-center, at constant volume, and is adiabatic. Conditions at the end of compression for both cases are: T = 700 K, p = 1000 kPa, v = 0.2 m3/kg air in the original mixture; the equivalence ratio is 1.0. The fuel can be modeled as isooctane. (b) The compression ratio is 8. The compression stroke work is 300 kJ/kg air in the original mixture. Find the indicated work per cycle for the compression and expansion strokes, per kilogram of air in the original mixture, for these two cases. (c) Briefly explain how you would increase the work per cycle with 30 percent burned gas fraction in the unburned mixture to the value obtained with 10 percent burned gas fraction, with fixed engine geometry. (A qualitative answer, only, is required here.) 116. The following cycle has been proposed for improving the operation of a four-stroke cycle engine. Its aim is to expand the postcombustion cylinder gases to a lower pressure and temperature by extending the expansion stroke, and hence extract more work per cycle. The cycle consists of: (I) an intake stroke; (2) a compression stroke, where the inlet valve remains open (and the cylinder pressure is constant) for the first portion of the stroke; (3) a combustion process, which occurs rapidly close to toptenter; (4) an expansion stroke, where the exhaust valve remains closed until the end of the stroke; (5) an exhaust stroke, where the cylinder pressure blows down to the exhaust pressure rapidly and most of the remaining combustion products are expelled as the piston moves from the BC to the TC position. Thus, for this engine concept, the compression ratio rc (ratio of cylinder volume at inlet valve closing to clearance volume) is less than the expansion ratio re (ratio of cylinder volume at exhaust valve opening to clearance volume). (a) Sketch a pV diagram for the cylinder gases for this cycle operating unthrottled, (b) Using the charts in SI units developed for fuel-air cycle calculations, carry out an analysis of an appropriate ideal model for this cycle where the compression ratio r, is 8 and the expansion ratio r,is (1) 8; (2) 16. Assume the following: Pressure in the cylinder at inlet valve close 1 atm Mixture temperature at inlet valve close 300 K Mixture equivalence ratio = 1.0 Fuel :isooctane C,H,, Lower heating d u e = 44.4 MJ/kg Residual gas mass fraction at inlet valve close 0.05 Stoichiometricfuellair ratio = 0.066 FIGURE PSI4 Calculate the indicated work per cycle per kg of air in the original mixture (the standard chart units) and the indicated mean effective pressure for these two expansion ratios. Base the mean effective pressure on the volume displaced by 202 INTERNAL COMBUSTION ENGINE FUNDAMENTALS IDEAL MODELS OF ENGINE CYCLES the piston during the expansion stroke. Tabulate your answers. (Note: You are given the initial conditions for the cycle calculation; changing the value of requires only modest changes in the cycle calculation.) (c) Comment briefly on the effect of increasing the ratio r,/r, above 1.0 with thjj concept on engine eficiency and specific power (power per unit engine weight). Additional calculations are not required. 5.17.
In a direct-injection stratified-charge (DISC) engine fuel is injected into the engine cylinder just before top-center (like a diesel); a spark discharge is then used to initiate the combustion process. A four-stroke cycle version of this engine has a displa& volume of 2.5 liters and a compression ratio of 12. At high load, the inlet pressure is boosted by a compressor to above atmospheric pressure. The compressor is geared directly to the engine drive shaft. The exhaust pressure is 1 atm. This DISC engine is to replace an equal displacement conventional naturally aspirated spark-ignition (SO engine, which has a compression ratio of 8. (a) Draw qualitative sketches of the appropriate constant-volume ideal cycle pressure-volume diagrams for the complete operating cycles for these two engines at maximum load. (b) Use available fuel-air results to estimate how much the DISC engine inlet pres sure must be boosted above atmospheric pressure by the compressor to provid the same maximum gross indicated power as the naturally aspirated SI engin The SI engine operates with an equivalence ratio of 1.2; the DISC engine limited by smoke emissions to amaximum equivalence ratio of 0.7. (c) Under these conditions, will the brake powers of these engines be the same, giv that the mechanical rubbing friction is the same? Briefly explain.
(d) At part load, the ST engine operates at an equivalence ratio of 1.0 and in1 pressure of 0.5 atm. At part load the DISC engine has negligible boost an operates with an inlet pressure of 1.0 atm. Use fuel-air cycle results to determin the equivalence ratio at which the DISC engine must be operated to provide t same net indicated mean effective pressure as the SI engine. What is the ratio DISC engine net indicated fuel conversion efficiency to SI engine efficiency these conditions? 5.18. The earliest successful reciprocating internal combustion engine was an engine de oped by Lenoir in the 1860s. The operating cycle of this engine consisted of strokes (i.e., one crankshaft revolution). During the first half of the first stroke, as piston moves away from its top-center position, fuel-air mixture is drawn into cylinder through the inlet valve. When half the total cylinder volume is filled wl fresh mixture, the inlet valve is closed. The mixture is then ignited and bums rapidly. During the second half of the first stroke, power is delivered from the high-pressure burned gases to the piston. With the piston in its bottom-center position, the e x h d valve is opened. The second stroke, the exhaust stroke, completes the cycle as piston returns to top-center. (a) Sketch a cylinder pressure versus cylinder volume diagram for this engine. (b) Using the charts in SI units developed for fuel-air cycle calculations, carry out cycle analysis and determine the indicated fuel conversion efficiency and m a P effective pressure for the Lenoir engine. Assume the following: % +' Inlet pressure = 1 atm Inlet mixture temperature = 300 K Mixture equivalence ratio = 1.0 203 Fuel: isooctane C,H,, Lower heating value = 44.4 MJFg Clearance volume negligible (c) Compare these values with typical values for the constant-volume fuel-air cycle. Explain (with thermodynamic arguments) why the two cycles have such different indicated mean effective pressures and efficiencies. (d) Explain briefly why the real Lenoir engine would have a lower efficiency than the value you calculated in (b) (the actual brake fuel conversion efficiency of the engine was about 5 jm&nt). 5.19. Estimate from fuel-air cycle results the indicated fuel conversion efficiency, the indicated mean effective pressure, and the maximum indicated power (in kilowatts) at wide-open throttle of these two four-stroke cycle spark-ignition engines: A six-cylinder engine with a 9.2cm bore, 9-cm stroke, compression ratio of 7, operated at an equivalence ratio of 0.8 A six-cylinder engine with an 8.3-cm bore, 8-cm stroke, compression ratio of 10, operated at an equivalence ratio of 1.1 Assume that actual indicated engine efficiency is 0.8 times the appropriate fuel-air cycle efficiency.The inlet manifold pressure is close to 1 atmosphere. The maximum permitted value of the mean piston speed is 15 m/s. Briefly summarize the reasons why: (a) The efficiency of these two engines is approximately the same despite their different compression ratios. (b) The maximum power of the smaller displacement engine is approximately the same as that of the larger displacement engine. 5.20. The constant-volume combustion fuel-air cycle model can be used to estimate the effect of changes in internal combustion engine design and operating variables on engine efficiency. The following table gives the major differences between a diesel and a spark-ignition engine both operating at half maximum power. Compression ratio Fuellair equivalence ratio Inlet manifold pressure Diesel engine Spark-ignition engine 16:l 0.4 9:l 1 atm 0.5 atm 1.o (a) Use the graphs of fuel-air cycle results (Figs. 5-9 and 5-10) to estimate the ratio of the diesel engine brake fuel conversion efficiency to the spark-ignition engine brake fuel conversion efficiency. (b) Estimate what percentage of the higher diesel brake M conversion eficiency comes from: (1) The higher diesel compression ratio (2) The leaner diesel equivalence ratio (3) The lack of intake throttling in the diesel compa~edwith the spark-ignition engine 204 INTERNAL COMBUSTION ENGINE FUNDAMENTALS The values of fuel conversion efficiency and mean effective pressure given the graphs are gross indicated values (i.e., values obtained from j p dV over the compression and expansion strokes only). You may assume, if necessary, that for the real engines, the gross indicated efficiency and gross indicated mean effective pressure are 0.8 times the fuel-air cyck values. Also, the mechanical rubbing friction for each engine is 30 percent of the mt indicated power or mep. CHAPTER REFERENCES 1. Taylor, C. F.: The Internal Combustion Engine in Theory and Practice, vol. 1: Thmmodynamicr, Fluid Flow, Pdormame, 2d ed., chaps. 2 and 4,1966. 2. Lancaster, D. R, Krieger, R. B., and Lienesch, I. H.: "Measurement and Analysis of Engim Pressure Data," SAE paper 750026, SAE Trans., vol. 84, 1975. 3. Edson, M. H.: "The Influence of Compression Ratio and Dissociation on Ideal Otto Cy& E n d e Thermal Efficiency," Digital Calculations of Engine Cycles, SAE Prog. in Technology,vol 7, 49-64,1964. 4. Edson, M. H., and Taylor, C. F.: "The L i t s of Engine Perfomance-Comparison of Actual and Theoretical Cycles," Digital Calculations of Engine Cycles, SAE Prog. in Technology, vol. 7. pp. 6541,1964. 5. Keenan, I. H.: Thermodynamics, John Wiley, New York, 1941; MIT Press, Cambridge, Mas., 1970. 6. Haywood, R. W.: "A Critical Review of the Theorems of Thermodynamic Availability, wilh Concise Formulations; Part 1.
Availability," J. Mech.
Engng Sci., vol. 16, no. 3, pp.
16173.1974. 7. Haywood, R. W.: "A Critical Review of the Theorems of Thermodynamic Availability, wilh Concise Formulations; Part 2.
Irreversibility," J. Mech. Engng Sci., vol. 16, no. 4, pp. 258-267, 1974. 3 8. Flynn, R. F., Hoag, K.
L., Kamel, M. M., and Primus, R. J.: "A New Perspective on D i d Ennine Evaluation Based on Second Law Analysis," SAE paper 840032, SAE Trans., vol. 93, & .? 1984. 9. Clarke, J. M.: "The Thermodynamic Cycle Requirements for Very High Rational Efiiciaci~%- 2 paper C53/76, Institution of Mechanical Engineers, J. Mech. Engng Sci., 1974. 10.
Traupel, W.: "Reciprocating Engine and Turbine in Internal Combustion Engineering" in Pr* i. CIMAC Int. Congr. on Combustion Engines, Zurich, pp. 39-54,1957. 11. Clarke, J. M.: "Letter: Heavy Duty Diesel Fuel Economy," Mech. Engng, pp. 105-106, M a d + 1983.
12. Caris, D. F., and Nelson, E. E.: "A New Look at High Compression Engines," SAE Tram.. v d % 67, pp. 112-124,1959. 13. Kerley.
R. V., and Thurston. K. W.: "The Indicated Performance of Otto-Cycle Engine%"SAT %6 ~ r a k .vol. , 70, pp. 5-37, 1962. 14. Bolt, J. A., and Holkeboer, D. H.: "Lean Fuel-Air Mixtures for High-Compression S@ Ignition Engines," SAE Trans., vol. 70, p. 195,1962.
.p: GAS EXCHANGE PROCESSES ip. 3 * $:, ' I2 This chapter deals with the fundamentals of the gas exchange processes-intake and exhaust in four-stroke cycle engines and scavenging in two-stroke cycle engines. The purpose of the exhaust and inlet processes or of the scavenging process is to remove the burned gases at the end of the power stroke and admit the fresh charge for the next cycle. Equation (2.38) shows that the indicated power of an internal combustion engine at a given speed is proportional to the mass flow rate of air. Thug inducting the maximum air mass at wide-open throtth or full load and retaining that mass within the cylinder is the primary goal of the gas exchange processes. Engine gas exchange processes are characterized by overall parameters such as volumetric eficiency (for four-stroke cycles), and scavenging eficiency and trapping eficiency (for two-stroke cycles). These overall Brameters depend on the design of engine subsystems such as manifolds, valves, and Ports, as well as engine operating conditions. Thus, the flow through individu1. components in the engine intake and exhaust system has been extensively fludied also. Supercharging and turbocharging are used to increase air flow engines, and hence power density. Obviously, whether the engine is natuRlly aspirated or supercharged (or turbocharged) significantly affects the gas ('change The above topics are the subiect of this chaoter -For processes. -r ---spark-ignition engines, the fresh charge is fuel, air, and (if used for mission control) recycled exhaust, so mixture preparation is also an important goal of the intake process. Mixture preparation includes both achieving the appropriate mixture composition and achieving equal distribution of air, fuel, and recycled exhaust amongst the different cylinders. In diesels, only air (or air plus recycled exhaust) is inducted. Mixture preparation and manifold flow phenomena are discussed in Chap. 7. A third goal of the gas exchange procesm is to set up the flow field within the engine cylinders that will give a fast-enough combustion process for satisfactory engine operation. In-cylinder flows are the subject of Chap. 8. 6.1 INLET AND EXHAUST PROCESSES IN THE FOUR-STROKE CYCLE In a spark-ignition engine, the intake system typically consists of an air filter, a carburetor and throttle or fuel injector and throttle or throttle with individual fuel injectors in each intake port, and intake manifold. During the induction process, pressure losses occur as the mixture passes through or by each of these components. There is an additional pressure drop across the intake port and valve. The exhaust system typically consists of an exhaust manifold, exhaust pipe, often a catalytic converter for emission control, and a-mutller or silencer.
Figure 6-1 illustrates the intake and exhaust gas flow processes in a conventional sparkignition engine. These flows are pulsating. However, many aspects of these flows can be analysed on a quasi-steady basis, and the pressures indicated in the intake system in Fig.
6-la represent time-averaged values for a multicylinder engine. The drop in pressure along the intake system depends on engine speed, the flow resistance of the elements in the system, the cross-sectional area through which the fresh charge moves, and the charge density. Figure 6-ld shows the inlet and exhaust valve lifts versus crank angle. The usual practice is to extend the valve open phases beyond the intake and exhaust strokes to improve emptying and charging of the cylinders and make the best use of the inertia of the gases in the intake and exhaust systems. The exhaust process usually begins 40 to 60" before BC. Until about BC the burned cylinder gases are discharged due to the pressure difference between the cylinder and the exhaust system. After BC, the cylinder is scavenged by the piston as it moves toward TC. The terms blowdown and displacement are used to denote these two phases of the exhaust process Typically, the exhaust valve closes 15 to 30" after TC and the inlet valve opens 10 to 20" before TC. Both valves are open during an overlap period, and when pJp, < 1, backflow of exhausted gas into the cylinder and of cylinder gases into the intake will usually occur. The advantage of valve overlap occurs at high engine speeds when the longer valve-open periods improve volumetric ef'liciency. As the piston moves past TC and the cylinder pressure falls below the intake pressure, gas flows from the intake into the cylinder. The intake valve remaim openuntil 50 to 70" after BC so that fresh charge may continue to flow into the cylinder after BC. In a diesel engine intake system, the carburetor or EFI system and t k throttle plate are absent. Diesel engines are more frequently turbocharged A hake and exhaust promu. for four-stroke cycle spark-ignition engine: (a) intake system and average pressures within it; (b) vahe timing and pressure-volume diagrams; (c) exhaust system; (d) cylinder pressure p and valve lift Lv v e n u crank angle 0. Solid ha are for wide-opcn throttle, dashed for part throttle; po, To,atmospheric conditions; Ap,,, = pressure losses in air cleaner; Ap" = k k e losses upstream of throttle; Apt,,. = l o w s across throttle; A p v S ,= l o n a across the intake valve.' 6 3 VOLUMETRIC EFFICIENCY volumetric efficiencyis used as an overall measure of the effectiveness of a fourstrokecycle engine and its intake and exhaust systems as an air pumping device. is defined [see Sec. 2.10, Eq. (2.2711 as "'4 = 2m,, V,N Pa.0 (6.1) The air density pa,, can be evaluated at atmospheric conditions; qu is then the overall volumetric efficiency.Or it can be evaluated at inlet manifold conditions; qD then measures the pumping performance of the cylinder, inlet port, and valve alone.
This discussion will cover unthrottled (wide-open throttle) engine operation only. It is the air flow under these conditions that constrains maximum engine power. Lesser air flows in SI engines are obtained by restricting the intake system flow area with the throttle valve. Volumetric efficiency is affected by the following fuel, engine design, and engine operating variables : I. Fuel type, fuellair ratio, fraction of fuel vaporized in the intake system, and fuel heat of vaporization 2. Mixture temperature as influenced by heat transfer 3. Ratio of exhaust to inlet manifold pressures 4. Compression ratio 5. Engine speed 6. Intake and exhaust manifold and port design 7. Intake and exhaust valve geometry, size, lift, and timings FIGURE 6-2 Intake and exhaust process for turbocharged four-stroke cycle engine. The turbocharger compressor C raises air pressure and temperature from ambient po, To to p,, T,. Cylinder pressure during intake is less than p,. During exhaust, the cylinder gases flow through the exhaust manifold to the turb charger turbine T. Manifold pressure p, may vary during the exhaust process and lies between cylinder pressure and ambient.' similar set of diagrams illustrating the intake and exhaust processes for a turbocharged four-stroke diesel is shown in Fig. 6-2. When the exhaust valve openf the burned cylinder gases are fed to a turbine which drives a compressor which compresses the air prior to entry to the cylinder. Due to the time-varying valve open area and cylinder volume, gas inerb effects, and wave propagation in the intake and exhaust systems, the pressures the intake, the cylinder, and the exhaust during these gas exchange processes VW in a complicated way. Analytical calculation of these processes is diEcuIt (* Secs. 7.6.2 and 14.3 for a review of available methods). In practice, these proce@ are often treated empirically using overall parameten such as volumetric ciency to define intakd and exhaust system performance. * 8 $$ 5 i >" The effects of several of the above groups of variables are essentially quasi steady in nature; i.e., their impact is either independent of speed or can be described adequately in terms of mean engine speed. However, many of these variables have effects that depend on the unsteady flow and pressure wave phenomena that accompany the time-varying nature of the gas exchange processes. 6.2.1 Quasi-Static Effects VOLUMETRIC EFFICIENCY OF AN IDEAL CYCLE For the ideal cycles of Fig. 5-26 and e, an expression for volumetric eRciency can be derived which is a function of the following variables: intake mixture pressure pi, temperature I;, and fuel/air ratio (FJA); compression ratio re; exhaust pressure p.; and molecular Weight M and y for the cycle working fluid. The overall volumetric efficiency is 210 GAS EXCHANGE PROCESSES INTERNAL COMBUSTION ENGINE FUNDAMENTALS where m is the mass in the cylinder at point 1 in the cycle. Since R pi v1 = m - TI M and P,,O = P.,O R %o Ma 211 For conventional liquid fuels such as gasoline the effect of fuel vapor, and fuellair ratio, is small. For gaseous fuels and for methanol vapor, the volumetric efficiency is significantly reduced by the fuel vapor in the intake mixture. and Eq. (5.38) relates TI to T,, the above expression for q, can be written FRACTION FUEL VAPORIZED, HEAT OF VAPORIZATION, AND HEAT TRANSFER.For a constant-pressure flow with liquid fuel evaporation and with heat transfer, the steady-flow energy equation is For (pJpi) = 1, the term in { 1is unity.
EFFECT OF FUEL COMPOSITION, PHASE, AND FUELIAIR RATIO. In a spark- ignition engine, the presence of gaseous fuel (and water vapor) in the intake system reduces the air partial pressure below the mixture pressure. For mixtures of air, water vapor, and gaseous or evaporated fuel we can write the intake manifold pressure as the sum of each component's partial pressure: where x, is the mass fraction evaporated and the subscripts denote: a, air properties;f, fuel properties; L, liquid; V, vapor; B before evaporation; A after evaporation. Approximating the change in enthalpy per unit mass of each component of the mixture by cpAT, and with hj,, - h,,, = hjSLv (the enthalpy of vaporization), Eq. (6-4) becomes which with the ideal gas law gives The water vapor correction is usually small (10.03). This ratio, pa,Jpi, for several common fuels as a function of (m,/ma) is shown in Fig. 6-3. Note that (mf/ma) only equals the engine operating fuellair ratio if the fuel is fully vaporized. 3 FIGURE M 0.5 1.O Equivalence ratio 6 Effect of fuel (vapor) on inlet air partial pressure. Ratio of air inlet pressure pa,, to mixture inlet pressure p, versus fuel/air equivalence ratio 4 for iso1.5 octane vapor, propane, methane, methanol vapor. and hydrogen. Since c,,.
% 2cp.a the last term in the denominator can often be neglected. If no heat transfer to the inlet mixture occurs, the mixture temperature decreases as liquid fuel is vaporized. For complete evaporation of isooctane, with 4 = 1.0, TA- TB= - 19•‹C. For methanol under the same conditions, TA- T, would be - 128•‹C.In practice heating occurs; also, the fuel is not necessarily fully evaporated prior to entry to the cylinder. Experimental data show that the decrease in air temperature that accompanies liquid fuel evaporation more than offsets the reduction in air partial pressure due to the increased amount of fuel vapor: for the same heating rate, volumetric efficiency with fuel vaporization is higher by a few per~ent.~ The ideal cycle equation for volumetric efficiency [Eq. (6.2)] shows that the effect of gas temperature variations, measured at entry to the cylinder, is through the factor (T,,,lT,). Engine test data indicate that a square root dependence of volumetric efficiencyon temperature ratio is closer to real engine behavior. The square root dependence is a standard assumption in engine test data reduction (see Sec. 2.12). EFFECT OF INLET .4\m EXHAUST PRESSURE RATIO AND COMPRESSION RATIO. As the pressure ratio (pJp,) and the compression ratio are varied, the fraction of the cylinder volume occupied by the residual gas at the intake pressure varies. As this, volume increases so volumetric efficiency decreases. These effects on ideal-cycle volumetric efficiency are given by the {) term in Eq. (6.2). For Y = 1.3 these effects are shown in Fig. 6-4.
212 INTERNAL COMBUSTION ENGINE FWAMENTALS here Aj and A, are the component minimum flow area and the piston area, Hence, the total quasi-steady pressure loss due to friction is ~ ~ u a t i o(6.6) n indicates the importance of large component flow areas for reducing frictional losses, and the dependence of these losses on engine speed. Figure 6-5 shows an example of the pressure losses due to friction across the air cleaner, carburetor, throttle, and manifold plenum of a standard four-cylinder I FIGURE 6-4 Eflect of exhaust to inlet pressure ratio on ideal-cycle volumetric efficiency. Air cleaner nrottle I 63.2 Combined Quasi-Static and Dynamic Effects When gas flows unsteadily through a system of pipes, chambers, ports, and valves, both friction, pressure, and inertial forces are present. The relative importance of these forces depends on gas velocity and the size and shape of these passages and their junctions. Both quasi-steady and dynamic effects are usually significant.
While the effects of changes in engine speed, and intake and exhaust manifold, port and valve design are interrelated, several separate phenomeha which affect volumetric efficiency can be identified. FRICIlONAL LOSSES. During the intake stroke, due to friction in each part of the intake system, the pressure in the cylinder p, is less than the atmospheric pressure ,p by an amount dependent on the square of the speed. This total pressure drop is the sum of the pressure loss in each component of the intake system: air filter, carburetor and throttle, manifold, inlet port, and inlet valve. Each loss is a few percent, with the port and valve contributing the largest drop.
As a result, the pressure in the cylinder during the period in the intake process when the piston is moving at close to its maximum speed can be 10 to 20 percent lower than atmospheric.
For each component in the intake (and the exhaust) system, Bernoulli's equation gives where 6 is the resistance coeficient for that component which depends on it^ Ramre lona in the intake system of a four-stroke cycle spark-ignition engine d e t e d n d under *ady flow conditions.' Stroke = 89 mm.Bore = 84 mm. automobile engine intake system. These steady flow tests, conducted over the fun engine speed range: show that the pressure loss depends on speed squared. Equivalent flow-dependent pressure losses in the exhaust system result in the exhaust port and manifold having average pressure levels that are higher than atmospheric. Figure 6-6 shows the time-averaged exhaust manifold gauge pressure as a function of inlet manifold vacuum (which varies inversely to load) and r 1 I 0 Inlet manifold vacuum, kP8 2 0 3 0 4 0 5 I I I 0 I ~ 7 0 ,peed for a four-cylinder automobile spark-ignition engine.4 At high speeds and loads the exhaust manifold operates at pressures substantially above atmospheric. hi EFFECT. The pressure in the inlet manifold varies during each cylinder's intake process due to the pi

different exhaust valve and port combinations, are given in Fig. 6-18. A sharp-cornered isolated poppet valve (i.e., straight pipe downstream, no port) gives the best performance FIGURE 6 1 8 Discharge coefficient as function of valve lit for several exhaust valve and port designs.I6 a,20 b,lJ r?O d.21 valves, however. Exhaust valves operate over a wide range of pressure ratios (1 to 5). For pressure ratios greater than about 2 the flow will be choked, but the effect of pressure ratio on discharge coefficient is small and confined to higher lifts (e.& & 5 percent at LJD, = 0.3).15 6.4 RESIDUAL GAS FRACTION The residual gas fraction in the cylinder during compression is determined by the exhaust and inlet processes. Its magnitude affects volumetric efficiency and engine performance directly, and efficiencyand emissions through its effect on workingfluid thermodynamic properties. The residual gas fraction is primarily a function of inlet and exhaust pressures, speed, compression ratio, valve timing, and exhaust system dynamics. - .-f 2 3w 400 500 600 700 Manifold pressure, mmHg abs Manifold pressure, mmHg abs 1 M 2 0 r 1 1 i I I I 1 \ The residual gas mass fraction x, (or burned gas fraction if EGR is used) is Usually determined by measuring the CO, concentration in a sample of gas from the cylinder during the compression stroke. Then where the subscripts C and e denote compression and exhaust, and &,, are mole fractions in the wet gas. Usually C 0 2 volume or mole fractions are measured in dry gas streams (see Sec. 4.9). A correction factor K, ?zo where y is the molar hydrogen/carbon ratio of the fuel and ji.z0,, are dry mole fractions,can be used to convert the dry mole fraction measurements. Residual gas measurements in a spark-ignition engine are given in Fig. 6-19, which shows the effect of changes in speed, valve overlap, compression ratio, and air/fuel ratio for a range of inlet manifold pressures for a 2-dm3, 88.5-mm bore, four-cylinder engine.22 The effect of variations in spark timing was negligible. Inlet pressure, speed, and valve overlap are the most important variables, though the exhaust pressure also affects the residual fra~tion.'~Normal settings for inlet valve opening (about 15" before TC) and exhaust valve closing (about 12" after TC) provide sufficient overlap for good scavenging, but avoid excessive backflow from the exhaust port into the cylinder. Residual gas fractions in diesel engines are substantially lower than in SI engines because inlet and exhaust pressures are comparable in magnitude and the compression ratio is 2 to 3 times as large. Also, a substantial fraction of the residual gas is air. \ 6 5 EXHAUST GAS FLOW RATE AND TEMPERATURE VARIATION 0' L 5 k L 7 k Manifold pressure, mmHg abs Airlfuel ratio FIGURE 6-19 Residual gas fraction for 2dm3 four-cylinder sparkignition engine as a function of intake madd pressure for a range of speed., compression ratios. and valve overlaps: also as a function of d r p ratio for a ran& of volumetric efficiencies. Operating conditions, unless noted: speed = 1400 rev/* A/F = 14.5, spark timing set to give 0.95 maximum torque, compression ratio = ~ . 5 . ~ ' The exhaust gas mass flow rate and the properties of the exhaust gas vary significantly during the exhaust process. The origin of this variation for an ideal exhaust process is evident from Fig. 5-3. The thermodynamic state (pressure, temperature, etc.) of the gas in the cylinder varies continually during the exhaust blowdown phase, until the cylinder pressure closely approaches the exhaust manifold pressure. In the real exhaust process, the exhaust valve restricts the flow out of the cylinder, the valve lift varies with time, and the cylinder volume changes during the blowdown process, but the principles remain the same. Measurements have been made of the variation in mass flow rate through 'he exhaust valve and gas temperature at the exhaust port exit during the exhaust Process of a spark-ignition engine.24 Figure 6-20 shows the instantaneous mass flow rate data at three different engine speeds. The blowdown and displacement 232 INTERNAL COMBUSTION ENGINE FUNDAMENTALS Crank angle, deg FIGURE 6-20 Instantaneous mass flow rate of exhaust gas through the valve versus crank angle: equivalena ratio = 1.2, wide-open throttle, compression ratio = 7. Dash-dot line is onedimensional compressible s flow model for blowdown and incompressible displacement model for exhaust stroke.24 $ 2 phases of the exhaust process are evident. Simple quasi-steady models of these phases give good agreement with the data at lower engine speeds.

The blowdown model shown applies orifice flow equations to the flow across the exhaust valve using the measured cylinder pressure and estimated gas temperature for upstream stagnation conditions. Equation (C.9) is used when the pressure ratio across the valve exceeds the critical value. Equation (C.8) is used when the pressure ratio is less than the critical value. The displacement model assumes the gas in the cylinder is incompressible as the piston moves through the exhaust stroke. As engine speed increases, the crank angle duration of the blowdown phase increases. There is evidence of dynamic effects occurring at the transition between the two phases The peak mass flow rate during blowdown does not vary substantially with speed since the flow is choked. The mass flow rate at the time of maximum piston speed during displacement scales approximately with piston speed. As the inlet manifold pressure is reduced below the wide-open throttle value, the proportion of the charge which exits the cylinder during the blowdown phase decreases but the mass flow rate during displacement remains essentially constant. The exhaust gas temperature varies substantially through the exhaat process, and decreases due to heat loss as the gas flows past the exhaust v a k and through the exhaust system. Figure 6-21 shows the measured cylinder pressure, calculated cylinder temperature and exhaust mass flow rate, and measured gas temperature at exhaust port exit for a single-cylinder spark-ignition engine at mid-load and speed.25 The average cylinder-gas temperature falls rapidly during blowdo and continues to fall during the exhaust stroke due to heat transfer to the cylin- Crank angle Measured cylinder pressure p,, calculated cylinder-gas temperature T,, ethaust mass flow rate me, and measured gas temperature at exhaust port exit T,, for single-cylinder spark-ignition engine. Speed = 1000 rev/min, imep = 414 kPa, equivalence ratio = 1.2, spark timing = 10"BTC,r, = 7.2.25 der walls. The gas temperature at the port exit at the start of the exhaust flow pulse is a mixture of hotter gas which has just left the cylinder and cooler gas which left the cylinder at the end of the previous exhaust process and has been stationary in the exhaust port while the valve has been closed. The port exit temperature has a minimum where the transition from blowdown flow to displacement occurs, and the gas comes momentarily to rest and loses a substantial fraction of its thermal energy to the exhaust port walls. Figure 6-22 shows the effect of varying load and speed on exhaust port exit temperatures. Increasing load (A + B -,C) increases the mass and temperature in the blowdown pulse. Increasing speed (B - D) raises the gas temperature throughout the exhaust process. These effects are the result of variations in the relative importance of heat transfer in the cylinder and heat transfer to the exhaust valve and port. The time available for heat transfer, which depends on engine speed and exhaust gas flow rate, is the most critical factor. The exhaust temperature variation with equivalence ratio follows from the variation in expansion stroke temperatures, with maximum values at q5 = 1.0 and lower values for leaner and richer mixtures.24Diesel engine exhaust temperatures are significantly 234 INTERNAL COMBUSTION ENGINE FUNDAMENTALS 1 6.6 SCAVENGING IN TWO-STROKE CYCLE ENGINES 6.6.1 Two-Stroke Engine Configurations Crank angle FIGURE 6-22 Measured gas temperature at exhaust port exit as a function of crank angle, single-cylinder sparkignition engine, for different loads and speeds. Curve A: imep = 267 kPa, 1000 rev/min; curve B: imep = 414 kPa, 1000 rev/min; curve C: imep = 621 kPa, 1000 revlmin; curve D :imep = 414 kPa, 1600 rev/min. Equivalence ratio = 1.2,spark timing = 10" BTC, compression ratio = 7.2.15 In tw~-strokecycle engines, each outward stroke of the piston is a power stroke.

achieve this operating cycle, the fresh charge must be supplied to the engine cylinder at a high-enough pressure to displace the burned gases from the previous cycle.

Raising the pressure of the intake mixture is done in a separate pump or blower or compressor. The operation of clearing the cylinder of burned gases and filling it with fresh mixture (or a i r b t h e combined intake and exhaust process-is called scavenging. However, air capacity is just as important as in the four-stroke cycle; usually, a greater air mass flow rate must be achieved to obtain the same output power. Figures 1-12, and 1-5 and 1-24 show sectioned drawings of a two-stroke spark-ignition engine and two two-stroke diesels. The different categories of two-stroke cycle scavenging flows and the port (and valve) arrangements that produce them are illustrated in Figs. 6-23 and 6-24. Scavenging arrangements are classified into: (a) cross-scavenged, (b) loopscavenged, and (c) unifow-scavenged conJigurations.

The location and orientation of the scavenging ports control the scavenging process, and the most common arrangements are indicated. Cross- and loop-scavenging systems use exhaust and inlet ports in the cylinder wall, uncovered by the piston as it approaches BC.27 The uniflow system may use inlet ports with exhaust valves in the cylinder head, lower than spark-ignition engine exhaust temperatures because ofthe lean operating equivalence ratio and their higher expansion ratio during the power stroke. The average exhaust gas temperature is an important quantity for determining the performance of turbochargers, catalytic converters, and particulate traps. The time-averaged exhaust temperature does not correspond to the average energy of the exhaust gas because the flow rate varies substantially. An enthalpy-averaged temperature is the best indicator of exhaust thermal energy. Average exhaust gas temperatures are usually measured with a thermocouple. Thermocouple-averaged temperatures are close to time-averaged temperatures. Mass-averaged exhaust temperatures (which are close to f if c, variations are small) for a spark-ignition engine at the exhaust port exit are about 100 K higher than time-averaged or thermocoupledetermined temperatures. Mass-average temperatures in the cylinder during the exhaust process are about 200 to 300 K higher than mass-averaged port temperatures. All these temperatures increase with increasing speed, load, and spark retard, with speed being the variable with the largest impact.26 Cross-scavenged, (b) loopscavenged, and (c) uniflow-scavenged two-stroke cycle flow configurations. (0) \ Scavenging 1 FIGURE 6-24 Common porting arrangements that go with (a)cross-scavenged, (b) loop-scavenged, and (c) uniflowscavenged configurations.

or inlet and exhaust ports with opposed pistons. Despite the different flow patterns obtained with each cylinder geometry, the general operating principles are similar. Air in a diesel, or fuel-air mixture in a spark-ignition engine, must be supplied to the inlet ports at a pressure higher than the exhaust system pressure.

Figure 6-25 illustrates the principles of the scavenging process for a uniflow engine design. Between 100 and 110" after TC, the exhaust valve opens and a blowdown discharge process commences. Initially, the pressure ratio across the exhaust valve exceeds the critical value (see App. C) and the flow at the valve will be sonic: as the cylinder pressure decreases, the pressure ratio drops below the critical value. The discharge period up to the time of the scavenging port opening is called the blowdown (or free exhaust) period. The scavenging ports open between 60 and 40" before BC when the cylinder pressure slightly exceeds the scavenging pump pressure. Because the burned gas flow is toward the exhaust valves, which now have a large open area, the exhaust flow-continues and no backflow occurs. When the cylinder pressure falls below the inlet pressure, air enters the cylinder and the scavenging process starts. This flow continues as long as the inlet ports are open and the inlet total pressure exceeds the pressure in the cylinder. As the cylinder pressure rises above the exhaust pressure, the fresh charge flowing into the cylinder displaces the burned gases: a part of the fresh charge mixes with the burned gases and is expelled with them. The exhaust valva usually close after the inlet ports close. Since the flow in the cylinder is toward the exhaust valve, additional scavenging is obtained. Figure 1-16 illustrates the k~ir from compressor PC (0) (6) FIGURE 625 Gas exchange process in two-stroke cycle uniflow-scavenged diesel engine: (a) valve and port timing and pressurevolume diagram; (b) pressure, scavenging port open area A,, as functions of crank angle.' and exhaust valve lift L, similar sequence of events for a loopscavenged engine. Proper flow patterns for the fresh charge are extremely important for good scavenging and charging of the cylinder. Common methods for supercharging or pressurizing the fresh charge are shown in Fig. 6-26. In large two-stroke cycle engines, more complex combinations of these approaches are often used, as shown in Fig. 1-24.

6.6.2 Scavenging Parameters and Models The following overall parameters are used to describe the scavenging pro~ess.'~ The delivery ratio A: A= mass of delivered air (or mixture) per cycle reference mass (6.20) 238 INTERNAL COMBUSTION ENGINE FLXDAMEMALS The charging eflciency qch: qch = mass of delivered air (or mixture) retained displaced volume x ambient density (6.24) indicates how effectively the cylinder volume has been filled with fresh air (or mixture). Charging eficiency, trapping efficiency,and delivery ratio are related by When the reference mass in the definition of delivery ratio is the trapped cylinder mass m,, (or closely approximated by it) then FIGURE 6-26 Common methods of pressurizing the fresh charge in two-stroke cycle engines: left, crankcase cornpression; center, roots blower; right, centrifugal compressor,' compares the actual scavenging air mass (or mixture mass) to that required in an ideal charging process.? The reference mass is defined as displaced volume x ambient air (or mixture) density. Ambient air (or mixture) density is determined at atmospheric conditions or at intake conditions. This definition is useful For experimental purposes.

For analytical work, it is often convenient to use the trapped cylinder mass 4, as the reference mass. The trapping efficiency qtr: mass of delivered air (or mixture) retained mass of delivered air (or mixture) = . (6.2 1) indicates what fraction of the air (or mixture).supplied to the cylinder is retained in the cylinder. The scavenging efficiency qse: = mass of delivered air (or mixture) retained mass of trapped cylinder charge mass of air in trapped cylinder charge mass of trapped cylinder charge qtr = 1 for A < 1 and (6.27) q , = A for A>1 and For the complete mixing limit, consider the scavenging process as a quasisteady flow process. Between time t and t dt, a mass element dm,, of air is delivered to the cylinder and is uniformly mixed throughout the cylinder volume. An equal amount of fluid, with the same proportions of air and burned gas as the cylinder contents at time t, leaves the cylinder during this time interval. Thus the mass of air delivered between t and t + dt which is retained, dm,, ,is given by qsc = A qsc = 1 + (6.22) indicates to what extent the residual gases in the cylinder have been replaced with fresh air. The purity of the charge: Purity = In real scavenging processes, mixing occurs as the fresh charge displaces the burned gases and some of the fresh charge may be expelled. Two limiting ideal models of this process are: (1) perfect displacement and (2) complete mixing. Perfect displacement or scavenging would occur if the burned gases were pushed out by the fresh gases without any mixing. Complete mixing occurs if entering fresh mixture mixes instantaneously and uniformly with the cylinder contents. For pegect displacement (with m,, as the reference mass in the delivery ratio), - (6.23) Assuming m,, is constant, this integrates over the duration of the scavenging Process to give -mar =I-expe) mtr Thus, for complete mixing, with the above definitions, indicates the degree of dilution, with burned gases, of the unburned mixture in the cylinder. t If scavenging is done with fuel-air mixture, as in spark-ignition engines, then mixture mass is used instead of air mass.

Figure 6-27 shows qrc and q,, for the perfect displacement and complete mixing assumptions as a function of A, the delivery ratio. -Perfect displacement --Perfect mixing 0 0 1.o 2.0 Delivery ratio, A FIGURE 6-27 Scavenging efficiency q , and trapping efficiency q,, versus delivery ratio A for perfect displacement and complete mixing models. An additional possibility is the direct flow of fresh mixture through the cylinder into the exhaust without entraining burned gases. This is called shortcircuiting; it is obviously undesirable since some fresh air or mixture is wasted. There is no simple model for this process. When short-circuiting occurs, lower scavenging efficiencies result even though the volume occupied by the shortcircuiting flow through the cylinder does displace an equal volume of the burned gases. Another phenomenon which reduces scavenging eficiency is the formation of pockets or dead zones in the cylinder volume where burned gases can become trapped and escape displacement or entrainment by the fresh scavenging flow. These unscavenged zones are most likely to occur in regions of the cylinder that remain secluded from the main fresh mixture flow path.

6.63 Actual Scavenging Processes Several methods have been developed for determining what occurs in actual cylinder scavenging processes.'' Accurate measurement of scavenging efficiency is dificult due to the problem of measuring the trapped air mass.

Estimation of & from indicated mean effective pressure and from gas sampling are the most reliable methods.' Flow visualization experi~nents'~-~~ in liquid analogs of the cylinder and flow velocity mapping techniques3' have proved useful in providing a qualitative picture of the scavenging flow field and identifying problems such as short-circuiting and dead volumes. Flow visualization studies indicate the key features of the scavenging process.

Figure 6-28 shows a sequence of frames from a movie of one liquid scavenging another in a model of a large two-stroke cycle loop-scavenged >a & 8$- $ diesel.29 The physical variables were scaled to maintain the same values of the appropriate dimensionless numbers for the liquid analog flow and the real engine flow. The density of the liquid representing air (which is dark) was twice the density of the liquid representing burned gas (which is clear). Early in the scavenging process, the fresh air jets penetrate into the burned gas and displace it first toward the cylinder head and then toward the exhaust ports (the schematic gives the location of the ports). During this initial phase, the outflowing gas contains no air; pure displacement of the burned gas from the cylinder is being achieved. Then short-circuiting losses start to occur, due to the damming-up or buildup of fresh air on the cylinder wall opposite the exhaust ports. The short-circuiting fluid flows directly between the scavenge ports and the exhaust ports above them. Since this damming-up of the inflowing fresh air back toward the exhaust ports continues, short-circuiting losses will also continue. While the scavenging front remains distinct as it traverses the cylinder, its turbulent character indicates that mixing between burned gas and air across the front is taking place. For both these reasons (short-circuiting and short-range mixing), the outflowing gas, once the "displacement" phase is over, contains an increasing amount of fresh air. Outflowing fluid composition measurements from this model study of a Sulzer two-stroke loop-scavenged diesel engine confirm this sequence of events. At 24 crank angle degrees after the onset of scavenging, fresh air due to shortcircuiting was detected in the exhaust. At the time the displacement front reached the exhaust port (65" after the onset of scavenging), loss of fresh air due to scavenging amounted to 13 percent of the scavenge air flow. The actual plot of degree of purity (or q,) versus delivery ratio (A) closely followed the perfect displacement line for A c 0.4. For A > 0.4, the shape of the actual curve was similar in 9 shape to the complete mixing curve.

Engine tests confirm these results from model studies. Initially, the ,; exhausted gas contains no fresh air ar mixture; only burned gas is being dis- ; placed from the cylinder. However, within the cylinder both displacement and ';' mixing at the interface between burned gas and fresh gas are occurring. The departure from perfect scavenging behavior is evident when fresh mixture first appears in the exhaust. For loop-scavenged engines this is typically when A zz 0.4. For uniflow scavenging this perfect scavenging phase lasts somewhat longer; for cross-scavenging it is over sooner (because the short-circuiting path is shorter). The mixing that occurs is short-range mixing, not mixing throughout the cylinder volume. The jets of scavenging mixture, on entering the cylinder, mix readily with gases in the immediate neighborhood of the jet efflux. More efficient scavenging-i.e., less mixing-is obtained by reducing the size of the inlet PO* while increasing their numbex." It is important that the jets from the inlet PO* slow down significantly once they enter the cylinder.

Otherwise the scavenging 4 front will reach the exhaust ports or valves too early. The jets are frequently directed to impinge on each other or against the cylinder wall. Swirl in uniflowscavenged systems may be used to obtain an equivalent result. The most desirable loop-scavenging flow is illustrated in Fig. 6-29. The X 3 I=- & Desirable air flow in loop-scavenged engine: air from the entering jets impinges on far cylinder wall and flows toward the cylinder head." :cavenging jets enter symmetrically with sufficient velocity to fill up about half the cylinder cross section, and thereafter flow at lower velocity along the cylinder wall toward the cylinder head. By proper direction of the scavenging jets it is possible to achieve almost no outflow in the direction of the exhaust from the cross-hatched stagnation zone on the opposite cylinder wall. In fact, measurement of the velocity profile in this region is a good indicator of the effectiveness of the scavenging flow. If the flow along the cylinder wall toward the head is stable, i.e., if its maximum velocity occurs near the wall and the velocity is near zero on the plane perpendicular to the axis of symmetry of the ports (which passes through the cylinder axis), the scavenging flow will follow the desired path. If there are "tongues" of scavenging flow toward the exhaust port, either in the center of the cylinder or along the walls, then significant short-circuiting will In uniflow-scavenged configurations, the inlet ports are evenly spaced around the full circumference of the cylinder and are usually directed so that the xavenging jets create a swirling flow within the cylinder (see Fig.

6-24). Results of measurements of scavenging front location in rig flow tests of a valved uniflow two-stroke diesel cylinder, as the inlet port angle was varied to give a wide range of swirl, showed that inlet jets directed tangentially to a circle of half the cylinder radius gave the most stable scavenging front profile over a wide range of condition~.~~ Though the scavenging processes in spark-ignition and diesel two-stroke engines are similar, these two types of engine operate with quite different delivery ratios. In mixture-scavenged spark-ignition engines, any significant expulsion of fresh fluid with the burned gas results in a significant loss of fuel and causes high hydrocarbon emissions as well as 10s of the energy expended in pumping the 244 INTERNAL COMBUSTION ENGINE FUNDAMENTALS flow which passes straight through the cylinder. In diesels the scavenging medium is air, so only the pumping work is lost. One consequence of this is that twostroke spark-ignition engines are usually crankcase pumped. This approach pro"ides the maximum pressure and thus also the maximum velocity in the scavenging medium at the start of the scavenging process just after the cylinder pressure has blown down; as the crankcase pressure falls during the scavenging process, the motion of the scavenging front within the cylinder also slows down Figure 6-30 shows the delivery ratio and trapping, charging, and scavenging eficiencies of two crankcase-scavenged spark-ignition engines as a function of engine speed. These quantities depend significantly on intake and exhaust port design and open period and the exhaust system configuration.3c36 For twostroke cycle spark-ignition engines, which use crankcase pumping, delivery ratios vary between about 0.5 and 0.8. Figure 6-31 shows scavenging data typical of large two-stroke diesek3' The purity (mass of air in trapped cylinder charge/mass of trapped cylinder charge) is shown as a function of the delivery ratio. The different scavenging configurations have different degrees of effectiveness, with uniflow scavenging being the most efficient. These diesel engines normally operate with delivery ratios in the range 1.2 to 1.4. 01 0.4 I 0.6 I 0.8 I 1.O I 1.2 I 1.4 1.6 Delivery ratio A FIGURE 6-31 Purity as a function of delivery ratio A for diierent types of large marine two-stroke diesel engines." 6.7 FLOW THROUGH PORTS Speed, revlmin FIGURE 630 Delivery ratio A, trapping efficiency q,,, charging efficiency qch.

and scavenging efficiency ir at fd load, as functions of speed for two single-cylinder two-stroke cycle spark-imition engins. Solid W' 147 an3displacement engine." Dashed line is loopscavenged 246 an3displacement engine." 5 The importance of the intake and exhaust ports to the proper functioning of the two-stroke cycle scavenging process is clear from the discussion in Sec.

6.6. The crank angle at which the ports open, the size, number, geometry, and location of the ports around the cylinder circumference, and the direction and velocity of the jets issuing from the ports into the cylinder all affect the scavenging flow. A summary of the information available on flow through piston-controlled ports can be found in Annand and Roe.16 Both the flow resistance of the inlet and exhaust port configurations, as well as the details of the flow pattern produced by the port system inside the cylinder during scavenging, are important. Figure 6-32 defines the essential geometrical characteristics of inlet ports. Rectangular ports make best use of the cylinder wall area and give precise timing control. Ports can be tapered, and may have axial and tangential inclination as shown. Figure 6-33 illustrates the flow patterns expected downstream of pistoncontrolled inlet ports. For small openings, the flow remains attached to the port Walls. For fully open ports with sharp corners the flow detaches at the upstream comers. Both a rounded entry and converging taper to the port help prevent flow detachment within the port. Discharge coefficients for ports have been measured as a function of the open fraction of the port, the pressure ratio across the port, x 1, corner radius r L Height / * Axial convergence Y//h 0 Sharp entry, circular ports h, Open height X Sharp enuy. square ports I I 0.2 0.4 0.6 1.o FIGURE 6 3 4 Discharge coefficients as a function of port open fraction (uncovered height/port height) for different inlet port designs. Pressure ratio across port = 2.35.1•‹ FIGURE 6 3 2 Parameters which define geometry of inlet port^.'^ and port geometry and inclination (see Ref. 16 for a detailed summary). The most appropriate reference area for evaluating the discharge coefficient is the open area of the port (see Fig.

6-32). For the open height h, less than (Y - r) but greater than r this is (6.30) A, = Xh, - 0.43r2 -3 B where Y is the port height, X the port width, and r the corner radius. For h, = Y, 33 4 the reference area is ** (6.31) % AR = X Y - 0.86r2 The effect of variations in geometry and operating conditions on the discharge coefficient C, can usually be interpreted by reference to the flow patterns illustrated in Fig. 6-33.

The effects of inlet port open fraction and port geometry on CD are shown in Fig. 6-34: geometry effects are most significant at small ad large open fraction^.^' CD varies with pressure ratio, increasing as the pressure ratio increases. Empirical relations that predict this variation with pressure ratio have been de~eloped.~' Tangentially inclined inlet ports are used when swirl is desired to improve scavenging or when jet focusing or impingement within the cylinder off the cylinder axis is required (see Sec. 6.6.3). The discharge coelfcient decreases as the jet tangential inclination increases. The jet angle and the port angle can deviate significantly from each other depending on the details of the port design and the open fraction.31 In piston-controlled exhaust ports, the angle of the jet from a thin-walled cxhaust port increases as indicated in Fig. 6-35.31 In thick ports, the walls are 4) I I I I - - - Uli - fQ F i O I I 20 40 I 60 I 80 100 Uncovered pon height, % (a) I 0.8 Port opm fraction &R Axial inclination 1 0.60 (b) FIGURE 6 3 3 Flow pattern through piston-controkd inlet ports: (a) port axis perpendicult to w d ; small 0and large opening witb sharp and rounded entry; (b) port axis inclined.16 n C U ~635 ~ b& o f i t exiting exhaust p n as a function of open port height." Port open fraction FIGURE 636 Discharge coefficient of a single rectangular exhaust port (7.6 mm wide x 12.7 mm high) in the wall d a 51-nun bore cylinder as a function of open fractipn and pressure ratio. Steady-ilow rig tests a 21.C p, = cylinder pressure, pe =; exhaust system usually tapered to allow the outward flow to diffuse. The pressure ratio acros the exhaust ports varies substantially during the exhaust process. The pressure ratio has a significant effect on the exhaust port discharge coefficient, as shown in Fig.

6-36. The changes in exit jet angle and separation point explain the effects d increasing open fraction and pressure ratio. The discharge coefficient also increases modestly with increasing gas temperature.39 6.8 SUPERCHARGING AND TURBOCHARGING 6.8.1 Methods of Power Boosting The maximum power a given engine can deliver is limited by the amount of fud that can be burned eficiently inside the engine cylinder. This is limite amount of air that is introduced into each cylinder each cycle. If the ind is compressed to a higher density than ambient, prior to entry into the the maximum power an engine of fixed dimensions can deliver will be incre This is the primary purpose of supcnharging; Eqs. (2.39) to (2.41) show b power, torque, and mean effective pressure are proportional to inlet air de& # -F 3 The term supercharging refers to increasing the air (or mixture) density by increasingits pressure prior to entering the engine cylinder. Three basic methods used to accomplish this. The first is mechanical supercharging where a %prate pump or blower or compressor, usually driven by power taken from the engine,provides the compressed air. The second method is turbocharging, where turbocharger-a compressor and turbine on a single shaft-is used to boost the inlet air (or mixture) density. Energy available in the engine's exhaust stream is used to drive the turbocharger turbine which drives the turbocharger compressor which raises the inlet fluid density prior to entry to each engine cylinder. The method-pressure wave supercharging-uses wave action in the intake and exhaust systems to compress the intake mixture. The use of intake and exhaust tuning to increase volumetric efficiency (see Sec. 6.2.2) is one example of this method of increasing air density. An example of a pressure wave supercharging device is the Comprex, which uses the pressure available in the exhaust stream to compress the inlet mixture stream by direct contact of the fluids in narrow flow channels (see Sec.

6.8.5). Figure 6-37 shows typical arrangements of the different supercharging and turbocharging systems. The most common arrangements use a mechanical supercharger (Fig. 6-37a) or turbocharger (Fig. 6-376). Combinations of an engine-driven compressor and a turbocharger (Fig. 6-37c) are used (e.g., in large marine engines; Fig. 1-24). Two-stage turbocharging (big. 6-374 is one viable approach for providing very high boost pressures (4 to 7 atm) to obtain higher engine brake mean effective pressures. Turbocompounding, i.e., use of a second turbine in the exhaust directly geared to the engine drive shaft (Fig. 6-37e), is an alternative method of increasing engine power (and cfkiency). Charge cooling with a heat exchanger (often called an aftercooler or intercooler) after compression, prior to entry to the cylinder, can be used to increase further the air or mixture density as shown in Fig. 6-371: Supercharging is used in four-stroke cycle engines to boost the power per unit displaced volume. Some form of supercharging is necessary in two-stroke cycle engines to raise the fresh air (or mixture) pressure above the exhaust pressure so that the cylinder can be scavenged effectively. With additional boost in two-stroke cycle engines, the power density is also raised. This section reviews the operating characteristics of the blowers, compressors, turbines, and wavecompression devices used to increase inlet air or mixture density or convert exhaust-gas availability to work. The operating characteristics of suprcharged and turbocharged engine systems are discussed in Chap. 15. 6.8.2 Basic Relationships Expressions for the work required to drive a blower or compressor and the work Produced by a turbine are obtained from the first and second laws of thermodynamics. The first law, in the form of the steady flow energy equation, applied to a c0Nrol volume around the turbomachinery component is 0 is the heat-transfer rate into the control volume, @is the shaft workrnnsfer rate out of the control volume, m is the mass flow, h is the specific enthjpy, c2/2 is the specific kinetic energy, and gz is the specific potential energy (whichis not important and can be omitted). A stagnqtion or total enthalpy, ho ,can be defined as C2 ho=h+2 (6.33) For an ideal gas, with constant specific heats, a stagnation or total temperature follows from Eq. (6.33): C2 &=Ti-(6.34) *cP A stagnation or total pressure is also defined: it is the pressure attained if the gas is isentropically brought to rest: Q in Eq. (6.32) for pumps, blowers, compressors, and turbines is usually small enough to be neglected. Equation (6.32) then gives the work-transfer rate as - *=M ~ o . out ho. ~ n) (6.36) A component eficiency is used to relate the actual work-transfer rate to the work-transfer rate required (or produced) by an equivalent reversible adiabatic device operating between the same pressures. The second law is then used to determine this reversible adiabatic work-transfer rate, which is that occurring in an isentropic process. For a compressor, the compressor isentropic eflciency qc is 'lc = reversible power requirement actual power requirement Figure 6-38 shows the end states of the gas passing through a compressor on an h-s diagram. Both static (p,, p,) and stagnation (pol, po2) constant-pressure lines are shown. The total-to-total isentropic eficiency is, from Eq. (6.37), which, since cp is essentially constant for air, or fuel-air mixture, becomes VCTT = FlGURE 637 Suprchnrging and turboeharging configurations: (a) mechanical supercharging;(b) turbochar&&; (4 en&edriuen compressor and turbocharger; (d) two-stage turboeharging; (e) turbochar&& turbocompounding; (f)turbocharger with intercooler. C Comprasor. E Engine, 1 inter-cooler* Turbine. To,. - To1 T,, - To, Since the process 01 to 02s is isentropic, the blower or compressor. Thus the power required to drive the device, - Wc,, , d l be ,&ere q, is the blower or compressor mechanical efficiency.

Figure 6-39 shows the gas states at inlet and exit to a turbine on an h-s diagram. State 03 is the inlet stagnation state; 4 and 04 are the exit static and states, respectively. States 4s and 04s define the static and stagnation efit states of the equivalent reversible adiabatic turbine. The turbine isentropic 4ciency is defined as FIGURE 6-38 Enthalpy-entropy diagram for compressor. lnld state 01, exit state 2; equivalent isentropic wm. Dressor exit state 2s. ' actual power output "= reversible power output n u s , the total-to-total turbine eficiency is Equation (6.39) becomes If the exhaust gas is modeled as an ideal gas with constant specific heats, then Eq. (6.45) can be written In deriving Eq. (6.40) it has been tacitly assumed that the kinetic energy pressure head (p, - p,) can be recovered. In internal combustion engine applications the compressor feeds the engine via a large manifold, and much of this kinetic energy will be dissipated. The blower or compressor should be designed for effective recovery of this kinetic energy before the exit duct. Since the kinetic energy of the gas leaving the compressor is not usually recovered, a more realistic definition of efficiency is based on exit static c ~ n d i t i o n s : ~ ~ Note that for exhaust gas over the temperature range of interest, e, may vary significantlywith temperature (see Figs. 4-10 and 4-17).

This is termed the total-to-static efficiency. The basis on which the efficiency b s$ Ecalculated should always be clearly stated. 3" The work-transfer rate or power required to drive the compressor b 9 3: obtained by combining Eq. (6.36), the ideal gas model, and Eq. (6.40): @ A where the subscript i denotes inlet mixture properties.

If q,, is used to define compressor performance, then p, replaces po, in Eq. (6.42). Equation (6.42)$ the thermodynamic power requirement. There will also be mechanical loss6 s FIGURE 6-39 Enthaipy-entropy diagram for a turbine. Inlet state 03, exit state 4; equivalent isentropic turbine exit state 4s. 254 MTERNAL COMBUSTION ENGINE FUNDAMENTALS For a particular device, the dimensions are fixed and the value of R is fixed. SO it Since the kinetic energy at the exit of a turbocharger turbine is usually wasted, a total-to-static turbine isentropic effciency, where the reversible batic power output is that obtained between inlet stagnation conditions and the exit static pressure, is more realistic:40 Vns = bas become the convention to plot (To~/To~) - h04 - T03 - T04 - 1 - @4/pO3)"- ''IY To, - Tk ho3 - h, h03 in is referred to as the corrected mass flow; N /& is referred to as the corrected speed. The disadvantage of this convention of removing D and R is that the groups of variables are no longer dimensionless, and performance plots or maps relate to a specific machine. Compressor characteristics are usually plotted in terms of the pressure ratio @02/p01) or (PJPOI)against the corrected mass flow (lit&/po,) along lines of ~ ~ n s t a corrected nt s p e d (N/&). Contours of constant effciency are superposed. Similar plots are used for turbines: po3/p4 against lit&/po3 along lines of constant N/&. Since these occupy a narrow region of the turbine performance map, other plots are often used (seeSec. 6.8.4). h&~po, I The power delivered by the turbine is given by [Eqs. (6.36) and (6.4611 where the subscript e denotes exhaust gas properties. If the total-to-static turbine efficiency(qns) is used in the relation for wT, then p4 replaces po4 in Eq. (6.48). With a turbocharger, the turbine is mechanically linked to the compressor. Hence, at constant turbocharger speed, * - where q, is the mechanical efficiency of the turbocharger. The mechanical losses are mainly bearing friction losses. The mechanical effciency is usually combined with the turbine efficiency since these losses are difficult to separate out. It is advantageous if the operating characteristics of blowers, compressors, and turbines can be expressed in a manner that allows easy comparison between different designs and sizes of devices.

This can be done by describing the performance characteristics in terms of dimensionless numbers?' The most important dependent variables are: mass flow rate m, component isentropic efficiency q.

and temperature diffqrence across the device ATo. Each of these are a function d the independent variables : po. in ,po,out (or pout),T,,in , N(speed), ~(characteisf~ dimension), R(gas constant), y (cJc,),and p(viscosity); i.e., By dimensional analysis, these eight independent variables can be reduced to four dimensionless groups : ND RT,, PO.in Po.out , (6.51) PO,in ' PD ' The Reynolds number, rh/(pD), has little effect on performance and y is fixed by $1 P' t the gas. Therefore these variables can be omitted and Eq. (6.51) becomes.

ND PO.i n D Z TO,in RTo,in PO.in 6.83 Compressors practical mechanical supercharging devices can be classified into: (1) sliding vane compressors, (2) rotary compressors, and (3) centrifugal compressors.

The first two types are positive displacement compressors; the last type is an aerodynamic compressor. Four different types of positive displacement compressors are illustrated in Fig. 6-40.

In the sliding vane compressor (Fig. 6-40a), deep slots are cut into the rotor to accommodate thin vanes which are free to move radially. The rotor is mounted eccentrically in the housing. As the rotor rotates, the centrifugal forces acting on the vanes force them outward against the housing, thereby dividing the crescent-shaped space into several compartments. Ambient air is drawn through the intake port into each compartment as its volume increases to a maximum.

The trapped air is compressed as the compartment volume decreases, and is then discharged through the outlet port. The flow capacity of the sliding vane compressor depends on the maximum induction volume which is determined by the housing cylinder bore, rotor diameter and length, eccentricity, number of vanes, dimensions of the inlet and outlet ports. The actual flow rate and pressure rise at constant speed will be reduced by leakage. Also, heat transfer from the moving vanes and rotor and stator surfaces will reduce compression efficiency unless cooling is used to remove the thermal energy generated by friction between the vanes, and the rotor and stator. l 3 e volumetric efficiency can vary between 0.6 and 0.9 depending on the size of the machine, the quality of the design, and the method of lubrication and cooling employed. The displaced volume V, is given by .here r is the rotor radius, E the eccentricity, and 1 the axial length of the cornp w o r . The mass flow rate parameter is + = constant x piq,,N~l(Zr ~0lpstd *here qc is the device volumetric efficiency,N its speed, and the subscripts i, 0 and std refer to inlet, inlet stagnation, and standard atmospheric conditions, nspectively. Figure 6-41 shows the performance characteristics of a typical vane compressor. The mass flow rate at constant speed depends on the pressure ratio only through its (weak) effect on volumetric efficiency. The isentropic is relatively low.41 An alternative positive displacement supercharger is the roots blower (Fig. w b) . The two rotors are connected by gears. The working principles are as follows.

Air trapped in the recesses between the rotor lobes and the housing is carried toward the delivery port without significant change in volume. As these recesses open to the delivery line, since the suction side is closed, the trapped air is suddenly compressed by the backflow from the higher-pressure delivery line. This intermittent delivery produces nonuniform torque on the rotor and pressure pulses in the delivery line. Roots blowers are most suitable for small pressure ratios (about 1.2). The volumetric efficiency depends on the running clearances, rotor length, rotational speed, and pressure ratio. In the three-lobe machines shown (two lobes are sometimes used) the volume

air pressure ratio plotted versus net air volume flow rate (total air flow less scavenging air flow).46 274 INTERNAL COMBUSTION ENGINE FUNDAMENTALS PROBLEMS 6.1. A conventional spark-ignition engine operating with gasoline will not run smoothfy (due to incomplete combustion) with an equivalence ratio leaner than about = 0.8. It is desirable to extend the smooth operating limit of the engine to leaner equivalence ratios so that at part-throttle operation (with intake pressure less than 1 atmosphere) the pumping work is reduced. Leaner than normal operation can k a ~ h i e ~ eby d adding hydrogen gas (H,) to the mixture in the intake system. The addition of H, makes the fuel-air mixture easier to bum. (a) The fuel composition with "mixed" fuel operation is H, C8H18--one mole of hydrogen to every mole of gasoline, which is assumed the same as is~octan~. What is the stoichiometric air/fuel ratio for the "mixed" fuel? (b) The lower heating value of Hz is 120 MJ/kg and for isooctane is 44.4 MJ/kg What is the heating value per kilogram of fuel mixture? (c) Engine operation with isooctane and the mixed (H, + C,H,,) fuel is Compared in a particular engine at a part-load condition (brake mean effective pressure of 275 kPa and 1400 revfmin). You are given the following information about the engine operation: + Fuel Equivalence ratio Gross indicated fuel conversion efficiency Mechanical rubbing friction mep Inlet manifold pressure Pumping mep C8HV3 0.8 0.35 138 kPa 46 kPa 55 kPa Hz + C8H18 0.5 0.4 138 kPa ? ? Estimate approximately the inlet manifold pressure and the pumping mean effective pressure with (H, + C,H,,) fuel. Explain your method and assumptions clearly. Note that mechanical efficiency q, is defined as bmep lmep, qm=-= bmep bmep + rfmep + pmep Hydrogen is a possible future fuel for spark-ignition engines. The lower heating value of hydrogen is 120 MJ/kg and for gasoline (C,H,,) is 44 MJ/kg. The stoichio. metric air/fuel ratio for hydrogen is 34.3 and for gasoline is 14.4. A disadvantage of hydrogen fuel in the SI engine is that the partial pressure of hydrogen in the Hz-air mixture reduces the engine's volumetric efficiency, which is proportional to the partial pressure of.air. Find the partial pressure of air in the intake manifold downstream of the hydrogen fuel-injection location at wide-open throttle when the total intake manifold pressure is 1 atmosphere; the equivalence ratio is 1.0. Then estimate the ratio of the fuel energy per unit time entering a hydrogen-fueled engine operating with a stoichiometric mixture to the fuel energy per unit time entering an identical gasoline-fueled engine operating at the same speed with a stoichiometric mixture(Note that the "fuel energy" per unit mass of fuel is the fuel's heating value.) 6.3. Sketch (a) shows an ideal cycle p-V diagram for a conventional throttled sparkignition engine, 1-2-345-6-7-1. The gas properties c,, c,, y, R throughout the cydc are constant. The mass of gas in the cylinder is m. The exhaust pressure is p,. Sketch (b) shows an ideal cycle p V diagram 1-2-3-4-5-6-8-1 for a sparkignition engine with novel inlet valve timing. The inlet manifold is unthrottled; it h s essentially the same pressure as the exhaust. To reduce the mass inducted at @ &4. 6.2. 65. 6-6. 6.7. load, the inlet valve is closed rapidly partway through the intake stroke at point 8. The gas in the cylinder at inlet valve closing at 8 is then expanded isentropically to 1 with the inlet valve closed. The pressure p , at the start of compression is the same for both cycles. (a) Indicate on p V diagrams the area that corresponds to the pumping work per cycle for cycles (a) and (b). Which area is greater? (b) Derive expressions for the pumping work per cycle Wp in terms of m, c,, y, TI, (pJp,), and the compression ratio r, for cycles (a) and (b). Be consistent about the signs of the work transfers to and from the gas. (c) For y = 1.3, r, = 8, and (pJp,) = 2 find the ratio Wp(b)/Wp(a),assuming the values of T, and m are the same in both cases. For four-stroke cycle engines, the inlet and exhaust valve opening and closing crank angles are typically: IVO 15" BTC; IVC 50" ABC; EVO 55" BBC; EVC 10' ATC. Explain why these valve timings improve engine breathing relative to valve opening and closing at the beginnings and ends of the intake and exhaust strokes.

Are there additional design issues that are important? Estimate approximately the pressure drop across the inlet valve about halfway through the intake stroke and across the exhaust valve halfway through the exhaust stroke, when the piston speed is at its maximum for a typical four-stroke cycle spark-ignition engine with B = L = 85 mm at 2500 and 5000 revfmin at WOT. Assume appropriate values for any valve and port geometric details required, and for the gas composition and state.

Using the data in Fig. 6-21, estimate the fraction of the original mass left in the cylinder: (a) at the end of the blowdown process and (b) at the end of the exhaust stroke. Compare the engine residual gas fraction data in Fig. 6-19 with ideal cycle estimates of residual gas fraction as follows. Using Eq. (5.47) plot the fuel-air cycle residual mass fraction x, against pip, for re = 8.5 on the same graph as the engine data in Fig. 6-19 at 1400 revlmin and 27" valve overlap. Assume T, = 1400 K and (y - 1)/ ./ = 0.24 in Eq.(5.47).

Suggest an explanation for any significant difference. INTERNAL COMBUSTION ENGINE FUNDAMENTALS One concept that would increase SI engine efficiency is early intake valve closing (EIVC) where the intake valve closes before the piston reaches BC o n the intake stroke, thus limiting the amount of charge inducted into the cylinder. (a) Explain why EIVC improves engine efficiency a t part load. (Hint: consider what must happen to the inlet manifold pressure in order to maintain constant mass in the cylinder as the intake valve is closed sooner.) (b) This part load reduction in charge could be achieved by using late intake valve closing where the intake valve is not closed until the compression stroke has pushed some of the cylinder gases back out into the intake manifold. Based on a comparison of p-V diagrams, is this method inferior to EIVC? 6.9. An eight-cylinder turbocharged aftercooled four-stroke cycle diesel engine operata with a n inlet pressure of 1.8 atmospheres a t its maximum rated power a t 2000 rev/ min. B = 128 mm, L = 140 mm, q, (based o n inlet manifold conditions of 1.8 atm and 325 K after the aftercooler) = 0.9. T h e compressor isentropic efficiency is 0.7. (a) Calculate the power required to drive the turbocharger compressor.

(b) If the exhaust gas temperature is 650•‹Ca n d the turbocharger isentropic efficiency is 0.65, estimate the pressure at turbine inlet. The turbine exhausts to the atmosphere.

SAERecommended Practice, "Engine Terminology and Nomenclaturdeneral," in SAE Handbook, J604d. . 6.10. The charging efficiency of two-stroke cycle diesel engines can be estimated from measurement of the concentration of 0, a n d CO, in the burned gases within the cylinder, o r in the exhaust blowdown pulse prior t o any mixing with fresh air. The engine bore = 125 mm, stroke = 150 mm, compression ratio = 15. The fuel flow rate a t 1800 revlmin is 1.6 g/s per cylinder. T h e conditions used to evaluate the air density for the reference mass are 300 K a n d 1 atm. The molar concentrations (dry) of CO, a n d 0, in the in-cylinder burned gases are 7.2 and 10.4 percent (see Fig. 4-22). T h e scavenging air flow rate is 8 0 g/s. Evaluate (a) the charging efficiency, (b) the delivery ratio, and (c) the trapping efficiency (assuming the trapped mass equals the reference mass). REFERENCES 1. Khovakh, M.: Motor Vehicle Engines, English Translation, Mir Publishers, Moscow, 1976. 2. Matsuoka, S., Tasaka, H., and Tsuruta, J.: "The Evaporation of Fuel and Its Effect on Volumetric Efficiency," JAR1 technical memorandum no. 2, pp. 17-22, 1971. 3. Takiuawa, M., Uno, T., Oue, T., and Yura, T.: "A Study of Gas Exchange Process Simulation of an Automotive Multi-Cylinder Internal Combustion Engine," SAE paper 820410, SAE T r m vol. 91, 1982. 4. Kay, I. W.: "Manifold Fuel Film Effects in an SI Engine," SAE paper 780944, 1978. 5. Ohata, A., and Ishida, Y.: "Dynamic Inlet Pressure and Volumetric Efficiency of Four Cycle Four Cylinder Engine," SAE paper 820407, SAE Trans., vol. 91,1982. 6. Benson, R. S., and Whitehouse, N. D.: Internal Combustion Engines, vol. 2, Pergamon Press, 1979.

7. Tavlor., C. F.: The Internal-Combustion Engine in Theory and Practice, vol. 1,2d ed., revised, M1T Press, Cambridge, Mass., 1985.

8. Hofbauer, P., and Sator, K.: "Advanced Automotive Power Systems, Part 2: A Diesel for Subcompact Car," SAE paper 770113, SAE Trans., vol. 86,1977. 9. Annstrong, - D. L., and Stirrat, G. F.: "Ford's 1982 3.8L V6 Engine," SAE paper 820112, SAE Trans, vol. 91, 1982. 10. Chapman, M., Novak, J. M., and Stein, R. A.: "Numerical Modeling of Inlet and Exhaust n o m in Multi-Cylinder Internal Combustion Engines," in Flows in Internal Combustion En9iws Winter Annual Meeting, ASME, New York, 1982. 14. Kstner, L. J, Williams, T. J., and White, J. B.: "Poppet Inlet Valve Characteristics and Their influence on the Induction P ~ ~ C ~ SProc. S , " Instn Mech. Engrs, vol. 178, pt. 1, no. 36, pp. 951-978, 1963-1964. 15, woods, W. A., and Khan, S. R.: "An Experimental Study of Flow through poppet valvW" h. [u r n Mech. E w s , vol. 180, pt. 3N, . pp. . 3241,1965-1966. 16. ~nnand,W.J. D., and Roe, G. E.: Gas Flow in the Internal Combustion Engine, Haessner Publishing, Newfoundland, NJ., 1974. 17. Tanaka, K.: "Air Flow through Exhaust Valve of Conical Seat," Int. Congr. Appl. Mech., vol. 1, 00. 287-295,1931. . 18. Bicen, A. F., and Whitelaw, J. H.:"Steady and Unsteady Air Flow through an Intake Valve of a ~eciprocatingEngine," in Flows in Internal Combustion Engines-41, FED-"01.20, Winter Annual Meeting, ASME, 1984. 19. Fukutani, I., and Watanabe, E.: "An Analysis of the Volumetric Efficiency Characteristics of +Stroke Cycle Engines Using the Mean Inlet Mach Number Mim," SAE paper 790484, SAE Trans., vol. 88, 1979. 3. Wallace, W. B.: "High-Output Medium-Speed Diesel Engine Air and Exhaust System Flow Losses," Proc. Instn Mech. Engrs, vol. 182, pt. 3D, pp. 134-144,1967-1968. 21. Cole, B. N., and Mills, B.: "The Theory of Sudden Enlargements Applied to Poppet ExhaustValve, with Special Reference to Exhaust-Pulse Scavenging," Proc. Instn Mech. Engrs, pt. lB, pp. 364-378.1953. 22. Toda, T., Nohira, H., and Kobashi, K.: "Eva!uation of Burned Gas Ratio (BGR) as a Predominant Factor to NO,," SAE paper 760765, SAE Trans., vol. 85,1976. 23. Benson, J. D., and Stebar, R. F.: "Effects of Charge Diluation on Nitric Oxide Emission from a Single-CylinderEngine," SAE paper 710008, SAE Trans., vol. 80,1971. 2 4 Tabaczynski, R. J., Heywood, J. B., and Keck, J. C.: "Time-Resolved Measurements of Hydrocarbon Mass Flow Rate in the Exhaust of a Spark-Ignition Engine," SAE paper 720112, SAE Trans., vol. 81. 1972. 25. Caton, J. A., and Heywood, J. B.: "An Experimental and Analytical Study of Heat Transfer in an Engine Exhaust Port," Int. J. Heat Mass Transfer, vol. 24, no. 4, pp. 581-595,1981.

26. Caton, J. A.: "Comparisons of Thermocouple, Time-Averaged and Mass-Averaged Exhaust Gas Temperatures for a Spark-Ignited Engine," SAE paper 820050,1982. 27. Phatak, R. G.: UA New Method of Analyzing Two-Stroke Cycle Engine Gas Flow Patterns," SAE paper 790487, SAE Trans., vol. 88,1979. 28. Rizk, W.: "Experimental Studies of the Mixing Processes and Flow Configurations in Two-Cycle Engine Scavenging," Proc. Instn Mech. Engrs, vol. 172, pp. 417437,1958. 29. Dedeoglu, N.: "Scavenging Model Solves Problems in Gas Burning Engine," SAE paper 710579, SAE Trans., vol. 80, 1971. 30. Sher, E.: "Investigating the Gas Exchange Process of a Two-Stroke Cycle Engine with a Flow Visualization Rig," Israel J. Technol, vol. 20, pp. 127-136,1982. 31. Jante, A.: "Scavenging and Other Problems of Two-Stroke Cycle Spark-Ignition Engines," SAE paper 680468, SAE Trans.. vol. 77,1968. 32. Kannappan, A.: "Cumulative Sampling Technique for Investigating the Scavenging Process in Two-Stroke Engine," ASME paper 74-DGP-11, 1974. 33. Ohigashi, S., Kashiwada, Y., and Achiwa, J.: "Scavenging the 2-Stroke Diesel Engine," Bull. JSME, vol. 3, no. 9, pp. 13&136,1960. 34 Huber, E. W.: "Measuring the Trapping Eficiency of Internal Combustion Engines through Continuous Exhaust Gas Analysis," SAE paper 710144, SAE Trans., vol. 80,1971. Blair, G. P., and Kenny, R. G.: "Further Developments in Scavenging Analysis for Two-Cycle Engines," SAE paper 800038, SAE Trans., vol. 89,1980. . * - 36. Baudequin. F, and Rochelle, P.: "Some Scavenging Models for Two-Stroke Engines," Proc. lwn Mech. Engrs, Automobile Division, vol. 194,no. 22,pp. 203-210,1980. 37. Gyssler, G.:"Problems Associated with Turbocharging Large Two-Stroke Diesel Engines," proc. C~MAC,paper B.16,1965. 38. Armand, W. J. D.: "Compressible Flow through Square-Edged Orifices: An Empirical Approx. imation for Computer Calculations;" J. Mech. Engng Sci, vol. 8,p. 448,1966.

39. Benson, R. S.: "Experiments on a Piston Controlled Port," The Engineer, vol. 210,pp. 875-g~ .- CHAPTER 1960. M. S.: Turbocharging the Internal Combustion Engine, Wiley-Intersdena publications, John Wdey, New York, 1982. 41. F. S.: "Supercharging Compressors-Problems and Potentid of the Various Altema. .-.Bhinder, tives," SAE paper 840243,1984. 42 Bhinder. F.S.: "Some Fundamental Considerations Concerning the Pressure Charging of S m a Diesel Engines," SAE papa 830145,1983. 43. Brandstetter, W, and Dziggel, R.: "The 4- and 5-Cylinder Turbocharged Diesel Engines for Volkswagen and Audi," SAE paper 820441,SAE Trans., vol. 91,1982 44. SAE Recommended Practice, "Turbocharger Nomenclature and Terminolo%y," in SAE Hadbook,J922. 45. Flynn, P. F.: "Turbocharging Four-Cycle Diesel Engines," SAE paper 790314,SAE Trans., vol 88,1979. 46. Gyannathy. G.: "How D&S the Comprex PressunWave Supercharger Work?" SAE paper 830234,1983. 47. Kollbmnner, T. A.: "Comprex Supercharging for Passenger Diesel Car Engines," SAE paper 800884,SAE Trans., vol. 89,1980. dn. Watson. .. -- ,N...

and Janota, SI ENGINE FUEL METERING AND MANIFOLD ' 7.1 SPARK-IGNITION ENGINE MIXTURE REQUIREMENTS The task of the engine induction and fuel systems is to prepare from ambient air and fuel in the tank an air-fuel mixture that satisfies the requirements of the engine over its entire operating regime. In principle, the optimum airlfuel ratio for a spark-ignition engine is that which gives the required power output with the lowest fuel consumption, consistent with smooth and reliable operation. In practice, the constraints of emissions control may dictate a different airlfuel ratio, and may also require the recycling of a fraction of the exhaust gases (EGR) into the intake system. The relative proportions of fuel and air that provide the lowest fuel consumption, smooth reliable operation, and satisfy the emissions requirements, at the required power level, depend on engine speed and load. Mixture requirements and preparation are usually discussed in terms of the airlfuel ratio 0' fuellair ratio (see Sec. 2.9) and percent EGR [see Eq. (4.2)]. While the fuel metering system is designed to provide the appropriate fuel flow for the actual air flow at each speed and load, the relative proportions of fuel and air can be stated more generally in terms of the fuellair equivalence ratio 4, which is the actual fuel/air ratio normalized by dividing by the stoichiometric fuellair ratio [Eq. SI ENGME FUEL METERING AND MANIFOLD PHENOMENA (3.8)]. The combustion characteristics of fuel-air mixtures and the properties of combustion products, which govern engine performance, efficiency, and emissions, correlate best for a wide range of fuels relative to the st~ichiometfi~ mixture proportions. Where appropriate, therefore, the equivalence ratio will be used as the defining parameter. A typical value for the stoichiometric air/fuel ratio of gasoline is 14.6.t Thus, for gasoline, The effects of equivalence ratio variations on engine combustion, emission% and performance are discussed more fully in Chaps. 9, 11, and 15. A brief summary is sufficient here. Mixture requirements are different for full-load (wideopen throttle) and for part-load operation. At the former operating condition, complete utilization of the inducted air to obtain maximum power for a given displaced volume is the critical issue. Where less than the maximum power at a given speed is required, efficient utilization of the fuel is the critical issue. At wide-open throttle, maximum power for a given volumetric efficiency is obtained with rich-of-stoichiometric mixtures, 4 x 1.1 (see the discussion of the fuel-air cycle results in Sec. 5.5.3). Mixtures that are richer still are sometimes used to increase volumetric efficiency by increasing the amount of charge cooling that accompanies fuel vaporization [see Eq. (6.5)], thereby increasing the inducted air density. At part-load (or part-throttle) operating conditions, it is advantageous to dilute the fuel-air mixture, either with excess air or with recycled exhaust gas. This dilution improves the fuel conversion efficiency for three reasons:' (1) the expansion stroke work for a given expansion ratio is increased as a result of the change in thermodynamic properties of the burned gases-see Sees. 5.5.3 and 5.7.4; (2) for a given mean effective pressure, the intake pressure increases with increasing dilution, so pumping work decreases-see Fig. 5-10; (3) the heat losses to the walls are reduced because the burned gas temperatures are lower. In the absence of strict engine NO, emission requirements, excess air is the obvious diluent, and at part throttle engines have traditionally operated lean.

When tight control of NO,, HC, and CO emissions is required, operation of the engine with a stoichiometric mixture is advantageous so that a three-way catalyst$ can be used to clean up the exhaust.

The appropriate diluent is then recycled exhaust gases which significantly reduces NO, emissions from the engine itself. The amount of diluent that the engine will tolerate at any given speed and load depends on the details of the engine's combustion process. Increasing excess ah 281 the amount of recycled exhaust slows down the combustion process and *eases its variability from cycle to cycle. A certain minimum combustion npeatability or stability level is required to maintain smooth engine operation.

Deterioration in combustion stability therefore limits the amount of dilution an can tolerate. As load decreases, less dilution of thefresh mixture can be tolerated because the internal dilution of the mixture with residual gas increases (S Sec. 6.4). At idle conditions, the fresh mixture will not usually tolerate any EGR and may need to be stoichiometric or fuel-rich to obtain adequate combustion stability. Mixture composition requirements over the engine load and speed range illustrated schematically for the two approaches outlined above in Fig. 7-1. If sloichiometri~operation and EGR are not required for emissions control, as load increases the mixture is leaned out from a fuel-rich or close-to-stoichiometric composition at very light load. As wide-open throttle operation is approached at each engine speed, the mixture is steadily enriched to rich-of-stoi~hiomet~ic at the maximum bmep point. With the stoichiometric operating conditions required for three-way-catalyst-equipped engines, when EGR is used, the percentage of recycled exhaust increases from zero at light load to a maximum at mid-load, and then decreases to zero as wide-open throttle conditions are approached so maximum bmep can be obtained. Combinations of these strategies are possible. For example, lean operation at light load can be used for best efficiency, and Mid 1 / - 12 High speed -14 - 4 F 16 - 18 V 100% Intake mass Row rate CURE t Typical value only.

Most gasolines have (AIF), in the range 14.4 to 14.7. (AIF), could lie betw14.1 and 15.2. t A three-way catalyst system, when operated with a close-to-stoichiomtrk mixture, achier6 sub stantial reductions in NO,, CO, and HC emissions simultaneously;see Sec. 11.6.2. 7-1 mixture requirements for two common operating strategies: Top diagram shows equinlenc. nt10 Vanation with intake mass flow rate (percent of maximum flow at rated speed) at constant low, and high engine speeds. Bottom diagram shows recycled exhaust (EGR) schedule as a function of ntdi~ flow rate, for low, mid, and high speeds for stoichiometricoperation. 282 INTERNAL COMBUSTION ENGINE FUNDAMENTALS stoichiometric mixtures (with a three-way catalyst) and/or EGR can be used at mid loads to control NO, emissions. In practical spark-ignition engine induction systems, the fuel and air dL, tribution between engine cylinders is not uniform (and also varies in each individ, ual cylinder on a cycle-by-cycle basis). A spread of one or more airffuel ratior between the leanest and richest cylinders over the engine's load and speed ran& is not uncommon in engines with conventional carburetors. The average mixture must be chosen to avoid excessive combustion variability in the leanest operating cylinder. Thus, as the spread in mixture nonunifomity increases. the mean equivalence ratio must be moved toward stoichiometric and away from the equivalence ratio which gives minimum fuel consumption. FIGURE 7-2 Schematic of elementary carburetor. 1 Iniet section 2 Venturi throat 3 Float chamber 4 Pressure equalizing passage 5 Calibrated orifice 6 Fuel discharge tube 7 Throttle plate 7.2 CARBURETORS 7.2.1 Carburetor Fundamentals A carburetor has been the most common device used to control the fuel flow int the intake manifold and distribute the fuel across the air stream. In a carburet0 the air flows through a converging-diverging nozzle called a venturi. The pressun difference set up between the carburetor inlet and the throat of thenozzle (which depends on the air flow rate) is used to meter the appropriate fuel flow for that air flow. The fuel enters the air stream through the fuel discharge tube or ports in the carburetor body and is atomized and convected by the air stream past the throttle plate and into the intake manifold. Fuel evaporation starts within the carburetor and continues in the manifold as fuel droplets move with the air flow and as liquid fuel floks over the throttle and along the manifold walls. A modem carburetor which meters, the appropriate fuel flow into the air stream over the complete engine operating range is a highly developed and complex device.

Then are many types of carburetors; they share the same basic concepts which we will now examine. Figure 7-2 shows the essential components of an elementary carburetor. The air enters the intake section of the carburetor (1) from the air cleaner which removes suspended dust particles. The air then flows into the carburetor venturi (a converging-diverging nozzle) (2) where the air velocity increases and the pn* sure decreases. The fuel level is maintained at a constant height in the flea chamber (3) which is connected 'via an air duct (4) to the carburetor i section (I). The fuel flows through the main jet (a calibrated orifice) (5) as a of the pressure difference between the float chamber and the venturi throa through the fuel discharge nozzle (6) into the venturi throat where the air st atomizes the liquid fuel. The fuel-air mixture flows through the diverging set of the venturi where the flow decelerates and some pressure recovery occurs. flow then passes the throttle valve (7) and enters the intake manifold. Note that the flow may be unsteady even when engine load and speed constant, due-to the periodic filling of each of the engine cylinden which dr air through the carburetor venturi. The induction time, 1/(2N) (20 ms at rcv/min), is the characteristic time of this periodic cylinder filling process. Generally, the characteristic times of changes in throttle setting are longer; it takes several engine operating cycles to reestablish steady-state engine operation after a It is usually assumed that the flow processes sudden change in throttle p~sition.~ in the carburetor can be modeled as quasi steady. FLOW THROUGH THE VENTURI. Equation (C.8) in App. C relates the mass flow rate of a gas through a Row restriction to the upstream stagnation pressure and temperature, and the pressure at the throat. For the carburetor venturi: where C,, and AT are the discharge coellicient and area of the venturi throat, respectively. If we assume the velocity at the carburetor inlet can be neglected, $.

(7.2) can be rearranged in terms of the pressure drop from upstream condilions to the venturi throat for the air stream, Apa = p, - pT,as h,, = C, Ad2p,, Ap,J112@ where @= [(A) - @dpJ2" - (~T/PO)'' + "" - (PT/Po) 1 'I2 and accounts for the effects of compressibility. Figure C-3 shows the value of @ as a function of pressure drop. For the normal carburetor operating range, where APJPOS 0.1, the effects of compressibility which reduce 8 below 1.0 are small. FLOW THROUGH THE FUEL ORIFICE. Since the fuel is a liquid and therefore antially incompressible, the fuel flow rate through the main fuel jet is given by 284 INTERNAL COMBUSTION ENGINE FUNDAMENTALS ' Eq. (C.2) in App. C as (7.5) = CDoA,(~P,AP,)"~ where CDoand A, are the discharge coefficient and area of the orifice, respa. tively, Ap, is the pressure difference across the orifice, and the orifice area h assumed much less than the passage area. Usually, the fuel level in the float chamber is held below the fuel discharge nozzle, as shown in Fig. 7-2, to prevent fuel spillage when the engine is inclined to the horizontal (e.g., in a vehicle on a slope). Thus, where his typically of order 10 mm.

The discharge coeficient CDein Eq. (7.5) represents the effect of all deviations from the ideal one-dimensional isentropic flow. It is influenced by many factors of which the most important are the following: (1) fluid mass flow rate; (2) orifice lengthldiameter ratio; (3) orifice/approach-area ratio; (4) orifice surface area; (5) orifice surface roughness; (6) orifice inlet and exit chamfers; (7) fluid specific gravity; (8) fluid viscosity; and (9) fluid surface tension. The use of the orifice Reynolds number, Re, = pVD,/p, as a correlating parameter for the discharge coeficient accounts for effects of mass flow rate, fluid density and viscosity, and length scale to a good first approximation. The discharge coefficient of a typical carburetor main fuel-metering system orifice increases smoothly with increasing Re, .3 18 I 0 1 I I I 2 3 4 I 5 Ap, kN/rn2 FIGURE 7-3 Performance of elementary carburetor: variation of CD,, CD., @, m, (AIF),, ma,and equivalence ratio 9 with venturi pressure drop. is given by give a stoichiometric mixture at an air flow rate corresponding to I kN/m2 venturi pressure drop (middle graph in Fig. 7-3). At higher air flow rates, the carburetor will deliver a fuel-rich mixture; at very high flow rates it will eventually deliver an essentially constant equivalence ratio. At lower air flow rates, the mixture delivered leans out rapidly. Thus, the elementary carburetor cannot provide the variation in mixture ratio which the engine requires over the complete load range at any given speed (see Fig.

7-1). The deficiencies of the elementary carburetor can be summarized as follows: and the equivalence ratio I. At low loads the mixture becomes leaner; the engine requires the mixture to be enriched at low loads. 2. At intermediate loads, the mixture equivalence ratio increases slightly as the CARBURETOR PERFORMANCE. The air/fuel ratio delivered by this carburetor 4 [=(A/F)](A/F)] (AIF), C,, 4 = -5- (J2J(:y2(l by - " syi2 where (AIF), is the stoichiometric airlfuel ratio. The terms A,, AT, p,, and P, are all constant for a given carburetor, fuel, and ambient conditions. Also, except for very low flows, p,gh 4 Ap,,. The discharge coeficients CDoand C,,, and @ vary with flow rates, however. Hence, the equivalence ratio of the mixtun delivered by an elementary carburetor is not constant. Figure 7-3 illustrates the performance of the elementary carburetor. The top set of curves shows how @, CD,, and CDotypically vary with the venturi pressun drop? Note that for Ap,, < p,gh there is no fuel flow. Once fuel starts to flow* a consequence of these variations the fuel flow rate increases more rapidly than the air flow rate. The carburetor delivers a mixture of increasing fuellair equivalence ratio as the flow rate increases. Suppose the venturi and orifice are r i d lo * air flow increases. The engine requires an almost constant equivalence ratio. 3. As the air flow approaches the maximum wide-open throttle value, the equivalence ratio remains essentially constant.

However, the mixture equivalence ratio should increase to 1.1 or greater to provide maximum engine power. 4. The elementary carburetor cannot compensate for transient phenomena in the intake manifold. Nor can it enrich the mixture during engine starting and warm-up. 5. The elementary carburetor cannot adjust changes ambient air density (due primarily to changes in altitude). 7.2.2 Modern Carburetor Design The changes required in the elementary carburetor so that it provides Ihce ratio versus air flow distribution shown in Fig. 7-1 are: the equiva- SI ENGINE FUEL METERING AND MANIFOLD PHENOMENA 286 INTERNAL COMBUSTION ENGINE FUNDAMENTALS 1. The w i n metering system must be compensated to provide essentially constat lean or stoichiometric mixtures over the 20 to 80 perant air flow range. 2. An idle system must be added to meter the fuel flow at idle and light loads. 3. An enrichment system must be addel so the engine can provide its maximu. power as wide-open throttle is approached. 4. An accelerator pump which injects additional fuel when the throttle is o p n d rapidly is required to maintain constant the equivalence ratio delivered to t k engine cylinder. 5. A &ke must be added to enrich the mixture during engine starting a d warm-up to ensure a combustible mixture within each cylinder at the t h e d ignition. 6. Altitude compensation is required to adjust the fuel flow to changes in & density. In addition, it is necessary to increase the magnitude of the pressure dr available for controlling the fuel flow.

Two common methods used to achieve t are the following. BOOST VENTURIS The carburetor venturi should give as large a vacuum at the throat as possible at maximum air flow, within the constraints of a low prenun loss across the complete venturi and diffuser. In a single venturi, .as the d i a m ~ of the throat is decreased at a given air flow to increase the flow velocity and hence the metering signal at the throat, the pressure loss increases. A hi@ vacuum signal at the venturi throat and higher velocities for improved atom ization can be obtained without increasing the overall pressure loss through tb8 use of multiple venturis. Figure 7-4 shows the geometry and the pressure distribv tion in a typical double-venturi system. A boost venturi is positioned upstream d the throat of the larger main venturi, with its discharge at the location d maximum velocity in the main venturi. Only a fraction of the air flows thmuP the boost venturi. Since the pressure at the boost venturi exit equals the pnnun 287 the main venturi throat, a higher vacuum Ap, = p, gh, is obtained at the boost ,,ntu. throat which can be used to obtain more precise metering of the fuel (p, [he manometer fluid density). Best results are obtained with the boost venturi slightly upstream (z5 mm) of the main venturi throat. Because only a fratlion of the total air flow goes through the boost venturi, the use of multiple ,,nturis makes it possible to obtain a high velocity air stream (up to 200 m/s) *here the fuel is introduced at the boost venturi throat, and adequate vacuum, and to reduce the pressure loss across the total venturi system, without increasing the height of the carburetor. The fuel is better atomized in the smaller boost ,cntun with its higher air velocity, and since this air and fuel mixture is discharged centrally into the surrounding venturi, a more homogeneous mixture rnu1ts. The vacuum developed at the venturi throat of a typical double-venturi is about twice the theoretical vacuum of a single venturi of the same flow area.5A triple-venturi system can be used to give further increases in metering The overall discharge coefficient of a multiple-venturi carburetor is lower than a single-venturi carburetor of equal cross-sectional area. The throat area of [he main venturi in a multiple-venturi system is usually increased, therefore, above the single-venturi size to compensate for this. Some decrease in air stream velocity is tolerated to maintain a high discharge coefficient (and hence a high volumetric efi~iency).~ , SIULTIPLE-BARRELCARBURETORS. Use of carburetors with venturi systems in parallel is a common way of maintaining an adequate part-load metering signal, high volumetric efficiency at wide-open throttle, and minimum carburetor height as engine size and maximum air flow increases. As venturi size in a single-barrel carburetor is increased to provide a higher engine air flow at maximum power, the venturi length increases and the metering signal generated at low flows decreases. Maximum wide-open throttle air flow is some 30 to 70 times the idle air flow (the value depending on engine displacement). Two-barrel carburetors usually consist of two single-barrel carburetors mounted in parallel. Four-barrel carburetors consist of a pair of two-barrel carburetors in parallel, with throttle plates compounded on two shafts. Air flows through the primary banel(s) at low intermediate engine loads. At higher loads, the throttle plate(s) on the sec~"ary banel(s) (usually of larger cross-sectional area) start to open when the air flow exceeds about 50 percent of the maximum engine air flow. There are many different designs of complete carburetors.

The operating principles of the methods most commonly used to achieve the above listed modibtions will now be reviewed. Figure 7-5 shows a schematic of a conventional modern carburetor and the names of the various components and fuel passages. COMPENSATIONOF MAIN METERING SYSTEM. Figure 7-6 shows a main fuel- FIGURE 7-4 Schematic of carburetor double-venturi sysfm metering system with air-bleed compensation. As the pressure at the venturi k m t decreases, air is bled through an orifice (or wries of orifices) into the main well. This flow reduces the pressure difference across the main fuel-metering 4fice which no longer experiences the full venturi vacuum. The mixing of bleed and does not significantly affect the composition of the mixture. The airmass flow rate is given by Fuel I mab = CD, - P ~) P J " ~ (7.8) ,,here CDband A, are the discharge coefficient and the area of the air-bleed The fuel mass flow rate through the fuel orifice is given by where The density of the emulsion p,, in the main well and nozzle is usually approximatedby FIGURE 7-5 Schematic of modern carburetor. 8 Throttle plate 1 Main venturi 9 Idle air-bleed orifice 2 Boost venturi 10 Idle fuel orifice 3 Main metering spray tube or n o d e 11 Idle mixture orifice 4 Air-bleed orifice 12 Transition orifice 5 Emulsion tube or well 13 Idle mixture adjusting screw 6 Main fuel-metering orifice 14 Idle throttle setting adjusting screw 7 Float chamber Fuel enters the air stream from the main metering system through (3). At idle, fuel enters air at (11). During transition, fuel enters at (1I), (12),and (3). (CourtesyS.p.A.E. Weber.) % air with the fuel forms an emulsion which atomizes more uniformly to smaller drop sizes on injection at the venturi throat.

The schematic in Fig.

7-6 illustrates the operating principle. When the engine is not running, the fuel is at the same level in the float bowl and in the main well. With the engine running, as the throttle plate is opened, the air flow and the vacuum in the venturi throat increase. For Ap,(=po - p,) c p,ghl, there is no fuel flow from the main metering system.

For p,ghl < Ap, < p,gh,, only fuel flows through the main well and nozzle, and the system operates just like an elementary carburetor. For Ap, > p,gh,, air enters the main well together with fuel. The amount of air ente.ng the well is controlled by the size of the main air-bleed orifice. The amount of air FIGURE 7-6 Schematic of main metering system with air-bkrd compensation. Since typical values are pf = 730 kg/m3 and pa = 1.14 kg/m3, usually p, & p pa. Thus, as the air-bleed flow rate increases, the height of the column of becomes less significant. However, the decrease in emulsion density due 10 increasing air bleed increases the flow velocity, which results in a significant presswe drop across the main nozzle. This pressure drop depends on nozzle length and diameter, fuel flow rate, bleed air flow rate, relative velocity between fuel and bleed air, and fuel properties. It is determined empirically, and has been found to correlate with p,, [as defined by Eq. (7.10)].2. The pressure loss at the main discharge nozzle with two-phase flow can be several times the pressure loss with single-phase flow.

Figure 7-7 illustrates the behavior of the system shown in Fig. 7-6: ma, m,, and the fuellair equivalence ratio 4 are plotted against Ap,. Once the bleed system is operating (Ap, > pf gh,) the fuel flow rate is reduced below its equivalent elementary carburetor value (the A, = 0 line). As the bleed orifice area is increased, in the limit of large A, and neglecting the pressure losses in the main nozzle, the fuel flow rate remains constant (A, + a).An appropriate choice of bleed orifice area A, will provide the desired equivalence ratio versus pressure drop or air flow characteristic. Additional control flexibility is obtained in practice through use of a second orifice, or of a series of holes in the main well or emulsion tube as shown in Fig. 7-5.

Main metering systems with controlled air bleed provide reliable and stable control of mixture composition at part throttle engine operation. They are simple, have considerable design flexibility, and atomize the fuel effectively. In Some carburetor designs, an additional compensation system consisting of a Wered rod or needle in the main metering orifice is used. The effective open area of the main metering orifice, and hence the fuel flow rate, can thus be directly related to throttle position (and manifold vacuum). A wide range of two-phase flow patterns can be generated by bleeding an air flow into a liquid flow. Fundamental studies of the generation and flow of SI ENGINE FUEL METERING AND MANIFOLD PHENOMENA INTERNAL COMBUSTION ENGINE FUNDAMENTALS 291 ,,Slem~are coupled, they interact and the main system behavior in this transition is modified by the fuel flow through the idle system. The total combined fuel flow ~rovidesa rich (or close-to-stoichiometric) mixture at idle, a progressive of the mixture as air flow increases, and eventually (as the main system lakes over full control of the fuel flow rate) an approximately constant mixture PO~YERENRICHMENT SYSTEM. This system delivers additional fuel to enrich ,he mixture as wide-open throttle is approached so the engine can deliver its maximum power. The additional fuel is normally introduced via a submerged which communicates directly with the main discharge nozzle, bypassing the metering orifice. The valve, which is spring loaded, is operated either mechanic a l ~through ~ a linkage with the throttle plate (opening as the throttle approaches its wide-open position) or pneumatically (using manifold vacuum). FIGURE 7-7 Metering characteristics of system with air-bled compensation: mass flow rate of air m,, mass flow rate of fuel m,, and equivalence ratio 4 as functions of venturi pressure drop for diferen~~ air-bleed orifice are as^, . two-phase mixtures in small diameter tubes with bleed holes similar to those used in carburetors have been carried out.' For a given pipe and bleed hole size, the type of flow pattern set up depends on the flow rates of the two phases.

IDLE SYSTEM. The idle system is required because at low air flows through the carburetor insufficient vacuum is created at the venturi throat to draw fuel into the air stream. However, at idle and light loads, the manifold vacuum is high with the pressure drop occ

The electrolyte is yttria (Y,03)-stabilized zirconia (ZrO,) ceramic which separates two gas chambers (the ex%aust manifold and the atmosphere) which have different oxygen partial pressures.
The cell can be represented as a series of interfaces as follows: Exhaust I Metal 1 Ceramic I Metal (Air p& is the oxygen partial pressure of the air (s2O kN/m2) and pb2 is the equi- librium oxygen partial pressure in the exhaust gases. An electrochemical reaction takes place at the metal electrodes: md the oxygen ions transport the current across the cell. The open-circuit output *ohage of the cell V. can be related to the oxygen partial pressures p& and p& through the Nernst equation: wOT 4400 revlmin ~ 6 . 6m 7 s 4 Injector A ~njectorB 0 'here F is the Faraday constant. Equilibrium is established in the exhaust gases the catalytic activity of the platinum metal electrodes. The oxygen partial Preme in equilibrated exhaust gases decreases by many orders of magnitude as [he equivalence ratio changes from 0.99 to 1.01, as shown in Fig. 7-17a. Thus the *"SO[output voltage increases rapidly in this transition from a lean to a rich SI ENGINE FUEL METERING AND MANIFOLD PHENOMENA 303 positive electrical Rich Lean Rich Lean Relative aidfuel ratio X FIGURE 7-17 Oxygen-sensor characteristics.Variation as a function of relative airlfuel ratio and temperature of: (a) oxygen partial pressure in equilibrated combustion products; (b)sensor output voltage." mixture at the stoichiometric point, as shown in Fig.
7-176. Since this transition is not temperature dependent, it is well suited as a sensor signal for a feedback system.'' Figure 7-18 shows a cross-section drawing of a lambda sensor, screwed into the wall of the exhaust manifold. This location provides rapid warm-up of the sensor following engine start-up. It also gives the shortest flow time from the fud injector or carburetor location to the sensor-a delay time v the operation of the feedback system. The sensor body is made of Zr02 ceramic stabilized with Y20, to give adequate low-temperature electrical conductivity. The inner and outer electrodes arre 10.-pm thick poroi platinum layers provide the required catalytic equilibration. The outer electrode which is exposed to the exhaust gases is protected against corrosion and erosion by a loo-@ spinal coat and a slotted shield. Air passes to the inner electrode through holes in the protective sleeve. The shield, protective sleeve, and housing are made from heat- and corrosion-resistant steel alloys. Such sensors were first developed for air/fuel ratio control at close to the stoichiometric value. Use of a similar sento control airlfuel ratios at lean-of-stoichiometric values during part-throt* engine operation is also feasible. For closed-loop feedback control at close-to-stoichiometric, use is made d the sensor's low-voltage output for lean mixtures and a high-voltage output for rich mixtures. A control voltage reference level is chosen at about the mid-poin(of the steep transition in Fig. 7-17b. In the electronic control unit the s e w signal is compared to the reference voltage in the comparator as shown in F* 7-19a.
The comparator output is then integrated in the integral controller wbm , output varies the fuel quantity linearly in the opposite direction to the sign of the comparator signal. There is a time lag 7, in the loop composed of the transport rime of fuel-air mixture from the point of fuel admission in the intake system to the sensor location in the exhaust, and the sensor and control system time delay. Because of this time lag, the controller continues to influence the fuel flow rate in the same direction, although the reference point) = 1.0 has been passed, as shown in Fig. 7-19b.
Thus, oscillations in the equivalence ratio delivered to the engine exist even under steady-state conditions of closed-loop control. This behavior of the control system is called the limit c y c k The frequency f of this limit cycle is given by 7, h - - ~ - ~ ~ h i Time o m - Lean e t FIGURE 7-19 Operation of electronic control unit for rclosed-loop i c feedback: (a) sensor signal compared with reference level; (b) controlkr output voltage-the integrated comparator output.12 304 SI ENGINE FUEL METERING AND MANIP INTERNAL COMBUSTION ENGINE FUNDAMENTALS and the change in equivalence ratio peak-to-peak is A4 =~ KT, where K is the integrator gain (in equivalence ratio units per unit time). Depending on the details of the three-way catalyst used for cleanup of all three pollutants (CO, HC, and NO3 in the exhaust, the optimum average equivalence ratio may not be precisely the stoichiometric value. Furthermore, the reference voltage for maximum sensor durability may not correspond exactly to the stoichiometri~point or the desired catalyst mean operating point. While a small shift (- + 1 percent) in operating point from the stoichiometric can be obtained by varying the reference voltage level, larger shifts are obtained by modifying the control loop to provide a steady-state bias. One method of providing a biasasymmetrical gain rate biasing1'-uses two separate integrator circuits with dif. ferent gain rates K + and K - to integrate the comparator output, depending on whether the comparator output is positive (rich) or negative (lean). An alternative biasing technique incorporates an additional delay time T , so that the controller output continues decreasing (or increasing) even though the sensor signal has switched from the high - to the low level (or vice versa). By introducing this additional delay only on the negative slope of the sensor signal, a net lean bias is produced. Introducing the additional delay on the positive slope of the sensor signal produces a net rich bias.12 Note that the sensor only operates at elevated temperatures. During engine start-up and warm-up, the feedback system does not operate and conventional controls are required to obtain the appropriate fuel-air mixture for satisfactory engine operation. (a) 20' throttle plate angle -- --4 (b) 30" throttle plate angle 7 5 FLOW PAST THROTTLE PLATE Except at or close to wide-open throttle, the throttle provides the minimum flow area in the entire intake system. Under typical road-load conditions, more than 90 percent of the total pressure loss occurs across the throttle plate. The minimum-to-maximum flow area ratio is large--typically of order 100. Throttle (c) 45' throttle plate angle - (d) 60' throttle plate angle FICCRE 7-21 Photographs of flow in two-dimensional hydraulic analog of carburetor venturi, throttle plate, and manifold plenum floor at different throttle plate angles." Closed Open to angle J. FIGURE 7-20 Throttle plate geometry.' plate geometry and parameters are illustrated in Fig. 7-20. A throttle plate of conventional design such as Fig. 7-20 creates a :hree-dimensional flow field. At part-throttle operating conditions the throttle plate angle is in the 20 to 45' range and jets issue from the "crescent moonw-shaped open areas on either side of the throttle plate. The jets are primarily two dimensional. Figure 7-21 shows photographs taken of a two-dimensional hydraulic analog of a typical carburetor 306 lNTF.RNAL COMBUSTION ENGINE FUNDAMENTALS SI ENGINE FUEL METERING AND MANIFOLD PHENOMENA (c-g)]. For pressure ratios across the throttle less than the critical value (pTlp0= 0.528), the mass flow rate is given by venturi and throttle plate in steady flow at different throttle angles. The path lines traced by the particles in the flow indicate the relative magnitude of the flow velocity."
The flow accelerates through the carburetor venturi (separation occun at the corners of the entrance section); it then divides on either side of the throttle plate. There is a stagnation point on the upstream side of the throttle plate. ne wake of the throttle plate contains two vortices which rotate in opposite directions. The jets on either side of the wake (at part throttle) are at or near sonic velocitv. There is little or no mixing between the two jets. Thus, if maldistributi~~ of the fuel-air mixture occurs above the throttle plate, it is not corrected immediately below the throttle plate. In analyzing the flow through the throttle plate, the following Tactors should be considered:'. 19. O' 1. The throttle plate shaft is usually of sufficient size to affect the throttle open area. 2. To prevent binding in the throttle bore, the throttle plate is usually completely closed at some nonzero angle (5, 10, or 15"). 3. The discharge coeficient of the throttle plate is less than that of a smooth converging-diverging nozzle, and varies with throttle angle, pressure ratio, and throttle plate Reynolds number. 4. Due to the manufacturing tolerances involved, there is usually some minimum leakage area even when the throttle plate is closed against the throttle bore. This leakage area can be significant at small throttle openings.
5. The measured pressure drop across the throttle depends (+ 10 percent) on the circumferential location of the downstream pressure tap. 6. The pressure loss across the throttle plate under the actual flow conditions (which are unsteady even when the engine speed and load are constant, see Fig. 7-8) may be less than under steady flow conditions. 307 where A,, is the throttle plate open area [Eq. (7.1831, po and T,,are the upstream p~ssureand temperature, p, is the pressure downstream of the throttle plate equal to the pressure at the minimum area: i.e., no pressure r a o v e v wsurs), and CD is the discharge coeficient (determined experimentally). For pressure ratios greater than the critical ratio, when the flow at the thmttle plate is choked, The relation between air flow rate, throttle angle, intake manifold pressure, and engine speed for a two-barrel carburetor and a 4.7-dm3 (288-in3) displacement eight-cylinder production engine is shown in Fig. 7-22. While the lines are from a quasi-steady computer simulation, the agreement with data is excellent. The figure shows that for an intake manifold pressure below the critical loo - Throttle angle 3 80- The throttle plate open area A,,, as a function of angle $ for the geometry in Fig. 7-20, is given by2 -) l,b0* + 2 [AJ/ (COS' cos2 $0)'1' cos * sin-' rzi: f ') - a(1 - a')'" + sin-' cos ?.!!!= (1 - cos ID' J - a2 COS 7I -- $0 COS a I (7.18) where a = d/D, d is the throttle shaft diameter, D is the throttle bore diameter. and $O is the throttle plate angle when tightly closed against the throttle bore When J/ = cos-' (a cos $,), the throttle open area reaches its maximum value (=nD2/4 - do).The throttle plate discharge coeficient (which varies with A J and minimum leakage area, must be determined experimentally. The mass flow rate through the throttle valve can be calculated from standard orifice equations for com~ressiblefluid flow [see App. C, Eqs. (C-8) and e U E "- *' 40- 20 - 0- 0 50 Intake manifold pressure, cmHg 60 70 FIGURE 7-22 Variation in air flow rate past a throttle, with inlet manifold pressure, throttle angle, and engine speed. 4.7dm3 displacement eight-cylinder engint2 308 INTERNAL COMBUSTION ENGINE FUNDAMENTALS value (0.528 x pa,, = 53.5 kN/mZ = 40.1 crnWg) the air flow rate at a given throttle position is independent of manifold pressure and engine speed because the flow at the throttle plate is choked.' 7.6 FLOW IN INTAKE MANIFOLDS 7.6.1 Design Requirements The details of the air and fuel flow in intake manifolds are extremely complex. The combination of pulsating flow into each cylinder, different geometry flow paths from the plenum beneath the throttle through each runner and branch of the manifold to each inlet port, liquid fuel atomization, vaporization and transport phenomena, and the mixing of EGR with the fresh mixture under steadystate engine operating conditions are difficult enough areas to untangle. During engine transients, when the throttle position is changed, the fact that the processes which govern the air and the fuel flow to the cylinder are substantially different introduces additional problems. This section reviews our current understanding of these phenomena.
Intake manifolds consist typically of a plenum, to the inlet of which bolts the throttle body, with individual runners feeding branches which lead to each cylinder (or the plenum can feed the branches directly). Important design criteria are: low air flow resistance; good distribution of air and fuel between cylinders; runner and branch lengths that take advantage of ram and tuning effects; sufficient (but not excessive) heating to ensure adequate fuel vaporization with carbureted or throttle-body injected engines. Some compromises are necessary; e.g., runner and branch sizes must be large enough to permit adequate flow without allowing the air velocity to become too low to transport the fuel droplets. Some of these design choices are illustrated in Fig. 7-23 which shows an inlet manifold and carburetor arrangement for a modem four-cylinder 1.8-dm3 engine. In this design the four branches that link the plenum beneath the carburetor and throttle with the inlet ports are similar in length and geometry, to provide closely comparable flow paths. This manifold is heated by engine coolant as shown and uses an electrically heated grid beneath the carburetor to promote rapid fuel e~aporation.~' Exhaust gas heated stoves at the floor of the plenum are also used in some intake manifolds to achieve adequate fuel vaporization and distribution. Note that with EGR, the intake manifold may contain passages to bring the exhaust gas to the plenum or throttle body. With port fuel-injection systems, the task of the inlet manifold is to control the air (and EGR) flow. Fuel does not have to be transported from the throttle body through the entire manifold.
Larger and longer runners and branches, with larger angle bends, can be used to provide equal runner lengths and take greater advantage of ram and tuning effects. With port fuel injection it is not norm all^ necessary to heat the manifold. A large number of different manifold arrangements are used in practice. Different cylinder arrangements (e.g., four, V-six, in-line-six, etc.) provide quite different air and fuel distribution problems. Air-flow phenomena in manifolds c a EGR gas passage' senjon A-A -C&nt FIGURE 7-23 Inlet manifold for four-cylinder 1.8-dm3displacement spark-ignitionengine? be considered as unaffected by the fuel flow. The reverse is definitely not the case: the fuel flow-liquid and vapor4epends strongly on the air flow. These two topics will therefore be reviewed in sequence. 7.6.2 Air-Flow Phenomena I % 8 3 The air flow out of the manifold occurs in a series of pulses, one going to each cylinder. Each pulse is approximately sinusoidal in shape. For four- and eightcylinder engines, these flow pulses sequence such that the outflow is essentially zero between pulses. For six-cylinder arrangements the pulses will overlap. When the engine is throttled, backflow from the cylinder into the intake manifold occurs during the early part of the intake process until the cylinder pressure falls below the manifold pressure. Backflow can also occur early in the compression stroke before the inlet valve closes, due to rising cylinder pressure. The flow at the throttle will fluctuate as a consequence of the pulsed flow out of the manifold into the cylinders. At high intake vacuum, the flow will be continuously inward at the throttle and flow pulsations will be small. When the outflow to the cylinder which is undergoing its intake stroke is greater than the flow through the throttle, the cylinder will draw mixture from the rest of the intake manifold. During the portion of the intake stroke when the flow into the cylinder is lower than the flow through the throttle, mixture will flow back into the rest of the manifold. At wide-open throttle when the flow restriction at the throttle is a minimum, flow Pulsations at the throttle location will be much more pronounced.'g The air flows to each cylinder of a multicylinder engine, even under steady operating conditions, are not identical. This is due to differences in runner and SI ENGINE FUEL METERING AND MANIFOLD PHENOMENA 311 Ti,s the manifold, the pressure level in the manifold increases more slowly than would be the case if steady-state conditions prevailed at each throttle position. Thus, the pressure difference across the throttle is larger than it would be under steady flow conditions and the throttle air flow overshoots its steady-state value. The air flow into each cylinder depends on the pressure in the manifold, so this lags the throttle air flow. This transient air-flow phenomenon affects fuel metering. For throttle-body injection or a carburetor, fuel flow should be related to throttle air flow. For port fuel injection, fuel flow should be related to cylinder air flow. Actual results for the air flow rate and manifold pressure in response to an opening of the throttle (increase in throttle angle) are shown in Fig. 7-24. The overshoot in throttle air flow and lag in manifold pressure as the throttle angle is increased are evident. Opposite effects will occur for a decrease in throttle angle. TABLE 7.1 Parameters that characterize manifold air flow I-4t v-83 33 9.4 30 16 300 500 Range of speeds, etc Maximum Minimum Crankshaft, rev/min Peak air velocity in manifold branch, m/s Peak Reynolds number in manifold branch Duration of individual cylinder intake process, ms 5000 650 1307, 100$ 15 4 5 x 10.' Engine geometry Typical flow-path distance between throttle bore and intake valve, cm Average intake-passage flow area, cm2 Volume of one direct flow path from throttle bore to intake valve, cm3 1.8-dm3fourcylinder in-line SI engine?' t 5.6-drn3 V eight-cylindcr SI engine?' 6 lo5 46 AIR-FLOW MODELS.Several models of the flow in an intake manifold have been pr~posed.'~," One simple manifold model that describes many of the above phenomena is the plenum or filling and emptying model. It is based on the assumption that at any given time the manifold pressure is uniform. The continuity equation for air flow into and out of the intake manifold is , 'here ma., is the mass of air in the manifold, and ma,,.
and 4. are the air, mass flow rates past the throttle and into each cylinder, respectively.
The flow me past the throttle is given by Eq. (7.19) or (7.20). For manifold pressures S~acientlylow to choke the flow past the throttle plate, the flow rate is independent of manifold pressure. The mass flow rate to the engine cylinders can be modeled at several levels of accuracy. The air flow through the valve to each 9linder can be computed from the valve area, discharge coeEcient, and pressure 312 INTERNAL COMBU~TION ENGINE FUNDAMENTALS difference across the valve; or a sine wave function can be assumed. In general case, Eq. (7.21) must be combined with the first law for an open sy (see Sec. 14.2.2). For calculating the manifold response to a change in loa throttle setting, simplifying assumptions can be made. A quasi-steady appro imation for the cylinder air flow: C m a , cyl = s o pa. m 2 VsN The& is usually adequate, and the air temperature can be assumed con~tant.'~ using the ideal gas law for the manifold, pmVm= ma,, R, Tm, Eq. (7.21) can k written as d~m qvVdN RTm Pm = m a , th dt 2Vm vm + Both and ma,, have some dependence on pm[e.g., see Eq. (6.2)].
In the absence of this weak dependence, Eq. (7.22) would be a first-order equation for p, with a time constant .r = 2VJ(q0 V, N) x VdvCy,,which is 2 to 4 times the intake stroke duration. The smooth curves in Fig. 7-24 are predictions made with Eq. (7.22) and show good agreement with the data. The plenum model is useful for investigating manifold pressure variations that result from load changes. It provides no information concerning pressure variations associated with momentum effects. Helmholtz resonator models for the intake system have been proposed. This type of model can predict the resonant frequencies of the combined intake and engine cyGnder system, and hence the engine speeds at which increases in air flow due to intake tuning occur. It does not predict the magnitude of the increase in volumetric efficiency. The Helmholtz resonator theory analyzes what happens during one inlet stroke, as the air in the manifold pipe is acted on by a forcing function produced by the piston motion. As the piston moves downward during the intake stroke, a reduced pressure occurs at the inlet valve relative to the pressure at the open end of the inlet pipe.
A rarefraction wave travels down the intake pipe to the open end and is reflected as a compression wave. A positive tuning effect occurs when the compression wave arrives at the inlet valve as the valve is ~losing.~' A single-cylinder engine modeled as a Helmholtz resonator is shown in Fig. 7-251.
The effective resonator volume V,,, is chosen to be one-half of the displaced volume plus the clearance volume; the piston velocity is then close to its maximum and the pressure in the inlet system close to its minimum The tuning peak occurs when the natural frequency of the cylinder volume coupled to the pipe is about twice the piston frequency. For a single-cylinder,fed by a single pipe open to the atmosphere, the resonant tuning speed N, is given by where a is the sound speed (m/s), A the effective cross-sectional area of the in system (cm'), 1the effective length of the inlet system (cm), K a constant equal about 2 for most engines, and V,,, = V'r, + 1)/[2(rc - I)] (~ m ~) . ~ ~ ~ G C R E7-25 ~ ~ l ~ h oresonator ltz models for (a) singlecylinder engine and (b)multicylinder engine.27 he. Helmholtz theory for multicylinder engines treats the pipes of cylinders not undergoing induction as an additional volume. The two pipes, (I,, A,) and (I ? . A,), and two volumes, V1 and &, in Fig. 7-25b form a vibrating system with two degrees of freedom and two resonant frequencies. The following equation, based on an electrical analog (in which capacitors represent volumes and inductors pipes), gives the two frequencies at which the manifold shown in Fig. 7-25b would be tuned:" where a = L,/Ll, i3 = CJC,, C1 = I.:, C2 = &, L, = (l/A),, L, = (IIA),, and I;,, = V,. The Helmholtz theory predicts the engine speeds at which positive tuning resonances occur with reasonable accuracy." The dynamics of the flow in multicylinder intake (and exhaust) systems can bc modeled most completely using one-dimensional unsteady compressible flow equations. The standard method of solution of the governing equations has been the method of characteristics (see Ben~on'~).Recently, finite difference techniques which are more efficient have been used.30The assumptions usually made in this type of analysis are: I. The intake (or exhaust) system can be modeled as a combination of pipes, junctions, and plenums. 2.
Flow in the pipes is one dimensional and no axial heat conduction occurs.
3. States in the engine cylinders and plenums are uniform in space. 4 Boundary conditions are considered quasi steady.
5. Coefficients of discharge, heat transfer, pipe friction, and bend losses for steady flow are valid for unsteady flow. 6 The gases can be modeled as ideal gases. This approach to intake and exhaust flow analysis is discussed more fully in Ec. 14.3.4. 314 SI ENGINE FUEL METERING AND MANIFOLD PHENOMENA INTERNAL COMBUSTION ENGINE FUNDAMENTALS 7.63 Fuel-Flow Phenomena TRANSPORT PROCESSES. With conventional spark-ignition engine liquid metering systems, the fuel enters the a& stream as a liquid jet. The liqui atomizes into droplets. These mix with the air and also deposit on the w the intake system components. The droplets vaporize; vaporization of the fuel on the walls occurs. The flow of liquid fuel along the walls can be signi The transport of fuel as vapor, droplets, and liquid streams or films can important. The fuel transport processes in the intake system are obvio extremely complex. The details of the fuel transport process are different for multipoint injection systems than for carburetor and throttle-body injection systems.
For latter systems, fuel must be transported past the throttle plate and through complete intake manifold. For the former systems, the liquid fuel is injected in inlet port, toward the back of the intake valve. For all these practical fuel met ing systems, the quality of the mixture entering the engine is imperfect. The air, recycled exhaust, mixture is not homogeneous; the fuel may not be vaporized as it enters the engine. The charge going to each cylinder is not us uniform in fuel/air ratio throughout its volume, and the distribution of fud between the different engine cylinders is not exactly equal.
During engine sients, when engine fuel and air requirements and manifold conditions chan is obvious that the above fuel transport processes will not all vary with time the same way. Thus, in addition to the transient non-quasi-steady air-flow nomena described above, there are transient fuel-flow phenomena. These ha be compensated for in the fuel metering strategy. Since gasoline, the standard spark-ignition engine fuel, is a mixture of large number of individual hydrocarbons it has a boiling temperature ran rather than a single boiling point. Typically, this range is 30 to 200•‹C.Individ hydrocarbons have the saturation pressure-temperature relationships of a p substance. The lower the molecular weight, the higher will be the saturated vapol pressure at a given temperature. The boiling point of hydrocarbons depends marily on their molecular weight: the vapor pressure also depends on mo structure. The equilibrium state of a hydrocarbon-air mixture depends th on the vapor pressure of the hydrocarbon at the given temperature, the re amounts of the hydrocarbon and air, and the total pressure of the mixture. equilibrium fraction of fuel evaporated at a given temperature and pressure be calculated from Bridgeman charts3' and the distillation characteristics of fuel (defined by the ASTM distillation curve"). Figure 7-26a shows the effa mixture temperature on percent of indolene fuel (a specific gasoline) eva at equilibrium at atmospheric pressure. Figure 7-26b shows the effect of manifold pressure on the amount evaporated.ls While insuficient time is us available in the manifold to establish equilibrium, the trends shown are indica of what happens in practice: lower pressures increase the relative amount 0 vaporized and charge heating is usually required to vaporize a substantial tion of the fuel. Fuellair ratio Fuel evaporated at reduced pressure Fuel maporated at atmospheric pressure (4 (b) n(;ckE 7-26 I,I pcrcentage of indolene fuel evaporated at equilibrium at 1 atmosphere pressure. (6) Effect of p u r e on amount of indolene fuel evaporated.ls For carbureted and throttle-body injection systems, the fuel path is the following.
Until the throttle plate is close to fully opened, most of the fuel metered tnto the air stream impacts on the throttle plate and throttle-body walls. Only a modest fraction of the fuel vaporizes upstream of the throttle. The liquid i s reentrained as the air flows at high velocity past the throttle plate. The fuel does nor usually divide equally on either side of the throttle plate axis. The air undergoes a 90•‹bend in the plenum beneath the throttle; much of the fuel which has aot evaporated is impacted on the manifold floor. Observations of fuel behavior In intake manifolds with viewing ports or transparent sections show that there is wbstantial liquid fuel on the walls with carburetor fuel metering systems. Figure 7-27 shows the engine conditions under which liquid fuel was observed on the floor of the manifold plenum beneath the throttle plate and in the manifold Nnners, in a standard four-cylinder production engine.23 This manifold was bled by engine coolant at 90•‹C. The greatest amount of liquid was present at h h engine loads and low speeds. Heating the manifold to a higher temperature bith steam at llS•‹Cresulted in a substantial reduction in the amount of liquid: fiere Was no extensive puddling on the plenum floor, liquid Pms or rivulets were in a zone bounded by 120 mmHg vacuum and 2500 revjmin, and there 'ere no films or rivulets in the manifold runner. Depending on engine operating "nditions, transport of fuel as a liquid film or rivulet in the manifold and vaporQtion from these liquid fuel films and rivulets and subsequent transport as 'Wr may occur. vaporized fuel and liquid droplets which remain suspended in the air - i g 300 3 200 1 Liquid films or rivulets liquid fuel droplets decreases rapidly (by up to about 30"C35), and the bjction of the fuel vaporized is small (in the 2 to 15 percent range35.36). Liquid fuel drops, due to their density being many times that of the air, will follow the air flow. Droplet impaction on the walls may occur as the ~hangesdirection, and the greater inertia of the droplets causes them to move across the streamlines to the outer wall. Deposition on the manifold floor due to gavity may also occur. The equation of motion for an individual droplet flowing gas stream is No liquid films or rivulets No liquld films or rlvulets ,, 200 B 5 B -4 ,, loo Oo ocm Engine speed, revlmin Engine speed, revlrnin (a) (b) &ere Dd is the droplet diameter, pl and p, are liquid and gas densities, v, and p, sre the droplet and gas velocities, a is the droplet acceleration, g acceleration due to gavity, and CDis the drag coefficient.For 6 < Re < 500 the drag coefficient of an evaporating droplet is a strong function of the Reynolds number, Re: e.g., FIGURE 7-27 Regions of engine load and speed range where extensive pools or puddles, liquid films, or rivulw were observed: (a) on manifold plenum floor and (b) in manifold runner. Four-cylinder automob& engine. Manifold heated by coolant at 90"CZ3 stream will be transported with the air stream. However, droplet deposition 00 the manifold walls may occur due to gravitational settling and to inertial effect) as the flow goes round bends in the manifold. The fuel transport processes for port fuel-injection systems are different will depend significantly on the timing and duration of the injection pulse. Fu injected onto the back of the inlet valve (and surrounding port wall), usu while the valve is closed or only partly open.
Vaporization of liquid fuel off valve and walls occurs, enhanced by the backflow of hot residual gases from cylinder (especially at part load).
There is evidence that, even under fully w a r d up engine conditions, some fuel is carried as liquid drops into the cylinder.33 FUEL DROPLET BEHAVIOR. With carburetor and throttle-body injection systems, the liquid fuel atomizes as it enters the air stream. In the carburetor venturi this occurs as the fuel-air emulsion from the fuel jet(s) enters the hi& velocity (> 100 m/s) air stream. With an injector, the velocity of the liquid jet as it exits the nozzle is high enough to shatter the flowing liquid, and its interaction with the coaxial air flow further atomizes the fuel. Typical droplet-size distributions are not well defined; size would vary over the load and speed range Droplet diameters in the 25 to 100 pm range are usually assumed to be representafive: larger drops are also produced. The liquid fuel drops are accelerated bY the surrounding air stream and start to vaporize. Vaporization rates have calculated using established formulas for heat and mass transfer between 8 droplet and a surrounding flowing gas stream (see Ref. 34 for a review of m e t h d of calculating droplet vaporization rates). Calculations of fuel vaporization in a ~arburetorventuri and upstream of the throttle plate show that the temperatun g iP 5 *? Z 1 "< iL &! 3 $ where Re = @, Dd Ivd - v, Ih,). Studies of droplet impaction and evaporation using the above equations typical manifold conditions and geometries indicate the following.26*3 5 ' 3 7 For 90" bends, drops of less than 10 pm diameter are essentially carried by the gas stream (< 10 percent impaction); almost all droplets larger than 25 pm Impact on the walls. Droplet sizes produced first in the carburetor venturi or fuel rnjector spray and then by secondary atomization as liquid fuel is entrained from the throttle plate and throttle-body walls depend on the local gas velocity: higher local relative velocities between the gas and liquid produce smaller drop sizes. Approximate estimates which combine the two phenomena outlined above show that at low engine air flow rates, almost all of the fuel will impact first on the throttle plate and then on the manifold floor as the flow turns 90" into the manifold runners. At high air flows, because the drops are smaller, a substantial fraction of the drops may stay entrained in the air flow. Secondary atomization a t the throttle at part-load operating conditions is important to the fuel transport process: the very high air velocities at the edge of the throttle plate produce droplets of order or less than 10 pm diameter. However, coalescence and deposition on the walls and subsequent reentrainment probably increase the mean droplet size. In the manifold, gravitational settling of large (> 100 pm) droplets would occur at low air flow rates,38 but these drops are also likely to impact the walls due to their inertia as the flow is turned.
Estimates of droplet evaporation rates in the manifold indicate the follow1". With a representative residence time in the manifold of about one crank revolution (10 ms at 6000 revlmin, 100 ms at 600 rev/min), only drops of size less lhan about 10 pm will evaporate at the maximum speed; 100 pm droplets will O"f vaporize fully at any speed. Most of these large droplets impact on the wails, anyway. Drops small enough to be carried by the air stream are likely to vaporize in the manifold.26 318 MTERNAL COMBUSTION ENGINE FUNDAMENTALS FUELFILM BEHAVIOR. The fuel which impacts on the wall will also va and, depending on where in the manifold deposition occurs and the local fold geometry, may be transported along the manifold as a liquid film or n If the vaporization rate off the wall is sufficiently high, then a liquid film w build up. Any liquid film or pool on the manifold floor or walls is imp because it introduces additional fuel transport processes-deposition, transport, and evaporation-which together have a much longer time constapt than the air transport process. Thus changes in the air and the fuel flow into each engine cylinder, during a change in engine load, will not occur in phase with each other unless compensation is made for the slower fuel transport. Several models of the behavior of liquid-fuel wall-films have been dev& oped. One approach analyzes a liquid puddle on the floor of the manifold plenum.38 Metered fuel enters the puddle; fuel leaves primarily through vapor. ization. The equation for rate of change of mass of fuel in the puddle is where mf,, is the mass of fuel in the puddle, m,, ,is the metered fuel flow and x is the fraction of the metered flow that enters the puddle. It is assumed the reentrainment/evaporation rate is proportional to the mass of fuel in puddle divided by the characteristic time T of the reentrainment/evaporatio process. The puddle behavior predicted by this model in response to a s increase in engine load is shown in Fig.
7-28a. Because only part (1 - x) of fuel flows directly with the air, as the throttle is opened rapidly a lean air/ ratio excursion is predicted. Figure 7-286 shows that this behavior (without a metering compensation) is observed in practice. Estimates of the volume of fuel the puddle (for a 5-liter V-8 engine) are of order 1000 mm3, and increase wi "f. m + A "f. m Metered fuel flow - Time (4 FIGURE 7-28 (a) Predicted behavior of the fuel film for an uncompensated step change in engine operating tions. (b) Observed variation in air/fuel ratio for uncompensated throttle opening at 1600 rev/rab which increased manifold pressure from 48 to 61 c ~ n H g . ~ ~ toe & ~ i ~ A filmd FIGURE 7-29 Schematic of fuel flow paths in the manifold when liquid film flows along the manifold runner Boor. v ~ u k vapor l - ,ncreasingload and speed. The time constant is of order 2 seconds for a fully ,,armed-up engine; it varies with engine operating conditions and is especially Knsitiveto intake manifold temperature. Such models have been used primarily lo develop fuel metering strategies which compensate for the fuel transport lag.38 An alternative model, for liquid film flow in the manifold runner and bran&, has been de~eloped.~' Fuel is deposited on the manifold walls and forms a film which flows toward the cylinder due to the shear force at the gaspiquid lnlerfaceas shown in Fig. 7-29. Vaporization from the film also occurs. An of the dynamics of the fuel film leads to expressions for steady-state film belocityand thickness. As air and metered fuel flows change due to a throttle position change, the characteristic time for reestablishing steady state is 1/(2uf?, where 1 is the manifold length and uf the average film velocity. This characterist~c response time is of order 1 second for typical manifold conditions, in approximate agreement with values obtained from transient engine experiments. A more extensive analysis of both fuel droplet and film evaporation in a complete carburetor, throttle, manifold system,35 with a multicomponent model lor gasoline based on its distillation curve, indicates the following phenomena are important. Secondary atomization of the liquid fuel at the throttle, which produces the smallest droplet sizes when the throttle open angle is small, significantly increases the fraction of fuel evaporation in the manifold. Increasing inlet air temperature increases the fraction of fuel vaporized; this effect is larger at lower loads since secondary atomization under these conditions increases the liquid fuel surface area significantly. Heating the wall, which heats the liquid film on the wall directly, provides a greater increase in fraction evaporated than does - equivalent heating of the air flow upstream of the carburetor. Due to the multicomponent nature of the fuel, the residual liquid fuel composition changes significantly as fuel is transported from the carburetor to the manifold exit. Of the full boiling range liquid composition at entry, all the light ends, most of the midrange components, but only a modest amount of the high boiling point fraction have evaporated at the manifold exit. The predicted fuel fraction evaporated ranged from 40 to 60 percent for the conditions examined. One set of measurements of the fraction of fuel vaporized in the manifold of a warmed-up fourcylinder engine showed that 70 to 80 percent of the fuel had vaporized, confirming that under these operating conditions "most" but not necessarily *all" the fuel enters the cylinder in vapor form.39 The engine operating range where fuel puddling, fuel films, and rivulets are observed (see Fig. 7-27) can now be explained. At light load, secondary atom- 320 INTERNAL COMBUSTION ENGINE FUNDAMENTALS ization at the throttle and the lower manifold pressure would reduce the am0 of liquid fuel impinging on the manifold plenum floor. Also, typical mani heating at light load substantially exceeds the heat required to vaporize the completely,40 and manifold floor temperatures are of order 15•‹Chigher tha full load. All the above is consistent with less liquid on the floor and none in runners at light load, compared to what occurs at full load. At high speed, drop sizes produced in the carburetor are much smaller, so impingement on the walk is much reduced. The fuel flow to each cylinder per cycle is not exactly the same. There b pometric variation where fuel is not divided equally among individual cylinden There is also a time variation under steady-state engine conditions where the air/fuel ratio in a given cylinder varies cycle-by-cycle?' Data on time-averagd air/fuel ratios in each cylinder of multicylinder engines show that the extent d the maldistribution varies from engine to engine, and for a particular engine varies over the load and speed range. Spreads in the equivalence ratio (maximum to minimum) of about 5 percent of the mean value are typical at light load fa carbureted engines. Largest variations between cylinders usually occur at wide open throttle. WOT spreads in the equivalence ratio of about 15 percent of t b mean appear to be typical, again for carbureted engines, while spreads as high u 20 to 30 percent are not uncommon at particular speeds for some engines.2'** Time - -. variations are less well defined; the limited data available suggest they could be of comparable magnit~de.~' With multipoint port fuel-injection systems, the fuel transport processes substantially different and are not well understood. Air-flow phenomena are corn parable to those with carbureted or throttle-body injection systems. However, manifold design can be optimized for air flow alone since fuel transport from (hc throttle through the manifold is no longer a design constraint. Because the manufacture and operation of individual fuel injectors are not identical, there is still some variation in fuel mass injected cylinder-to-cylinder and cycle-to-cycle. Si individual cylinder air flows depend on the design of the manifold, whereas amount of fuel injected does not, uniform air distribution is especially impor with port injection systems. The fuel vaporization and transport processes depend on the duration of injection and the timing of injection pulse(s) relati* to the intake valve-lift profile. Some of the injected fuel will impinge on the port walls, valve stem, and backside of the valve, especially when injection towa closed valve occurs. Backflow of hot residual gases at part-load operation have a substantial effect on fuel vaporization. Compensation for fuel lag du transient engine operation is still required; sudden throttle openings are acc panied by a "lean spike" in the mixture delivered to the engine, comparable though smaller than that shown in Fig. 7-28 for a throttle-body fuel-injecd system. Thus wall wetting, evaporation off the wall, and liquid flow along wall are all likely to be important with port fuel-injection systems also. With port fuel-injection systems, liquid fuel enters the cylinder and drop are present during intake and compression. Limited measurements have made of the distribution, size, and number density of these fuel droplets. Du the droplet number density in the clearance volume increased to a @,imum at the end of injection (the injection lasted from 45 to 153' ATC) and decreased due to evaporation during compression to a very small value at Ibc time of ignition. Average droplet size during intake was 10 to 20 pm in diamde,; it increased during compression as the smaller drops in the distribution ,,porated.
At the conditions tested, some 10 to 20 percent of the fuel was in dropletform at the end of injection. At ignition, the surviving droplets contained negligible fraction of the fuel. During injection, the distribution of droplets laoS~the clearance volume was nonuniform. It became much more uniform with ,,me,after injection ended.33 , PROBLEMS 7.1. The equivalence ratio in a conventional spark-ignition engine varies from no load (idle) to full load, at a fixed engine speed, as shown at the top of Fig. P7-1. (By load is meant the percentage of the maximum brake torque at that speed.) Also shown is the variation in total friction (pumping plus mechanical rubbing plus accessory friction).Using formats similar to those shown, draw carefully proportioned qualitatioe graphs of the following parameters versus load (0 to 100 percent): Combustion efficiency, rl, Gross indicated fuel conversion eficiency, Gross indicated mean effective pressure, imep, Brake mean effective pressure, bmep Mechanical efficiency, q, Indicate clearly where the maximum occurs if there is one, and where the value is zero or unity or some other obvious value, if appropriate. Provide a briejjustification for the shape of the curves you draw.
7.2 The four-cylinder spark-ignition engine shown in the figure uses an oxygen sensor in the exhaust system to determine whether the exhaust gas composition is lean or rich of the stoichiometric point, and a throttle-body injection system with feedback to maintain engine operation close to stoichiometric. However, since there is a time delay between a change in the fuellair ratio at the injector location and the detection of that change by the sensor (corresponding to the flow time between the injector and the sensor), the control system shown results in oscillations in fuevair ratio about the stoichiometricpoint. (a) Estimate the average-flowtime between the injector and the sensor at an engine speed of 2000 revlmin. INTERNAL COMBUSTION ENGINE FUNDAMENTALS + (b) The sensor and control unit provide a voltage V of V, volts when the fuel/& equivalence ratio 4 is less than one and a voltage of - V, volts when 6 is greab than one. The feedback injection system provides a fuellair ratio (FIA) given by);( )(; = (1 t=o + cvn where t is the time (in seconds) after the voltage signal last changed sim (FIA),,, is the fuellair

In the eng* cylinder, the flow involves a complicated combination of turbulent shear l a m recirculating regions, and boundary layers. The flow is unsteady and may exhi? substantial cycle-to-cycle fluctuations. Both large-scale and small-scale t u r b d d motions are important factors governing the overall behavior of the flow.' An important characteristic of a turbulent flow is its irregularity 0' domness. statistical methods are therefore used to define such a flow field. The normally used are: the mean velocity, the fluctuating velocity about mean, and several length and time scales. In a steady turbulent flow situation, the instantaneous local fluid velocity U (in a specific direction) is written: For steady flow, the mean velocity 0 is the time average of U(t): ~ h fluctuating c velocity component u is defined by its root mean square value, the turbulence intensity, u': Alternatively, since the time average of (uo) is zero. In engines, the application of these turbulence concepts is complicated by the fact that the flow pattern changes during the engine cycle. Also, while the overall features of the flow repeat each cycle, the details do not because the mean flow can vary significantly from one engine cycle to the next. There are both cycle-to-cycle variations in the mean or bulk flow at any point in the cycle, as well as turbulent fluctuations about that specific cycle's mean flow. One approach used in quasi-periodic flows such as that which occurs in the engine cylinder is ensemble-averaging or phase-averaging.

Usually, velocity measurements are made over many engine cycles, and over a range of crank angles. Thc instantaneous velocity at a specific crank angle position 9 in a particular cycle i can be written as The ensemble- or phase-averaged velocity, 0(9), is defined as the average of *dues at a specific phase or crank angle in the basic cycle. Figure 8-5 shows this approach applied schematically to the velocity variation during a two-stroke engine cycle, with small and large cycle-to-cycle variations. The ensemble3Vwaged velocity is the average over a large number of measurements taken at the same crank angle (two such points are indicated by dots): N , is the number of cycles for which data are available. By repeating this CHARGE MOTION WITHIN THE CYLINDER (a) Low 333 cycle-to-cycle variation FIGURE 8 4 (b) Large cycle-to-cycle variation Ensemble average Schematic of jet created by flow through the intake valve indicating its turbulent struct~re.~. . FIGURE 8-5 Schematic of velocity variation with crank angle at a fixed location in the cylinder during !wo consecutive cycles of an engine. Dots indicate measurements of instantaneous velocity at the same crank angle. Ensemble- or phase-averaged velocity obtained by averaging over a large number of sucb measurements shown as solid smooth line. Top graph: low cycle-to-cycle flow variations. Here I k individual-cycle mean velocity and ensemble-averaged velocity are closely comparable. Bollom graph: large cycle-to-cycle variations. Here the individual-cycle mean velocity (dotted line) is ditTertal from the ensemble-averaged mean by 0.The turbulent fluctuation u is then defined in relation to l k individual-cycle .', process at many crank angle locations the ensemble-averaged velocity pr~fil over the complete cycle is obtained. The ensemble-averaged mean velocity is only a function of crank since the cyclic variation has been averaged out. The difference between the velocity in a particular cycle and the ensemble-averaged mean velocity over man cycles is defined as the cycle-by-cycle variation in mean velocity: O(0, i) = U(8, i) - UEA(0) Thus the instantaneous velocity, given by Eq. (8.4), can be split into three co Figure 8-5 illustrates this breakdown of the instantaneous velocity into an ensemble-averaged component, an individual-cycle mean velocity, and a component which randomly fluctuates in time at a particular point in space in a single cycle. This last component is the conventional definition of the turbulent velocity fluctuation. Whether this differs significantly from the fluctuations about ~hcensemble-averaged velocity depends on whether the cycle-to-cycle fluctuations are small or large.

The figure indicates these two extremes.? In turbulent flows, a number of length scales exist that characterize different aspects of the flow behavior. The largest eddies in the flow are limited in size by the system boundaries. The smallest scales of the turbulent motion are limited by molecular diffusion. The important length scales are illustrated by the schematic of the jet issuing into the cylinder from the intake valve in Fig. 8-6. The eddies responsible for most of the turbulence production during intake are the large eddies in the conical inlet jet flow. These are roughly equal in size to the local jet thickness. This scale is called the integral scale, I,: it is a measure of the largest scale structure of the flow field. Velocity measurements made at two points separated by a distance x significantly less than I, will correlate with each other; with x % I , , no correlation will exist. The integral length scale is, therefore, defined as the integral of the autocorrelation coeficient of the fluctuating velocity 31 two adjacent points in the flow with+respect to the variable distance between - 'There is considerabledebate as to whether the fluctuating components of the velocity U(0,i) defined E q (8.7) (cycle fluctuations in the mean velocity and fluctuations in time about the individual cycle are physically distinct phenomena. The high-frequency fluctuations are generally attributed to the variations in the mean dOw k u e e n individual cycles, a phenomenon that is well established. Whether this distinction is ad has yet to be resolved. -n) 334 CHARGE MOTION WITHIN THE CYLINDER INTERNAL COMBUSTION ENGINE FUNDAMENTALS 335 , 1 FIGURE 8-7 Spatial velocity autocorrelationR, as a f u n ~ od n x, detining the integral length scale I, and H 0 I IM micro length scale I,. 'I the points, as shown in Fig. 8-7: i.e., 1, = [R , where R, = dx 1 9 u(xo)u(xo+ x) Nm- 1 U'(X~)U'(X~ + X) i= 1 This technique for determining the integral scale requires simultaneous measuments at two points. Due to the d i c u l t y of applying such a technique in most efforts to determine length scales have first employed correlations to de mine the integral time scale, T,. The integral time scale of turbulence is defined a correlation between two velocities at a fixed point in space, but separated time : 7, = [be isotropic (have no preferred direction) than are the large eddies, and have a yncture like that of other turbulent flows. The dissipation of turbulence energy ukes place in the smallest structures. At this smallest scale of the turbulent motion, called the Kolntogorov scale, molecular viscosity acts to dissipate smallkinetic energy into heat. If s is the energy dissipation rate per unit mass and ,,he kinematic viscosity, Kolmogorov length and time scales are defined by (8.1 1) The ~(olmogorovlength scale indicates the size of the smallest eddies. The);olmogor~vtime scale characterizes the momentum-diffusion of these smallest dructures. A third scale is useful in characterizing a turbulent flow. It is called the mjcroscale (or Taylor microscale). The micro length scale,1 is defined by relating the fluctuatingstrain rate of the turbulent flow field to the turbulenac intensity: 11 can be determined from the curvature of the spatial correlation curve at the & i n ,as shown in Fig. 8-7.'.' More commonly, the micro time scale TM is determined from the temporal autocorrelation function of Eq. (8.9): For turbulence which is homogeneous (has no spatial gradients) and is isotropic (has no preferred direction), the microscales,1 and ,T are related by R, dt where 1 u(to)u(to + t) R, = N m - 1 i = ul(to)u'(to+ t) and N, is the number of measurements. Under conditions where the turbul pattern is convected past the observation point without significant distortion the turbulence is relatively weak, the integral length and time scales are rela by 1, = Orl In flows where the large-scale structures are convected, r, is a measure of it takes a large eddy to pass a point. In flows without mean motion, the int time scale is an indication of the lifetime of an eddy.5* Superposed on this large-scale flow is a range of eddies of sm smaller size, fed by the continual breakdown of larger eddies. Since the eddies respond more rapidly to changes in local flow pattern, they are mo These different scales are related as follows. The turbulent kinetic energy per unit mass in the large-scale eddies is proportional to u". Large eddies lose a substantial fraction of this energy in one "turnover" time 1,/u1. In an equilibrium situation the rate of energy supply equals the rate of dissipation: ut3 11 EX- Thus, ' 'here Re, is the turbulent Reynolds number, ull,/v.

Within the restrictions of homogeneous and isotropic turbulence, an energy can be used to relate 1, and ';1 . , 336 INTERNAL COMBUSnON ENGINE FUNDAMENTALS CHARGE MOTION WITHIN THE CYLINDER Fi where A is a constant of order 1. Thus, 337 d d t y fluctuation is 112 ~ ~ j l I 2 I,=($) 1, These restrictions are not usually satisfied within the engine cylinder dUrhr intake. They are approximately satisfied at the end of compression. 8.2.2 AS has already been explained, this definition of fluctuation intensity [the mamble-averaged rms velocity fluctuation, Eq. (8.18)] includes cyclic variations the mean flow as well as the turbulent fluctuations about each cycle's mean flow.7 ~t is necessary to determine the mean and fluctuating velocities on an ,ndividual-~y~le basis to characterize the flow field more completely. The critical p ~ of~ this t process is defining the mean velocity at a specific crank angle (or %;thina small window centered about that crank angle) in each cycle.

Several have been used to determine this individual-cycle mean velocity (e.g., moving window, low-pass filtering, data smoothing, conditional sampling; see ~ c f7.for a summary). A high data rate is required. In this individual-cycle velocity analysis the individual-cycle time-averaged or mean velocity o(8, 0 is first determined.'." The ensemble average of this mean velocity Application to Engine Velocity Data , As has been explained above, it is necessary to analyze velocity data on an in& vidual cycle basis as well as using ensemble-averaging techniques. The basic nitions for obtaining velocities which characterize the flow will now be develow The ensemble-averaged velocity has already been defined by Eq. (8.5). ~h~ ensemble-averaged fluctuation intensity uk, is given by eEA u;, EA(@ = ,, {- x [U(&')i {- x [~ (e ill2} , 1 Nc Nc i=1 112 1 Nc Nc i=1 - oEA(e)2]r12 (8.16) It includes all fluctuations about the ensemble-averaged mean velocity. Use of Eqs. (8.5) and (8.16) requires values for U and u at each specific crank angle under consideration. While some measurement techniques (e.g., hot. wire anemometry) provide this, the preferred velocity measurement method (doppler anemometry) provides an intermittent signal. With laser doppler mometry (LDA), interference fringes are produced within the small volume created by the intersection of two laser beams within the flow field. When a small particle passes through this volume, it scatters light at a frequency proportio to the particle velocity. By seeding the flow with particles small enough to camed without slip by the flow and collecting this scattered light, the flow velocity is determined.9 A signal is only produced when a particle moves through the measurement volume; thus one collects data as velocity crank angle pairs. It h necessary, therefore, to perform the ensemble-averaging over a finite crank angle window A8 around the specific crank angle of interest, 8. The ensemble-averad velocity equation becomes is identical to the ensemble-averaged value given by Eq. (8.17). The root mean square fluctuation in individual-cycle mean velocity can then be determined from This indicates the magnitude of the cyclic fluctuations in the mean motion. The instantaneous velocity fluctuation from the mean velocity, within a specified window A0 at a particular crank angle 0, is obtained from Eq. (8.4). This instantaneous velocity fluctuation is ensemble-averaged, because it varies substantially cycle-by-cycle and because the amount of data is usually insufficient to give reliable individual-cycle results: where Ni is the number of velocity measurements recorded in the window during the ith Cycle, N , is the number of cycles, and N, is the total number of measu* ments.t The corresponding equation for the ensemble-averaged root mean squa* t This need to ensemble-average over a finite crank angle window introduces an error called angle broadening, due to change in the mean velocity across the window. This error depends on velocity gradient, and can be made negligibly small by suitable choice of window me?-'' I ! i This quantity is the ensemble-averaged turbulence intensity. Several different techniques have been used to measure gas velocities within [he engine cylinder (see Refs. 13 and 14 for brief reviews and references). The 'ehnique which provides most complete and accurate data is laser doppler anemometr~.~ Sample results obtained with this technique will now be reviewed t o CHARGE MOTION WITHIN THE CYLINDER 339 9 illustrate the major features-of the in-c must be interpreted with caution since where the geometry and flow have been modi their interiretation easier. Also, the flow withi in nature. It takes measurements at many poi of a flow visualization technique to characterize the flow adequately. Figure 8-8 shows ensemble-averaged velocities throughout the engine at two measurement locations in a special L-head engine designed to gene swirling flow within the cylinder. The engine was motored at 300 rev/min, a mean piston speed of 0.76 m/s. Figure 8-8b of the swirling intake flow within the clear High velocities are generated during the inta then decreasing in response to the "..-..-, ---- - - is a motored engine cyclc A cornparism with an equivalent firing ycle showed close agreement.'' The expansi yLra.,."... - . . - -0 Intake Compression Expansion Exhaust Crank angle, deg 180 . . 5w , , , >w 1 .-- ~ntakeCompression Exhaust Ex~msio" Crank angle, deg E -SnwotJ~edensemble --- Cycle by cycle Crank angle, deg (a) b 2 Intake Compression Expansion Exhaust Crank angle, deg (b) (l(;cRE 8 9 temrhk-averaged rms velocity fluctuation and ensemble-averagedindividual-cycle turbulence inten-1, ds a function of crank angle: (a)at location bin Fig. 8-8a; (b)at location c in Fig. 8-8a.l' p l h a ~ ~stroke t velocities are not typical of firing engine behavior, h0wever.t [lgurc 8-8c shows the mean velocity in the clearance volume in the same direcrlon but on the cylinder axis. At this location, positive and negative flow veloc,rlsswere measured. Since this location is out of the path of the intake generated b w , velocities during the intake stroke are much lower. The nonhomogeneous character of this particular ensemble-mean flow is evident. Figure 8-9 shows the ensemble-averaged rms velocity fluctuation (which tncludcs contributions from cycle-by-cycle variations in the mean flow and rurbulence) and the ensemble-averaged individual-cycle turbulence intensity at rhcw same two locations and directions. The difference between the two curves in c~rhgraph is an indication of the cycle-by-cycle variation in the mean flow [see 1q. 18.7)].

During the intake process, within the directed intake flow pattern, the c)cle-by-cycle variation in the mean flow is small in comparison to the high ~urbulcncelevels created by the intake flow. Outside this directed flow region, again during intake, this cycle-by-cyclecontribution is more significant relative to the turbulence. During compression, the cycle-by-cycle mean flow variation is comparable in magnitude to the ensemble-averaged turbulence intensity. It is 'hmfore highly significant. Two important questions regarding the turbulence in the engine cylinder m whether it is homogeneous (i.e., uniform) and whether it is isotropic (i.e., Inhendent of direction). The data already presented in Figs. 8-8 and 8-9 show during intake the flow is far from homogeneous. Nor is it isotropic.ll (b) \ FIGURE 8-8 lgine cycle in motored four-stroke L-head engin Ensemble-averaged velocities roughout the el ! schematic showing measurement locations ad rev/min, mean piston speed 0.

m/s. (a)Engine th; (c) velocity at c on cylinder axis.'' intake flow pal ity directions; (b) velocity at b ' increase in velocity when the exhaust valve opens is due to the flow of gas into the cylinder bust. due primarily to heat losses, the cylinder pressure is then below 1 a m . 340 INTERNAL COMBUSTION ENGINE FUNDAMENTALS However, it is the character of the turbulence at the end of the com process that is most important: that is what controls the fuel-air mi burning rates. Only limited data are available which relate to these With open disc-shaped combustion chambers, measurements at differen tions in the clearance volume around TC at the end of compression show turbulence intensity to be relatively homogeneous. In the absence of an in generated swirling flow, the turbulence intensity was also essentially isotr near TC.16 These specific results support the more general conclusion that inlet boundary conditions play the dominant role in the generation of the flow and turbulence fields during the intake stroke. However, in the ab swirl, this intake generated flow structure has almost disappeared by the compression process commences. The turbulence levels follow this t mean flow, with the rapid decay process lasting until intake valve closing. ~a in the compression process the turbulence becomes essentially homogeneous.11 When a swirling flow is generated during intake, an almost solidrotating flow develops which remains stable for much longer than the inlet generated rotating flows illustrated in Fig. 8-3.

With simple disc-shaped cham bers, the turbulence still appears to become almost homogeneous at the end d compression. With swirl and bowl-in-piston geometry chambers, however, (bC flow is more complex (see Sec. 8.3). The flow through the intake valve or port is responsible for many featurn of the in-cylinder motion. The flow velocity through the valve is proportional 10 the piston speed [see Eq. (6.10) for pseudo valve flow velocity, and Eq. 2.10)]. % would be expected therefore that in-cylinder flow velocities at different en@ speeds would scale with mean piston speed [Eq. (2.1111. Figure 8-10 show) ensemble-averaged mean and rms velocity fluctuations, normalized by the mean piston speed through the cycle at three different engine speeds. The measuremest location is in the path of the intake generated swirling flow (point b in Fig. 8-84 An the curves have approximately the same shape and magnitude, indicating ths I 0: ' 2 4 I I I 6 I 8 1 Mean piston speed, m/s nCURE 8-11 .. ~~ridual-cycle turbulence intensity u;,, (OX) and ensemble-averaged rms fluctuation velocity symbols) at TC at the end of compression, for a number of different flow configurations chamber geometries as a function of mean piston speed.'6 Two data sets for two-stroke ported mpncs. Four data sets with intake generated swirl. of this velocity scaling.? Other results support this conclusion, though in the absence of an ordered mean motion such as swirl when the ensemble-averaged mean velocities at the end of compression are low, this scaling k r the mean velocity does not always hold.16 Figure 8-11 shows a compilation of cnscmble-averaged rms fluctuation velocity or ensemble-averaged individualcycle turbulence intensity results at TC at the end of compression, from 13 different flow configurations and combustion chamber geometries. Two of these sets of r~ultsare from two-stroke cycle ported configurations. The measured fluctuating wlocities or turbulence intensities are plotted against mean piston speed. The l~navrrelationship holds well. There is a substantial variation in the proportionality constant, in part because in most of these studies (identified in the figure) the ensemble-averaged rms fluctuation velocity was the quantity measured. Since this includes the cycle-by-cycle fluctuation in the mean velocity, it is larger (by up to a htor of 2) than the average turbulence intensity u;, A consensus conclusion is emerging from these studies that the turbulence lnlmity at top-center, with open combustion chambers in the absence of swirl, a maximum value equal to about half the mean piston speed:'" ' that because of the valve and combustion chamber of this particular engine, the ratio of ff to 5 u kher than is typical of normal engine geometries. 342 INTERNAL COMBUSTION ENGINEFUNDAMENTALS The available data show that the turbulence intensity at TC with swirl is usua higher than without swirl16 (see the four data sets with swirl in Fig. 8-11). some data, however, indicate that the rms fluctuation intensity with swirl may be lower.18 The ensemble-averaged cyclic variation in individual-cycle mean veloriv at the end of compression also scales with mean piston speed. This quantity be comparable in magnitude to the turbulence intensity. It usually decrease 'when a swirling flow is generated within the cylinder during the intake pr0cess.l l6 During the compression stroke, and also during combustion while tk cylinder pressure continues to rise, the unburned mixture is compressed. Turbulent flow properties are changed significantly by the large and rapidly imposed distortions that result from this compression. Such distortions, in the absence dissipation, would conserve the angular momentum of the flow: rapid comprsion would lead to an increase in vorticity and turbulence intensity. There evidence that, with certain types of in-cylinder flow pattern, an increase in turbu. lence intensity resulting fro-m piston motion and combustion does occur toward the end of the compression process. The compression of large-scale rotating flow can cause this increase due to the increasing angular velocity required to con. serve angular momentum resulting in a growth in turbulence generation by shear.19 Limited results are available which characterize the turbclence time and length scales in automobile engine flows. During the intake process, the integral length scale is of the order of the intake jet diameter, which is of the order of the valve lift (510 mm in automo-bile-size engines). During compression the flow relaxes to the shape of the combusion,chamber. The integral time scale at the end of compression decreases with increasing engine speed. It is of order 1 ms at engine speeds of about 1000 revlmin. The integral length scale at the end of compression is believed to scale with the clearance height and varies little with engine speed. It decreases as the piston approaches TC to about 2 mm (0.2 x clearance height). The micro time scale at the end of compression is of order 0.1 ms at 1000 revlmin, and decreases as engine speed increases (again in automobile-size engine cylinders).

Micro length scales are of order 1 mm at the end of compression and vary little with engine speed. Kolmogorov length scales mm.8*20. 21 at the end of compression are of order CHARGE MOTION WITHIN M E CYLINDER 343 the injected fuel. Swirl is also used to-speed up the combustion process in ,park-igniti~nengines. In two-stroke engines it is used to improve scavenging. In wme designs of prechamber engines, organized rotation about the prechamber ,is is also called swirl. In prechamber engines where swirl within the precombustion chamber is important, the flow into the prechamber during the compresion process creates the rotating flow. Prechamber flows are discussed in Sec. 8.5. 1 Swirl Measurement The nature of the swirling flow in an actual operating engine is extremely difficult to determine. Accordingly, steady flow tests are often used to characterize the swirl.

Air is blown steadily through the inlet port and valve assembly in the cylinder head into an appropriately located equivalent of the cylinder. A common technique for characterizing the swirl within the cylinder has been to use a light paddle wheel, pivoted on the cylinder centerline (with low friction ~bearings), mounted between 1 and 1.5 bore diameters down the cylinder. The paddle wheel diameter is close to the cylinder bore. The rotation rate of the paddle wheel is used as a measure of the air swirl. Since this rotation rate depends on the location of the wheel and its design, and the details of the swirling flow, this t e h nique is being superseded by the impulse swirl meter shown in Fig. 8-12. A honeycomb flow straightener replaces the paddle wheel: it measures the total torque exerted by the swirling flow. This torque equals the flux of angular 8 3 SWIRL Swirl is usually defined as organized rotation of the charge about the cyli axis. Swirl is created by bringing the intake flow into the cylinder with an ini angular momentum. While some decay in swirl due to friction occurs during engine cycle, intake generated swirl usually persists through the compressio~ combustion, and expansion processes. In engine designs with bowl-in-pi combustion chambers, the rotational motion set up during intake is substant modified during compression. Swirl is used in diesels and some stratified-char engine concepts to promote more rapid mixing between the inducted air charge Ld Restraining torque FIGURE 8-12 Schematic meter.22 of steady-flow impulse torque swirl 344 INTERNAL COMBUSTION ENGINE FUNDAMENTALS momentum through the plane coinciding with the flow-straightener upstr face. For each of these approaches, a swirl coeflcient is defined which essent compares the flow's angular momentum with its axial momentum. For paddle wheel, the swirl coefficient C, is defined by C, = o B produced under corresponding conditions of flow and valve lift Ibe mains in the cylinder. Steady-state impulse torque-meter flow rig data can be to estimate engine swirl in the following manner.23Assuming that the port valve retain the same characteristics under the transient conditions of the mgineas on the steady-flow rig, the equivalent solid-body angular velocity o, at :he end of the intake process is given by 00 - where w, is the paddle wheel angular velocity (=2nNp, where N, is the rotatio a1 speed) and the bore B has been used as the characteristic dimension. characteristic velocity, vO, is derived from the pressure drop across the v using an incompressible flow equation: uO = poi pPljI2 *here Q1 and 6, are crank angles at the start and end of the intake process and ,hc torque T and mass flow rate m are evaluated at the valve lift corresponding , [he local crank angle. Using Eq. (8.27) for T, Eq. (6.11) for m, assuming vo and ,,are constant throughout the intake process, and introducing volumetric effi,jfncy q, based on intake manifold conditions via Eq. (2.27), it can be shown that or a compressible flow equation: vo= {-- 27 Po (Y- 1) Po - P(C$- 1)ty]}112 where the subscripts 0 and c refer to upstream stagnation and cylinder values, respectively. The difference between Eqs. (8.25) and (8.26) is usually small. With the impulse torque meter, characteristic velocity and length scales must also k introduced. Several swirl parameters have been defined.22.23 The simplest is 8T rhvo B C, = - where T is the torque and m the air mass flow rate. The velocity oO,defined by Eq. (8.25) or Eq. (8.26), and the bore have again been used to obtain a dimensionless coefficient.

Note that for solid-body rotation of the fluid within the cylinder at the paddle wheel speed o,, Eqs. (8.24) and (8.27) give identical swirl coefficients. In practice, because the swirling flow is not solid-body rotation and because the paddle wheel usually lags the flow due to slip, the impulse torqw meter gives higher swirl coefficient^.^^ When swirl measurements are made in an operating engine, a swirl ratio is normally used to define the swirl. It is defined the angular velocity of a solid-body rotating flow o s , which has equal angular momentum to the actual flow, divided by the crankshaft angular rotational speed : W, R, = 2nN During the induction stroke in an engine the flow and the valve open a m and consequently the angular momentum flux into the cylinder, vary with angle. Whereas in rig tests the flow and valve open area are fixed and the a n d u momentum passes down the cylinder continuously, in the engine intake p r e where A,CD is the effective valve open area at each crank angle. Note that the crank angle in Eq. (8.29) should be in radians. Except for its (weak) dependence on q,, Eq. (8.29) gives R, independent of operating conditions directly from rig (61results and engine geometry. The relationship between steady-flow rig tests (which are extensively used because of their simplicity) and Wual engine swirl patterns is not fully understood. Steady-flowtests adequately describe the swirl generating characteristics of thc intake port and valve (at fixed valve lift) and are used extensively for this purpose. However, the swirling flow set up in the cylinder during intake can change significantly during compression. 83.2 Swirl Generation during Induction Two general approaches are used to create swirl during the induction process. In one, the flow is discharged into the cylinder tangentially toward the cylinder wall, ahere it is deflected sideways and downward in a swirling motion. In the other, the swirl is largely generated within the inlet port: the flow is forced to rotate about the valve axis before it enters the cylinder. The former type of motion is achieved by forcing the flow distribution around the circumference of the inlet valve to be nonuniform, so that the inlet flow has a substantial net angular momentum about the cylinder axis.

The directed port and deflector wall port in Fig. 8-13 are two common ways of achieving this result. The directed port brings the flow toward the valve opening in the desired tangential direction. Its passage straight, which due to other cylinder head requirements restricts the flow area and results in a relatively low discharge coefficient. The deflector wall port uses 'he pon inner side wall to f o m the flow preferentially through the outer peripht'Y of the valve opening, in a tangential direction. Since only one wall is used to Obtain a directional effect, the port areas are less restrictive. " CHARGE MOTION WITHIN THE CYLINDER Shrouded 347 Masked FIGURE 8-14 shrouded inlet valve and masked cylinder head approaches for producing net incylinder angular momentum. FIGURE 8-13 Dierent types of swirl-generating inlet ports: (a) deflector wall; (b) directed; (c) shallow ramp helical; (d) steep ramp Flow rotation about the cylinder axis can also be generated by masking off or shrouding part of the peripheral inlet valve open area, as shown in Fig. 8-14. Use is often made of a mask or shroud on the valve in research engines because changes can readily be made. In production engines, the added cost and weight, problems of distortion, the need to prevent valve rotation, and reduced volumetric eficiency make masking the valve an unattractive approach. The more practical alternative of building a mask on the cylinder head around part of the inlet valve periphery is used in production spark-ignition engines to generate swirl. It can easily be incorporated in the cylinder head casting process. The second broad approach is to generate swirl within the port, about the valve axis, prior to the flow entering the cylinder. Two examples of such helical ports are shown in Fig. 8-13. Usually, with helical ports, a higher flow discharge coefficient at equivalent levels of swirl is obtained, since the whole periphery or the valve open area can be fully utilized. A higher volumetric efficiency resultr Also, helical ports are less sensitive to position displacements, such as can occur in casting, since the swirl generated depends mainly on the port geometry above the valve and not the position of the port relative to the cylinder axis. Figure 8-15 compares steady-state swirl-rig measurements of examples the ports in Fig. 8-13. The rig swirl number increases with increasing valve reflecting the increasing impact of the port shape and decreasing impact of the flow restriction between the valve head and seat. Helical ports normally more angular momentum at medium lifts than do directed ports.23v2s Th ratios for these ports calculated from this rig data using Eqs. (8.27) and (8.29) are: 2.5 for the directed port, 2.9 for the shallow ramp helical, and 2.6 for the steep ramp helical. Vane swirl-meter swirl ratios were about 30 percent less. These { impulse-swirl-meter derived engine swirl ratios arewithin about 20 percent of the solid-body rotation rate which has equal angular momentum to that of the cylinder charge determined from tangential velocity measurements made within the cylinder of an operating engine with the same port, at the end of the induction process." Valve lift Valve diameter Steady-state torque meter swirl measurements of directed, shallow ramp, and steep ramp helical ports as a function of inlet valve lift/diameter ratio.23 348 INTERNAL COMBUSTION ENGINE NNDAMEN~ALS Directed and deflector wall ports, and masked valve or head designt produce a tangential flow into the cylinder by increasing the flow resistanfc through that part of the valve open area where flow is not desired. A highly nonuniform flow through the valve periphery results and the flow into the cylinder has a substantial v, velocity component in the same direction about the cylin. &r axis. In contrast, helical ports produce the swirl in the port upstream of the valve, and the velocity components v,, and v, through the valve opening, and v, about the valve axis are approximately uniform around the valve open area.

Figure 8-16 shows velocity data measured at the valve exit plane in steady-flow rig tests with examples of these two types of port. The valve and cylinder waU locations are shown. In Fig. 8-16a, the deflector wall of the tangentially oriented port effectively prevents any significant flow around half the valve periphery. contrast, in Fig. 8-166 with the helical port, the air flows into the cylinder around CHARGE MOTION WITHIN THE CYLINDER 349 lhc full valve open area.

The radial and axial velocities are essentially uniform ,round the valve periphery. The swirl velocity about the valve axis (anticlockwise *hen viewed from above) for this helical port is relatively uniform and is about hdlf the magnitude of the radial and axial velocities. The swirling air flow within the cylinder of an operating engine is not ,,ifom The velocities generated at the valve at each point in the induction Crwessdepend on the valve open area and piston velocity. The velocities are highest during the first half of the intake process as indicated in Fig.

6-15. Thus, [he swirl velocities generated during this portion of the induction stroke are hleher than the swirl generated during the latter half of the stroke: there is swirl slratificati~n. Also, the flow pattern close to the cylinder head during induction is disorganized, and not usually close to a solid-body rotation. It of a system of vortices, created by the high-velocity tangential or spiraling intake jet. Further down the cylinder, the flow pattern is closer to solid-body with the swirl velocity increasing with increasing radius.23.24 This more ordered flow directly above the piston produces higher swirl velocities in that region of the cylinder. As the piston velocity decreases during intake, the swirl pattern redistributes, with swirl speeds close to the piston decreasing and swirl ' speeds in the center of the cylinder increasing." Note that the axis of rotation of rhc in-cylinder gases may not exactly coincide with the cylinder axis. 833 Swirl Modification within the Cylinder Radial 1 - 1 = 50 mls FIGURE 8-16 Swirl, axial, and radial velocities measured 2 mm from cylinder head around the valve circul~fie for (a) tangential deflector-wall port and (b)helical port; magnitude of velocity is given by the dis along a radial line (from valve axis), from valve outline to the respective curve scaled27by the refe length (examples of radial velocity indicated by two arrows); valve lift = 12.8 The angular momentum of the air which enters the cylinder at each crank angle during induction decays throughout the rest of the intake process and during the compression process due to friction at the walls and turbulent dissipation within the fluid.

Typically one-quarter to one-third of the initial moment of momentum about the cylinder axis will be lost by top-center at the end of compression. However, swirl velocities in the charge can be substantially increased during compression by suitable design of the combustion chamber. In many designs of direct-injection diesel, air swirl is used to obtain much more rapid mixing between the fuel injected into the cylinder and the air than would occur in the absence of swirl. The tangential velocity of the swirling air flow set up inside the cylinder during induction is substantially increased by forcing most of the air into a compact bowl-in-piston combustion chamber, usually centered on the cylinder "is, as the piston approaches its top-center position. Neglecting the effects of friction, angular momentum is conserved, and as the moment of inertia of the air is decreased its angular velocity must increase. However, the total angular momentum of the charge within the cylinder does decay due to friction at the chamber walls. The angular momentum of the cylinder charge T, changes with time according to the moment of momentum conservation equation: 350 INTERNAL COMBUSTION ENGW FUNDAMENTALS where Ji is the flux of angular momentum into the cylinder and T, is the torquc due to wall friction. At each point in the intake process Jiis given by Ji = 1. U n F ,tial velocity v, at the wall varies with radius, the shear stress should be o;iluated at each radius and integrated over the surface: e.g.,29 pruBY dA, where dA, is an element of the valve open area, as defined in Fig. 8-17. While t angular momentum entering the cylinder during the intake process is the actual angular momentum within the cylinder at the end of induction will be less, due to wall friction during the intake process.

Friction continues through the compression process so the total charge angular momentum at the end of cornpression is further reduced. There is friction on the cylinder wall, cylinder head, and piston crown (including any combustion chamber within the crown). This friction can be esti. mated with sufficient accuracy using friction formulas developed for flow over a flat plate, with suitable definition of characteristic length and velocity scales. Friction on the cylinder wall can be estimated from the wall shear stress: where o, is the equivalent solid-body swirl.

The friction factor C, is given by the flat plate formula: CF = 0.0371(~eJ-O.~ (8.33) where 1is an empirical constant introduced to allow for differences between the flat plate and cylinder wall (1 zz 1.5)28and Re, is the equivalent of the flat plate Reynolds number [Re, = p(Boj2)(xB)/A. Friction on the cylindrical walls of a piston cup or bowl can be obtained from the above expressions with D,, the bowl diameter, replacing the bore.

Friction on the cylinder head, piston crown, and piston bowl floor can be estimated from expressions similar to Eqs. (8.32) and (8.33). However, since the FIGURE 8-17 Definition of symbols in equation for a n g m momentum flux into the cylinder [Eq. (8.31)l. sith *here CI is an empirical constant (~0.055).

An alternative approximate is to evaluate these components of the wall shear stress at the mean ndi~s.'~ Next, consider the effectson swirl of radially inward displacement of the air &rge during compression. The most common example of this phenomenon murs with the bowl-in-piston combustion chamber design of medium- and highdirect-injection diesels (see Sec. 10.2.1). However, in spark-ignition engines shere swirl is used to increase the burning rate, the shape of the combustion chamber close to top-center can also force radially inward motion of the charge. For a given swirling in-cylinder flow at the end of induction and neglecting the ~Rectsof friction, as the moment of inertia of the air about the cylinder axis is dt-creased the air's angular velocity must increase to conserve angular momentum. For example, for solid-body rotation of the cylinder air charge of mass m,, the initial angular momentum and solid-body rotation a,,, are related at bottom-center by where I, is the moment of inertia of the charge about the cylinder axis. For a disc-shaped combustion chamber, Zc = mc B2/8 and is constant. For a bowl-inpiston combustion chamber, where DB and h, are the diameter and depth of the bowl, respectively, and z is the distance of the piston crown from the cylinder head. At TC crank position, z x 0 and I, % m, D28. At the end of induction, I, x m, B2/8.

Thus, in the absence of frictionw, would increase by usually a factor of about 4. In an operating engine with this bowl-in-piston chamber design, the observed increase in swirl in the bowl is less; it is usually about a factor of 2 to 3.23.25 This is because of wall friction, dissipation in the fluid due to turbulence and velocity gradients, and the fact that a fraction of the fluid remains in the clearance height above the piston crown. The loss in angular momentum due to these effects will vary with geometric details, initial swirl flow pattern, and engine speed. Swirl velocity distributions in the cylinder at the end of induction show the tangential velocity increasing with radius, except close to the cylinder wall where friction causes the velocity to decrease. While the velocity distribution is not that of a solid-body rotation, depending on port design and operating conditions it is 352 CHARGE MOTION WITHIN THE CYLINDER INTERNAL COMBUSTION ENGINE FUNDAMENTALS often close to solid-body rotation.23*25 Departures from the solid-body ve distribution are greater at higher engine speeds, suggesting that the flow p in the cylinder at this point in the cycle is still developing with time.23.30 absence of radially inward gas displacement during compression, the flow p continues to develop toward a solid-body distribution throughout the corn sion stroke.25Swirl ratios of 3 to 5 at top-center can be achieved with the shown in Fig. 8-13, with flat-topped pistons (i.e., in the absence of any amplification during compressi~n).~~.

25 With combustion chambers where the chamber radius is less than the cy der bore, such as the bowl in piston, the tangential velocity distribution wia radius will change during compression. Even if the solid-body rotation assump tion is reasonable at the end of induction, the profile will distort as gas move into the piston bowl. Neglecting the effects of friction, the angular momentum d each fluid element will remain constant as it moves radially inward. Thus t k increase in tangential velocity of cach fluid element as it moves radially inward proportional to the change in the reciprocal of its radius. Measurements of th swirl velocity distribution within the cylinder of bowl-in-piston engine desim support this description. The rate of displacement of gas into the bowl depenQ on the bowl volume VB, cylinder volume V, and piston speed S,, at that parti* lar piston position: ".= dt "(-)(3 L VB)sp V V The gas velocity into the bowl will therefore increase rapidly toward the end the compression stroke and reach a maximum just before TC (see Sec. 8.4 w this radial "squish" motion is discussed more fully). Thus, there is a increase in u, in the bowl as the crank angle approaches TC. The lower lay the bowl rotate slower than the upper layers because that gas entered the earlier in the compression process.23.25 Velocity measurements illustrating the development of this radial dist tion in tangential velocity are shown in Fig. 8-18. These measurements made by analysing the motion of burning carbon particles in the cylinder o operating diesel engine frog movies of the combustion process. The figure the engine geometry and the data compared with a model based on gas di ment and conservation of angular momentum in each element of the charge is displaced inward. Different swirl velocity profiles exist within and outside bowl as the piston approaches TC. Swirl velocities within the bowl TC is approached, roughly as predicted by the ideal model. Outside th swirl velocity decreases with increasing radius due to the combine friction and inward gas displacement as the clearance height decreases. Swirl ratios in bowl-in-piston engine designs of up to about 15 ca achieved with DBx 0.5B, at top-center. Amplification factors relative to topped piston swirl &retypically about 2.5 to 3, some 30 percent lower than ideal factor of (BJDJ' given by Eq. (8.35) as z + 0. This difference is due to tbr mass remaining within the clearance height which does not enter the bowl, Radius, mm 353 Radius, mm ~ G U R E818 ~ ~ l ~ cmeasurements ity as a function of radius across the combustion chamber of a firing, bowl-inprlon. direct-injection diesel engine. Schematic shows the chamber geometry. Solid lines are calcubtions based on the assumption of constant angular momentum for fluid elements as they move d ~ a l l yinward." the effects of wall friction (enhanced by the higher gas velocities in the bowl). Sometimes the bowl axis is offset from the cylinder axis and some additional loss in swirl amplification results.25 The effect of swirl generation during induction on velocity fluctuations in the combustion chamber at the end of compression has been e~arnined.~'The ~urbulenceintensity with swirl was higher than without swirl (with the same chamber geometry).'Integral scales of the turbulence were smaller with swirl than without. Cyclic fluctuations in the mean velocity are, apparently, reduced by swirl. Also, some studies show that the ensem

flow during later stages of exhaust stroke. Growing vortex in the piston face-cylinder wall corner and turbulent outflow toward the valve are apparent at 60•‹ BTC. At 20" BTC,the vortex has grown to of order 0.28 diameter.42 sp & g This vortex flow has been observed in an operating engine. Figure 8-33 shows schlieren photographs taken during the exhaust stroke in a special squarecross-section flow visualization spark-ignition engine. The accompanying schematic identifies the vortex structure which is visible in the photo because the cool boundary-layer gas is being scraped off the cylinder wall by the upward-moving piston and "rolled up." The vortex diameter as the piston approaches TC is about 20 percent of the bore. PROBLEMS 8.1. (a) Estimate the ratio of the maximum gas velocity in the center of the hollow cone inlet jet to the mean piston speed from the data in Fig. 8-1. (b) Compare this ratio with the ratio of inlet valve pseudo flow velocity determined from Fig.
6-15 to the mean piston speed at the same crank angle. The engine is that of Fig. 1-4. (c) Are the engine velocity data in (a) consistent with the velocity calculated from the simple piston displacement model of (b)? Explain. E.2. Given the relationship between turbulence intensity and mean piston speed [Eq. (8.23)] and that the turbulence integral scale is 0.2 x clearance height, use Eqs. (8.14) and (8.15) to estimate the following quantities for a spark-ignition engine with bore = stroke = 86 mm,r, = 9, at 1000 and 5000 rev/min and wide-open throttle: (a) Mean and maximum piston speed, maximum gas velocity through the inlet valve (see Prob. 8.1) (b) Turbulence intensity, integral length scale, micro length scale, and Kolmogorov length scale, all at TC = 0.002 I@ to' 16 Reynolds number t FIGURE 8-32 Ratio of area of vortex in piston faa-cylinder wall corner to square of stroke, as a function Reynolds number based on piston velocity, for piston moving toward the cylinder head.u INTERNAL COUBUSTION ENGINE FUNDAMENTALS The swirl ratio at the end of induction at 2000 rev/min in a direct-injection d i w engine of bore Istroke = 100 mm is 4.0. What is the average tangential velocity (evaluated at the inlet valve-axis radial location) required to give this swirl ratio?
What is the ratio of this velocity to the mean piston speed and to the mean flow velocity through the inlet valve estimated from the average valve open area and open time? (a) Derive a relationship for the depth (or height) h, of a disc-shaped bowl-in-piston direct-injection diesel engine combustion chamber in terms of compression ratio r.., bore B, stroke L,.bowl diameter D,, and top-center cylinder-head to pistoncrown clearance c. For B = L = 100 mm, r, = 16, D, = 0.5B, c = 1 mm find the fraction of the air charge within the bowl at TC. (b) If the swirl ratio at the end of induction at 2500 rev/min is 3 find the swirl ratio and average angular velocity in the bowl-in-piston chamber of dimensions given above. Assuple the swirling flow is always a solid-body rotation. Compare the tangential velocity at the bowl edge with the mean piston speed. Neglect any friction effects. (c) What would the swirl ratio be if the top-center clearance height was zero? 85. Using Eq. (8.37) and Fig. 8-20b plot the squish velocity divided by the mean piston speed at 10" BTC (the approximate location of the maximum) as a function of squish area expressed as a percentage of the cylinder cross section, Aj(nB2/4)x 100, from 50 to 0 percent. r, = 10, c/B = 0.01, B/L = 1, R = l/a = 3.5. 8.6. Figure 8-24 shows the velocity at the prechamber nozzle throat during compression for dimensions typical of a small swirl chamber indirect-injection diesel. Assuming that the swirl chamber shape is a disc of height equal to the diameter, that the n o d e throat is at 0.8 x prechamber radius, and that the flow enters the prechamber tangentially, estimate the swirl ratio based on the total angular momentum about the swirl chamber axis in the prechamber at top-center. Assume B = L; neglect friction. 8.7. The total crevice volume in an automobile spark-ignition engine is about 3 percent of the clearance volume. If the gas in these crevice regions is close to the wall temperature (450 K) and at the cylinder pressure, estimate the fraction of the cylinder mass within these crevice regions at these crank angles: inlet valve closing (50' ABC), spark discharge (30" BTC), maximum cylinder pressure (15" ATC), exhaust valve opening (60' BBC), TC of the exhaust stroke. Use the information in Fig. 1-8 for your input data, and assume the inlet pressure is 0.67 atm. . REFERENCES 1. Bi&n, A. F., Vafidis, C., and Whitelaw, J. H.: "Steady and Unsteady Airflow through the Intake Valve of a Reciprocating Engine," ASME Trans., J. Fluids Engng, vol. 107,pp. 413-420,1985. 2. Namazian, M., Hansen, S. P., Lyford-Pike, E.
J., Sanchez-Barsse, J., Heywood, J. B., and Rife. J.: "Schlieren Visualization of the Flow and Density Fields in the Cylinder of a Spark-Igniuon Engine," SAE paper 800044,SAE Trans., vol. 89,1980. 3. Ekchian, A., and Hoult, D. P.: "Flow Visualization Study of the Intake Process of an Internal Combustion Engine," SAE paper 790095,SAE Trans., vol. 88,1979. 4. Hirotomi, T., Nagayama, I., Kobayashi, S., and Yamamasu, M.: "Study of Induction Swirl in a Spark Ignition Engine," SAE paper 810496,SAE Trans., vol.
90,1981. 5. Reynolds, W.
C.: 'Modeling of Fluid Motions in Engines-An Introductory Overview," in J. N. Mattavi and C A. Amann (eds.), Combustion Modelling in Reciprocating Engines, pp.
69-124. Plenum Press, 1980. 6. Tennekes, H., and Lumley, J. L.: A First Course in Turbulence, MIT Press, 1972. 7. ask, R. B.: "Laser Doppler Anemometer Measurements of Mean Velocity and Turbulence in Internal Combustion Engines," ICALEO '84 Confmnce Proceedings, vols. 45 and 47,I ~ P C ~ , , , ~ ~ a s u r e m e and n t Control and h e r Diagnostics and Photochemistry, Laser Institute of AmBoston, November 1984. g, ~abaczynski.R. J.: "Turbulence and Turbulent Combustion in Spark-Ignition Engin-" Frog. Energy Combust. Sci., vol. 2, pp. 143-165.1976. 9.
Witze, P. 0.:"A Critical Comparison of Hot-wire Anemometry and Laser Doppler Velodmetry for LC. Engine Applications," SAE paper 800132,SAE Trans., vol. 89,1980. 10 Witze, P. O., Martin. J. K., and Borgnakke, C.: "Conditionally-Sampled Velocity and Turbul%feasuremmtsin a Spark Ignition Engine," Combust. Sci. Technol., vol. 36,pp. 301-317,1984. I 1. ask, R. B.: "Comparison of Window, Smoothed-Ensemble, and Cycle-by-Cycle Data Reduction Techniques for Laser Doppler Anemometer Measurements of In-Cylinder Velocity," in T. MOM R.
P. Lohmann, and J. M. Rackley (eds.), Fluid Mechanics of Combustion Systems, pp. 11-% ASME. New York, 1981. 12 Lioy T-M, and Santavicca, D. A.: "Cycle Rwolved LDV Measurements in a Motorad IC ~ngine,"ASME Ttmu., J. Fluids Engng, vol. 107,pp. 232-240,1985. 13. Amann, C. A.: "Classical Combustion Diagnostics for Engine Research," SAE paper 850395. in Engine Combustion Analysis: New Approaches, P-156,SAE, 1985. 14. Dyer, T. M.: "New Experimental Techniques for In-Cylinder Engine Studiw" SAE paper 850396, in Engine Combustion Analysis: New Ap~roaches. P-156. -.SAE, 1985. -15. Rask, R. B.: "Laser Doppler Anemometer Measurements in an Internal Combustion Engin%" SAE paper 790094,SAE Trans., vol. 88,1979. 16. Liou, T.-M., Hall, M., Santavicca,D. A, and Bracco, F. V.: "Laser Dopper Velocimetry Measurements in Valved and Ported Engines," SAE paper 840375,SAE Trans., vol. 93,1984. I f . Arcournanis, C., and Whitelaw, J. H.: "Fluid Mechanics of Internal Combustion Engines: A Review," Proc. Imtn Mech. Engrs, vol. 201,pp.
57-74.1987. 18. Bopp, S., Vafidis C., and Whitelaw, J.
H.: "The Effectof Engine Speed on the TDC Flowfield in a Motored Reciprocating Engine," SAE paper 860023,1986. 19. Won& V. W., and Hoult, D. P.: "Rapid Distortion Theory Applied to Turbulent Combustio~" SAE paper 790357. SAE Trans., vol. 88.1979. 20. Fraser, R. A.. Felton, P. G., and Bracco, F. V.: "Preliminary Turbuhce Length Scale Measurements in a Motored IC Engine," SAE paper 860021,1986. 21. Ikegami, M., Shioji, M., and Nishimoto, K.: "Turbulena Intensity and Spatial Integral Scale during Compression and Expansion Strokes in a Fow-cycle Reciprocating Engine," SAE p a p 870372.1987. 22. ~ z k a n ; ~ .Borgnakke, , C., and Morel, T.: "Characterization of Flow Produced by a High-Swirl Inlet Port," SAE D a m 830266. 1983.
23. Monaghan, M. L, tnd ~ettifer,H. F.: "Air Motion and Its Effects on Diesel Performance and Emissions," SAE paper 810255,in Diesel Combustion and Emissions, pt. 2, SP-484, SAE Trans., vol. 90,1981. 24.
Tindal, M. J., Williams, T.
J., and Aldoory. M.: "The Effect of Inlet Port Design on Cylinder Gas Motion in Direct Injection Died Engines," in Flows in Internal Combustion Engines. pp. 101-11 1, ASME, New York, 1982. 25. Brand], F., Revmncic, I., Cartellieri, W., and Dent, J. C.: "Turbulent Air Flow in the Combustion Bowl of a D.I. Diesel Engine and Its Effect on Engine Pdormana," SAE paper 790040, SAE Trans,, vol. 88,1979.
26. Brandstiitter, W, Johns, R J. R., and Wigley, G.: "Calculation of Flow Roduced by a Tangential Inlet Port," in International Symposium on Flows in Internal Combustion Engines-III, FED voL 28,pp. 135-148,ASME, New York, 1985. 27.
Brandstiitter, W, Johns. R. J. R., and Wigley, G.: "The Effect of Inlet Port Geometry on InCylinder Flow Structure," SAE paper 850499,1985.
28. Davis, G.C.. and Kent, J. C.: "Comparison of Model Calculations and Experimental Measurements of the Bulk Cylinder Flow Processes in a Motored PROCO Engine," SAE paper 790290, 1979. 370 INTERNAL COMBUSTION ENGME FLINDAMENTALS 29. Borgnakke, C., Davis, G. C, and T a b a c z ~ s b R. , J.: "Predictions of In-Cylinder Swirl Ve1odt). and Turbulence Intensity for an Open Chamber Cup in Piston Engine," SAE paper 810224,SU Trans., vol. 90, 1981. 30. Arcoumanis, C., Bicen, A. F, and Whitelaw, J. H.: "Squish and Swirl-Squish Interaction b Motored Model Engines." Trans. ASME, J. Fluids Engng, vol. 105,pp. 105-112,1983. 31. Ikegami, M., Mitsuda, T., Kawatchi, K., and Fujikawa, T.: "Air Motion and Combustion . Direct Injection Diesel Engines," JAM technical memorandum no.
2, pp. 231-245,1971. 32. Lieu, T.-M., and Santavicca, D. A.: "Cycle Resolved Turbulence Measurements in a p o w Engine With and Without Swirl," SAE paper 830419,SAE Trans., vol. 92,1983. 33.
Fitzgeorge, D., and Allison, J.
L.: "Air Swirl in a Road-Vehicle Diesel Engine," Proc, Instn ,+frch Engrs (AD.), no. 4,pp. 151-168,1962-1963. 34. Lichty, L. C.: Combustion Engine Processes, McGraw-Hill, 1967. 35. Shinamoto, Y., and Akiyama, K.: "A Study of Squish in Open Combustion Chambers of a Engine," Bull. JSME, vol.
13,no. 63,pp. 1096-1103,1970. 36. Dent, J. C., and Derham, J. A.: "Air Motion in a Four-Stroke Direct Injection D i e d EnginGq Proe. Instn Mech. Engrs, vol. 188,21/74,pp. 269-280, 1974.
37. Asanuma, T., and Obokata, T.: "Gas Velocity Measurements of a Motored and Firing Engine Laser Anemometry," SAE paper 790096,SAE Trans., vol. 88,1979. 38. Asanuma, T., Babu, M. K. G., and Yagi, S.: "simulation of Thermodynamic Cycle of Three-Val* Stratified Charge Engine," SAE paper 780319,SAE Trans., vol. 87,1978. 39.
Hires, S. D., Ekchian, A.. Heywood. J. B, Tabaaynski. R. J., and Wall, J. C.: "Performance and NO, Emissions Modelling of a Jet Ignition Prechamber Stratified Charge Engine," SAE papa 760161,SAE Trans., vol. 85,1976. 40.
Zmmerman, D. R.: "Laser Anemometer Measurements of the Air Motion in the Prechamber of an Automotive Diesel Engine," SAE paper 830452,1983. 41. Meintjes, K, and Alkidas, A. C.: "An Experimental and Computational Investigation of the Flow in Diesel Prechamben," SAE paper 820275,SAE Trans., vol.
91, in Diesel Engine Combustig -Emissions, and Particulates, P-107,SAE, 1982. 42. Namazian, M., and Heywood, J. B.: 'Flow in the Piston-Cylinder-Ring Crevices of a SparkIenition Engine: Effect on Hydrocarbon Emissions, Efficiency and Power," SAE paper 820088. ~ A ~rans.,vol. E 91,1982. 43. Wentworth, J. T.: "Piston and Ring Variables Affect Exhaust Hydrocarbon Emissions," SAE paper 680109,SAE Trans., vol.
77,1968. 44. Tabaaynski, R.
J., Hoult, D. P., and Keck, J. C.: "High Reynolds Number Flow in a Movins Corner," J. Fluid Mech, vol. 42,pp. 249-255,1970. 45. Daneshyar, H. F., Fuller, D. E., and Deckker, B. E. L.: "Vortex Motion Induced by the Piston d an Internal Combustion Engine," Int. J. Mech. Sci., vol. 15,pp. 381-390, 1973. CHAPTER COMBUSTION IN SPARK-IGNITION ENGINES 9.1 ESSENTIAL FEATURES OF PROCESS In a conventional spark-ignition engine the fuel and air are mixed together in the intake system, inducted through the intake valve into the cylinder, where mixing with residual gas takes place, and then compressed. Under normal operating conditions, combustion is initiated towards the end of the compression stroke at the spark plug by an electric discharge. Following inflammation, a turbulent flamedevelops, propagates through this essentially premixed fuel, air, burned gas mixture until it reaches the combustion chamber walls, and then extinguishes. Photographs of this process taken in operating engines illustrate its essential features. Figure 9-1 (color plate) shows a sequence of frames from a high-speed color movie of the combustion process in a special single-cylinder engine with a glass piston crown.' The spark discharge is at - 30". The flame first becomes visible in the photos at about -24'. e. flame, approximately circular in outline in this n C U ~9-1~(On color plate opposite p. 498) mane of spark-ignition engine combustion process, taken glass piston crown.
Ignition timing 30" BTC, light load, 1430 revlmin, (AIF) = 19.' Color photograph. from hia-spacd lb%h 371 view through the piston, then propagates outward from the spark plug locatioe The blue light from the flame is emitted most strongly from the front. The irregular shape of the turbulent flame front is apparent. At TC the flame diameter is about two-thirds of the cylinder bore.
The flame reaches the cylinder wall farthat from the spark plug about 15" ATC, but combustion continues around parts the chamber periphery for another 10". At about 10" ATC, additional radiation-initially white, turning to pinky-orange-centered at the spark plug location is evident. This afterglow comes from the gases behind the flame which burned earlier in the combustion process, as these are compressed to the highest ternperatures attained within the cylinder (at about 15" ATC) while the rest of the charge burns.'. Additional features of the combustion process are evident from the data in Fig.
9-2, taken from several consecutive cycles of an operating spark-ignition engine. The cylinder pressure, fraction of the charge mass which has burned (determined from the pressure data, see Sec. 9.2), and fraction of the cylinder volume enflamed by the front (determined from photographs like Fig.
9-1) are shown, all as a function of crank angle.4 Following spark discharge, there is a period during which the energy release from the developing flame is too small for the pressure rise due to combustion to be discerned. As the flame continues to grow and propagate across the combustion chamber, the pressure then steadily rises above the value it would have in the absence of combustion. The pressure reaches a maximum after TC but before the cylinder charge is fully burned, and then decreases as the cylinder volume continues to increase during the remainder of the expansion stroke. The flame development and subsequent propagation obviously vary, cycleby-cycle, since the shape of the pressure, volume fraction enflamed, and mass fraction burned curves for each cycle differ significantly. This is because flame growth depends on local mixture motion and composition. These quantities vary in successive cycles in any given cylinder and may vary cylinder-to-cylinder. Especially significant are mixture motion and composition in the vicinity of the spark plug at the time of spark discharge since these govern the early stages of flame development. Cycle-by-cycle and cylinder-to-cylinder variations in combustion are important because the extreme cycles limit the operating regime of the engine (see Sec. 9.4.1). Note that the volume fraction enflamed curves rise more steeply than the mass fraction burned curves. In large part, this is because the density of the unburned mixture ahead of the flame is about four times the density of the burned gases behind the flame. Also, there is some unburned mixture behind the visible front to the flame: even when the entire combustion chamber is fully enflamed, some 25 percent of the mass has still to bum. From this description it is plausible to divide the combustion process into four distinct phases: (1) spark ignition; (2) early flame development; (3) flame propagation; and (4) flame termination.
Our understanding of each of these phases will be developed in the remainder of this chapter. The combustion event must be properly located relative to top-center to oi Crank angle, deg FIGURE 9-2 Cylinder pressure, mass fraction b u d , and volume fraction enflamed for five vcnsccutive c ~ l inn a sPark-imitionengine as a function of crank angle. IgnXon timing 30' BTC, widaopn throtUe, IOU rev/min, q5 = 0.98.4 COMBUSTION IN SPARK-IGNITION ENGINE obtain the maximum power or torque. The combined duration of the flame development and propagation process is typically between 30 and 90 crank angk degrees. Combustion starts before the end of the compression stroke, continues through the early part of the expansion stroke, and ends after the point in the cycle at which the peak cylinder pressure occurs. The pressure versus crank angk curves shown in Fig. 9-3a allow us to understand why engine torque (at given engine speed and intake manifold conditions) varies as spark timing is varied relative to TC. If the start of the combustion process is progressively advanced before TC, the compression stroke work transfer (which is from the piston to the cylinder gases) increases. If the end of the combustion process is progressively delayed by retarding the spark timing the peak cylinder pressure occurs later in the expansion stroke and is reduced in magnitude. These changes reduce the expansion stroke work transfer from the cylinder gases to the piston. The optimum timing which gives the maximum brake t o r q u ~ a l l e dmaximum brake torque, or MBT, timing--occurs when the magnitudes of these two opposing trends just offset each other. Timing which is advanced or retarded from this optimum gives lower torque. The optimum spark setting will depend on the rate of flame development and propagation, the length of the flame travel path across the combustion chamber, and the details of the flame termination process after it reaches the wall. These depend on engine design and operating conditions, and the properties of the fuel, air, burned gas mixture. Figure 9-3b shows the effect of variations in spark timing on brake torque for a typical spark-ignition engine. The maximumis quite flat.
b a r k advance = 50 deg - 0 10 Crank angle, deg 20 30 Spark advance, deg FIGURE 9-3 (a) Cylinder pressure versus crank angle for overadvanad spark timing (109, MBT timing (30'). retarded timing (lo0).(b) EBect of spark advance on brake torque at constant speed and (All3 8' wide-open throttle. MBT is maximum brake torque timing.' 375
Empirical rules for relating the mass burning profile and maximum cylinder pressure to crank angle at MBT timing are often used. For example, with optimumspark timing: (1) the maximum pressure occurs at about 16" after TC; (2) half the charge is burned at about 10" after TC. In practice, the spark is often Rtarded to give a 1 or 2 percent reduction in brake torque from the maximum value,to permit a more precise definition of timing relative to the optimum. SO far we have described normal combustion in which the spark-ignited flame moves steadily across the combustion chamber until the charge is fully consumed.However, several factors-e.g., fuel composition, certain engine design and operating parameters, and combustion chamber deposits-may prevent this normal combustion process from occurring. Two types of abnormal combustion have been identified: knock and surface ignition. Knock is the most important abnormal combustion phenomenon. Its name comes from the noise that results from the autoignition of a portion of the fuel, air, residual gas mixture ahead of the advancing flame.
As the flame propagates across the combustion chamber, the unburned mixture ahead of the flamethe end gas-is compressed, causing its pressure, temperature, and density 10 increase.
Some of the end-gas fuel-air mixture may undergo chemical reactions prior to normal combustion. The products of these reactions may then autoignite: i.e., spontaneously and rapidly release a large part or all of their chemical energy. When this happens, the end gas burns very rapidly, releasing its energy at a rate 5 to 25 times that characteristic of normal combustion. This causes highfrequency pressure oscillations inside the cylinder that produce the sharp metallic noise called knock. The presence or absence of knock reflects the outcome of a race between the advancing flame front and the precombustion reactions in the unburned end gas. Knock will not occur if the flame front consumes the end gas before these reactions have time to cause the fuel-air mixture to autoignite. Knock will occur if the precombustion reactions produce autoignition before the flame front arrives.
The other important abnormal combustion phenomenon is surface ignition. Surface ignition is ignition of the fuel-air charge by overheated valves or spark plugs, by glowing combustion-chamber deposits, or by any other hot spot in the engine combustion chamber: it is ignition by any source other than normal spark ignition. It may occur before the spark plug ignites the charge (preignition) or after normal ignition (postignition).
It may produce a single flame or many flames. Uncontrolled combustion is most evident and its effects most severe when it results from preignition. However, even when surface ignition occurs after the spark plug fires (postignition), the spark discharge no longer has complete control of the combustion process. Surface ignition may result in knock. Knock which occurs following normal Spark ignition is called spark knock to distinguish it from knock which has been Preceded by surface ignition. Abnormal combustion phenomena are reviewed in more detail in Sec. 9.6. . 376 COMBUSTION IN SPARK-IGNITION ENGINES INTERNAL COMBUSTION ENGINE FUNDAMENTALS 377 tions in the burned and unburned gas are then determined by conservation of mass : 9.2 THERMODYNAMIC ANALYSIS OF SI ENGINE COMBUSTION 9.2.1 Burned and Unburned Mixture States - Because combustion occurs through a flame propagation process, the changes in state and the motion of the unburned and burned gas are much more complex than the ideal cycle analysis in Chapter 5 suggests. The gas pressure, temperature, and density change as a result of changes in volume due to piston motion.
During combustion, the cylinder pressure increases due to the release of the fuel's chemical energy. As each element of fuel-air mixture bums, its density decreases by about a factor of four. This combustion-produced gas expansion compresses the unburned mixture ahead of the flame and displaces it toward the combustion chamber walls. The combustion-produced gas expansion also compresses those parts of the charge which have already burned, and displaces them back toward the spark plug. During the combustion process, the unburned gas elements move away from the spark plug; following combustion, individual gas elements move back toward the spark plug.
Further, elements of the unburned mixture which burn at different times have different pressures and temperatures just prior to combustion, and therefore end up at different states after combustion. The thermodynamic state and composition of the burned gas is, therefore, non-uniform. A first law analysis of the spark-ignition engine combustion process enables us to quantify these gas states. Consider the schematic of the engine cylinder while combustion is in progress, shown in Fig. 9-4.
Work transfer occurs between the cylinder gases and the piston (to the gas before TC; to the piston after TC). Heat transfer occurs to the chamber walls, primarily from the burned gases. At the temperatures and pressures typical of spark-ignition engines it is a reasonable approximation to assume that the volume of the reaction zone where combustion is actually occurring is a negligible fraction of the chamber volume even though the thickness of-the turbulent flame may not be negligible compared with the chamber dimensions (see Sec. 9.3.2). With normal engine operation, at any point in time or crank angle, the pressure throughout the cylinder is close to uniform. The condi- and conservation of energy: where V is the cylinder volume, m is the mass of the cylinder contents, o is the specific volume, xb is the mass fraction burned, Uo is the internal energy of the cylinder contents at some reference point 80, u is the specific internal energy, W is the work done on the piston, and Q is the heat transfer to the walls. The subscripts u and b denote unburned and burned gas properties, respectively. The work and heat transfers are 4 %: 5 where 0 is the instantaneous heat-transfer rate to the chamber walls. To proceed further, models for the thermodynamic properties of the burned and unburned gases are required. Several categories of models are described in Chap. 4. Accurate calculations of the state of the cylinder gases require an equilibrium model (or good approximation to it) for the burned gas and an ideal gas mixture model (of frozen composition) for the unburned gas (see Table 4.2). However, useful illustrative results can be obtained by assuming that the burned and unburned gases are different ideal gases, each with constant specific heats;6 l.e., Combining Eqs. (9.1) to (9.5) gives FIGURE 9-4 II W 11 Schematic of flame in the engine cylinder during combustion: unburned gas (U) to left of burned gas to right. A denotes adiabatic burned-gaJ core, BL denotes thermal boundary layer in burned gas, is work-transfer rate to piston, is heattransfer rate to chamber walls.
where 378 INTERNAL COMBUSTION ENGINE COMBUSTION IN SPARK-IGNITION ENGINES FUNDAMENTALS 379 are the mean temperatures of the burned and unburned gases. Equations and (9.7) may now be solved to obtain and R, - T --T,+ - Rb pV - mRuTu mRb xb If we now assume the unburned gas is initially uniform and undergoes tropic compression, then -40 This equation, with Eqs. (9.8) and (9.9) enables determination of both xb and ?, from the thermodynamic properties of the burned and unburned gases, and known values of p, V, m, and 0. Alternatively, if xb is known then p can k determined. Mass fraction burned and cylinder gas pressure are uniquely related. While Eq. (9.9) defines a mean burned gas temperature, the burned gas is not uniform. Mixture which bums early in the combustion process-is further compressed after combustion as the remainder of the charge is burned. Mixture which burns late in the combustion process is compressed prior to combustion and, therefore, ends up at a different final state. A temperature gradient exists across the burned gas with the earlier burning portions at the higher tern. perat~re.~.Two limiting models bracket what occurs in practice: (1) a fully mixed model, where it is assumed that each element of mixture which burns mixes instantaneously with the already burned gases (which therefore have a uniform temperature), and (2) an unmixed model, where it is assumed that no mixing occurs between gas elements which burn at different times. In the fully mixed model the burned gas is uniform, T, = and the equations given above fully define the state of the cylinder contents. In the unmixed model, the assumption is made that no mixing occurs between gas elements that burn at different times, and each burned gas element is therefore isentropically compressed (and eventually expanded) after combustion.t Thus: z, t This model applies to burned gas regions of the chamber away from the walls. Heat transfer to tht walls results in a thermal boundary layer on the walls which grows with time. The gas in the bounb ary layer is not isentropically compressed and expanded. I -20 d ~ l l l 0 20 40 Crank angle, deg l I 60 0 FIGURE 9-5 Cylinder pressure, mass fraction burned, and gas temperatures as functions of crank angle during combustion. T, is unburned gas temperature, T, is burned gas temperature, the subscripts e and I denote early and late burning gas elements, and is the mean burned gas temperature.' (Reprinted with permission. Copyright Chemical Society.) 1973, American where &(x;, xb) is the temperature of the element which burned at the pressure p(.r;) when the pressure is p(x,), and is the temperature resulting from isenthalpic combustion of the unburned gas at T&(xb),p(xb). An example of the temperature distribution computed with this model is s h w n in Fig.
9-5. A mixture element that burns right at the start of the combustion process reaches, in the absence of mixing, a peak temperature after combustion about 400 K higher than an element that burns toward the end of the combustion process. The mean buroed gas temperature is closer to the lower of these temperatures.
These two models approximate respectively to situations where the time scale that characterizes the turbulent mixing process in the burned gases is (1) much less than the overall burning time (for the fully mixed model) or (2) much longer than the overall burning time (for the unmixed model). The real situation lies in between.
Measurements of burned gas temperatures have been made in engines using spectroscopic techniques through quartz windows in the cylinder head. Examples of measured temperatures are shown in Fig. 9-6. The solid lines marked A, B, and C are the burned gas temperatures measured by Rassweiler and Withrow7 using 'he sodium line reversal technique in an L-head engine, for the spark plug end (4,the middle (B), and the opposite end (C) of the chamber, respectively. Curves labeled W2and W, were measured by Lavoie8 through two different windows, W, a d W3 (with W, closer to the spark), again in an L-head engine. Each set of exPerimental temperatures shows a temperature gradient across the burned gas to that predicted, and the two sets have similar shapes. ' INTERNAL COMBUSTION ENGINE FUNDAMENTALS COMBUSTION IN SPARK-IGNITION ENGINES m e with a constant burning velocity propagates outward from the center of a sphericalcontainer. Applying this gas motion model to an engine, it can be concluded that a window in the cylinder head initially views earlier burned gas (of higher temperature and entropy) and that as more of the charge burns, the ,&jow views later burned gas of progressively lower entropy. The experimental fit this description: they cross the constant entropy lines toward lower Note that the gradient in temperature persists well into the expansion indicating that the "unmixed" model is closer to reality than the "fully " model. More accurate calculations relating the mass fraction burned, gas pressure, and gas temperature distribution are often required. Note that the accuracy of calculatio~l~ depends on the accuracy with which the time-varying heat loss to the chamber walls can be estimated (see Sec. 12.4.3) and whether flows into and out of crevice regions are significant (see Sec. 8.6), as well as the accuracy of the models used to describe the thermodynamic properties of the gases. Appropriate more accurate models for the thermodynamic properties are: an equilibrium model for the burned gas, and specific heat models which vary with temperature for each of the components of the unburned mixture (see Secs. 4.1 and 4.7). In the absence of significant crevice effects, Eqs. (9.1) and (9.2) can be written as FIGURE 9-6 Burned gas temperatures measured using spectroscopic techniques through windows in the cylinder head, as a function of cylinder pressure Temperatures measured closer to spark plug have higher values. Dashed lines show isentropic behavior.'. In the unmixed model, the temperature of each burned gas element follows a different isentropic line as it is first compressed as p increases to p,. and then expanded as the pressure falls after p,,. The measured temperature curves in Fig. 9-6 do not follow the calculated isentropes because of gas motion past the observation ports. As has already been mentioned, the expansion of a gas element which occurs during combustion compresses the gas ahead of the flame and moves it away from the spark plug. At the same time, previously burned gas is compressed and moved back toward the spark plug. Defining this motion in an engine requires sophisticated tiow models, because the combustion chamber shape is rarely symmetrical, the spark plug is not usually centrally located, and often there is a bulk gas motion at the time combustion is initiated. However, the gas motion in a spherical or cylindrical combustion bomb with central ignition which can readily be computed illustrates the features of the combustion-induced motion in an engine. Figure 9-7 shows calculated particle trajectories for a stoichiometric methane-air mixture, initially at ambient conditions, as a laminar g , -1 < where :: 1 Eb = Xb N o d 4 radius xb ub d x and I' E,, = -Xb 0 0,.
dx xb and similar definitions hold for iib and ii,. For a given equivalence ratio, fuel and burned gas fraction : and FIGURE 9-7 Particle trajectories in unburned and burned Bar as flame propagates outward at constant vebc1r)l from the center of a spherical combustion bomb Stoichiometric methamair mixture initially at 1 atm and 300 K. 381 - ii, = h, - pfi, - fib = hb - ptb (9.1 7 4 b) TO simplify the calculations, it is convenient to assume that, for the burned gas, 6, = ub(pb, p) and Eb = vb(Tb, p). This corresponds to the fully mixed assumption described above. The effect of neglecting the temperature distribution in the calculation of mass fraction burned is small. In addition, the heat losses from the unburned gas can usually be neglected; the unburned gas is then compressed ' , is specified for some initial state of the unburned gas (where isentropically.
F ' 382 COMBUSTION IN SPARK-IGNITION ENGINES INTERNAL COMBUSTION ENGINE FUNDAMENTALS 383 xb = 0) by p o , V,, M u ,and the mass of charge m.
Then, since for any isentr process Tucan be determined. Equations (9.13) to (9.18) constitute a Set of nine equations for the unknowns Ir,, Irb,ii,, iib,&, 5, T,, Tb,and x, or p. One convenient sol method is to eliminate xb from Eqs. (9.13) and (9.14) to obtain fib - i),, fib - ii, where U = UO- W - Q. can then be solved using a obtained from Eq. (9.13). An of pressure dp/dO and equat found in Ref. 10. Some exa measured pressure data, wi With accurate pressure versus crank angle rec burned should be close to but lower than unity, usually in the range 0.93 the difference from unity is the combustion inefftcency for lean mixtures (3-9) and incomplete oxygen utilization for rich mixtures (see Fig. 4-20). More accurate burned gas temperature c presence of a thermal boundary layer (of order 1 mm thick) around th bustion chamber walls (see Sec.
12.6.5). The burned gas region in Fig. 9-4 FIGURE 9-9 Calculated temperature distribution in the adiabatic core of the burned gas zone for the unmixed model assuming thermodynamic equilibrium. 4 = 1.0. Dashed line is temperature of each element just aIter it bums. ., 10 5 15 20 Pressure, am divided into an adiabatic core and a boundary layer that grows in thickness with tune.
In the adiabatic core, in the absence of mixing between gas elements that burn at different times, burned gas is compressed and then expanded isentropially. The burned gas temperature distribution can be calculated as follows. Gwen the pressure versus crank angle data, the unburned mixture state can be determined using Eq. (9.18) above. Each small element of unburned mixture burns in a constant-enthalpy constant-pressure process. So the burned state of an clcment of unburned charge, which burns at p = p i , can be obtained from the &lation After combustion, this element which burned at p = p i is compressed and txpanded along the isentropic: An example of the temperature distribution computed in this manner for this mixed model in the burned gas adiabatic core is shown in Fig. 9-9.
The &men1 ignited by the spark is compressed to the highest peak temperature at L,.The temperature difference across the bulk of the charge (0.05 < xb < 0.95) hit 200 K. Degrees after spark (4 FIGURE 9-8 Mass fraction burned curves determined from measured cylinder pressure data uing two-# bustion model: (a) gasoline; (b)methanol. 4 = fuelfair equivalence ratio." '-22 Analysis of Cylinder Pressure Data qlindfl pressure changes with crank angle as a result of cylinder volume change, -bustion, heat transfel to the chamber walls, flow into and out of crevice and leakage.
The first two of these effects are the largest. The effect of 3&1 INTERNAL COMBUSTION ENGINE FUNDAMENTALS volume change on the pressure can readily be accounted for; thus, combustion rate information can be obtained from accurate pressure data provided models for the remaining phenomena can be developed at an appropriate level of approximation. The previous section has developed the fundamental basis for such calculations. Cylinder pressure is usually measured with piezoelectric pressure transducers. This type of transducer contains a quartz crystal. One end of the crystal is exposed through a diaphragm to the cylinder pressure; as the cylinder pressure increases, the crystal is compressed and generates an electric charge which is proportional to the pressure. A charge amplifier is then used to produce an output voltage proportional to this charge. Accurate cylinder pressure versus crank angle data can be obtained with these systems provided the following steps are carried out: (1) the correct reference pressure is used to convert the measured pressure signals to absolute pressures; (2) the pressure versus crank angle (or volume) phasing is accurate to within about 0.2"; (3) the clearance volume is estimated with sufficient accuracy; (4) transducer temperature variations (which can change the transducer calibration factor) due to the variation in wall heat flux during the engine cycle are held to a minimum. Log p versus log V plots can be used to check the quality of cylinder pressure data. The first three of the above requirements can be validated using log p-log V diagrams for a motored engine. If the effects of thermal cycling are significant, the expansion stroke on the log plog V plot for a firing engine shows excessive curvature.I2 Figure 9-10 shows pressure-volume data from a firing spark-ignition engine on both a linear p-V and a log p-log V diagram. O n the log p-log V diagram the compression process is a straight line of slope 1.3. The start of combustion can be identified by the departure of the curve from the straight line. The end of com- bustion can be located approximately in similar fashion; the expansion stroke following combustion is essentially linear G t h slope 1.33. Since both the compression of the unburned mixture prior to-combustion and the expansion of the burned gases following the end of combustion are close to adiabatic isentropic prmsses (for which pVY = constant; y = cJc,,), the observed behavior is as More extensive studies12.l 3 show that the compression and expansionare well fitted by a polytropic relation: pVn = constant (9.20) n e exponent n for the compression and expansion processes is 1.3 (f0.05) for conventional fuels. It is comparable to the average value of y, for the unburned mixture over the compression process, but is larger than y, for the burned gas mixture during expansion due to heat loss to the combustion chamber walls (see Figs.4-13 and 4-16). Log p-log V plots such as Fig. 9-10 approximately define the start and end of combustion, but do not provide a mass fraction burned profile. One wellestablished technique for estimating the mass fraction burned profile from the pressure and volume data is that developed by Rassweiler and W i t h r ~ w They .~ correlated cylinder pressure data with flame photographs, and showed how Eq. (9.20) could be used to account for the effect of cylinder volume change on the pressure during combustion.
Assuming that the unburned gas filling the volume V, ahead of the flame at any crank angle during combustion has been compressed polytropically by the advancing flame front, then the volume K , , it occupied at time of spark is Similarly, the burned gas behind the flame filling the volume V, would, at the end of combustion, fill a volume V,, given by , The mass fraction burned x, is equal to 1 - (K. d V ,) and to V,, /V,, where Vo amd V, are the total cylinder volumes at time of spark and at the end of combustion, respectively.
Since V = + V,, Eqs. (9.21) and (9.22) then give: Fraction of maximum volume (4 FIGURE 9-10 (a) Pressure-volumediagram; (b)log 4 = 0.8, r, = 8.72, propane fueLL2 Fraction of maximum volume (b) rev/min, MBT timing imep = This method is widely used, though it contains several approximations. Heat-transfer effects are included only to the extent that the polytropic exponent fi in Eq. (9.22) differs appropriately from y. The pressure rise due to combustion is Proportional to the amount of fuel chemical energy released rather than the mass of mixture burned. Also, the polytropic exponent n is not constant during combustion. Selecting an appropriate value for n (whether n is assumed to be con- 386 COMBUSTION IN S

of the size of the large energy-containing structures of the flow. The Kolmogorov scale 1, [Eq. (8.11)] defines the smallest structures of the flow where small-scale kinetic energy is dissipated via molecular viscosity. Several dimensionless parameters are used to characterize turbulent premixed flames. The dimensionless parameter used to define the turbulence is the turbulent Reynolds number, Re, = ulll/v. For homogeneous and isotropic (no Preferred direction) turbulence, the integral and Kolmogorov scales are related by Eq. (8.14): I& = Re;". A characteristic turbulent eddy turnover time 7, can be defined as 396 COMBUSTION IN SPARK-IGNITION ENGINES m E R N A L COMBUSTION ENGINE FUNDAMENTALS A characteristic chemical reaction time is the residence time in a laminar flame: 6, r, =- SL The ratio of the characteristic eddy turnover time to the laminar burning time b called the Damkohler number: Da = ' .= =L ($I($) It is an inverse measure of the influence of the turbulent flow on the chemid processes occurring in the flame. Other ratios are of interest. The ratio 6 J , is measure of the stretch or local distortion to which a laminar flame is subjected b the turbulent flow.
Unless 1,/6, 9 1 the concept of a localized flame region little significance. The ratio ut/SL is a measure of the relative strength of t~rbulence.~~ Different regimes of turbulent flames are apparent in the plot of Damk ler number versus turbulent Reynolds number in Fig.
9-18.22It has been that DL z v and that the relationships for homogeneous isotropic turbu valid. Two regimes--distributed reactions and reaction sheets-are norm identified. In the distributed reaction regime, chemical reactions proceed in d tributed reaction zones and thin-sheet flames do not occur.
A sufficient condit for this regime is I , 4 6,. In the reaction sheet regime, propagating react fronts are wrinkled and convoluted by the turbulence. A sufficient condition the existence of reaction sheets is I , % 6,. For Re, > 1, there is a region in Fi 9-18 where I, > 6, > l K : the characteristics of flames in this regime are unclear. 397 Values of Da and Re, for a typical spark-ignition engine (the cross-hatched Ngion in Fig. 9-18) lie predominantly in the reaction sheet flame regime. Engine ,Fration at high speed (the lower right boundary) and low load (the lower left boundary)gives values of Da and Re, which fall below the IJ6, = 1 line. This is hrgely due to the low values of laminar flame speed that result from the high mounts of residual gas and EGR under these conditions (see Sec. 9.3.4 and Fig. 6-19). Whether the flame structure under these conditions is significantly different is not known. Observations of engine flames to date, described below, lie above the 1J6, = 1 line, within the reaction sheet regime. One would expect, then, the Structureof the flame in a spark-ignition engine, once developed, to be that of a thin reaction sheet wrinkled and convoluted by the turbulent flow. Detailed observations have been made of flame structure from ignition to flame extinguishing at the far cylinder wall. A flame develops from the spark discharge which causes ignition as follows. In the initial breakdown phase of ignition, a cylindrical discharge between the spark plug electrodes is establi~hed.'~ As electrical energy is fed into the discharge, the arc expands and exothermic chemical reactions capable of sustaining a propagating flame develop. Figure 9-19 shows how this development of a flame kernel occurs, with a set of shadowgraph photographs taken at 40-ps intervals of the spark plug electrode gap in one cylinder of a 2-liter conventional engine. The first photograph is between 20 and Sops after the spark breakdown occurred. The complete sequence (-200 ys) corresponds to 1.3 crank angle degrees. The outer boundary of this developing flame kernel is approximately spherical and is smooth with modest irregularities, corresponding to a thin reaction zone with hightemperature gases inside. As this developing sheetlike flame grows it interacts with the turbulent flow field in the vicinity of the spark plug: the flame outer surface becomes increasingly convoluted and the flame center can be convected away from the plug in a direction and with a velocity that can vary substantially cycle-by-cycle, as seen in Fig. 9-20?. l7 The structure of the flame continues to develop as it propagates across the chamber.
Evidence, largely from schlieren photographs and studies of flame structure with laser diagnostics, shows that early in the burning process the flame FIGURE 9-18 1 l@ lo4 lo6 lo' Turbulent Reynolds number R ~ T Different turbulent Bame regimes Damkohler number versus turbulence number, u' is turbulence intensity; SL flame speed; I,, I,, and 6, are integral mogorov scale, and laminar flame (From Abraham et a1.") CURE 9-19 s b d ~ ~ g r a pphotographs h of spark-generated kernel between the spark plug electrodes First pho'"~aphon left, 20 to 50 p after breakdown; 40 ps between photos. Stoichiometnc mixture, 1100 Avhin.(Courtesy A. Douad, Institut Francais du Petrole.) 398 COMBUSTION IN SPARK-IGNITION ENGINES INTERNAL COMBUSTION ENGINE FUNDAMENTALS 399 FIGURE 9-20 Schlieren photographs of developing flame, 5" after spark discharge, showing different con" processes in two different cycles. Spark plug wires 0.8 rnm diameter. 1400 rev/min; 0.5 atm pressure; propane fuel; 4 = 0.9; spark advance 45" BTC." is a thin, moderately wrinkled but simply connected, front or reaction sh between unburned and burned gas. The thickness of the front is about 0.1 which is comparable to the thickness of a laminar flame under the prevaili conditions. The scale of the wrinkles is typically about 2 mm at engine speeds 1000 to 2000 rev/min. As the flame propagates across the chamber, the thickn of the reaction sheet front remains roughly constant, the flame front beco more convoluted, and the scale of the wrinkles tends to decrease with time.24 Further evidence that the thin reaction sheet front becomes highly wink and convoluted by the turbulent flow field into a thick turbulent flame " brus is provided by the schlieren photographs in Fig. 9-21. These show a flame gating across the combustion chamber of a square-cross-section singleengine with a special transparent piston crown containing a 13-mm wide to isolate a small section of the flame." The flame on the left is for a propanemixture; that on the right is hydrogen-air.
The energy density per unit volume mixture and the flow field are comparable for each fuel. The effective thick this turbulent flame-the average distance between the region ahead of the where only unburned mixture exists, and the region behind the flame, where 0 (4 FIGURE 9-22 Enlrrged schlieren photographs of (a) flame front and (b) flame back in square-cross-section cylinder mginc with two glass side walls. 1400 rev/min, 0.5 atm inlet pressure, propane fuel, 4 = 0.9.17 burned mixture exists-is apparent.?
It was 4 to 5 mm for propane and 1.5 mm for hydrogen. The difference is due to the substantially higher laminar flame speed for the hydrogen, air, burned gas mixture (see Sec. 9.3.4) which increases [he Damkohler number and shifts the flame toward the weak-turbulence (i.e., less winkled) flame regime in Fig. 9-18. Additional insight into the structure of the developed engine flame can be obtained by enlarging photographs of the leading and trailing edges of the flame, obtained with the schlieren or shadowgraph technique.
Figure 9-22a shows the front of the flame 40' after the spark, when it has propagated about halfway across the chamber. It shows the irregular but smoothly curved surfaces which Wmprise the leading edge of the flame. Figure 9-226 shows the back of the flame 70' after the spark, when the front of the flame has just reached the wall of the mmbustion chamber farthest from the spark plug. It shows large clear regions of burned gas behind the flame and smaller clear regions connected by a lacelike FIGURE 9-21 Schlieren photographs of flame in square-cross-section cylinder engine, with narro crown (at bottom of pictures) which permits observation of 13-mm wide section 0 fuel, spark timing 36" BTC, photograph at 14" ATC, flame thickness z 4.6 mm. spark timing 3" BTC, photograph at 10' ATC, flame thickness z 1.5 mm. Stoic 1380 rev/min, 0.5 atm inlet press~re.~' 'Th. photographs were selected from a large number to give the minimum flame thickness corre- Wndink! to the flame front perpendicular to the channel length. 400 COMBUSTION INTERNAL COMBUSTION ENGME FLJNDAMENTALS 30 29 28 Flame radius, mm 27 FIGURE 9-23 Upper picture: oscillogram of output of opt multichannel analyzer showing the intensity light scattered from a narrow laser beam as a tu tion of distance through the flame. Intensity it measure of gas density. Lower picture: schema of flame structure corresponding to this signal. revjmin, 1 atm inlet pressure, propane 4 = 1.0.~~ structure within which the remaining regions of unburned mixture are being con sumed." The analogy with a crumpled sheet of paper is appropriate. Laser scattering experiments, where "snapshots" of the density profit along a laser beam passed through the flame were obtained using Rayleigh scat tered light from the gas molecules, provide explicit evidence of this structure." Figure 9-23 shows an oscillogram of the output of the optical analyzer. Each do represents the intensity of the scattered light which is a.
measure of the g density. The signal on the left corresponds to unburned gas. The flame is gating from right to left. The oscillogram shows a thin transition zone o 0.25 mm between unburned and burned gas, followed at a distance of 1.5 an "island" of unburned gas. The fraction of oscillograms showing sue "islands" varied from 0 at 300 revlmin to 20 percent at 1800 revlmin. An int pretation of this signal consistent with the available photographic evidence shown ~nderneath.'~ The above results suggest that increasing engine speed, which incre turbulence levels in the unburned charge, increasingly convolutes and p multiply-connects the thin reaction sheet flame front. Enlarged schlieren tographs of a 9-mm diameter section of the developed engine flame, vi normal to the flame surface, indicate that increasing turbulence intensity a decreasing turbulence scales result in increasingly finely wrinkled flame St tures. Figure 9-24 shows a set of such photographs, arranged in order of incr ing turbulent Reynolds number. Increases in turbulence intensity, which measured, were achieved by increases in engine speed and by modifying the in valve. Relevant parameters for each photograph are given in Table 9.1. The above theoretical discussion and experimental evidence indicates IN SPARK-IGNITION ENGINES 4 1 flCURE 9-24 shadowgraph photographs, with light beam normal to flame front, of 1 G m m diameter section of flame. photographs, arranged in order of increasing turbulent Reynolds number, suggest this is an jppropriate scaling parameter (see Table 9.1).17 developed turbulent flames in spark-ignition engines, under normal operating conditions, are highly wrinkled and probably multiply-connected thin reaction sheets. The overall thickness of the turbulent flame "brush," front to back, is of order 1 cm. The thickness of the thin reaction sheet is comparable to estimates of the laminar flame thickness under the prevailing unburned mixture conditions which are of order 0.1 mm. The scale of the wrinkles is of order 1 mmZ4Direct evidence to date is limited to the low to mid engine speed and low to high engine TABLE 9.1 Parameters for shadowgrapb photographs in Fig. 9-24 htograph o b c Engine speed, revlmin 300 600 300 d 900 f 1200 600 9 h 900 1200 Turbulence intensity, Re, m/s Valve Re, 0.44 0.88 1.07 1.33 S S US 106 157 173 229 503 611 S S US US US 193 224 234 285 333 760 1024 1117 1658 2263 1.80 1.95 2.90 4.0 Valve: S shrouded; US, unshrouded (produced higher turbulence due to km Orderedflow).Re, = I,u'/v; Re, = I,U'/Y (see Sec. 8.21).27 COMBUSTION IN SPARK-IGNITION ENGINES eated as negligibly thin. Laminar burning velocities for methane, propane, isotane, methanol, gasoline, and hydrogen-premixed with air-at pressures, temperatures, and equivalence ratios which occur in engines have been measured using this t e ~ h n i q u e . ~ ' -Also, ~ ~ the effect of a burned gas diluent on laminar burning velocity with gasoline-air mixtures has been deter~nined.~' Correlations derived from these data are the most accurate means available for estimating laminar burning velocities for mixtures and conditions relevant to spark-ignition load ranges. Whether the structure becomes significantly different at high engine speed is not known. Models of this turbulent flame development and propagation process are reviewed in Chap. 14.
9 3 3 Laminar Burning Speeds An important intrinsic property of a combustible fuel, air, burned gas mixture is its laminar burning velocity. This burning velocity is defined as the velocity, relative to and normal to the flame front, with which unburned gas moves into the front and is transformed to products under laminar flow conditions. Some details of flame structure help explain the significance of this quantity. A flame is the result of a self-sustaining chemical reaction occumng within a region of space called the flame front where unburned mixture is heated and converted into products. The flame front consists of two regions: a preheat zone and a reaction zone. In the preheat zone, the temperature of the unburned mixture is raised mainly by heat conduction from the reaction zone: no significant reaction or energy release occurs and the temperature gradient is concave upward (d2T/ ax2 > 0). Upon reaching a critical temperature, exothermic chemical reaction begins. The release of chemical energy as heat results in a zone where the temperature gradient is concave downward (a2T/ax2 < 0). The region between the temperature where exothermic chemical reaction begins and the hot boundary at the downstream equilibrium burned gas temperature is called the reaction zone. The thicknesses of the preheat and reaction zones can be calculated for onedimensional flames from conservation equations of mass and energy. The thickness of the preheat zone 6,. is 403 The effect of the mixture fuellair equivalence ratio on laminar burning for several hydrocarbon fuels and methanol is shown in Fig. 9-25. The burning velocity peaks slightly rich of stoichiometric for all the fuels shown. The ~aluesfor isooctane and gasoline are closely comparable. Data at higher pressures and temperatures have been fitted to a power law of the form: where To = 298 K and po = 1 atm are the reference temperature and pressure, and SL,o , a, and B are constants for a given fuel, equivalence ratio, and burned gas diluent fraction. For propane, isooctane, and methanol, these constants can be represented by FI ,, p = -0.16 and !t + 0.22(4 - 1) (9.34b) St,o = Bm f B&$ - 43' (9.35) is the equivalence ratio at which S, , is a maximum with value Bm. where ,,$t where and 2, are the mean thermal conductivity and specific heat at constant pressure in the preheat zone and S, is the laminar burning velocity." Thus, the factors which govern the laminar burning velocity of a specific unburned mixturethe velocity at which this flame structure propagates relative to the unburned gas ahead of it-are the temperature and species concentration gradients within the flame and the mixture transport and thermodynamic properties. Laminar burning velocities at pressures and temperatures typical of unburned mixture in engines are usually measured in spherical closed vessels by propagating a laminar flame radially outward from the vessel center. The laminar burning velocity is then given by dm,/dt SL = (9.32) A, P U where the mass burning rate is determined from the rate of pressure rise in the vessel and Af is the flame area. Because the laminar flame thickness [e.g., given by Eq. (9.3111 under engine conditions is of order 0.2 and is therefore much less than characteristic vessel dimensions, in applying Eq. (9.32) the flame can be I5 0.6 A I I I I I 0.8 1.0 1.2 1.4 1.6 Fuellair equivalence ratio $ FIGURE 9-25 Laminar burning velocity for several fuels as funo tion of equivalence ratio, at 1 atm and UK) K. Lines are least-squares polynomial fits to data.". TABLE 9.2 +-, Parameters Fuel B,, and B, for Eq. + B,, cm/s B,, em/s Ref. 1.11. 36.9 - 140.5 30 Methanol Propane Isooctane Gasoline -.- . A n " 3 , , Note: Values of S , , given by Eq. (9.35) arc obtained from least-squarm fits of Eq. (9.33) to data over the range L 0 0 Values of 4,,,B,,, , and B1 are given in Table 0 7 30 gasoline with average molecular weight of 107 ~USU tional data were available and were correlated by3' a, = 2.4 For @solinela reference -. - 0.27143.51 r ...."- (9.36a) For methane, simple equations such as (9 . 3 4 ~b) do not adequately correlate the data over the range of p and T relevant to engines.
However, laminar burning nave velocity data from a spherical constant-volum. WUW the obtained along an unburned gas isentropic path, as the pressure inalnn~ rises during combustion. Variation in laminar burning velocity L-== ---unburned gas isentropes does correlate with a power law: .
S,, = s ,o (Puo ~) s= Values for SL, and E from the literature are summarized in Table 9.3. TABLE 9.3 Parameters for methane& burning velocity correlation laminar m.(93711 t At 298 K initial temperature. $ S a Fig. 9-25. Mole 0.1fraction diluent 0.2 f b 0.3 FIGURE 9-26 Effect of burned gas mole fraction P, in unburned ~ i i i n e .on ~ ~ laminar burning velocity. Fuel: gasmixture The presence of burned gas in the unburned cylinder charge due to residual gases and any recycled exhaust gases causes a substantial reduction in the laminar burning velocity. Any burned gas in the unburned mixture reduces the heating value per unit mass of mixture and, thus, reduces the adiabatic flame temperature. It acts as a diluent.
The effect of increasing burned gas or diluent fraction on laminar flame speed is shown in Fig. 9-26. The diluent used was a mixture of CO, and N2, chosen to match the heat capacity of actual gasoline-air combustion products.f The proportional reduction in laminar burning velocity is essentially independent of the unburned mixture equivalence ratio, pressure, and temperature over the range of interest in engines. The data in Fig. 9-26 are correlated by the relation: where & is the mole fraction of burned gas diluent. Other studies corroborate the magnitude of this burned gas effect.3Z Note that for equal heat capacity added to the unburned mixture, burned gases have a much larger effect on laminar burning velocity than does excess air. For example, the laminar burning velocity of a stoichiometric mixture as it is leaned to 9 = 0.8 is reduced by 23 percent. The excess air required has a heat capacity of about 0.2 times that of the combustion products of the undiluted mixture. Adding the same heat capacity by adding stoichiometric burned gmes (which requires a burned gas mole fraction of 0.175) reduces the laminar burning f The water in actual residual and exhaust gas was omitted. A mixture of 80 percent N. percent CO, ,by volume, was used. nnd 3n 406 INTERNAL COMBUSTION ENGINE FUNDAMENTALS velocity by 55 percent.32 Proper allowance for the burned gas fraction in ing laminar burning velocities for spark-ignition engines is most important. The above correlations define the laminar burning velocity as a functi unburned mixture thermodynamic properties and composition, only. It has assumed that flame thickness and curvature effects are negligible.28 Our in laminar burning velocity is twofold: first, it is used to define the char chemical reaction time of the mixture in Eq. (9.30); second, a presumed c quence of the wrinkled thin-reaction-sheet turbulent-flame structure is locally, the sheet propagates at the laminar burning velocity. The above corre tions adequately characterize a quiescent burning process. Ho flame propagation can be influenced by the local flow field If the flame thickness is less than the Kolmogorov scale, the of straining which affects both the flame area (usually referred to as ing for an area increase) and the local (laminar) burning velocity. While this problem is not yet well understood, it is known that straining can affect the laminar burning velocity and can cause flame extinction.
The laminar burning velocity decreases with increasing strain rate, and the Lewis number of the unburned mixture has a significant influence on this rate of decrease. The Lewis number is the ratio of diffusivities of heat and mass. For stoichiometric mixtures it is close to one; it increases above about unity as the unburned fuel-air mixture is leaned out. Thus the local flow field may 'have a discernable effect on the local burning velocity of the thin laminarlike reaction-sheet flame, especially for lean or dilute mixtures.34 93.4 Flame Propagation Relations If the heat-release or mass burning rate analysis of Sec. 9.2.2 is coupled with an analysis of flame geometry data, substantial additional insight into the behavior of spark-ignition engine flames is obtained. Flame photographs (such as those in Figs. 9-1,9-14, and 9-16 and Refs. 4 and 35) effectively define the position of the front or leading edge of the turbulent engine flame. The "shadow" of the enflamed zone, under normal engine conditions, is close to circle: only in the presence of very high swirl does substantial distortion of the flame shape occur.'" Thus, to a good approximation, the surface which d e h e s the leading edge of the turbulent flame (ahead of which only unburned mixture exists) is a portion of the surface of a sphere. Figure 9-27 indicates the geometrical parameters which define this flame surface: rc,ac,z, ,the coordinates of the flame center; rf , the radius of the best-fit circle to the flame front silhouette; and the geometry of the cornbustion chamber walls. The flame is initiated at the spark plug; however, it may move away from the plug during the early stages of its development as shown, We d e h e theframefront area Af as the spherical surface of radius rf coinciding with the leading edge of the flame contained within the combustion chamber, and the enframed volume Vf as the volume within the chamber behind this flame front. The thermodynamic analysis of cylinder pressure data allows us to define additional geometrical parameters. The burned gas radius rb is the radius of the COMBUSTION IN SPARK-IGNITION ENGINES -R spark 0 Distance 407 FIGURE 9-27 Schematic of spherical h e front in engine cornbustion chamber identifying parameters which define flame geometry. (From Beretta et a13 spherical surface within the combustion chamber which would contain all the burned gas behind it; i.e., a r b , rc, a,, 2,) = UP, (9.39) The spherical burning area A, is the area of this spherical surface; i.e., A, = a Urb ,rc ac , 2,) arb 9 (9.40) The laminar burning area A, is the surface area the flame would have if it burned at the laminar flame speed, i.e., dmddt A, = P, SL (9.41) speed in the unburned mixture ahead of the flame Several velocities can be defined. The mean expansion speed of the front uf uf = dAs/dt Ls (9.42) 408 INTERNAL COMBUSTION ENGIN6 W A M E N T A L S where A, is the "shadow" area enclosed by the " best-fit" circle through the! leading edge of the flame and is the arc length within the chamber of this " best-fit " circle. The mean expansion speed of the burned gas u, is This derivative is taken with the piston position fixed since only burned volume changes due to combustion are of interest. The burnina sneed Sl is defined bv The mean gas speed just ahead of the flame front u, is u, = U b - Sb Note that combining Eqs.
(9.41) and (9.44) gives the relation Sb A, = SLA, Also, it follows from Eqs. (9.29), (9.43), and (9.44) that As x, and y, + 0, ub/Sbapproaches the expansion ratio p J p , . As x, and y, -r 1, u$Sb approaches unity. The variation of the above quantities during the engine combustion , shows results from an analysis of cylinder pressure data and the corresponding flame front location information (determined from high-speed movies through a window in the piston) of several individual engine operating cycles. The combustion chamber was a typical wedge design with a bore of 102 mm and a com~ressionratio of 7.86. The flame radius initially grows at a rate that increases tually rf - r, goes to an essentially constant value of about 6 mm for r, >, 30 mm. This difference, r, - r,, is approximately half the thickness of the turbulent : 410 C O M B U ~ O Nm SPARK-IGNITION ENGINES INTERNAL C O M B U ~ O NENGINE FUNDAMENTALS 411 3.5 Normalized enflamed and burned volumes, and flame front area and laminar burning area, are shown in Fig. 9-28c.
Volumes are normalized by the cylinder volume, and areas by nRh, where h is the average clearance height and R the cylinder radius. Discontinuities occur in the flame area a, at the points where the flame front contacts first the piston face and then the near cylinder wall. The laminar area A, is initially close to the flame area A, and then increases rapidly as the flame grows beyond 10 mm in radius. During the rapid burning combustion phase Cv, 2 0.2) the value of y, is significantly greater than y,.
During this phase, the laminar area exceeds the flame area by almost an order of magni. tude. These observations indicate the existence of substantial pockets of unburned mixture behind the leading edge of the flame.4 The ratio of the volume of the unburned mixture within the turbulent flame zone (V, - h)to the reaction-sheet area within the flame zone (AL- A,) defines a characteristic length IT = V' - v, A, - 4 which can be thought of as the scale of the pockets of unburned mixture within the flame.
For the data set of Fig. 9-28,1T is approximately constant and of order 1 mmZ4 These flame geometry results would be expected from the previous photographic observations of how the flame grows from a small approximately spherical smooth-surfaced kernal shortly after ignition to a highly wrinkled reaction-sheet turbulent flame of substantial overall thickness. Initially, the amount of unburned gas within the enflamed volume is small. During the rapid burning phase of the combustion process, however, a significant fraction (some 25 percent; see Fig. 9-2) of the gas entrained into the flame zone is unburned. The front expansion speed u,, burning speed S,, and laminar flame speed S, are shown in Fig. 9-281. The expansion speed increases as the flame develops to a maximum value that is several times the mean piston speed of 3.1 m/s and is comparable to the mean flow velocity through the inlet valve of 18 m b Z 4The burning speed increases steadily from a value close to the laminar flame speed at early times to almost an order of magnitude greater than S, during the rapid burning phase.
During this rapid burning phase, since (r, - r,) is approximately constant, the flame front expansion speed and the mean burned gas expansion speed are essentially equal. The difference between u, x u, and S, is the unburned gas speed u, just ahead of the flame front. Note that the ratio u//Sb (%udSb) decreases monotonically from a value equal to the expansion ratio @,,/pb) at spark to unity as the flame approaches the far wall, as required by Eq. (9.47). The effect of flame propagation on the flow field in the unburned mixture ahead of the flame is important because it is the turbulence just ahead of the flame that determines the local burning velocity. Measurements of mean velocities, rms fluctuation velocities, and turbulence intensities have been made using laser doppler anemometry (see Sec. 8.2.2) at different locations within engine combustion chambers (e.g., Refs. 36 and 37). Such data are difficult to interpret - 3.0 342 346 350 354 358 362 Crank angle, deg FIGURE 9-29 Laser doppler anemometer measurements of ensemble-averaged mean velocity a,, [EQ.(8.2011, m s fluctuation in individual-cycle mean velocity U,, p q . (8.21)] and turbulence intensity u; CEq. (8.22)], close to the cylinder axis, from before ignition to after flame amval. Disc-shaped chamber, spark plug in cylinder wall, measurement at x / B = 0.57, B = 76 m a 300 rev/min. $p = 0.83 rnls.36 because the mean flow varies cycle-by-cycle, the turbulence is not homogeneous, and the flame motion and shape show substantial cyclic variations. The results in Fig.
9-29 were taken in a special single-cylinder engine with a disc-shaped combustion chamber where the spark plug was located in the cylinder liner.
Shown are the ensemble-averaged mean velocity, cyclic variation in mean velocity, and the turbulence intensity, normal to the front, during the major portion of the combustion process, close to the chamber center. The mean velocity normal to the front increases steadily from shortly after ignition, as the combustion-produced gas expansion displaces unburned mixture toward the wall. It peaks as the flame arrives at the measurement location. The cyclic variation in mean velocity and the turbulence intensity normal to the front remain essentially constant until a few degrees before the flame arrival. These two quantities are comparable in magnitude; thus the turbulence intensity is lower than the rms fluctuation velocity (in this case by about a factor of 2) (see Sec. 8.2.2). Whether the increase in turbulence as the flame approaches is due to rapid distortion resulting from the compression of the unburned mixture which occurs during combustion or is the result of inadequate resolution of cycle-to-cycle flow variations is unclear. Rapidly imposed distortions of a turbulent flow field, such as those imposed by combustion-produced gas expansion, would lead to an increase in vorticity and turbulence intensity. Other studies, e.g., Ref. 37, indicate there is little or no increase in turbulence intensity ahead of the flame. The variation of burning speed with engine speed has also been carefully examined in a study where flame position was determined from high-speed movies, mass burning rates from cylinder pressure, and turbulence information 412 INTERNAL COMBUSTION ENGINE FUNDAMENTALS from experiments at equivalent motored condition^.^^ The turbulence q obtained during motoring experiments was the ensemble-averaged root square velocity fluctuation defined by Eq. (8.18). Values of Sb/SLand ~ $ 3 , determined at two points in the combustion process: at a flame radius of (the end of the flame development process) and at mass fraction burned eq 0.5 (halfway through the rapid burning phase). To correct the motored tu lence data for the higher pressure levels corresponding to engine firing tions, a simple rapid distortion model (see Sec.
14.4.2) based on conservati angular momentum in turbulent eddies was used. A linear correlation between S, and uk results, as shown in Fig. 9-30, for the rapid burning combustion phase.
Note that as u;/SL goes to zero, SJSL approaches a value close to unity.
Once the flame front reaches the far cylinder wall (see Fig. 9-27) the front can no longer propagate: however, combustion continues behind the front until all the unburned mixture entrained into the enflamed region is consumed. This final burning or termination phase of the combustion process can be approximated by an exponential decay in the mass burning rate with a characteristic time constant z, of order 1 ms.
Since these "islands" or "pockets" of unburned mixture behind the leading edge of the flame have a characteristic scale I, based on the laminar flame area [Eqs. (9.41) and (9.48)], it follows that I, = rbSL In summary, the above flame data analysis procedures show that the relationships between r j and r,, V/ and 6 ,Aj and A,, u,, S, and SL are distinctly different in the three phases of combustion: (1) the development phase, where a highly wrinkled reaction-sheet " thickv-overall turbulent flame evolves from the essentially spherical flame kernal established by the spark discharge; (2) the rapid-burning phase, where this thick "developed" turbulent flame propagates across the combustion chamber to the far wall, during which most of-the mass is burned; and (3) the termination phase after the flame front has reached the far wall and propagation of the front is no longer possible, when the remaining unburned mixture within the flame bums up. The burning velocity, in the rapid-burning phase of the combustion process, scales with turbulence intensity, which in turn scales with engine speed. . 35 30- ..... d*:! 25 - @I* ..I *. *: 20 15 lo: 5 0 ~ 51 115 ' 10 1 ($)@ 0'15 ' 20 1 FIGURE 9-30 Variation of burning speed with turbulena intensity. The ensemble-averaged rms velocity fluctuation was measured during motoring engine operation. The ratio p/p, (firing pressure1 motoring ' pressure) corrects for the eff'ect of additional compression on the turbulence intensity. Range of engine speeds and spark timing.35 COMBUS~ONIN S P A R K - I G ~ N ENGMES 413 ARIATIONS IN BURNING, , PARTIAL 9.4.1 Observations and Definitions observation of cylinder pressure versus time measurements from a spark-ignition engine, for successive operating cycles, shows that substantial variations on a cycle-by-cy~lebasis exist. Since the pressure development is uniquely related to the combustion process, substantial variations in the combustion process on a cycle-by-cyclebasis are occurring. In addition to these variations in each individual cylinder, there can be significant differences in the combustion process and pressure development between the cylinders in a multicylinder engine. Cyclic variations in the combustion process are caused by variations in mixture motion within the cylinder at the time of spark cycle-by-cycle, variations in the amounts of air and fuel fed to the cylinder each cycle, and variations in the mixing of fresh mixture and residual gases within the cylinder each cycle, especially in the vicinity of the spark plug.
Variations between cylinders are caused by differences in these same phenomena, cylinder-to-cylinder.
Cycle-by-cycle variations in the combustion process are important for two reasons. First, since the optimum spark timing is set for the "average" cycle, faster-than-average cycles have effectively overadvanced spark-timing and slower-than-average cycles have retarded timing, so losses in power and e6ciency result. Second, it is the extremes of the cyclic variations that limit engine operation. The fastest burning cycles with their overadvanced spark timing are most likely to knock.
Thus, the fastest burning cycles determine the engine's fuel octane requirement and limit its compression ratio (see Sec. 9.6.3). The slowest burning cycles, which are retarded relative to optimum timing, are most likely to burn incompletely. Thus these cycles set the practical lean operating limit of the engine or limit the amount of exhaust gas recycle (used for NO emissions control) which the engine will tolerate. Due to cycle-by-cycle variations, the spark timing and average air/fuel ratio must always be compromises, which are not necessarily the optimum for the average cylinder combustion process.
Variations in cylinder pressure have been shown to correlate with variations in brake torque which directly relate to vehicle driveability. An example of the cycle-by-cycle variations in cylinder pressure and the variations in mixture burning rate that cause them are shown in Fig. 9-31.
Pressure and gross heat-release rate [calculated from the cylinder pressure using Eq. (9.2711 for several successive cycles at a mid-load, mid-speed point are shown as a function of crank angle. The maximum heat-release rate and the duration of the heat release or burning process vary by a factor of two from the slowest to the fastest burning cycle shown. The peak cylinder pressure varies accordingly. The faster burning cycles have substantially higher values of maximum pressure than do the slower burning cycles; with the faster burning cycles peak pressure occurs The heat-release rate data in Fig. 9-31 show that there are cycle-by-cycle variations in the early stages of flame development (from zero to a few percent of COMBUSTION M SPARK-IGNITION ENGINES point of efficiency,hydrocarbon emissions, torque variations, and rough^ness. e partial-burn and misfire regimes are discussed in Sec. 9.4.3. various measures of cycle-by-cycle combustion variability are used. It can defined in terms of variations in the cylinder pressure between different cycles, or terms of variations in the details of the burning process which cause the &fferenCc?Sin pressure. The following quantities have been used: 35 30 B g B & 25 20 1. pressure-related parameters. The maximum cylinder pressure p,,,; the crank angle at which this maximum pressure occurs 8;, the maximum rate of pressure rise (dpld6)-; the crank angle at which (dp/d8), occurs; the indicated mean effective pressure [which equals j p dV/&, see Eqs. (2.14), (2.15), and (2.19)l. 2. Burn-rate-related parameters. The maximum heat-release rate (net or gross, see Sec. 9.2.2); the maximum mass burning rate; the flame development angle AB, and the rapid burning angle, Ad, (see Sec. 9.2.3).
3. Flame front position parameters. Flame radius, flame front area, enflamed or burned volume, all at given times; flame arrival time at given locations. 15 10 5 0 -. g 50 - 40 - 30 - 4% 2010 - - 10 1 -150 I -100 -50 I I 0 50 100 150 Degrees ATC FIGURE 9-31 Measured cylinder pressure and calculated gross heat-release rate for ten cycles in single-cylinder spark-ignition engine operating at 1500 rev/min, 4 = 1.0, p,,,,, = 0.7 am, MBT timing 25" BTC.14 the total heat release) and in the major portion of the combustion process-the rapid-burning phase-indicated by the v&ations in the maximum b;rning rate. As the mixture becomes leaner with excess air or more dilute with a higher burned gas fraction from residual gases or exhaust gas recycle, the magnitude of cycle-by-cycle combustion variations increases. Eventually, some cycles become sufficiently slow burning that combustion is not completed by the time the exhaust opens: a regime where partial burning occurs in a fraction of the cycles is encountered. For even leaner or more dilute mixtures, the misfire limit is reached.
At this point, the mixture in a fraction of the cycles fails to ignite. While sparkignition engines will continue to operate with a small percentage of the cycles in the partial-burn or misfire regimes, such operation is obviously undesirable from Pressure-related quantities are easiest to determine; however, the relation between variations in combustion rate and variations in cylinder pressure is complex.38 Equation (9.26) defines the factors that govern this relationship. Because the rate of change of pressure is substantially affected by the rate of change of cylinder volume as well as rate of burning, changes in the phasing of the combustion process relative to TC (e.g., which result from changes in flame development angle) as well as changes in the shape and magnitude of the heatrelease rate profile affect the pressure. Figure 9-32 illustrates how the magnitude of the maximum cylinder pressure p,, and the crank angle at which it occurs e? vary as the crank angle at which combustion effectively starts (e.g., 8 at whch 1 percent of the cylinder mass has burned) and the burning rate are varied. vary for a k e d fast-burning heat-release Curve CABE shows how p,, and 8, profile (the duration of the heat-release process and its maximum value are held Fast bum FIGURE 9-32 Schematic of variation in maximum cylinder pressure and crank angle at which it occurs, in individual cycles. CABE typical of fast heat-release process; CA'B'D'E' typical of slow heat-release process. (From Matekunas.") 416 I ~ R N A L C O M B U ~ O NENGINE FUNDAMENTALS constant), as the phasing of this combustion process relative to TC is varied. corresponds to MBT timing where the start of combustion is phased to maximum brake torque, B corresponds to retarded timing, and C to advanced timing. C'A'B'D'E' is a similar curve for a slow-burning heatprofile. A' corresponds to MBT timing, and B' and D' to increasingly timing. Note that with a suficiently slow-burning heat-release profile, beyond gl, om, decreases as the bum process is increasingly retarded. This occurs when the rate of increase of pressure due to combustion becomes so low that it is more than offset by the pressure decrease due to volume increase: eventually for extremely slow and late burning, the maximum pressure approaches the motored pressure at TC. The dashed lines show the constant start-of-combustion timing relative to MBT for each burn rate curve. Note that dm, for constant relative timing varies little as the heat-release profile or bum rate varies3' We can now explain the effects of variations in the heat-release profile (both in the development stage of the burning process, which effectively changes the location of the start of combustion, and in the rate of burning throughout the process) on p, and 8*,, when the spark timing occurs at a fixed crank angle. For a fixed burning rate profile (duration of bum and maximum burning rate) as the start of combustion is delayed to be closer to TC, p,, decreases and 8initially increases (A to B or A' to B'). This is the effect of a change in relative timing or phase of the burning process due to a slower initial rate of flame development with fixed spark timing. If, in addition to the flame development being slower, the heat-release rate throughout the burning process is lower, then that combustion process is even more retarded from the optimum and p,,, decreases and 8, increases further, to their values at Dr. The effect of a faster initial flame development and faster burning rate, with fixed spark time, is the opposite. The magnitudes of the changes in p,, and 8depend, obviously, on the extent of the cyclic variations; they also depend on whether the average burn process is fast or slow. For fast-burning engines, a larger fraction of the heat release occurs near TC when the chamber volume is changing relatively slowly. Thus pressure variations are mainly due to combustion variations. With slow-burning engines, where a significant fraction of the energy release occurs well after TC, the effect of volume change also becomes significant and augments the effect of combustion variations. For large variations and a slow average burning process, p,, can fall below E', and Om, then decreases. A fast-burning combustion process significantly reduces the impact of cyclic combustion variations on engine perf~rmance.~' We can now evaluate the various measures of combustion variability. The maximum pressure variation has been shown to depend on both changes in phasing and burning rate. The magnitude of this variation depends on whether the combustion chamber is faster or slower burning, on average. It also depends on whether the burning process is substantially retarded relative to MBT. It depends, too, on cyclic cylinder fuel and air charging variations. Thus the interpretation of variations in p , [or in the maximum rate of pressure rise (dp/dO)] in terms of variations in the rate and phasing of the burning process C O M B U ~ O NIN SPARK-IGNITION ENGINES 417 One important measure of cyclic variability, derived from pressure data, is the cofficient of variation in indicated mean effective pressure. It is the standard deviation in imep divided by the mean imep, and is usually expressed in percent: COV,,, * x 100 (9.50) lmeP ~tdefines the cyclic variability in indicated work per cycle, and it has been found that vehicle driveability problems usually result when COV,,, exceeds about 10 = between p,,, 8 and imep for 120 cycles of an engine cylinder at fixed operating conditions and three different spark timings.38 The MBT timing data show a spread in imep at a fixed value of d,,. This imep data band is relatively flat and is centered around Omax z 16"; only at later values of 8does imep fall off significantly. The vertical spread in = 16" is due to variations in the amount of fuel entering the imep around 8cylinder each cycle; normal variations in the bum profile under these conditions, which effectively change the phasing of the combustion process, produce only modest reductions in imep. For early 8(the extreme upper left of Fig. 9-33a), the variations in p,, are also due mainly to these fuel-charging variations, cycleby-cycle; these are the fastest burning c

the pattial-burning regime, the most common type of incomplete-combustion cycle was a slow-burning cycle which required more time to complete burning than was available: flame extinguishment during expansion was much less common. Engine performance measurements showed that the engine stability limit--evidenced by minimum fuel consumption and onset of rapid increase in HC emissions--occurred at 4 = 0.65, just before the partial-burn limit line where some slow-burning cycles occur but combustion is still complete in all cyclesP4 From the above it is clear that flame initiation is a necessary but not sufficient condition for complete combustion. Too-slow flame development and prop- 95 SPARK IGNITION In spark-ignition engines, the electrical discharge produced between the spark plug electrodes by the ignition system starts the combustion process close to the end of the compression stroke.
The high-temperature plasma kernel created by the spark develops into a self-sustaining and propagating flame front-a thin reaction sheet where the exothermic combustion chemical reactions occur. The function of the ignition system is to initiate this flame propagation process, in a repeatable manner cycle-by-cycle, over the full load and speed range of the engine at the appropriate point in the engine cycle. Shadowgraph and schlieren photographs of the kernel created by the discharge between the plug electrodes, the growth of that kernal, and its transition to a propagating flame have already been presented in Figs. 9-19 and 9-20, and described in the accompanying text. A spark can arc from one electrode to another when a sufficiently high voltage is applied.
Ignition systems commonly used to provide this spark are: battery ignition systems where the high voltage is obtained with an ignition coil (coil ignition systems); battery systems where the spark energy is stored in a capacitor and transferred as a high-voltage pulse to the spark plug by means of a special transformer (capacitive-discharge ignition systems); and magneto ignition systems where the magneto-a rotating magnet or armaturegenerates the current used to produce a high-voltage pulse. This section reviews our basic understanding of electrical discharges in inflammable gas mixtures relevant to engine ignition (Sec. 9.5.1), the major design and operating characteristics of conventional engine ignition systems (Sec. 9.5.2), and, briefly, some alternative approaches to generating a propagating flame (Sec. 95.1 Ignition Fundamentals Equivalence ratio FIGURE 9-38 Actual limiting combustion regimes for lean-operating engine. 1200 revlmin, volumetric efficiency 60 percent, methane fuel, 40 m.J spark energy, 2.5 ms spark duration.u A spark can arc from one plug electrode to the other only if a sufficiently high voltage is applied. In a typical spark discharge, the electrical potential across the electrode gap is increased until breakdown of the intervening mixture occurs. Ionizing streamers then propagate from one electrode to the other.
The impedance of the gap decreases drastically when a streamer reaches the opposite electrode, and the current through the gap increases rapidly. This stage of the 428 INTERNAL COMBUSTION ENCiINE FUNDAMENTALS discharge is called the breakdown phase. It is followed by the arc phase, where thin cylindrical plasma expands largely due to heat conduction and diffusion a with inflammable mixtures, the exothermic reactions which lead to a propagat] flame develop. This may be followed by a glow discharge phase where, de on the details of the ignition system, the energy storage device (e.g., the coil) will dump its energy into the discharge circuit.52*53 Figure 9-39 shows the behavior of the discharge voltage and current as a function of time for a conventional coil ignition system. Typical values are shown; actual values depend on the details of the electrical components. The breakdown phase is characterized by a high-voltage (- 10 kV), high-peak current (-200 A), and an extremely short duration (- 10 ns). A narrow (-40 pm diameter) cylindrical ionized gas channel is established very early. The energy supplied is transferred almost without loss to this plasma column. The temperature and pressure in the column rise very rapidly to values up to about 60,000 K and a few hundred atmospheres, respectively. A strong shock or blast wave propagates outward, the channel expands, and, as a result, the plasma temperature and pressure fall. Some 30 percent of the plasma energy is carried away by the shock wave; however, most of this is regained since spherical blast waves transfer most of their energy to the gas within a small (-2 mm diameter) sphere into which the breakdown plasma soon expands.52.5 3 A breakdown phase always precedes arc and glow discharges: it creates the electrically conductive path between the electrodes.
The arc phase voltage is low COMBUSTION IN SPARK-IGNITION ENGINES (< 100 V), though the current can be as high as the external circuit permits. In contrast to the breakdown phase where the gas in the channel is fully dissociated and ionized, in the arc phase the degree of dissociation may still be high at the anter of the discharge, but the degree of ionization is much lower (about 1 percent). Voltage drops at the cathode and anode electrodes are a significant fraction of the arc voltage, and the energy deposited in these electrode sheath which is conducted away by the metal electrodes, is a substantial fraction of the total arc energy (see Table 9.4 below). The arc requires a hot cathode spot, so evaporation of the cathode material occurs. The arc increases in size due prirnarily to heat conduction and mass diffusion. Due to these energy transfers the gas temperature in the arc is limited to about 6000 K: the temperature and degree of dissociation decrease rapidly with increasing distance from the arc axis. Currents less than 200 mA, a large electrode voltage drop at the cathode (300 to 500 V), a cold cathode, and less than 0.01 percent ionization are typical for the glow discharge. Energy losses are higher than in the arc phase, and peak equilibrium gas temperatures are about 3000 K.52 About 0.2 mJ of energy is required to ignite a quiescent stoichiometric fuelair mixture at normal engine conditions by means of a spark. For substantially leaner and richer mixtures, and where the mixture flows past the electrodes, an order of magnitude greater energy (-3 mJ) may be required.54 Conventional ignition systems deliver 30 to 50 mJ of electrical energy to the spark. Due to the physical characteristics of the discharge modes discussed above, only a fraction of the energy supplied to the spark gap is transmitted to the gas mixture. The energy balance for the breakdown, arc, and glow phases of the discharge is given in Table 9.4. Radiation losses are small throughout.
The end of the breakdown phase occurs when a hot cathode spot develops, turning the discharge into an arc; heat losses to the electrodes then become substantial. The breakdown phase reaches the highest power level (- 1 MW),but the energy supplied is small (0.3 to 1 mJ). The glow discharge has the lowest power level (- 10 W) but the highest energy (30 to 100 mJ), due to its long discharge time. The arc phase lies between. The proportions of the electrical energy supplied, which can be transferred to the plasma in these three phases of the discharge, are shown in Fig. 9-40.53.55 The different transfer capabilities for breakdown arc and glow discharges arise TABLE 9A Energy distribution for breddown, arc, and glow dischargest Time, s FIGURE 9-39 Schematic of voltage and current variation with time for conventional coil spark-ignition system. Typical values for energy and voltage in the three phases-breakdown, arc, and glow discharge-are given.= 429 Radiation loss Heat loss to electrodes Total losses Plasma energy Breakdown, % Are, % Glow, % 100 atm) Eq. (10.24) overpredicts penetration.
densities COMBUSTION IN COMPRESSION-IGNITION ENGINES 300 300 Measurement po = 10 MW I Measurementpa = 531 2 MW 1L 0.5 0.3 0.03 0.05 0.1 o . + l l l 0.3 0.5 1 3 0.3 0.030.05 0.1 5 0.3 0.5 1 3 5 Time, rns T i e , ms FIGURE 10-26 Spray tip penetration as function of time at various ambient pressures (pJ and injection pressures (P,,). Fuel jets injected into quiescent air at room temperature." seconds, S and d, in meters, Ap in pascals, p, in kilograms per cubic meter, and T, in kelvins. More detailed studies have examined the spray tip location as a function of time, following start of a diesel injection process in high-pressure bombs. Data taken by Hiroyasu et al.,19 shown in Fig. 10-26, illustrate the sensitivity of the spray tip position as a function of time to ambient gas state and injection pressure for fuel jets injected into quiescent air at room temperature. These data show that the initial spray tip penetration increases linearly with time t (i e the spray tip velocity is constant) and, following jet breakup, then increase as Injection pressure has a more significant effect on the initial motion before breakup; ambient gas density has its major impact on the motion after breakup. Hiroyasu et al. correlated their data for spray tip penetration S(m) versus time as 4. 2Ap 112t t < tbreak: S = 0.39(-) t > tbreak: S = 2.95e)Ip(dn t)'~' where tbreak = 2 % ~dn Ap)'I2 and Ap is the pressure drop across the nozzle (pascals), p, and p, are the liquid and gas densities, respectively (in kilograms per cubic meter), dn is the nozzle a v 4600 7500 I I I I 0.5 1.O 1.5 2.0 T i e , ms (b) FIGURE 10-27 (a) Measured outer boundary of sprays injected into swirling air flow.(b) Spray tip penetration as a function of time for different swirl rates. Solid lines show Eq.(10.27).29 diameter (meters), and t is time (seconds).
The results of Reitz and Bracco25 indicate that the breakup or intact length depends on nozzle geometry details in addition to the diameter (see Fig. 10-25b). Note that under high injection pressures and nozzle geometries with short lengthldiameter ratios, the intact or breakup length becomes very short; breakup can occur at the noale exit plane. The effect of combustion air swirl on spray penetration is shown in Fig.
10-27.
Figure 10-27a shows how the spray shape and location changes as swirl is increased; Fig. 10-27b shows how spray tip penetration varies with time and swirl rate-29These authors related their data on spray tip penetration with swirl, s,, through a correlation factor to the equivalent penetration, S, without swirl given (10.27) 532 INTERNAL COMBUSTION ENGINE FUNDAMENTALS COMBUSTION IN COMPRESSION-IGNITIONENGINES 533 where R, is the swirl ratio which equals the swirl rate in revolutions per mi divided by the engine speed N (revolutions per minute), and vj is the initial jet velocity (meters per second). The curves in Fig. 10-27b correspond to (10.27).
Swirl both reduces the penetration of the spray and spreads out the s more rapidly. 10.55 Droplet S i z e Distribution combustion chamber is important, atomization of the liquid fuel into number of small drops is also necessary to create a large surface area which liquid fuel can evaporate. Here we review how the drop size distribu the fuel spray depends on injection parameters and the Since the measurement of droplet characteristics in an opera Droplet diameter Dd, pm perature. During the injection period, the injection conditions such as inje sure, nozzle orifice area, and injection rate may vary. Consequently, size distribution at a given location in the spray may also chan during the injection period. In addition, since the details of the process are different in the spray core and at the spray edge, and the trajecto of individual drops depend on their size, initial velocity, and location within spray, the drop size distribution will vary with position within the s of these variations has yet been adequately quantified. The aerodynamic theory of jet breakup in the atomization regime s marized in Sec. 10.5.3 (which is based on work by G. I. Taylor) leads to prediction that the initial average drop diameter Dd is proportional of the most unstable surface waves:?' 211.1s Pg0, dd= C 7A* where u is the liquid-fuel surface tension, pg is the gas den velocity between the liquid and gas (taken as the mean injection ve a constant of order unity, and A* is the dimensionless wavelength growing wave. A* is a function of the dimensionless number @Jpg)(Rej/W where the jet Reynolds and Weber numbers are given by Re, = pl vidJyl Wel = plv: d j u and d, is the nozzle orifice diameter. A* goes to 312 as number increases above unity. Near the edge of the spray close to the nozzle, equation predicts observed drop size trends with respect to injection velocity, properties, nozzle Lid, and nozzle diameter, though measured mean drop s are larger by factors of 2 to 3.30 However, within the dense early region of spray, secondary atomization phenomena-coalescence and breakup-oc Droplet size distribution in diesel fuel spray injected through throttling pintle nozzle into quiescent room-temperature air at 11 atrn.
Nozzle opening pressure 9.9 MPa. Pump speed 500 revlmin. Drop lets are sampled well downstream of injector at given radial distances from spray axis.32 which will change the droplet size distribution and mean diameter. The downstream drop size in the solid-cone sprays used in diesel-injection systems is markedly influenced by both drop coalescence and breakup. Eventually a balance is reached as coalescence decreases (due to the expansion of the spray) and breakup ceases (due to the reduced relative velocity between the drops and the entrained Measurements of droplet size distributions within a simulated diesel spray indicate how size varies with location. Figure 10-28 shows the variation in drop size distribution with radial distance from the spray axis, at a fixed axial location. The drop sizes were measured with a liquid immersion technique where a sample of drops is collected in a small cell filled with an immiscible liquid. Size distributions can be expressed in terms of: 1. The incremental number of drops An within the size range Dd - AD62 < Dd < Dd ADJ2 2.
The incremental volume AV of drops in this size range 3. The cumulative number of drops n less than a given size Dd + 4 The cumulative volume V of drops less than a given size Dd Since the drops are spherical: dn 6 dV dDd - nD; dDd 534 INTERNAL COMBUSnON ENGINE FUNDAMENTALS COMBUSTION IN COMPRESSION-IGNITION ENGINES 535 100 R i 80 B 7 .-9 ?"E .a 60 E,, o 0.1 MPa 40 20 1; Droplet diameter Injection pressure, MPa 9 4 (b) FIGURE 10-29 Normalized drogsize cumulative frequency distribution in spray injected into ambient-temperat air for air pressures from 0.1 to 5 MPa. Throttling pintle nozzle with nozzle opening pressure 9.9 MPa. Median drop diameter Dm = 1.2240, .32 The distributions shown in the figure are frequency distributions of drop volume.32 The peak in the distribution shifts to larger drop diameters as the radial position decreases: on average, the drops are smaller at the periphery of the spray. To characterize the spray, expressions for drop size distribution an diameter are desirable. An appropriate and commonly used mean diameter is Sauter mean diameter: DSM= (5 (5 D: dn)/ D: dn) where dn is the number of drops with diameter D, in the range D, - dDJ2 < D, < D, + dDJ2. The integration is usually carried out by summing appropriate number of drop size groups. The Sauter mean diameter is t eter of the droplet that has the same surface/volume ratio as that of spray. Various expressions for the distribution of drop sizes in liquid sprays hav been proposed. One proposed by Hiroyasu and K a d ~ t abased ~ ~ on the chisquare statistical distribution fits the available experimental data. Figure 10-29 shows how the chi-square distribution with a degree of freedom equal to 8 fits well to experimental measurements of the type shown in Fig. 10-28. Here Dm is the median drop diameter which for this chi-square curve is 1.224Ds,. The nondimensional expression for drop size distribution in sprays injected through hole nodes, pintle nozzles, and throttling pintle nozzles given by the chi-square distribution is empirical expression for the Sauter mean diameter DsM (in micrometers) for ical diesel fuel properties given by Hiroyasu and K a d ~ t is a~~ D~~ = A(&)-o.I~s 0.121~0.131 Pa f (10.32) where Ap is the mean pressure drop across the nozzle in megapascals, pa is the air density in kilograms per cubic meter, and V, is the amount of fuel delivered per cycle per cylinder in cubic millimeters per stroke. A is a constant which equals 25.1 for pintle nozzles, 23.9 for hole nozzles, and 22.4 for throttling pintle nozzles. Other expressions for predicting D, can be found in Ref. 17. The effects of injection pressure, nozzle geometry and size, air conditions, and fuel properties on Sauter mean diameter in sprays obtained with diesel fuelinjection nozzles have been extensively studied. Various immersion, photographic, and optical techniques for making such measurements have been used.'' Some of the major effects are illustrated in Figs. 10-30 and 10-31 which show v = 0.7 - 1.4 X m21s Injection pressure, MW Injection pressure, MPa (b) Effect of (a) liquid viscosity v and (b) liquid surface tension u on Sauter mean drop diameter as a function of injection pressure. Air conditions: 3 MPa and ambient temperature." 7 - 1 Temperature liquid Time FIGURE 10-33 Schematic of variation of mass, diameter, t perature, evaporation rate, heat-transfer rat air, and heat-transfer rate to liquid dro function of time during evaporation individual drop in diesel environment of injection. As the droplet temperature increases due to heat transfer, the fuel vapor press increases and the evaporation rate increases. As the mass transfer rate of va away from the drop increases, so the fraction of the heat transferred to the dr surface which is available to increase further the drop temperature decreases. the drop velocity decreases, the convective heat-transfer coefficient between air and the drop decreases. The combination of these factors gives the beha shown in Fig. 10-33 where drop mass, temperature, velocity, vaporization rate con&ntration in the air within the spray. As fuel vaporizes, the local air temperature will decrease and the local fuel vapor pressure will increase. Eventually thermodynamic equilibrium would pertain: this is usually called adiabatic satura- thiH equilibrium situation may not be reached within the spray, these results ar useful for understanding the temperature distribution within an evaporatin spray. To quantify accurately the fuel vaporization rate within a diesel fuel spra requires the solution of the coupled conservation equations for the liquid drop - 540 COMBUSTION IN COMPRESSION-IGNITION ENGINES INTERNALCOMBUSTION ENGINE FUNDAMENTALS injection is usually taken as the time when the injector needle lifts off its s (determined by a needle-lift indicator). The start of com to determine precisely. It is best identified from the change i release rate, determined from cylinder pressure data us described in Sec. 10.4, which occurs at ignition. Depending the combustion process, the pressure data alone may ind change due to combustion first occurs; in DI engines und ignition is well defined, but in ID1 engines the ignition point is harder to identi Flame luminosity detectors are also used to determine the first appearance oft flame. Experience has shown that under normal conditions, the point of appe ante of the flame is later than uncertainty or error in determining the ignition po Both physical and chemical processes must take pla fraction of the chemical energy of the injected liquid fuel is released. processes are: the atomization of the liquid fuel jet; the vaporizati droplets; the mixing of fuel vapor with air. The chemical processes are the combustion reactions of the fuel, air, residual gas mixture which le tion. These processes are affected by engine design and operating variables, an fuel characteristics, as follows. Good atomization requires high fuel-injection pressure, small injector ho diameter, optimum fuel viscosity, and high cylinder air pressure at the time injection (see Sec. 10.5.3). The rate of vaporization of the fuel droplets depends the size of the droplets, their distribution, and their velocity, the pressure a temperature inside the chamber, and the volatility of the fuel. The mixing is controlled largely by injector and combustion chamber design. So combustion chamber and piston head shapes are designed to amplify swirl create turbulence in the air charge during compression. Some engine designs a prechamber or swirl chamber to create the vigorous air motion necessary rapid fuel-air mixing (see Sec. 10.2). Also, injector design featu number and spatial arrangement of the injector holes determine the fuel pattern. The details of each nozzle hole affect the spray c tion of the spray depends on the size of the fuel droplets, the i the air density, and the air-flow characteristics. The arrangement of the the spray cone angle, the extent of spray penetration, and the air flow all the rate of air entrainment into the spray. These physical aspects of fuel-inj and fuel-spray behavior are reviewed in Sec. 10.5. The chemical component of the ignition delay is co bustion reactions of the fuel. A ne0u.q hydrocarbon oxidation i Since the diesel engine combustion process is heterogeneou ignition process is even more complex. Though ignition occurs in regions, oxidation reactions can proceed in the liquid phase as well fuel molecules and the oxygen dissolved in the fuel droplets large hydrocarbon molecules to smaller molecules is occurri processes depend on the composition of the fuel and the cylinder charge te Sql rature and pressure, as well as the physical processes described above which vern the distribution of fuel throughout the air charge. Since the ignition characteristics of the fuel affect the ignition delay, this fuel is very important in determining diesel engine operating chartics such as fuel conversion efficiency, smoothness of operation, misfire, emissions, noise, and ease of starting. The ignition quality of a fuel is cetane number. Cetane number is determined by comparing the of the fuel with that of primary reference fuel mixtures in a stane test (see below). For low cetane fuels with too long an ignition st of the fuel is injected before ignition occurs, which results in very ing rates once combustion starts with high rates of pressure rise and ressures. Under extreme conditions, when autoignition of most of the injected fuel occurs, this produces an audible knocking sound, often referred to as "diesel knock." For fuels with very low cetane numbers, with an exceptionally long delay, ignition may occur sufficientlylate in the expansion process for the burning process to be quenched, resulting in incomplete combustion, reduced power output, and poor fuel conversion efficiency. For higher cetane number fuels, with shorter ignition delays, ignition occurs before most of the fuel is injected. The rates of heat release and pressure rise are then controlled primarily by the rate of injection and fuel-air mixing, and smoother engine operation 10.6.2 Fuel Ignition Quality The ignition quality of a diesel fuel is defined by its cetane number. The method used to determine the ignition quality in terms of cetane number is analogous to that used for determining the antiknock quality of gasoline in terms of octane tane number scale is defined by blends of two pure hydrocarbon 1s. Cetane (n-hexadecane, C,,H,,), a hydrocarbon with high ignition ity, represents the top of the scale with a cetane number of 100. An isocetane, ameth~lnonane(HMN), which has a very low ignition quality, represents the e scale with a cetane number of 15.1 Thus, cetane number (CN) is CN = percent n-cetane + 0.15 x percent HMN (10.33) The engine used in cetane number determination is a standardized singlecylinder, variable compression ratio engine with special loading and accessory equipment and instrumentation. The engine, the operating conditions, and the test procedure are specified by ASTM Method D613.37 The operating requirements include: engine speed-900 revlmin; coolant temperature--100•‹C; intake air temperatured5.6"C (150•‹F); injection timing-13" BTC; injection In the onma1 ~rocedurea-methylnapthalene (C,,H,,) wrth a mane number of zero represented scale. Heptamethylnonane, a more stable compound, has replaced it. 542 COMBUSTION IN COMPRESSION-IGNITIONENGINES INTERNAL COMBUSTION ENGINE FUNDAMENTALS pressure--10.3 MPa (1500 lb/in2). With the engine operating under these con tions, on the fuel whose cetane number is to be determined, the compression ra is varied until combustion starts at TC: i.e., an ignition delay (2.4 ms at 900 rev/min) is produced. The above procedure is then repeated reference fuel blends. Each time a reference fuel is tried, the compression r adjusted to give the same 13" ignition delay. When the c required by the actual fuel is bracketed by the values required blends differing by less than five cetane numbers, the cetane number of the fue determined by interpolation between the compression ratios required by the t reference blends. Because of the expense of the cetane number test, many correlations predict ignition quality based on the physical properties of diesel fuels have developed.38.39 A calculated cetane index (CCI) is often used to estimate i quality of diesel fuels (ASTM D97640). It is based on API gravity and the boiling point (temperature 50 percent evaporated). It is applicable to straightfuels, catalytically cracked stocks, and blends of the two. Its use is suitable most diesel fuels and gives numbers that correspond quite closely to cet number. A diesel index is also used. It is based on the fact that ignition linked to hydrocarbon composition: n-paraffins have high ignition quality aromatic and napthenic compounds have low ignition quality. The aniline (ASTM D61 14'-the lowest temperature at which equal volumes of t aniline become just miscible) is used, together with the API gravity, to give th diesel index : Diesel index = aniline point ("F)x The diesel index depends on the fact that aromatic hydrocarbons mix with aniline at comparatively low temperatures, whereas paraffins require siderably higher temperatures before they are completely miscible. Simil high API gravity denotes low specific gravity and high paraffinicity, and, good ignition quality. The diesel index usually gives values slight1 cetane number. It provides a reasonable indication of ignition qu (but not all) cases. 10.63 Au toignition Fundamentals Basic studies in constant-volume bombs, in steady-flow reactors, and in ra compression machines have been used to study the autoignition characteristic fuel-air mixtures under controlled conditions. In some of these studies the and air were premixed; in some, fuel injection was used. Studies t API gavity is based on specific gravity and is calculated from: API gravity, deg = (141.5fs gravity at 60•‹F) - 131.5. 0 543 d = 0.:3 A qi = 0.:I 0 4 = 0.' 7 0 +=I.(I - Light oil No.. 2 diesel 0.3 I 0.9 1.0 I I I I I I 1.1 1.2 1.3 1.4 1.5 1.6 x 1 I I I 0.4 0.8 1.2 1.6 102 Temperature' I 2.0 x K - ~ (b) (a) ~gnitiondelay as function of reciprocal air temperature for light oil spray injected into constant(b) Ignivolume combustion bomb. Injection pressure 9.8 MPa (100 atrn). Air pressures tion delay x @ressure)' measured in steady-flow reactor for No. 2 diesel fuel as function of reciprocal temperature. Fuelfair equivalence ratio 4 varied from 0.3 to tion into constant-temperature and pressure environments have shown that the temperature and pressure of the air are the most important variables for a given fuel composition. Ignition delay data from these experiments have usually been correlated by equations of the form: (10.35) where rid is the ignition delay (the time between the start of injection and the start of detectable heat release), EA is an apparent activation energy for the fuel autoignition Process, fi is the universal gas constant, and A and n are constants dependent on the fuel (and, to some extent, the injection and air-flow Figure 10-35~shows ignition delay data obtained by injecting liquid fuel sprays into a high-pressure heated constant-volume bomb.42 Figure 10-35b shows ignition delay data from a steady-flow high-pressure reactor where vaporized fuel was mixed rapidly with the heated air ~trearn.4~ The match between the form of Eq. (10.35) and the data is clear. Figure 10-391also shows an equivalence ratio dependence of the ignition delay. Representative values for A, n, and E, for Eq. (10.35), taken from these and other studies, are given in Table 10.3. Ignition delay times calculated with these formulas for various diesel engines are given in COMBUSTION IN COMPRESSION-IGNlITON ENGINES 545 546 COMBUSTION IN COMPRESSION-IGNITION ENGINES INTERNALCOMBUSTIONENGINE FUNDAMENTALS 10.6.4 547 Physical Factors Afiecting Delay The physical factors that affect the development of the fuel spray and th charge state (its pressure, temperature, and velocity) will influence the igm delay. These quantities depend on the design of the fuel-injection system combustion chamber, and the engine operating conditions. The injection variables affecting the fuel-spray development are injection timing, q velocity, rate, drop size, and spray form or type.
The relevant charge co depend on the combustion system employed, the details of the combusti chamber design, inlet air pressure and temperature, compression ratio, injecti timing, the residual gas conditions, coolant and oil temperature, and en speed. Data on these interactions are available for different types of di engines. The trends observed with the different diesel combustion systems generally similar, though some of the details are different. In this section ignition delay trends during normal (fully warmed-up) engine operation are c sidered. The dependence of the ignition delay on engine design and opera variables during engine starting and warm-up is also very important, and m different from fully warmed-up behavior due to lower air temperature and sure. INJECTION TIMING. At normal engine conditions (low to medium speed, full warmed engine) the minimum delay occurs with the start of injection at about 1 to 15" BTC?' The increase in the delay with earlier or later injection tirnin occurs because the air temperature and pressure change significantly close to T If injection starts earlier, the initial air temperature and pressure are lower so delay will increase. If injection starts later (closer to TC) the temperature pressure are initially slightly higher but then decrease as the delay proceeds. most favorable conditions for ignition lie in between. INJECTION QUANTITY OR LOAD. Figure 10-36 shows the effect of increas injection quantity or engine load on ignition delay. The delay decreases appr imately linearly with increasing load for this DI engine. As load is increased, t residual gas temperature and the wall temperature increase. This results in hi charge temperature (and also, to a lesser extent, charge pressure) at injection, shortening the ignition delay. When adjustment is made for this increa perature, it is found that increasing the quantity of fuel injected has no significan effect on the delay period under normal operating conditions. Under engine ing conditions, however, the delay increases due to the larger drop in m temperature associated with evaporating and heating the increased amoun This latter result should be expected since it is the first part of the injecte fuel which ignites first; subsequent injected fuel (above the minimum required maintain the fuel-air mixture within the flammability limits during the del does not influence the delay. DROP SIZE, INJECI'ION VELOCITY, AND RATE. These quantities are dete mined by injection pressure, injector nozzle hole size, nozzle type, and geomet bmep, kh FIGURE 10-36 Ignition delays measured in a small four-stroke cycle DI diesel engine with r, = 16.5 as a function of load at 1980 rev/min. Fuel cetane numbers 3439, and 52.48 Experiments by Lyn and V a l d m a n i ~have ~ ~ shown that none of these factors has a significant effect on the delay. At normal operating conditions, increasing injection pressure produces only modest decreases in the delay. Doubling the nozzle hole diameter at constant injection pressure to increase the fuel flow rate (by a factor of about 4) and increase the drop size (by about 30 percent) had no significant effect on the delay. Studies of different nozzle hole geometries showed that the lengthldiameter ratio of the nozzle was not significant; nor did changes in nozzle type (multihole, pintle, pintaux) cause any substantial variation in delay at normal engine conditions. INTAKE AIR TEMPERATURE AND PRESSURE. Figure 10-35 showed values of ignition delay for diesel fuels plotted against the reciprocal of charge temperature for several charge pressures at the time of injection. The intake air temperature and pressure will affect the delay via their effect on charge conditions during the delay period. Figure 10-37 shows the effects of inlet air pressure and temperature as a function of engine load. The fundamental ignition data available show a strong dependence of ignition delay on charge temperatures below about 1000 K at the time of injection. Above about 1000 K, the data suggest that the charge temperature is no longer so significant. Through this temperature range there is an effect of pressure at the time of injection on delay: the higher the pressure the shorter the delay, with the effect decreasing as charge temperatures increase and delay decreases. Since air temperature and pressure during the delay period are such important variables, other engine variables that affect the relation between the inlet air state and the charge state at the time of injection will influence the delay. Thus, an increase in the compression ratio will decrease the ignition delay, COMBUstrON IN COMPRES!3ION-IGNITION ENGINES 549 INTERNAL COMBUSTION ENGINE FUNDAMENTALS -With wall --- with - - - Without wall 100 L = 100mm bmep, kF'a (b) FIGURE 10-37 Effect of inlet air pressure and temperature on ignition delay over load ran& of small DI diesel at 1980 revlmin. (a) Engine naturally aspirated and with 1 atm boost; inlet air temperature = 25•‹C; 50 cetane number fuel. (b) Engine naturally aspirated; = 25 and 66•‹C;34 and 50 cetane number I 0.1 I II I l wall Without wall l 0.3 0.5 1 3 5 Ambient pressure, MPa (0) 10 I 0.1 \ \ \ \ T, = 44O0C L=100mm 0.3 0.5 1 3 5 Ambient pressure, MPa (b) from nozzle on ignition delay from combustion bomb ction of air pressure; T, = KL. (b) Effect of wall temperature at 44•‹Cair ternperat~e.~~ and injection timing will affect the delay (as was discussed earlier), largely due to the changes in charge temperature and pressure at the time of injection. ENGINE SPEED. Increases in engine speed at constant load result in a slight decrease in ignition delay when measured in milliseconds; in terms of crank angle ~ change in engine speed changes degrees, the delay increases almost l i n e a r l ~ ?A the temperature/time and pressure/time relationships. Also, as speed increases, injection pressure increases. The peak compression temperature increases with increasing speed due to smaller heat loss during the compression stroke.47 COMBUSTION CHAMBER WALL EFFECIS. The impingement of the sp the combustion chamber wall obviously affects the fuel evaporation and mixi processes. Impingement of the fuel jet on the wall occurs, to some extent, almost all of the smaller, higher speed engines. With the "M" system, t impingement is desired to obtain a smooth pressure rise. The ignition del the " M " system is longer than in conventional DI engine designs.47 Engine combustion bomb experiments have been carried out to examine the effec wall impingement on the ignition delay. Figure 10-38 shows the effect of impingement on ignition delay measured in a constant-volume c bomb, for a range of air pressures and temperatures, and wall temperat The wall was perpendicular to the spray and was placed 100 mm fr tip. The data shows that the presence of the wall reduces the delay a pressures and temperatures studied, but has no significant effect at the high pressures and temperatures more typical of normal diesel operation. Engine experiments where the delay was measured while the jet impingement process was varied showed analogous trends. The jet impingement angle (the angle between the fuel jet axis and the wall) was varied from almost zero (jet and wall close to parallel) to perpendicular. The delay showed a tendency to become longer as the impingement angle decreased. The most important result is not so much the modest change in delay but the difference in the initial rate of burning that results from the differences in fuel evaporation and fuel-air mixing rates. SWIRL RATE. Changes in swirl rate change the fuel evaporation and fuel-air mixing processes. They also affect wall heat transfer during compression and, hence, the charge temperature at injection.
Only limited engine studies of the effectof swirl rate variations on ignition delay have been made. At normal operating engine speeds, the effect of swirl rate changes on the delay are small. Under engine starting conditions (low engine speeds and compression temperatures) the effect is much more important,47 due presumably to the higher rates of evaporation and mixing obtained with swirl.
OXYGEN CONCENTRATION. The oxygen concentration in the charge into which the fuel is injected would be expected to influence the delay. The oxygen concentration is changed, for example, when exhaust gas is recycled to the intake 550 INTERNAL COMBUSTION ENGINB FUNDAMENTALS } Base fuel: 25%nsetane n-paraffins A '--- A p varied, fq constant fq varied, P cO- 0 0.5 1 1.5 Relative oxygen density 0 Cycloalkanes x Aromatics + 75% i-octane 5-20. by wlume in base fuel FIGURE Irk3 Effect of oxygen density in gas on ignition delay in singlecylinder DI engine of 1.3-dm3 disp1acmeat with re = 15 at 1800 rtv/min.Oxygen &ity changed by recycling exhaust gas at constant inla density and by varying inlet pressure from 0.5 to 3 atm with air.49 for the control of oxides of nitrogen emissions (see Chap. 11). Results of a study carried out in a single-cylinder DI engine operated at a constant airlfuel ratio (30 : I), manifold temperature, injection timing, and speed (1800 revtmin), where the oxygen concentration was varied by recirculating known amounts of cooled exhaust, are shown in Fig.
10-39.49 Oxygen density is normalized by the naturally aspirated no-recirculation test value. As oxygen concentration is decreased, ignition delay increases. 10.65 Effect of Fuel Properties Since both physical and chemical processes take place durhg the ignition delay, the effects of changes in the physical and chemical properties of fuels on the delay period have been studied. The chemical characteristics of the fuel are much the more important.
The ignition quality of the fuel, defined by its cetane number, will obviously affect the delay. The dependence of cetane number on fuel molecular structure is as follows. Straight-chain parafinic compounds (normal alkanes) have the highest ignition quality, which improves as the chain length increases. Aromatic compounds have poor ignition quality as do the alcohols (hence, the difliculties associated with using methanol and ethanol, possible alternative fuels, in compression-ignition engines). Figure 10-40 illustrates these effects. A base fuel was blended with pure paraffinic (normal, iso-, and cycloalkanes), aromatic, and olefinic hydrocarbons ,of various carbon numbers, by up to 20 percent by volume. The base fuel, a blend of 25 percent n-hexadecane and 75 percent isooctane, had a cetane number of 38.3. The figure shows that the resulting ignition delays correlate well as a function of cetane number at constant compression ratio and engine operating conditions. Addition of normal alkanes (excluding n-pentane and 10 carbon number alkanes) improve the ignition quality. As the chain length of added paraffin gets longer (higher carbon number) the cetane number impr Observed cetane number FIGURE 10-40 Effect of type of hydrocarbon structure on ignition quality of fuels in DI diesel combustion process at constant compression ratio and engine operating conditions.s0 ment increases. Isoalkanes, depending on the degree of branching, degrade ignition quality (unless the branching is concentrated at one end of the molecule, when these types of isoalkanes improve ignition quality). Cycloalkanes and aromatics generally reduce the cetane number, unless they have a long n-alkane chain attached to the ring. The cetane number of a fuel (a measure of its ability to autoignite) generally varies inversely with its octane number (a measure of its ability to resist autoignition; see Fig. 9-69 for the effect of hydrocarbon structure on knock). The cetane number of commercial diesel fuel is normally in the range 40 to 55. Engine ignition delay data with diesel fuels of different cetane number, at various constant loads and speeds, shown in Fig. 10-41, demonstrate similar trends. Within the normal diesel fuel cetane number range of 40 to 55, an approximately linear variation is evident. However, decreasing fuel cetane number below about 38 may result in a more rapid increase in ignition delay. Cetane number is controlled by the source of crude oil, by the refining process, and by additives or ignition accelerators. Just as it is possible to reduce the tendency to knock or autoignite in spark-ignition engine fuels by adding antiknock agents, so there are additives that improve the ignition quality of compression-ignition engine fuels. Generally, substances that increase the tendency to knock enhance ignition, and vice versa. Ignition-accelerating additives include organic peroxides, nitrates, nitrites, and various sulfur compounds. The most important of these commercially are the alkyl nitrates (isopropyl nitrate, COMBUSTION IN COMPRESSION-IGNITIONENGINES ""I o Engine 1 2000 revlmin, 112 load b 2000 rev/min, full load L 1000 rev/min, 114 load 1 35 ' 600 revhin, idle 40 45 NGURE 10-42 Comparison of engine ignition delays predicted with Eq. (10.37) with corresponding measured values.54 Measured delay, ms - 50 55 Cetane number FIGURE 10-41 Effect of fuel cetane number on ignition delay over the load and speed range of 6.2-dm3eight-cylinder ID1 swirl-chamber diesel engine. Top curve indicates typical fit between data and least-squares straight line over this cetane number range.'' primary amyl nitrates, primary hexyl nitrates, octyl nitrate).52 Typically, about 0.5 percent of these additives by volume in a distillate fuel gives about a 10 cetane number increase in a fuel's ignition quality, though their effectiveness may depend on the composition of the base fuel. The incremental effect of increasing amounts of ignition-accelerating additives on cetane number decreases?' Usually, the ignition delay obtained with cetane improved blends are found to be equivalent to those obtained with natural diesel fuels of the same cetane number. Two potential practical uses for ignition accelerators are in upgrading the ignition characteristics of poorer quality diesel fuel and (in much larger amounts) making possible the use of alcohols in compression-ignitionengines.
The physical characteristics of diesel fuel do not significantly affect the ignition delay in fully or partially warmed-up engines.
Tests with fuels of different front-end volatility (over the cetane number range 38 to 53), and with substantially different front-end ignition quality for the same average cetane number, showed no discernible differences. Fuel viscosity variations over a factor of 2.5 were also tested and showed no significant effect.48 Thus, in p,warmed-up engine, variations in fuel atomization, spray penetration, and vaporization rate over reasonable ranges do not appear to influence the duration of the delay period significantly (see also Sec. 10.5.6 on fuel vaporization). 10.6.6 Correlations for Ignition Delay in Engines Many correlations have been proposed for predicting ignition delay as a function of engine and air charge variables. These usually have the form of Eq. (10.35) and have been based on data from more fundamental experiments in combustion bombs and flow reactors. An important factor in assessing the appropriateness of any correlation is how it is to be used to predict the magnitude of the delay.
If an equation for predicting the complete delay process (including all the physical and chemical processes from injection to combustion) is required, then the data show that such a simple form for the equation is unlikely to be adequate for the full range of engine conditions (see Table 10.4). However, if a model for the autoignition process of a premixed fuel-air mixture during the delay period is required, for use in conjunction with models for the physical processes of fuel evaporation and fuel-air mixing, then correlations such as those listed in Table 10.3 may be sufficiently accurate. An empirical formula, developed by Hardenberg and H a s P for predicting the duration of the ignition delay period in DI engines, has been shown to give good

"Disintegrating Process and Spray Characterization Fuel Jet Injected by a Diesel Nozzle," SAE paper 840275, SAE Trans., vol. 93,1984. 19. Kamimoto, T., Kobayashi, H., and Matsuoka, S.: "A Big Size Rapid Compression Machine Fundamental Studies of Diesel Combustion," SAE paper 811004, SAE Trans., vol. 90,1981. 20. Balles, E.: " Fuel-Air Mixing and Diesel Combustion in a Rapid Compression Machine," Ph. Thesis, Department of Mechanical Engineering, MIT, June 1987. 21. Browne, K. R., Partridge, I. M., and Greeves, G.: "Fuel Property Effects on FueljAir Mixing i an Experimental Diesel Engine," SAE paper 860223,1986. 22. Bracco, F. V.: "Modeling of Engine Sprays," SAE paper 850394,1985. 23. Kuo, T., and Bram, F.
V.: "Computations of Drop S h in Pulsating Sprays and of Liquid-Co no. 10, pp. 1730-1742,1982. 25. Reitz, R D., and Bracco, F. V.: "On the Dependence of Spray Angle and Other Spray Para eters on Nozzle Design and Operating Conditions," SAE paper 790494, 1979. 26. Wu, K.-J., S y C.-C., Steinberger, R. L., Santavicca, D.
A., and Bracco, F. V.: "Measurements Penetration," SAE paper 710571, SAE Trans., vol. 80,1971. 29. Hiroyasu, H., Kadota, T., and Arai, M.: "Supplementary Comments: ~ u e lSpray ~h ization in Diesel Engines," in James N. Mattavi and Charles A.
Amann (eds.), Combustion the Nozzle in Atomizing Liquid Jets," Phys. Fluids, vol. 29, no. 4, pp. 941-951, 1986. 31. Reitz, R. D., and Diwakar, R.: "Effect of Drop Breakup on Fuel Sprays," SAE paper 8 1986. 32. Hiroyasu, H., and Kadota, T.: "Fuel Droplet Size Distribution in Diesel Combustion Cham SAE paper 740715, SAE Trans., vol. 83,1974. 33. El Wakil, M. M., Myers, P. S., and Uyehara, 0. A.: "Fuel Vaporivltion and 1dtion Diesel Combustion," in Bwning a Wide Range of Fuels in Diesel Engines, SAE hogre Technol., vol. 11, pp. 30-44, SAE, 1967. COMBUSTION IN COMPRESSION-IGNITION ENGINES 565 Bornan, G. L., and Johnson, J. H.: "Unsteady Vaporization Histories and Trajectories of Fuel Drops Injected into Swirling Air," in Burning a Wide Range of Fuels in Diesel Engines, SAE Progress in Technology, vol. 11, pp.
13-29, SAE, 1967; also SAE paper 598C, 1962. Kamimoto, T., and Matsuoka, S.: "Prediction of Spray Evaporation in Reciprocating Engines," SAE paper 770413, SAE Trans., vol. 86,1977. , Kuo, T., Yu, R. C., and Shahed, S.
M.: "A Numerical Study of the Transient Evaporating Spray Mixing Process in the Diesel Environment," SAE paper 831735, SAE Trans., vol. 92,1983. . ASTM Method D613, Cetane Test Procedure. . Henein, N. A., and Fragoulis, A. N.: "Correlation between Physical Properties and Autoignition parameters of Alternate Fuels," SAE paper 850266, 1985.
9. ~ u f d e r0. , L., Glavincevski, B., and Burton, G. F.: "Ignition Quality Rating Methods for Diesel ota, T., and Hiroyasu, H.: "Spontaneous Ignition Delay of Fuel Sprays in High us Environments," Trans. Japan Soc. Mech. Engrs, vol. 41, no. 345, pp. 24-31, 3. ~padaccini, L. J., and TeVelde, J. A.: "Autoignition Characteristics of Aircraft-Type Fuels," Combust. Flame, vol. 46, pp. 283-300, 1982. 44. Plee, S. L., and Ahmad, T.: "Relative Roles of Premixed and Diffusion Burning in Diesel Combustion," SAE paper 831733, SAE Trans., vol. 92,1983. 45. stringer, F. W., Clarke, A. E., and Clarke, J.
S.: "The Spontaneous Ignition of Hydrocarbon Fuels in a Flowing System," Proc. lnstn Mech. Engrs, vol. 184, pt. 35, 1969-1970. 46. Wolfer, H.
H.: "Ignition Lag in Diesel Engines," VDI-Forschungsheft 392, 1938; Translated by Royal Aircraft Establishment, Farnborough Library No. 358, UDC 621436.047, August 1959.
47.
Lyn, W.-T., and Valdmanis, E.: "Effects of Physical Factors on Ignition Delay," SAE paper 48. Won& C. L., and Steere, D. E.: "The Effects of Diesel Fuel Properties and Engine Operating Conditions on Ignition Delay," SAE paper 821231, SAE Trans., vol.
91,1982. 49. Andm, A., and Pachernegg, S. J.: "Ignition Conditions in Diesel Engine" SAE paper 690253, SAE Trans., VOI.78, 1969. 50. Glavincevski, B., Gilder, 0.L, and Gardner, L.: "Cetane Number Estimation of Diesel Fuels from Carbon Type Structural Composition," SAE paper 841341, 1984. 1. Olree, R., and Lenane, D.: "Diesel Combustion Cetane Number Effects," SAE paper 840108, SAE Trans., vol. 93, 1984. and Hardenberg, H. 0.: "Ignition Improvers for Ethanol Fuels," SAE paper o., and Hase, F. W.: "An Empirical Formula for Computing the Pressure ~i~ Delay of a Fuel from its Cctane Number and from the Relevant Parameters of Direct-Injection Diesel Engines," SAE paper 790493, SAE Trans, vol. 88,1979. Dent, J.
C., and Mehta, P. S.: "Phenomenological Combustion Model for a Quiwcent Diesel Engine," SAE paper 811235, SAE Trans., vol. 90,1981. 5. Y-J., Kobayashi, H., Matsuzawa, K, and Kamimoto, T.: "A Photographic study of soot Formation and Combustion in a Diesel Flame with a Rapid Compression Machine," in Diagnostics and Modeling of Combustion in Reciprocating Engines, pp. 149-157, COMODIA 85, Proceedings of Symposium, Tokyo, Sept. 4-6,1985. 6. Lakshminara~an,P. A., and Dent, J. c.:"~nterferometricStudies of Vaporising and Combustion Sprays," SAE paper 830244, SAE Trans., vol. 92,1983. 7. Colella, K.J., E. N., Ekchian, J. A., C h a & W. K., and Heywood, J. B.: "A Rapid cornpression Machine Study of the Influence of Charge Temperature on Diesel Combustion;" SAE paper 870587,1987.
Monk C. J., and Dent, J. C.: "The Simulation of Air Fuel Mixing in High Swirl Open Chamber Died Engines," Proc. Instn Mech.
Engrs, vol. 190, no. 47/76, pp. 503-513, 1976. Rife, J., and Heywood, J. B.: "Photographic and Performance Studies of mesel ~ ~ ~with b ~ ~ t i 566 INTERNAL COMBUSTION ENGINE FUNDAMENTALS a Rapid Compression Machine," SAE paper 740948, SAE Trans., vol. 83,1974. 60. Whitehousc, N. D., Cough, E, and Jeje, A. B.: "The Study of Combustion in a Quiescent CHAPTER co bustion Chamber Diesel Engine," ASME paper 82-HT-35,1982. 61. Nightinple, D. R.: "A Fundamental Investigation into the Problem of NO Formation in Engines," SAE paper 750848, SAE Trans., vol. 84,1975. 62. Bennethum, J. E., Mattavi, J. N., and Toepel, R. R.: "Diesel Combustion Cha Hardware, Procedures, and Data Interpretation," SAE paper 75084%SAE Trans 63. Rhee, K . T., Myers, P. S., and Uyehara, 0. A.: " T i e - and ~ ~ a c g ~ e s o l v e d nation in Di-1 Combustion Using Continuous Flow Gas Sampling," SAE P Trans., vol. 87,1978. 64. Shipinsky, J, Uyehara, 0. A, and Myers, P. S.: "Experimental Correlation between Ratemo Injection and Ratt-of-Heat-Release in a Diesel Engine," ASME paper 6-P-11,1968. 65. Grigg, H. C., and Syed, M. H.: "The Problem of Predicting Rate of Heat Release in Di Engine," Proc. lnstn Mech. Engrs, V O ~ .184, pt. 3J, 1969-1970. 66. Whitehouse, N. D., Clough, E., and Way, J. B.: "The Effect of Changes in Design and Opera Conditions on Heat Release in Direct-Injection Diesel Engines," SAE paper 740085, 1974.
67. Meguerdichian, M., and Watson, N.: "Prediction of Mixture Formation and Heat Re1 D i e 1 Engines," SAE paper 780225,1978. 68. Kamimoto, T., Aoyagi Y, Matsui, Y., and Matsuoka, S.: "The Effects of Some Engine on Measured Rates of Air Entrainment and Heat Release in a DI Diesel Engine," S 8000253, SAE Trans., vol. 89,1980. 69.
Dent, J. c., Mehta, P. S., and Swan, J.: " A Predictive Model for Automotive DI Di Performance and Smoke Emissions," paper C126/82, presented at the International on Diesel Engines fir Passenger Cars and Light Duty Vehicles, Institution of Me& neers, London, England, Oct. 5-7, 1982. POLLUTANT FORMATION AND CONTROL NATURE AND EXTENT OF ark-ignition and diesel engines are a major source of urban air pollution. The k-ignition engine exhaust gases contain oxides of nitrogen (nitric oxide, NO, small amounts of nitrogen dioxide, NO,--collectively known as NOJ, on monoxide (CO), and organic compounds which are unburned or partially ed hydrocarbons (HC). The relative amounts depend on engine design and ating conditions but are of order: NO,, 500 to 1000 ppm or 20 g/kg fuel; 1 to 2 Percent or 200 g/kg fuel; and HC, 3000 ppm (as C,) or 25 g/kg fuel. on blowby gases, and fuel evaporation and release to the atmosphere through ents in the fuel tank and carburetor after engine shut-down, are also sources of ed hydrocarbons. However, in most modem engines these nonexhaust are effectively controlled by returning the blowby gases from the crankne intake system and by venting the fuel tank and carburetor float wl through a vapor-absorbing carbon cannister which is purged by some of intake air during normal engine operation.
In diesel engine exhaust, ons of NO, are comparable to those from SI engines. Diesel hydroon emissions are significant though exhaust concentrations are lower by ut a factor of 5 than typical SI engine levels. The hydrocarbons in the exhaust Y also condense to form white smoke during engine starting and warm-up. -7 Specific hydrocarbon compounds in the exhaust gases are the source of dies; odor. Diesel engines are an important source of particulate emissions; betwee about 0.2 and 0.5 percent of the fuel mass is emitted as small (-0.1 pm diameter particles which co&t primarily of soot with some additional absorbed hydro: carbon material. Diesel engines are not a sigmficant source of carbon mo Use of alcohol fuels in either of these engines substantially incre hyde emissions. While these are not yet subject to regulation, aldehyde a significant pollutant if these fuels were to be used in quantities c gasoline and diesel. Currently used fuels, gasoline and diesel, contain s oline in small amounts (5600ppm by weight S), diesel fuel in la (10.5 percent).
The sulphur is oxidized (or burned) to produce sulfur $SO_,$, of which a fraction can be oxidized to sulfur trioxide, $SO_,$, which c with water to form a sulfuric acid aerosol. In general, the concentrations of these pollutants in intern engine exhaust differ from values calculated assuming chemical equilibrium. the detailed chemical mechanisms by which these pollutants form an kinetics of these processes are important in determining emission 1 pollutant species, e.g., carbon monoxide, organic compounds, the formation and destruction reactions are intimately coupled with the fuel combustion process.
Thus an understanding of the formation of thes requires knowledge of the combustion chemistry. For nitrogen oxides oxides, the formation and destruction processes are not part of the fuel bustion vrocess.
However, the reactions which produce these species take pl an envirkmment created by the combustion reactions, so the two pr still intimately linked. A summary of the mechanisms by which the form in internal combustion engines provides an introduction to t subsequent sections, the details of the basic formation mechanisms of each pollutant-and the application of these mechanisms to the combustion process both spark-ignition and compression-ignition engines will be developed. The processes by which pollutants form within the cylinder of a co a1 spark-ignition engine are illustrated qualitatively in Fig. 11-1. The shows the combustion chamber during four different phases of the engme o ating cycle: compression, combustion, expansion, and exhaust. Nitric oxid forms throughout the high-temperature burned gases behind the flame th chemical reactions involving nitrogen and oxygen atoms and molecules, which not attain chemical equilibrium. The higher the burned gas temperatu higher the rate of formation of NO. As the burned gases cool during the ex sion stroke the reactions involving NO freeze, and leave NO concentrations far in excess of levels corresponding t o equilibrium at exhaust co monoxide also forms during the combustion process. With rich fuel-air there is insufficient oxygen to burn fully all the carbon in the fuel to COz; also, the high-temperature products, even with lean mixtures, dissociation ensur there are significant CO levels. Later, in the expansion stroke, the CO oxidat' process also freezes as the burned gas temperature falls. The unburned hydrocarbon emissions have several different sour - NO forms in high-tempemhue \ CO present at high temperature and if fuel rich burned gas Unburned mixture. forced into crevices (a) Compression (6) Combustion I1 Deposits desorb HC Entrainment of HC from wall into bulk gas HC iium crevices; some HC burns (d) Exhaust ollutant formation mechanisms i n a spark-ignition engine.
combustion, the increasing cylinder pressure forces nder into crevices, or narrow volumes, connected to the mbustion chamber : the volumes between the piston, rings, and cylinder wall e the largest of these. M8 ost of this gas is unburned fuel-air mixture; much of it 570 INTERNAL COMBUSTION ENGINE FUNDAMENTALS escapes the primary combustion process because the entrance to these cr too narrow for the flame to enter. This gas, which leaves these crevices the expansion and exhaust processes, is one source of unburned hydr emissions. Another possible source is the combustion chamber layer containing unburned and partially burned fuel-air mixture is left at when the flame is extinguished as it approaches the wall. While it has bee that the unburned HC in these thin (50.1 mm)layers burn up rapidly when combustion chamber walls are clean, it has also been shown that th deposits on the walls of engines in actual operation do increase engine HC e sions. A third source of unburned hydrocarbons is believed to be any engine left in a thin film on the cylinder wall, piston and perhaps on the cylinder h These oil layers can absorb and desorb fuel hydrocarbon components, before after combustion, respectively, thus permitting a fraction of the fuel to escape primary combustion process unburned. A final source of HC in engines plete combustion due to bulk quenching of the flame in that fraction of engine cycles where combustion is especially slow (see Sec. 9.4.3). Such conditi are most likely to occur during transient engine operation when the ai spark timing, and the fraction of the exhaust recycled for emis not be properly matched. The unburned hydrocarbons exit the cylinder by being entrained in bulk-gas flow during blowdown and at the end of the exhaust st piston pushes gas scraped off the wall out of the exhaust valv tion of the hydrocarbons which escape the primary combustion the above processes can occur during expansion and exh oxidation depends on the temperature and oxygen concentration time histori these HC as they mix with the bulk gases. One of the most important variables in determining spa emissions is the fuellair equivalence ratio, 4. Figure 11-2 shows qu NO, CO, and HC exhaust emissions vary with this parameter. The engine has normally been operated close to stoichiometric, ensure smooth and reliable operation. Figure 11-2 shows th give lower emissions until the combustion quality becomes poor misfire occurs), when HC emissions rise sharply and engine operation erratic. The shapes of these curves indicate the complexities of emission In a cold engine, when fuel vaporization is slow, the fuel flow provide an easily combustible fuel-rich mixture in the cylinder. engine warms up and this enrichment is removed, CO and HC emissions high. At part-load conditions, lean mixtures could be used which lower HC and CO emissions (at least until the combustion q and moderate NO emissions. Use of recycled exhaust to dilute t mixture lowers the NO levels, but also deteriorates comb gas recirculation (EGR) is used with stoichiometric mixtu control systems.
Note that the highest power levels are obtained with slightly rich-of-stoichiometric mixtures and no recycled exh incoming charge. As we will see, several emission control techniques are Wuir 3 Fuellair equivalence ratio FIGURE 11-2 Variation of HC,CO, and NO concentration in the exhaust of a conventional spa&-ignition engine with fuellair equivalence ratio. to reduce emissions of all three pollutants, over all engine operating modes, and achieve acceptable average levels. In the diesel engine, the fuel is injected into the cylinder just before cornbustion starts, so throughout most of the critical parts of the cycle the fuel distibution is nonuniform. The pollutant formation processes are strongly dependent on the fuel distribution and how that distribution changes with time due mixing. Figure 11-3 illustrates how various parts of the fuel jet and the flame affect the formation of NO, unburned HC, and soot (or particulates) during d " phases of diesel combustion in a directde forms in the high-temperature burned s regions as before, but temperature and fuellair ratio distributions within the urned gases are now nonuniform and formation rates are highest in the close- ~ ~of ~t~i~i~~ tO-stoichiometricregions. Soot forms in the rich ~ n b u r n e d - f ~ ~ l core the fuel sprays, within the flame region, where the fuel vapor is heated by with hot burned gases. Soot then oxidizes in the flame zone when it contacts llburned oxygen, giving rise to the yellow luminous character of the flame. Hydrocarbons and aldehydes originate in regions where the flame quenches both On the walls and where excessive dilution with air prevents the combustion mpletion. Fuel that vaporizes from the s of combustion is also a source of HC. d by the early part of the combustion mediately following the ignition-delay POLLUTANT FORMATION AND CONTROL Lean flme-out region: HC \ / Initial rapid combustion: noise 573 Rate constants for NO formation mechanism1 Fuel jet mixing with air: rich mixture + (1) 0 N, + NO + N (-~)N+No+N,+o + 0,+ N O + o (-2) 0 + NO + 0, + N (3) N + OH +NO + H (-3) H + NO + OH + N (2) N Premixed Rate constant, cm3/mol.s Temperature nnge, K Uncertainty, factor of or % 7.6 x loi3 exp [-38,000/TJ 1.6x10i3 2000-5000 300-5000 2 6.4 x lo9 T exp [- ~ I S O / T ~ 300-3000 1.5 x 10' T exp [-19,50O/Tj 1000-3000 4.1 x lo1= 2.0 x loi4 exp [-23,65O/T] 300-2500 22004500 20% at 300 K 2 at 2000-5000 K *30% 3m-1500 K 2 at 3000 K f 30% at 1000 K 2at3000K *80% 2 Flame on wal FIGURE 113 Summary of pollutant fo mechanisms in a direct-i controlled" combustion W i g controlled 11.2 NITROGEN OXIDES 11.21 Kinetics of NO Formation While nitric oxide (NO) and nitrogen dioxide (NO,) a as NO, emissions, nitric oxide is the predominant inside the engine cylinder. The principal source of NO is the oxidation spheric (molecular) nitrogen.
However, if the fuel the oxidation of the fuel nitrogen-~ontainingCOmpO of NO. Gasolines contain negligible amounts of nitrogen; although d contain more nitrogen, current levels are not significant. The mechanism of N O formation from atmospheric nitrogen has studied extensively.' It is generally accepted that in combustion of stoichiometrjc fuel-& mixtures the principal reactions governing the of NO from molecular nitrogen (and its destruction) are? The forward and reverse rate constants (k: and k;, respectively) for these reactions have been measured in numerous experimental studies. Recommended values for these rate constants taken from a critical review of this published data are given in Table 11.1. Note that the equilibrium constant for each reaction, Kc,i (see Sec. 3.7.2), is related to the forward and reverse rate constants by Kc,i = k:/k;. The rate of formation of NO via reactions (11.1) to (11.3) is given by [see Eqs. (3.55) and (3.58)] 2] N+OH=NO+H called the extended Zeldovich mechanism. Zeldovichl was the first to suggest importance of reactions (11.1) and (11.2). Lavoie et al.' added reaction (11.3) to the mechanism; d m contribute significantly. MCOH] k, mO][O] - k;mO][H] (11.4) where [1 denote species concentrations in moles per cubic centimeter when ki have the values given in Table 11.1. The forward rate constant for reaction (11.1) and the reverse rate Constants for reactions (11.2) and (1 1.3) have large activation energies which results in a strong temperature dependence of NO formation - k;mOIml- A similiar relation to (1 1.4) can be written for d[N]/dt: 21 - k:PJl[02] - k$m][OH] -k;mOIM O+N,=NO+N N+02=NO+0 + k: + k ; w m O] + k;pJO][H] (11.5) Since N is much less than the concentrations of other species of interest (-lo-' mole fraction), the steady-state approximation is appropriate: d[a/dt is set equal to zero and Eq. (1 1.5) used to eliminate N. The NO formation rate 1 - mo12/(KCo21CN21) 1 + k; CNOl/(k: [O2]+ k: [OH]) + hi^ is here K = (k:/k;)(k:/k;). (11.6) 574 INTERNAL C O M B O N E POLLUTANT FORMATION AND CONTROL N FUNDAMENTALS TABLE 11.2 Typical values of R,, R1/R2, and Rll(R2 575 + R3)t Equivalence ratio Rd RJRz RiI(Rz 0.8 1O . 1.2 5.8 x 2.8 x lo-' 7.6 x 1.2 2.5 9.1 0.33 0.26 0.14 +Rd t At 10 atm pressure and 2600 K. $ Units gmol/cm3~s.
NO forms in both the flame front and the postflame gases. In engines however, combustion occurs at high pressure so the flame reaction zo extremely thin (-0.1 mm) and residence time within this zone is short. Als cylinder pressure rises during most of the combustion process, so burned produced early in the combustion process are compressed to a higher perature than they reached immediately after combustion.
Thus, NO fo in the postflame gases almost always dominates any flame-front-produce is, therefore, appropriate to assume that the combustion and NO formation p cesses are decoupled and to approximate the concentrations of 0, O,, OH, and N, by their equilibrium values at the local pressure and equilibrium temperature. TO introduce this equilibrium assumption it is convenient to use the notation R, = k:[O],CN,], = k;CNO],N,, where [1, denotes equilibrium concentration, for the one-way equilibrium rate for reaction (11.1), with similiar definitions for R, = k:CNIe[O21.
= k~CNOI,COI, and R3 = k:Ne[Ofle = k;CNO],[H], . Substituting [Ole, [O,],, [OH],, and CNzI, for [Ol, [O,], [OH], [HI, and CN,] in Eq. (11.6) yields [a,, dm01-dt 2R1{1 - (CN01/CN01e)2) 1 + (CNOIICNOle)RII(R~+ R3) Typical values of R,, RJR, and Rl/(R2 + R3) are given in able 11.2. The difierence between R,/R, and R,/(R, + R3) indicates the relative importance of adding reaction (11.3) to the mechanism. The strong temperature dependence of the NO formation rate can be 4], demonstrated by considering the initial value of dCNO]/dt when ~ 0] / ~ 0 1. Then, from Eq. (11.7), -dCNol dt - 2Rl = 2k:[o].CN J.
The equilibrium oxygen atom concentration is given by Cole = K 0 COzlt'z ;Rnl/2 FIGURE 11-4 Initial NO formation rate, mass fraction per second (for mOl/CNOl, 4 I), as a function of temperature for different equivalence ratios (4)and 15 atm pressure.
Dashed line shows adiabatic flame tmperature for kerosene combustion with 700 K, 15 atm air.= where K,(,, is the equilibrium constant for the reaction 30, = 0 (-'f") KHo, = 3.6 x lo3 exp -- atmli2 (11.10) The initial NO formation rate may then be written [combining Eqs. (11.8), (11.9), and (11.10) with k: from Table 11.11 as dB01 6 x 1016 - 69,090 exp (~) ~ o ~ I ~ ~ c N mol/cm3. , I . s (11.11) The strong dependence of dPJO]/dt on temperature in the exponential term is evident. High temperatures and high oxygen concentrations result in high NO formation rates. Figure 11-4 shows the NO formation rate as a function of gas temperature and fuellair equivalence ratio in postflame gases. Also shown is the adiabatic flame temperature attained by a fuel-air mixture initially at 700 K at a constant pressure of 15 atm. For adiabatic constant-pressure combustion (an appropriate model for each element of fuel that burns in an engine), this initial NO formation rate peaks at the stoichiometric composition, and decreases rapidly as the mixture becomes leaner or richer. A characteristic time for the NO formation process, , ,T can be defined by -=- z& 1 dl301 ; , l CNoIe dt (11.12) 578 INTERNAL COMBUSTION ENOME FUNDAMENTALS 6000-I I I I 1 l l POLLUTANT FORMATION AND CONTROL I SI engine I I (I I 579 1.0 -80 // 11 12 I I I I I 0 13 14 15 16 17 18 19 Airlfuel ratio (a) FIGURE 116 (a) NO and NO, concentrations in SI engine exhaust as function of air/fuel ratio, 1500 rev/min, wide-open throttle; (b) NO, as percent of total NO, in diesel exhaust as function of load and speed.' Figure 11-6 shows examples of NO and NO, emissions data from a sparkignition and a diesel engine. The maximum value for the ratio (NO,/NO) for the SI engine is 2 percent, at an equivalence ratio of about 0.85. For the diesel this ratio is higher, and is highest at light load and depends on engine speed. It is customary to measure total oxides of nitrogen emissions, NO pl NO,, with a chemiluminescence analyzer and call the combination NO,. It always important to check carefully wheth given in terms of mass of NO or mass of N 30 and 46, respectively. 11.2.3 NO Formation in Spark-Ignition Engines In conventional spark-ignition engines the fuel and air (and any recycled exha are mixed together in the engine intake system, and vigorous mixing with residual gas within the cylinder occurs dur air ratio and the amount of diluent (resid approximately uniform throughout the ch bustion.? Since the composition is essentially uniform, the nature of the NO mation process within the cylinder can be understood by coupling the kine mechanism developed in Sec. 11.2.1 with the burned gas temperature distributio and pressure in the cylinder during the combustion and expansion processes. Th t It is well known that the mixture composition within the cylinder is not completely uniform varies from one cycle to the next Both these factors contribute to cycle-by-cycle combustion v tions. For the present discussion,the assumption of mixture uniformity is adequate. Crank angle, deg FIGURE 11-7 Illustration of SI engine NO formation model: (a) measured cylinder pressure p and calculated mass fraction burned x,; (b) calculated temperature of unburned gas T, and burned gas T, in early- and lateburning elements; (c) calculated NO concentrations in early- and late-burning elements for ratecontrolled model and at equilibrium.' temperature distribution which develops in the burned gases due to the passage of the flame across the combustion chamber has been discussed in Sec.
9.2.1. Mixture which burns early is compressed to higher temperatures after combustion, as the cylinder pressure continues to rise; mixture which bums later is compressed primarily as unburned mixture and ends up after combustion at a lower burned gas temperature. Figure 11-7a and b shows measured cylinder pressure data from an operating engine, with estimates of the mass fraction burned (x,) and the temperatures of a gas element which burned at the end of the burning process. The model used to estimate these temperatures assumed no mixing between mixture elements which burn at different times. This assumption is more realistic than the 580 INTERNAL COMBUSTION ENGINE F U ~ A M E N T A L S POLLUTANT FORMATION AND CONTROL alternative idealization that the burned gases mix rapidly and are thus uniform (see Sec. 9.2.1). If the NO formation kinetic model [Eq. (11.7)] is used to calculate NO concentrations in these burned gas elements, using the equilibrium concen. trations of the species 0 , 0,, N,, OH, and H corres~ondingto the average fuellair equivalence ratio and burned gas fraction of the mixture and these pressure and temperature profiles, the rate-limited concentration profiles in Fig. 11-7c are obtained. Also shown are the NO concentrations that would correspond to chemical equilibrium at these conditions. The rate-controlled concentrations rise from the residual gas NO concentration, lagging the equilibrium levels, then cross the equilibrium levels and "freeze " well above the equilibrium values corresponding to exhaust conditions. Depending on details of engine operating conditions, the rate-limited concentrations may or may not come close to equilibrium levels at peak cylinder pressure and gas temperature. Also, the amount of decomposition from peak NO levels which occurs during expansion depends on engine as well as whether the mixture element burned early or late.' Once the NO chemistry has frozen during the early part of the expansion stroke, integration over all elements will give the final average NO concentration in the cylinder which equals the exhaust concentration. Thus, if {NO} is the local mass fraction of NO, then the average exhaust NO mass fraction is given by 1 {W} = {NO) o dxb where {NO} is the final frozen NO mass fraction in the element of charge which burned when the mass fraction burned was xb. Note that {NO} = ~ O I M N ~ P , where M,, = 30, the molecular weight of NO. The average exhaust Concentration of NO as a mole fraction is given by - Mcxh x lo6. The earlier burning fratand the exhaust concentration in ppm is tions of the charge contribute much more to the exhausted NO than do later burning fractions of the charge: frozen NO concentrations in these early-burning elements can be an order of magnitude higher than concentrations in lateburning elements. In the absence of vigorous bulk gas motion, the highest No concentrations occur nearest the spark plug. Substantial experimental evidence supports this description of NO formation in spark-ignition engines. The NO concentration gradient across the burned gas in the engine cylinder, due to the temperature gradient, has been &monstrated using gas sampling techniquess. and using measurements of the chemiluminescent radiation from the reaction NO 0 + NO, + hv to determine the local NO concentration.
Figure 11-8 shows NO concentration data as a function of crank angle, taken by ~ a v o i e through '~ two different windows in the cylinder head of a specially constructed Ghead engine where each window was a different distance from the spark plug. The stars indicate the estimated initial NO concentration that results from mixing of the residual gas with the fresh charge, at the + I - _ I I I I I I Experiment W2 0 Experiment W3 ---Kinetic solutions * I*- -7 - ,' - d = 0.9 ~ o -20 - ~ oCrank angle, 20 40 deg 31 ~ ~ 60 FIGURE 11-8 Swctrosco~ically measured NO concentrations through two windows W3 and W, in special L-head SI engine (W, is closer to spark than w3). The asterisks mark estimated initial conditions and flame arrival times. The dashed lines are calculated ratelimited of I ~ I ~ concentrations I ~ for parts I charge burning at these flame arrival times with zero initial NO concentration.1•‹ time of arrival of the flame at each window. The observed NO mole fractions rise smoothly from these initial values and then freeze about one-third of the way through the expansion process. NO levels observed at window W,, closest to the spark plu& were substantially higher than those observed at window w,. The dashed lines show calculated NO concentrations obtained using the NO formation kinetic model with an "unmixed" thermodynamic analysis for elements that burned at the time of flame arrival at each window.
Since the calculated values started from zero NO con~entrationat the flame front (and not the diluted residual gas NO level indicated by the star), the calculations initially fall below the data- However, the differencebetween the two measurement locations and the frozen levels are predicted with reasonable accuracy. Thus, the rate-limited formation Process, freezing of NO chemistry during expansion, and the existence of NO concentration gradients across the combustion chamber have all been The most important engine variables that affect NO emissions are the fuel/ air equivalence ratio, the burned gas fraction of the in-cylinder unburned mixture, and spark timing. The burned gas fraction depends on the amount of &luent such as recycled exhaust gas (EGR) used for NO, emissions control, as well as the residual gas fraction. Fuel properties will affect burned gas conditions; the effect of m X I d variations in gasoline properties is modest, however. The effect of variahons in these parameters can be explained with the NO formation mechani~mdescribed above: changes in the time history of temperature and oxygen concentration in the burned gases during the combustion process and early part of the expansion stroke are the important factors." 'Qun*mNc~RATIO. Figure 11-9 show the effect of variations in the fuellair equivalence ratio on NO emissions.
Maximum burned gas temperatures occur at 582 POLLUTANT FORMATION AND CONTROL INTERNAL C O M B U ~ O NE N G ~ EFUNDAMENTALS . 0~14 ' 16 18 " 4 F FIGURE 1 1 3 Variation of exhaust NO concentration with AIF and fuellair equivalence ratio. Spark-ignition engine, 1600 rev/min, q, = 50 percent, MBT timing." EGR, % 583 FIGURE 11-10 Variation of exhaust NO concentration with percent recycled exhaust gas (EGR). Spark-ignition engine, 1600 revlmin, q, = 50 percent, MBT timing.'' 4 -, 1.1; however, at this equivalence ratio oxygen concentrations are low. As the mixture is enriched, burned gas temperatures fall.
As the mixture is leaned out, increasing oxygen concentration initially offsets the falling gas temperatures and NO emissions peak at 4 -,0.9. Detailed predictions of N O concentrations in the burned gases suggest that the concentration versus time histories under fuel-lean conditions are different in character from those for fuel-rich conditions. In lean mixtures NO concentrations freeze early in the expansion process and little NO decomposition occurs. In rich mixtures, substantial NO decomposition occurs from the peak concentrations present when the cylinder pressure is a maximum. Thus in lean mixtures, gas conditions at the time of peak pressure are especially significant.' heat capacity of the cylinder charge, per unit mass of fuel. Figure 11-11 shows the effect of different diluent gases added to the engine intake flow, in a singlecylinder engine operated at constant speed, fuel flow, and air flow.13~h~ data in Fig.
l-lla show that equal ~0lumepercentages of the different diluents produce differentr~ductionsin NO emissions. The same data when plotted against diluent heat capacity (diluent mass flow rate x specific heat, c,) collapse to a single BURNED GAS F~ACTION.The unburned mixture in the cylinder contains fu vapor, air, and burned gases. The burned gases are residual gas cycle and any exhaust gas recycled to the intake for NO, emis residual gas fraction is influenced by load, valve timing (especially the extent valve overlap), and, to a lesser degree, by speed, airffuel r ratio as described in Set. 6.4. The burned gases act as a dil mixture; the absolute temperature reached after combustion varies the burned gas mass fraction. Hence increasing the burned gas fr N O emissions levels. However, it also reduces the combustion rate makes stable combustion more difficult to achieve (see Secs. 9.3 and 9.4). Figure 11-10 shows the effect of increasing the burned gas fraction by cling exhaust gases to the intake system just below the throttle plate. Subst reductions in NO concentrations are achieved with 15 to 25 perce is about the maximum amount of EGR the engine will t0ler part-throttle conditions. Of course, increasing the EGR at fixed engine lo speed increases the inlet manifold pressure, while fuel flow and air flow approximately constant. The primary effect of the burned gas diluent in the unburned mixture on t NO formation process is that it reduces flame temperatures by increasing t 0 0.2 Diuent in intake mixture, 96 vol (4) 0.4 0.6 Ar 0.8 1.0 Diluent heat capacity iwp, JK.
(b) ass NO emissions with various diuents. (b)correlation o f ~ .
reduction with dihent heat capacity. Spark-ignition engine operated at 1600 revlmin, brake load (intakePressure -0.5 atm), with MBT spark timing,'J 584 INTERNAL COMBUSTION ENGINE FUNDAMENTALS A similiar study where the burned gas fraction in the ~ d ~ r n char ed was varied by changing the valve overlap, compression ratio, and EGR, se ately, showed that, under more realistic engine operating conditions, capacity of the total fluent mass in the in-cylinder mixture that Whether the diluent mass is changed by varying the valve overlap, the compression ratio is not important.14 EXCESS AIR AND EGR Because of the above, it is possible to correlate the influ- ence of engine operating variables (such as airlfuel ratio, engine speed, and load) and design variables (such as valve timing and compression ratio) on NO emissions with two parameters which define the in-cylinder mixture composition: the fuellair equivalence ratio (often the airlfuel ratio is used instead) and the w/fuel ratio. The gas/fuel ratio (GIF) is given by G - total mass in cylinder = " (1 + ~) F fuel mass in cylinder F 1 - x, where xb is the burned gas fraction [Eq. (4.311.
These together ckfine the relative proportions of fuel, air, and burned gases in the in-cylinder mixture, and hence Oaslfuel ratio FIGURE 11-12 Correlation between gasjfuel ratio (G/F')and i d cated specific NO, emissions at various aidfuel ratios (AIF) and volumetric efficiencies (q,,). Sparkignition engine operated at 1400 revlrnin with spark timing retarded to give 0.95 of maximum brake torque,' t someof the scatter in Fig. 11-11 is due to the fact that the residual gas fraction is slightly for each diluent. POLLUTANT FORMATION AND CONTROL 9 5 correlate NO emissions.? Figure 11-12 shows the correlation of specific NO from a fourcylinder engine, over a wide range of engine operating ~onditionswith the airlfuel ratio and gaslfuel ratio. Lines of constant air/fuel and volumetric efficiency are shown; the direction of increasing dilution with residual gas and EGR at constant air/fuel ratio is to the right. Excessive dilution results in poor combustion quality, partial burning, and, eventually, misfire (see Sec. 9.4.3).
Lowest NO emissions consistent with good fuel consumption (avoiding the use of rich mixtures) are obtained with a stoichiometric mixture, with as much dilution as the engine will tolerate without excessive detenoration in combustion quality.15 Comparisons between predictions made with the NO formation model (described at the beginning of this section) and experimental data show good agreement with normal amounts of dilution.16 With extreme dilution, at NO levels of about 100 ppm or less, the NO formed within the flame reaction zone cannot, apparently, be neglected. Within the flame, the concentrations of radicals such as 0 , OH, and H can be substantially in excess of equilibrium levels, resulting in much higher formation rates within the flame than in the postflame gases. It is believed that the mechanism [reactions (11.1) to (11.311 and the formation rate equation (1 1.6) are valid. However, neglecting flame-front-formed NO is no longer an appropriate assumption.17 SPARK TIMING. Spark timing significantly affects NO emission levels. Advancing the timing so that combustion occurs earlier in the cycle increases the peak cylinder pressure (because more fuel is burned before TC and the peak pressure moves closer to TC where the cylinder volume is smaller); retarding the timing decreases the peak cylinder pressure (because more of the fuel burns after TC). Higher peak cylinder pressures result in higher peak burned gas temperatures, and hence higher NO formation rates. For lower peak cylinder pressures, lower NO formation rates result. Figure 11-13 shows typical NO emission data for a spark-ignition engine as a function of spark timing. NO emission levels steadily decrease as spark timing is retarded from MBT timing and moved closer to TC. Since exact determination of MBT timing is difficult (and not critical for fuel consumption and power where the variation with timing around MBT is modest), there is always considerable uncertainty in NO emissions at MBT timing. Often, therefore, an alternative reference timing is used, where spark is retarded from MBT timing to the point where torque is decreased by 1 or 2 percent from the maximum value. Great care with spark timing is necessary to obtain accurate NO emissions measurements under MBT-timing operating con- t Spark timing also affects NO emissions, as discussed next. The above discussion relates to engines run with timing at M

benzenes Ortho- and pamadialkyl benzenes Cyclic paraff~ns 2 Ethylene Meta-dialkyl benzenes Aldehydes 5 1-olefins (except ethylene) Diolefins Tri- and tetraalkyl benzenes 10 Internally bonded olefins 30 Internally bonded olefins with substitution at the double bond Cycloolefins hin the flame. Quenching of the flame occurs under several trical configurations: the flame may be propagating normal to, or at an angle to the wall; the flame may quench at the entrance to a thin volume with a narrow entrance to the combustion chamber such tween the piston crown and the cylinder wall. When the flame bon emissions depends on the extent can subsequently be oxidized.) hing processes are analyzed by relating the heat release within t loss to the walls under conditions where quenching just a Peclet number (Pe), is approximately constant for any given etrical configuration. The simplest configuration for study is the two-plate ch process, where the minimum spacing between two parallel plates through ch a flame will propagate is determined.

The Peclet number for this two-plate figuration is given by: 100 t General Motors Reactivity Scale (0-100). Based on the NO, formation rate for the hydrocarbon relative to the NO, fonnation rate for 2,3dimethyl-2-benzene?' in the fuel, indicating that significant pyrolysis and synthesis occur during the combustion process. Oxygenates are present in engine exhaust, and are known to partici the formation of photochemical smog. Some oxygenates are also irrita odorants. The oxygenates are generally categorized as carbonyls, phen other noncarbonyls. The carbonyls of interest are low molecular weight hydes and aliphatic ketones. The volatile aldehydes are eye and res irritants. Formaldehyde is a major component (5 2 0 percent of total Carbonyls account for about 10 percent of the HC emissions fro senger car engines, but only a few percent of spark-ignition engine Phenols are odorants and irritants: levels are much lower than alde Other noncarbonyls include methanol, ethanol, nitromethane, met Whether these are significant with conventional hydrocarbon fuels is unclear Use of alcohol fuels increases oxygenate emissions. Both methanol and aldehy emissions increase substantially above gasoline-fueled levels with methanol-fuel spark-ignition engines. hich is approximately constant over a wide range of conditions. p, S,, c,, T , k are the density, laminar flame speed, specific heat at constant pressure, gas onductivity, respectively, with the subscripts u and f ed and flame conditions. d,, is the two-plate quench distance. re and unburned gas temperature are assumed to be equal; ropriate in the engine context since there is ample stroke for a thermal boundary layer to build up to a al correlations for two-plate quenchnly limited data for liquid hydrocarbon els such as isooctane are available. The data in the pressure range 3 to 40 atm where P is the pressure in atmospheres and 4 is the fuel/& equivalence ratio. The two-plate quench distance d,, is then obtained from Eq. (11.27) and Prandtl number and viscosity relations for the flame conditions (see Sec. 4.8 or Ref. 36). ize crevice region into which a flame will propagate can be For the process of a flame front quenching on a single wall, there are many ssible geometries. The simplest is where the flame front is parallel to the wall 600 INTERNAL COMBUSTION ENGINE FUNDAMENTALS and approaches it head on. The one-wall quench distance d,,, defined as position of closest approach of the reaction zone to the wall, scales with fl properties in a similar way to the two-plate quench distance. Thus, a one. Peclet number relation can be formed: where the subscript u denotes properties evaluated at unburned gas conditio Using the wall temperature as representative of the unburned gas perature (because the thermal boundary-layer thickness is greater than t quench distances), Lavoie showed that Pe 4 2 Pe2 is a reasonable fit to the single-wall quench data. Typical two-wall quench d A = -_L = 0.2 are, therefore, in the range 0.04 to 0.2 mm. While a fraction of the fuel hydrocarbons can escape the bustion process unburned or only partially reacted, oxidation of hydrocarbons can occur during the expansion and exhaust processes. H bon oxidation rates have been determined in a number of different stu several different empirical correlations of the data in the form of overall rea rate equations have been proposed. A reasonable fit to the experimental data unburned HC burnup is the rate expression? , and jt,, where [1 denotes concentration in moles per cubic centimeter,, % the mole fractions of HC and O , , respectively, t is in seconds, T in kelvins, the density term (p/RT)has units of moles per cubic centimeter. The the data about this equation is substantial, however. Studies of combustion of premixed fuel-air mixtures at high p closed vessels or bombs have been useful in identifying the mechanism hydrocarbons escape complete combustion. The residual unburned hy left in the bomb following a combustion experiment have been shown to primarily from crevices in the bomb walls. Unburned HC levels w a1 to total crevice volume, and decreased to very low values (- 10 p the crevices were filled with solid material. Thus wall quench h apparently diffuse into the burned gases and oxidize following the quen event.37 Analytical studies of the flame quenching process, and ~ o s t ~ u e n c h sion and oxidation with kinetic models of the hydrocarbon oxidatio in agreement with these bomb data.38 Flame quenching can be thought of two-stage process. The first step is the extinction of the flame at a short dist from the cold wall, determined by a balance between thermal conduction of POLLUTANT FORMATION AND CONTROL 601 hot reaction zone to the wall and heat released in the reaction zone by flame reactions. The second step is the postquench diffusion and oxidation time scale of one or a few milliseconds after quenching. The diffuxidation process ultimately reduces the mass of wall quench hydrocarens to several orders of magnitude below its value at the time of quenching. Closed-vessel combustion experiments have also been used to show that oil layers on the walls of the bomb cause an increase in residual unburned HC levels after combustion is complete. The additional HC that result in experiments with oil films present are primarily (> 95 percent) fuel molecules, and are directly proprtional to the amount of oil placed on the walls of the reactor and the solubility of the specific fuel in the oil. These results show that absorption of fuel in the oil occurs prior to ignition. This dissolved fuel is then desorbed into the burned gases well after combustion is complete. Thus fuel absorption into and from any oil layers is a potentially important engine HC mecha- C Emissions from Spark-Ignition Unburned hydrocarbon levels in the exhaust of a spark-ignition engine under normal operating conditions are typically in the range 1000 to 3000 ppm C,. This corresponds to between about 1 and 23 percent of the fuel flow into the engine; the engine combustion efficiency is high. As indicated in Fig. 11-2, HC emissions rise rapidly as the mixture becomes substantially richer than stoichiometric. When combustion quality deteriorates, e.g., with very lean mixtures, HC emissions can rise rapidly due to incomplete combustion or misfire in a fraction of the engine's operating cycles. As outlined in Sec. 11.1, there are several mechanisms that contribute to total HC emissions. Also, any HC escaping the primary combustion process may oxidize in the expansion and exhaust processes. While a complete description of the HC emissions process cannot yet be given, there are sufficientfundamental data available to indicate which mechanisms are likely to be most important, and thus how major engine variables influence HC emission Four possible HC emissions formation mechanisms for spark-ignition where the fuel-air mixture is essentially premixed) have been proposed: ame quenching at the combustion chamber walls, leaving a layer of rned fuel-air mixture adjacent to the wall; (2) the filling of crevice volumes urned mixture which, since the flame quenches at the crevice entrance, he primary combustion process; (3) absorption of fuel vapor into oil e cylinder wall during intake and compression, followed by desorpapor into the cylinder during expansion and exhaust; (4) incomplete combustion in a fraction of the engine's operating cycles (either partial burning ete misfire), occurring when combustion quality is poor (e.g., during nts when AIF, EGR, and spark timing may not be adequately). In addition, as deposits build up on the combustion chamber walls, 602 4 INTERNAL COMBUSTION ENGINE FUNDAMENTALS 1 20 LI 340 Crank angle, deg 0 380 g i FIGURE 11-24 Variation in HC concentration and HC mass flow rate at the exhaust valve during the exhaust process.

SI engine operating at 1200 revlmin and 4 = 1.2, unthrottled* HC emissions increase. Whether the deposits constitute an additional mechanis or merely modify one of the above mechanisms is unclear. All these processes (except misfire) result in unburned hydrocarbons clo to the combustion chamber walls, and not in the bulk of the cylinder gases. Thus, the distribution of HC in the exhaust gases would not be expected to be uniform Experiments have been done to determine the unburned HC concentration dis tribution in the exhaust port during the exhaust process to provide insight into the details of the formation mechanisms. Gas concentrations were measured wit a rapid-acting sampling valve placed at the exhaust port exit. Figure 11-24 sho results from these time-resolved HC concentration measurements. HC concent tions vary significantly during the exhaust process. Gas which remains in the ~xhaust -.------ - nort r - - - between exhaust vulses has a high HC concentration, so techniques where air or nitrogen was bled into the exhaust port wer The displace this high HC gas while the exhaust valve was closed.

.. . concentration in the blowdown exhaust gases is clearly discernible, as is the rise in HC concentration toward the end of the exhaust stroke. The cylinde HC concentrations were then multiplied by the instantaneous exhaust gas flow rate to obtain the instantaneous HC mass emission rate from the cy throughout the exhaust process, also shown in Fig. 11-24. The unburned HC exhausted in two peaks of approximately equal mass: the first of these coinci with the exhaust blowdown mass flow pulse (which removes the majority of m cvlinder): .. c -s from -- - -- the . ,- the second occurs toward the end of the exhau; where HC concentrations are very high and the mass flow rate is relatively low. Other experiments have confirmed these observations?1 Clearly, mixing - - rned HC with the bulk cylinder gases occurs during expansion and/or the ust blowdown process. Then, the final stages of piston motion during the aust stroke push most of the remaining fraction of the cylinder mass with its h HC concentration into the exhaust.

This would be expected to leave a high ation of HC in the residual gas in the cylinder. Experiments conducted the valve mechanism of a single-cylinder engine was arranged to disenng operation and trap residual gases in the cylinder confirm this. For one set of typical engine operating conditions, approximately one-third of the hydrocarbons left unburned in an engine combustion event was retained in the cylinderand re~ycled.~' FLAME QUENCHING AT THE WALLS. The existence of quench layers on the combustion chamber walls of a spark-ignition engine was shown photopphically by Photographs of the flame region immediately after flame arrival at the wall through a window in the cylinder head showed a thin nonradiating layer adjacent to the wall. The quench layer thicknesses measured were in the range 0.05 to 0.4 mm (thinnest at high load), in rough agreement with predictions based on experiments in combustion bombs. However, more recent work in bombs and engines indicates that diffusion of hydrocarbons from the :h layer into the burned gases and its subsequent oxidation occur on a time scale of a few milliseconds, at least with smooth clean combustion chamber walls. The constant-volume combustion bomb data which suggested this conclusion and the kinetic calculations which support this explanation of why quench layers are not significant with smooth clean walls have alreadv been described in Sec. 11.4.2. The following evidence shows these conclusions are also valid in an engine. A special rapid-acting poppet valve was used in a single-cylinder engine to sample the gases from a torus-shaped region, of height of order 0.25 mm and diameter about 6 mrn, adjacent to the wall over a 1-ms period. Sampling was repeated every cycle to provide a steady stream of sampled gases for anal ysis. Figure 11-25 shows the variation in concentrations of HC species through the combustion, expansion, and exhaust processes. The fuel was propane' (c3H8). The fuel concentration drops rapidly to a low value when the flame arrives at the alve; at the same time, intermediate hydrocarbon product concentrations rise then fall sharply to values below 1 ppm. Beginning at 60" ATC, all HC centrations rise and vary somewhat during the remainder of the cycle in a ay that depends strongly on engine operating conditions. The observed rapid in partial oxidation products immediately after flame arrival is consistent the flame quenching short of the wall. The presence of C H 2 0 and CH3CH0 significant quantities indicates that low-temperature oxidation processes are ccurring. However, since all HC product concentrations fall rapidly within 2 ms flame arrival to very low values, the unburned HC in the quench layer diffuse o the bulk burned gases and oxidize. The increase in HC concentrations later the cycle results from the sampling of hydrocarbons from sources other than 11m"oh I-..-..- 44 604 POLLUTANT F O R M A ~ O NAND CONTROL INTERNAL COMBUSTION ENGINE FUNDAMENTALS ame amves at each crevice, it can either propagate into the crevice and fully or 1 and air within the crevice or it can quench at the crevice trance. Whether the flame quenches depends on crevice entrance geometry, the m~ositionof the unburned mixture, and its thermodynamic state as described mval and quenching, burned gases will flow into each der pressure starts to decrease. Once the crevice gas presre is higher than the cylinder pressure, gas flows back from each crevice into 104 g I@ d g I@ ". s g 605 10 5 2 I 0 100 200 300 Crank angle, deg ATC no EGR.U Though quench layers on clean smooth combustion chamber walls are not a significant source of unburned hydrocarbons, it has been shown that wall surface finish does affect exhaust I%2 levels. Comparisons have been made between the standard "rough" as-cast cylinder head surfaces and the same cylinder heads when smoothed. The average exhaust HC concentration decreased by 103 ppm C, or 14 percent; the smoothed surface area was 32 percent of the total combustion &amber surface area45 Buildup of deposits on the combustion chamber surfaces also affect HC emission levels, as will be discussed later. CREVICE HC MECHANISM.The crevices in the combustion chamber walls- small volumes with narrow entrances-into which the flame is un etrate have been shown to be a major source of unburned HC.

The these crevice regions is the volumes between the piston, piston rings, an wall. Other crevice volumes in production engines are the threads aroun spark plug, the space around the plug center electrode, crevices arou and exhaust valve heads, and the head gasket crevice. Table 8.1. shows the and relative importance of these crevice regions in one cylin V-6 engine determined from measurements of cold-engine ComP crevice volume is a few percent of the clearance volume and the pack crevices are the dominant contributor. The important crevice processes occurring during the engine cycle are following. As the cylinder pressure rises during compression, unb forced into the crevice regions. Since these volumes are thin they h surface/volume ratio; the gas flowing into each crevice cools by heat close to the wall temperature. During combustion, while the P to rise, unburned mixture continues to flow into the crevice v~hmes.When ant of these crevices, the volumes between the piston, pisn rings, and cylinder wall, is shown schematically in Fig. 8-27. This crevice nsists of a series of volumes, connected by flow restrictions such as the ring side whose geometry changes as the ring moves up and down ther at the top or bottom ring surface. The gas flow, ng motion are therefore coupled, and their behavior mpression and expansion strokes has already been discussed in Sec. compression and combustion, mass flows into the volumes in this region. Once the cylinder pressure starts to decrease (after about 15" s out of the top of these crevice regions in Fig. 8-27 into the cylinnt to the cylinder wall. The important result is that the er charge (5 to 10 percent) trapped in these regions at ressure escapes the primary combustion process. Most the cylinder during the expansion process. Depending spark plug location in relation to the position of the top ring gap, well above percent of this gas can be unburned fuel-air mixture. Its potential contribution unburned H C emissions is obvious. There is substantial evidence to support the above description of crevice iston ring crevice region in particular. Visualization have identified the spark plug crevice outflow, lowansion out of the volume above the fist ring after the time of d the jet-like flows through the top ring gap later in the expanprocess when the pressure difference across the ring changes sign.46 Gas ling from the volume above the top ring, using a rapid-acting sample valve unted in the piston crown, has shown that the gas composition in this region fuel-air mixture until flame arrival at the crevice o the sampling valve location. Next, product gases enter the vice as the cylinder pressure continues to rise. Then, during expansion as gas gion, the composition of the gas sampled reverts back toward t of the unburned mixture which enters the crevice region earlier?' Direct evidence that the piston and ring crevice regions are a major contribr to exhaust HC emissions comes from experiments where the volume of this substantially changed.

W e n t w ~ r t halmost ~ ~ completely elimithis crevice by moving the top piston ring as close to the crown of the as possible, and sealing this ring at top and bottom in its groove with 0 sealed ring-orifice design in a production engine showed uctions of between 47 and 74 percent from baseline HC levels over a range of POLLUTANT FORMATION AND CONTROL @@ O-ring piece Gap seal 1.8. 1.6. rg 1.4. 612- er'.

.; c 1.0. '8 0.8: g -2 0.6. . -fj 0.4. a' ;: , ./ . ./. Scaled-ring designs Second compression ring 0.2. ' 0 2 '0:4 '0:6 ' 0:8 ' 1:o ' 112 '1.4 Oil consumption rate, mgls sealed-ring orifice ring design FIGURE 11-28 correlation between exhaust hydrocarbon emissions and oil consumption rate. Production piston rings and sealed &g-orifice ring designs. SI engine at 1600 revlmin, imep = 422 k ~ a equivalence , ratio = 0.9, r, = 8.0, intake pressure = 54 kPa, MBT spark tbingS7 study of this problem-the one-dimensional cyclic absorption and desorption of a dilute amount of gas in a thin (constant thickness) isothermal liquid layer diffusion effects are important-has been carried out. It suggests that oil wall could be a significant contributor to HC emksion levels. on the correlations between engine oil consumption and exhaust HC emissions provide a perspective on the relative importance of oil absorptionldesorption and crevice mechanisms. Wentworth measured oil consumption and HC emissions in a spark-ignition engine for a range of piston ring designs." Some of these designs were of the sealed ring-orifice type which effectively eliminates all the crevices between the piston, piston rings, and cylinder, and Prevents any significant flow into or out of the ring region.

HC emissions increase with increasing consumption for both production ring designs and the sealed ring-orifice designs as shown in Fig 11-28. Extrapolation to zero oil consumption from norma1 sumption levels shows a reduction in exhaust HC levels, but this decrease is significantly less than the difference in emission levels between the production and the sealed ring-orifim designs which effectively remove the major mvice region. The production piston used had a chamfered top land. The HC emissions for a normal piston top-land design would probably be higher. POOR COMBUSTION QUALITY. Flame extinction in the bulk gas, before all the flame front reaches the wall, is a source of HC emissions under certain 611 ~ ~ e r a t i nconditions. g As the cylinder pressure falls during the expansion stroke, the temperature of the unburned mixture ahead of the flame decreases. This slows the burning rate [the laminar flame speed decreases so the burning rate in Eq. (9.52) decreases]. If the pressure and temperature fall too rapidly, the flame can be extinguished. This type of bulk quench has been observed in spark-ignition engines; it results in very high HC concentrations for that particular cycle. Engine conditions where bulk quenching is most likely to occur are at idle and light load where engine speed is low and the residual gas fraction is high, with high dilution with excessive EGR or overly lean mixtures, and with substantially retarded combustion. Even if steady-state engine calibrations of AIF, EGR, and spark-timing are such that bulk quenching does not occur, under transient engine operation these variables may not be appropriately set to avoid bulk quenching in some engine cycles due to the different dynamic characteristics of the engine subsystems which control these variables. The existence of zones of stable and unstable engine operation with lean or dilute mixtures has already been discussed (see Sec. 9.4.3). Detailed engine combustion studies have shown that, as mixture composition becomes more dilute (e.g., by increasing EGR) and unburned gas temperature and pressure during combustion become lower, combustion quality (or variability) and engine stability deteriorate. The standard deviation in a parameter such as indicated mean effective pressure (which depends for its magnitude on the proper timing of the start of combustion and on the duration of the combustion process) increases due first to an increase in the number of slower burning cycles, then as conditions worsen to the occurrence of partial burning cycles, and finally to some misfiring cycles. Figure 9-36 showed how unburned hydrocarbon emissions from a sparkignition engine rise as the EGR rate is increased at constant load and speed, and combustion quality (defined by the ratio of standard deviation in imep to the average imep) deteriorates. Initially the increase in HC is modest and is caused by changes in the other HC emission mechanisms described above. However, when partial burning cycles are detected, HC emissions rise more rapidly due to incomplete combustion of the fuel in the cylinder in these cycles. When misfiring cycles-no combustion--occur the rise in HC becomes more rapid still. The relative importance of bulk gas quenching in a fraction of the engine's operating cycles due to inadequate combustion quality as a source of HC, compared with the other sources described in this section, has yet to be established. However, one obvious technique for reducing its importance, burning the mixture faster so that combustion is completed before conditions conducive to slow and partial burning exist in the cylinder, does reduce engine exhaust HC emissions. Figure 11-29 shows a comparison of HC emissions from a moderate burn rate engine with HC emissions with a faster burn rate [i.e., with improved combustion quality-lower coefficientof variation in imep, COVimcp,Eq. (9.50)], achieved by the use of two spark plugs instead of one." The exhaust measurements show lower HC emissions when significant amounts of EGR are used for NO, control for the faster, and hence less variable, combustion process. Such evidence s w p t s that occasional partial burning cycles may occur, even under 612 INTERNAL C O M B U ~ O NENGINE FUNDAMENTALS 30 '0 10 20 30 40 EGR rate, % FIGURE 11-29 Effect of increasing burn rate on tolerance to recycled exhaust gas (EGR) and HC and NO, emissions levels. COV,,,, defined by Eq. (9.50). SI engine at 1400 revjmin, 324 kPa imep, equivalence ratio = 1.0, MBT timing.58 conditions where combustion appears to be ' ' n ~ ~ a l ,a" is important in practice. E F F E OF ~ DEPOSITS. Deposit buildup on the combustion chamber walls (which occurs in vehicles over several thousands of miles) is known to increase unburned HC emissions. With leaded gasoline operation, the increase in HC emissions varies between about 7 and 20 percent. The removal of the deposits results typically in a reduction in HC emissions to close to clean engine levels. With unleaded gasoline, while the deposit composition is completely different (carbonaceous rather than lead oxide), the increase in HC emissions with accumulated mileage is comparable. Soft sooty deposits, such as those which accumulate after running the engine on a rich mixture, also cause an increase in HC emissions. Again, when the deposits were removed the emission rate fell about 25 percent to the original level." Studies with simulated deposits (pieces of metalfoam sheet 0.6 mm thick) attached to the cylinder head and piston also showed increases in HC emissions. The increase varied between about 10 and simulated deposit area. The effect for a given area of deposit 100 ppm c / ~of* varied with deposit location. Locations close to the exhaust valve, where the flow direction during the exhaust process would be expected to be directly into the exhaust port, showed the highest increase in emissions.45 1t is believed that absorption and desorption of hydrocarbons by these surface deposits is the mechanism that leads to an increase in emissions. Deposits can also build up in the piston ring crevice regions. A reduction in volume of these crevice regions would decrease HC emissions (and such a decrease has been observed). However, changes in piston-cylinder wall ckarance due to deposits can affect the flame-quenching process and could increase emissions.4' HYDROCARBON TRANSPORT MECHANISMS. AU of the above mechanisms (except misfire) result in high hydrocarbon concentrations adjacent to the cornbustion &amber walls. While any jet-type flows out of crevices during the expan- FIGURE 11-30 Schematic of flow Processes by which ring crevice HC and HC desorbed from cylinder film exit the cylinder: (a) exhaust blowdown process; (b)during exhaust stroke; (c) end of exhaust stroke.60 sion and exhaust strokes can transport unburned HC into the bulk gases, most of the HC will remain near the wall. Two mechanisms by which gas near the cylinder wall exits the cylinder have been demonstrated. One is entrainment in the vigorous gas flow out of the cylinder which occurs during the exhaust blowdown Process. The other is the vortex generated in the piston crown-cylinder wall corner during the exhaust stroke. Figure 11-30 illustrates these flow processes. In Fig. 11-30a the engine cylinder is &own as the exhaust valve opens during the blowdown process. ~t this time the ~ d ~ r n HC e d from the ring crevice regions, laid along the wall during expansion (and possibly HC from the oil film on the cylinder wall), is expanding into the cylinder as the cylinder pressure falls. Some of this material will be entrained by the bulk gases in the rapid motion which occurs during exhaust blowdown (see SIX- 6.5). The rapid thinning of the thermal boundary-layer on the combustion chamber walls during blowdown, which would result from entrainment of the denser hydrocarbon-containing gas adjacent to the wall, has been observed in schlieren movies taken in a transparent engine.46 This process, plus entrainment of any HC from the spark plug and head gasket crevjms, would contribute to unburned HC in the blowdown gases which contain half the total HC emissions (see Fig. 11-24). During the exhaust stroke this gas enf~ah'Ientp~ocess continue, exhausting additional unburned HC, as shown in Fig. 11-30b. 614 POLLUTANT FORMAT1[ON AN1 INTERNAL COMBUSTION ENGINE FUNDAMENTALS The second mechanism starts at the beginning of the exhaust stroke in t piston crown-cylinder wall comer. The piston motion during the exhaust str scrapes the boundary-layer gases off the cylinder wall (which contain the rem der of the piston and ring crevice hydrocarbons), rolls them up into a vortex, an pushes them toward the top of the cylinder. This piston crown-cylinder wall comer flow is discussed in Sec. 8.7, and has been observed in transparent engines as well as in water-flow engine analog studies. At the end of the exhaust stroke, the height of this vortex is comparable to the engine clearance height. As shown in Fig. 11-30c, a recirculation flow is likely to build up in the upper comer of the cylinder away from the exhaust valve, causing the vortex to detach from the wall la and partly sweep out of the cylinder. In the comer nearest the valve, the flow is deflected around the valve, also tending to pull part of the vortex out of the chamber. In this way it is possible for a large part of the vortex, which now contains a substantial fraction of the unburned HC originally located adjacent to the cylinder wall, to leave the cylinder at the end of the exhaust stroke.

This vortex flow is thought to be the mechanism that leads to the high HC concentrations measured at the end of the exhaust process, which contributes the other half of the exhausted HC mass (see Fig. 11-24), and to be responsible for the HC concentrations measured in the residual gases being much higher than average exhaust HC levek4' This study showed that at close to wide-open-throttle conditions, only about two-thirds of the HC which fail to oxidize inside the cylinder were exhausted, though 95 percent of the gas within the cylinder flows out through the exhaust valve. The residual gas HC concentration was about 11 times the average exhaust level. At part-throttle conditions, where the residual gas fraction is higher, it has been estimated that only about half of the unreacted HC in the cylinder will enter the exhaust6' 1 E I Post-combustion in-cyl'ider mixing I 3 I+ Oxidation products ' Oxidation products Exhaust POI? I Exhaust pipe FIGURE 11-31 Schematic of complete SI engine HC formation and oxidation mechanism within the cvlinder and exhaust system.62 HYDROCARBON OXIDATION. Unburned hydrocarbons which escape the primary engine combustion process by the mechanisms described above must then survive the expansion and exhaust process without oxidizing if they are to appear in the exhaust. Since the formation mechanisms produce unbumed HC at temperatures close to the wall temperature, mixing with bulk burned gas must take place fmt to raise the HC temperature to the point where reaction can occur. The sequence of processes which links the source mechanisms to hydrocarbons at the exhaust exit is illustrated in Fig. 11-31; it involves mixing and oxidation in both the cylinder and the exhaust system. There is considerable evidence that substantial oxidation does occur. The oxidation of unbumed HC in the quench layers formed on the combustion chamber walls on a time scale of order 1 ms after the flame is extinguished has already been discussed. Because the quench layers are thin, diffusion of HC into the bulk burned gas is rapid. Because the burned gases are still at a high ternDerature, oxidation then occurs quickly. Measurements of in-cylinder HC con: centrations by gas sampling prior to exhaust valve opening show levels about 1.5 to 2 times the average exhaust l e ~ e l . ~ "The . ~ ~exhaust unburned HC are a mixture of fuel hydrocarbon compounds and pyrolysis and partial oxidation pro- Unburned HC sources: Cnvices (Wall phenomena ducts. While the relative proportion of fuel compared to reaction product hydrocarbon compounds varies substantially with engine operating conditions, an average value for passenger car vehicle exhausts is that fuel compounds comprise 40 percent of the total HC. Though partially reacted HC are ~roducedin the flame-quenching process, these are closest to the high-tempel bum and are likely to mix and burn rapidly. That such a laree >fthe a . frat --------- -HC are reaction products indicates that substantial postformation HC reactions are occurring. There is direct evidence that HC oxidation in the exhaust system occurs.64 Since in-cylinder gas temperatures are higher, it is likely that mixing of unburned HC with the bulk cylinder gases limits the amount of oxidation rather than the reaction kinetics directly. Overall empirically based expressions for the rate of oxidation of hydrocarinbons of the form of Eq. (11.31) have been developed and used to examine .. cylinder and exhaust burnup. A characteristic time, z for this burnup process can be defined : - - ~ - 3 .-a- ."--..=a- 'i Using an expression similar to Eq. (11.31) for d[HC]/dt, Weiss and K e ~ have k ~ ~ shown that any HC mixing with the burned gases in the cylinder prior to exhaust 616 INTERNAL COMBUSTION ENGINE FUNDAMENTALS blowdown will oxidize. The in-cylinder gas temperature prior to blowdown gen. erally exceeds 1250 K; the characteristic reaction time, ,z is then less than 1 ms. During blowdown the temperature falls rapidly to values typically less than 1000 K; , ,z is then greater than about 50 ms. An experimental study of HC exiting from a simulated crevice volume has shown that complete HC oxidation only occurs when the cylinder gas temperature is above 1400 K . ~ 'Thus a large fraction of the HC leaving crevice regions or oil layers during the exhaust process can be expected to survive with little further oxidation. Gas-sampling data show little decrease in inzylinder HC concentrations during the exhaust stroke, thus supporting this conclu~ion?~. 63 Overall, probably about half of the unburned HC formed by the source mechanisms described above will oxidize within the engine cylinder (the exact amount cannot yet be predicted with any accuracy; it is likely to depend on engine design and operating conditions6'). As shown schematically in Fig. 11-31, oxidation of HC in the exhaust system can occur. Often this is enhanced by air addition into the port region to ensure that adequate oxygen for burnup is available. However, since the gas temperature steadily decreases as the exhaust gases flow through the exhaust port and manifold, the potential for HC burnup rapidly diminishes. To oxidize the hydrocarbons in the gas phase, a residence time of order 50 ms or longer at temperatures in excess of 600•‹C are required.

To oxidize carbon monoxide temperatures in excess of 700•‹C are required.

Average exhaust gas temperatures at the cylinder exit (at the exhaust valve plane) are about 800•‹C;average gas tempratures at the exhaust port exit are about 600"C.t Figure 6-21 shows an example of the measured cylinder pressure, measured gas temperature at the exhaust port exit, and estimated mass flow rate into the port and gas temperature in the cylinder, during the exhaust process at a part-throttle operating condition. port residence time and gas temperatures vary significantly through the Process.

precise values of these variables obviously depend on engine operating con&tions. ~t is apparent that only in the exhaust port and upstream end of the minifold can any significant gas-phase HC oxidation ~ ~ u r . The importance of exhaust gas temperature to exhaust system emissions burnup is illustrated by the results shown in Fig. 11-32.66 The exhaust system of a four-cylinder engine was modified by installing a section of heated and insulated pipe to maintain the exhaust gas temperature constant in the absence of any HC or CO burnup. The exhaust temperature entering this test section was varied by adjusting the engine operating conditions.

The figure shows CO and HC concentrations as functions of residence time in the exhaust test section (or effectively as a function of distance from the engine). T, is the entering gas tern* prature. m e exhaust composition was fuel lean with 3 percent 0, in the burned t ~~t~ that there is a significant variation in the temperature of the exhaust gases throughout the exhaust process. The gas exhausted first is about 100 K hotter than the gas exhausted at the end of the process (see Sec. 6.5). Residence time, ms FIGURE 11-32 Effect of exhaust gas temperature on HC and co burnup in the exhaust. SI engine at 1600 rev/min, engine air flow = 7.7 dm3/s, lean mixture with 3% 0, and 13% (CO + CO,) i n e x h a u ~ t .

~ ~ gas stream. HC oxidation starts immediately (for T 2 600•‹C),the rate of oxidation increasing rapidly with increasing temperature. Under fuel-lean conditions, incomplete HC oxidation can result in an increase in CO levels.

CO oxidation commences later, when the gas temperature rises above the entering value due to heat released by the already occurring HC oxidation. The further heat released by CO oxidation accelerates the CO burnup process. These data underline the importance of the exhaust port heat-transfer and mixing processes. ~ 0 t mixing h between the hotter blowdown gases (with their lower HC concentration) and the cooler end-of-exhaust gases (with their higher HC concentration) and &xing between burned exhaust gas and secondary air are important. Engine everiments where the exhaust gas reactions were quenched by timed injection of cold carbon dioxide at selected locations withjn the exhaust Port have shown that significant reductions in HC concentration in the port can occur. Parallel modeling studies of the HC burnup process (based on instantaneOW mass flow rate, estimated exhaust gas temperature, and an overall hydrocarban reaction-rate expression), which predicted closely comparable magnitudes and trends, inckated that gas temperature and port residence time are the critical variables. The percent of unburned HC exiting the cylinder which reacted in the exhaust system (with most of the reaction occurring in the port) varied between a few and 40 Percent. Engine operating conditions that gave highest exhaust ternperatures (stoichiometric operation, higher speeds, retarded spark timing, lower compression ratio) and longest residence times (lighter load) gave relatively higher Percent reductions. Air injection at the exhaust valve-stem base, phased to coincide with the exhaust process, showed that for stoichiometric and slightly rich conditions secondary air flow rates up to 30 percent of the exhaust flow substantially increased the degree of burnup. The timing of the secondary air flow relative to the exhaust flow and the location of the air injection point in the port are known to be critical.64 Reductions in exhaust port heat losses through the use of larger port crosssectional areas (to reduce flow velocity and surface area per unit volume), inser- 618 INTERNAL COMBUSTJON ENGINE FUNDAMENTALS tion of port liners to provide higher port wall temperatures, and attention to port design details to minimize hot exhaust gas impingement on the walls are known to increase the degree of reaction occurring in the port. POLLUTANT FORMATION AND CONTROL critical factors and engine variables in HC emissions mechanisms 1. Formation of HC SUMMARY. It will be apparent from the above that the HC emissions formation process in spark-ignition engines is extremely complex and that there are several paths by which a small but important amount of the fuel escapes combustion. It is appropriate here to summarize the overall structure of the spark-ignition engine hydrocarbon emission problem and identify the key factors and engine variables that influence the different parts of that problem. Table 11.7 provides such a summary. The total process is divided into four sequential steps: (1) the formation of unburned hydrocarbon emissions; (2) the oxidation of a fraction of these HC emissions within the cylinder, following mixing with the bulk gases; (3) the flow of a fraction of the unoxidized HC from the cylinder into the exhaust; (4) the oxidation in the exhaust system of a fraction of the HC that exit the cylinder.

The detailed processes and the design and operating variables that influence each of these steps in a significant way are listed. The four separate formation mechanisms identified in step 1 have substantial, though as yet incomplete, evidence behind them. They are listed in the most likely order of importance.

Each has been extensively described in this section. It is through each of these mechanisms that fuel or fuel-air mixture escapes the primary combustion process. That fuel must then survive the expansion and exhaust processes and pass through the exhaust system without oxidation if it is to end up in the atmosphere as HC emissions. The rate of mixing of these unburned HC with the hot bulk cylinder gases, the temperature and composition of the gases with which these HC mix, and the subsequent temperature-time and composition-time histories of the mixture will govern the amount of in-cylinder oxidation that occurs. The distribution of these HC around the combustion chamber is nonuniform (and changes with time); they are concentrated close to the walls of the chamber. The fraction of these HC that will exit the chamber during the exhaust process will depend on the details of the in-cylinder flow patterns that take them through the exhaust valve.

Overall, the magnitude of the residual fraction will be one major factor; the residual gas is known to be much richer in HC than the average exhaust. In particular, the flow patterns in the cylinder toward the end of the exhaust stroke as the gas scraped off the cylinder wall by the piston moves toward the exhaust valve will be important. Finally, a fraction of the unburned HC which leave the cylinder through the exhaust valve will bum up within the exhaust system. Gas-phase oxidation in the exhaust ports and hotter parts of the exhaust manifold is significant. The amount depends on the gas temperature, composition, and residence time. If catalysts or a thermal reactor are included in the exhaust system, very substantial additional reduction in HC emission levels can occur. These devices and their operating characteristics are described in Sec. 11.6. (1) Crevice volume (2) Crevice location (relative to spark plug) (4) Crevice wall temperature (5) Mixture compositiont (1) Oil consumption (2) Wall temperature (c) Incomplete combustion (1) Bum rate and variability (2) Mixture compositiont (4) Spark timing$ (d) Combustion chamber walls (1) Deposits (2) Wall roughness 3. Fraction HCflowing (a) Residual fraction (2) Exhaust pressure (3) Valve overlap (4) Compression ratio (b) In-cylinder flow during exhaust stroke (1) Valve overlap (2) Exhaust valve size and (3) Combustion chamber shape (4) Compression ratio 2. In-cylinder mixing and oxidation (a) Mixing rate with bulk gas (1) Speed (2) Swirl ratio (3) Combustion chamber shape (b) Bulk gas temperature during expansion and exhaust (1) speed (2) Spark timing$ (3) Mixture compositiont (4) Compression ratio (5) Heat losses to walls (c) Bulk gas oxygen concentration (1) Equivalence ratio (4 Wall temperature (1) Important if HC source near wall (2) For crevices: importance depends on geometry 4. Oxidation in exhaust system (a) Exhaust gas temperature (1) Speed (2) Spark timing$ (3) Mixture compositiont (4) Compression ratio (5) Secondary air flow (6)Heat losses in cylinder and exhaust (b) Oxygen concentration (1) Equivalence ratio (2) Secondary air flow and addition point (c) Residence time (1) Speed (2) Load (3) Volume of critical exhaust system component (d) Exhaust reactor9 (1) Oxidation catalyst (2) Three-way catalyst (3) Thermal reactor Fuel/air cquivalcn= ratio and burned gas fraction (residual PIUS wclcd exhaust gas). f Relative to MBT timing. Of at leastas ~ r c a an t importance as engine details if present ia total emission control system.

sa scf. 11.6. 619 620 INTERNAL COMBUSTION ENGINE FUNDAMENTALS Hydrocarbon Emission Mechanisms in Diesel Engines 11.4.4 BACKGROUND. Diesel fuel contains hydrocarbon compounds with higher boiling points, and hence higher molecular weights, than gasoline. Also, substantial pyrolysis of fuel compounds occurs within the fuel sprays during the diesel combustion process. Thus, the composition of the unburned and partially oxidized hydrocarbons in the diesel exhaust is much more complex than in the spark-ignition engine and. extends over a larger molecular size range. Gaseous hydrocarbon emissions from diesels are measured using a hot particulate filter (at 190•‹C) and a heated flame ionization detector. Thus the HC constituents vary from methane to the heaviest hydrocarbons which remain in the vapor phase in the heated sampling line (which is also maintained at about 190•‹C).Any hydrocarbons heavier than this are therefore condensed and, with the solid-phase soot, are filtered from.the exhaust gas stream upstream of the detector. The particulate emission measurement procedure measures a portion of total engine hydrocarbon emissions also. Particulates are collected by filtering from a diluted exhaust gas stream at a temperature of 52•‹C or less. Those hydrocarbons that condense at or below this temperature are absorbed onto the soot. They are the extractable fraction of the particulate: i.e.,

ratio of 100 m2/g, so the measured value is about twice the superficial area. Approximating a particle of agglomerated spherules by a single sphere of 200 nm diameter gives a surface/mass ratio of 15 m2/g.70These data and estimates of superficial area per unit mass indicate that diesel soot has low porosity. SOLUBLE FRACTION COMPONENTS.The extractable organic fraction of diesel FIGURE 11-40 Lattice-imaging micrograph of a diesel particulate." olefins, and aromatics-contributed to the particulate emissions; as a group, aromatics were the greatest contributors.
Eighty percent of the carbon-14 used to tag individual fuel compounds was found in the insoluble fraction and 20 percent in the soluble particulate fra~tion.~' In addition to the elements listed in Table 11.8, trace amounts of sulfur, zinc, phosphorus, calcium, iron, silicon, and chromium have been found in particulates. Sulfur and traces of calcium, iron, silicon, and chromium are found in diesel fuel; zinc, phosphorus, and calcium compounds are frequently used in lubricating oil additives70 A lattice image of a diesel particle is shown in Fig. 11-40; it suggests a concentric lamellate structure arranged around the center of each spherule. This arrangement of concentric lamellas is similar to the structure of carbon black. This is not surprising; the environment in which diesel soot is produced is similar to that in which oil furnace blacks are made. The carbon atoms are bonded together in hexagonal face-centered arrays in planes, commonly referred to as platelets. As illustrated in Fig. 11-41, the mean layer spacing is 0.355 nm (only slightly larger than graphite). Platelets are arranged in layers to form crystallites. Typically, there are 2 to 5 platelets per crystallite, and on the order of lo3 crys- Platelet Crystdlite Mcle FIGURE 11-41 Substructure of carbon particulate emissions includes compounds that may cause health and environmental hazards. Thus chemical and biological characterization of the soluble organic fraction are important. Both soxhlet and sonification methods are used to extract the organic fraction from particulate samples. Because the particulates are mixtures of polar and nonpolar components, full extraction requires different solvents; any one solvent is a compromise. Methylene chloride is the most commonly used extractant, however.
Since a complex mixture of organic compounds is associated with diesel particulates, a preliminary fractionation scheme is used to group similar types of compounds before final separation and identification.
The scheme most frequently used results in seven fractions generally labeled as: basics, acidics, paraffins, aromatics, transitionals, oxygenates, and ether insolubles. Table 11.9 indicates the types of components in each fraction and the approximate proportions. The biological activity of the soluble organic fraction and its subfractions is most commonly assessed with the Ames Salmonella/microsomal test. With this test, a quantitative dose-response curve showing the mutagenicity of a sample compound is obtained. The Ames test uses a mutant strain of Salmonella typhimurium that is incapable of producing histidine. Mutagenicity is defined as the ability of a tested compound to revertback-mutate-this bacterium to its wild state, where it regains its ability to produce histidine.j5 115.3 Particulate Distribution within the Measurements have been made of the particulate distribution within the combustion chamber of operating diesel engines. The results provide valuable information on the particulate formation and oxidation processes and how these relate to the fuel distribution and heat-release development within the combustion chamber. Techniques used to obtain particulate concentration data include: use of rapid-acting poppet or needle valves which draw a small gas sample from the cylinder at a specific location and time for analysis (e.g., Refs. 21 632 INTERNAL COMBUSTION ENGINE FUNDAMENTALS TABLE 113 Components of the soluble organic fraction3' Fraction Componeots of fraction Acidic Aromatic or aliphatic Acidic functional groups Phenolic and carboxylic acids Aromatic or aliphatic Basic functional groups Amines Aliphatics, normal and branched Numerous isomers From unburned fuel and/or lubricant From unburned fuel, partial combustion, and recombination of combustion products; from lubricants Single ring compounds Polynuclear aromatics Polar functional groups but not acidic or basic Aldehydes, ketones, or alcohols Aromatic phenols and quinones Aliphatic and aromatic Carbonyl functional groups Ketones, aldehydes, esters, ethers Aliphatic and aromatic Hydroxyl and carbonyl groups High molecular weight organic species Inorganic compounds Glass fibers from filters Basic Paraffin Aromatic Oxygenated Transitional Insoluble Percent of total 3-15 < 1-2 34-65 3-14 7-15 1-6 -20 TC 20 40 60 80 Crank angle, deg ATC 100 6-25 and 74), optical absorption techniques (e.g., Refs. 75 and 76), and cylinder dumping where the cylinder contents are rapidly emptied into an evacuated tank at a preset time in the cycle (e.g., Ref. 77). Both DI and ID1 engines have been studied. Of course, concentration data taken at specific locations in the cylinder during the engine cycle are not necessarily representative of the cylinder contents in general; nor do they represent the time history of a given mass of gas. The fuel distribution, mixing and heat-release patterns in the cylinder are highly nonuniform during the soot-formation process, and the details of gas motion in the vicinity of the sampling location as the piston changes position are usually unknown. In direct-injection diesel engines, the highest particulate concentrations found in the core region of each fuel spray where local average equivalence are very rich (see Secs. 10.5.6 and 10.7.2). Soot concentrations rise rapidly after combustion starts. Figure 11-42 shows a set of sample-valve sootconcentration data from a large (30.5-cm bore, 38.1-cm stroke), quiescent, direct- FIGURE 11-42 Pmculate concentrations, in g/m3 at standard temperature and pressure, in vanous regons of the fuel spray as a function of crank angle in quiescent DI dresel engine, measured with rapid sampling valve. Merent sample valve locations m combustion chamber and spray inhcated on left. Cylinder bore = 30.5 cm,stroke = 38.1 cm, r, = 12.9, engine speed = 500 rev/mn, bmep = 827 kPa." injection diesel engine which illustrates these point^.'^ The particulate concentrations on the fuel spray axis close to the injector orifice are remarkably high (-200 to 400 g/m3 at standard temperature and pressure). This corresponds to a large fraction of the fuel carbon in the extremely rich fuel vapor core being sampled as particulate (as soot and condensed HC species). Such high particulate fractions of the local fuel carbon (- 50 percent) have also been found in the very fuel rich cores of high-pressure liquid-fueled turbulent diffusion flames. Pyrolysis of the fuel is therefore an important source of soot. These very high local soot concentrations decrease rapidly once fuel injection ceases and the rich core mixes to leaner equivalence ratios.
Soot concentrations in the spray close to the piston bowl outer radius and at the cylinder wall rise later, are an order of magnitude less, and decay more slowly. Away from the fuel spray core, soot concentrations 3E! 634 INTERNAL COMBUSTION ENGINE FUNDAMENTALS POLLUTANT FORMATION AND CONTROL 635 2! 2 .' Ignition 'j p -10 TC H Injection FIGURE 11-43 \,\'--:=--. 10 20 30 40 50 Crank angle, deg decrease rapidly with increasing distance from the centerline. A use son with these soot concentrations is the fuel concentration in a ~toichiometri~ mixture, about 75 g fuel/m3.
Approximate estimates of the mean soot concentration inside the cylinder through the combustion process suggests that almost all (over 90 percent) of the soot formed is oxidized prior to exhaust. Similar results have been obtained in a small direct-injection engine with 79 Peak soot concentrations in the outer regions of the fuel spray were comparable (- 10 gi m3). Measurements were not made in the spray core near the injector orifice; however, based on the equivalence ratio results in Fig. 10-46, soot concentrations would be expected to be lower due to the more rapid mixing with air that occurs with swirl.
Similar data are available from sampling in the prechamber of an ID1 swirl chamber engine.21 Figure 11-43 shows soot concentrations 2, 10, and 15 mm from the wall of the prechamber. Equivalence ratio distributions from this study have already been shown in Fig. 11-17. Concentrations peak 5 to 10' ATC at levels -2 g/m3; these are substantially lower than DI engine peak soot concentrations (presumably due to the more rapid mixing of fuel and air in the ID1 engine). Concentrations in the prechamber at these locations then decrease substantially. A better indication of average concentrations within the cylinder is given by total cylinder sampling experiments. Measurements of the total number of soot particles and soot volume fraction through the combustion process have been made in an ID1 passenger car diesel. The contents of the engine cylinder, at a preselected point in the cycle, were rapidly expelled through a blowdown port, diluted, and collected in a sample bag. Figure 11-44 shows one set of results. Particles first appear shortly after the start of combustion (4 to 5" ATC). The number density rises to a maximum at 20" ATC and then falls rapidly as a result of particle coagulation and, possibly, oxidation. The exhaust particulate number density is less than one-tenth of the peak value. The volume fraction soot data (soot mass concentration is proportional to volume fraction) show a much flatter maximum earlier in the combustion process and a decrease (due to oxidation) from 20 to 40" ATC to about one-third of the peak value. Oxidation apparently ceases at about 40" ATC at these conditions. O Crank angle, deg FIGURE 11-44 Cylinder-average particle-number density N and particle-volume fraction F,, as a function of crank angle in ID1 diesel engine determined from cylinder-dumping experiments. 1000 rev/min, 9 = 0.32, injection starts at 3.5' BTC. Gas volumes at standard temperature and pressure.77 115.4 Soot Formation Fundamentals The soot particles, whose characteristics have been described in the above two sections, form primarily from the carbon in the diesel fuel. Thus, the formation process starts with a fuel molecule containing 12 to 22 carbon atoms and an H/C ratio of about 2, and ends up with particles typically a few hundred nanometers in diameter, composed of spherules 20 to 30 nrn in diameter each containing some 10' carbon atoms and having an H/C ratio of about 0.1. Most of the information available on the fundamentals of soot formation in combustion comes from studies in simple premixed and diffusion flames, stirred reactors, shock tubes, and constant-volume combustion bombs. A recent reviews0 summarizes the extensive literature available from such studies.
Also, the production of carbon black requires a high yield of soot from pyrolysis of a hydrocarbon feedstock, and the literature from that field has much to contribute (see Ref. 81). However, the characteristics of diesel combustion which make it unsuitable for more fundamental studies-the high gas temperatures and pressures, complex fuel composition, dominance of turbulent mixing, the unsteady nature of the process, and the three-dimensional geometry-also make it difficult to interpret fundamental ideas regarding soot formation in the diesel context. There is much about the soot formation process in diesel engines, therefore, that is poorly and incompletely understood. Soot formation takes place in the diesel combustion environment at temperatures between about 1000 and 2800 K, at pressures of 50 to 100 atm, and with suflkient air overall to bum fully all the fuel. The time available for the formation of solid soot particles from a fraction of the fuel is in the order of milliseconds. The resulting aerosoldispersed solid-phase particles in a gas-an be characterized by the total amount of condensed phase (often expressed as the soot volume fraction, F v , the volume of soot/total volume), the number of soot particles per unit volume (N), and the size of the particles (e.g., average diameter d). F,, N, and d are mutually dependent [e.g., for spherical particles Fv = 636 POLLUTANT FORMATION AND CONTROL INTERNAL COMBUSTION ENGINE FUNDAMENTALS (x/6)~d3],and any two of these variables characterize the system. It is mo convenient to consider N and Fv as the independent variables since they ea relate to the "almost-separate" stages of soot particle generation (the source N) and soot particle growth (the source of Fv). These stages can be summarized as follows 1. Particle formation, where the first condensed phase material arises from the fuel molecules via their oxidation and/or pyrolysis products.
These products typically include various unsaturated hydrocarbons, particularly acetylene and its higher analogues (C2,,H,), and polycyclic aromatic hydrocarbons (PAH).
These two types of molecules are considered the most likely precursors of soot in flames. The condensation reactions of gas-phase species such as these lead to the appearance of the first recognizable soot particles (often called nuclei). These first particles are very small (d < 2 m)and the fotmation of large numbers of them involve negligible soot loading in the region of their formation. 2. Particle growth, which includes both surface growth, coagulation, and aggregation. Surface growth, by which the bulk of the solid-phase material is generated, involves the attachment of gas-phase species to the suIface of particles and their incorporation into the particulate phase. Figure 11-45, where the 1% of the molecular weight of a species is plotted against its hydrogen mole fraction z,, illustrates some important points about this process.
Starting with a fuel molecule of f , 0.5 ~ it is apparent that neither purely polyacet~lenechain 9 637 growth nor purely PAH growth would lead to soot particles which have 2, in the range 0.1 to 0.2. What is required is condensation of species with the right hydrogen content, or condensation of species with higher hydrogen content followed by dehydrogenation, or a combination of both these processes. Obviously some polyacetylenes and some PAH can satisfy these requirements, as can saturated platelets (e.g., C27H2, ; see Sec. 11.5.2). Surface growth reactions lead to an increase in the amount of soot (Fv) but the number of particles (N) remains unchanged. The opposite is true for growth by coagulation, where the particles collide and coalesce, which decreases N with Fv constant. Once surface growth stops, continued aggregation of particles into chains and clusters can occur. These stages of particle generation and growth constitute the soot formation process. At each stage in the process oxidation can occur where soot or soot precursors are burned in the presence of oxidizing species to form gaseous products such as CO and CO,. The eventual emission of soot from the engine will depend on the balance between these processes of formation and burnout. The emitted soot is then subject to a further mass addition process as the exhaust gases cool and are diluted with air. Adsorption into the soot particle surface and condensation to form new particles of hydrocarbon species in the exhaust gases occurs in the exhaust system and in the dilution tunnel which simulates what happens in the atmosphere. Figure 11-46 illustrates the relationship between these processes.70 Although they are illustrated as discrete processes, there is some overlap, and they may occur concurrently in a given elemental mixture region within the diesel combustion chamber. Of course, due also to the nonhomogeneous nature of the mixture and the duration of fuel injection and its overlap with combustion, at any given time different processes are in progress in different regions or packets of fluid. The fundamentals of each of these processes will now be reviewed. I Nucleation Dehydrogenation Oxidation Oxidation .- u" Oxidation d 0 condensation FIGURE 11-45 paths to soot formation on plot of species molecular weight M versus hydrogen mole fraction %t.80 FIGURE 11-46 Processes leading to net production of diesel particulate^.'^ 638 INTERNAL COMBUSTION ENGINE FUNDAMENTALS SOOT PARTICLE FORMATION. Empirically, it has been found useful to defi the composition of the fuel-oxidizer mixture at the onset of soot formation flames by the carbon/oxygen ratio. Equilibrium considerations indicate that so formation should occur when, in n C, H, + yo, - ,2, CO Hz (m - 2y)Cs +5 + m becomes larger than 2y: i.e., the C/O ratio exceeds unity. The corresponding fuellair equivalence ratio is given by FIGURE 11-47 Mechanistic model for formation of soot from aromatic and aliphatic hydrocarbon c~mpounds.'~ (3 4 = 2 - (i+6) where 6 = n/(4m); 4 is 3 for (C/O) = 1, with n/m = 2. The experimentally observed critical C/O ratios are less than unity, however, varying with fuel composition and details of the experimental setup from about 0.5 to 0.8. The critical C/O ratio for soot formation increases with increasing temperature but is only weakly dependent on pressure. Beyond the carbon formation limit, the yield of soot increases rapidly with increasing C/O ratio and is strongly enhanced by increasing pre~sure.'~ It is obvious that soot formation is a nonequilibrium process. Yet despite decades of study, the precise details of the chemistry leading to the establishment of soot nuclei still elude investigators. Several different theories have been advanced to explain the pyrolysis process-the extensive decomposition and atomic rearrangement of the fuel molecules-that culminates in nucleation. Reviews of these theories can be found in Refs. 73,80, and 81.Often-cited mechanisms are thermal cracking that results in fragmentation of fuel molecules into smaller ones, condensation reactions and polymerization that result in larger molecules, and dehydrogenation that lowers the H/C ratio of the hydrocarbons destined to become soot. Three different paths to the production of soot appear to exist, depending on the formation temperature. At the lowest temperatures (51700 K) only aromatics or highly unsaturated aliphatic compounds of high molecular weight are very effective in forming solid carbon through pyrolysis. At intermediate temperatures typical of diffusion flames (21800 K), all normally used hydrocarbon fuels produce soot if burned at sufficientlyrich stoichiomet but appear to do so by following a different path. At very high temperature above the range of interest for diesel combustion, a third nucleation proces seems likely that involves carbon vapor.70 A simple mechanistic model for nucleation in the low and intermediate te perature ranges which has considerable experimental support for its b tures has been advanced by Graham et al." It is illustrated in Fig. 11-47. At temperatures, an aromatic hydrocarbon can produce soot via a relatively direct route that involves condensation of the aromatic rings into a gra structure. Above about 1800 K, however, a slower, less-direct route i that entails ring breakup into smaller hydrocarbon fragments. These fr then polymerize to form larger unsaturated molecules that ultimate1 soot nuclei. Aliphatic molecules can only follow this latter less-direct route.
~xperimentalmeasurements in flames suggest that polyunsaturated hydrocarbon compounds are involved in nucleation, and acetylenes and polyacetylenes have been detected that decrease in concentration as the mass of carbon formed increases. Such observations fit the indirect path in Fig. 11-47. Results of studies of pyrolysis of benzene between 1300 and 1700 K support a physical condensation mechanism for the low-temperature path. This mechanism begins with the transformation of the initial hydrocarbon into macromolecules by a gas-phase reaction. The partial pressure of these macromolecules grows until supersaturation becomes sufficient to force their condensation into liquid micr~droplet~. ese become nuclei, and subsequently formed gaseous macromolecules then ntribute to nuclei growth.'O SOOT PARTICLE GROWTH. Nucleation produces a large number of very small particles with an insignificant soot loading. The bulk of the solid-phase material is generated by surface growth, which involves the gas-phase deposition of hydrocarbon intermediates on the surfaces of the spherules that develop from the nuclei. A qualitative description of the changes that occur as a function of time in a premixed flame during nucleation and surface growth is shown in Fig. 11-48. The soot fraction F v , in units of soot volume per unit volume of gas, is related to the number density N and the volume-mean diameter of the soot particles by A F --Nd3 '-6 (11.37) d is the actual diameter of the spherules, or the diameter of a sphere of equivalent v ~ h m eto an agglomerated particle. The rate of change of particle number density with time t can be written . -dN =N,-N, dt (11.38) POLLUTANT FORMATION AND CONTROL INTERNAL COMBUSTION ENGINE FUNDAMENTALS 641 ion and surface growth rates have diminished, the resulting particles resemble a luster in which the original spherules retain much of their individual identity. After surface growth essentially ceases, continued coalescence of the soot particles results in the formation of chainlike structures of discrete spherules. This suggests forces are significant. Positive charge measured on these particle chains is claimed to be the cause of their chainlike 73 This latter once surface growth ceases is termed aggregation. It has been shown experimentally that during coagulation the rate of decrease of particle number density was proportional to the product of a coagulation coefficient and the square of the number density: Time - J dN - KNZ dt FIGURE 11-48 Variation in soot volume fraction F,, particle number density N, particle size d, and soot hydrogen/carbon ratio with time in a flame.'' where N, is the rate at which fresh nuclei appear and fi, is the rate of agglomeration of spherules or particles that collide and stick. At the peak of the N curve, Nn= N,. To the left of the peak, fin > N,,the particle diameter remains essentially constant at the minimum detectable diameter and the (small) rise in soot volume is dominated by nucleation. To the right of the peak in the N curve, fi,> N,. The number of agglomerating collisions is high because of the high number density; at the same time nucleation ends because there is enough dispersed surface area for gaseous deposition of hydrocarbon intermediates so the probability of generating new nuclei falls to zero. With nucleation halted slightly to the right of the N curve peak, all the subsequent increase in soot volume fraction (the majority) stems from surface growth. To the right of the N curve peak, the number density falls in the case illustrated by three orders of magnitude. This is the result of agglomeration, which is responsible for a portion of the increase in particle diameter. Agglomeration does not contribute to the rise in soot volume fraction, F , . Surface growth that takes place on nuclei and on spherules is responsible for forming the concentric shells (somewhat distorted and warped) that constitute the outer portions of spherules and which are distinct from the less-organized spherule center (see Figs. 11-40 and 11-41). Surface growth on agglomerated particles may partly fill in the crevices at the junctures of adjoining spherules to provide the nodular structure evident in Fig. 11-40.~' Once particles have formed, interparticle collisions can lead to agglomeration, thereby decreasing the number of particles and increasing their size. Three types of agglomeration have been identified in soot formation. During the early stages of particle growth, collision of two spherical particles may result in their coagulation into a single spheroid. This is easy to visualize in hydrocarbon p~rolysis where the beginnings of a soot particle may have the viscosity of a tarry Also, when the individual particles are small, rapid surface growth will quickly restore the original spherical shape.73 This process occurs up to dia* eters of about 10 nm. On the other hand, if spherules have solidified before colli ' (11.39) This is the Smoluchowski equation for coagulation of a liquid colloid. Based on brownian motion, this equation is applicable when the Knudsen number (ratio of mean free path to particle diameter) exceeds 10. K depends on such fadors as article size and shape, size distribution, and the temperature, pressure, and density of the gas. Equation (11.39) has been used to predict coagulation rates in lo~-preSSUresooting f l i ~ n e s It. ~has ~ ~also ~ ~ been modified so that it applies where the particle size and mean free path are comparable by using a more complex expression for K (see Ref. 83). These studies show that under conditions approximating those in engine flames, the fraction of the initial number density No remaining at time t is given approximately by N x (KN, t)-' (11.40) No Thus as t increases, N/No decreases rapidly. Although these coagulation calculations are simplistic (in that many of the assumptions made are not strictly valid since Soot particles are not initially distributed homogeneously in the combustion space, they are not monodisperse, and surface growth and oxidation may be taking place during agglomeration), an overall conclusion is that the rate of coagulation of spherules and particles to larger particles is very sensitive to number density. Thus the number of particles decreases rapidly with advancing crank angle in the diesel engine during the early part of the expansion process (see Fig. 11-44) and agglomeration is essentially complete well before the exhaust valve opens. Throughout the soot formation process in a flame, the H/C ratio of the hydrocarbons formed in the pyrolysis and nucleation process and of the soot particles continually decreases. The H/C ratio decreases from a value of about 2, typical of common fuels, to of order 1 in the youngest soot particles that can be sampled, and then to 0.2 to 0.3 once surface growth has ceased in the fully agglomerated The latter stages of this process are indicated in Fig. 11-48. The addition of mass to the soot particles occurs by reaction with gas-phase molecules. The reacting gas-phase hydrocarbons appear to be principally acetylen% with larger polymers adding faster than the smaller. Small polyacetylenes 642 MTERNAL COMBUSTION ENGINE FUNDAMENTALS undergo further polymerization in the gas phase, presumably by the same mec nism leading to nucleation. As a result of preferential addition of the larger po mers, the H/C ratio of the particles decreases toward its steady-state value.
most of the polyacetylenes added must be of very high molecular weight or drogenation must also take place.73,80 Rate constants for Nagle and StricklandConstable soot oxidation mechanism84 115.5 Soot Oxidation In the overall soot formation process, shown schematically in Fig. 11-46, oxidation of soot at the precursor, nuclei, and particle stages can occur. The engine cylinder soot-concentration data reviewed in Sec. 11.5.3 indicate that a large frat.
tion of the soot formed is oxidized within the cylinder before the exhaust process commences. In the discussion of diesel combustion movies in Sec. 10.3.1, dark brown regions were observed in the color photographs (see color plate, Fig. 10-4); these were interpreted as soot particle clouds, and were seen to be surrounded by a diffusion flame which appeared white from the luminosity of the high-temperature soot particles consumed in this flame. As air mixed with this soot-rich region, the white flame eradicated the dark soot clouds as the particles were burned up. In general, the rate of heterogeneous reactions such as the oxidation of soot depends on the diffusion of reactants to and products from the surface as well as the kinetics of the reaction. For particles less than about 1 pm diameter, dfiusional resistance is minimal. The soot oxidation process in the diesel cylinder is kinetically controlled, therefore, since particle sizes are smaller than this limit. There are many species in or near the flame that could oxidize soot: examples are 739 have con0, , 0 , OH, CO,, and H,O. Recent reviews of soot cluded that at high oxygen partial pressures, soot oxidation can be correlated with a semiempirical formula based on pyrographite oxidation studies. For fuelrich and close-to-stoichiometriccombustion products, however, oxidation by OH has been shown to be more important than 0, attack, at least at atmospheric pressure. It is argued on the basis of structural similarities that the rates of oxidation of soot and of pyrographites should be the same. This is a significant simplfication. It has proved difficult to follow the oxidation of soot aerosols in flames, and if care is taken to avoid diffusional resistance, studies of bulk samples of pyrographite can then be used as a basis for understanding soot oxidation. The semiempirical formula of Nagle and Strickland-Constable has been shown84 to correlate pyrographite oxidation for oxygen partial pressures PO, < 1 atm and temperatures between 1100 and 2500 K. This formula is based on the conce that there are two types of sites on the carbon surface available for 0, att For the more reactive type A sites, the oxidation rate is controlled by the frac of sites not covered by surface oxides (and therefore is of mixed order, between and 1 in p,,). Type B sites are less reactive, and react at a rate which is first orde in po2. A thermal rearrangement of A sites into B sites is also allowed (with constant k,). A steady-state analysis of this mechanism gives a surface mass Rate constant Units k, = 20 exp (- 15,10O/T) k, = 4.46 x exp (- 7640/T) g/cm2.s .atm k, = 1.51 x lo5 exp (-48,800p) k, = 21.3 exp (2060/T) g h 2 .s g/un2.s .
atm atm-' dation rate w (g C/cmZ.s): (+ + k*p02)x kBpo,(l - x) (1 1.41) 1 kz PO, where x is the fraction of the surface occupied by type A sites and is given by = (x = I+- PoykJ1 (11.42) The empirical rate constants determined by Nagle and Strickland-Constable for this model are listed in Table 11.10. According to this mechanism, the reaction is first order at low oxygen partial pressures, but approaches zero order at higher pressures.
At a given oxygen pressure, the rate initially increases exponentially with temperature (equivalent activation energy is kA/kz or 34,100 cal/mol). Beyond a certain temperature the rate decreases as the thermal rearrangement favors formation of less reactive B sites. When, at sufficiently high temperature, the surface is completely covered with B sites, the rate is first order in oxygen partial pressure and increases again with t e m p e r a t ~ r e . ~ ~ Park and leton' on'^ have compared this formula with oxidation rate data obtained from pyrographite samples, carbon black particles, and with the available flame soot oxidation data. Figure 11-49 shows both the soot oxidation rate predicted by Eqs. (11.41) and (11.42) as a function of temperature and oxygen partial pressure, and the above-mentioned data. The formula correlates the data shown to within a factor of 2.
Under diesel engine conditions, the 0, partial Pressure can be high (-several atmospheres), as can the temperatures of close-tostoichiometric mixtures (52800 K). Equations (11.41) and (11.42) have been used to estimate the amount of soot that can be oxidized in a typical ID1 diesel engine. It was assumed that soot was Present in stoichiometric combustion products at selected times in the cycle and that mixing with air leaned out the burned gas mixture at differentrates until the overall fuel/air equivalence ratio was reached. The surface recession rate during this Process was computed. Figure 11-50 shows sample results at an engine speed of 1600 rev/min and an overall cylinder equivalence ratio of 0.58. Fast, intermediate, and slow mixing occurred in 30, 70, and 140", respectively. The surface recession rate rises to a maximum as po2 increases and then decreases as the 644 INTERNAL COMBUSTION ENGINE FUNDAMENTALS I T,K 4000 3000 -1 I 1600 2000 I I 0.15 I } 1 I 1400 1200 I I I I Intermediate mixing rate Nagle and StricklandConstable formula Crank angle, deg (b) FIGURE 11-50 Soot particle burnup rate in diesel combustion environment: (a) in early- and late-burned fuel-air elements with intermediate mixing rate; (b)for fast and slow mixing for early-burning eleme~ts.~' c I -7 0.04. - 0.1 3 4 Lee, Thring, and Beer 5 6 8 7 9 x lo-4 Reciprocal temperature, K-' more important. For the late mixing element shown (mixing lean of stoichiometric at 40" ATC), the total carbon mass oxidized is only 40 percent of that for the early mixing calculation. This is due primarily to the decreasing gas temperatures as the expansion stroke proceeds, and not the longer time available for b ~ r n u p . * ~ For a spherical particle, the mass burning rate w (g/cm2.s) can be converted to a surface recession rate using Nagle and Strickland-Constable T = 2500 f 100 K o Soot radius ? = 4.5 nm .. A Soot radius f = 18 nm 0.1 1 10 Oxygen partial pressure pq, aim 100 FIGURE 11-49 Specific soot oxidation rate measurements and predictions as a function of temperature and oxygen partial pre~sure.'~ falling gas temperature more than offsets the increasing oxygen concentration. While the shape of the recession rate versus time curves depends on the mixing rate, the total amount of carbon burned (the area under each curve in Fig. 11-50b) is about the same (0.1 pg/mm2).
However, the point in the cycle at which the soot-containing burned gas mixture passes through stoichiometric is much where p is the density (FZ 2 g/cm3).The integrated values of w(t) when divided by p then give the maximum radius of a soot particle that can be burned up. Integrated values of 0.1 pg/mm2 (estimated for TC start of burnup) correspond to a radius of about 50 nm or diameter of 100 nrn. Individual spherule diameters are about 30 nm, so soot which mixes with air early in the expansion stroke is likely to be fully burned. Thus the soot present in the exhaust would be expected tp come from regions which mix with air too late for the oxidation rate to be sufficient for particle burnup. Agglomeration will have an indirect influence on the amount of soot oxidized through its effect on surface area. In the limiting case of a spherical cluster, n monodisperse spherules (10 5 n 5 100) can be imagined as compacted into a single solid sphere of equal volume. Alternatively, the same n spherules can be imagined compacted into a cylinder of diameter equal to that of the original spherules. Since oxidative attack is essentially an exterior surface phenomenon, the surface/volume ratio is the appropriate measure of the effect of particle shape on soot mass burnup rate. It can be shown that the surface/volume ratios for the 646 INTERNAL COMBUSTION ENGINE FUNDAMENTALS single sphere, cylinder, and individual spherule are in the ratio n-'I3, 3, and respectively. Thus agglomeration will decrease the relative oxidation rate. In th limit spherical clusters are less desirable than a chain; the larger the cluster th bigger the relative reduction in surface area. However, the densely packed spher ule limit does not appear to be approached in practice. A specific surface area, of about 200 m2/g for diesel soot, has been mea~ured.'~A smooth-surfaced 30-nm diameter spherule with a 2-g/cm3 density has a surface/mass ratio of 100 m2Ig; the measured value is about twice this value, indicating low porosity and an agglomerate structure which is loosely rather than densely packed.83 Equation (11.41) shows a maximum recession rate in combustion products corresponding to a fuellair equivalence ratio of about 0.9. Recent evidence shows that in an atmospheric pressure environment with rich and close-to. stoichiometric combustion products where 0, mole fractions are low, oxidation by OH radical attack is much more significant than oxidation by 0 or 0,. The OH radical may be important in oxidizing soot in the flame zone under close-to. stoichiometric conditions. 115.6 Adsorption and Condensation The final process in the particulate formation sequence illustrated in Fig. 11-46 is adsorption and condensation of hydrocarbons. This occurs primarily after the cylinder gases have been exhausted from the engine, as these exhaust gases are diluted with air.
In the standard particulate mass emission measurement process this occurs in a dilution tunnel which simulates approximately the actual atmospheric dilution process. A diluted exhaust gas sample is filtered to remove the particulate. After equilibrating the collection filter at controlled conditions to remove water vapor, the particulate mass is obtained by weighing. In the prescribed EPA procedure, the Alter temperature must not exceed 52•‹C.For a given exhaust gas temperature, the filter (and sample) temperature depends on the dilution ratio, as shown in Fig. 11-51. The effect of the dilution ratio (and the dependent sample temperature) on collected particulate mass is shown in Fig. 11-52 for a standard dilution tunnel, m0 2 4 6 8 Dilution ratio 1 J 0 FIGURE 11-51 Effect of exhaust gas dilution ratio on the temperature of the collected particulate sample as a function of engine exhaust temperature T,." Dilution ratio FIGURE 11-52 Typical effect of dilution ratio on particulate mass emission and its partitioning between extractable and nonextractablefractions.'O where the total sample is partitioned into extractable and nonextractable fractions. The nonextractable fraction is the carbonaceous soot generated during combustion and is not affected by the dilution process. With no dilution (dilution ratio of unity) the difference between the total and nonextractable mass is small; the bulk of the extractable fraction is acquired after the exhaust gas is mixed with dilution air. Extensive studies of this dilution process have shown that both adsorption and condensation occur.
Adsorption involves the adherence of molecules of unburned hydrocarbons to the surfaces of the soot particles by chemical or physical (van der Waals) forces. This depends on the fraction of the available particle surface area occupied by hydrocarbons and on the partial pressure of the gaseous hydrocarbons that drives the adsorption process. As the dilution ratio increases from unity, the effect of decreasing temperature on the number of active sites dominates and, as shown in Fig. 11-52, the extractable fraction increases. At high dilution ratios, the sample temperature becomes insensitive to the dilution ratio (see Fig. 11-51) but the decreasing hydrocarbon partial pressure causes the extractable mass to fall again. Condensation will occur whenever the vapor pressure of the gaseous hydrocarbon exceeds its saturated vapor pressure. Increasing dilution decreases hydrocarbon concentrations and hence vapor pressure. However, the associated reduction in temperature does reduce the saturation pressure. High exhaust concentrations of hydrocarbons are the conditions where condensation is likely to be most significant, and the hydrocarbons most likely to condense are those of low volatility. Sources of low-volatility hydrocarbons are the high-boiling-point end of the fuel, &burned hydrocarbons that have been pyrolyzed but not consumed in the combustion process, and the lubricating oil." Experiments with a passenger car ID1 diesel, where the oil was tagged with a radioactive tracer, have shown that the oil can contribute from 2 to 25 percent of the total particulate mass, with the greatest contribution occurring at high speed. On average, over half of the extractable mass was traceable to the oil. All the material traceable to the oil was found in the extractable fraction, indicating that the oil did not participate in the combustion process. However, the oil is not POLLUTANT FORMATION AND always a significant contributer: in another engine, fuel was the dominant soul of extractable material.'O* " 11.6 EXHAUST GAS TREATMENT 11.6.1 Available Options Our discussion so far has focused on engine emissions. Further reductions in emissions can be obtained by removing pollutants from the exhaust gases in the engine exhaust system. Devices developed to achieve this result include catalytic converters (oxidizing catalysts for HC and CO, reducing catalysts for NO,, and three-way catalysts for all three pollutants), thermal reactors (for HC and CO), and traps or filters for particulates. The temperature of exhaust gas in a spark-ignition engine can vary from 300 to 400OC during idle to about 900•‹C at high-power operation.
The most common range is 400 to 6WC. Spark-ignition engines usually operate at fuellair equivalence ratios between about 0.9 and 1.2 (see Sec. 7.1). The exhaust gas may therefore contain modest amounts of oxygen (when lean) or more substantial amounts of CO (when rich). In contrast, diesel engines, where load is controlled by the amount of fuel injected, always operate lean. The exhaust gas therefore contains substantial oxygen and is at a lower temperature (200 to 500•‹C).
Removal of gaseous pollutants from the exhaust gases after they leave the engine cylinder can be either thermal or catalytic. In order to oxidize the hydrocarbons in the gas phase without a catalyst, a residence time of order or greater than 50 ms and temperatures in excess of 600•‹C are required.
To oxidize CO, temperatures in excess of 700•‹C are required. Temperatures high enough for some homogeneous thermal oxidation can be obtained by spark retard (with some loss in efficiency) and insulation of the exhaust ports and manifold. The residence time can be increased by increasing the exhaust manifold volume to form a thermal reactor (see Sec. 11.6.3). However, this approach has limited application. Catalytic oxidation of CO and hydrocarbons in the exhaust can be achieved at temperatures as low as 250•‹C. Thus effective removal of these pollutants occurs over a much wider range of exhaust temperatures than can be achieved with thermal oxidation. The only satisfactory method known for the removal of NO from exhaust gas involves catalytic processes. Removal of NO by catalytic oxidation to NO, requires temperatures p, .I That two different definitions of indicated output are in common use follows from two different approaches to determining friction work or power. In the standard engine test code procedures2 friction power is measured in a hot motoring test: the engine is motored with water and oil temperatures held at the firing engine values, with the throttle setting unchanged from its firing engine position (in an SI engine). This measures (approximately) the sum of pumping, rubbing friction, and auxiliary power.
The sum of brake power, and friction power determined in this way, is the gross indicated power. Alternatively, when an accurate record of cylinder pressure throughout the whole cycle is available, pumping power can be determined directly: the sum of rubbing friction and accessory power is then the difference between the net indicated powerdetermined from !p dV over the whole cycle-and the brake power. For the reasons explained in Sec. 2.4, the gross indicated output is preferred and used in this text. The distinction is most important for SI engines at part load where the pumping power and rubbing friction power are comparable in magnitude. For unthrottled engines at low speeds, the distinction becomes less important (Fig. 13-1 shows the relative importance of pumping work under both these conditions). 133 FRICTION FUNDAMENTALS The friction losses outlined in Sec.
13.1 can be classified into two groups, depending on the type of dissipation which occurs. One type is friction between two metal surfaces in relative motion, with a lubricant in between.
The other type is turbulent dissipation. 133.1 Lubricated Friction A primary problem in understanding friction between lubricated surfaces in engines is the wide variation in the magnitude of the forces involved.
Thus BJ 7 716 ENGINE FRICTION AND LUBRICATION INTERNAL COMBUSTION ENGINE FUNDAMENTALS 717 Oil I Load 7 .-LZJ-q Li F=F Supporting oil film Hydrodynamic lubrication , Mixed lubrication + Boundary lubrication Bearing Supporting oil film FIGURE 13-2 Schematic of a lubricated journal and a slider bearing. various regimes of lubrication can occur.
Figure 13-2 shows the operating con&tions of two common geometries for lubricated parts: a journal and a slider bearing.
The different regimes of lubricated friction can be illustrated by means of the Stribeck diagram shown in Fig. 13-3, where the coefficient of friction f (tangential force/normal force) for a journal bearing is plotted against a dimensionless duty parameter pN/a, where p is the dynamic viscosity of the lubricant, N is the rotational speed of the shaft, and a is the loading force per unit area. For sliding surfaces the dimensionless duty parameter becomes pU/(ob), where U is the relative velocity of the two surfaces and b is the width of the sliding pad in the direction of motion. The coefficient of friction can be expressed as f = a f , + (l . where f, is the metal-to-metal coefficient of dry friction,fL is the hydrodynamic coefficient of friction, and a is the metal-to-metal contact constant, varying between 0 and 1. As a + 1,f +f, and the friction is called boundary, i.e., close to solid friction. The lubricating film is reduced to one or a few molec

control piston temperatures by assisting in heat transfer to the cylinder walls and coolant. Automobile engines normally use three rings, though two-ring designs exist. Larger diesel engines may use four rings. Many designs of compression ring are employed,13 the differences between them being in the cross-sectional shapes (and hence relative flexibility) and in their use of wear-resistant surface treatments. Top compression rings are usually made of cast iron. The axial profiles are chosen to facilitate hydrodynamic lubrication. Common shapes are a rectangular cross section with inner and outer edges chamfered to prevent sticking in the groove, or with a barrel-shaped working surface which can accommodate the rotation of the piston which occurs with short piston skirts. Wear-resistant coatings (either a hard chromium-plated overlay or a molybdenum-filled inlay) are usually applied to the outer ring surface. The second compression ring serves principally to reduce the pressure drop across the top ring. Since the operating environment is less arduous, the 730 INTERNAL COMBUSTTON ENGINE FUNDAMENTALS second ring can be made more flexible to give better oil control. The objective i to compensate for the torsional deflection of the ring under load so that topedg contact with the cylinder liner is avoided. Top-edge contact tends to pump toward the combustion chamber, detracting from the performance of the oil control ring. Bottom-edge contact provides an oil scraping action on the down. stroke. The oil control ring meters and distributes the oil directed onto the cylinder liner by the crankshaft system, returning excess oil to the crankcase sump. it must exert ~ ~ c i epressure nt against the cylinder, possess suitably shaped wiping edges (usually two thin steel rings), and provide adequate oil drainage. Slotted or composite rings are normally used.14 The tension in all the piston rings holds them out against the cylinder wall and hence contributes to friction. The gas pressure behind the compression rings increases this radial force. The gas pressures behind the second ring are substantially lower than behind the first ring. The gas pressures behind the rings are a function of speed and load. An approximate rule for estimating ring friction is that each compression ring contributes about 7 kPa (1 lb/in2) mep.' Oil rings, due to their substantially higher ring tension, operate under boundary lubrication; they contribute about twice the friction of each compression ring." The piston assembly is the dominant source of engine rubbing friction. The components that contribute to friction are: compression rings, oil control rings, piston skirt, and piston pin. The forces acting on the piston assembly include: static ring tension (which depends on ring design and materials); the gas pressure forces (which depend on engine load); the inertia forces (which are related to component mass and engine speed). The major design factors which influence piston assembly friction are the following: ring width, ring face profile, ring tension, ring gap (which governs inter-ring gas pressure), liner temperature, ringland width and clearances, skirt geometry, skirt-bore ~learance.~, Piston assembly friction is dominated by the ring friction. The forces acting on a typical compression ring, lubricated by a thin oil film, are shown in Fig. 13-18. The analysis of this hydrodynamic contact is complex because the forces acting on the ring vary with time and slight changes in ring face geometry can have large effects on the computed results. Cylinder pressure p, normally acts on the top and back of the ring. The inter-ring gas pressure p , (which depends on cylinder pressure and the geometry of the lands, ring grooves, and ring, especially the ring gap), acts on the oil film and bottom part of the ring. The character of the gas flow into and out of the inter-ring regions and its effect on ring motion were discussed in Sec. 8.6. Late in the expansion stroke, pressure reversals can occur which may cause the ring to move to the upper surface of the groove or to flutter in between.
Ring tension acts to force the ring against the liner. The pressure in the lubricating oil film is generated as shown by the surface A-B in Fig. 13-18 as the ring moves downward. It is believed that the film cavitates between B and C so the pressure decreases to a low value and then increases to p,. When the direction of motion is reversed, C-B becomes the pressure-generating surface. Models for the ring and oil film behavior have been developed. For the practical case where the oil film thickness h is much less than the ring width, the Combustion chamber FIGURE 13-18 Schematic of pressure distribution in the lubricating oil film and around a compression ring during expansion stroke. Pressure profile in the oil film indicated by horizontal shading.' Navier-Stokes equation for the liquid film motion reduces to a Reynolds equation of the form : (13.14) where h is the local film thickness, p the liquid viscosity, and U the relative velocity between the two surfaces. This equation, along with the appropriate force balances on the ring, can then be solved for the coupled film and ring behavior (e.g., see Ref. 15). Measured oil film thicknesses in an operating direct-injection diesel engine are shown in Fig. 13-19. A capacitance technique with electrodes embedded in the top compression ring was used to make the measurements.16 At topcenter during combustion, the thickness is a minimum (x 1 F); it then increases as gas loading on the rings decreases and piston velocity increases during the expansion stroke to a value an order of magnitude higher. Higher engine load results in higher gas loading on the rings. It also results in higher lubricant temperatures and lower viscosity, which reduce the film thickness during intake, compression, and exhaust.
This large change in film thickness over one cycle is the reason the ring friction regime changes from boundary lubrication to thick-film hydrodynamic lubrication. When the oil film thickness drops below about 1 m, asperity contact will begin.? An analysis of the side thrust between the piston and cylinder wall helps explain piston design trends. A force balance on the cranklconnecting rod mechanism of Fig. 2-1 leads to the following. An axial force balance relates the piston t The critical film thickness depends on both the cylinder liner and ring surface finish. ENGINE FRICTION AND LUBRICATION 733 ,No load (ro = 10.5 mm2/s) Half load (vo = 9.5 mm21s) / \ ,Gas pressure Half load -300 Crank angle, deg FIGURE 13-19 F, Rings done without pressure 6 Rings alone with compression pressure Fj Ring belt body alone Measured oil film thickness between top ring and cylinder liner of a DI diesel engin 1300 rev/min. Bore = 139.7 mm, stroke = 152.4 mm.v, is estimated oil viscosity. mission of the Society of Tribologists and Lubrication Engineers (STLE), formerly the American Society of Lubrication Engineers (ASLE).16 -270 -180 -90 0 90 180 270 Crank angle, deg mass m and acceleration to the net axial force: FIGURE 13-20 Measured frictional force on cylinder liner of 137 rnm bore and 135 mm stroke single-cylinder DI diesel engine. 1200 rev/min, coolant temperature 80"C,cylinder liner inside temperature 97"C.18 where 4 is the angle between the cylinder axis and connecting rod, and p is the rvlinder onaooe nressure. A transverse force balance gives dS nB2 F, = F, sin 4 = (- ~ - $ + , P T F , Here F, is the force in the connecting rod (positive when in compression) and F, is the friction force on the piston assembly (- when piston is moving toward the crank; + when piston moves away from the crank). dSJdt is the piston acceleration obtained by differentiating the equation for piston velocity [Eq. (2.1 l)] : dS dt 2= d2s = dt2 + RZ cos 28 (R2 - sin2 The side thrust F, given by Eq. (13.16) is transmitted to the liner vi rings and piston skirt. It changes direction as the piston passes through t o p and bottom-center positions. Since the friction force changes sign at these locations and the gas pressure during expansion is greater than during compression, the side thrust during expansion is greater. The piston skirt carries part of this side thrust so it contributes to piston assembly friction. The large contact area between the skirt and liner, relative to the ring contact area, results in lighter loading (forcetarea) and promotes hydrodynamic lubrication. Piston skirt areas have been reduced substantially in recent years to reduce piston mass (which reduces side thrust) and contact area. An additional reduction in side thrust, leading to reduced skirt friction, has been achieved with the use of an offset wrist-pin. By offsetting the pin axis by 1 to 2 mrn without changing its vertical location, the crank angle at which the piston traverses the bore and "slaps" the other side of the cylinder is advanced so it occurs before combustion has increased the cylinder gas pressure significantly." Direct measurements of the friction force associated with the piston assembly have been made. The most common technique involves the use of a special engine where the axial force on the cylinder liner is measured directly with a load transducer (e.g., Ref 18). Figure 13-20 shows the friction forces measured in such an engine (a DI diesel enpine) through the engine's operating cycle. Friction forces are highest just before and after top-center at the end of the compression stroke. The high values at the start of the expansion stroke under firing conditions are caused by the piston slap impulse and the high side-thrust force as well as the combustion gas pressure loading on the rings. Bishop" has developed correlations for piston and ring friction in the following categories: boundary condition friction (primarily between the rings and 734 iNTERNAL m M B u s n o N ENGINE FUNDAMErnALS ENGINE FRICTION AND LUBRICATION 735 the cylinder wall due to ring tension, and gas pressure behind the compression rings) and viscous ring and piston friction. He argued that boundary condition friction was primarily due to breakdown of the oil film between the rings and cylinder wall over part of the piston travel. Assuming that the transition to boundary lubrication occurred at a critical speed, he showed that fmep due to boundary friction was proportional to stroke/bore2,i.e.: (fmep),,d,, a loading x L BZ The ring loading has two components. The component due to ring tension is essentially constant. The component due to gas pressure behind the rings will depend on load. Bishop assumed it to be proportional to inlet manifold pressure. The viscous piston friction-friction between the piston and rings and cylinder wall under hydrodynamic lubrication conditions-was correlated by FIGURE 13-21 (he~Ayd,yn a S A Schematic of hydrodynamically lubricated journal bearing.3 ,eff pLi2 where A , eff is the effective area of the piston skirt in contact with the cylinder liner. The relative importance of the boundary lubrication piston and ring friction, and viscous piston and ring friction over the load and speed range, is as follows. The viscous friction component increases in importance with increasing speed. The boundary lubrication friction component increases with increasing load as the cylinder gas pressures increase. 13.6.4 Crankshaft Bearing Friction Crankshaft friction contributions come from joumal bearings (connecting rod, main and accessory or balance shaft bearings) and their associated seals. A schematic of a journal bearing operating under hydrodynamic lubrication is shown in Fig. 13-21. Large loads can be camed by journal bearings with low energy losses under normal operating conditions, due to the complete separation of the two surfaces in relative motion by the lubricant film. Loads on crankshaft journal bearings vary in magnitude and direction because they result primarily from the inertial loads of the piston/connecting rod mechanism and the cylinder gas loads [see Eq. (13.15)]. Typical loads and the resulting journal eccentricity diagram for a connecting rod bearing are shown in Fig. 13-22. From the journal eccentricity diagram the minimum oil film thickness is determined. This quantity, the minimum separation distance between the journal and bearing surfaces, is a critical bearing design parameter. If the 6lm thickness is too low, asperities will break through the oil film and substantially increase the friction and wear. Journal bearings are usually designed to provide minimum film thicknesses of about 2 lun. Lacation of minimum oil film thickness Polar load diagram for Connecting rod bearing Ecceaeicity of journal in wnnecting rod bearing ElGURE 13-22 Typical engine journal bearing load and eccentricity diagrams3 736 ENGINE FRICTION AND LUBRICATION INTERNAL COMBUSTION ENGINE FUNDAMENTALS The friction force F, in the bearing is given approximately by the product nf the hearing area the oil viscositv. and the mean velocity nradient in the oil: ~ y p k oHC, direct-acting OHC, I).pe U:end pivot rocker 737 m OHC,m: center pivot mcker where Db and Lb are the bearing diameter and length, i is the mean radial clearance, and N is the shaft rotational speed. A more sophisticated analysis of the friction in a hydrodynamically lubricated bearing yields the relationlg lypc IV: OHC, center pivot rocker with lifter Qpe v: push rod where E is the eccentricity ratio (fi - h3/6 and h, is the minimum clearance. The first term closely matches the approximation given in Eq. (13.20). The factor 1/(1 - ez)'/z and the second term correct for the offset of the journal center relative to the bearing center: W is the bearing load and 4 the attitude angle. To first order, with hydrodynamic lubrication the friction power does not depend significantly on the bearing load. If a is the loading per unit projected area of the bearing TWNL DA1. then the coefficient of frictionf is given by FIGURE 13-23 Different valve train c~nfigurations.~' For a given bearing, or series of geometrically similar bearings, the friction coefficient is proportional to pN/a. However, at low values of pN/a the hydrod pressure in an actual bearing will be insufficient to support the shaft load and the oil film becomes incomplete. The friction coefficient increases rapidly as mixed lubrication then occurs. Bishop" summed the friction power loss in all crankshaft and con rod journal bearings and divided by the displaced volume per unit time to obtain the following correlation for bearing friction mep (in kilopascals): fmep (bearings) = 41.4 (:)-(LO)- where In Eq. (13.24), Dmb is the main bearing diameter, L,, the total main bearing length t number of cylinders, D,, the rod bearing diameter, Lrb the rod bearing length, m the number of pistons per rod bearing, D, the accessory shaft bearing diameter, L, the total length of all accessory shaft bearings + number of cylinders, and all dimensions are in millimeters. The similarity between engines is such that K x 0.14 for spark-ignition engines and K x 0.29 for diesel engines. The front and rear main bearing sealsZ0 also contribute to crankshaft assembly friction. At 1500 rev/min they are responsible for about 20 percent of the friction attributable to the crankshaft.1•‹ 13.65 Valve Train Friction The valve train carries high loads over the entire speed range of the engine. Loads acting on the valve train at lower speeds are due primarily to the spring forces, while at higher speeds the inertia forces of the component masses dominate. Valve train designs can be classified by type of configuration, as indicated in Fig. 13-23.
Large valves and high rated speeds generally increase spring and inertia loads and friction. Friction differences between these systems are difficult to quantify. For example, measurements of valve train friction mean effective pressure for several of these valve train types showed signilkant variations (+ 30 percent): see Fig. 1 3 - 2 4 ~ . ' ~However, .~~ when the data were adjusted to a common spring load, Fig. 13-246, the low-speed friction mep values converged and the high-speed fmep differences were reduced. l o The total valve train friction can be broken down by critical contact regions: camshaft journal bearings, rocker arm/fulcrum and cam/tappet interface. 738 INTERNAL COMBUSTION ENGINE FUNDAMENTALS ENGINE FRICTION AND LUBRICATION 40- 739 rocker arm fulc~um~ .-----m-tcnsion, low-mass Roller followers (tappets) Valvespring and retainers gk 105 - O,- 0 0 1A *& 4d00 5d00 3d00 Engine speed, mrlmin (4 I I I I 2000 3000 4000 Engine speed, d m i n 1000 5000 (b) FIGURE 13-24 (a) Total valve train friction mean effective pressure as a function of speed for four engines with different valve configurations (see Fig. 13-23). (b)Valve train friction torque for three of these engines after adjusting to common valve spring load.1•‹ The shape of the valve train mep versus speed curve indicates that the predominant regime of lubrication in the valve train at lower engine speeds is boundary lubrication. The -/lifter interface usually contributes the largest friction loss due to the very high loads and small contact areas." Effective methods of reducing valve train friction are: (1) spring load and valve mass reduction; (2) use of tappet roller cam followers; (3) use of rocker arm fulcrum needle bearings. One such low-friction valve train design is shown in Fig. 13-25.22The roller cam-followers provide the largest benefit especially at lower speeds: reductions of order 50 percent in valve train friction can be achieved. Bishoplz developed a correlation for valve train friction from design data on valve spring loads and valve weights, and experimental data from dynamometer tests of push rod engines. He shows that fmep (valve train) = C[1 - 0.133(N/1000)]niv Dk7' B~L where niv is the number of inlet valves per cylinder, Div is the inlet valve head diameter, and B and L are bore and stroke. This relation does not include camshaft bearing friction, which is included in Eq. (13.23). The functional form of Eq. (13.25) is an acceptable fit to more modem engine data. Bishop's value for C (1.2 x 104 with fmep in kilopascals, N in revolutions per minute, and dimensions in millimeters) gives valve train fmep values (which exclude camshaft bearing losses) about two-thirds the total valve train friction of current production engines. This is consistent with the data in Fig. 13-24. LOW friction valve train.12 13.7 ACCESSORY POWER REQUIREMENTS The coolant water pump and oil pump are built-in accessories, essential to engine operation, and are normally considered part of the basic engine.2 A fully equipped engine usually includes additional accessories-a fan and generator; in automobile use it often includes a power-steering pump, an air conditioner, and an air pump for emission control. The power delivered by the fully equipped engine (the net power) is lower than the power delivered by the basic engine due to the power requirements of these additional accessories. The friction mean effective pressures associated with driving the water pump and alternator, and oil pump are shown in Fig. 13-14a. Together they comprise about 20 percent of the total (motored) engine friction. The water pump is typically less than about 7 kPa at 1500 rev/min;1•‹the oil pump 4 to 10 kPa at this speed;" the alternator requires 7 to 10 kPaeZ3These numbers vary significantly with component design details. The generator power depends on the electrical load to be met and the generator blower design. A requirement of about two-thirds of the peak is indicated for average generator power.23 The power requirements for a fan, generator, and power-steering pump typical of a 5.7-liter engine are shown in Fig. 13-26.
The fan requirements are the largest and with a direct drive increase with the cube of the speed. Alternative couplings such as a viscous drive reduce the fan speed at high engine speed and thereby reduce its power significantly.
The power-steering pump is only required to provide high pressures intermittently. Here only the fluid pumping losses are charged against the engine. Air-conditioning is standard on a majority of U.S. cars; additional power is required for the air-conditioning compressor. Also, since the compressed refrigerant is condensed in a second radiator, a larger-than-standard fan is required to pull additional air through the combined radiator systems. An air pump which pumps air into the engine exhaust ports may be part of an SI engine emission INTERNAL COMBUSTION ENGINE FUNDAMENTALS ENGINE FRICTION AND LUBRICATION ! I I ! FIGURE 13-26 Power requirements for engine fan, generator, and power-steering pump typical of 5.7-liter eightEngine speed, revlmin cylinder 24 control system (see Sec.
11.6). Its power requirements (- 1 kW at normal engine speeds) must then be added to the accessory friction requirements. 1 sump 2 Suction pipe 3 Lube oil pump 4 O i l pressure control valve 5 Pressure pipe 6 Bypass pipe or alternative 7 Cooling coil or, alternatively: 8 Block-type oil cooler 9 Oil filter 10 Safcty valve 11 Main oil gallety 12 Main be-g 13 Big end bearing 14 Camshaftbearing 15 lhppet (with timing groove to pulse-lubricaterocker arm) 16 Push rod (hollow, used as rocker arm oil feed pipe) 17 Rocker arm bearing 18 Metering plug (to control valve lubrication) 19 Push rod duct (used as cylinder-head-to-crankcase oil return pipe) 20 Splash hole to lubricate timing gears 741 21 Fi8ton cooling nozzle 22 Oil prrssure gauge adaptor 23 Oil pressure gauge FIGURE 13-27 13.8 LUBRICATION Lubrication system layout for air-cooled DI diesel engine. (Courtesy Kliiekner-Humboldt-Deutz AG.) The lubricant and the lubricating system perform the following functions:25 1. Reduce the frictional resistance of the engine to a minimum to ensure maximum mechanical efficiency. 2. Protect the engine against wear. 3. Contribute to cooling the piston and regions of the engine where friction work is dissipated.
4. Remove all injurious impurities from lubricated regions. 5. Hold gas and oil leakage (especially in the ring region) at an acceptable minimum level. through the tappets and pushrods. For cooling pistons and lubricating cylinders, oil is thrown against the underside of the piston through nozzles connected to the main bearings. Spring-loaded ball valves incorporated in the nozzles interrupt the jet cooling at low engine speeds to insure that the oil pressure remains above a safe level. The gears of the main timing train are splash-lubricated. The oil is returned from the injection pump and rocker chamber cover to the sump. 13.8.2 Lubricant Requirements 13.8.1 Lubrication System Table 13.1 lists the qualities required of engine oils to perform the main lubrication system functions. These qualities can be summarized under the following headings.25 The principle moving parts of an engine are positively lubricated by introducing a supply of oil from a pressurized system. An example of a lubrication system (for an air-cooled diesel engine) is shown in Fig. 13-27. The oil pump draws oil from the engine sump and delivers it through a control valve to the oil cooler. The oil then passes through the filter to the main oil gallery. From the main oil gallery it is branched to the main, the big end, and the camshaft bearings. Oil is also ducted to the injection pump. Through a passage in the camshaft bearing the oil flows to the tappet bridges. As the oil passages of tappets and tappet bridges line up during tappet motion, rocker arms and valve stems are pulse-lubricated OXIDATION STABILITY. The temperature of the oil and engine parts it contacts, the presence of oxygen, the nature of the metal surfaces and debris, and the products of the fuel combustion, all influence the oxidation of the hydrocarbon components in lubricating oil. High temperatures are the primary factor, and the top piston ring groove and the crankcase are the critical regions.
The temperature of the top ring groove can easily reach 250•‹C.The lubricating oil when subject to these conditions must not, through oxidation, contribute to deposit formation, even after long periods of running. These deposits would eventually TABLE 13,1 ENGINE FRICTION AND LUBRICATTON 743 Functionsi and qualities required of engine oils r e q a Where md when Q11.litics required Reduce frictional resistance During cold-starting Low enough viscosity to provide good and avoid undue cranking resistance Minimum viscosity without risk of metal-to-metal contact under the varying conditions of templratn, speed, and load S~•'6cientlyhigh viscosity at high temperatures; good lubrication property outside the hydrodynamic condition. esoecialli - .at toPcenter Antiseizure properties, especially during the run-in period Protect against corrosion and wear Between con-rod/ crankshaft bearings, and journals Between pistons, rings, and cylinders During shutdown or when running at low temperature In normal running Assist sealing In the ring zone, especially at TC DETERGENCY/DISPERSION.
Except for deposits formed in the combustion Must protect metallic surfaces against corrosive action of fuel decomposition products (water, SO,, HBr, HCI, etc.) Must resist degradation (resist oxidation, have good thermal stability) Must counteract action of fuel and lubricant decomposition products at high temperatures, especially on non-ferrous metals By intervention in the friction mechanism must reduce the consequences of unavoidable metal-tometal contact Must resist deposit formations which would affect lubrication (detergency or dispersive action) Must contribute to the elimination of dust and other contaminants (dispersive action) chamber, deposits in the oil are controlled by its detergency. The amount of deposits formed depends on the fuel used, the quality of combustion, the temperature of the lubricating oil and coolant, and on the effectiveness of gas sealing at the piston rings. The detergency property is given to straight mineral oils by additives; the function of the detergent additive is to reduce the amount of deposits formed and make their removal easier. At low temperatures, deposits are mainly byproducts of fuel combustion, and the detergency function is to keep them in suspension or solution in the oil. At high temperatures, deposits come from the oxidized fractions of the oil. The detergency function here is both to keep these products in suspension and to inhibit the reactions that lead to the formation of varnishes and lacquers. In addition, in diesel engines, the detergency helps in neutralizing the acidic reaction products from the sulfur compounds in the fuel. Must have sufficient viscosity at high temperatures and low volatility Must limit ring and liner wear Must not contribute to formation of deposits in ring grooves and must prevent such formation Contribute to cooling - Chiefly of pistons, rings, and con-rod bcarlngs Must have good thermal stability and oxidation resistance Must have low volatility Viscosity must not be too high Facilitate the elimination of undesirable products During oil drains to eliminate atmospheric dust, soot from diesel engines, Pb salts, wear debris, organic products from burned fuel and lubricants, and other contaminants which promote deposits or accelerate wear Must be able to maintain in fine suspension all solid material (dispersivity)whatever the temperature and physical and chemical conditions (water) Must be able to solubiize certain organic compounds, particularly heavy oxidation products Source: From Schilling." lead to ring sticking which results in excessive blowby. At high temperatures, deposits are related to the oxidized fraction of the oil. The oil temperature in the crankcase is 120 to 130•‹C,or higher. Oil maintained at this temperature should neither form any acid products capable of attacking the bearing alloys nor form insoluble products which form deposits. Good-quality mineral oils cannot withstand these temperatures, so antioxidant and anticorrosive additives are used to control these problems. While antioxidants help to reduce deposit formation, detergentldispersant additives are required to maintain any insoluble materials formed through oxidation in suspension. Z WEAR REDUCTION. Wear is due to the individual and combined effects of corrosion, adhesion (i.e., metal-to-metal contact), and abrasion. Corrosive attack by acidic products of combustion is one of the chief causes of cylinder and ring wear. The effect is worst at low cylinder wall temperatures.
In diesel engines, the sulfur in the fuel increases the corrosive wear. Corrosive wear is effectively prevented by the use of detergent oils which neutralize the corrosive acids as they form, and by designing the cooling system to give appropriate metal temperatures.
Adhesive wear affects certain parts of the engine. In the upper cylinder, metal-to-metal contact between piston, rings, and cylinder walls takes place each time the engine is started (most significant during cold-starts) because there is i n ~ ~ c i e oil n t in the top portion of the engine. Oils with antiwear additives and low viscosity at low temperatures provide a partial remedy. Adhesive wear also occurs on components such as cams, tappets, drive gears, rocker arm ends, and valve stems. Abrasion results from the presence of atmospheric dust, and metallic debris from corrosive and adhesive wear, in the lubricating oil. Efficient air filtration is therefore most important (see Ref. 26 for a discussion of air filters). Elimination of 744 ENGINE FRICTION AND LUBRICATTON INTERNAL COMBUSTION ENGINE NNDAMENTALS 745 abrasive particle impurities from the oil system by filtration and periodic oil change is essential. For low resistance to cranking and ease of starting, and rapid distribution of the oil while the engine is cold, a low oil viscosity at low ambient temperatures is required.
When the engine (and oil) is fully warmed up, viscosity in the proper range is important for adequate sealing of the piston, acceptable oil consumption, and low friction losses. The viscosity of the oil at both low and normal engine temperatures (a spread of some 200 K) is, therefore, important. The viscosity of lubricating oils decreases with increasing temperature. The pour point, viscosity, and viscosity index are used to characterize the behavior of a lubricating oil for these aspects of engine operation. The pour point is determined by cooling a sample of oil in a test jar until, when the jar is rotated from the vertical to the horizontal, no perceptible movement of the oil will occur within 5 s; 5•‹F above this temperature is the pour point. The viscosity of lubricating oils is determined by measuring the time required for a specified volume of oil to flow through a capillary tube or orifice, contained in a constant temperature water bath.
The kinematic viscosity, v (v = PIP),is determined by this method. Use of a Saybolt tube with an orifice of specified diameter is the standard U.S. measurement practice. The viscosity is then given by the time t (in seconds) required to flow 60 cm3 of oil, and is expressed as Saybolt universal seconds, SUS. Approximate conversion to centim2/s)can be obtained via stokes (1 centistoke = VISCOSITY. v=at-- b t where for 115 > t > 34 s, a = 0.224 and b = 185; for 215 > t > 115 s, a = 0.223 and b = 155; and for t > 215 s, a = 0.2158 and b = 0." The viscosity of lubricating oils decreases with increasing temperature. Since engine oils must operate over a range of temperatures, a measure of the rate of decrease is important. The viscosity index, an empirical number indicating the effect of temperature changes on viscosity, is used for this purpose;" a low viscosity index indicates a relatively large change of viscosity with temperature.
To increase the viscosity index, lubricating oils incorporate additives called "viscosity-index improvers." These are high molecular weight compounds (molecular weight = lo3 to lo4) whose primary function is to reduce the viscosity variation with temperature. The lubricating oil classification used most extensively is the SAE classificati~n.?~ It depends solely on the viscosity of the oil. The seven different classification numbers 5W, low, 20W, 20, 30, 40, and 50 correspond to viscosity ranges; increasing numbers correspond to increasing viscosity, as shown in Fig. 13-28. SAE numbers followed by W (abbreviation for winter) refer to oils for use in cold climates, and viscosity is determined at -18•‹C(0•‹F). SAE numbers without W are applied to engine oils commonly used under warmer conditions; 3 2 -34 0;. -18 a , , 0 20 1 . , 40 60 ,.I 80 100 b ~ m p e OC~ , ,.I, Viscosity versus temperature curves illustrating SAE lubricating oil classilicati~n.'~ they are based on viscosity at 99•‹C (210•‹F). Multigrade oils (for example, 10W-40) satisfy service requirements at low as well as high temperatures in terms of the SAE classification. The first number indicates the viscosity at - 18•‹C;the second number at 99•‹C.Examples are shown in Fig. 13-28. Multigrade oils have a higher viscosity index than single-grade oils, which make them more attractive for engine use. PROBLEMS 13.1. (a) Show how friction mean effective pressure for a four-stroke cycle engine can be obtained from the brake power P,, engine speed N, displaced volume V,, and p dV over the compression and expansion strokes (= W,,,,). (b) How is pumping mean effective pressure related to j p dV over the compression and expansion strokes and j p dV over the full four-stroke cycle? (c) Find the brake power, total friction power, total friction imep, and pumping imep for a fourstroke cycle SI engine operating at 1800 rev/min with a measured brake torque of 32 N.m, a gross imep of 933 kPa, and a net imep of 922 k P a V, = 0.496 dm3. 13.2. Three categories of friction are described in Sec. 13.3: boundary friction, hydrodynamic (or fully lubricated) friction, and turbulent dissipation. By means of Eq. (13.6), estimate the relative proportion of total friction work per cycle in each category for a fourcylinder automobile spark-ignitionengine operating at 3000 revtmin. 133. For four-stroke cycle naturally aspirated multicylinder spark-ignition and diesel automobile engines at full load and one-third full load, at mid speed (2000 revlmin), give approximate estimates of the percentages of total friction mep in these three categories: pumping mep, rubbing friction mep, and accessory friction mep.
State explicitly how you develop these estimates and what you include as accessories. INTERNAL COMBUSTION ENGINE FUNDAMENTALS All of the friction measurement procedures except the differencebetween brake and gross indicated power or mep measured directly assume that motored engine friction and firing engine friction are closely comparable. This is not an accurate assumption for the pumping component. Summarize the differences between the gas exchange processes under motoring and firing conditions for a spark-ignition engine at a fixed part-load throttle setting that will result in the pumping work being significantly different under these two conditions. On separate accurately proportioned sketches of the piston, cylinder, connecting rod, and crank mechanism (similar to Fig. 2-I), during the intake stroke (at 120' ATC), compression stroke (at 60"BTC), expansion stroke (at 60' ATC), and exhaust stroke (at 120" BTC), draw an arrow for each of the forces acting on the piston (pressure forces, force from connecting rod, friction force, inertia force).
Mark clearly the positive direction of each force.
Express each force in terms of cylinder pressure p,, crankcase pressure p,, ,friction force F,, piston area A,, effective piston (and part of connecting rod) mass m,, piston acceleration a, connecting rod force F,. (a) For the DI diesel engine for the friction force data in Fig. 13-20, estimate the maximum pressure force on the piston (under full-load conditions) and the approximate magnitude of the inertia force [mass of piston plus part of the connecting rod (7 kg) x $, x (N/4)]. Compare these forces with the piston friction force at time of peak pressure. (b) Figure 13-6 shows the variation in friction force acting on the piston of a DI diesel engine under no-load and full-load firing conditions. Carefully sketch the shape (indicating direction and rough magnitude) of the cylinder pressure force on the piston, the piston velocity, and the piston acceleration, as functions of crank angle on the same graph as these friction forces. Use these graphs to explain the variation of piston friction force throughout the four strokes of the cycle. (a) Show by dimensional analysis of the variables that govern the friction in a journal bearing (friction force F,, oil viscosity p, bearing diameter D,, length L,, mean clearance I;, shaft rotational speed N) that What additional physical assumptions are then required to obtain an equation of the form of (13.20)? (b) Under what conditions can Eq. (13.23), an empirically developed relation for engine bearing fmep, be obtained from Eq. (13.20)? Explain whether each of the following components of engine friction would be expected to depend on (1) crankshaft rotational speed N, (2) mean piston speed S,, (3) or both of these variables. Crankshaft journal bearings, connecting rod bearings, valve train, piston rings, piston skirt, water pump, fan, valve flow loss (resistance to flow through the inlet and exhaust valves). REFERENCES 1. Ball,W.F., Jackson, N. S., Piey, A. D., and Porter, B. C.: "The Friction of a 1.6 Litre Automotive Engine-Gasoline and Diesel," SAE paper 860418,1986. 2. SAE ~ L s Code t J816b. ENGINE FRICITON AND LUBRICATION 747 3. Rosenberg, R. C.: "General Friction Considerations for Engine Design," SAE paper 821576, 1982 4. Schilling, A.: Automobile Engine Lubrication, Scientific Publication, 1972. 5. Millington, B. W., and Hartles, E. R.: "Frictional Losses in Diesel Engines," paper 680590,SAE Trans., vol.
77,1968.
6. Barnes-Moss, H. W.: "A Designer's Viewpoint," in Passenger Car Engines, Conference Proceedings, pp. 133-147,Institution of Mechanical Engineers, London, 1975.
7.
Lancaster, D. R., Krieger, R. B., and Lienesch, J. H.: "Measurement and Analysis of Engine Pressure Data," paper 750026,SAE Trans., vol. 84,1975. 8. Gish, R. E., McCullough, J. D., Retzloff, J. B, and Mueller, H.
T.: "Determination of T N Engine ~ Friction," SAE Trans., vol. 66, pp. 649-661,1958. 9. Brown, W.L.: "The Caterpillar IMEP Meter and Engine Friction," paper 730150,SAE Trans., vol.
82,1973. 10. Kovach, J. T., Tsakiris, E.
A,, and Won& L. T.: "Engine Friction Reduction for Improved Fuel Economy," SAE paper 820085,1982. 11. Cleveland, A. E., and Bishop, I. N.: "Several Possible Paths to Improved Part-Load Economy of Spark-Ignition Engines," SAE paper 150A, 1960. 12. Bishop, I. N.:"Effect of Design Variables on Friction and Economy," SAE Trans., vol. 73, pp. 334-358,1965.
13.
Piston Rings, Mobil Technical Bulletin. 14. Nunney, M. J.: The Automotive Engine, Newnes-Butterworths, London, 1974. 15.
Furuhama, S., Takiguchi, M., and Tomizawa, K.: "Effect of Piston and Piston Ring Designs on the Piston Friction Forces in Diesel Engines," SAE paper 810977,SAE Trans., vol. 90,1981. 16. Fumhama, S., Ashi, C., and Hiruma, M.: "Measurement of Piston Ring Oil Film Thickness in an Operating Engine," ASLE p r e p ~ 82-LC-6C-1,1982. t 17.
McGeehan, J. A.: "A Literature Review of the Effects of Piston and Ring Friction and Lubricating Oil Viscosity on Fuel Economy," SAE paper 780673,SAE Trans., vol.
87,1978. 18. Fumhama, S., and Takiguchi, M.: "Measurement of Piston Frictional Force in Actual Operating Diesel Engine," SAE paper 790855,SAE Trans., vol. 88,1979.
19. Cameron, A.: The Principles of Lubrication, Wiley, New York, 1966. 20. McGeehan, J.
A.: "A Survey of the Mechanical Design Factors Affecting Engine Oil Consump tion," SAE paper 790864,SAE Trans., vol. 88,1979. 21. Armstrong, W. B., and Buuck, B. A.: "Valve Gear Energy Consumption: Effect of Design and Operational Parameters," SAE paper 810787,1981. 22. Staron, J. T., and Willermet, P. A.: "An Analysis of Valve Train Friction in Terms of Lubrication Principles," SAE paper 830165,SAE Trans., vol. 92,1983. 23. Burke, C. E., Nagler, L. H., Campbell, E. C., Lundstrom, L. C, Zierer, W. E., Welch, H. L., Kosier, T. D., and McConnell, W. A.: "Where Does All the Power Go," SAE Trans., vol. 65,pp.
713-737,1957. 24. Dean, J. W., and Casebeer, H. M.: "Chrysler 340 Cu In. V-8 Engine Produces 275 HP at 5000 RPM," SAE paper 680019,1968.
25. Schilling, A.: Motor Oils and Engine Lubrication, Scientific Publications, 1968.
26.
Annand, W.J., and Roe, G.
E.: Gas Flow in the Internal Combustion Engine, Haessner Publishing, 1974. 27. ASTM Standards, Part 17,Petroleum Products. 28.
ASTM D2270-64. 29. SAE J300a. MODELING REAL ENGINE FLOW AND COMBUSTION PROCESSES F 749 trends and tradeoffs, and, if the model is sufficiently accurate, to optimize design and control; 4 Providing a rational basis for design innovation.
i; 14.1 PURPOSE AND CLASSIFICATION OF MODELS In engineering, modeling a process has come to mean developing and using the appropriate combination of assumptions and equations that permit critical features of the process to be analyzed. The modeling of engine processes continues to develop as our basic understanding of the physics and chemistry of the phenomena of interest steadily expands and as the capability of computers to solve complex equations continues to increase. Modeling activities can make major contributions to engine engineering at different levels of generality or detail, corresponding to different stages of model development, by: 1. Developing a more complete understanding of the process under study from the discipline of formulating the model; 2. Identifying key controlling variables to provide guidelines for more rational and therefore less costly experimental development efforts; 3.
Predicting engine behavior over a wide range of design and operating variables to screen concepts prior to major hardware programs, to determine 748 Each of these contributions is valuable. Whether a model is ready to pass from one stage to the next depends on the accuracy with which it represents the actual process, the extent to which it has been tested and validated, and the time and effort required to use the model for extensive sets of calculations and to interpret the results. This chapter reviews the types of models and their primary components that are being developed and used to describe engine operating and emissions characteristics. These models describe the thermodynamic, fluid-flow, heattransfer, combustion, and pollutant-formation phenomena that govern these performance aspects of engines. Many of the building blocks for these models have been described in the previous chapters. The purpose here is to show how fluid dynamics, heat-transfer, thermodynamics, and kinetics fundamentals can be combined at various levels of sophistication and complexity to predict, with varying degrees of completeness, internal combustion engine combustion and emissions processes, and hence engine operating characteristics. For the processes that govern engine performance and emissions, two basic types of models have been developed. These can be categorized as thermodynamic or fluid dynamic in nature, depending on whether the equations which give the model its predominant structure are based on energy conservation or on a full analysis of the fluid motion. Other labels given to thermodynamic energyconservation-based models are: zero-dimensional (since in the absence of any flow modeling, geometric features of the fluid motion cannot be predicted), phenomenological (since additional detail beyond the energy conservation equations is added for each phenomenon in turn), and quasidimensional (where specific geometric features, e.g., the spark-ignition engine flame or the diesel fuel spray shapes, are added to the basic thermodynamic approach). Fluid-dynamicbased models are often called multidimensional models due to their inherent ability to provide detailed geometric information on the flow field based on solution of the governing flow equations. Some general observations about models of engine processes provide a context for the details that follow. The processes themselves are extremely complex.
While much is known about these processes, they are not adequately understood at a fundamental level. At present, it is not possible to construct models that predict engine operation from the basic governing equations alone.
Thus the objectives of any model development effort should be clearly defined, and the structure and detailed content of the model should be appropriate to these objectives. It is impractical to construct models that attempt to describe all important aspects of engine operation: more limited objectives are appropriate. Due to this complexity of engine processes and our inadequate understanding at a fundamental level, most engine models are incomplete. Empirical relations and ad hoc

The compatability relationships are expressed in terms of variables (called Riemann invariants) which are constant along the position characteristics for constant-area homentropic flow, though they vary if these restrictions do not apply. Thus, the solution of the mass and momentum conservation equations for this one-dimensional unsteady flow is reduced to the solution of a set of ordinary differential equations. The equations are usually solved numerically using a rectangular grid in the x and t directions. The intake or exhaust system is divided into individual pipe sections which are connected at junctions. A mesh is assigned to each section of pipe between junctions. From the initial values of the variables at each mesh point at time t = 0, the values of the Riemann variables at each mesh point at subsequent time steps are then determined. Gas pressure, density, and temperature can then be calculated from the energy conservation equation and the ideal gas law. Additional details of the method are given by Benson et al.5.6 + Additional simplifications are possible. Expanding Eq. (14.16) and using the mass and momentum conservation equations yields If u can be represented by c, T and Rlc, rearranged and simplified to give =y - 1 is constant, Eq. (14.17) can be where the sound speed a for an ideal gas is given by If friction and heat-transfer effects are small enough to be neglected, Eqs. (14.15) and (14.18) can be considerably simplified. In the absence of these effects the flow is isentropic; it has uniform entropy which is constant with time and is often called hornentropic flow.6 If the duct area can be neglected then the continuity equation, (14.13), can be simplified also. FINITE DIFFERENCE METHODS. Finite difference methods for solving the onedimensional unsteady flow equations in intake and exhaust manifolds are proving more efficient and flexible than the method of characteristics. The conservation equations, (14.13), (14.14), and (14.16), can be rearranged and written in INTERNAL COMBUSTION ENGINE FUNDAMENTALS 6 0 t [3 t n + 2 TABLE 14.1 Boundary conditions for unsteady onedimensionalfinite element analysis9 pipe ends Out-flow Time n + 1,j n+l ,,/ At n.
I \'-*\ /" &AX- j-1 \'. 'xu j + l j x - Distance FIGURE 14-4 Mesh in timedistance plane for application of one-step Lax-Wendroff method to intake or exhaust pipe. Mass Energy In-flow matrix form as ~ l U l A l =P2 U2A2 UZ cPTl + L = ~ , T 2 2 +-v2: Isobaric PZ = P3 Mass plUlA1 Energy c , T3 = c, T, Isentropic p21p: = P ~ / P $ Mass ap V-=XP~U,A~ , at = P2 UzAz + -2u2 = C, Tl A d 2 - v: +2 3 l 3 pipe . -junctions Energy at Pressure The fluid viscous shear is small relative to friction at the wall in the momentum equation, and heat conduction and viscous dissipation prove negligible relative to convective heat transfer at the wall in the energy conservation equation.
These equations have the vector form: a F aG --+-=H ax at where G and H are functions of F only. Several finite difference methods have been used to solve Eq. (14.21) (see Refs. 7, 8, and 9). The one-step Lax-Wendroff method will be illu~trated.~ Equation (14.21) can be developed into a Taylor series with respect to time, and the time and space derivatives approximated by central differences around the mesh point, shown in Fig. 14-4, as FYf' 1 At 2Ax = F; - - - (GY+1 - GjA- ') [(Gy+ + AtH; + Gy)(G;+ 1 - G;) - (Gy + Gy- ,KG; - GY- (14.22) where G' = BGJdF. This equation is first-order accurate, unless H is small. For stability in the integration process, the time step and mesh size must satisfy the requirement that where C is the Courant number. p1 - Apl = pz + Ap2 = p3 + Ap3 = ... These finite difference solution methods usually require the introduction of some form of dissipation or damping to prevent instabilities and large nonphysical oscillations from occurring with nonlinear problems with large gradients (e.g., a shock wave in the exhaust system). Amplification of the physical viscosity and the addition of artificial viscosity, damping, and smoothing terms to Eq. (14.22) are frequently used technique^.^, The boundary conditions at pipe ends and junctions are obtained from the appropriate conservation equations and pressure relations, as illustrated in Table 14.1. Out-flows and in-flows obviously conserve mass and energy. For the flow out through a restriction, there is no pressure recovery downstream: for flow in through a restriction, the flow upstream of the restriction is isentropic. For pipe junctions, the conservation equations are applied to the control volume contained within the dashed line in the sketch in the table.
The pressure boundary conditions are most easily estimated by modifying the simple constant-pressure assumption with pressure losses at each pipe exit or entry, calculated from experimentally determined loss coefficients (see Fig. 6-5).' Calculations of intake and exhaust flows using these techniques predict the variations in intake and exhaust manifold pressure with crank angle (as shown, for example, in Fig. 6-7), in single and multicylinder engines, with acceptable accuracy.'. Measured volumetric efficiency variations with engine speed, manifold design, and valve dimensions and timing are adequately predicted also. Figure 1 4 % shows the instantaneous exhaust and intake mass flow rates for cylinder number 1 of a four-cylinder spark-ignition engine at wide-open throttle at 1500 rev/min. Note how gas dynamic effects distort the exhaust flow. Note also the "reverse" flows into the cylinder past the exhaust valve and out of the MODELING REAL ENGINE FLOW A N D COMBUSTION PROCESSES Thermodynamic analysis of cylinder contents 763 Phenomenological process models valve geomeuy 2. Thermodynamic ,c 0.6 Experiment Model Plenum ---- properties Compression I Combustion a 3. Flow rates '. 5. Transport properties Crank angle, deg (4 Speed, revlmin (b) 6. Combustion rate Exhaust FIGURE 14-5 4 (a) Predicted mass flow rate through the exhaust valve me and through the intake valve m, in cylinder 1, four-cylinder four-stroke-cycle spark-ignition engine at wi*open throttle and 1500 rev/min. Flows into cylinder are positive; flows out are negative.
(b) Predicted and measured volumetric efficiency at wide-open throttle for fow-cylinder spark-ignition engine. Solid line: one-dimensional unsteady flow model. Dashed line: quasi-steady flow calculation based on infinite plenums for manifolds.' cylinder past the intake valve at the end of the exhaust process, and the larger reverse flow at the end of the intake process at this low engine speed.
Figure 14-5b shows the volumetric efficiency for this engine based on these predicted mass flow rates, as a function of speed. Experimental values and values predicted with quasi-steady flow equations and infinite plenums for manifolds are also shown. These results clearly demonstrate the important role that intake and exhaust system gas dynamics play in determining both the engine speed at which peak breathing efficiency occurs and the air charging characteristics over the full engine speed range.' 14.4 THERMODYNAMIC-BASED IN-CYLINDER MODELS 14.4.1 7. Emissions mechanisms FIGURE 14-6 Logic structure of thermodynamic-based simulations of internal combustion engine operating cycle.
The starting point for these cycle simulations is the first law of thermodynamics for an open system, developed in Sec.
14.2. This is applied to the cylinder volume for the intake, compression, combustion, expansion, and exhaust processes that in sequence make up the engine's operating cycle. The structure of this type of engine simulation is indicated in Fig. 14-6. Then, during each process, submodels are used to describe geometric features of the cylinder and valves or ports, the thermodynamic properties of the unburned and burned gases, the mass and energy transfers across the system boundary, and the combustion process. During intake and compression, the cylinder volume is modeled as a single open system. Application of the conservation equations in the form of Eqs. (14.1), (14.3), and (14.10) or (14.11) for the intake and then the compression process givesZ Intake: Background and Overall Model Structure If the mass transfer into and out of the cylinder during intake and exhaust, the heat transfer between the in-cylinder gases and the cylinder head, piston, and cylinder liner, and the rate of charge burning (or energy release from the fuel) are all known, the energy and mass conservation equations permit the cylinder pressure and the work transfer to the piston to be calculated. Engine models of this type have been developed and used extensively to predict engine operating characteristics (indicated power, mean effective pressure, specific fuel consumption, etc.) and to define the gas state for emission calculations. These models effectively follow the changing thermodynamic and chemical state of the working fluid through the engine's intake, compression, combustion, expansion, and exhaust processes; they are often called engine cycle simulations. where m is the mass of gas in the cylinder, mi and me are the mass flow rates through the inlet valve and the exhaust valve, and f is the fuel fraction m,/m. The subscripts i and e denote properties of the flow through the intake and exhaust valves, respectively. The thermodynamic properties for these flows are the values upstream of the valves and therefore depend on whether the flow is into or out of the cylinder. 764 MODELING REAL ENGINE FLOW AND COMBUSTION PROCESSES INTERNAL COMBUSTION ENGINE FUNDAMENTALS 765 Compression : Exhaust : The pressure is then determined from Eq. (14.9). During intake and compression, the working fluid composition is frozen.
The composition and thermodynamic properties can be determined using the models described in Secs. 4.2 and 4.7. Mass flows across open valves are usually calculated using one-dimensional compressible flow equations for flow through a restriction (see App. C and Secs. 6.3.2 and 14.3.2) or filling and emptying models (Sec. 14.3.3). The more accurate unsteady gas dynamic intake (and exhaust) flow models described in Sec. 14.3.4 are sometimes used to calculate the mass flow into the engine cylinder in complete engine cycle simulations when the variation in engine flow rate with speed is especially important :lo the disadvantage is much increased computing time. Heat transfer during intake and compression is calculated using one of the Nusselt-Reynolds number relations for turbulent convective heat transfer described in Sec. 12.4.5. The transport properties, viscosity, and thermal conductivity used in these correlations can be obtained from relations such as Eqs. (4.52) to (4.55).
During combustion which starts with the spark discharge in spark-ignition engines and with spontaneous ignition of the developing fuel-air jets in compression-ignition engines, the actual processes to be modeled become much more complex.
Many approaches to predicting the burning or chemical energy release rate have been used successfully to meet different simulation objectives. The simplest approach has been to use a one-zone model where a single thermodynamic system represents the entire combustion chamber contents and the energy release rate is defined by empirically based functions specified as part of the simulation input.
At the other extreme, quasi-geometric models of turbulent premixed flames are used with a two-zone analysis of the combustion chamber contents-an unburned and a burned gas region-in more sophisticated simulations of spark-ignition engines. In compression-ignition engines, multiple-zone models of the developing fuel-air jets have been used to provide more detailed predictions of the combustion process and nonuniform cylinder composition and state. These combustion models will be reviewed in the following sections (14.4.2 and 14.4.3) and the appropriate conservation equations for the combustion process will be developed there. In diesels, radiation heat transfer becomes important during the combustion process (see Sec. 12.5). The expansion process is either treated as a continuation of the combustion process or, once combustion is over, can use the form of the mass, fuel, and energy conservation equations which hold during compression [Eqs. (14.27) and (14.2811. The exhaust process conservation equations for a one-zone open-system model of the cylinder contents are2 where he, the enthalpy of the flow through the exhaust valve, is the cylinder average enthalpy for flow out of the cylinder and the exhaust system gas enthalpy if reverse flow occurs. The engine operating cycle should end with the working fluid at the same state that it started out.
For the first calculations of the sequence of processes in Fig. 14-6, property values defining the initial state of the fluid in the cylinder were assumed. If the values of these properties at the end of the first cycle differ from the assumed values, the cycle calculation is repeated with the appropriate new initial values until the discrepancy is sufficiently small. Convergence with these cycle simulations occurs within a few iterations. The working fluid state is now defined throughout the operating cycle. The work transfer to the piston per cycle can now be obtained. From W , , the masses of fuel and air inducted, m, and ma, and engine speed N, all the engine indicated performance parameters can be calculated: power, torque, mean effective pressure, specific fuel consumption, fuelconversion efficiency; as well as volumetric efficiency, residual gas fraction, total heat transfer, etc. With a friction model, the indicated quantities can be converted to brake quantities. The more sophisticated of these thermodynamic-based engine cycle simulations define the working fluid state throughout the cycle in sufficient detail for useful predictions of engine emissions to be made. The discussion in Chap. 11 of emission-formation mechanisms indicates that our understanding of how some of these pollutants form (e.g., NO,, CO) is reasonably complete, and can be modeled accurately. The formation processes of the other pollutants (unburned hydrocarbons and particulates) are not adequately understood, though modeling activities are continuing to contribute to that understanding. The key features of models for predicting engine emissions were discussed in Chap.
11. Cycle simulations and combustion models which have been developed for spark-ignition engines, where the fuel, air, residual gas mixture is essentially uniformly mixed, are discussed in Sec. 14.4.2. Compression-ignition engine simulations and combustion models are then discussed in Sec. 14.4.3. The special features required for prechamber engine models are reviewed in Sec. 14.4.4. Finally, thermodynamic-based models for more complex engine systemsmulticylinder, turbocharged, and turbocompounded engines-are discussed in Sec. 14.4.5. 766 MODELING REAL ENGINE FLOW AND COMBUSTlON PROCESSES INTERNAL COMBUSTTON ENGINE FUNDAMENTALS 767 14.43 Spark-Ignition Engine Models These models have usually followed the conceptual structure indicated in Fig. 14-6. Our focus here is on the combustion submodels that have been developed and used successfully. Features of the spark-ignition engine combustion process that permit major simplifying assumptions for thermodynamic modeling ire: (t) the fuel, air, residual gas charge is essentially uniformly premixed; (2) the volume occupied by the reaction zone where the fuel-air oxidation process actually occurs is normally small compared with the clearance volume-the flame is a thin reaction sheet even though it becomes highly wrinkled and convoluted by the turbulent flow as it develops (see Sec. 9.3); thus (3) for thermodynamic analysis, the contents of the combustion chamber during combustion can be analyzed as two zones-an unburned and a burned zone. Useful combustion chamber design information can be generated with simple geometric models of the flame. In the absence of strong swirl, the surface which defines the leading edge of the flame can be approximated by a portion of the surface of a sphere. Thus the mean burned gas front can also be approximated by a sphere. Then, for a given combustion chamber shape and assumed flame center location (e.g., the spark plug), the spherical burning area A, [see Eq. (9.40)], the burned gas volume V, [see Eq. (9.3911, and the combustion chamber surface "wetted" by the burned gases can be calculated for a given flame radius r, and piston position (defined by crank angle) from purely geometric considerations.? The practical importance of such "model" calculations is that (1) the mass burning rate for a given burning speed S, (which depends on local turbulence and mixture composition) is proportional to the spherical burning area A, as given by Eq. (9.44); (2) the heat transfer occurs largely between the burned gases and the walls and is proportional to the chamber surface area wetted by the burned gases A , , [see Eq. (12.2111. Using the fact that the density ratio across the flame p Jp, is approximately constant and equal to 4, the unburned and burned gas volumes and h can be related to the unburned and burned mass fractions (1 - x,) and x,, respectively. Examples of the results of such flame geometry calculations are shown in Figs. 14-7 and 14.8." Figure 14-7a shows spherical flame areas A, as a function of flame radius r, for two different chambers and two plug locations and the TC piston position.
The much larger flame area and shorter flame travel length of the central plug location are obvious. Such area data can be plotted as a function of burned gas volume 5, as shown in Fig. 14-7b, so that comparisons of Ab(rb)for different chambers at the same mass fraction burned can be made. The advantage of a more compact chamber with higher central clearance height is apparent. Figure 14-8 shows that burned-gas-wetted wall area on the cylinder head, cylin- t Note that the center of this sphere may be convected away from the spark plug location, especially if some swirl is p-t. However, only strong swirling and squish flows produce major distortions to the flame surface shape. / 0.4 - / - Disc, center - 0.2 7 1 . , Disc, side ignition \ 0 I 0.2 I '\ 0.4 I 0.6 '% I 0.8 \ 1.0 Bawl-in-piston 0.6 -*- Center FIGURE 14-7 Calculated spark-ignition engine spherical flame surface area: (a) as a function of h e radius for different combustion chamber shapes and spark plug locations and (b) as a function of entlamed volume. Piston in top center position.l1 der wall, and piston as a function of flame radius and crank angle for an open chamber with central ignition. The cylinder head and piston are the dominant areas early in the expansion stroke when the burned gas temperatures and heat fluxes are highest. Mass fraction burned versus crank angle profiles determined from a first law analysis of cylinder pressure data, as shown in Fig.9-2,9-5, and 9-8, have an essentially universal dimensionless shape, as indicated in Fig. 9-13. Much useful 768 MODELING ReAL ENGINE FLOW AND COMBUSTION PROCESSES INTERNAL COMBUSTION ENGINE FUNDAMENTALS 769 4Z0 Piston Cylinder wall i 0 / ~ n n -.-7 I /,$-140 o-.A. 0.6 ..
Flame radius Bore 0.8 1.0 FIGURE 14-8 Calculated burned-gas-wetted wall area as a function of radius based on spherical flame model of an open-chamber SI engine with center plug location, for piston locations of O0,42", and 70•‹." TC Crank angle, deg 23 analysis has been done with engine simulations where this universal combustion profile has been used as a calculation input. The S-shaped mass fraction burned ~rofileis often represented by the Wiebe function: where 8 is the crank angle, 8, is the start of combustion, A8 is the total combustion duration (x, = 0 to x, m I), and a and m are adjustable parameters which fix the shape of the curve. Actual mass fraction burned curves have been fitted with a = 5 and m = 2." The conservation equations for an open system [Eqs. (14.1) and (14.10) or (14.11)] are now applied to the unburned gas zone ahead of the flame and to the burned zone behind the flame, in turn (see Fig. 9-4). For premixed engines,f and $ are zero. During combustion, m and m, in Eq. (14.10) or Eq. (14.11) are the mass flow rate across the flame sheet. This is -mb for the unburned zone system and +mb for the burned zone system; m, is given by mk,, with 5 obtained by differentiating Eq. (14.32). To calculate the effect of heat transfer on the burned gas state more accurately, the burned gas zone in Fig. 9-4 can be modeled in two parts: an adiabatic core and a boundary-layer region. The intent here is to account for the fact that heat loss to the walls primarily cools the burned gas adjacent to the wall, and only indirectly affects the core gas through the change in pressure that results FIGURE 14-9 Cylinder pressure p, mass fraction burned x,, unburned and burned gas temperatures (T,= unburned, T, = adiabatic burned core, 'i;= mean burned gas temperatures), heat-transfer rate 0, (normalized by fuel 5ow rate x heating value), thermal boundary-layer thickness a, and mean nitric oxide concentration in the burned gases, through a four-stroke engine operating cycle, predicted by thermodynamic-based cycle simulation. 5.7-dm3displacementeight-cylinder engine operating at wideopen throttle, 2500 revlmin, with equivalence ratio = 1.1. Gross indicated mean effective pressure is 918 kPa and specific fuel consumption is 254 g/kW h.I3 from heat loss. The open-system conservation equations, (14-1) and (14.10) or (14.11), are now applied to the core and boundary-layer region separately. The boundary-layer region covers that portion of the combustion chamber wall wetted by the burned gases, as shown in Fig.
9-4, and is of thickness a,, which increases with time.
The temperature of the boundary-layer zone (assumed uniform) is usually taken to be the mean of the wall temperature and burned gas core temperature. Equation (14.10) or Eq. (14.11) is used to relate the enthalpy flux due to the mass flow across the inner edge of the boundary layer (which has an enthalpy equal to the core gas enthalpy), the heat transfer to the wall, the changing energy within the boundary-layer system due to its increasing mass and changing state, and the work transfer due to its changing volume. An example of predictions of cylinder pressure, unburned and burned gas temperatures, heat-transfer rate, and boundary-layer thickness, based on an assumed 50" total burn duration for a 5.7dm3 eight-cylinder engine at wide-open throttle and 2500 rev/min is shown in Fig. 14-9.13 Appropriately based predictions of overall engine performance parameters made with this type of thermodynamic model agree well with engine data. Figure 14-10 shows predictions of indicated spec5c fuel consumption and exhaust gas temperature as a function of MODELING REAL ENGINE FLOW AND COMBUSTION PROCESSES 420 - 771 MBT timing 400200 I Experiment: MBT A MBT + 101 380 - - Calculated FIGURE 14-10 Equivalence ratio 4 Predicted and measured indicated specific fuel consumption and exhaust temperature as a function of the fuellair equivalence ratio for a spark-ignition engine operated at 1250 rev/min and imep of 379 kPa. MBT: maximum brake torque timing. MBT + 10%: combustion timiig retarded to give 10 percent fuel consumption penalty.14 m 80 0 the fuellair equivalence ratio at fixed load and speed. The isfc predictions and data agree well (except for very lean mixtures with retarded timing where cycleby-cycle combustion variations are sufficiently large so predictions based on the average cycle lose accuracy); the predicted curves for exhaust temperature show the same trends as the experimental data. However, they are higher due to underestimation of the heat losses during the exhaust process.14 The output from such thermodynamic-based cycle simulations has replaced the fuel-air cycle as a predictor of effects of major variables on engine performance and efficiency. An instructive example of the value of such predictions is shown in Fig. 14-11, where fuel consumption at constant equivalence ratio, load, and speed has been computed as a function of total bum duration and heat loss to the chamber walls: increasing burn duration and heat loss both worsen fuel wns~mption.'~ Such data can be used to assess the efficiency improvements that should result from reduced heat transfer (e.g., reduced chamber surface area) and increased bum rate. Obviously the dependence of burn rate on engine design and operating parameters has not been modeled; the bum rate profile was a calculation input. Such models are most useful either (1) when the burn rate profile is not critical to the problem under study or (2) when predictions for a range of assumed bum rate profiles provide the required information. So far we have discussed engine cycle simulations where details of the combustion process have been specified as input. The same thermodynamic-based simulation structure can be used in conjunction with a combustion model which predicts the rate of fuel burning. Various combustion models have been proposed and used for this purpose. Some of these are empirically based; some are based on the highly wrinkled, thin reaction-sheet flame model described in Sec. 9.3. All FIGURE 14-11 Predicted brake spedic fuel consumption as a function of heat transfer per cycle to the combustion chamber walls (as a percent of the fuel's heating value) and total bum duration [A9 in Eq.(14.3211. 1250 rev/min, 262 kPa bmep, fuellair equivalence ratio = 0.91, maximum brake torque spark timing.I5 20 40 60 Total bum duration, deg 100 these models assume that the overall flame shape approximates a portion of a sphere centered at or near the spark plug. Empirical flame models have difficulty appropriately describing the three phases of the combustion process-flame development, rapid burning, and termination-with sufficient generality to be widely useful. One such model, based on the experimental data shown in Fig. 9-30, has been used successfully to evaluate different combustion chambers.16*l 7 The burning speed S, [defined by Eq. (9.441 is related empirically to the laminar flame speed S, (see Sec. 9.3.3), the local rms velocity fluctuation u; [see Eq. (8.22)] under motored engine conditions, the firing and motored cylinder pressure at the same crank angle, and spark advance. While a good fit to the data in Fig.
9-30 for engine flames during their turbulent rapid-buming phase was obtained, during the flame development period a correction factor was required to fit the data. Spark-ignition engine combustion models with a more fundamental framework have been developed and used. Based on coupled analysis of flame front location and cylinder pressure data, Keck and c o ~ o r k e r s ' " ~have ~ derived the following burning law : 772 INTERNAL COMBUSTION ENGINE FUNDAMENTALS -. MODELING REAL ENGINE now AND COMBUSTION PROCESSES 773 SL (14.363) + SL (14.36~) 2. Initially, as t -+ 0, s b $:I;:: .... , 3. Quasi-steady state, dpldt x 0, Sb X , .:.,I,, :.:,:.: .... .
.. .. UT 4. Final burning stage after the flame front reaches the wall, t 2 t , (when A -,01, , . +.'. . :... ., ..
.. . . , . ..~ .. . .
I , , ... :. .: . + , I L litb - e - (r - t w) / ~ b mb(tw) - FIGURE 1412 Schematic of turbulent premixed spark-ignition engine flame, illustrating the physical basis for burning law of ~ q s (14.33) . to (14.35). The approximately spherical front of the "thick" turbulent flame (dashed line) diffuses outward at the laminar flame speed S,. Fresh mixture also crosses this front at a characteristic velocity u, due to turbulent convection.
Schematic on left shows detailed flame structure:6, is a reactionsheet thickness, I , is characteristicscale of wrinkles in the sheet.
/ where / p = me - mb = p N f - GI = pp,M A L - A,) is a parametric mass (interpreted as the mass entrained within the flame region that has yet to burn), u, a characteristic speed, and rb = lT/SLis a characteristic burning time. I, A,, 5,A,, b a r e defined in Sec. 9.3.4. Figure 14-12 illustrates the physical basis for this model. The first term in Eq. (14.33) represents the laminar (diffusive) propagation forward of the approximately spherical front of the "thick" turbulent flame; the second term represents the burning of mixture already entrained within this flame front. In Eq. (14.34), which describes the rate of change of unburned mixture mass p within the flame zone, the &st term represents the turbulent convection of unburned mixture across the spherical front of the flame and the second term represents the mass rate of burning of entrained but not yet burned mixture which is contained within the "wrinkles" and "islands," which the distorting and stretching of the thin reaction sheet by the turbulent flow produces. This has been called an "entrainment " or "eddy-burning " model for the above reasons. The exponential term in brackets in Eq. (14.34) allows for the fact that the flame sheet initially is spherical and laminarlike: it requires a time of about r, to develop into a turbulent flame. The behavior of Eqs. (14.33) and (14.34) in four important limits is: 1. For a quiescent mixture, u, + 0 or 1, -,m, s b -,SL (14.36d) To apply Eqs. (14.33) and (14.34), the quantities u, and rb (or 1, = zbSJ must be evaluated. Two approaches have been taken: (1) use of empirical correlations for these variables, derived from engine flame data (such as that described in Sec. 9.3.4); (2) use of more fundamental models to predict these quantities. Keck has derived the following correlations for u, and I,, based on the application of Eqs. (14.33) and (14.34) to several sets of engine combustion data: ' (9"' (Y4 6 u, = O.08tri (14.37) 1, = 0.8Lh - (14.38) u, was found to be proportional to (at time of spark) and to correlate well with mean inlet gas speed ii, = q&AdAiv)SP,where q, is volumetric efficiency, A, is piston area, A, is the maximum open area of the inlet valve, S, is mean piston speed. 1, appears to scale with valve lift, L,; it decreases with increasing density at a rate proportional to p t 3 l 4 . While u, and 1, are not constant during the combustion process, their variation is modest." A quantitative comparison of predicted and measured flame radius as a function of time is shown in Fig.
14-13 for hydrogen and propane fuel-air mixtures which exhibit widely different behavior:18 the figure indicates both the behavior and validity of the model. Predicted burned gas expansion speeds u, [see Eq. (9.43)] are shown in Fig. 14-13a as a function of burned gas radius; the parameters u, and 1, were chosen to fit the propane data. Figure 14-13b shows that the measured flame front radii, r,, are in good agreement with the predicted flame and burned gas radii, rf and r,, for these two fuels. The initial expansion speed of hydrogen is about 10 times that of propane.
Since r, x rb for early times, Sbx SL and this ratio is expected. As rb become large, (r, - r,) -,u, rb, which is several times smaller for hydrogen mixtures than for propane mixtures. An adaption of this approach developed by Tabaaynski and coworkers2'. 22 is based on the following model of turbulent flame propagation.
The vorticity in the turbulent flow field is concentrated in vortex sheets which are 774 MODELING R W L ENGINE FLOW AND COMBUSTION PROCESSES INTERNAL COMBUSTION ENGME FUNDAMENTALS Thus, in Eqs. (14.33) and (14.34), uT and 7, are 775 given by where I,, the microscale, is determined from the integral scale and the turbulent Reynolds number via Eq. (8.15), assuming that the turbulence is homogeneous and isentropic. The task therefore becomes one of evaluating u' and I,. One approach used is to relate the turbulence intensity at the start of the combustion process to the mean intake flow velocity through the valve: e.g.,23 Far wall ESL I Oo I 20 I I I 40 I I 60 80 Burned gar radius rb, mm where S, is the mean piston speed, B the bore, and L,, and Div the lift and diameter of the inlet valve. It is assumed that the integral length scale at the start of combustion, IIp0,is proportional to a characteristic flow dimension, usually the clearance height h. Then, during combustion, the unburned portion of the charge is assumed to undergo isentropic compression sufficiently rapidly that the angular momentum of the "eddies" is conserved and the length scale follows the eddy size, i.e., a simple rapid distortion process occurs: This model predicts an increase in turbulence intensity and decrease in length scale with compression, which is only partly confirmed by experiment. A more sophisticated approach is to describe the dynamic behavior of the turbulence with one or more rate equations for the key turbulence parameters: k the turbulent kinetic energy and e the dissipation rate of k. Turbulence is generated, diffused, and dissipated by the flow field, so the rate of change of turbulent kinetic energy k can be written: Degrees affcr spark FIGURE 14-13 (a) Calculated burned gas expansion speed u, for stoichiometric hydrogen-air and propaneair mixtures as a function of burned gas radius r,. (b) Comparison of experimentally measured (points) and calculated (dashed curve) flame radii r, for these mixtures as a function of crank angle. Also shown (solid curve) is the burned gas radius r, ." of a size comparable to the Kolmogorov scale 1, [see Eq. (8-ll)]. These vortex sheets are assumed to have a characteristic spacing which is of the order of the Taylor microscale I,, which is a function of the integral length scale I, and the turbulent Reynolds number as indicated by Eq. (8.15). From these turbulence assumptions it is argued that ignition sites propagate along the vortex sheets with a velocity u' + S,, where u' is the local turbulence intensity. The propagation of the reaction front between the vortex sheets is assumed to be a laminar process. where the term P, represents the volumetric production of turbulence and the diffusion term Dk can be modeled as a gradient diffusion with an effective turbulent viscosity which dominates the laminar diffusion process. In this application, Eq. (14.42) is integrated over the combustion chamber (or a region of the chamber) to provide spatially averaged turbulence predictions. Then the diffusion terms become boundary fluxes: e.g., the transport of kinetic energy across the combustion chamber boundary due to flow through the inlet or exhaust valve. The dissipation rate E is related to the integral length scale via I, can be taken as proportional to the clearance height (I, x 0.22 h), or an additional rate equation for a second turbulence parameter, the dissipation rate E, can 776 INTERNAL COMBUSTION ENGINE FUNDAMENTALS 0 MODELING REAL ENGINE FLOW AND COMBUSnON PROCESSES 777 Normal lift 114 normal lii FIGURE 1416 Crank angle after spark, deg -400 -200 0 200 Crank angle, deg 400 FIGURE 1414 Predicted turbulence intensity u' as a function of crank angle and valve lift in engine operating at 1500 rev/min, 414 kPa imep, with a compression ratio of be used.
In the more complete of these k - e turbulence models,24the E equation is similar to the k equation with production, diffusion, and dissipation terms. These k - E turbulence models are discussed more fully in Sec. 14.5.2. The application of this turbulence model to the spark-ignition engine combustion chamber becomes complicated and the reader is referred to references for the detail^.^'-^' Considerable success with predicting trends in mass burning rate has been achieved with this type of model. Design variables examined include: swirl, squish, valve lift, borelstroke ratio.
The advantage of such models is that they are straightforward computationally so that extensive parametric sets of calculations are feasible. The major disadvantage is the ad hoc nature of the turbulence and flame models which involve plausible but arbitrary assumptions. Sample predictions are shown in Figs. 14-14 and 14-15.27.28Figure 14-14 shows the variation in turbulence intensity u' in an engine with a disc-shaped combustion chamber, throughout the operating cycle.
A normal valve-lift profile and :;I Comparisons of predicted and measured mass fraction burned versus crank angle profiles for same swirl levels and plug locations as Fig. 14-15.28 reduced maximum valve-lift profile (one-quarter normal) are shown. The high levels of turbulence generated during the first half of the intake process decay substantially before the latter stages of the compression stroke produce some amplification. Reduced valve lift produces higher levels of turbulence intensity at combustion, as is well known.29 Figure 14-15 shows the predicted turbulence behavior during combustion for a disc-shaped chamber for different swirl levels and plug locations. Swirl is shown to increase the turbulence intensity. Comparison of predicted and measured mass fraction burned profiles versus crank angle for different swirl levels and plug locations are shown in Fig. 14-16. The large flame area effects (shown here in the two limiting plug locations: side wall and center) and significant though lesser effect of swirl are correctly modeled. Such models are useful for relating changes in spark-ignition engine design and operating variables to changes in engine performance, via predictions of changes in flame development and propagation. The above type of combustion model has been used to obtain explicit relations for the flame development and rapid burning angles as functions of engine design and operating variables.30 The equation for the mass burning rate, (14.33), was effectively integrated over the relevant portion of the total combustion process; the turbulent characteristic velocity was assumed proportional to S,, the mean piston speed. The flame development angle was found to vary as 3.0 .-6 a 2.6 \ -.- 8 Central spark, high swirl spark, high swirl Central spark, 'Zero" swirI -Wall , 2.0 - 0 --- 20 40 60 Crank angle, deg 80 FIGURE 1415 Predicted turbulence intensity during combustion for high and "zero" swirl levels for central and cylinder wall spark plug locations. Same engine and operating conditions as in Fig. 14-14.28 where v is the kinematic viscosity (v = pip) and h is the clearance height at ignition. C is a constant which depends on engine geometry and is determined by matching Eq. (14.44) with engine data. The rapid bum angle (here taken as the crank angle between x, = 0.01 and 1.0) is given by where C' is a constant which depends on engine geometry, B is the bore, the subscript i denotes the value at ignition, and the superscript * denotes the value MODELING REAL ENGINE FLOW AND COMBUSTION PROCESSES at cylinder conditions where xb = 0.5. These expressions show reasonable agreement with observed trends in A8, and A8,. 14.43 Direct-Injection Engine Models In direct-injection compression-ignition and stratifiedcharge engines, the liquid fuel is injected into the cylinder as one or several jets just prior to ignition.
In large direct-injection compression-ignition engines, the air flow is essentially quiescent.
However, in medium and smaller size DI engines, the air flow is usually swirling about the cylinder axis at up to 10 times the crankshaft rotational speed; this air-flow pattern increases the rate of entrainment of air into the fuel jet to increase the fuel-air mixing rate. Thus modeling of the ignition and combustion processes for direct-injection types of engines is much more complex than for premixed-charge spark-ignition engines. The unsteady liquid-fuel jet phenomena-atomization, liquid jet and droplet motion, fuel vaporization, air entrainment, fuel-air mixing, and the ignition chemistry-all play a role in the heat-release process (see Chap. 10). It is not yet possible to model all these phenomena from a fundamental basis, even with the most sophisticated fluid-dynamicbased codes now available (see Sec. 14.5), since many of these processes are not yet adequately understood. However, models at various levels of detail and empiricism have been developed and have proven useful in direct-injection diesel and stratified-charge engine analysis. This section reviews the important features of single-zone heat-release models and phenomenological jet-based combustion models.
Their relative simplicity and modest computer time requirements make them especially useful for diesel cycle simulation and more complex engine system studies. Single-zone models assume that the cylinder contents can be adequately described by property values representing the average state, and use one or more algebraic formulas to define the heat-release rate. The functional forms of these formulas are chosen to match experimentally observed heat-release profiles (see Sec.
10.4.2). Coefficients in these formulas, which may vary with engine design details and operating conditions, are determined empirically by fitting with data. The phenomenological description of diesel combustion developed by Lyn (see Sec. 10.3) comprises three primary phases: the ignition delay period, the premixed fuel-burning phase, and the mixing-controlled fuel-burning phase. Ignition delay correlations are reviewed in Sec. 10.6.6. Here models for the second and third phases, when the major heat release occurs, are summarized (see Ref. 31 for a more extensive review). The attraction of the one-zone heat-release approach is its simplicity: however, since it cannot fully describe the complex phenomena which comprise the compression-ignition engine combustion process, substantial empirical input must be used. Several one-zone heat-release models have been proposed and used (e.g., Refs. 32 to 34). These use simple equations to describe the rate of release of the fuel's energy, sometimes modeled on the presumed controlling physical or chemical process and always calibrated by comparison with data. 779 One extensively used model of this type developed by Watson et ~ 1 is . especially appropriate for use in total diesel system simulations where the combustion process details are not the primary focus. It is based on Lyn's description of compression-ignition combustion-a rapid premixed burning phase followed by a slower mixing controlled burning phase. The fraction of the injected fuel that burns in each of these phases is empirically linked to the duration of the ignition delay. One algebraic function is used to describe the premixed heatrelease phase and a second function to describe the mixing-controlled heatrelease phase. These two functions are weighted with a phase proportionality factor, fl, which is largely a function of the ignition delay. Thus: where m f , , is the mass of fuel burned, m,,, is the total fuel mass injected per cycle per cylinder, and t' is time from ignition non-dimensionalized by total time allowed for combustion [=(t - tign)/Atcomb].t The premixed-burning function is fi = 1 - (1 - trK1)K2 (14.47) and the mixing-controlled function is f2= 1 - exp (- K, ttK4) (14.48) where K,, K,, K,, and K, are empirical coeficients. The proportionality factor fl is given by where 4 is the overall fuellair equivalence ratio and a, b, and c are empirical constants. Correlation with data from a typical turbocharged truck engine gave the following values for K, to K,: + 1.25 x 10-'(qd K, =2 K, = 5000 where z,, the ignition delay, is in milliseconds and N, engine speed, is in revolutions per minute. It also gave these ranges for a, b, c:jS 0.8 c a < 0.95; 0.25 c b c 0.45; 0.25 < c < 0.5 t The combustion duration at At,,, is an arbitrary period within which combustion must be completed.
A value of 125" was used above.
~ ~ MODELING REAL ENGINE FLOW AND COMBUSTION PROCESSES INTERNAL COMBUSTION ENGINE FUNDAMENTALS Such single-zone heat-release models are useful because of their simplicity. They obviously cannot relate engine design and operating variables explicitly to the details of the combustion process. Experience indicates that those models with only one function are not usually able to fit experimentally determined heat. release profiles with sufficient accuracy. All single-zone heat-release models should be checked against experimentally derived heat-release profiles, and recal. ibrated if necessary, before being used for predictions. Many thermodynamic-based direct-injection engine simulations incorporate an explicit model for each fuel spray which attempts to describe how the spray develops with time. The spray starts out as a liquid fuel jet which then vaporizes, entrains air and (later) burned gases. Mixture preparation can be limited by the availability of either fuel vapor or air, the former limited by droplet evaporation and the latter by air entrainment. While there is evidence in the literature to support both of these phenomena as rate-limiting, more recent studies36 show that most (70 to 95 percent) of the injected fuel is in the vapor phase at the start of combustion, whereas only 10 to 35 percent of the vaporized fuel is mixed to within the combustion limits (equivalence ratio between 0.3 and 3).
This suggests that the combustion process in typical heavy-duty directinjection compression-ignition engines is mixing controlled rather than vaporization controlled. While spray geometry is an essential aspect of the fuel-air mixing process, it may not be necessary to model the precise details of the actual configuration. For the

describing the mass and energy flows between components and the heat and work transfers within each component, total system behavior can be studied. In such engine simulations, the reciprocator cylinders, the intake manifold, and the various sections of the exhaust system are treated as connected open systems. The flows into and out of these volumes are usually analyzed using the quasisteady emptying and filling approach described in Sec. 14.3.3, using the opensystem conservation equations of Sec. 14.2. The reciprocator cycle is treated as a sequence of processes within each cylinder: intake, compression, combustion (including expansion), and exhaust. These are modeled using the approaches described previously in Secs. 14.4.1 to 14.4.4. Heat transfer has, of course, an important effect on the in-cylinder processes.
It also is important in the exhaust system since the performance of the turbocharger turbine and of any compounded turbine depends on the gas state at the turbine inlet. The performance of the turbomachinery components is normally defined by maps that interrelate efficiency, pressure ratio, mass flow rate, and shaft speed for each component (see Secs. 6.8.2 to 6.8.4). Special provisions are usually required in the logic of the turbomachinery map interpolation routines to avoid problems with the compressor surge and turbine choking operating limits of these devices. When the reciprocator is coupled with turbomachinery its manifolds no longer connect directly with the atmosphere: matching procedures are required to ensure that the pressure levels and mass flow rates of the compressor and turbines match with those of the engine.
The following matching process is typical of those used for turbocharged engines (one compressor and one turbine only). At a given time, the values of the variables describing the state of the rotor speed according to the turbocharger dynamics equation n Turbocharger w 8 Inter AP 4 wa84gate I 5 1 7 1244 7 Intake manifold Multicylinder diesel engine 6 Exhaust manifold Qf Engine friction FIGURE 14-24 Block diagram of turbocharged turbocompounded diesel engine system. various system components are known (from integration of the system governing equations over the previous time step). These include the intake and exhaust manifold pressures and the turbocharger rotor speed. The compressor inlet pressure is atmospheric pressure less the intake air-filter pressure drop.
The turbine exit pressure is atmospheric plus the muffler pressure drop. By relating the compressor discharge pressure to the intake manifqld pressure and the turbine inlet pressure to the exhaust manifold pressure (through suitable pressure drops) the pressure ratio across each machine is determined. Hence, the compressor and turbine maps can be entered using the calculated pressure ratios, and the rotor speed (same for both turbomachines) as inputs. The output from the map interpolation routines determines the mass flow rate and efficiency of each component for the next time step. From these the power required to drive the compressor (- wc) and to drive the turbine (wT) are determined from Eqs. (6.42) and (6.48), respectively. Any excess power (or power deficiency) will result in a change of where ITc is the rotational inertia of the turbocharger, o is angular velocity, and B is the rotational damping. The values of the other state variables for the next time step are determined from the solution of the mass and energy conservation equations for each open system, with the compressor and turbine mass flows taken from the output of the turbomachinery map interpolation routines. This approach can be used to establish the steady-state engine operating characteristics from an assumed initial set of state variables. (Of course, due to the pulsating nature of the flows into and out of the cylinders, these state variables will vary in a periodic fashion throughout the engine cycle at a fixed engine load and speed.) This approach can also be used to follow transient engine behavior as load or speed is varied from such a steady-state condition.35 The additional inputs required are the fuel pump delivery characteristics as a function of fuel pump rack position and speed, with the latter evaluated from an appropriate model for dynamic behavior of the g~vernor.'~ From the brake torque of the engine (determined by subtracting friction torque from the indicated torque), the torque required by the load TL, the inertia of the engine and load I , and I , , the dynamic response of the engine and load to changing fuel rate or engine speed can be obtained from An example of the output from this type of engine model is shown in Fig.
14-25. The response of a turbocharged DI diesel engine to an increase in load from 0 to 95 percent of full load is shown. The predictions come from a model of the type shown in Fig. 14-24, and engine details correspond to the experimental configuration.55 The simulation follows the data through the engine transient with reasonable accuracy. Note that with the assumed constant governor setting, during this transient the equivalence ratio of the trapped mixture rises to close to stoichiometric because the increase in air flow lags the increase in fuel flow. This would result in excessive smoke emissions. Such models prove extremely useful for exploring the effect of changes in engine system design on transient response.56 For two-staged turbocharged or turbocompounded systems the engineturbocharger matching process is more complicated. The division of the pressure ratio between the exhaust manifold and atmosphere between the two turbines in Fig. 14-24 is not known a priori. Nor, with two compressors, is the intake pressure ratio distribution known. Iterative procedures based on an assumed mass flow rate are used to determine the pressure level between the two turbines such that mass flow and pressure continuity through the exhaust system is satisfied (e.g., Ref. 2). 792 MODELING REAL ENGINE FLOW AND COMBUSTION PROCESSES 793 INTERNAL COMBUSTION ENGINE FUNDAMENTALS TABLE 143 Available energy equations for various processes 1500' -Measured MeehPnism Eqllntioo Work transfer Heat transfer Gas transfer Liquid fuel transfert Control volume storage dA, = dW dAQ = dQ(1 - To/T) dA, = dm,[(h - h,) - To(s- so)] dA, = dm,-(1.O338Qw) dA, = d{m,[(u - u,) - To(s- so) + p,(v - v,)}] t The availability of the he1 is 1.0338 times its lower heating value; see Sec. 5.7. bustion engine processes has already been developed in Sec. 5.7. The change in availability of any system undergoing any process where work, heat, and mass transfers across the system boundary occur (see Fig. 5.13) can be written: Tie, s FIGURE 14-25 Predicted (---) and measured (-1 increase in load.5s T i ,s response of a turbocharged direct-injection diesel engine to an 14.4.6 Second Law Analysis of Engine Processes The first-law-based methods for evaluating power plant performances do not explicitly identify those processes within the engine system that cause unrecoverable degradation of the thermodynamic state of the working fluid. However, second-law-based analysis methods do provide the capability to identify and quantify this unrecoverable state degradation. Thus, cause and effect relationships which relate these losses to individual engine processes can be determined. The first law analysis approaches summarized in this section (14.4) are based on the fact that energy is conserved in every device and Process. Thus, they take account of the conversion of energy from one form to another: e.g., chemical, thermal, mechanical. Although energy is conserved, second law analysis indicates that various forms of energy have differing levels of ability to do useful mechanical work. This ability to perform useful mechanical work is defined as availability. The availability of a system at a given state is defined as the amount of useful work that could be obtained from the combination of the system and its surrounding atmosphere, as the system goes through reversible processes to equilibrate with the atmosphere. It is a property of the system and the environment with which the system interacts, and its value depends on both the state of the system and the properties of the atmosphere. Availability is not a conserved property; availability is destroyed by irreversibilities in any process the system undergoes. When availability destruction occurs, the potential for the system to do useful mechanical work is permanently decreased.
Thus to make a proper evaluation of the processes occurring within an engine system both energy and availability must be considered concurrently. The basis for an availability analysis of realistic models of intexd corn- AA = - Adcstroycd (14.53) where A,,, and A,,, represent the availability transfers into and out of the system across the boundary. Since availability is not a conserved quantity, this equation can only be used to solve for the availability destruction term, AdeStmye,.Table 14.2 summarizes the equations for the availability change of the system and the availability transfers associated with work, heat and mass transfer across the system boundary, developed in Sec. 5.7. This availability balance is applied to the internal combustion engine operating cycle as follows. A first-law-based cycle analysis of the type described above in this section (14.4) is used to define the variation in working fluid themodynamic state, and the work, heat, and mass transfers that occur in each of the processes that make up the total engine cycle. Integration of the availability balance over the duration of each process then defines the magnitude of the availability destruction that occurs during that process. To illustrate this procedure, consider the operating cycle of a 10-liter sixcylinder turbocharged and aftercooled direct-injection four-stroke cycle compression-ignition engine, operating at its rated power and speed of 224 kW and 2100 rev/min. The variations in temperature, energy, and entropy are determined with a first-law-based analysis. Figure 14-26 shows the T-sdiagram for the working fluid as it goes through the sequence of processes from air inlet from the atmosphere (state 1) to exhaust gas exit to the atmosphere (state The incoming air is compressed (with some irreversibility) in the turbocompressor to state 2 and cooled with an aftercooler to state 3. The air at state 3 is drawn into the cylinder and mixed (irreversibly) with residual gases until, at the end of the intake, the cylinder gases are represented by state 4. That mixture is subsequently compressed (with modest heat loss) to state 5. Fuel addition commences close to state 5; subsequent burning increases the combustion chamber pressure and ternperature along the line 5-6. At 6 the heat release, heat transfer, and volume change rate are such that the maximum cylinder pressure is reached (a few degrees after TC). From 6 to 7 combustion continues to completion, the burned 794 INTERNAL COMBUSTION ENGME FUNDAMENTALS MODELING REAL ENGINE FLOW AND COMBUSTION PROCESSES 20001 1 795 TABLE 143 Comparison of first and second law analysis for sixcylinder 14-liter naturally aspirated and -mbocbarged diesel engine at 2100 rev/mins8 FIGURE 14-26 T-s diagram for the working fluid as it goes through the sequence of processes from air inlet to exhaust in turbocharged aftercooled DI compressionignition engine. The 10-liter six-cylinder engine is operated at its rated power (224 kW)and speed (2100 rev/min).
The text relates processes to numbered end Entropy, kcallkg K gases continue to expand, doing work on the piston and losing heat to the walls. At state 7 the exhaust valve opens initiating a rapid pressure equilibration with the exhaust manifold to a pressure corresponding to point 8. Gases are expelled from the cylinder to the exhaust manifold. After the intake valve opens, cylinder residual gases are mixed with incoming air at state 3 to yield gases at state 4 to complete the in-cylinder cycle. The exhaust gases that have been expelled from the cylinder experience additional thermodynamic losses and can be represented by state 9. These gases then pass through the turbocharger turbine to state 10 to provide the work to drive the compressor. A first law and second law analysis of a naturally aspirated diesel engine are compared in Table 14.3. Also shown is a second law analysis of a turbocharged version of the naturally aspirated diesel. These results illustrate the value of defining the losses in availability that occur in each process. Consider the first and second law analysis results for the naturally aspirated engine. While 25.1 percent of the fuel energy leaves the combustion chamber in the form of heat transfer, the availability transfer corresponds to 21.4 percent of the fuel's availability. It is this latter number that indicates the maximum amount of the heat transfer that can be converted to work. The table shows that 34.6 percent of the fuel energy is carried out of the engine in the exhaust gases. However, the second law analysis shows that the exhaust contains only 20.4 percent of the available energy of the fuel. The ratio of these quantities shows that only about 60 percent of the exhaust energy can be converted to work using ideal thermodynamic devices.? The exhaust gas leaves the system in a hightemperature, ambient pressure state and therefore has high entropy (relative to the p o , To reference state). This, via the gas-transfer equation in Table 14.2, reduces the available energy of the exhaust gas stream. t Of course, real thennodynamicdevices will produce less work than ideal devices. NatnraUy aspirated First law, % fuel energy Turboehvged Second hw, % fwl availability Indicated work? Combustion loss Cylinder heat transfer Internal valve throttling Exhaust valve throttling Loss in compressor Loss in turbine Exhaust to ambient Total Brake power, kW 185 185 220 - f Note that the indicated work for the second law balance is a lower percentage than for the first law. This occurs because the availability of the fuel is 1.0317 times the fuel's heating value. The quantity referred to as combustion loss in Table 14.3 is determined from an availability balance for the combustion chamber over the duration of the combustion period. The "availability destroyed" term in Eq. (14.53) then represents the deviation of the actual combustion process from a completely reversible process. The second law analysis shows that the availability loss associated with the combustion irreversibilities is 15.9 percent of the fuel's availability. This loss depends on the overall equivalence ratio at which the engine is operating, as indicated in Fig. 5-17. Combustion of leaner airlfuel ratios would give a higher fractional availability loss due to mixing of the fuel combustion products with increased amounts of excess air and the lower bulk temperature. Overall, the most important point emerging from this comparison is that the work-producing potential of the heat loss to the combustion chamber walls and the exhaust mass flow out of the engine is not as large as the magnitude of the energy transferred: some of these energy transfers, even with ideal thermodynamic work-producing devices, must ultimately be rejected to the environment as heat. A comparison of the second and third columns in Table 14.3, both obtained with a combined first and second law analysis, illustrates how turbocharging improves the performance of a naturally aspirated engine. The brake fuel conversion efficiency of the turbocharged engine is considerably improved-from 33.9 to 39.2 percent. The table indicates that through turbocharging, the availability transfers associated with the heat loss and exhaust gas flow are reduced from 41.8 7% MODELING REAL ENGINE FLOW AND COMBUSTION PROCESSES INTERNAL COMBUSTION ENGINE FUNDAMENTALS to 31.7 percent (a differenceof 10.1 percentage points), while the combustion and added turbomachinery availability losses increase from 15.9 to 21.4 percent (a difference of 5.5 percentage points). By turbocharging, advantage has been taken of the following changes. While the leaner air/fuel ratio operation of the turbo. charged engine increases the combustion availability losses due to the use of a greater portion of the chemical energy of the fuel to mix with and heat excess air, the lower burned gas temmrature this produces results in reduced heat losses and lower cvlinder exhaust temperature. ~naddition,the turbocharger transfers available energy from the cylinder exhaust to the inlet air. The reduced heat loss and lower final exhaust availability level give a substantial performance improvement." To interpret the second law analysis results, one must remember that the desired output is brake work and increases in this quantity (for a given fuel flow) represent improved performance.
All other availability terms represent losses or undesirable transfers from the system; decreasing these terms constitutes an improvement. These undesirable available energy transfer and destruction terms fall into five categories: (1) heat transfer, (2) combustion, (3) fluid flow, (4) exhaust to ambient, (5) mechanical friction.
The available energy flows identified as heat transfer represent the summation of all availability transfers that occur due to heat transfers. The most significant of these are the in-cylinder and aftercooler heat rejection.
The combustion loss represents the amount of available energy destroyed due to irreversibilities occurring in releasing the chemical potential of the fuel as thermal energy and mixing the combustion products with any excess air. The fluid flow losses include the available energy destroyed within the working fluid in the compressor, aftercooler, intake valve, exhaust valve, exhaust manifold, and turbine due to fluid shear and throttling. The availability destroyed due to fluid shear and mechanical rubbing, exterior to the working fluid, are contained in the mechanical friction category. The effect of variations in engine load and speed on these five categories of losses or transfers will now be described. Figure 14-27 shows the availability transfers or losses in each of these categories for a turbocharged six-cylinder 10-liter displacement direct-injection diesel engine, expressed as a percentage of the fuel availability, as a function of engine load. The percentage of fuel availability associated with the heat transfers varies 100 Total heat transfer + d 80 Combustion losses nuid flow losses - 100 3BR Total heat transfer 80- Combustion losses Fluid flowlosses Z ..-.
~ O 0 Brake work l 20 l l 40 l l 60 Losd,%max ' r 80 I ' 100 FIGURE 14-27 Distribution of available energy into major categories for the engine of Fig. 14-26 as a function of engine load." 797 Brake w r k 1 0 1300 I I 150 I I 1700 I I 1900 I I 2100 Engine speed, revlmin FIGURE 14-28 Distribution of available energy into major categories for the engine of Fig. 14-26 as a function of engine speed.57 little over the load range. The combustion loss increases from 21.8 to 32.5 percent as load is decreased due to an increasingly lean operation of the engine. Fluid friction losses, as a percentage, increase slightly as load increases due to larger mass flow rates. Since friction is approximately constant in absolute magnitude, its relative importance increases drastically as the brake output goes to zero. Exhaust flow available energy decreases from 12.2 to 8 percent as load is decreased from 100 to 0 percent.'' The effect of varying engine speed (at full load) is shown in Fig. 1428. The availability associated with heat transfers changes over the speed range shown from 15.6 to 21 percent: more time during each cycle is available for heat transfer at lower speeds. Fluid flow and friction losses decrease with decreasing speed. Other availability losses remain essentially constant as a percentage of the fuel's availability.57 145 FLUID-MECHANIC-BASED MULTIDIMENSIONAL MODELS 14.5.1 Basic Approach and Governing Equations The prediction of the details of the flow field within engines, and the heat-transfer and combustion processes that depend on those flow fields, by numerical solution of the governing conservation equations has become a realizable goal. Such methods have been under development for more than a decade, during which time they have steadily improved their ability to analyze the flow field in realistic engine geometries. While the overall dynamic characteristics of intake and exhaust flows can usefully be studied with one-dimensional unsteady fluid dynamic computer calculations (see Sec. 14.3.4), flows within the cylinder and in intake and exhaust ports are usually inherently unsteady and three dimensional. Recent increases in computing power, coupled with encouraging results with twodimensional calculations, indicate that useful three-dimensional calculations are now feasible. However, they still do not have the capability to predict accurately 798 INTERNAL COMBUSTION ENGINEFUNDAMENTALS all the features of real engine processes of interest.
Gas-flow patterns can be pre. dicted best; predictions of fuel spray behavior are less complete, and combustion calculations mesent considerable difficulties. These lomputational, fluid dynamic, engine process analysis codes solve the partial differential equations for conservation of mass, momentum, energy, and species concentrations. To apply a digital computer to the solution of a continuum problem (such as the flow field inside the cylinder), the continuum must be represented by a finite number of discrete elements. The most common method of discretization is to divide the region of interest into a number of small zones or cells. These cells form a grid or mesh which serves as a framework for constructing finite volume approximations to the governing partial differential equations. The time variable is similarly discretized into a sequence of small time intervals called time steps, and the transient solution is "marched out" in time: the solution at time t,,, is calculated from the known solution at time t,. Threedimensional formulations of the finite difference equations are required for most practical engine calculations; two-dimensional (or axisyrnmetric) formulations can be useful, however, under simpler flow situations, and have been more extensively used to date due to their simpler models and computer codes and requirement for less computer time and storage capacity. The principal components of these multidimensional engine flow models are the following:59 1. The mathematical models or equations used to describe the flow processes. Especially important is the turbulence model, which describes the small-scale features of the flow which are not accessible to direct calculation. 2. The discretization procedures used to transform the differential equations of the mathematical model into algebraic relations between discrete values of velocity, pressure, temperature, etc., located on a computing mesh which (ideally) conforms to the geometry of the combustion chamber with its moving valves and piston. 3. The solution algorithm whose function is to solve the algebraic equations. 4. The computer codes which translate the numerical algorithm into computer language and also provide easy interfaces for the input and output of information. The basic equations for all existing in-cylinder flow calculation methods are the differential equations expressing the conservation laws of mass, momentum (the Navier-Stokes equations-a set of three), energy, and species concentrations. These equations, in the above order, may be written: i MODELING REAL ENGINE FLOW AND COMBUSTION PROCESSES 799 The first term on the right gives the source terms, the second term the diffusive transport. The D/Dt operator provides the convective transport terms and is Here, p is the density, u, the ith velocity component, e the internal energy per unit mass, and Y, the concentration of species a per unit mass. In the IC engine context, the thermal energy source term Q involves a viscous term and source terms arising from chemical reaction of the fuel. Both Q and the species source term, S,, will depend upon the chemical rate equations, which must be known to close the problem. Note that diffusion of the various species contributes to the diffusive flow of internal energy, q,, in addition to conductive heat diffusion. The fact that turbulent flows exhibit important spatial and temporal variations over a range of scales (dictated at the upper end by chamber dimensions and at the lower end by viscous dissipative processes, see Sec. 8.2.1) makes direct numerical solution of these governing equations impractical for flows of engine complexity. Recourse must therefore be made to some form of averaging or filtering which removes the need for direct calculation of the small-scale motions. Two approaches have been developed for dealing with this turbulence modeling problem: full-field modeling (FFM), sometimes called statistical flux modeling; and large-eddy simulation (LES) or subgrid-scale simulation. In FFM, one works with the partial differential equations describing suitably averaged quantities, using the same equations everywhere in the flow. For periodic engine flows, time averaging must be replaced by ensemble or phase averaging (see Sec. 8.2.1). The variables include the velocity field, thermodynamic state variables, and various mean turbulence parameters such as the turbulent kinetic energy, the turbulent stress tensor, etc. In FFM, models are needed for various averages of the turbulence quantities. These models must include the contributions of all scales of turbulent motion.s9, 60 Large-eddy simulation (LES) is an approach in which one actually calculates the large-scale three-dimensional time-dependent turbulence structure in a single realization of the flow. Thus, only the small-scale turbulence need be modeled. Since the small-scale turbulence structure is more isotropic than the large-scale structure and responds rapidly to changes in the large-scale flow field, modeling of the statistical fluxes associated with the small-scale motions is a simpler task than that faced in FFM where the large-scale turbulence must be included. An important difference between FFM and LES is their definition of "turbulence." In FFM the turbulence is the deviation of the flow at any instant from the average over many cycles of the flow at the same point in space and oscillation phase [i.e., the fluctuation velocity defined by Eq. (8.16) or (8.18)]. Thus, FFM "turbulence" contains some contribution from cycle-by-cycle flow variations. LES defines turbulence in terms of variations about a local average; hence in LES turbulence is related to events in the current cycle.60 800 INTERNAL COMBUSTION ENGINE FUNDAMENTALS MODELING REAL ENGINE FLOW AND COMBUSl7ON PROCESSES 145.2 Turbulence Models In full-jeld modeling (FFM), equations for the averaged variables are formed from Eqs. (14.54).
With periodic engine flows, phase or ensemble averaging must be used (see Secs. 8.2.1 and 8.2.2).
Since the flow during the engine cycle is cornpressed and expanded, mass-weighted averaging (called Favre averaging) can be used to make the averaged compressible-flow equations look almost exactly like the averaged equations for incompressible flows. The combined ensemble-Favre averaging approach works as follo~s.~' We denote the phase-averaging process by {), i.e.: 1 {p(x, t) = lim N-m C p(x, t + nr) n=1 where z is the cycle period. We also write {p) = P, and decompose p into p = ?, + p'. The mass-weighted phase-averaged quantities (indicated by an overbar) are defined by N p(x, t a x , t)f(x, t) = lim + nr)f (x, t + nz) (14.57) perature, {Q) will be strongly influenced by temperature fluctuations. These issues are discussed more fully in Secs. 14.5.5 and 14.5.6. which represent turbuThe momentum equations contain terms, -p&;, lent stresses (and are often called the Reynolds stresses). These terms must be modeled with additional equations before the set of equations, (14.59), is "closed" and can be solved. The most widely used turbulence model or equation set is the k-E r n ~ d e l . ~ " -This - ~ ~assumes a newtonian relationship between the turbulent stresses and mean strain rates, and computes the (fictitious) turbulent viscosity appearing in this relationship from the local turbulent kinetic energy k (= u, uJ2) and its dissipation rate E. An equation governing k can be developed by multiplying the u, equation in Eq. (14.54) by u,, subtracting from this the equation formed by multiplying the iii equation in Eq. (14.59) by ii,, and phaseaveraging the result. The equation so obtained is - p= -u!u' aii.
=x (pf 9) = {pfgh) = af3 + m - fififi+fg'h'+ 3- + 6f 7+ fg'h') - where P is the rate of turbulence production per unit mass N-w n = l where all flow variables (except density and pressure) have been decomposed as f =f +f .
Note that {p') is zero, {f) the mass-weighted phase average off is zero, but { f)is not zero. With these definitions: 801 a j ax, and J , represents diffusive transport. In the most commonly used two-equation k-E model, all the unknown turbulence quantities are modeled in terms of the turbulent velocity scale k1I2 and the turbulence length scale k31Z/&obtained from the definition of the energy dissipation rate, via (14.58) Phase-averaging Eq. (14.54), one obtains6' The rationale is that the rate of energy dissipation is controlled by the rate at which the large eddies feed energy to the smaller dissipative scales which in turn adjust to handle this energy.'jO A turbulent viscosity pT is defined: where where Co is a model constant. The turbulent stress terms appearing in Eqs. (14.59) and (14.61) are then modeled in a quasi-newtonian manner: The terms on the left-hand side in Eq. (14.59) involve only the solution variables and hence require no modeling. However, all of the terms on the 3, ii,, 5, and right, particularly the last terms that represent turbulent transport, involve turbulence fluctuation quantities and must be modeled in terms of the solution variables. The source terms {Q) and (Sa} present special difficulties to the engine modeler. Due to the exponential dependence of the heat release Q on tem- x, - pu; u; = $kdij + spT V where Si, is the strain rate of the iii field: iidij - 2 ~ 5,, (14.64) 802 INTERNAL COMBUSTION ENGINE FUNDAMENTALS The viscous-stress terms in the momentum equations are evaluated using a newtonian constitutive relation. The turbulent-diffusion terms in the various transport equations are modeled using the turbulent diffusivity. The diffusing flux of a quantity 4 is given by tains terms for production and decay of q and for its convection and diffusion. In the KIVA engine code,67this equation has the form: where a+ is a turbulent Prandtl number for 4. The model is completed with a transport equation for E. An exact equation can be developed by suitable manipulation of the Navier-Stokes equations. All E equation models are of the form6' where o is the turbulent stress tensor, p the turbulent viscosity, C a constant of order unity, and L a characteristic length on the order of twice the mesh spacing. @ is a source term representing the production of turbulence by the motion of fuel droplets in situations where fuel sprays are important. The physical meaning of the terms in Eq. (14.69) are as follows. The term V (pqu) is the convection of the turbulence by the resolved (large-scale) velocity field.
The term - 3 ~ q V u is a compressibility term that is the turbulent analog of p dV work.
The term o : Vu represents the production of turbulence by shear in the resolved velocity field; V (pVq) is the selfdiffusion of the turbulence with diffusivity pip. The term -CpL-'q3l2 represents the decay of turbulent energy into thermal energy. This term appears with opposite sign as a source term in the thermal internal energy equation in place of o : Vu, which can be thought of as the rate at which kinetic energy of the resolved motions is dissipated by the turbulence.
Before it is dissipated, the kinetic energy of the resolved velocity field is first converted into subgrid scale turbulent energy q, which is then converted into heat by the decay term CpL-1q3/2.67 Under most circumstances, the velocity and temperature boundary layers in an engine cylinder will be too thin to be resolved explicitly with a computing mesh that is practical on present-day computers. However, these layers are important because they determine the wall shear and heat flux which are essential boundary conditions for the numerical simulation, and are of practical irnportance (see Secs. 8.3 and 12.6.5).
Special submodels for these boundary layers, referred to as wall functions, are used to connect the wall shear stresses, heat fluxes, wall temperatures, etc., to conditions at the outer edge of the boundary layer. This removes the need to place grid points within the layer.
Since the boundary layers are usually turbulent, the logarithmic "turbulent law of the wall" is commonly used. Key assumptions made are: that the finite difference mesh point nearest the wall lies in the law-of-the-wall region and that the law-ofthe-wall relation for steady flow past a plane wall is valid under engine cylinder conditions. While these may not be valid assumptions, it is not yet feasible to resolve the flow details within the boundary layer.68 where W is the source term and Hi is the diffusive flux of ,% which is modeled similarly to the other diffusion terms. The appropriate form of W is the subject of much debate. For an incompressible flow, W can be modeled adequately by C, and C, are constants: the C, term produces the proper behavior of homogeneous isotropic turbulence and the C, term modifies this behavior for homogeneous shear. However, for a flow with compression and expansion, an additional term in Eq. (14.68) is needed to account for changes in E produced by dilation. Several forms for this additional term have been p r o p o ~ e d ~ '(for .
~ ~example, C, ~ E V ii) and compared.63 The goal is to construct a W that predicts the appropriate physical behavior under the relevant engine conditions. While different choices for modeling these terms do affect the results (especially the behavior of the turbulence length scale during the cycle6'), the predictions of mean flow and turbulence intensity do not differ very ~ignificantly.~~ One other FFM that has been applied to engines is the Reynolds stress model (RSM) which, in its most general form, comprises seven simultaneous partial differential equations for the six stress components and the dissipation rate E. This obviously imposes a much greater computing burden compared with the two-equation k-E model. The limited results a ~ r i i l a b l eindicate ~~ that RSM predictions of the flow field are closer to corresponding measured data than k-E model prediction^.^^ The large-eddy simulation (LES) approach to turbulence modeling66 has also been applied to engines. Since here one calculates the large-scale threedimensional time-dependent flow structure directly, only the turbulence smaller in scale than the grid size need be modeled. Hence these are often referred to as subgrid-scale models. A new dependent variable q, which represents the kinetic energy per unit mass of the turbulent length scales that are too small to resolve in the mesh, is introduced. This variable satisfies a transport equation which con- . 1453 Numerical Methodology The three important numerical features of multidimensional methods are: the computational grid arrangement, which defines the number and positions of the locations at which the flow parameters are to be calculated; the discretization practices used to transform the differential equations of the mathematical model *. into algebraic equations; and the solution algorithms employed to obtain the flow parameters from the discrete equations.59*65 COMPUTING MESH.The requirements of the computing mesh are: 1. It adequately fits the topography of the combustion chamber and/or inlet port, including the moving components.
2. It allows control of local resolution to obtain the maximum accuracy with a given number of grid points.
3. It has the property that each interior grid point is connected to the same number of neighboring points. The first requirement obviously follows from the need to simulate the effects of changes in engine geometry. The second'requirement stems from the fact that computing time increases at least linearly with the number of mesh points. Thus it is desirable that the mesh allow concentration of grid points in regions where steep gradients exist such as jets and boundary layers. The third requirement comes from the need for the mesh to be topologically rectangular in some transformed space so that highly efficient equation solvers for such mesh systems can be utilized. Early engine models used a grid defined by the coordinate surfaces of a cylindrical-polar frame. Such an approach is adequate provided the combustion chamber walls also coincide with coordinate surfaces.
This only occurs for a restricted number of practical chambers (e.g., disc and centered cylindrical bowlin-piston shapes); even for these, the inlet and exhaust valve circumferences would in general cut across the grid (see Fig. 14-29a). While procedures have been devised for modifying the difference equations for such grids to allow for noncoincident boundaries, the preferred approach is to employ some form of flexible " body-fitting" coordinate frame/grid whose surfaces can be shaped to the chamber geometry, as illustrated in Fig.
14-29b, which shows a diesel engine combustion chamber fitted by a mesh which is orthogonal-curvilinear in the bowl. This enables the bowl shape to be accurately represented and the boundary layers on its surfaces to be resolved in greater detail. The region between the piston crown and cylinder head surfaces is fitted with a bipolar system which expands and contracts axially to accommodate the piston motion. The orthogonality constraint of this mesh limits its usefulness: the generation of orthogonal meshes for general three-dimensional geometries is cumbersome and the resulting mesh often far from optimal. These problems are largely surmounted by " arbitrary " nonorthogonal lagrangianeulerian meshes like that used in KIVA,~' illustrated in Fig. 14-29c. This has the additional advantage that the mesh points in the swept volume are not constrained to move axially: their motion can be arbitrarily pre~cribed.~' DISCRETIZATION PRACIICES.These multidimensional engine flow models are time-marching programs that solve finite difference approximations to the gov- Plan view Elwation view (b) FIGURE 1429 Different types of computing mesh arrangements for engine combustion chambers. (a) Cylindrical polar mesh: dashed line shows valve head ~ircumference.~'(b) Bodyatted orthogonal curvilinear mesh fitted to DI diesel combustion chamber bowL6' (c) Arbitrary nonorthogonal lagrangian-eulerian (ALE) mesh for offset diesel combustion bowL6' INTERNAL COMBUSTION ENGINE FUNDAMENTALS erning differential equations. The individual cells formed by the mesh or grid serve as the spatial framework for constructing these algebraic finite difference equations. The time variable is similarly discretized into a sequence of small time intervals called time steps: the solution at time t,,, is calculated from the known solution at time t,. The spatial differencing is made conservative wherever passible. The procedure used is to difference the basic equations in integral form, with the volume of a typical cell used as the control volume and the divergence terms transformed into surface integrals using the divergence theorem.67 The discretized equations for any dependent variable 4 are of the general form : A P 4 r 1= x n A,&,+' + s+,,V, + A:I#: (14.70) where the A's are coefficients expressing the combined influences of convection and diffusion, S+, V, is the source integral over the cell volume Vp, the subscript p denotes a typical node point in the mesh, the summation is over its (six) nearest neighbors, and the superscripts i 1 and i denote " new" and "old" values, at times t + 6t and t, respectively, where 6t is the size of the time step.69 Until recently all methods involved similar spatial approximations to calculate convective and diffusive transport, using a blend of first-order upwind differencing for the former and second-order central differencing for the latter. Unfortunately, all discretization practices introduce inaccuracies of some kind, and the standard first-order upwind scheme produces spatial diffusion errors which act in the same way as real diffusion to "smooth" the solutions. The magnitude of the numerical diffusion reduces as the mesh density is increased, but even with as many as 50 mesh points in each coordinate direction, the effect is not eliminated. A recent development has been the introduction of "higher order" spatial approximations which, in the past, had a tendency to produce spurious extrema. This problem has been overcome by the use of " flux blending" techniques. First-order upwind and higher-order approximations are blended in appropriate proportions to eliminate the overshoots of the latter. Even with these schemes, however, true mesh-independent solutions could not be achieved with densities of up to 50 nodes in each coordinate direction; so there is still a need for further impr~vernent.~~ , + SOLUTION ALGORITHMS. Numerical calculations of compressible flows are inefficient at low Mach numbers because of the wide disparity between the time scales associated with convection and with the propagation of sound waves. While all methods use first-order temporal discretization and are therefore of comparable accuracy, they differ in whether forward or backward differencing is employed in the transport equations leading to implicit or explicit discrete equations, respectively. In explicit schemes, this inefficiency occurs because the time steps needed to satisfy the sound-speed stability condition are much smaller than those needed to satisfy the convective stability condition alone. In implicit schemes, the inefficiency manifests itself in the additional computational labor needed to solve the implicit (simultaneous) system of equations at each time step. This solution is usually performed by iterative techniques. The computing time requirements of these two approaches scale with the number of equations n and the number of mesh points m, as follows. For explicit methods, computing time scales as nm, but the time step is limited by the stability condition as summarized above. For implicit methods, computing time scales as n3m and At is only limited by accuracy considerations. One procedure used, a semi-implicit method, is the acoustic subcycling method. All terms in the governing equations that are not associated with sound waves are explicitly advanced with a larger time step At similar to that used with implicit methods. The terms associated with acoustic waves (the compression terms in the continuity and energy equations and the pressure gradient in the momentum equation) are explicitly advanced using a smaller time step St that satisfies the sound-speed stability criterion p q . (14.23)], and of which the main time step is an integral multiple.
While this method works well in many IC engine applications where the Mach number is not unduly low, it is unsuitable for very low Mach number flows since the number of subcycles (At/&) tends to infinity as the Mach number tends to zero.
For values of At/& greater than 50 an implicit scheme becomes more efficient. Pressure gradient scaling can be used to extend the method to lower Mach numbers. The Mach number is artificially increased to a larger value (but still small in an absolute sense) by multiplying the pressure gradient in the momentum equation by a time-dependent scaling factor l/a(t)2, where a(t) > 1. This reduces the effective sound speed by the factor a. This does not significantly affect the accuracy of the solution because the pressure gradient in low Mach number flows is effectively determined by the flow field and not vice versa. Coupling pressure gradient scaling with acoustic subcycling reduces the number of subcycles by a.67 The implicit equations that result from forward differencing consist of simultaneous sets for all variables and thus require more elaborate methods of solution. However, they contain no intrinsic stability constraints. Fully iterative solution algorithms for solution of these equation sets are being replaced with more efficient simultaneous linear equation solvers.65 145.4 Flow Field Predictions To illustrate the potential for multidimensional modeling of IC engine flows, examples of the output from such calculations will now be reviewed. A large amount of information on many fluid flow and state variables is generated with each calculation, and the processing, organization, and presentation of this information are tasks of comparable scope to its generation! Flow field results are usually presented in terms of the gas velocity vectors at each grid point of the mesh in appropriately selected planes. Arrows are usually used to indicate the direction and magnitude (by length) of each vector. Examples of such plots--of the flow pattern in the cylinder during the intake process-are shown in Fig. 1430.70The flow field is shown 60" ATC during the intake stroke. A helical intake MODELING REAL ENGINE FLOW AND C O M B U F N PROCBSSES 809 FIGURE 14-30 Computed velocity field within the cylinder at 60" ATC during the intake stroke. Top left: plane through cylinder and inlet valve axes.
Bottom left: orthogonal plane through valve axis. Right: circumferential-radial plane halfway between piston and cylinder head. Reference vector arrow corresponds to velocity of 132 m/s. Letters denote centers of toroidal flow structures.70 port is used to general swirl, and the flow through the valve curtain area (see Sec. 6.3.2)-the inlet boundary condition for the calculation-was determined by measurement. The calculation used a curvilinear, axially expanding and contracting grid with about 16,000 mesh points of the type shown in Fig. 14-296. It employed a fully iterative solution algorithm with standard upwind differencing and the k-E turbulence model. Shown in Fig.
14-30 are the plane through the valve and cylinder axis (top left), the perpendicular plane through the valve axis (bottom left), and a circumferential radial plane halfway between the cylinder head and the piston (right). The major features of the conical jet flow through the inlet valve into the cylinder are apparent (see Sec. 8.1).
However, the off-cylinder-axis valve and the swirl generated by the helical port produce substantial additional complexity. The letters on the figures show regions of local recirculation. Regions A and B correspond to the rotating flow structures observed in simpler geometries (see Fig. 8-3): however, regions CF indicate that the swirling motion is far from solidbody r~tation.~' Figures 14-31 and 14-32 show comparisons of thiee-dimensional predictions of in-cylinder flow fields with data. The computational and experimental geometries have been matched, as have the inlet flow velocities through the valve open area and engine speed. Figure 14-31 shows predicted and measured mean flow velocities and turbulence intensities within the cylinder, with a conventional inlet port and valve configuration, at 68' ATC during the intake stroke.71 The experimental values come from LDA measurements (see Sec. 8.2.2). The general features of the mean flow are reproduced by the model with reasonable accuracy, though some details such as the flow along the cylinder toward the head in the FIGURE 1431 Comparison of (a) measured and predicted axial velocity profiles and (b) measured and predicted turbulence intensity pro6les at 68O ATC during the intake stroke. Data: line with points. Predictions: line without points. Each interval on the scale on cylinder axes corresponds to 2 times the mean piston speed." (a) 72' ATC u u' - Measurement (b) 166' ATC Prediction ------ FIGURE 14-32 Comparison between measured and predicted swirl velocities and turbulence intensities at 72 and 166" ATC during the intake stroke. Engine equipped with helical ports9 MODELING REAL ENGINE FLOW AND COMBUSTION PROCESSES 810 811 INTERNAL COMBUSTION ENGINE FUNDAMENTALS symmetry plane are not predicted. The approximate magnitude of

was used and results in a thick "turbulent" flame with an approximately cylindrical front surface.
Flame front propagation speeds are a&quately predicted; the flame is not modeled in suficient detail to describe its actual structure (see Sec.
9.3.2). Practical use is now being made of these cornbustion codes for both spark-ignition engine (e.g., Refs. 83, 86, and 87) and compression-ignitionengine studies.84s References 1. Streit, E. E., and Borman, G. L.: "Mathematical Simulation of a Large Turbocharged TwoStroke Diesel Engine," SAE paper 710176, SAE Trans., vol. 80,1971. 2 Assanis, D. N., and Heywood, J. B.: "Development and Use of Computer Simulation of the Turbocompounded Diesel System for Engine Performance and Component Heat Transfer Studies," SAE paper 860329,1986. 3. Watson, N., and Janota, M. S.: Turbocharging the Internal Combustion Engine, John Wiley, New York, 1982. 4. Janota, M. S., Hallam, A. J., Brock, E. K., and Dexter, S. G.: "The Prediction of Diesel Engine Performance and Combustion Chamber Component Temperatures Using Digital Computers," Proc. Instn Mech. Engrs, vol. 182, pt. 3L, pp. 58-70, 1967-1968. 5. Benson, R. S., Garg, R. D., and Woollatf D.: "A Numerical Solution of Unsteady Flow Problems," Int. J. Mech. Sci., vol. 6, pp. 117-144, 1964. 6. Benson, R. S.: In J. H. Horlock and D. E. Winterbone (eds.), The Thermodynmnics and Gas Dynamics of Internal Combustion Engines, vol. 1, Clarendon Press, Oxford, 1982. 7. Chapman, M., Novak, J. M., and Stein, R.
A.: "Numerical Modeling of Inlet and Exhaust Flows in Multi-Cylinder Internal Combustion Engines," in T. Uzkan (ed.), Flows in Internal Combustion Engines, ASME, 1982. 8. Bulaty, T., and Niessner, H.: "Calculation of 1-DUnsteady Flows in Pipe Systems of LC. Engines," ASME paper ASME-WA7,1984. 9. Takizawa, M., Uno, T., Oue, T., and Yura, T.: "A Study of Gas Exchange Process Simulation of an Automotive Multi-Cylinder Internal Combustion Engine," SAE paper 820410, SAE Trans., vol. 91,1982. 10. Baruah, P.
C., Benson, R. S., and Balouch, S. K.: "Performance and Emission Predictions of a Multi-Cylinder Spark Ignition Engine with Exhaust Gas Recirculation," SAE paper 780663,1978. 11. Poulos, S. G., and Heywood, J. B.: "The Effect of Chamber Geometry on Spark-Ignition Engine Combustion," SAE paper 830334, SAE Trans., vol. 92,1983. 12. Heywood, J. B., Higgins, J. M., Watts, P.
A., and Tabaczynski, R. I.: "Development and Use of a Cycle Simulation to Predict SI Engine Efficiency and NO, Emissions," SAE paper 790291,1979. 13. Watts, P. A., and Heywood, J. B.: "Simulation Studies of the Effects of Turbocharging and Reduced Heat Transfer on Spark-Ignition Engine Operation, SAE paper 800289, 1980. 14. Lavoie, G. A., and Blumberg, P. N.: "A Fundamental Model for Predicting Fuel Consumption, NO, and HC Emissions of the Conventional Spark-Ignited Engine," Combust. Sci. and Technol., vol. 21, pp. 225-258, 1980. 15. Novak, J. M, and Blumberg, P. N.: "Parametric Simulation of Significant Design and Operating Alternatives Affecting the Fuel Economy and Emissions of Spark-Ignited Engines," SAE paper 780943, SAE Trans., vol. 87,1978. 16. Groff, E. G., and Matekunas, F. A.: "The Nature of Turbulent Flame Propagation in a Homogeneous Spark-Ignited Engine," SAE paper 800133, SAE Trans., vol. 89,1980. 17. Mattavi, J. N.: "The Attributes of Fast Burning Rates in Engines," SAE paper 800920, SAE Trans., vol. 89, in SP-467, The Piston EngiwMeeting the Challenge of the 80s, 1980. 18. Keck, J. C.: "Turbulent Flame Structure and Speed in Spark-Ignition Engines," Proceedings of Nineteenth Symposium (Internationa[) on Combustion, pp. 1451-1466, The Combustion Institute, 1982. 19. Beretta, G.
P., Rashidi, M., and Keck, J.
C.: "Turbulent Flame Propagation and Combustion in Spark Ignition Engines," Combust. Flame, vol. 52, pp. 217-245,1983. 20. Keck, J. C., Heywood, J. B., and Noske, G.: "Early Flame Development and Burning Rates in Spark-Ignition Engines," SAE paper 870164,1987. 21. Tabaczynski, R. J., Ferguson, C. R., and Radhakrishnan, K.: "A Turbulent Entrainment Model for Spark-Ignition Engine Combustion," SAE paper 770647, SAE Trans., vol. 86,1977. 22.
Tabaczynski, R. J., Trinker, F. If., and Shannon, B. A. S.: "Further Refinementand Validation of a Turbulent Flame Propagation Model for Spark-Ignition Engines," Combust. F l m , vol. 39, pp. 111-121,1980. 23. Borgnakke, C.: "Flame Propagation and Heat-Transfer Effects in Spark-Ignition Engines," in J. C.
Hilliard and G. S. Springer (eds.), Fuel Economy in Road Vehicles Powered by Spark Ignition Engines, chap. 5, pp. 183-224, Plenum Press, 1984. 24. Launder, B. E., and Spalding, D. B.: Lectures in Mathematical Models of Turbulence, Academic Press, 1972. 25. Borgnakke, C., Arpaci, V. S., and Tabaczynski, R.
J.: "A Model for the Instantaneous Heat Transfer and Turbulence in a Spark Ignition Engine," SAE paper 800287,1980. 26. Borgnakke, C., Davis, G. C., and Tabanynski, R. J.: "Predictions of In-Cylinder Swirl Velocity and Turbulence Intensity for an Open Chamber Cup in Piston Engine," SAE paper 810224, SAE Trans., vol. 90,1981. 27. Davis, G. C., Tabaaynski, R. J., and Belaire, R. C.: "The Effect of Intake Valve Lift on Turbulence Intensity and Burnrate in S.I. Engines," SAE paper 840030, SAE Trans., ~01.93,1984.
28.
Davis, G. C., Mikulec, A., Kent, J. C., and Tabaaynski, R. J.: "Modeling the Effect of Swirl on Turbulence Intensity and Burn Rate in S.I. Engines and Comparison with Experiment," SAE paper 860325,1986. 29.
Stivender, D.
L.: "Sonic Throttling Intake Valves Allow Spark-Ignition Engine to Operate with Extremely Lean Mixtures," SAE paper 680399, SAE Trans., vol. 77,1968. 30. Hires, S.
D., Tabaczynski, R. J., and Novak, J. M.: "The Prediction of Ignition Delay and Combustion Intervals for a Homogeneous Charge, Spark Ignition Engine," SAE paper 780232, SAE Trans., vol. 87, 1978. 31. Primus, R.
J., and Won& V. W.: "Performance and Combustion Modeling of Heterogeneous Charge Engines," SAE paper 850343,1985. 32. Shipinski, J., Uyehara, 0. A., and Myers, P. S.: "Experimental Correlation between Rate of Injection and Rate of Heat Release in Diesel Engine," ASME paper 68-DGP-11,1968. 33. Whitehouse, N. D., and Way, R J. B.: "Simple Method for the Calculation of Heat Release Rates in Diesel Engines Based on the Fuel Injection Rate," SAE paper 710134,1971. 34. Woschni, G., and Anisits, F.: "Experimental Investigation and Mathematical Presentation of Rate of Heat Release in Diesel Engines Dependent Upon Engine Operating Conditions," SAE paper 740086,1974. 35.
Watson, N., Pilley, A. D., and Marzouk, M.: "A Combustion Correlation for Diesel Engine Simulation," SAE paper 800029,1980. 36. Kuo, T., Yu, R. C., and Shahed, S. M.: "A Numerical Study of the Transient Evaporating Spray Mixing Process in the Diesel Environment," SAE paper 831735, SAE Trans., vol. 92,1983. 37. Chiu, W. S., Shahed, S. M., and Lyn, W. T.: "A Transient Spray Mixing Model for Diesel Combustion," SAE paper 760128, SAE Tram., vol. 85,1976. 38. Rife, J.
M., and Heywood, J. B.: "Photographic and Performance Studies of Diesel Combustion with a Rapid Compression Machine," SAE paper 740948, SAE Trans., vol. 83,1974. 39. Sinnamon, J. F., Lancaster, D. R., and Steiner, J. C.: "An Experimental and Analytical Study of Engine Fuel Spray Trajectories," SAE paper 800135, SAE Trans., vol. 89,1980. 40. Kobayashi, H., Yagita, M., Kaminimoto, T., and Matsuoka, S.: "Prediction of Transient Diesel Sprays in Swirling Flows Via a Modified 2-D Model," SAE paper 860332,1986. 41. Ricou, F.
P., and Spalding, D.
B.: "Measurements of Entrainment by Axisymrnetric Turbulent Jets," J . Fluid Mech., vol. 9, pp. 21-32, 1961. 42. Abramovich, G. M.: The Theory of Turbulent Jets, MIT Press, Cambridge, Mass., 1963. 43. Shahed, S. M, Flynn, P. F., and Lyn. W. T.: "A Model for the Formation of Emissions in a Direct-Injection Diesel Engine," in J. N. Mattavi and C. A. Amann (eds.), Combustion Modeling in Reciprocating Engines, pp. 345-368, Plenum Press, 1980. 44. Hiroyasu, H., Kadota, T., and Arai, M.: "Development and Use of a Spray Combustion Modeling to Predict Diesel Engine Efficiency and Pollutant Emission," paper 214-12, Bull. JSME, vol. 26, no. 214, pp. 569-575.1983. 45. Hiroyasu, H., Kadota, T., and Arai, M.: "Development and Use of a Spray Combustion Modeling to Predict Diesel Engine Efficiency and Pollutant Emissions, " paper 214-13, Bull. JSME, vol. 26, no. 214, pp.
576-583,1983. 46.
Hiroyasu, H.: "Diesel Engine Combustion and Its Modeling," in Proceedings of International Symposium on Diagnostics and Modeling of Combustion in Reciprocating Engines, COMODIA 85, pp. 53-75, Tokyo, September 46,1985. 47. Blumber~.P. N., Lavoie, G. A., and Tabaczynski R. J.: "Phenomenological Models for Reciprocating Internal Combustion Engines," Prog. E w g y Combust. Sci., vol. 5, pp.
123-167,1979. 48. Hires, S. D., Ekchian, A, Heywood, J.
B., Tabaaynski R. J., and Wall, J. C.: "Performance and NO, Emissions Modeling of Jet Ignition Prechamber Stratified Charge Engine," SAE paper 760161, SAE Trans., vol. 85,1976. 49. Hiroyasu, H, Yoshimatsu, A., and Arai, M.: "Mathematical Model for Predicting the Rate of Heat Release and Exhaust Emissions in ID1 Diesel Engines," paper C102182, Proceedings of Conference on Diesel Engines for Passenger Cars and Light Duty Vehicles, Institution of Mechanical Engineers, London, 1982 50. Watson, N, and Kamel, M.: "Thermodynamic Efficiency Evaluation of an Indirect Injection Diesel Engine," SAE paper 790039, SAE Trans., vol. 88,1979. 51. Mansou& S. H., Heywood, J. B., and Radhakrishnan, K.: "Divided-Chamber Diesel Engine, Part I: A CycleSimulation which Predicts Performance and Emissions," SAE paper 820273, SAE Trans, vol.
91, 1982. 52. Mansoun, S. H., Heywood, J.
B, and Ekchian, J. A., "Studies of NO, and Soot Emissions from an ID1 Diesel using an Engine Cycle Simulation," paper C120/82, in Diesel Engines for Passenger Cars and Light Duty Vehicles, Institution of Mechanical Engineers Conference Publication 1982-8, pp. 215227,1982. 53. Syed, S.
A., and Bracco, F. V.: "Further Comparisons of Computed and Measured DividedChamber Engine Combustion," SAE paper 790247,1979. 54. Meintjes, K., and Alkidas, A.
C.: "An Experimental and Computational Investigation of the Flow in Diesel Prechambers," SAE paper 820275, SAE Trans., vol. 91,1982.
55.
Watson, N., and Manouk, M.: "A Non-Linear Digital Simulation of Turbocharged Diesel Engines under Transient Conditions," SAE paper 770123, SAE Trans., vol. 86,1977. 56. Manouk, M., and Watson, N.: "Load Acceptance of Turbocharged Diesel Engines," paper C54/78, Proceedings of Conference on Turbocharging and Turbochargers, Institution of Mechanical Engineers, London, 1978. 57. Primus, R. J., and Flynn, P. F.: "Diagnosing the R d Performance Impact of Diesel Engine Design Parameter Variation (A Primer in the Use of Second Law Analysis)," in Proceedings of International Symposium on Diagnostics and Modeling of Combustion in Reciprocating Engines, COMODIA 85, pp. 529-538, Tokyo, September 44,1985. 58. Primus, R. J., Hoag, K. L., Flynn, P. F., and Brands, M. C.: "An Appraisal of Advanced Engine Concepts Using Second Law Analysis Techniques," SAE paper 841287, SAE Trans., vol. 93,1984. 59. Gosman, A. D.: "Computer Modeling of Flow and Heat Transfer in Engines, Progress and Prospects,'' in Proceedings oflnterrurtional Symposium on Diagnostics and Modeling of Combustion in Reciprocating Engines, COMODIA 85, pp. 15-26, Tokyo, September 46,1985. 60. Reynolds, W. C.: "Modeling of Fluid Motions in Engines-An Introductory Overview," in J. N. Mattavi and C. A. Amann (eds.), Combustion Modeling in Reciprocating Engines, pp. 41-68, Plenum Press, 1980. 61.
El Tahry, S. H.: "k-e Equation for Compressible Reciprocating Engine Flows," J. Energy, vol. 7, no. 4 pp. 345-353, 1983. 62. Morel, T., and Mansour, N. N.: "Modeling of Turbulence in Internal Combustion Engines," SAE paper 820040,1982. 63.
Ahmadi-Befrui, B., Gosman, A. D., and Watkins, A. P.: "Prediction of In-Cylinder Flow and Turbulence with Three Versions of k-e Turbulence Model and Comparison with Data," in T. Uzkan (ed.), Flows in Internal Combustion E n g i n e s l l , FED-vol. 20, p. 27, ASME, New York, 1984. 64. El Tahry, S. H.: "Application of a Reynolds Stress Model to Engine Flow Calculations," in T. Uzkan (ed.), Flows in Internal Combustion E n g i n e s l l , FED-vol. 20, pp. 39-46, ASME, New York, 1984. 65. Gosman, A. D.: "Multidimensional Modeling of Cold Flows and Turbulence in Reciprocating Engines," SAE paper 850344,1985. 66. Ferzieger, J. H.: "Large Eddy Simulationsof Turbulent Flows," AIAA paper 76-347,1976. 67. Amsden, A. A., Butler, T. D., O'Rourke, P. J, and Ramshaw, J. D.: "KIVA-A Comprehensive Model for 2-D and 3-D Engine Simulations," SAE paper 850554,1985. 68. Butler, T. D., Cloutman, L. D., Dukowicz, J. K., and Ramshaw, J. D.: "Multidimensional Numerical Simulation of Reactive Flow in Internal Combustion Engines," in Prog. Energy Combust. Sci., vol.
7, pp. 293-315, 1981. 69. Gosrnan, A. D., Tsui, Y. Y., and Watkins, A. P.: "Calculation of Three Dimensional Air Motion in Model Engines," SAE paper 840229, SAE Trans., vol. 93, 1984. 70.
Brandstatter, W., Johns, R. J. R., and Wigley, G.: "The Effect of Inlet Port Geometry on InCylinder Flow Structure," SAE paper 850499,1985. 71. Gosman, A. D., Tsui, Y. Y., and Watkins, A. P.: "Calculation of Unsteady Three-Dimensional Flow in a Model Motored Reciprocating Engine and Comparison with Experiment," presented at Fifth International Turbulent Shear Flow Meeting, Cornell University, August 1985. 72. Schapertons, H., and Thiele, F.: "Three-Dimensional Computations for Flowfields in DI Piston Bowls," SAE paper 860463,1986. 73. Isshiki, Y., Shimamoto, Y., and Wakisaka, T.: "Numerical Prediction of Effect of Intake Port Configurations on the Induction Swirl Intensity by Three-Dimensional Gas Flow Analysis," in Proceedings of International Symposium on Diagnostics and Modeling of Combustion in Reciprocating Engines, COMODIA 85, pp. 295-304, Tokyo, September 4-6, 1985. 74. Wakisaka, T., Shimamoto, Y., and Isshiki, Y.: "Three-Dimensional Numerical Analysis of InCylinder Flows in Reciprocating Engines," SAE paper 860464,1986. 75. Diwakar, R.: "Multidimensional Modeling of the Gas Exchange Processes in a UniflowScavenged Two-Stroke Diesel Engine," in T. Uzkan, W. G. Tiederman, and J. M. Novak (eds.), International Symposium on Flows in Internal Combustion Engines-Ill, FED--vol. 28, pp. 125134, ASME, New York, 1985. 76. Yamada, T., Ilioue, T., Yoshimatsu, A, Hiramatsu, T., and Konishi, M.: "In-Cylinder Gas Motion of Multivalve EngincThree Dimensional Numerical Simulation," SAE paper 860465, 1986. 77. Gosman, A. D., and Johns, R. J. R.: "Computer Analysis of Fuel-Air Mixing in Direct-Injection Engines," SAE paper 800091, SAE Trans., vol. 89,1980. 78. Watkins, A. P., Gosman, A. D., and Tabrizi, B. S.: "Calculation of Three Dimensional Spray Motion in Engines," SAE paper 860468,1986. 79. Butler, T. D., Cloutman, L. D., Dukowicz, J.
K., and Ramshaw, J. D.: "Toward a Comprehensive Model for Combustion in a Direct-Injection Stratified-Charge Engine," in J. N. Mattavi and C. A. Amann (eds.), Combustion Modelling in Reciprocating Engines, pp. 231-260, Plenum Press, 1980. 80. Bracco, F. V.: "Modeling of Engine Sprays," SAE paper 850394,1985. 81. Cartellieri, W., and Johns, R. J. R.: Multidimensional Modeling of Engine Processes: Progress and Prospects," paper presented at the Fifteenth CIMAC-Congress, Paris, June 1,1983. 822 INTERNAL COMBUSTION ENGINE FUNDAMENTALS 82. Amsden, A. A., Ramshaw, J. D., Oaourke, P.
J., and Dukowicz, J. K.: "KIVA: A Cornpuler Program for Two- and Three-Dimensional Fluid Flows with Chemical Reactions and Fuel Sprays," report LA-10245-MS, LQS Alamos National Laboratory, Lm Alamos, New Mexico, February 1985. 83. ~hmadikefrui,B., Gosman, A. D, Lockwood, F. C., and Watkins, A. P.: " M ~ l t i d i i s i ~ ~ ~ l Calculation of Combustion in an I d e a l i i Homogeneous Charge Engine: A Progress Report," SAE paper 810151, SAE Trans., vol. 90,1981. 84. ~osn&, A. D., and Harvey, P. S.: ''Computer Analysis of Fuel-Air Mixing and Combustion in an Axisymmetric D.I. Diesel," SAE paper 820036, SAE Trans., vol. 91,1982. 85. Basso, A., and Rinolfi, R.: "Two-Dimensional Computations of Engine Combustion: Compafi. sons of Measurements and Predictions," SAE paper 820519,1982. 86. Basso, A.: 'Optimization of Combustion Chamber Design for Spark Ignition Engines," SAE paper 840231,1984. 87. Schapertons, H., and Lee, W.: "Multidiensional~Modeling of Knocking Combustion in S1 Engines," SAE paper 850502,1985. 88. Cheng, W. K., and Theobald, M. A.: "A Numerical Study of Diesel Ignition," paper 87-FE-2, presented at the ASME Energy-Sources Technology Conference, Dallas, February 1987. CHAPTER ENGINE OPERATING CHARACTERISTICS This chapter reviews the operating characteristics of the common types of sparkignition and compression-ignition engines.
The performance, efficiency, and emissions of these engines, and the effect of changes in major design and operating variables, are related to the more fundamental material on engine combustion, thermodynamics, fluid flow, heat transfer, and friction developed in earlier chapters. The intent is to provide data on, and an explanation of, actual engine operating characteristics. 15.1 ENGINE PERFORMANCE PARAMETERS The practical engine performance parameters of interest are power, torque, and specific fuel consumption. Power and torque depend on an engine's displaced volume. In Chap. 2 a set of normalized or dimensionless performance and emissions parameters were defmed to eliminate the effects of engine size. Power, torque, and fuel consumption were expressed in terms of these parameters (Sec. 2.14) and the significance of these parameters over an engine's load and speed range was discussed (Sec. 2.15). Using these normalized parameters, the effect of engine size can be made explicit. The power P can be expressed as: P = mep ApSJ4 (four-stroke cycle) P = mep APSJ2 (two-stroke cycle) (15.1) ENGINE OPERATING CHARACTERISTICS 825 The torque T is given by T = mep V,,/(~A) (four-stroke cycle) T = mep Vd(2x) (two-stroke cycle) (15.2) Thus for well-designed engines, where the maximum values of mean effective pressure and piston speed are either flow limited (in naturally aspirated engines) or stress limited (in turbocharged engines), power is proportional to piston area and torque to displaced volume. Mean effective pressure can be expressed as for four-stroke cycle engines [Eq. (2.41)], and as for two-stroke cycle engines [Eqs. (2.19), (2.38), and (6.2511. The importance of high fuel conversion efficiency, breathing capacity, and inlet air density is clear. Specific fuel consumption is related to fuel conversion efficiencyby Eq. (2.24): Engine speed, revlmin 1 sfc = V/ QHV These parameters have both brake and indicated values (see Secs.
2.3, 2.4, and 2.5). The difference between these two quantities is the engine's friction (and pumping) requirements and their ratio is the mechanical efficiency t],,, . The relative importance of these parameters varies over an engine's operating speed and load range. The maximum or normal rated brake power (see Sec. 2.1) and the quantities such as bmep derived from it (see Sec. 2.7) define an engine's full potential. The maximum brake torque (and bmep derived from it), over the full speed range, indicates the ability of the designer to obtain a high air flow through the engine over the full speed range and use that air effectively. Then over the whole operating range, and most especially those parts of that range where the engine will operate for long periods of time, engine fuel consumption and efficiency, and engine emissions are important. Since the operating and emissions characteristics of spark-ignition and compression-ignition engines are substantially different, each engine type is dealt with separately. 15.2 INDICATED AND BRAKE POWER AND MEP The wide-open-throttle operating characteristics of a production spark-ignition automotive engine are shown in Fig. 15-1. The power shown is the gross power for the basic engine; this includes only the built-in engine a~cessories.~ The maximum net power for the fully equipped engine with the complete intake and exhaust system and full cooling system is about 14 percent lower. The indicated Engine speed, nvlmin FIGURE 151 Gross indicated, brake, and friction power (P,, P,, PI), indicated, brake, and friction mean effective pressure, indicated and brake specific fuel consumption, and mechanical efficiency for 3.8-dm3 sixcylinder automotive spark-ignition engine at wide-open throttle. Bore = 96.8 mm, stroke = 86 nun, r, = 8.6.' power was obtained by adding the friction power to the brake power; it is the average rate of work transfer from the gases in the engine cylinders to the pistons during the compression and expansion strokes of the engine cycle (see Sec. 2.4). The indicated mean effective pressure shows a maximum in the engine's midspeed range, just below 3000 revlmin. The shape of the indicated power curve follows from the imep curve.
Since the full-load indicated specific fuel consumption (and hence indicated fuel conversion efficiency) varies little over the full speed range, this variation of full-load imep and power with speed is primarily due to the variation in volumetric efficiency, t], [see Eq. (15.3)]. Since friction mean effective pressure increases almost linearly with increasing speed, friction power will increase more rapidly. Hence mechanical efficiency decreases with increasing speed from a maximum of about 0.9 at low speed to 0.7 at 5000 rev/ min. Thus bmep peaks at a lower speed than imep. The brake power shows a maximum at about 4300 revlrnin; increases in speed above this value result in a decrease in P,. The indicated fuel conversion efficiency increases by about 10 percent from 0.31 to 0.34 over the speed range 1000 to 4000 revlmin. This is primarily due to the decreasing importance of heat transfer per cycle with increasing speed. At part load at fixed throttle position, these parameters behave similarly; however, at higher speeds torque and mean effective pressure decrease more rapidly with increasing speed than at full load. The throttle chokes the flow at lower and lower speeds as the throttle open area is reduced, increasingly limiting the air flow (see Fig.
7-22). The pumping component of total friction also increases as the engine is throttled, decreasing mechanical efficiency (see Figs.
13-9 and 13-10). Figure 15-2 shows full-load indicated and brake power and mean effective pressure for naturally aspirated DI and ID1 compression-ignitionengines. Except at high engine speeds, brake torque and mep vary only modestly with engine speed since the intake system of the diesel can have larger flow areas than the intake of SI engines with their intake-system fuel transport requirements. The part-load torque and bmep characteristics (at fixed amount of fuel injected per cycle) have a similar shape to the full-load characteristics in Fig. 15-2. The decrease in torque and bmep with increasing engine speed is due primarily to the increase in friction mep with speed (see Figs. 13-7, 13-11, and 13-12).
Decreasing engine heat transfer per cycle and decreasing air-flow rate, as speed increases, have modest additional impacts.
153 OPERATING VARIABLES THAT AFFECT SI ENGINE PERFORMANCE, EFFICIENCY, AND EMISSIONS The major operating variables that affect spark-ignition engine performance, efficiency, and emissions at any given load and speed are: spark timing, fuellair or air/fuel ratio relative to the stoichiometric ratio, and fraction of the exhaust gases that are recycled for NO, emission control. Load is, of course, varied by varying the inlet manifold pressure.
The effect of these variables will now be reviewed. 153.1 Spark Timing Figure 9-3 and the accompanying text explain how variations in spark timing relative to topcenter affected the pressure development in the SI engine cylinder. If combustion starts too early in the cycle, the work transfer from the piston to the gases in the cylinder at the end of the compression stroke is too large; if combustion starts too late, the peak cylinder pressure is reduced and the expan- 828 INTERNAL COMBUSTION ENGINE FUNDAMENTALS sion stroke work transfer from the gas to the piston decreases. There exists a particular spark timing which gives maximum engine torque at fixed speed, and mixture composition and flow rate. It is referred to as MBT-maximum brake torquetiming. This timing also gives maximum brake power and minimum brake specific fuel consumption.
Figure 15-3a shows the effect of spark advance variations on wide-open-throttle brake torque at selected speeds between 1200 and 4200 rev/min for a production eight-cylinder engine. At each speed, as spark is advanced from an initially retarded setting, torque rises to a maximum and then decreases. MBT timing depends on speed; as speed increases the spark must be advanced to maintain optimum timing because the duration of the combustion process in crank angle degrees increases. Optimum spark timing also depends on load.
As load and intake manifold pressure are decreased, the spark timing must be further advanced to maintain optimum engine performance. The maximum in each brake torque curve in Fig. 15-3a is quite flat. Thus accurate determination of MBT timing is dimcult, but is important because NO and HC emissions vary significantly with spark timing. In practice, to permit a more precise definition of spark timing, the spark is often retarded to give a 1 or 2 percent reduction in torque from the maximum value. In Fig. 15-3a the mixture composition and flow rate were held constant at each engine speed. If the mixture flow rate is adjusted to maintain constant brake --I BLspark advance 1.o 10 20 30 40 Spark advance, deg BTC (a) 9 = 1.0, A& = 60•‹, 0% EGR except where noted 5 -20 -10 -5 MBT +5 Retard AdvanffiI Spark advance Mixture Composition The unburned mixture in the engine cylinder consists of fuel (normally vaporized), air, and burned gases. The burned gas fraction is the residual gas plus any recycled exhaust used for NO control. Mixture composition during combustion is most critical, since this determines the development of the combustion process which governs the engine's operating characteristics. While substantial efforts are made to produce a uniform mixture within the cylinder, some nonuniformities remain (see Sec. 9.4.2).
In a given cylinder, cycle-by-cycle variations in average charge composition exist. Also, within each cylinder in a given engine cycle, the fuel, air, EGR, and residual gas are not completely mixed, and composition nonuniformities across the charge may be significant.t These together produce variations in composition at the spark plug location (the critical region since the early stages of flame development influence the rest of the combustion process) which can be of order f 10 percent peak-to-peak (see Fig. 9-34). In addition, in multicylinder engines, the average air, fuel, and EGR flow rates to each cylinder are not identical. Typical cylinder-to-cylinder variations have standard deviations of 5 percent of the mean for air flow rate and fuel flow rate (giving a + (b) FIGURE 154 (a) Variation in brake torque with spark advance, eight-cylinder automotive spark-ignition engine at wide-open throttle, at engine speeds from 1200 to 4200 rev/min. 1 percent torque loss from MBT and spark advance for borderline knock are shown.5 (b) Predicted variation in brake specw& fuel wnsumption (normalized by MBT value) with spark retard at several different part-load engine wnditiom6* ' ' 15.3.2 1% loss tine 420 TC torque, the effect of spark timing variations on fuel consumption at constant engine load can be evaluated. Figure 15-3b shows results obtained with a computer simulation of the engine operating cycle.6. The curves for several different part-load operating conditions and burn durations (from fast to slow) have been normalized and fall essentially on top of each other. Five degrees of retard in spark timing have only a modest effect on fuel consumption; for 10 to 20" retard, the impact is much more sigdicant. Spark timing affects peak cylinder pressure and therefore peak unburned and burned gas temperatures (see Sec. 9.2.1). Retarding spark timing from the optimum reduces these variables.
Retarded timing is sometimes used therefore for NO, emission control (see Fig. 11-13 and accompanying text) and to avoid knock (see Sec. 9.6.1). The exhaust temperature is also affected by spark timing. Retarding timing from MBT increases exhaust temperature; both engine eficiency and heat loss to the combustion chamber walls (see Fig. 12-27) are decreased. Retarded timing is sometimes used to reduce hydrocarbon emissions by increasing the fraction oxidized during expansion and exhaust due to the higher burned gas temperatures that result (see Sec. 11.4.3). Retarded timing may be used at engine idle to bring the ignition point closer to TC where conditions for avoiding misfire are more favorable. t This aspect of mixture nonuniformity is least well defined. Mixing of the b h mixture (fuel, air, and EGR) with residual gas is likely to be incomplete (see Fig. 14-36), especially at light load when the residual gas fraction is highest. With intakeport fuel-injection systems, there is evidence of incomplete fuel-air mixing due to the fact that the air flow and fuel flow proare not in phase? When the engine is wld, fuel distribution within the cylinder is known to be nonuniform. + 7 percent variation in the air/fuel ratio) for steady-state engine operation. EGR cylinder-to-cylinder flow rates may have higher variability. Under unsteady engine operating conditions all these variations can be higher. It is necessary to consider the effect of mixture composition changes on engine operating and emissions characteristics in two regimes: (1) wide-open throttle (WOT) or full load and (2) part throttle or load. At WOT, the engine air flow is the maximum that the engine will induct.7 Fuel flow can be varied, but air flow is set by engine design variables and speed. At part throttle, air flow, fuel flow, and EGR flow can be varied. Evaluation of mixture composition changes at part load should be done at fixed (brake) load and speed, i.e., under conditions where the engine provides the desired torque level at the specified speed. To maintain torque (or load or bmep) constant as mixture composition is varied normally requires changes in throttle setting (and if EGR is varied, changes in EGR flow-control valve setting). This distinction between part-load comparisons at specified torque or bmep, rather than at constant throttle settings (which gives essentially constant air flow), is important because the pumping work component of engine friction will vary at constant engine load as mixture composition changes. At constant throttle setting and speed, the pumping work remains essentially unchanged. AIR/FUEL OR EQUIVALENCE RATIO CHANGES. Mixture composition effects are usually discussed in terms of the airlfuel ratio (or fuellair ratio) because in engine tests, the air and fuel flow rates to the engine can be measured directly and because the fuel metering system is designed to provide the appropriate fuel flow for the actual air flow at each speed and load.
However, the relative proportions of fuel and air can be stated more generally in terms of the fuellair equivalence ratio 4 [the actual fuellair ratio normalized by dividing by the stoichiometric fuellair ratio, see Eq. (3.811 or the relative airlfuel ratio 1 [see Eq. (3.911. The combustion characteristics of fuel-air mixtures and the properties of combustion products, which govern engine performance, efficiency, and emissions, correlate best for a wide range of fuels relative to the stoichiometric mixture proportions.
Where appropriate, therefore, the equivalence ratio will be used as the defining parameter. Equation (7.1) converts the airlfuel ratio with gasoline to the equivalence ratio. The theoretical basis for understanding the effect of changes in the equivalence ratio is the fuel-air cycle results in Figs. 5-9 and 5-10, where the indicated fuel conversion efficiency and mean effective pressure are shown as a function of the fuellair equivalence ratio, 4. The mean effective pressure peaks slightly rich of stoichiometric, between 4 = 1 and 1.1. Due to dissociation at the high temperatures following combustion, molecular oxygen is present in the burned gases under stoichiometric conditions, so some additional fuel can be added and par- t EGR is normally zero at WOT,since maximum torque is usually desired.
tially burned. This increases the temperature and the number of moles of the burned gases in the cylinder. These effects increase the pressure to give increased power and mep. Fuel conversion efficiency decreases approximately as 114, as the mixture is richened above stoichiometric (4 > 1) due to the decreasing combustion efficiency associated with the richening mixture. For mixtures lean of stoichiometric, the theoretical fuel conversion eficiency increases linearly as 4 decreases below 1.0. Combustion of mixtures leaner than stoichiometric produces products at lower temperature, and with less dissociation of the triatomic molecules CO, and H,O.Thus the fraction of the chemical energy of the fuel which is released as sensible energy near TC is greater; hence a greaterfraction of the fuel's energy is transferred as work to the piston during expansion, and the fraction of the fuel's available energy rejected to the exhaust system decreases (see Sec. 5.7).
There is a discontinuity in the fuel conversion efficiency and imep curves at the stoichiometric point; the burned gas composition is substantially different on the rich and the lean sides of 4 = 1. Figure 15-4 shows gross indicated specific fuel consumption data for a sixcylinder spark-ignition engine at wide-open throttle and 1200 r e ~ / m i n ,and ~ values of gross indicated mean effective pressure and fuel conversion efficiency derived from the isfc data. In these engine tests, the fuel-air mixture was prepared in two different ways: (1) with the normal carburetor and (2) with a heated vaporizing tank to ensure intake-mixture uniformity. Shapes of the practical efficiency curves and the theoretical curves in Fig. 5-9 differ. Cylinder-to-cylinder air/fuel ratio maldistribution prevents the carbureted engine operating leaner than 4 x 0.85 (A/F x 17) without misfire under these conditions. While use of a fuel vaporizing and mixing tank essentially removes this maldistribution and extends the lean mis6re limit, qZ, does not continue to increase as 4 decreases. The reasons for this are that cycle-to-cycle pressure fluctuations and the total dura- FIGURE 154 Fuellair equivalence ratio Effect of the fuellair equivalence ratio variations on indicated mean effective pressure, specific fuel consumption, and fuel conversion efiiciency of six-cylinder spark-ignition engine at wideopen throttle and 1200 rev/ min. Data for standard carburetcd engine, and engine equipped with vapor tank which extends the lean operating limit, are shown.9 ENGINE OPERATING CHARACTERISTICS ~>m~act, high r,, chamber I I I I I UX) 0.6 0.7 0.8 0.9 1.0 I 1.1 1.2 1.3 Fuellair equivalence ratio Q) bmep = 325 kPa : MBT timing M D 310 - 290 270 1 1 1 1 0.6 0.7 0.8 0.9 1 1.0 1 1 1.1 1.2 Fuellair equivalence ratio (b) FIGURE 15-5 Effect of combustion chamber design and bum rate on spark-ignition engine brake specific fuel consumption. (a) l.6dm3 four-cylinder engine with wnventional combustion chamber and 1.5dm3 four-cylinder engine with compact fast-burning high-compressionratio chamber beneath the exhaust valve with re = 13, both at bmep of 250 kPa and 2400 rev/min.1•‹(b) Predictions from thermodynamicibased computer simulation of engine cycle for 5.7dm3 eightcylinder engine at bmep of 325 kPa and 1400 rev/min with MBT spark timing.6 tion of the burning process increase as the mixture becomes leaner: both these factors degrade engine efficiency. Since the spark advance is set for the average cycle, increasing cycle-to-cycle dispersion produces increasing imep (and hence q,, i) losses in "nonaverage * cycles due to nonoptimum timing. The lengthening burn duration directly decreases efficiency, even in the absence of cy'clic variations. Engine fuel consumption and efficiency well lean of stoichiometric depend strongly on the engine combustion chamber design. Figure 15-5 shows two sets of engine bsfc data, for a conventional combustion chamber and a compact highcompression-ratio chamber, at constant load and speed (250 kPa bmep and 2400 rev/min) as a function of equivalence ratio. Also shown are bsfc results obtained from a thermodynamiobased computer cycle simulation of the sparkignition engine operating cycle (at 325 kPa bmep and 1400 re~jmin).~ Though the load and speed are different, the behavior of the data and predictions for rich mixtures, 4 > 1, are comparable. On the lean side of stoichiometric, however, fuel consumption depends on the combustion characteristics of the chamber. The faster-burning compact high-compression-ratio chamber shows decreasing bsfc 833 until the lengthening bum duration and larger cycle-by-cycle variations cause bsfc to increase. For the slower-burning conventional chamber, this deterioration in combustion starts to occur almost immediately on the lean side of stoichiometric, and fuel consumption worsens for C$ 5 0.9. Thus the equivalence ratio for optimum fuel consumption at a given load depends on the details of chamber design (including compression ratio) and mixture preparation quality. It also varies for a given chamber over the partthrottle load and speed range. For lighter loads and lower speeds it is closer to stoichiometric since the residual gas fraction is higher and combustion quality is poorer with greater dilution and at lower speeds. At part load, as the &/fuel ratio is varied at constant brake load, the pumping work varies, and this also contributes to the brake specific fuel consumption and efficiency variation with equivalence ratio. Figure 15-6 shows the gross and net indicated fuel conversion efficiencies and brake efficiency as a function of equivalence ratio at a part-throttle constant load and speed point (325 kPa

To assess more broadly the effect of compression ratio variations on fuel conversion efficiency, several data sets have been normalized and compared in Fig. 15-13 which shows the ratio of fuel conversion efficiency at the given compression ratio divided by the efficiency at rc = 8, for wide-open-throttle engine operation. The agreement for rc 5 14 is good. Over the compression ratio range that is accessible to SI engines with available fuels (rc 12), fuel conversion efficiency increases by about 3 percent per unit of compression ratio increase.
Note, of course, that engine power increases by about the same amount. ~ f i,(CN) Vf, b 1100 / 1000 / 2000 revlmin WOT / MBT timing 8 10 12 14 16 Compression ratio 18 20 900 (CN) FIGURE 15-13 Wide-open throttle I I I I 8 10 12 14 I 16 I I I 18 20 22 Compression ratio r, : Relative fuel conversion efficiency improvement with increasing compression ratio, spark-ignition engines at wide-open throttle: CN," KT." A similar comparison of the effect of compression ratio increases on efficiency at part load is shown in Fig. 15-14.'' The figure shows brake fuel conversion efficiency data from engines of different cylinder volume. Both the compression ratio for maximum efficiency and the maximum efficiency depend on cylinder size. The wide-open-throttle and road-load data (top two curves17) confirm that the increase in efficiency with an increase in the compression ratio at part load apparently depends on the details of engine operation to a significant degree also. For the important compression ratio range of 9 to 11, the relative 15 mep, kPa 843 WOT (CNI /'+RL (CN) FIGURE 1512 Effect of compression ratio on indicated mean effective pressure and fuel conversion efficiency. 5.3-dm3eightcylinder spark-ignition engine at 2000 rev/min and wide-open throttle. Equivalence ratio and spark timing adjusted for maximum torque for mep data; adjusted for minimum fuel consumption for efficiency data.17 FIGURE 15-14 Vd, cm3/cylinder Compression ratio rc Relative brake fuel conversion eficiency improvement with increasing compression ratio of spark-ignition engines of diierent displaced volume per cylinder at part throttle (except top CN,I7 curve TO." at WOT).19 RL road load. 844 INTERNAL COMBUSTION ENGINE FUNDAMENTALS ENGnVE OPERATING CHARACIZRISnCS 845 efficiency improvement is between 1 and 3 percent per unit of compression ratio increase, depending on cylinder size and operating conditions. The exhaust temperature decreases as compression ratio and efficiency increase until the compression ratio corresponding to maximum efficiency is reached. It has also been shown that heat losses to the combustion chamber walls, as a fraction of the fuel's chemical energy, also decrease as the compression ratio and efficiency both increase." The effect of compression ratio changes on N O emissions is small. Some studies show a modest increase in specific NO emissions as the compression ratio increases at constant load and speed; other studies show a slight decrease. Increasing the compression ratio increases exhaust hydrocarbon emissions. Several trends could contribute: increased importance of crevice volumes at high r,; lower gas temperatures during the latter part of the expansion stroke, thus producing less HC oxidation in the cylinder; decreasing residual gas fraction, thus increasing the fraction of in-cylinder HC exhausted; lower exhaust temperatures, hence less oxidation in the exhaust system. 15.4 SI ENGINE COMBUSTION CHAMBER DESIGN 15.4.1 Design Objectives and Options There has always been extensive debate over the optimum SI engine combustion chamber design. There are a large number of options for cylinder head and piston crown shape, spark plug location, size and number of valves, and intake port design." Debate revolves around issues such as chamber compactness, surface/volume ratio, flame travel length, and use of swirl and squish types of mixture motion. Figure 15-15 shows examples of several common types of combustion chamber shapes. Over the past few years a consensus has developed which favors faster-burning combustion-chamber designs. A chamber design where the fuel burning process takes place faster, i.e., occupies a shorter crank angle interval at a given engine speed, produces a more robust and repeatable combustion pattern that provides emission control and efficiency gains simultaneously. A faster-burning chamber with its shorter burn time permits operation with substantially higher amounts of EGR, or with very lean mixtures, within the normal constraints of engine smoothness and response. Thus greater emissions control within the engine can be achieved, and at part load at this higher level of dilution a faster-burning chamber shows an improvement in fuel consumption due to the reduced pumping work, reduced heat transfer (due to lower burned gas temperatures), and reduced amount of dissociation in the burned gases.22 The major combustion chamber design objectives which relate to engine performance and emissions are: (1) a fast combustion process, with low cycle-bycycle variability, over the full engine operating range; (2) a high volumetric efficiency at wide-open throttle; (3) minimum heat loss to the combustion chamber walls; (4) a low fuel octane requirement. FIGURE 15-15 Examples of common spark-ignition engine combustion chamber shapes: (a) bathtub and wedge: (b) bowl-in-piston; (c) four-valve pent roof; (d) hnnispheri~al.~' Many methods for producing a "fast bum" have been proposed.
These include ways of making the combustion chamber shape more compact, moving the spark plug to a more central location within the chamber, using two plugs, and increasing in-cylinder gas motion by creating swirl during the induction process or during the latter stages of compression. A faster combustion process relative to more moderate bum rate engines does result in a direct engine efficiency gain, other factors being equal.
The magnitude of this direct gain is relatively modest. Experimental studies of the effect of an increase in burn rate from moderate to fast at constant engine load, speed, and mixture composition show that this effect is a few percent at most.23 Computer simulations of the engine operating cycle confirm these experimental observations: while a decrease in total burn duration from 100 to 60' (slow to moderate burn) does result in a 4 percent decrease in bsfc, a decrease in bum duration from 60 to 20" gives only a further 1.5 percent bsfc decrea~e.~ Of greater importance is the fact that the faster bum process is more robust and results in the engine being able to operate satisfactorily with much more EGR, or much leaner, without a large deterioration in combustion quality. Faster burning chamber designs exhibit much less cycle-by-cycle variability. This ability to operate with greater dilution at part load while maintaining a short burn duration and low cycle-by-cycle variability, permits much greater control of NO, within the engine with 20 or more percent EGR without any substantial increase in HC emissions (see Fig. 11-29), or permits very lean operation. In both cases the efficiency gain relative to moderate burn rate engines, which must operate with less dilution, is sizeable.24 High volumetric efficiency is required to obtain the highest possible power density. The shape of the cylinder head affects the size of valves that can be incorporated into the design. Effective valve open area, which depends on valve diameter and lift, directly affects volumetric efficiency.
Swirl is used in many modern chamber designs to speed up the burning process and achieve greater combustion stability.
Induction-generated swirl appears to be a particularly stable in-cylinder flow. Swirl results in higher turbulence inside the chamber during combustion, thus increasing the rate of flame development and propagation.
Generating swirl during the intake process decreases volumetric efficiency. Heat transfer to the combustion chamber walls has a significant impact on engine efficiency. It is affected by cylinder head and piston crown surface area, by the magnitude of in-cylinder gas velocities during combustion and expansion, by the gas temperatures and the wall temperatures. The heat-transfer implications of a combustion chamber should be included in the design process. Knock effectively limits the maximum compression ratio that can be used in any combustion chamber; it therefore has a direct impact on efficiency. Knock is affected by all the factors discussed above. It is the hardest of all the constraints to incorporate into the design process because of its obvious complexity. Knowledge of the fundamentals of spark-ignition engine combustion, incylinder gas motion, and heat transfer has developed to the point where a rational procedure for evaluating these factors for optimum combustion chamber development and design can be defined. The next two sections develop such a procedure. 15.4.2 Factors That Control Combustion Our understanding of the structure of the spark-ignition engine flame as it develops and propagates across the combustion chamber (see Secs.
9.3 and 9.4) allows us to relate the physical and chemical factors that control this process to the relevant engine design and operating parameters. The following factors affect the flame development and propagation processes: 1. Geometry. Combustion chamber shape and spark plug location. 2. Flow field characteristics. Mean velocity, turbulence intensity, and characteristic turbulence length scale in the unburned mixture during combustion. 3. Unburned mixture composition and state. Fuel, equivalence ratio, burned gas fraction, mixture pressure and temperature.
Geometry primarily affects combustion through the flame front surface area. It has a lesser effect on combustion development through its influence on in-cylinder motion. Geometric calculations (see Sec. 14.4.2), based solely on the assumption that the front surface of the flame can be modeled as a portion of a sphere centered at the spark plug, provide data on flame front area and the volume behind the flame front surface (the enflamed volume), contained within the combustion chamber at the appropriate flame radii and piston positions. Flame area varies significantly from one chamber shape to another for a given enflamed volume. In the example shown in Fig. 14-7, the bowl-in-piston chamber gives flame surface areas 30 to 45 percent larger than those for the disc chamber under equivalent conditions around top-center.
Hemispherical and open or clamshell chambers showed gains of about 30 percent relative to the equivalent disc configuration.
For a given chamber shape, flame area depends even more significantly on plug location.
Figure 14-7 shows that shifting the plug from a side to a center location for the bowl-in-piston chamber increased the peak flame area by 150 percent. For hemispherical and open chambers, the increases for a similar shift in plug location were 75 and 90 percent, respe~tively.~~ Maps of flame area as a function of radius at different crank angle locations indicate the following pattern. For chamber geometries with side ignition, as flame radius increases, the flame area first rises slowly, then remains approximately constant, and then decreases slowly to zero. In contrast, chambers with central ignition show, as flame radius increases, a rise in flame area to a peak during the major part of the flame travel followed by a rapid decrease as the flame encounters the chamber walls. Moving the plug location toward the center of the chamber produces a larger increase in flame front area than does making the chamber shape more compact (though this has a positive impact too). The effect of chamber geometry on bum rate has been examined using thermodynamic-based engine cycle simulations with various types of combustion model (e.g., the type developed by Keck and coworkers, see Sec. 14.4.2). Figure 15-16 shows results from one such study." The combustion characteristics of ten different chamber geometries were compared at fixed part-load engine operating conditions.
The flame development and propagation phases were separated into 0 to 10 and 10 to 90 percent mass fraction burned times.
These were then normalized by the equivalent burn times of the slowest burning chamber-the disc with side ignition. Chamber geometry has the greatest impact on the 10 to 90 percent burn time; its effect on 0 to 10 percent time is significant but substantially smaller. Total burn times can be reduced by between 20 to 30 percent by optimizing spark plug location-comparing worst to best location for each chamber shape. Comparing worst and best chamber shapes, total burn time with fixed plug location can be reduced by about 10 percent. Increased turbulence in the unburned mixture at the time of combustion increases the burning rate. Turbulence is usually increased by generating swirl during the induction process (see Sec. 8.3.2 and below). Cycle simulation studiesZSindicate that both the duration of the early stage of the burning process and of the main stage decrease when the turbulent velocity at the start of com- Spark plug location Disc, side Hemi. side I 0 I 0.2 I I 0.4 0.6 Bum angle ratio 1 0.8 I 1.0 FIGURE 15-16 Comparison of bum angles (0-10 percent burned, 10-90 percent burned, 0-90 percent burned; see Fig. 9-13) for ten different spark-ignition engine combustion chamber geometries and spark plug locations. Bum angles are normahxi by angles for slowest burning chamber: disc with side bustion is increased. The faster combustion process comes primarily from the higher turbulence intensity; however, the decreased characteristic turbulence scale that accompanies the increased turbulence is also significant since it results in a shorter characteristic burning time [see Eq. (14.39) and the accompanying text]. It is important to note that the fuel conversion eficiency of higherturbulence chambers at the same operating conditions can be lower than for normal chambers, despite the faster bum rates, due to the higher heat transfer that accompanies the higher in-cylinder velocities. For example, predictions based on the combustion model defined by Eqs. (14.33) to (14.35), where the characteristic mixture speed u, was increased by a factor of two, showed that the 0 to 10 percent and 10 to 90 percent bum durations decreased by about onethird. However, the indicated fuel conversion efficiency decreased by about 6 percent due to the predicted 15 percent increase in heat transfer." Mixture composition and state affect the bum rate through the dependence of laminar flame speed on temperature, pressure, fuellair equivalence ratio, and burned gas fraction (residual gas and EGR): see Sec. 9.3.3 and Eqs. (14.33) to (14.35).
Table 15.1 compares the burn durations for a stoichiometric mixture, a lean mixture with 4 = 0.8, and a stoichiometric mixture with 20 percent EGR. The values of the laminar flame speed at the time of spark are also given (conditions at spark as well as composition are different in each case). The longer bum durations of the more dilute mixtures are clear. Note that EGR as a diluent has a much more deleterious effect on combustion than does air at these approximately equal levels of dilution. All the above-described factors-flame geometry, fluid motion, and mixture composition-can vary cycle-by-cycle, and therefore contribute to combustion variability (see Sec.
9.4). Cyclic differences in gas motion in the vicinity of the spark plug result in differences in motion of the flame kernel during its early stages of development.
Differences in turbulence result in differences in the rates at which the initially smooth surface of the flame kernel becomes wrinkled and convoluted by the flow. Different initial flame center motions change the geometrical interaction of the flame front with the combustion chamber walls later in the flame propagation process. Differences in the amount of fuel, air, and EGR which enter each cylinder cycle-by-cycle, the nonuniformity in composition of the entering charge, and any incomplete mixing of that entering charge with the residual gases in the cylinder also contribute to combustion variability. These composition nonuniformities lead to differences in the early stages of flame development. The variations in the amounts of fuel, air, and EGR that enter each cylinder cycle-by-cycle and in the uniformity of that mixture are factors within the direct control of the engine designer. A fast combustion process reduces cyclic combustion variability for the following reasons. With a faster bum, optimum spark timing is closer to top-center: mixture temperature and pressure at the time of spark are higher, so the laminar flame speed at the start of combustion is greater. This, combined with the higher turbulence of most fast-bum concepts, results in faster flame kernel development. TABLE 15.1 Effect of excess air and recycled exhaust on burn dwation bun^ durations, degree EGR, 1.0 0.8 1.0 % 0.9 degree 040% 104% S L . 9.9 ~ an/s 0 0 20 340 336 324 22 26 31 17 21 28 75 52 23 400 aa3 per cylinder displaced volume, 80 mm bore, 8.5 compression ratio, disc chamber, center plug location. lSOO m/min, stoichiometric operation, 0, = spark timing (MBT), inlet pressure 0.5 atm, inlet temperature 350 K, S, = laminar flame speed." 850 INTERNAL COMBUSTION ENGINE FUNDAMENTALS More rapid initial flame growth results in less variation in flame center motion during the critical flame-development phase.
The resulting geometric variations in the flame frontlchamber wall interaction are therefore reduced; this decreases the variations in burn rate that result from these geometric variations. Also, the faster burning process ends earlier in the expansion stroke. Thus the problem of occasional slow burning cycles, partial burning cycles, and eventually misfire, which occurs with dilute mixtures under normal burning conditions due to quenching of the combustion process as gas temperatures fall during expansion, is largely avoided (see Sec. 9.4.3). 15.43 Factors That Control Performance VOLUMETRIC EFFICIENCY.Combustion chamber shape affects volumetric efi- ciency through its constraints on maximum valve size and through the degree of swirl (if any) that the chamber and port designs produce to achieve the desired combustion characteristics. To obtain maximum performance and to reduce pumping losses, the size of the valve heads should be as large as practical; the valve sizes that can be accommodated depend on cylinder head layout. Table 6.1 lists the typical maximum valve sizes that can be accommodated into several common chamber shapes (see Fig. 15-15). The approximate mean piston speed at maximum power is a measure of the maximum air flow that each engine design can pump. Note that of the two-valve configurations, the designs with inclined valve stems permit substantially greater maximum air flow. The four-valve pentroof design, which also has inclined valve stems, is the best of those listed since it accommodates the largest valve and port areas (there are other four-valve head designs which are comparable). Swirl can be generated during the intake process through suitable port, valve, and head design. It requires either that the flow through the intake valve be directed tangentially into the cylinder so that gas flows through one side of the valve opening preferentially (e.g., through the use of masks to restrict flow at the mask location or through the use of a tangentially directed port or a flow deflector in the port just upstream of the valve), or requires the use of a helical intake port that imparts an angular velocity to the flow before it enters the cylinder. In either case the inlet flow enters the cylinder with higher velocity than it would have in the absence of swirl; hence the pressure drop across the valve is increased, and maximum air flow through the cyiinder is reduced. Well-designed helical swirl-generating ports (see Sec. 8.3.2) appear to be the best way to create swirl. However, geometric and production constraints often prevent the incorporation of such ports into the cylinder head design, and other swirl-generating methods must be used. The engine maximum-power penalty associated with generating significant swirl is of order 5 to 10 per cent. Since swirl is only required at part-throttle operation when enhancement of the burn rate is most critical and is not usually required at full throttle when the flow restriction penalty is most significant, induction systems with a separate passage for the part-throttle air flow, where only this separate passage generates swirl, are an attractive option. However, the gains in volumetric efficiency are offset by a higher cost due to the additional complexity in port and manifold of the double passage and the individual throttle valves required in each port for flow control. Swirl can be intensijed during compression with bowl-in-piston combustion chambers by decreasing the moment of inertia of the in-cylinder charge as the piston moves toward top-center, and thereby increasing its angular velocity (see Sec. 8.3.3). An advantage here is that the swirl level generated during induction is less than would be required without the compression-produced radially inward motion of the charge. This approach can be used with combustion chamber designs that are axisymrnetric and compact. Swirl can also be generated by squish motion toward the end of compression with a suitable design of chamber. The advantage of this approach is that there is no induction-stroke swirl-generating volumetric efficiency penalty. However, the cylinder head geometries proposed to date for either intensifying or generating swirl have vertical valve stems, and hence have smaller valve sizes which in themselves restrict air flow. Also, the cylinder head geometry required to generate swirl during compression has a larger surface area than more open chamber designs and, therefore, has significantly higher heat losses. The impact of conventional radially inward squish motion (see Sec.
8.4) on in-cylinder turbulence, and hence combustion, is unclear. Chambers with significant squish are also more compact; for this reason alone they would be faster burning. HEAT TRANSFER. The convective engine heat transfer to the combustion chamber walls is described by equations of the form of (12.2): e.g., Eq. (12.21). The heat-transfer coefficient is usually correlated by expressions of the form of Eq. (12.3), which relate the Nusselt, Reynolds, and Prandtl numbers (see Sec. 12.4). Thus combustion chamber surface area, and especially the surface area in contact with the burned gases, is important. Gas velocity is also important; it influences the heat-transfer rate through the Reynolds number.
Various characteristic velocities have been used in the Reynolds number to scale heat transfer: mean piston speed, mean in-cylinder gas velocity, turbulence intensity, either individually or in combination. Both of these variables, area and velocity, are affected by combustion chamber design. Studies of engine performance using thermodynamic-based simulations of the engine's operating cycle (see Sec. 14.4) provide data that indicate the importance of changes in heat transfer. At part-throttle operating conditions, such simulation calculations show that a 10 percent change in combustion chamber heat losses results in a change of between 2 and 5 percent in brake specific fuel consumption; an average fuel consumption change of about one-third the magnitude of the heat-transfer change (and of opposite sign) is an appropriate rule of thumb.25*"At wide-open throttle, the effect on mean effective pressure is comparable: a 10 percent change in heat transfer results in about a 3 percent change in bmep. ENGINE OPERATING CHARACTERISTICS This impact of heat transfer on engine efficiency and performance underlines the importance of combustion chamber details that affect heat transfer. For the chamber shapes shown in Fig.
15-16, the total heat losses as a fraction of the fuel's energy, at fixed engine speed and intake conditions, were also calculated. Both chamber shape and spark plug details affect heat losses since together these govern the surface area of the hot burned gases in contact with the walls. The open and hemispherical chambers had least heat transfer. Geometries such as the bowl-in-piston, which obviously have a higher surface area, had about 10 percent higher heat transfer. The effect of shifting the plug from a side to center location depended on chamber shape. Open and bowl-in-piston chambers showed little change; the hemispherical chamber showed a 4 percent reduction. Given a general chamber shape choice, the details of the actual design are important also; it is easy to add substantial surface area with piston cutouts, plug bosses, and cylinder head masking or squish regions which will deteriorate chamber performance to a measurable degree. Higher in-cylinder velocities affect heat-transfer rates through the Reynolds number term in the heat-transfer coefficient correlation. Swirl- and squishgenerated flows increase in-cylinder gas velocities and will, therefore, increase heat-transfer rates. 15.4.4 Chamber Octane Requirement Knock limits an engine's compression ratio, and hence its performance and efficiency. The more fundamental aspects of knock were reviewed in Sec. 9.6. Knock occurs when the end-gas autoignites prior to its being burned up by the normal flame-propagation process.
The tendency to knock depends on engine design and operating variables which influence end-gas temperature, pressure, and time spent at high values of these two properties before flame arrival. The presence or absence of knock in an engine depends primarily on the antiknock quality of the fuel, which is defined by the fuel's octane number (see Sec. 9.6.3). It determines whether or not a fuel will knock in a given engine under given operating conditions: the higher the octane number, the higher the resistance to knock. The octane number requirement of an engine is defined as the minimum fuel octane number that will resist knock throughout its speed and load range. The following factors affect an engine's octane requirement: (1) composition of the fuel; (2) chamber geometry and size; (3) charge motion; (4) sparkadvance curve; (5) inlet air, intake manifold, and water jacket temperatures; (6) carburetor or fuel-injector air-fuel ratio calibration; (7) the ambient conditionspressure, temperature, and relative humidityduring the requirement determination. The following illustrates the interaction between fuel factors and engine operating variables.
Figure 15-17 shows the relation between spark advance, torque, and speed in an engine operating at wide-open throttle. The dashed lines, determined with a fuel of sufficiently high octane rating to avoid knock, show MBT timing as a function of speed, along with the spark-advance limits for con- 853 Torque loss - 1% ,- knock Retard V) Automatic spark advance I I 1 0 I I I 2000 I I 4000 I Engine speed, revlmin I FIGURE 15-17 Relation between spark advance, speed, and torque loss, for spark-ignition - engine a; wide-om throttle, showing knock limit for specific gasoline and typical spark-advance schedule that avoids knock problems.28 stant specified percentage torque reductions.
The upper solid line traces the spark advance for borderline knock with a particular commercial gasoline.
To avoid knock with this fuel, the spark advance must be set to lose one percent of engine torque at 800 rev/min, with the torque loss diminishing to zero at 1200 revlmin. Above that speed this particular fuel allows operation at MBT timing without knocking. The lower solid curve represents a typical spark-advance schedule at WOT. It lies below the borderline knock advance (and results in a significant torque loss) for the following reasons. One is that different commercial gasolines with the same research octane number can respond differently to variations in engine operating conditions. Calibrating the engine (i.e., specifying the schedules for spark advance, A/F, and EGR) must be done with sufficient margin of conservatism to avoid objectionable knock with the normal range of commercial gasoline~over the full operating conditions of the engine. A second reason is engine-to-engine production variability despite the close dimensional tolerances of modem production engineering. For example, the effective compression pressure in each cylinder of a multicylinder engine is not identical, due to geometric and ring-pack behavior differences. The cylinder with the highest compression pressure is most knock-prone. Allowing for corresponding effects of cylinder-tocylinder variations in AIF, EGR rates, and spark timing, it is obvious that for a given operating condition in a multicylinder engine, one cylinder is more likely to knock than the others.
It is that cylinder which limits the spark advance.? A third reason for the discrepancy between actual spark-advance calibration and the knock limit for a given engine and fuel is the octane requirement increase associated with the buildup of deposits on the combustion chamber walls over extended mileage (see Sec. 9.6.3). t There is no assurance that the same cylinder will be the principal offender in all engines of the same model, nor in a given engine at all operating conditions. 854 INTERNAL COMBUSTION ENGINE FUNDAMENTALS In the example shown above, it was the problem of knock at low engine speed which required the spark advance calibration to be retarded. Whether low-, medium-, or high-speed knock is the limiting factor in a particular engine depends on the sensitivity of the fuel, on engine design features, and especially upon the engine's spark-advance requirements for MBT. The knock-limited spark advance determined from road octane rating tests will vary with engine speed and fuel sensitivity, as shown in Fig. 15-18. Low sensitivity fuels will tolerate more severe engine operating conditions and vice versa. Figure 15-18b, c, and d shows a typical engine spark-advance characteristic superposed on the knocklimited spark-advance plot. Depending on the fuel sensitivity and shape of the spark-advance curve, the knock region may occur at low, medium, or high speed (or not at all). It will be apparent from the above discussion that defining the effect of combustion chamber geometry on knock can only be done in an approximate fashion. The importance of fuel composition details, differences in engine design, the variability between engines of the same type, and the effect of deposits all make the quantification of trends as chamber design is varied extremely difficult. One of the most important chamber variables is the compression ratio. Figure 15-19 shows the relationship between the octane requirement and compression ratio for a number of combustion chambers. The octane requirement was defined as the research octane number of the fuel required to operate the engine at WOT with the weakest mixture for maximum power with borderline / sensltvity Low sensitivity F High sensitivity Engine speed characteristic A- Region of knock Engine speed '3 .d advance characteriskic Engine speed Engine speed FIGURE 15-18 Diagrams showing knock-limited spark-advancecurves for fuels of different sensitivity and how these can give low-, medium-, and high-speed knock in the same engine.2g chambers 1 4-valve Compact chambers A .\\\{ v 0 I 1 9 It Compression ratio 13 FIGURE 15-19 Octane requirement (gasoline research octane number), at wide-open throttle and MBT timing, to avoid knock as a function of compression ratio for various combustion chamber designs.1•< (or light) knock coinciding with MBT timing at the given speed. As is well known, the octane requirement increases with increasing compression ratio; there are, however, differences in the octane requirement between different types of chamber at the same compression ratio.
The chambers studied were disc-shaped chambers, bathtub and four-valve (open chambers with squish) and compact high compression ratio chambers (bowl or cup-type chambers in the piston crown or in the cylinder head around one of the valves). In the 9 to 11 compression ratio range there are only modest differences between the chambers studied. At higher compression ratios, 11 to 13, the compact chambers show a lower octane requirement which gives them a 1 to 2 compression ratio advantage over the more open chambers.
This advantage for the compact (and high-turbulence) chambers comes largely from the increased heat-transfer rates in these chambers. Whether the higher turbulence is generated during intake or at the end of the compression stroke, it increases the heat transfer from the end-gas, reducing its temperature and therefore its propensity to knock. However, this higher heat transfer also reduces engine power and efficiency, so the benefits of the compression ratio advantage are reduced. There is some increase in the knock-limited compression ratio with a given fuel as bum time is decreased by using one, two, three, and then four spark plugs simultaneously, with a given chamber geometry, but the effect is much smaller than the differences suggested by Fig. 15-19.23 Spark plug location within the chamber is an important factor affecting octane requirement. More centrally located plug positions shorten the flame travel path to the cylinder walls and decrease the time between spark discharge and flame amval at the end-gas location. This decreases the octane requirement.
The position of the spark plug in relation to the exhaust valve is also important: it is advantageous to burn the unburned mixture which has been heated by contact with the hot exhaust valve early in the combustion process. 856 INTERNAL COMBUSTION ENGINE FUNDAMENTALS TABLE 15.2 Engine conditions affecting octane number requirement Octane number rep.irement tends to go yp when: octane number requirement tends to p down when: 1. Ignition timing is advanced. 2. Air density rises due to supercharging or a larger throttle opening or higher barometric pressure. 3. Humidity or moisture content of the air decreases. 4. Inlet air temperature is increased. 5. Coolant temperature is raised. 1. Ignition timing is retarded. 2. Engine is operated at highcr altitudes or smaller throttle opening or lower barometric pressure. 3. Humidity of the air increases. 6. Antifreeze (glycol) engine coolant is used. 7.
Engine load is increased. 4. Inlet air temperature is decreased.
5. Fuellair ratio is richer or leaner than that producing maximum knock. 6. Exhaust gas recycle system operates at part throttle. 7. Engine load is reduced. advance has a major impact on knock; since it is also easy to adjust, it is the engine variable most commonly used to control knock. Studies show that typically 0.5 to 1.0 RON reduction is achieved per degree of retard.30 Atmospheric conditions-pressure, temperature, and humidity-all affect the octane number req~irement.~~ The fuellair equivalence ratio affects the octane requirement of an engine. The highest requirement is for slightly rich mixtures; increasing richness and leanness about this point decrease the octane requirement substantially. Figure 15-20 shops the knock-limited compression ratio as a function of the relative air/fuel ratio (2 = 114; 2 > 1 for lean mixtures) for conventional and highturbulence chambers, for two fuels with different octane ratings. Substantially higher compression ratios can be used with lean mixtures, especially with the high-turbulence chamber which extends the lean limit. The coolant temperature affects the octane requirement. Higher coolant temperature increases the inlet mixture temperature, and reduces heat losses from the end-gas to a modest degree. 15.45 Operating variables that affect the temperature or pressure time histories of the end-gas during combustion or the basic autoignition characteristics of the unburned fuel, air, residual mixture will also affect the engine's octane requirement. The most important additional variables which increase or decrease octane requirement in a consistent manner are listed in Table 15.2. Relative spark Hi& turbulence Moderate turbulence Relative. aidfuel ratio X FIGURE 15-20 Knock l i t s and lean engine operating limits as function of compression ratio and relative air/fuel ratio I (I = 114) for moderate and high-turbulence engine combustion Chamber Optimization Strategy The discussion in the previous sections suggests that the following sequence of steps in a combustion chamber development process is most logical. First should come the selection of the best chamber geometry. Geometric optimization can result in substantial benefits and carries no significant penalties. Chamber geometry involves cylinder head and piston crown shape, and plug location. Open chambers such as the hemispherical or pent-roof cylinder head, and clamshell, with near central plug location, give close to the maximum flame front surface area (and hence a faster burn), have the lowest chamber surface area in contact with the burned gases (and therefore the lowest heat transfer), and have inclined valves which give high volumetric efficiency. Spark plug location close to the center of the chamber is especially important in obtaining a fast burn rate. More compact chamber shapes than the open chambers listed above, such as the bowl-in-piston or chamber-in-head designs, do produce a somewhat faster burn, but with lower volumetric efficiency and higher heat losses. Following this first step, two problem areas may remain: the chamber may have a higher octane requirement than is desired and the burn rate may not be fast enough to absorb the high dilution required at part load to meet the emissions and fuel consumption goals. Positioning the spark plug as close to the center as possible will have reduced the octane requirement for that particular chamber shape. Depending on chamber design details, some squish area could be introduced. However, the perceived octane advantage of chamber designs which contain substantial squish is offset, at least in part, by their higher heat losses. A unit compression ratio increase results in a 3 percent or less increase in efficiency at part load. However, if the measures required to increase the compression ratio from, say, 9 to 10 resulted in a 10 percent increase in heat transfer, engine efficiency would not improve. The next step should be to reduce the cyclic variability in the combustion process to the maximum extedt feasible, by improving the uniformity of the intake fuel, air, and EGR mixture. Delivery of equal amounts of each of these constituents to each cylinder, provision for good mixing between constituents in the intake manifold and port, and accurate control of mixture composition during engine transients are all especially important. Also important is achieving closely similar flow patterns within each engine cylinder during intake so as to obtain equal burn rates in all cylinders. Attention to these intake process and mixture preparation details will always improve engine operation and carries no performance penalties. However, the bum rate may still not be fast enough, especially during the critical early stages of flame development, and cyclic variability may still be too high to meet the engine's performance goals. Then higher turbxlence levels during combustion must be achieved. This is usually best done by creating swirl during the induction process.
The appropriate method for introducing swirl will depend on any geometric manufacturing constraints and cost issues. With no geometric constraints, use of helical swirl-generating ports or a divided intakeport system with valves to control the flow at light load are likely to have the lowest power penalties. It is especially important that only the minimum additional turbulence required to achieve the performance objectives be added at this stage. Higher than necessary gas velocities within the cylinder result in excessive heat losses and low volumetric efficiency. In summary, to meet the objectives of a fast, repeatable, and robust combustion process with high volumetric efficiency, low heat transfer, and acceptable octane requirement, combustion chamber development should proceed through the following steps.
1. Optimize the chamber geometry within the design constraints for the maximum flame front area, minimum burned gaslchamber wall contact area, and largest valve size. 2. Obtain additional reductions in the cyclic combustion variability by improving mixture distribution and uniformity and by creating flow patterns into each cylinder that are essentially identical. 3.
Achieve any additional improvement in bum rate and cyclic variability required to meet objectives by increasing turbulence to the minimum extent. This is usually best done by creating swirl during the induction process. Mean piston speed, mls 800 FIGURE 15-21 Performance map for 6 . W 3 eight-cylinder aircooled naturally aspirated medium-swirl DI diesel engine. Contours of constant bsfc in grams per Kilowatt-hour shown. Bore = 102 mm, stroke = 100 mm,r, = 18.
Multihole fuel Engine speed, m l m i n discussed in Sec. 15.2. Here we examine the part-load behavior of various types of naturally aspirated diesel engines. As with SI engines (see Sec. 15.3.3), performance maps where bsfc contours are plotted on a graph of bmep versus engine speed are commonly used to describe the effects of load and speed variations. Figure 15-21 shows the performance map for an air-cooled four-stroke cycle medium-swirl naturally aspirated DI diesel (similar to the engine in Fig. 1-23). Maximum rated power for this 6.54-dm3 displacement engine at 3200 revlmin is 119 kW, maximum bmep at 2000 revlmin is 784 kPa, and minimum bsfc (at 1600 revlmin and 580 kPa bmep) is 220 g/kW. h, which corresponds to a brake fuel conversion efficiency of 38.5 percent. The gross indicated fuel conversion efficiency would be about 48 percent. Figure 15-22 shows the performance map for a small high-swirl DI diesel which uses the M.A.N. combustion system with a single fuel jet sprayed tangentially into the swirling air flow. Due to the higher speed and higher swirl than the Mean piston speed, mls 4 8001 1 6 8 10 12 14 1 I I I I 155 VARIABLES THAT AFFECT CI ENGINE PERFORMANCE, EFFICIENCY, AND EMISSIONS 155.1 Load and Speed The performance of a naturally aspirated DI heavy-duty truck diesel engine and a small ID1 engine at full load over the engine speed range have already been 0 1 loo0 I 2000 3000 4ooo Engine speed, revlmin I 5000 FIGURE 1522 Performance map for 1.47-dm3 four-cylinder naturally aspirated DI diesel engine with high-swirl single-hole-nozzle M.A.N. combustion system. Contours of constant bsfc in grams per kilowatthour shown. Bore = 76.5 mm, stroke = 80 mm, re = 18.5.34 ENGINE OPERATING CHARACTERISTICS larger DI engine in Fig. 15-21, the maximum bmep is slightly lower. The best bsfc is about 10 percent higher largely due to higher friction mep, but in part due to higher heat losses resulting from the less favorable surface/volume ratio of the smaller bore engine and higher swirl, and lower heat-release rate of the M.A.N. system. Note that the maximum mean piston speed for this engine, 13.3 m/s at 5000 revlmin, is comparable to that of the larger medium-swirl engine in Fig.
15-21 (10.7 m/s). Figure 15-23 gives the performance characteristics of an automotive naturally aspirated swirl-chamber ID1 diesel engine. Maximum bmep values are usually higher than those of equivalent size DI engines because without the need to generate swirl during the intake process, the intake port and valve are less restrictive and volumetric efficiency is higher, and because the ID1 engine can be run at lower AIF without smoking.
The best bsfc values are usually some 15 percent higher than values typical of equivalent DI engines. The best brake fuel conversion efficiency of the engine of Fig. 15-23 is 32.5 percent. Comparisons between naturally aspirated DI and ID1 diesel engines of closely comparable design and size indicate that the DI engine is always more efficient, though the benefit varies with load. At full load, differences of up to 20 percent in bsfc have been noted, especially in engines with larger displacement per cylinder. At part load, the gain is less-of order 10 percent. Comparisons should be made at equal emission levels, a task that is dmcult to accomplish in practice. Emission control with the DI engine is more difficult, so this constraint reduces the benefit somewhat. Figure 15-24 shows a breakdown of the indicated efficiency differences between the two systems.
At full load (AIF = 18 to 20) the ID1 suffers a penalty of about 15 to 17 percent due in large part to the retarded timing of the ID1 combustion process and its long, late-burning, heat-release profile. At light load, about 300 kPa bmep (AIF = SO), these combustion effects are small and the indicated efficiency penalty of the ID1 (around 5 to 7 percent) is due to the higher heat losses associated with the larger surface area and highvelocity flow through the connecting nozzle of the divided-chamber geometry and due to the pumping pressure loss between the main and auxiliary chamber~.~~ Note that all these diesel engine performance maps are similar in general Mean piston speed, mls 4 O' 6 2& 8 & 10 12 - Engine s p e d , mrlmin 14 & FIGURE 15-23 Performance map for 1.987-dm3fivecylinder naturally aspirated ID1 swirl-chamber diesel engine. Contours of constant bsfc in grams per Kilowatthour shown. Bore = 76.5 stroke = 86.4 mm, r, = 23.35 mml 861 Effects of: ,Retard Airlfuel ratio F'IGURE 15-24 Factors which improve the indicated efficiency of naturally aspirated small DI diesel combustion systems relative to ID1 swirl-chamber combustion system, as a function of A/F or load.36 shape and when plotted against S, are quantitatively comparable. The increase in bsfc from the minimum value with increasing speed at constant load is due to the increase in friction mep, partly offset by the effect of decreasing importance of heat losses per cycle on efficiency. The increase in bsfc with decreasing load at constant speed is dominated by the decreasing mechanical efficiency as bmep is reduced. The indicated fuel conversion efficiency increase as the fuellair equivalence ratio is decreased partly offsets this. The trends in bsfc when increasing load at constant speed and increasing speed al constant load from the minimum are more modest. They are the net results of (1) the increase in mechanical efficiency and decrease in indicated fuel conversion efficiency as the load increases and (2) decreasing indicated efficiency due to increasing importance of heat losses and increasing mechanical efficiency as the speed decreases. The enrichment of the mixture at high load and low speed of spark-ignition engines is, of course, absent. Figure 15-25 shows the effect of load on NO, and HC emissions for naturally aspirated DI and ID1 diesel engines. For the DI engine NO, concentrations rise steadily as the fuellair ratio increases with increasing bmep at constant injection timing. The increasing quantity of fuel injected per cycle results in an increasing amount of close-to-stoichiometric combustion products near the peak pressure and temperature (see Sec. 11.2.4). The ID1 engine shows a similiar trend except that, at high load, NO, concentrations level off. These characteristics do not change substantially with engine speed.
The ID1 engine shows significantly lower HC emissions than the DI engine. The high HC at idle and light load are thought to result from fuel mixing to too lean an equivalence ratio. If diesel engines are overfueled at high load, HC emissions then rise rapidly. These HC mechanisms are described in Sec. 11.4.4.

may have sufficient margin of safety relative to knock to allow modest inlet-air boost, any substantial air compression prior to cylinder entry will require changes in engine design and/or operating variables to offset the negative impact on knock. The variables which are adjusted to control knock in turbocharged SI engines are: compression ratio, spark retard from optimum, charge air temperature, and fuellair equivalence ratio.? Figure 15-34 shows how the knock limits depend on charge pressure, temperature, fuellair equivalence ratio and compression ratio for given octane rating fuels. The difference in boost achievable with the premium and the regular quality gasoline is significant, as expected (Sec. 9.6.3). Charge-air temperature has a strong influence on allowable boost levels: lowering the compressed air temperature prior to entry to the cylinder with a charge-air cooler allows a substantially higher compression ratio to be used at a given boost level, with a corresponding impact on engine eficiency.3 The boost pressure benefits of the richer mixtures in Fig. 15-34a (4 = 1.1 compared with 0.9) are largely due to the cooling effect of the additional fuel on the air charge. For example, Fig. 15-34b shows that, with a rich mixture and charge cooling to 60•‹C, a charge pressure of 1.5 atm can be utilized at optimum spark timing with a compression ratio of 8.
Without charge cooling, the same charge pressure can only be used with a compression ratio of 6.4' In turbocharged SI engines, the knock limit is usually reached at spark timings retarded from the MBT optimum. Figure 15-35 shows the brake mean 1.2 20 1.2 40 60 80 100 120 Charge temperature, OC (4 6 7 8 Compression ratio (b) FIGURE 15-34 Dependence of SI engine knock limits on: (a) charge pressure, temperature, and equivalence ratio 4, with r, = 7, 2500 rev/min, MBT timing, 91 and 100 research octane number fuel; (b)charge pressure and compression ratio, without and with (to 60•‹C)charge air cooling, 2500 rev/min, MBT timing, 4 = 1.1, 100 RON fue1.49 effective pressure achievable at a fixed compression ratio as a function of charge pressure and ignition timing with and without charge-air cooling.
Additional retard allows higher boost pressures to be utilized; however, at a constant safety margin from the knock limit, the resulting gains in bmep decrease as retard is increased. To avoid an unnecessary fuel consumption penalty, retarded timing should only be used when the turbocharger does develop a high boost pressure. The above discussion illustrates why turbocharged spark-ignition engines normally have lower compression ratios than naturally aspirated engines, use substantial mixture enrichment (up to 4 = 1.3) at high boost to cool the charge, often use an intercooler to reduce the charge-air temperature, and operate with without CAC Valve timing changes are often made too. These are done primarily to improve low-speed torque where turbocharging has a limited impact. $ The turbocharged engine in Fig.
1-10 has an intercooler to reduce the inlet charge temperature. 140 Spark advance, deg BTC FIGURE 15-35 Brake mean effective pressure and knock limits for turbocharged SI engines as a function of spark advance and inlet pressure p, (in atmospheres). 2500 rev/min, r, = 7, 4 = 1.1, 99 RON fuel, without and with (AT = 45•‹C)charge-air c ~ o i i n ~ . * ~ retarded timing at high boost pressures. Since compression ratio reductions and retarded ignition timings result in losses in efficiency, and unintended knock with high boost pressures would be especially damaging, precise control of ignition timing is critical.
Most turbocharged SI engines now use a knock sensor and ignition-timing control system so that timing can be adjusted continuously to avoid knock without unnecessary retard. The sensor is usually an accelerometer which senses above-normal vibration levels on the cylinder head at the characteristic knock frequency. With a knock sensor, ignition timing can be automatically adjusted in response to changes in fuel octane rating and sensitivity, and ambient conditions. Turbocharged SI engines where fuel is mixed with the air upstream or downstream of the compressor, using carburetors or fuel-injection systems, have been developed and used. Most modern turbocharged engines use port fuel injection. This provides easier electronic control of fuel flow, avoids filling most of the pressurized manifold volume with fuel-air mixture, and improves the dynamic response of the system by reducing fuel transport delays. We now consider the performance of actual turbocharged spark-ignition engines. Examples of compressor outlet or boost pressure schedules as a function of speed at wide-open throttle for three turbocharges engines are shown in Fig. 15-36. The essential features of the curves are the same. Below about 1000 engine rev/min the turbocharger achieves negligible boost. Boost pressure then rises with increasing speed to 1.4 to 1.8 atm (absolute pressure) at about 2000 rev/min. Boost pressure then remains essentially constant with increasing engine speed. The rising portion of the curve is largely governed by the relative size of the turbine selected for a given engine. This is usually expressed in terms of the AIR ratio of the turbine-the ratio of the turbine's inlet casing or volute area A to the radius of the centroid of that area.
Lower AIR values (smaller-capacity turbines) give a more rapid boost pressure rise with increasing speed; however, they give higher boost pressures at high engine speed, which is ~ndesirable.4~. Avoidance of knock is the reason why boost must be limited at medium to FIGURE 15-37 Power and torque as a function of engine speed for two turbocharged and one naturally aspirated four-cylinder spark-ignition engine. See Table 15.3.52 high engine speed; the details of this problem have already been discussed above. Even with the use of very rich mixtures and spark retard at WOT, lower compression ratios for turbocharged engines, and intercooling, knock avoidance requires that boost pressures (which would continue to rise with increasing engine speed in the absence of any control) be maintained approximately constant.
This is normally achieved by reducing the exhaust flow through the turbine as speed increases by bypassing a substantial fraction of the exhaust around the turbine through the wastegate or flow control valve (see Sec. 6.8.4). A wastegate is a spring-loaded valve acting in response to the inlet manifold pressure on a controlling diaphragm. Although other methods of controlling boost can be the wastegate is the most common. About 30 to 40 percent of the exhaust bypasses the turbine at maximum engine speed and load. Figure 15-37 compares the performance of two turbocharged spark-ignition engines (four-cylinder, 2.1- and 2.3-dm3 displacement) with that of the base 2.3-dm3 engine in its naturally aspirated form. Table 15.3 gives details of these TABLE 153 Turbocharged spark-ignition engine performance5" FIGURE 15-36 0 1000 2000 3000 4000 5000 61 Engine speed, revlmin 1 Boost pressure schedules for three turbocharged spark-ignition engines: (a) 3.8-dm3 V-6 engine, 86.4 mm stroke, r, = 8;" (b) 2.2dm3 four-cylinder engine, 92 mm stroke, r, = 8.1;51(c) 2.32dm3 fourcylinder engine, 80 mm stroke, re = 8.7.52All schedules are wastegate controlled. Type 21-dm3 TC Displacement, dm3 Bore x stroke, mm Compression ratio Maximum power, kW at revlmin Maximum torque, N .m at revtmin Maximum bmep, kPa 2.127 92 x 80 7.5 98 at 5400 210 at 3800 1241 23-dm5N A L3dm3 TC/AC 2.316 2.316 % x 80 8.7 117 at 5300 250 at 2900 1356 % x 80 9.5 83 at 5400 184 at 2800 998 874 INTERNAL COMBUSTION ENGINE FUNDAMENTALS -lhrbocharged --- Naturally aspirated hsfc, g1kW.h Percent maximum mean piston speed I FIGURE 15-38 Comparison of bsfc contours (in grams per kilowatt-hour) on performance maps of turbocharged and naturally aspirated versions of the same spark-ignition engine, scaled to the same maximum torque and mean piston speeds3 three engines. The 2.1-dm3 turbocharged but not intercooled engine (which also does not have a knock sensor to control spark advance) requires a lower compression ratio and achieves less of a bmep gain than the 2.3-dm3 turbocharged intercooled engine with its knock-sensor spark-advance control, which together permit use of a higher compression ratio.
Turbocharging the naturally aspirated 2.3-dm3 engine, with the modifications indicated, results in a 36 percent increase in maximum engine torque and a flatter torque-versus-speed profile. The brake specific fuel consumption contours of an engine produced in both naturally aspirated and turbocharged versions are shown in Fig. 15-38. The data have been scaled to represent engines of different displaced volume but the same maximum engine torque. The smaller-displacement low-compression-ratio turbocharged engine (r, = 6.9) shows a reduction in bsfc at low speed and part load due to improved mechanical efficiency. At high speed and load the largerdisplacement naturally aspirated engine has an advantage in bsfc due to its higher compression ratio (8.2), less enrichment, and more optimum timing.53In a vehicle context, the low-speed part-load advantage of the smaller size but equal power turbocharged engine should result in an average fuel economy benefit relative to the larger naturally aspirated engine. This benefit has been estimated as a function of load. At full load the average efficiencies should be comparable; at half load, the turbocharged engine should show a benefit of about 10 percent, the benefit increasing as load is decreased.49 15.6.2 thermal loading of critical components can become limiting too. As boost pressure is raised, unless engine design and operating conditions are changed, maximum pressures and thermal loadings will increase almost in proportion. In practice, the compression ratio is often reduced and the maximum fuellair equivalence ratio must be reduced in turbocharged engines (relative to naturally aspirated engines) to maintain peak pressures and thermal loadings at acceptable levels. The fuel flow rate increases at a much lower rate than the air flow rate as boost pressure is increased. Limitations on turbocharged engine performance are discussed more fully by Watson and J a n ~ t a . ~ ' Small automotive indirect-injection (IDI) turbocharged engines are limited by structural and thermal considerations to about 130 atrn maximum swirl- or pre-chamber pressure, 14 m/s maximum mean piston speed, and 860•‹C maximum exhaust temperat~re.~~ Smoke and NO, emission standards are additional constraints. Figure 15-39 shows the full-load engine and turbocharger performance characteristics of a six-cylinder 2.38-dm3 displacement Comet V swirl-chamber automobile diesel engine. The maximum boost pressure is controlled by a poppet-valve-type wastegate to 0.75 bar above atmospheric. The fuel consumption map for this engine is shown in Fig.
15-40. Superimposed on the turbocharged engine map is the map for the base naturally aspirated swirlchamber ID1 engine of the same geometry and compression ratio (r, = 23). The turbocharged engine has a maximum torque 46 percent higher and a maximum power 33 percent higher than the naturally aspirated engine. The best bsfc values are closely comparable. The different methods of supercharging internal combustion engines were reviewed in Sec.
6.8. Turbocharging, mechanical supercharging with a Roots blower, and pressure wave supercharging with the Comprex are alternative methods of boosting the performance of a small automotive swirl-chamber ID1 Bwst pressure 20 I I Bosch smoke number I I I I 1001 OC 806040 350 ' Full load Four-Stroke Cycle CI Engines The factors that limit turbocharged diesel engine performance are completely different to those that limit turbocharged spark-ignition engines. The output of naturally aspirated diesel engines is limited by the maximum tolerable smoke emission levels, which occur at overall equivalence ratio values of about 0.7 to 0.8. Turbocharged diesel engine output is usually constrained by stress levels in critical mechanical components. These maximum stress levels limit the maximum cylinder pressure which can be tolerated under continuous operation, though the Engine speed, revls FIGURE 15-39 Engine and turbocharger characteristics of six-cylinder 2.38-dm3 swirl-chamber ID1 automotive diesel engine at full load.54 Mean piston speed, mls , 2 1.2 4 I 6 8 10 12 I I I I 0 10 I 20 30 40 1 I I I II 50 60 70 80 bsfc contours in glkW h I 14 Engine speed, rev/s FIGURE 15-40 Fuel consumption map (bsfc in grams per kilowatt-hour) for turbocharged ( ) and naturally aspirated (-- -) versions of 2.38-dm3six-cylinder swirl-chamber ID1 diesel engine.54 -..- 1.2-dm3Baseline (I) ----1.2-dm3'huh (4) -- 1.2-dm3Roots (2) -1 .6-dm3NA engine (5) 1 %dm3 Comprex, (3) -.
-. with intercooler -.
-without intercooler diesel engine. Figure 15-41 compares the torque and bsfc values obtained with each of these supercharging methods on a performance map for a 1.2-dm3 engine. Values for a 1.6-dm3 naturally aspirated ID1 diesel engine are also shown. All three approaches achieve close to the desired maximum power of the 1.6-dm3NA engine (40 kW at 4800 revlmin): e.g., l.2-dm3 turbo, 41.2 kW at 4500 revlmin; 1.2-dm3 Comprex with intercooler, 42.3 k W at 3500 revlmin; 1.2-dm3 Roots, 37.6 kW at 4000 revlmin. The Comprex system produces the highest torque at low engine speeds, even under unsteady engine operating conditions. The density of the charge air determines the amount of charge, and hence the torque. Chargeair pressure and temperature for the three supercharging systems are shown in Fig. 15-42. The Comprex (here without an intercooler) must have the highest charge pressure because it has the highest charge temperature. Intercooling would be particularly effective in this case.5s Small high-speed high-swirl turbocharged direct-injection diesel engines (e.g., suitable for automobile or light-truck applications) have similar performance maps to those of equivalent ID1 engines (Figs. 15-39 and 15-40).
Maximum bmep values are closely comparable: usually slightly higher boost is required to offset the lower volumetric efficiency of the high-swirl-generating port and valve of the DI engine. Best bsfc values for the DI engine are usually about 15 percent lower than of comparable ID1 engines (see Ref. 56). The operating characteristics of larger medium-swirl turbocharged DI diesel engines are illustrated by the data shown in Fig.
15-43. The engine is a 12-dm3 displacement six-cylinder heavy-duty truck engine. The combustion chamber is similar to that shown in Fig. 15-32c, with a square combustion cavity and relatively low levels of swirl. The swirl is generated by a helical port in one of the two intake ports and a tangential port in the other in the four-valve cylinder head. Both the engine's operating map and the turbocharger compressor map with the boost pressure curve superposed are shown for two different compressor impellers. The adoption of the backward-vaned rake-type impellor compared to a more conventional design significantly increases low- and medium-speed per- 1 Engine speed, rev/min FIGURE 15-41 Torque and brake specific fuel consump tion of naturally aspirated and supercharged l.2dm3 swirl-chamber ID1 diesel engine. Baseline (1): naturally aspirated. Supercharged with (2) Roots blower; (3) Comprex (with and without intercooler); (4) turbocharger. Larger displacement 1.6-dm3naturally aspirated engine (S)." 1 .o 0 -' 0.01 0.02 0.03 0.04 0.05 Air flow rate, m3/s 300 FIGURE 1542 Charge pressure and temperature with the ID1 diesel engine and different supercharging methods of Fig. 15-41.55 ENGINE OPERATING CHARACTERISTICS 879 Backward vaned Conventional Engine speed, revlmin (4 Percent maximum engine speed Air flow, m3/s (b) FIGURE 1544 Performance characteristics of medium-speed turbocharged aftercooled DI diesel engine.
(a) Torque, power, smoke number, and bsfc for V twelve-cylinder version. (b) Compressor characteristics and engine full-load line for V-8 cylinder version. Bore = 128 mm,stroke = 140 mm,r, = 15.58 (4 FIGURE 15-43 Performance characteristics of turbocharged 12dm3 six-cylinder medium-swirl heavyduty truck DI diesel engine, with two diermt compressor impellers: (a) fuel consumption maps; (b) compressor maps with MI-load boost operating line for engine with backward-vaned impellor superposed. Bore = 135 mm,stroke = 140 mm, r, = 16." formance by improving the compressor efficiency over the engine's boost pressure curve (Fig. 15-43b). A wastegate is then used to control the boost level at high engine speeds. The improvement in low-speed engine torque is apparent in Fig. 15-43a. The dependence of the maximum torque curve on both engine and turbocharger design details is clear. With boost pressure ratios limited to below 2, in the absence of air-charge cooling, maximum bmep values of 1.1 MPa are typical of this size and type of diesel engine. With structurally more rugged component designs, aftercooled turbocharged medium-speed diesel engines with swirl in this cylinder size range can utilize higher boost and generate much higher bmep. Wastegate control of boost is no longer required.
Figure 15-44 shows the performance characteristics of a V-8 cylinder engine with its compressor map and full-load boost characteristic. This turbocharged intercooled engine achieves a maximum bmep of about h between the maximum torque speed and 1.5 MPa and bsfc below 200 @ W e rated power. Boost pressure at full load increases continuously over the engine speed range." Examples of values of combustion-related parameters for this type of engine over the load range at its maximum rated speed are shown in Fig. 15-45 for a 14.6-dm3 six-cylinder turbocharged aftercooled Dl diesel engine with a boost pressure ratio of 2 at rated power. The ignition delay decreases to about 10" (0.9 ms at 1800 rev/min) as load is increased. The bmep at 100 percent rated load at this speed is 1.2 MPa. Exhaust temperature increases substantially with increasing load: maximum cylinder pressure increases to about 10 MPa at the rated load. In this particular study it was found that these operating parameters were relatively insensitive to fuel variations.
The cross-hatched bands show data for an additional nine fuels of varying sulfur content, aromatic content, 10 and 90 percent distillation temperatures.'' Higher outputs can be obtained with two-stage turbocharged aftercooled diesel engines, the arrangement shown in Fig. 6-371.The performance characteristics of such a high bmep (1.74 MPa) six-cylinder engine of 1Cdm3displacement are shown in Fig. 15-46. The high air flow requires an overall pressure ratio of 3 at sea level ambient conditions (rising to 4 at 3658 m altitude). This was obtained at lower cost with two turbochargers in series than with a multistage single turbocharger. At rated conditions, the maximum cylinder pressure is 12.7 MPa and the maximum mean piston speed is 10.6 m/s. Additional gains in efficiency with these heavy-duty automotive diesel engines can be achieved with turbocompounding: some of the available energy in the exhaust gases is captured in a turbine which is geared directly to the engine 880 ENGINE OPERATING CHARACIERISTICS INTERNAL COMBUS'llON ENGINE FUNDAMENTALS Cylinder pressure 200 i 20 Ignition delay ge .i lo Smoke I 0 460 I I 800 1200 I 1600 2000 3 2 % 8 P 0 gi drive shaft. The above discussion indicates that typical turbocharged DI diesel engines achieve bsfc levels of 210 to 220 g/kW.
h (brake fuel conversion efficiencies of 0.4 to 0.38). With the increased cylinder pressure capability, higher fuel-injection pressures, and lower-temperature aftercooling of the above higher bmep engines, bsfc values of 200 g/kW. h (0.42 brake efficiency) or lower can be achieved. With turbocompounding, bsfc values can be reduced another 5 to 6 percent to about 180 g/kW - h, or a brake efficiency of 0.47, at rated p ~ w e r . ~ ' The largest four-stroke cycle DI diesel engines are used for marine propulsion.
An example is the Sulzer 400 mm bore 480 mm stroke engine which produces 640 kW per cylinder at 580 rev/min (S,, = 9.3 m/~).Very high bmep levels (2.19 MPa) are achieved at maximum continuous rated power through progress in turbocharger design and engine improvements which allow higher maximum cylinder pressures. These, combined with optimization of gas exchange and combustion processes, achieve bsfc values of 185 to 190 g/kW h (45 to 46 percent brake efficien~y).~' Many diesel system concepts are being examined which promise even higher output and/or efficiency. Variable-geometry turbocharger-turbine nozzles improve utilization of exhaust gas available energy at low engine speeds. The hyperbar turbocharging system-essentially a combination of a diesel engine with a free-running gas turbine (a combustion chamber is placed between the engine and the turbocharger turbinebhas the potential of much higher bmep. Diesel systems with thermally insulated combustion chambers which reduce heat losses and increase the available exhaust energy have the potential for improving efficiency and for increasing power through additional exhaust energy recovery in devices such as compounded turbines and exhaust-heated Rankine cycle systems.48 a 1 2400 bmep, LPa FIGURE 15-45 Operating parameters of 14.6dm3 six-cylinder turbocharged aftercooled DI diesel engine as a function of load at maximum rated speed of 1800 revlmin. Maximum rated power = 261 kW at hmen ---- r = 1192 kPa. Points: standard diesel fuel. Shaded band: nine fuels of varying sulfur content, aromatic content, 10 and 90per cent distillation temperature~.~~ - - - - 15.6.3 , , i S 2 0 0 t , I I I I 800 lo00 1200 1400 1600 1800 2000 2200 Engine speed, rev/min 881 FlGURE 15-46 Operating characteristics of 14-dm3 sixcylinder two-stage- turbocharged aftercooled quiescent-chamber DI diesel engine.
Maximum bmep = 1.74 MPa. Boost pressure ratio at rated power = 3. Bore = 140 mrn, stroke = 152 mm.60 Two-Stroke Cycle SI Engines The two-stroke cycle spark-ignition engine in its standard form employs sealed crankcase induction and compression of the fresh charge prior to charge transfer, with compression and spark ignition in the engine cylinder after charge transfer.
The fresh mixture must be compressed to above exhaust system pressures, prior to entry to the cylinder, to achieve effective scavenging of the burned gases.
Twostroke cycle scavenging processes were discussed in Sec. 6.6. The two-stroke spark-ignition engine is an especially simple and light engine concept and finds its greatest use as a portable power source or on motorcycles where these advantages are important.
Its inherent weakness is that the fresh fuel-air mixture which short-circuits the cylinder directly to the exhaust system during the scavenging process constitutes a significant fuel consumption penalty, and results in excessive unburned hydrocarbon emissions. This section briefly discusses the performance characteristics of small crankcase compression two-stroke cycle SI engines. The performance characteristics (power and torque) of these engines depend on the extent to which the displaced volume is filled with fresh mixture, i.e., the charging efficiency mq. (6.2411. The fuel consumption will depend on both the trapping efficiency [Eq. (6.2111 and the charging efficiency. Figure 15-47~shows how the trapping efficiency qtr varies with increasing delivery ratio A at several engine speeds for a two-cylinder 347-cm3 displacement motorcycle crankcase compression engine. The delivery ratio increases from about 0.1 at idle conditions to 0.7 to 0.8 at wide-open throt1.o Speed, revlmin Rrfect mixing b 0.9 - 0.8 - C C 5 'E, 'C A 0.2 2iJxJ 3000 0 m rn MOO A 6000 400 3M) 0 1 b 0.7 loo0 3000 MOO 7000 Engine speed, revlmin 00 .B 0.5 - Delivery ratio A (4 (b) FIGURE 15-47 (a) Trapping and charging efficiencies as a function of the delivery ratio. (b) Dependence of brake mean effective pressure on freshcharge mass defined by charging efficiency. Two-cylinder 347-cm3 displacement two-stroke cycle spark-ignition engine.63 RGURE IS48 Performance characteristics of a three-cylinder 450-cm3 two-stroke cycle spark-ignition engine. Maximum bmep = 640 kPa. Bore = 58 mm. stroke = 56 mm.@ tle. Lines of constant charging efficiency qc, [which equals Aqtr; see Eq. (6.2511 are shown. Figure 15-47b shows bmep plotted against these charging efficiency values and the linear dependence on fresh charge mass retained is clear.
Performance curves for a three-cylinder 450-cm3 two-stroke cycle minicar engine are shown in Fig.
15-48. Maximum bmep is 640 kPa at about 4000 rev/ min. Smaller motorcycle engines can achieve slightly higher maximum bmep at higher speeds (7000 revlmin). Fuel consumption at the maximum bmep point is about 400 g/kW. h. Average fuel consumption is usually one-and-a-half to two times that of an equivalent four-stroke cycle engine. CO emissions from two-stroke cycle engines vary primarily with the fuellair equivalence ratio in a manner similar to that of four-stroke cycle engines (see Fig. 11-20). NO, emissions are significantly lower than from four-stroke engines due to the high residual gas fraction resulting from the low charging efficiency. Unburned hydrocarbon emissions from carbureted two-stroke engines are about five times as high as those of equivalent four-stroke engines due to fresh mixture short-circuiting the cylinder during scavenging. Exhaust mass hydrocarbon emissions vary approximately as A(1 - qt,)4, where 4 is the fuellair equivalence ratio.63 15.6.4 Charging efficiency $,h ;;, Two-Stroke Cycle CI Engines Large marine diesel engines (0.4 to 1 m bore) utilize the two-stroke cycle. These low-speed engines with relatively few cylinders are well suited to marine propulsion since they are able to match the power/speed requirements of ships with simple direct-drive arrangements. These engines are turbocharged to achieve high brake mean effective pressures and specific output. The largest of these engines can achieve brake fuel conversion efficiencies of up to 54 percent. An example of a large marine two-stroke engine is shown in Fig. 1-24.
Over the past 25 years 884 INTERNAL COMBUSTION ENGINE FUNDAMENTALS ENGINE OPERATING CHARACTERISTICS the output per cylinder of such engines has increased by a factor of more than two, and fuel consumption has decreased by 25 percent. These changes have been achieved by increasing the maximum firing pressure to 13 MPa, and by refining critical engine processes such as fuel injection, combustion, supercharging, and scavenging. The uniflow-scavenging process is now preferred to loop scavenging since it achieves higher scavenging efficiency at high strokepore ratios and allows increases in the expansion stroke.62 The performance characteristics of a 580 mm bore Sulzer two-stroke marine diesel engine with a strokepore ratio of 2.9 are shown in Fig. 15-49. The solid lines show the standard turbocharged engine characteristics. The rated speed for the engine is 125 revlmin, corresponding to a maximum mean piston speed of 7.2 m/s. The rated bmep is 1.66 MPa. The minimum bsfc is 175 g/kW. h which equals a brake fuel conversion efficiency of 48 percent. For larger lower-speed engines, the efficiency is higher. The dashed lines show how the performance of this engine can be improved by turbocompounding. A proportion of the engine's exhaust flow, at loads higher than 50 percent, is diverted from the turbocharger inlet to a separate turbine coupled to the engine power takeoff gear via an epicyclic speed-reduction gear and hydraulic coupling. The additional power recovered in this manner from the engine exhaust flow improves bsfc by 5 gJcW - h. At part load, when the full exhaust flow passes through the turbocharger, an efficiency gain is also obtained, due to the higher scavenging pressure (and therefore increased cylinder pressure) obtained with the full exhaust flow. 141 Crank angle,deg I I I 340 420 500 I , , 580 660 740 Engine speed, revlmin I 820 I I] 900 FIGURE 15-50 Injection, combustion, and performance characteristics of intermediate-size turbocharged twostroke cycle uniflow-scavenged DI diesel engine. Bore = 230.2 mm, stroke = 279.4 mm and r, = 16. Shallow dish-in-pistoncombustion chamber with swirl. At maximum rated power at 900 rev/min, bmep = 0.92-1.12 MPa depending on applicati~n.~~ Both two-stroke and four-stroke cycle diesel engines of intermediate size Percent maximum power FIGURE 15-49 Performance characteristics of large marine two-stroke cycle uniflowscavenged DI diesel engine. Bore = 580 mrn, stroke/bore = 2.9, maximum rated speed = 125 rev/min (mean piston speed = 7.2 m/s), bmep (at rated power) = 1.66 MPa. Solid line: standard turbocharged configuration. Dashed lines: parallel turbocompounded conliguration at greater than 50 percent load. bsac: brake specific air c o n s ~ m p t i o n . ~ ~ (200 to 400 mm bore) are used in rail, industrial, marine, and oil drilling applica- tions. The performance characteristics of a turbocharged two-stroke cycle uniflow-scavenged DI diesel engine (similar to the engine in Fig.
1-5), with 230.2 mrn bore, 279.4 mm stroke, and a compression ratio of 16, are shown in Fig. 15-50. Combustion in the shallow dish-in-piston chamber with swirl occurs smoothly yielding a relatively low rate of pressure rise. The pressure curve shown with peak pressure of 13.3 MPa is for full-load operation. The bmep at rated power at 900 rev/min is 0.92 to 1.12 MPa depending on application. The maximum mean piston speed is 8.4 m/s. The bsfc of 200 g/kW. h co&esponds to qf, = 0.42. , Engine speed, revlmin FIGURE 15-51 Brake power and specific fuel consumption (grams per kilowatt-hour) map of four-cylinder 3.48dm3 uniflow-scavenged two-stroke cycle DI diesel engine. Engine turbocharged at mid and high loads; Roots blown at low loads.
Maximum boost pressure ratio = 2.6. Bore = 98.4 mm, stroke = 114.3 mm,r, = Smaller turbocharged two-stroke cycle DI diesel engines also compete with four-stroke cycle engines in the marine, industrial, and construction markets. The fuel consumption map of such a four-cylinder 3.48-dm3 displacement uniflowscavenged two-stroke cycle diesel engine is shown in Fig. 15-51. The engine uses a Roots blower to provide the required scavenging air pressure for starting and light-load operation. At moderate and high loads the turbocharger supplies sacient boost and the blower is not needed; the blower is unloaded (air flow is bypassed around the blower) under these conditions. The engine generates 138 kW at its rated speed of 2500 rev/min (mean piston speed of 9.5 m/s) and a maximum bmep of 951 kPa at 1500 revfmin.
The best bsfc is 225 g/kW.h and the maximum boost pressure ratio is 2.6. 15.7 ENGINE PERFORMANCE SUMMARY The major performance characteristics of the spark-ignition and compressionignition engines described in previous sections of this chapter are summarized here to highlight the overall trends. Table 15.4 lists the major design features of these engines, the bmep at maximum engine torque, bmep and the value of the mean piston speed 3, at maximum rated power, and the minimum value of bsfc ENGINE OPERATING CHARACTERISTICS (a) Rank the chambers 1,2, 3 in the order of their volumetric efficiency (1 = highest and the corresponding brake fuel conversion efficiency.
It should be stressed that there are many different engine configurations and uses, and that for each of these there are variations in design and operating characteristics. However, these representative values of performance parameters illustrate the following trends: 1. Within a given category of engines (e.g., naturally aspirated four-stroke SI engines) the values of maximum bmep, and bmep and S, at maximum rated power, are closely comparable. Within an engine category where the range in size is substantial, there is an increase in maximum bmep and a decrease in minimum bsfc as size increases due to the decreasing relative importance of friction and heat loss per cycle. There is also a decrease in Sp at maximum power as engine size increases. Note the higher bmep of naturally aspirated SI engines compared to equivalent NA diesels "due to the fuel-rich operation of the former at wide-open throttle. 2.
Two-stroke cycle spark-ignition engines have sigmficantly lower bmep and higher bsfc than four-stroke cycle SI engines. 3. The effect of increasing inlet air density by increasing inlet air pressure increases maximum bmep values substantially.
Turbocharging with aftercooling gives increased bmep gains relative to turbocharging without aftercooling at the same pressure level. The maximum bmep of turbocharged SI engines is knock-limited. The maximum bmep of turbocharged compressionignition engines is stress-limited. The larger CI engines are designed to accept higher maximum cylinder pressures, and hence higher boost. 4. The best efficiency values of modern automobile SI engines and ID1 diesel engines are comparable. However, the diesel has a significant advantage at lower loads due to its low pumping work and leaner air/fuel ratio.
Small DI diesels have comparable (or slightly lower) maximum bmep to equivalent ID1 diesels. The best bsfc values for DI diesels are 10 to 15 percent better, however. 5. In the DI diesel category (which is used over the largest size rangeless than 100 mm bore to almost 1 m), maximum bmep and best brake fuel conversion efficiency steadily improve with increasing engine size due to reduced impact of friction and heat loss per cycle, higher allowable maximum cylinder pressure so higher boost can be used, and (additionally in the larger engines) through turbocompounding. 7l3 (b) Rank the chambers in order (1, 2, 3) of their flame frontal area (1 = highest) when the mass fraction burned is about 0.2 and the piston is at TC. (c) Given this relative flame front area ranking, discuss whether the ranking by mass burning rate dmddt will be different from the flame area ranking. (d) Briefly discuss the knock implications of these three chamber designs. Which is likely to have the worst knock problem? $ spark plug \ PROBLEMS 15.1. The schematics show three different four-stroke cycle spark-ignition engine combustion chambers. A and B are two-valve engines, C is a four-valve engine (two inlet valves which open simultaneously, two exhaust valves). Dimensions in millimeters are indicated. A and C have normal inlet ports and do not generate any swirl, B has a helical inlet port and generates substantial swirl. Spark plug locations are indicated. All three engines operate at the same speed (3000 revjmin), with the same inlet mixture composition, temperature, and pressure, and have the same displaced volume. 889 t/ ~ l o o - - - - - c j &-loo----j A. 2-valve Side plug Nonnal port 15.2 B. Zvalve Plug 16 am fmm axis Helical port +1oomm+ C. 4-valve Center plug No- ports FIGURE PI54 Figures 15-23 and 15-10 show the variation in brake specific fuel consumption (bsfc) for a swirl-chamber ID1 automobile diesel (D) and a conventional automobile spark-ignition (SI) engine as a function of load and speed, respectively. From these graphs determine, and then plot, brake fuel conversion efficiency: (1) as a function of speed at full load and (2) as a function of load at a mid-speed of 2500 revjmin. Both engines are naturally aspirated. Assume the engine details are: Diesel S I engine Compression ratio Equivalence ratio range Displacement, dm3 22 9 0.34.8 1.0-1.2 2.3 1.6 (a) List the major engine design and operating variables that determine brake fuel conversion efficiency. (b) Explain briefly the reasons for the shapes of the curves you have plotted and the relative relationship of the D and SI curves. (c) At 2500 revjmin, estimate which engine will give the higher maximum brake power. 153. The diesel system shown in the figure consists of a multicylinder reciprocating diesel engine, a turbocharger (with a compressor C and turbine T, mechanicaily connected to each other), an intercooler (I), and a power turbine (T,) which is geared to the engine drive shaft. The gas and fuel flow paths and the gas states at the numbered points are shown. You can assume that the specific heat at constant pressure c, of the gas throughout the entire system is 1.2 kJ/kg. K and y = cdc, = 1.333. The engine operates at 1900 revjmin. The fuel has a lower heating value of 42 MJ/kg of fuel, ENGINE OPERATING CHARACTERISTICS 891 .3 (a) What is the power (in kilowatts) which the turbocharger turbine (T,) must produce? What is the gas temperature at exit to the turbocharger turbine? (b) What is the power turbine power output?
(c) The heat losses in the engine are 15 percent of the fuel's chemical energy (mfQ,). Find the engine power output, the total system power output, and the total system brake fuel conversion efficiency (friction effects in the engine and power turbine are internal to these devices and do not need to be explicitly evaluated). Air 0.53 kgls ,FnLek.&,=qJ 2.5 a m T,, 1.5 atm Paker turbine I Fuel 675 K 0.018 kgls Gesred to drive shaft 1 atm Exhaust FIGURE PIS-3 15.4. The attached graph shows how the brake power and specific fuel consumption of a four-stroke cycle single-cylinder spark-ignition engine vary with the fuellair equivalence ratio at wide-open throttle. It also shows how the following efficiencies vary with equivalence ratio: The volumetric efficiency : q , The mechanical efficiency: q, [Eq. (2.17)] The combustion efficiency: q, [Eq.(3.27)] The indicated fuel conversion efficiency: qJ, [Eq. (2.23)] The indicated thermal conversion efficiency: qt, [Eq. (3.3111 (a) Derive a relation between the variables qJ,i , qc ,and qt, i . (b) Derive an equation which relates the brake power P, to q, ,q, ,tk, qr,i , and any other engine and fuel parameters required. (c) Explain briefly why the variations of qa, q,, q, , q / , i , qt, with equivalence ratio in the figure have the form shown (e.g., why the parameter is approximately constant, or has a maximum/minimum, or decreases/increases with increasing richness or leanness, etc.). 155. The diagram shows the layout of a low heat loss turbocharged turbocompounded diesel engine. The engine and exhaust system is insulated with ceramics t o reduce heat losses to a minimum. Air flows steadily at 0.4 kg/s and atmospheric conditions into the compressor C, and exits at 445 K and 3 atm. The air is cooled to 350 K in the intercooler I. The specific heat of air, c,, is 1 k J / k g K . In the reciprocating diesel engine, the fuel flow rate is 0.016 kg/s, the fuel heating value is 42.5 MJ/kg, and the heat lost through the ceramic walls is 60 kW. The exhaust gases leave the reciprocating engine at 1000 K and 3 atm, and enter the first turbine T,, which is mechanically linked to the compressor. The pressure between the two turbines is 1.5 atm. The second turbine T, is mechanically coupled to the engine drive shaft and exhausts to the atmosphere at 800 K. The specific heat of exhaust gases, c,, is 1.1 kJ/kg. K. (a) Analyze the reciprocating diesel engine E and determine the indicated power obtained from this component of the total system. If the engine mechanical efficiency is 0.9 what is the brake power obtained from component E? (b) Determine the power obtained from the power turbine T,. (c) Determine the total brake power obtained from the complete engine system and the fuel conversion efficiency of the system. You can neglect mechanical losses in the coupling between the power turbine and the engine drive shaft. 1.5 atm "5 I 3 am 350 K 0.8 1.0 1.2 1.4 Equivalence ratio 1.6 FIGURE PI54 1000 K 3atm 3 Fuel, 0.016 kgls FIGURE PIS-5 15.6. New automobile spark-ignition engines employ "fast-burn technology" to achieve an improvement in fuel consumption and reductions in hydrocarbon (HC) and oxides of nitrogen (NO3 emissions. This question asks you to explain the experimental data which shows that faster-burning combustion chambers do provide these benefits relative to more moderate bum-rate chambers. (a) Figure 9-36b shows the effect of increasing the percent of the exhaust gas recycled to the intake (for NO, control) in a moderate burn-rate engine at constant speed and load, stoichiometric air/fuel ratio, with timing adjusted for maximum brake torque at each condition. COV,, is the standard deviation in imep divided by the average imep, in percent. The different types of combustion are: misfre, partial burn, slow burn, normal burn, defined in Sec. 9.4.3. Frequency is percent of cycles in each of these categories. Use your knowledge of the sparkignition engine flame-propagation process and HC emission mechanism to explain these trends in COV,,, ,HC, and frequency as EGR is increased. (b) The fast-burn combustion chamber uses two spark plugs and generates swirl inside the chamber by placing a vane in the inlet port to direct the air to enter the chamber tangentially.
The swirl angular velocity in the cylinder at the end of intake is six times the crankshaft angular velocity. There is no swirl in the moderate burn-rate chamber which has a single spark plug and a relatively quiescent in-cylinder flow. The table shows spark timing, average time of peak pressure, average flame-development angle (0 to 10 percent mass burned) and rapid burning period (10 to 90 percent mass burned) for these two engines. Figures 11-29 and 15-9 show how the operating and emission characteristics of the fast bum and moderate burn-rate engines change as percent EGR is increased Explain the reasons for the differences in these trends in COV,,,, bsfc (brake specific fuel consumption), and HC, and similarity in NO,. The operating conditions are held constant at the same values as before. Fast 15.7. bw Moderate b m Spark timing 18' 40" BTC Crank angle for average,P &lo% burned 1&90% burned 15" 16" ATC 24" 35" 20" 50" Two alternative fuels, methanol and hydrogen, are being studied as potential future spark-ignition engine fuels which

"F calorie (thermo.)/g calorie (thermo.)/g ."C 2 3 4 To Multiply by To J/kg J/kr K J/kg J/kg.K Force dyne kilogram-force pound-force Force per unit length (includes sqtiace tension) dyne/centimeter N/m pound-force/inch N/m pound-force/foot N/m Fuel consumption (economy) pound/horsepower-hour gram/kilowatt-hour mile/gallon (U.S.) mile/gallon (Imp.) kg/J kg/J m/m3 m/m3 Heat flux (includes thermal conductivity) ~ t u i&. ft2. OF Btu (IT)/ft2 Btu (IT)/h. ft2. "F calorie (thermo.)/cm2 Length foot inch micron mile Mass Ounce pound ton (long or Imp., 2240 lb) ton (short, 2000 lb) tonne (metric) Mass per unit time wow) pound/second pound/minute pound/hour Mass per unit volume gradsallon (U.S.) pound/foot3 pound/iich3 pound/gallon (Imp.) pound/gallon (U.S.) Power, heat flow Btu O / h o u r horsepower (550R .lbf/s) horsepower (metric, CV, PS) 5 Multiply by - 1 To convert from 2 To Pressure, stress (force per unit area) atmosphere (normal, 760 tom) inch of mercury (WF) kilogram-force/centimeter2 mrn of mercury, O•‹C(ton) pound-force/foot a pound-force/inch2 (psi) Temperature interval degree Celsius degree Fahrenheit Temperature temperature ("C) temperature ("F) 3 Multiply by 4 To 101.3 3.377 98.07 133.3 47.88 6.895 0.5556 ("F- 32)/1.80 Torque kilogram-force meter pound-force foot 9.807 1.356 Velocity foot/second kilometerpour milehour 0.3048 0.2778 1.609 Viscosity centipoise centistoke poise stoke -- 5 M & ~ Yby 1.000 1.m 0.1000 100.0 Volwne barrel (42U.S. gallon) foot3 gallon (Imp.) gallon (U.S.) inch3 liter 0.1590 28.32 4.546 3.785 16.39 1 .ooO Volume per unit time foot3/minute (dm) foot3/second gallon (U.S.)/minute (gpm) 0.4719 28.32 63.09 Notes: 1. Derived units such as that for torque (newton-metre,N.m)arc written with a period betwan each component unit for clarity. In practice, the period is often omitted. 2 Derived from Mobil Technical Bulletin SI Units, The Modem Metric System. Copyright Mobil Oil Corporation, 1974. Sections reproduced courtesy Mobil Oil Corporation. APPENDIX B IDEAL GAS RELATiONSHIPS APPENDIX 903 B.2 THE MOLE It is convenient to introduce a mass unit based on the molecular structure of matter, the mole: The mole is the amount of substance which contains as many molecules as there are carbon atoms in 12 grams of carbon-12.t Thus, the number of moles n of gas is given by IDEAL GAS RELATIONSHIPS and Eq. (B.3) becomes Values for the universal gas constant in different units are given in Table B.1. In the SI system, the value is 8314.3 J/krnol K. TABLE El Values of universal grs constant a B.l IDEAL GAS LAW The gas species which make up the working fluids in internal combustion engines (eg., oxygen, nitrogen, carbon dioxide, etc.) can usually be treated as ideal gases. This Appendix reviews the relationships between the thermodynamic properties of ideal gases. The pressure p, specific volume v, and absolute temperature T of an ideal gas are related by the ideal gas law pv= RT B.3 THERMODYNAMIC PROPERTIES It follows from Eq. (B.l) that the internal energy US of an ideal gas is a function of temperature only: u = u(T) (B.1) For each gas species, R is a constant (the gas constant). It is different for each gas and is given by where a is the universal gas constant (for all ideal gases) and M is the molecular weight of the gas. Since v is given by V/m,where V is the volume of a mass of gas m, Eq. (B.l)can be rewritten as Since the enthalpy h is given by u (B.6) + pv, it follows also that h=YT) (B.7) t This is the SI system definition of the mole; it was'formerly called the gram-mole. The kilogrammole (kmol) is also used; it is 1000 timea as large as the mole.

2 The symbol u will be used for internal energy per unit mass, ii for internal energy per mole, and U for internal energy of a previously defined system of mass m. Similar notation will be used for enthalpy, entropy, and specific heats, per unit mass and per mole. APPENDIX B IDEAL GAS RELATIONSHIPS The specific heats at constant volume and constant pressure of an ideal gas, c, and cp,respectively, are defined by The ratio of specific heats, y, is a useful quantity: An additional restrictive assumption is often made that the specific heats are constants.

This is not a necessary part of the ideal gas relationships. In general, the internal energy and enthalpy of an ideal gas at a temperature T relative to its internal energy and enthalpy at some reference temperature To are given by T + B.4 MIXTURES OF IDEAL GASES The working fluids in engines are mixtures of gases. The composition of a mixture of ideal gases can be expressed in terms of the following properties of each component: Partial pressure pi.

The pressure each component would exert if it alone occupied the volume of the mixture at the temperature of the mixture. Parts by volume VJV.

The fraction of the total mixture volume each component would occupy if separated from the mixture, at the mixture temperature and pressure. Mass fraction xi. The mass of each component mi, divided by the total mass of mixture m. Mole fraction jEi. The number of moles of each component ni, divided by the total number of moles of mixture n. From Eq. (B.l) it follows that = uo 905 ~"(77dT (B.12) h = ho + J cp(T)dT (B.13) From Eq. (B.5) it follows that (B.16) The thermodynamic properties of mixtures of ideal gases can be computed from the following relationships: Molecular weight rT and (B.17) To The entropy at T, u, and p, relative to the entropy at some reference state To, v, , po ,can be obtained from the relationships Internal energy, enthalpy, and entropy On a mass basis : u = ~ x i u i h=xxihi (B.14) i i On a mole basis: which integrate to give ii = C &iii i (B.15a) and The properties u, h, and s can be evaluated on a per unit mass or per mole basis. On a mass basis, c,, c, , and R would have the units J F g . K (Btuflbm OR);on a mole basis u, h, and s are replaced by ii, I;, and 5.

R is then the universal gas constant a, c, and c, are replaced by E, and Z.,, and E,, E,, and a would have the units J/kmol. K (Btu/lb-mol .OR).

- h"= 1 zil;, i 3= x Zi3, i (B. 19a, b, c) APPENDIX C EQUATIONS FOR FLUID F W W THROUGH A RESTRICTION 907 APPENDIX I I EQUATIONS FOR FLUID FLOW THROUGH A RESTRICTION FIGURE C-1 Schematic of liquid flow through oriiice. C.1 LIQUID FLOW Consider the flow of a liquid through an orifice as shown in Fig. C-1. For the ideal flow, Bernoulli's equation can be written For an incompressible flow, continuity gives V I A l = V2A , and the ideal mass flow rate through an orifice is given by The real mass flow rate is obtained by introducing the discharge coefficient: The discharge coefficient is a function of orifice dimensions, shape and surface roughness, mass flow rate, and fluid properties (density, surface tension, and viscosity). The use of the orifice Reynolds number In many parts of the engine cycle, fluid flows through a restriction or reduction in flow area. Real flows of this nature are usually related to an equivalent ideal flow. The equivalent ideal flow is the steady adiabatic reversible (frictionless) flow of an ideal fluid through a duct of identical geometry and dimensions. For a real fluid flow, the departures from the ideal assumptions listed above are taken into account by introducing a flow coefficient or discharge coefficient C D ,where CD = actual mass flow ideal mass flow Alternatively, the flow or discharge coefficient can be defined in terms of an effective cross-sectional area of the duct and a reference area. The reference area AR is usually taken as the minimum cross-sectional area.

The effective area of the flow restriction A, is then the cross-sectional area of the throat of a frictionless nozzle which would pass the measured mass flow between a large upstream reservoir at the upstream stagnation pressure and a large downstream reservoir at the downstream measured static pressure. Thus C,,=- AE AR Re,=-=-pV2D2 bD2 /' V as a correlating parameter for the discharge coefficient accounts for the effects of m, p, v, and D2 to a good approximation.' C.2 GAS FLOW Consider the flow of an ideal gas with constant specific heats through the duct shown in Fig.

C-2. For the ideal flow, the stagnation temperature and pressure, T, and p,, are related to the conditions at other locations in the duct by the steady flow energy equation v2 To=T+- 2% and the isentropic relation 908 INTERNAL COMBUSTION ENGINE FUNDAMENTALS (C EQUATIONS FOR FLUID FLOW THROUGH A RESTRICnON 909 This ratio is called the critical pressure ratio. For (pT/po)less than or equal to the critical pressure ratio, I Throat I I The critical pressure ratio is 0.528 for y = 1.4 and 0.546 for y = 1.3. For a real gas flow, the discharge coefficient is introduced. Then, for subcritical flow, the real mass flow rate is given in terms of conditions at the minimum area or throat by po ideal For a choked flow, 1 FIGURE C-2 Pressure distribution for gas flow through a n o d e . Equation (C.8) can be rearranged in the form of Eq. (C.2) (with A, 4 A,) as litreal= C~ A ~ C 2 ~ 0 b-0 PT)I"~@ By introducing the Mach number M = V/a, where a is the sound speed (= the following equations are obtained: KT), (c. 10) where @ is given by (C. 11) The mass flow rate m is Figure C-3 shows the variation of @ and (m/m*),dealwith (po - pT)/po.m* is the mass flow rate through the restriction under choked flow conditions (when the Mach number at the throat is unity). For flow rates less than about 60 percent of the choked flow, the effects of compressibility on the mass flow rate are less than 5 percent. With the ideal gas law and the above relations for p and T, this can be rearranged as For given values of po and To, the maximum mass flow occurs when the velocity at the minimum area or throat equals the velocity of sound. This condition is called choked or critical flow. When the flow is choked the pressure at the throat, p,, is related to the stagnation pressure p, as follows: 1.0 0.9 0.8 0,7 P_T PO 0.6 0.;28 FIGURE C-3 Relative mass flow rate m/m* and wm~ressible flow function UJ [Eq.(C.11)]as function of n o d e or restriction pressure ratio for ideal gas with y = 1.4. (From Taylor.') Flow coefficients are determined experimentally and are a function of the shape of the passage, the Reynolds number and Mach number of the flow, and the gas properties. For a Mach number at the throat less than about 0.7 and for passages of similar shape, the flow coefficient is essentially a function of Reynolds number only. Orifice plates are frequently used to measure gas flow rates. Standard methods for determining flows through orifice plates can be found in Ref. 3. REFERENCES 1. Lichtarowicz, A., Duggins, R. K., and Markland, E.: "Discharge Codficients for Incompressible Non-Cavitating Flow through Long Orifices," J. Mech. Eng. Sci., vol. 7, no. 2, pp. 210-219,1965. 2. Taylor, C. F.: The Internal Combustion Engine in Theory and Practice, vol. I, p. 506, MIT Press, 1966. 3. Marks' Standmd Handbookjiw Mechanical Engineers, 8th ed., McGraw-Hi, 1978. APPENDIX DATA ON WORKING FLUIDS TABLE D.l TABLE D.2 Thermodynamic properties of air at low density? Standard entbalpy of formation and molecular weight of species Sped- Fornula oxygen Nitrogen Carbon Carbon monoxide Carbon dioxide Hydrogen Water Water Methane Propane Ismtane Isooctane Cetane Methyl alwhol Methyl alcohol Ethyl alcohol Ethyl alcohol 0, N, C CO Mokeolu mi* g/de 32.00 28.01 12.011 28.01 (Graphs, Tables, and Computational Equations for Forty Substances), by W. C. Reynolds, Published by the Department of Mechanical Engineering, Stanford University, Stanford,CA 94305,1979. gas gas solid gas CO, Hz Hz0 H2O CH4 C,H, C,H,, C,H,, CH,OH 2.016 18.02 18.02 16.04 44.10 114.23 114.23 226.44 32.04 liquid liquid gas CH,OH 32.04 liquid 46.07 liquid '16~34 gas gas liquid gas gas gaS C,H,OH C2H,0H t At 298.15 K (25•‹C)and I atrn. ' t Abstracted with permission from Thermodynamic Properties in SI Statet MJ/kmol @I kd/mol TABLE D3 Enthalpy of C, CO, CO, ,Hz, H,O, N, ,0, h'q I) -&298.ls), kcd/mol T(K) c CO CO, Ha Ha0 N, 0, Source: JANAF Tkmochemiul Tables, National Bureau of Standards Publication NSRDS NBS37.1971. qs3 * " dxxx u'u'du' - 1$81ap g g xSsTdS $3 "32 8 umumSu"u" 58 x INDEX Adiabatic flame temperature, 81,94 Air: constituents of, 65 table of thermodynamic properties, 912 Viscosity, 143 Air/fuel ratio: definition, 53 feedback control, 301-304 lambda sensor, 301-303 relative, 71 stoichiometric, 69-70,915 of gasoline, 280 Air pollution, automotive: emissions mechanisms, summary, 568-572 nature of problem, 5-6 sources of emissions, 567-568 (see also Carbon monoxide; NO, ; Particulates; Unburned HC emissions) Alcohols: antiknock rating, 476-477 composition, 68 methanol combustion, 382 oxygenates : emissions of, 598 as extenders, 476-477 stoichiometricequation, 72 Aldehyde emissions, 568,598 Alkyl compounds (acetylenes, napthenes, olefins, paraffins), 67-68 Aromatics, 68 Atkinson : cycle, 184-186 James, 3 Atomization of sprays: regimes ot, 525429,532 secondary, 532-533 Autoignition, 462470,542-545 chemistry of, 463-467 cool flames,465 of hydrogen, 463-464 induction-time correlations, 468,543-545 SheU model, 469-470 single-, two-stage, 465-466 Availability: analysis, 16193,792-797 balances, 191-192,196,793,795 combustion loss, 192-193,196,795 convemion efficiency, 84-85 definitions, 84,186188,792-793 distribution, by category, 796-797 losses, actual cycle, 196,796797 steady-flow function, 187,793 Balance, 20 Bearings: journal, 716 eccentricity, 735 friction, 717,736-737 load diagram, 734-735 schematic, 735 slider, 716 Beau de Rochas, Alphonse, 2-3 Blowby, 361-365 unburned HC emissions, 6n,567,606607 Brake parameters, definition, 46,4849 Bum angles (SI engines): flame development, 389-390,421-423,777 overall, 389-390 rapid-burning, 389-390,422423,777-778 variations in, 415,422-423 Bum rate (SI engines): and combustion chamber geometry, 847-848 effect on cycle-bycycle variations, 415417, 845-846,849-850 effect on performance, 195 EGR,effect of, 837-839 turbulence effects, 846-848 (see also Bum angles; Heat-release rate) Burned gas : composition: equilibrium, 93 low temperature, 104 fraction, 102-103 Burning rate analysis, Krieger and Bonnan, 511-514 (see also Heat-release analysis) Carbon monoxide: background, 6,567-57 1 diesels, 592 oxidation kinetics, 593-596 SI engines, 592-596,836 (see also Catalytic converters) Carburetors, 16-17,282-294 accelerator pump, 286,291 air-bleed compensation,287-290 altitude compensation, 286,292-293 boost venturis, 16,286-287 choke, 286,291-292 elementary, 282-285 idle system, 286,290-291 main metering system, 286290 modem design, 1617,285-294 multiple-barrel, 287 power enrichment, 286,291 transient effects, 293-294 Catalytic converters: catalyst conversion efficiency, 651652,656 catalytic materials, 649,651652,654,65565 7 degradation, poisoning, 651453 design of, 649-650 light-off temperature, 651,653 NO reduction, 654-655 oxidation, 649-654 three-way, 655-657 Cetane: index, 542 n-hexadecane, 541,915 number, 541,550-552 fuel structure dependence, 550-551 Charts (see Thermodynamic charts) Chemical equilibrium: computer codes, 90-92 constants, 87-90 general principles, 86-94 Chemical reaction : rate constants,96 rates, 92-96 steady state assumption, 96 Combustion: constant pressure, 7475,126,172 constant volume, 73-74,125,169 efficiency, 8143,509,601 inefficiency, 154,195,509 products composition: equilibrium, 93 low temperature, 104 stoichiometry, 68-72 (see also Flame development; Flame propagation; Flame structure; Flames) Combustion chambers: bowl-in-piston, 342,353-357,811,866-869 design of, SI engines: air breathing, 220-222,846,850-851 bum rate, 844-846 common types, 845 knock, 854-857 objectives, 844-846 optimization strategy, 857-858 swirl, 846,850-852 surface area, 44 Combustion (CI engines): consequence, of 492493 fuel-air mixing and burning rates. 558-562 models for, 504-508,779-780,782-784, 786788,816-818 phases of, 505-506 mixing-controlled phase, 506,558-562 premixed, rapid burning phase, 505, 558-560 (see also Ignition delay) photographs of, color plate (between 498 and 499), 497-502 role of, 493,555-558 summary of, 491493 (see also Diesel wmbustion systems; Ignition delay; Fuel sprays) Combustion modeling, 766778,779-780, 782-784,786788,81648 Combustion (SI engines): abnormal phenomena, 451 burned gas : mixed model, 378-381 temperatures, 379-384383 unmixed model, 378-381 composition effects, 395 cycle-byqcle variations, 413-424 bum rate effects, 415417,845-846,849-850 C~USCSof, 282,419-422 description of, 372-373,413415,829,832, 849-850 measures of, 415-418 cylinder-tocylinder variations, 282,413,420, 829430,831 description of, 371-373,376 factors that control, 846-850 leanfdilute operating limits, 424426 misfin, 414415,424427,611 motion produced by, 384411 partial burning, 414-415,424-427,611 speed, effects on, 394,400-402,41142 stages of, 372,389-390,39742,412 thermodynamics of, 376383 turbulent flame regimes, 396397 (seealso Flame propagation relations; Flame structure; Flames; Heat release; Knock; Spark ignition) Compression, crankcase, 11,238,244 Compression-ignition engines : operating cycle, 25-31 (see also Diesel engines) Compression ratio : definition, 43 effect on eEciency, 170,172,175,182,197, 841-844 effect on mep, 176,183,842 knock limited (critical), 470472,854357 typical values, 43,58,492,887 Compressors: centrifugal, 238,258-262,877-878 corrected mass flow, 255,262 corrected speed, 255,262 isentropic efficiency, 251 performance maps, 255,257-258,261-262, 270,273,878-879 roots blower, 15,256258,886 screw, 256-258 sliding vane, 255-257 velocity diagrams, 260 Comprex (see Supercharging) Conservation equations, open system: energy, 751-753 mass, 750-751 Coolant heat flow, 675675 Courant number, 760 Crank angle, definition, 44 Crevices: effect on performance, 195,387-388 flows in/out, 360-365 geometry, 361-362 model for, 387-388 piston/ring assembly, 361-363 unburned HC emissions, 604-608 Critical pressure ratio, 909 Cycles: Alkinson, 184-186 constant-pressure, 163-164, 178 constant-volume, 163-164,169-172, 178 availability analysis, 189-195 fuel conversion efficiency, 170,197 four-stroke, 10-1 1 fuel-air, 162, 177-183 assumptions, 177 CI engine, 181 results, 181-183, 197 SI engine, 178-180 ideal gas standard, 162, 169-177 availability analysis, 189-192 comparison, 173-177 entropy changes, 188-189,192 limited-pressure, 163-164, 178 Otto, 11 overexpanded, 183-186 two-stroke, 11-12 Cylinder pressure: analysis of: CI engines, 508-517 Rasswneir and Withrow method, 385-386 SI engines, 384389 (see also Heat release) cycle sample size, 418 data (CI engines), 504,513,885 data (SI engines), 162,372-374,384,414 with knock, 453-454.45942 measurement of, 384 p-, 8,-, 415418,829 Cylinder volume: equation for, 4 3 4 Damkohler number, 396,399 Delivery ratio, 237-24,244,882483 Diesel wmbustion systems: direct-injection,32-37,493494,496 bowl-in-piston, swirl multihole nozzle, 493494,496-501 M.A.N. " M ",494,496501 quiescent, 493-494,496500 9U) INDEX Diesel combustion systems (continued): indirect-injection,33-34,494-496 swirl prechamber, 494-502 turbulent prechamber, 494-497 (see also Combustion (CI engines); Fuel sprays) Diesel emissions: NOJparticulates trade off, 865-866 (see also Carbon monoxide; NO,; Particulates; Unburned HC emissions) Diesel engines: bur-stroke cycle air-cooled, 35-36.859 examples (DI), 32-36,877-881 examples (IDI), 33-34,875-877 large (marine), 3637,883-886 two-stroke cycle, 14,37,883-886 Diesel, Rudolf, 4 Droplets: equations for individual, 814-815 Sauter mean diameter, 434-436 size distribution, 352-354 vaporization, 536539,814815 Dynamometer, 45-46 Efficiency, definitions of: availability conversion, 84 catalyst conversion, 651652,656 charging, 239,244 combustion, 81-83 compressor isentropic, 251 fuel conversion, 52, 85,164,169 mechanical, 49,723 scavenging, 238,244 thermal conversion, 85 trapping, 238,244 turbine isentropic, 253 volumetric, 53-54 Emissions (see Carbon monoxide; NO,; Particulates; Unburned HC emissions) Emissions index, 56 Energy, available (see Availability) Energy balance, engine, 673-676 Engine processes: availability analysis of, 186193 thermodynamic relations for, 164-169 Engines: classification, 7-9 components, 12-15 compression-ignition (diesel), 25-37 energy balance, 673-676 historical, 1-7 maximum work, 83-85 multifuel, 39 prechamber (see Pmhamber engines) spark-ignition, 15-25 stratified~har~e (see Stratified-charge engines) Wankel (see Wankel engines) Enthalpy, 108-111,116,123-127,903-905 sensible, 113-114, 122 tables of, 914 stagnation, 251 Enthalpy of formation: datum reference state, 77 definition, 76 standard values, individual species, 77, 124, 913 of unburned mixture, 123-125 Equilibrium (see Chemical equilibrium) Equivalence ratio (see Fuellair equivalence ratio) Evaporative HC emissions, 6n,567 Exhaust: blowdown process, 166,206,231-233,613 displacement process, 167,206,231-233 (see also Intake and exhaust flow models) Exhaust gas: composition data, diesels, 148-149 data, SI engines, 146-148 equivalence ratio determination, 148-152 F/A nonuniformities, 152-154 measurement, 145-146 mass flow rate, 231-232 recycle, recirculation (EGR), 103 temperatures, 232-234,648 enthalpy-averaged, 234 equivalence ratio effects, 834-835 EGR, effects of, 837-838 thermodynamic state, 167 EGR tolerance, SI engines, 837-839 Exhaust gas treatment, 648-660 (see also Catalytic converters; Particulate traps; Thermal reactors) Exhaust manifold pressures, 214 Flame development process : effects of combustion chamber geometry, 846447 effects of mixture composition and state, 846, 848-849 effects of turbulence, 846-849 factors that control, 846-850 Flame ionization detector, 145-146,597n, 620 Flame photographs: CI engines, color plate (between 498 and 499) SI engine, 390-394,397-399,401,458450, color plate (between 498 and 499) Flame propagation data, 409,412,773-774 Flame propagation relations, 406-412 characteristic length, 410,412 "entrainment" burning laws, 771-778 flame areas,406409,766767 turbulent burning speed, 408-409,411412 velocity parameters, 408-412 Flame quenching, 599-601 Flame structure (CI engines): ignition, location of, 502,556557 species concentration data, 557-559 spraylflame photos, color plate (between 498 and 499), 502,523,525,527,537 (see also Combustion (CI engines); Diesel combustion systems) Flame structure (SI engines), 390-402 flame area, 394,406410,846-847 flame thickness, 398402,410 swirl, effect of, 393 Flame volume (SI engines): data, 372-373,409 relationships, 406-410 Flames: classification, 62-64.395-397 diffusion, 63 laminar, 63 premixed, 63 turbulence, effect on, 390-392,398402 turbulent, 63,395-397 Flow modeling (see Models, fluiddynamic based) Flows (i-cylinder): exhaust stroke vortex, 365-367 laser doppler anemometry, 336,808-809 piston/cylinder corner, 365-367,613-614 through intake valve, 224225,227,229, 326330 valve-jet driven, 327-330,807-809 velocities at intake valve, 326327,808-810 (see also Blowby; Crevices; Squish; Swirl; Turbulence) Flows through nozzles, orifices, restrictions, 906910 Four-stroke cycle : definition, 10-11 exhaust proass, 206-208 inlet process, 206-208 pV diagram, 47,162,284,727 Friction : accessory requirements (fan, generator, pumps), 739-740 background, 712-71 3 coefficient of, 716 boundary lubrication, 716-718 hydrodynamic lubrication, 718 mixed lubrication, 718 Stribcck diagram, 716-717 crankshaft, 734-737 difference, motorinB/firing, 720-721 losses, categories of, 713 measurement methods, 719-721 piston assembly, 730,732-734 pumping, 47,168-169,713-715,725,726728 throttling work, 727-728 valve flow work, 727-728 turbulent dissipation, 719 valve train, 737-739 Friction correlations: Bishop, 727,733,736,738 crankshaft, con rods, 736 piston and rings, 733-734 total friction mep, 719,722 valve train, 738 Friction data: diesels, 722,724,725 engine breakdown tests, 722,725-726 SI engines, 721,723 Friction definitions: accessory mep, power, work, 714-715 pumping mep, power, work, 47,714-715 rubbing friction mep, power, work, 714-715 total friction mep, power, work, 714-715 Fri~tion~lubrication regimes: boundary, 716718 mixed, 716 hydrodynamic, 716 Fuel-air cycle (see Cycles) Fuel-air equivalence ratio, 71 availability analysis, effect on, 192-193 from exhaust composition, 148-152 for optimum SI engine efficiency, 831-835 Fuel-air mixing, diesels, 493,504408, 555-558 and burning rates, 558-562 Fuellair ratio : definition, 53 stoichiometric,69 Fuel conversion efficiency: constant-volume cycle, 170, 182 compression ratio effects, 170,175,182,197 equivalence ratio effects, 182,197 constant-pressure cycle, 172, 175 definition, 52, 85 DI vs ID1 diesel, 860-861 limited-pressure cycle, 170, 175 overexpanded cycle, 184-185 Fuel conversion efficiency (SI engines): effect of: bum rate, 832-833 compression ratio, 841-844 Fuel conversion efficiency (SI engines) (continued): equivalence ratio, 830-834 Fuel injection (diesels): distributor pump, 30-32,518 in-line pump, 28,M,518 nozzle flow rate, 521 nozzle geometry, 526529 nozzles, 29,31,519-520 objectives, 518 single-barrel pump, 518-519 systems, 27-31,517-522 unit injectors, 520-521 Fuel injection (SI engines): injection timing, 298-299 injector design, 295-296 multipoint port systems, 16-17,294-299 air-flow meter, 297-299 fuel transport, 320-321 mechanical, 298 specddensity, 294296,299 single-point systems, 299-301 Fuel sprays: adiabatic saturation, 538-539 breakup, 522-523,530-531,532 evaporation, 535-539,814-815 and flame structure, 555-558 ignition sites, 525,556557 modeling, 538-539,780-784,813-816 equations for droplets, 814-815 1-D turbulent jet, 780-781 multidimensional, 813-816 multipackage, 782-784 multizone, 781-782 penetration, 529-532 photographs of, color plate (between 498 and 499),523,525,527,537 spray angle, 526528 structure, 522-527,529,535-537,555-558 swirl, effect of, 524-525,531-532.558 temperature distribution, 538-539 wall interaction, 523-524 (see also Atomization; Droplets) Fuels : additives: antiknock, 473,475-476 ignition-accelerating, 551-552 octane improvers, 476-477 API gravity, 542 distillate: cetane rating, 541-542 diesel index, 542 nitrogen content, 577 sulfur content, 568 enthalpy of formation, 913 gasoline: composition, 280,915 equilibrium vaporization, 314-3 15 " heating values, 78-90,915 hydrocarbons: classes of, 66-68 knocking tendency, 470-472 hydrogen, 915 autoignition of, 463464 cornbustion, 398,773-774 stoichiometric equation, 72 ignition quality of, 492,541-542,550-552 isooctane, 67,915 octane rating, 471 stoichiometry, 69-71 laminar flame speeds, 395,402406 primary reference, 475 properties : table of, 915 thermodynamic, 77,130-133 stoichiometric A/F, 70,915 (see also Alcohols; Cetane; Octane) Gas constant, 903 Gas properties: computer routines for, 130-140 isentropic compression functions, 113-115 molar and mass basis, 107,904-905 molecular weight, 106,136,905,913 polynomial functions fuels, 130-133 gas species, 130-131 ratio specfic heats, 134, 137,139,904 specific heats, 132,134,136,138,904 stagnation values, 251,907 tables, 127-129,912,914 unburned mixture, 130-135 (see also Ideal gas;Thermodynamiccharts; Transport properties) Gasoline (set Fuels, gasoline) Heat-release analysis: gross, net, 387-388,510-511 ID1 diesel engines, 514-517 one zone, 386-388.508-511 problems with (d'tesels), 508-509 two zone (SI engines), 376382 Heat-release rate: diesels: apparent, 509 data, 504,511,516-517,560-561 definition of, 497 mixingcontrolled, 560-562 variables, effects of, 560-562 Heat-release rate (continued): SI engines: cycle-bycycle variations, 414-415 results, 390,413414 Heat transfer: characteristicsof, in engines, 668470,672473 coefficient, 671 conduction, 670 convective, 670-671 dimensional analysis, 676-677 cycle-simulation predictions, 702-704,707, 769-771 effect of engine variables, 701-707 compression ratio, 703-704 coolant temperature, 704-705 equivalence ratio, 703 load, 702,796-797 spark timing, 704 speed, 673,675,679,702-703,797 squish, swirl, 704 wall material, 705-707 effect on performance, efficiency, 194-195, 770-771,851-852 exhaust system, 682683 intake system, 682 (see also Intake manifold) prechamber diesels, 787 radiation: apparent emissivity, 684-688 apparent flame temperature, 685-686 from gases, 683-684 monochromatic absorption coefficient, 687688 prediction formula 688-689 relative importance, 693-694 from soot, 683,684-689 Heat transfer correlations: evaluation of, 694-696 exhaust port, 682683 instantaneous local, 681482,695-696 instantaneous, spatial average, 67-80, 694-695 Annand, 678479,695 Woschni, 679-680,694-695 time-average, 677679 zonal models, 682,696,768-769 Heat transfer measurements: methods, 689-690 results, diesels, 692694 results, SI engines, 690-692 Heating values, 78-90,915 higher heating value, 78 lower heating value, 78 Humidity: effect on air properties, 67 psychrometric chart, 66 relative, 65 Hydrocarbon emissions (see Unburned HC emissions) Hydrocarbons: burnup, 600,614-618 classes of, 6668 knocking tendency, 470474 oxidation mechanism, 467 Hydrogen: autoignition of, 463-464 combustion, 773-774 stoichiometricequation, 72 Ideal gas: analytic model for, 109-1 12 law, 64,902 mixtures, 905 relationships, 107-109,902-905 thermodynamic properties, 903-905 (see also Burned gas; Gas properties; Unburned mixture; Working fluids) Ignition delay: correlations for, 543-545 in engines, 553-554 delinition, 505,539-540 factors affecting: air temperature, pressure, 547-548 chamber wall, 548-549 injection timing, 546 load, 546-548 oxygen concentration, 549-550 speed, 548 spray parameters, 546-547 swirl, 549 fuel property effects, 550-553 processes occurring, 540-541 (see also Autoignition; Cetane) Indicated parameters, dehition : gross, 47-49,714-715 net, 4749,714-715 Intake and exhaust flow models: boundary conditions, 761 example results, 311-312,761-762 finitedifferencemethods, 759-762 gas dynamic models, 313,756-762 homentropic flow, 758 . 1-D unsteady flow equations, 756758 manifold models: wing and emptying, 311-312,753-755 Helmholtz resonator, 312-313 method of characteristics, 759 quasi-steady models, 232,753-754 924 INDEX Intake manifold: air flow, 309-313 description of, 309-311 transient behavior, 310-312 (see also Intake and exhaust flow models) design, 308-309 fuel transport, 314-321 droplet behavior, 316-317 liquid films, 315-316,318-320 transient behavior, 310-312,318-321 vaporization, 314-321 pressure variation, 212-214,216,310-311 IC engines (see Engines) Internal energy, 108-1 11,116-127,903-905 sensible, 113-114, 122 Internal energy of formation: standard values, 124 of unburned mixture, 123-125 Knock : antiknock additives, 4,473,475-476 lead alkyls, 4,473,475-476 MMT, 475476 characterization of, 4-56 combustion photographs, 458-461 damage, 456457 deposit effects on, 477478 description of, 375,450-457 detection, 454 effect on heat transfer, 707 end gas, 457462,467470 temperature, 468-469 impact of, 456457,852-854 intensity, 45-56 pressure waves, 461-462 sensors, 872 theories : autoignition, 457458,462 detonation, 457458 (see also Autoignition; Compression ratio; Fuels; Octane) Laminar flame: speed, 395,402correlations, 403-406 data, 403-405 and SI engine combustion, 771-775, 777-778,848-849 straining effects, 406 thickness, 395,402 Langen, Eugen, 2 Lead alkyls, 4,473,475-476 Lenoir, J. J. E., 2 Lubricant: requirements, 741-745 SAE viscosity classification, 744-745 Lubrication: of bearings, 715-718,734-737 of piston assembly, 729-734 regimes of, 716-718 system layout, 740-741 (see also Friction; Bearings) Manifolds : tuning of, 215,217-218 (see also Exhaust manifold; Intake manifold) Mass fraction burned, SI engines: data, 372-373,382,777-778 equations for, 377-378,381-382390 Wiebe function, 390,768 Maximum work, 83-85 (see also Availability) Mean effective pressure: coefficient of variation (COV), 417,424-425 cycle-by-cycle variations, 417,425 definitions, 50,714-715 friction,-714-715,825-827 fuel-air cycle results, 183 ideal cycles, 171,173,176 importance of, 59,823-824 overexpanded cycle, 185-186 pumping, 169,714-715 relationships for, 50-51,57,823-824 Mean effective pressure (DI diesels): effect of: injection parameters, 863-864 load and speed, 858460,877-878 full load, 826-827 Mean effective pressure (ID1 diesels): effect of: injection parameters, 863-864 load and speed, 860,875-876 full load, 826-827 Mean effective pressure (SI engines): effect of: compression ratio, 842 equivalence ratio, 83C832 heat transfer, 851 wide open throttle, 824-827,839-840 Mechanical efficiency: definition, 49 values, SI engine, 722-723 Methanol combustion (SI engine), 382 Mixture nonuniformity, quality, 152-154,282, 314,829-832 Mixture requirements (SI engines), 279-282, 833-834 steady, transient, 834 typical schedules, 281-282 Models of engine processes, rationale, 748-750 Models, fluiddynamic based (multidimensional) for boundary layers, 803 of combustion, 816-818 flow field predictions, 360,807-813 concentration distributions, 811-813 particle traces, 810-812 velocities, 807-8 11 governing equations, 798-799 KIVA code, 803,804,815416 numerical methodology, 798,80-07 computing mesh, 804405,810 discretization practices, 804-8015 solution algorithms, 806-807 overview, 797-798 sprays, 813-816 turbulence models: full-field modeling, 799-802 k-Emodels, 775-777,801-802,808,810 largeeddy simulation, 799 Reynolds stress, 802 subgrid scale, 802-803 Models, thermodynamiobased (phenomenological,zero-dimensional): complex engine systems, 789-792 transient behavior, 791-792 turbocharged/turbocompounded, 789-792 DI diesels : model structure, 784-785 simulation results, 784-785 single zone combustion models, 778-780 spray models, 780-784 (see also Fuel sprays) emissions, 765,787-788 ID1 diesels, 784-788 prechamber phenomena, 784-787 simulation results, 787-788 open system conservation equations, 763-765 overall structure, 762-763 SI engines: combustion models, 766-778 cycle simulation results, 769-771 "entrainment " burning laws, 771-778 flame geometry models, 766-768 stochastic models, 787-788 turbulence intensity models, 775-777 (see also Mass fraction burned) Mole, 903 Molecular weights, values, 913 Moment of inertia of charge, 353 NO concentrations, in-cylinder: DI diesel, 587-589 ID1 diesel, 589-590 SI engines, 579-581 NO formation: description of, CI engines, 586587 equivalence ratio, effect of, 575-576 kinetics of, 572-576 rate constants, 573 Zeldovich mechanism, 572 model for, SI engines, 578-581 rate equation for, 573-574 temperature, effect of, 574-576 NO from fuel N, 577 Nitrogen, atmospheric, 65 NO, formation, 577-578 NO,, definition of, 567,572 NO, emissions (diesels): effect of: diluents, 590491,861-863 equivalence ratio, 588-589 EGR, 590-591,861-863 injection parameters, 863-867 load, 861-862 swirl, 866-867 flame temperature correlation, 591-592 (see also NO formation) NO, emissions (SI engines): effect of: compression ratio, 844 diluents, 582-584 equivalence ratio, 581-585,83-36 EGR, 582-585,836-838 load, speed, 840-841 spark timing, 585586,829 (see also Catalytic converters; NO formation) Noise, 5,571-572 Octane: antiknock index, 474 fuel sensitivity, 473-474 and knock, 854-855 number, 471474 motor method, 471473 requirement, 453,474,478,852-857 research method, 471473 road, 474 oxygenates as extenders, 476-477 ratings of fuels, 915 Odor, diesel, 568 Oil consumption rate, 610 Organic compounds: classes of, 66-68 (see also Fuels) Otto: cycle, 11 Otto (continued): Nicolaus, A., 2-3 Oxygen (lambda) sensor, 301-303 Oxygenate emissions, 568,598 Paralftns : ignition limits, 465-466 knocking tendency, 470472 molecular structure, 67 Part-throttle (SI engines): efficiency, 833-834,843-844 mixture requirements, 280-282,834 performance, 833 Particulate emissions (diesels): effect of: injection parameters, 864-866 load, 861-862 Particulate traps, 659-660 Particulates, diesels: Ames test, 631 composition of, 627430,647-648 distribution in cylinder, 631635 HC absorption, condensation, 646-648 measurement techniques, 626-627 dilution ratio effects, 646-647 oil, contribution from, 629430,647448 size, 628-63 1 soluble fraction, 629,646-648 soot formation fundamentals, 635-642 soot oxidation, 642-646 specific surface area, 631,646 spherules, 627428 structure, 627431 (see also Particulate missions; Soot formation; Soot oxidation) Particulates, SI engines, 626 Peclet number, 599600 Performance of engines, summary, 58,866-888 Performance maps: description of, 839 DI dies